



Max-Planck-Institut
für Kohlenforschung

tu technische universität
dortmund

Enantioinversion in der Gold(I)-katalysierten Hydroalkoxylierung von Allenen

&

Studien zur Totalsynthese von Chagosensine

Dissertation

Zur Erlangung des akademischen Grades eines

Doktors der Naturwissenschaften

(Dr. rer. nat.)

des Fachbereichs Chemie der Technischen Universität Dortmund

vorgelegt von

Marina Kristina Ilg

geboren am 22.02.1988

in Böblingen

Mülheim an der Ruhr, 2017

Eidesstattliche Versicherung (Affidavit)

Ilg, Marina Kristina

166176

Name, Vorname
(Surname, first name)

Matrikel-Nr.
(Enrolment number)

Belehrung:

Wer vorsätzlich gegen eine die Täuschung über Prüfungsleistungen betreffende Regelung einer Hochschulprüfungsordnung verstößt, handelt ordnungswidrig. Die Ordnungswidrigkeit kann mit einer Geldbuße von bis zu 50.000,00 € geahndet werden. Zuständige Verwaltungsbehörde für die Verfolgung und Ahndung von Ordnungswidrigkeiten ist der Kanzler/die Kanzlerin der Technischen Universität Dortmund. Im Falle eines mehrfachen oder sonstigen schwerwiegenden Täuschungsversuches kann der Prüfling zudem exmatrikuliert werden, § 63 Abs. 5 Hochschulgesetz NRW.

Die Abgabe einer falschen Versicherung an Eides statt ist strafbar.

Wer vorsätzlich eine falsche Versicherung an Eides statt abgibt, kann mit einer Freiheitsstrafe bis zu drei Jahren oder mit Geldstrafe bestraft werden, § 156 StGB. Die fahrlässige Abgabe einer falschen Versicherung an Eides statt kann mit einer Freiheitsstrafe bis zu einem Jahr oder Geldstrafe bestraft werden, § 161 StGB.

Die oben stehende Belehrung habe ich zur Kenntnis genommen:

Official notification:

Any person who intentionally breaches any regulation of university examination regulations relating to deception in examination performance is acting improperly. This offence can be punished with a fine of up to EUR 50,000.00. The competent administrative authority for the pursuit and prosecution of offences of this type is the chancellor of the TU Dortmund University. In the case of multiple or other serious attempts at deception, the candidate can also be unenrolled, Section 63, paragraph 5 of the Universities Act of North Rhine-Westphalia.

The submission of a false affidavit is punishable.

Any person who intentionally submits a false affidavit can be punished with a prison sentence of up to three years or a fine, Section 156 of the Criminal Code. The negligent submission of a false affidavit can be punished with a prison sentence of up to one year or a fine, Section 161 of the Criminal Code.

I have taken note of the above official notification.

Ort, Datum
(Place, date)

Unterschrift
(Signature)

Titel der Dissertation:
(Title of the thesis):

Enantioinversion in the Gold(I)-catalyzed Hydroalkoxylation of Allenes &

Studies Toward the Total Synthesis of Chagosensine

Ich versichere hiermit an Eides statt, dass ich die vorliegende Dissertation mit dem Titel selbstständig und ohne unzulässige fremde Hilfe angefertigt habe. Ich habe keine anderen als die angegebenen Quellen und Hilfsmittel benutzt sowie wörtliche und sinngemäße Zitate kenntlich gemacht.

Die Arbeit hat in gegenwärtiger oder in einer anderen Fassung weder der TU Dortmund noch einer anderen Hochschule im Zusammenhang mit einer staatlichen oder akademischen Prüfung vorgelegen.

I hereby swear that I have completed the present dissertation independently and without inadmissible external support. I have not used any sources or tools other than those indicated and have identified literal and analogous quotations.

The thesis in its current version or another version has not been presented to the TU Dortmund University or another university in connection with a state or academic examination.*

*Please be aware that solely the German version of the affidavit ("Eidesstattliche Versicherung") for the PhD thesis is the official and legally binding version.

Ort, Datum
(Place, date)

Unterschrift
(Signature)

1. Berichterstatter: Prof. Dr. Alois Fürstner
2. Berichterstatter: Prof. Dr. Norbert Krause

Die vorliegende Arbeit entstand unter der Anleitung von Prof. Dr. Alois Fürstner in der Zeit von Juni 2013 bis Januar 2017 am Max-Planck-Institut für Kohlenforschung in Mülheim an der Ruhr. Teile dieser Arbeit wurden bereits in folgenden Beiträgen veröffentlicht:

„A Striking Case of Enantioinversion in Gold Catalysis and Its Probable Origins“

M. K. Ilg, L. M. Wolf, L. Mantilli, C. Farès, W. Thiel, A. Fürstner, *Chem. Eur. J.* **2015**, *21*, 12279–12284.

„A Two-Component Alkyne Metathesis Catalyst System with an Improved Substrate Scope and Functional Group Tolerance: Development and Applications to Natural Product Synthesis“

S. Schaubach, K. Gebauer, F. Ungeheuer, L. Hoffmeister, M. K. Ilg, C. Wirtz, A. Fürstner, *Chem. Eur. J.* **2016**, *22*, 8494–8507.

Die praktischen Arbeiten erfolgten zum Teil in enger Zusammenarbeit mit Dr. Jakub Flasz, Dr. Aurélien Letort, M. Sc. Marc Heinrich und Samira Speicher (Kapitel 2). Die beschriebenen Ergebnisse bilden eine vollständige Darstellung dieser gemeinsamen Arbeiten. Die von diesen Mitarbeitern alleinverantwortlich erzielten Ergebnisse wurden als solche an entsprechender Stelle gekennzeichnet.

Danksagung

Mein herzlichster Dank gilt meinem Doktorvater, Prof. Dr. Alois Fürstner, für die Aufnahme in seinen Arbeitskreis, die Bereitstellung spannender und herausfordernder Forschungsthemen sowie das entgegengebrachte Vertrauen. Darüber hinaus möchte ich mich für die hilfreichen Diskussionen, die gewährte wissenschaftliche Freiheit und die exzellenten Arbeitsbedingungen bedanken. Für die freundliche Übernahme des Koreferats danke ich Prof. Dr. Norbert Krause von der Technischen Universität Dortmund.

Für die erfolgreiche Zusammenarbeit während des Gold-Projekts danke ich Dr. Larry Wolf und Dr. Christophe Farès. Weiterhin möchte ich Dr. Jakub Flasz, Marc Heinrich und Dr. Aurélien Letort für die hervorragende Kooperation bei der Bearbeitung des anspruchsvollen Synthese-Projekts danken sowie Marc Heinrich und Dr. John Murphy für die Fortführung des Projekts. Hervorheben möchte ich zudem Samira Speicher, die als Auszubildende eine wertvolle Unterstützung war.

Ferner möchte ich dem technischen Personal der Arbeitsgruppe Fürstner danken, das sich unermüdlich in allen Belangen des Laboralltags engagiert: Helga Krause, Sebastian Auris, Karin Radkowski, Saskia Schulthoff, Christian Wille, Daniel Laurich und Jennifer Lenartowicz. Roswitha Leichtweiß danke ich für die Hilfe bei der Verwendung der HPLC-Geräte und Monika Lickfeld für die Unterstützung in allen organisatorischen und administrativen Angelegenheiten. Ein weiterer Dank gilt den Mitarbeitern der analytischen Abteilungen für die gewissenhafte Messung und Auswertung zahlreicher Proben.

Lee Collins, Marc Heinrich, Yonghoon Kwon, John Murphy, Dragoş Roşca und Jens Willwacher danke ich herzlichst für das zügige und kritische Korrekturlesen dieser Arbeit. Bei allen aktuellen und ehemaligen Mitgliedern der Arbeitsgruppe möchte ich mich für die gute Atmosphäre im Labor und die wertvollen Diskussionen bedanken; insbesondere bei meinen langjährigen Box- und Bürokollegen Sebastian Auris, Dr. Lennart Brewitz, Dr. Konrad Gebauer, Marc Heinrich, Dr. Laura Hoffmeister, Dr. Nikolas Huwyler, Dr. Kévin Jouvin, Helga Krause, Dr. Aaron Lackner, Dr. Rudy Lhermet, Samira Speicher, Dr. Dieter Weber und Bernhard Wölfl – sowie bei Dr. Dragoş-Adrian Roşca und Dr. Sebastian Schaubach. Auch die gemeinsamen Unternehmungen außerhalb des Labors werden mir stets in Erinnerung bleiben; dafür danke ich besonders Jens, Laura, Konrad, Peter, (Kuschelrock-)Marc, *the serious postdoc* Alicia, Stephan, Michi, Minh Kong, Dr. Sommer, Niko, Aaron, Pepito, Teresa (no?!) und Rudy – Tschuuuus.

Außerdem danke ich meinen Freunden, die mich regelmäßig besucht und auch aus der Ferne immerzu unterstützt haben, allen voran Biggi und Eva. Meinen Volleyballmädeln und Guido danke ich für drei Jahre Spaß und Ausgleich im Training, an den Spieltagen und darüber hinaus.

Den größten Dank verdient meine Familie, die mir stets zugehört und bedingungslos den Rücken gestärkt hat. Neben meinen Eltern danke ich vor allem Jens für die liebevolle Unterstützung, die unendliche Geduld und das maximale Verständnis. Ihnen sei diese Arbeit gewidmet.

Meiner Familie und Jens

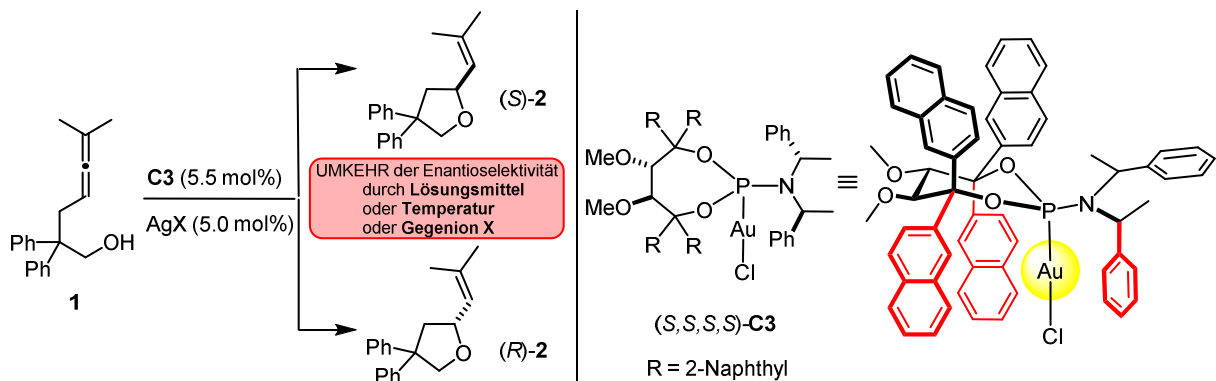
„Wer kämpft kann verlieren, wer nicht kämpft hat schon verloren.“

(Bertolt Brecht)

Inhalt

Enantioinversion in der Gold(I)-katalysierten Hydroalkoxylierung von Allenen

Chirale Phosphoramidit-Liganden mit TADDOL-basiertem Rückgrat haben sich in der asymmetrischen Goldkatalyse als äußerst erfolgreich erwiesen. Im Rahmen ihrer Anwendung in der intramolekularen Hydroalkoxylierung von Allenen wurde eine bemerkenswerte Entdeckung gemacht: die Enantioselektivität der Zyklisierung von Allenol **1** zu Tetrahydrofuran **2** konnte allein durch Variation von Lösungsmittel, Temperatur oder Gegenion unter Verwendung ein und desselben chiralen Gold-Komplexes **C3** von (*S*) nach (*R*) umgekehrt werden.



Das Phänomen der Enantioinversion, bei dem eine einzige chirale Quelle selektiv beide Enantiomere eines Produkts erzeugen kann, ist nicht unbekannt. Allerdings ist dessen Ursprung auf molekularer Ebene kaum verstanden. Der hier vorliegende Fall ist besonders eindrucksvoll, da es sich um das erste Beispiel handelt, bei dem drei verschiedene Parameter eine signifikante Inversion auslösen. Um Einblicke in den zugrunde liegenden Mechanismus zu erhalten, wurden detaillierte mechanistische Studien durchgeführt.

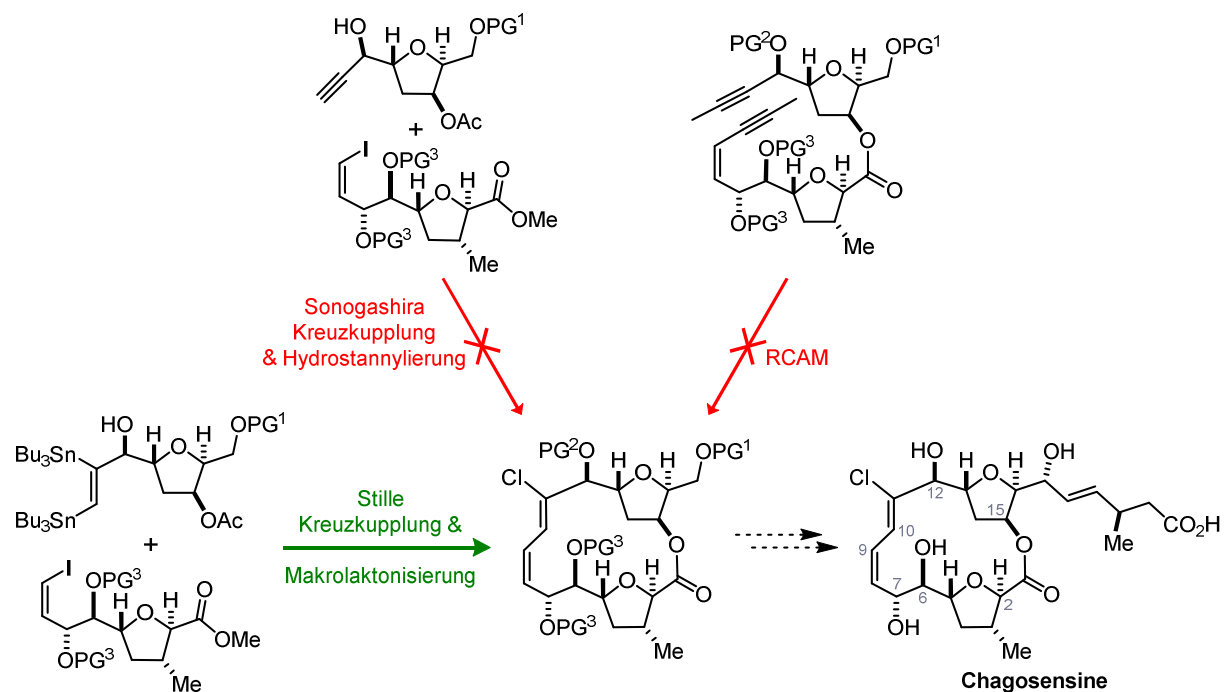
Präparative Untersuchungen, welche die ausführliche Analyse der Reaktionsparameter, Eyring-Studien sowie NMR-Experimente beinhalteten, konnten mithilfe von DFT-Rechnungen ein plausibles mechanistisches Szenario liefern. Der Hauptgrund für die Enantioinversion wurde im Vorliegen zweier kompetitiver Reaktionspfade gefunden: Im einen Fall ist die Protodeaurierung geschwindigkeitsbestimmend und das (*S*)-Produkt wird favorisiert, während im anderen Fall ein alternativer Pfad zugänglich ist, der durch assistierte Protodeaurierung bevorzugt das (*R*)-Produkt generiert. Eine solche Unterstützung kann entweder durch ein protisches Lösungsmittel, ein koordinierendes Gegenion oder ein zweites Substratmolekül erfolgen. Das Energieprofil erhält dadurch einen beachtlichen entropischen Beitrag, der den stereochemischen Verlauf maßgeblich bestimmt.

Diese Studie erklärt den ungewöhnlichen Effekt der Enantioinversion erstmals auf molekularer Ebene. Die Ergebnisse unterstreichen die Bedeutung der Entropie, die bei der Analyse von mehrstufigen Reaktionsmechanismen beachtet werden muss.

Studien zur Totalsynthese von Chagosensine

Die selektive und konsekutive Funktionalisierung von Alkinen wurde im Kontext eines anspruchsvollen Totalsynthese-Projekts erforscht. Die Anwendung einer Sequenz aus ringschließender Alkin-Metathese (RCAM), *trans*-Hydrostannylierung und Zinn/Chlor-Austausch sollte den Aufbau eines einzigartigen (*Z,Z*)-Chlorodiens im vielfältig substituierten Makrozyklus des marinen Polyketids Chagosensine ermöglichen.

Nach erfolgreicher Darstellung der benötigten Fragmente, wurde die geplante Reaktionsfolge untersucht. Die ringschließende Alkin-Metathese ließ sich jedoch nicht realisieren, vermutlich aufgrund erheblicher Ringspannung der konzipierten Enin-Makrozyklen und der außergewöhnlich hohen Dichte an koordinierenden funktionellen Gruppen. Der Versuch, diese gespannten Intermediate mittels ringschließender Dien-En-Metathese zu umgehen, schlug ebenfalls fehl. Auch der alternative Zugang über ein nicht-zyklisches Enin wurde durch ineffiziente Sonogashira Kreuzkupplung und erfolglose Hydrometallierung verwehrt.

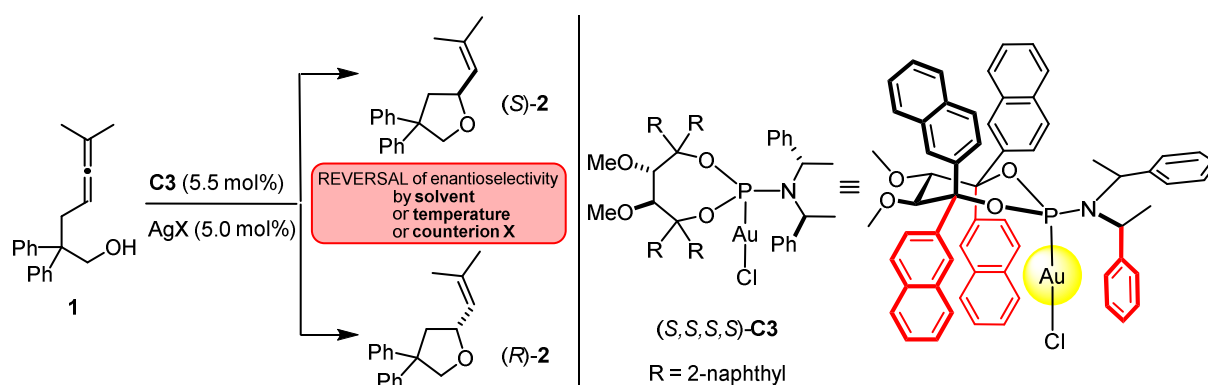


Trotz enormer Bemühungen und der Weiterentwicklung von Katalysatorsystemen versagten etablierte Methoden wie RCAM, RCM und Sonogashira Kreuzkupplungen im komplexen, hoch-oxygenierten Umfeld des Naturstoffs. Die Lösung wurde schlussendlich in der Funktionalisierung des Alkins vor der Fragmentkupplung gefunden: Bis-Metallierung des Nordsegments und anschließende selektive Stille Kreuzkupplung mit dem Südfragment gefolgt von Makrolaktomisierung lieferte in der vierten Strategie den Makrozyklus als Schlüsselintermediat. Damit ist die Fertigstellung der ersten Totalsynthese von Chagosensine in Reichweite gerückt.

Abstract

Enantioinversion in the Gold(I)-catalyzed Hydroalkoxylation of Allenes

Previously developed chiral phosphoramidite ligands comprising a TADDOL-related acyclic backbone have proven successful in asymmetric gold catalysis. While extending their applicability to the intramolecular hydroalkoxylation, a striking case of enantioinversion was observed: the sense of induction in the cyclization of allenol **1** to tetrahydrofuran **2** can be swapped from (*S*) to (*R*) solely by changing either the solvent or the temperature or the escorting counterion, while using the very same chiral gold complex **C3**.



The perplexing phenomenon of enantioinversion, in which a single chiral source delivers either enantiomer of a given product, is not uncommon. However, the understanding of its origins at the molecular level is quite limited. Moreover, the present case seemed particularly remarkable, since it represents the first reported example in which three different parameters are able to trigger a significant switch. Thus, a combined experimental and computational approach was conducted to gain insight into the underlying mechanism.

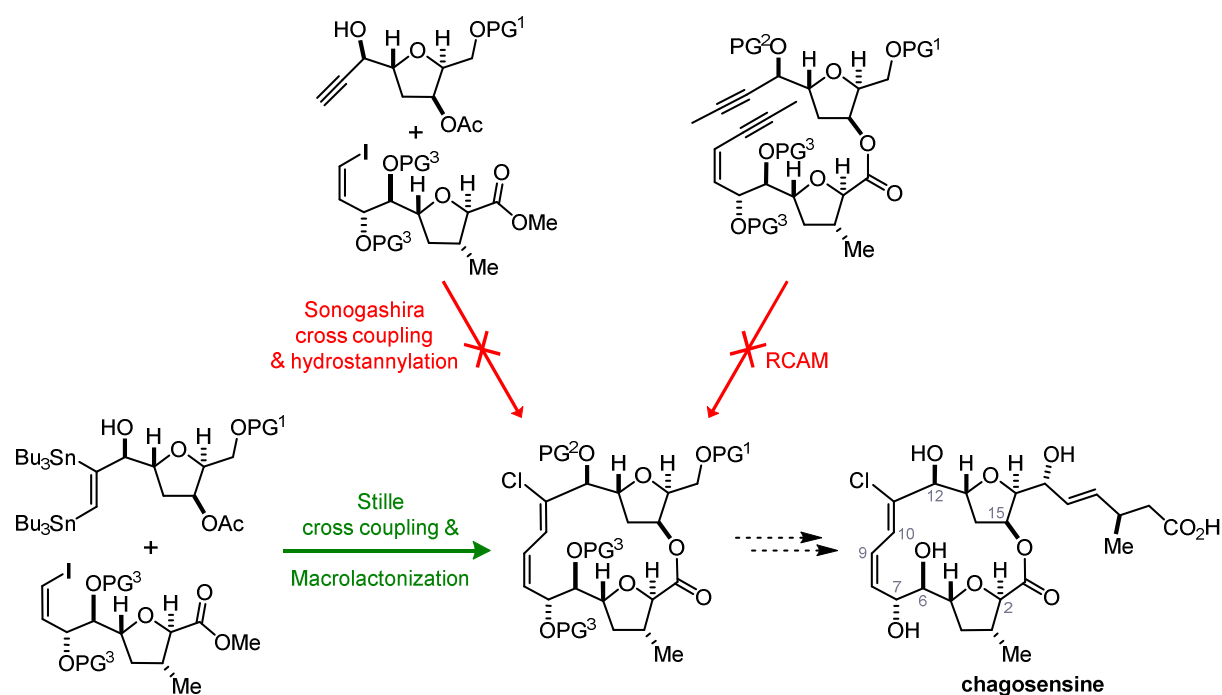
Preparative studies including thorough screenings, Eyring plots and NMR experiments in combination with DFT calculations provided a plausible mechanistic scenario. The major reason for the enantioinversion was found in the existence of two competing pathways: a pathway where proto-deauration is rate-determining favors the (*S*)-product, whereas an alternative outlet involving assisted proto-deauration preferably produces the (*R*)-product; such assistance can be provided either by a protic solvent, a coordinating counterion or a second substrate molecule. Consequently, the reaction free energy profile gains a significant entropic component that can ultimately dictate the stereochemical course.

This case study represents the first example, which explains the unusual effect of enantioinversion at the molecular level. The results highlight the importance of considering the entropy in the analysis of a multi-step reaction mechanism.

Studies Toward the Total Synthesis of Chagosensine

The selective and consecutive functionalization of alkynes was investigated in the context of a challenging total synthesis program. The marine polyketide chagosensine, isolated in 2003 from the Red Sea calcareous sponge *Leucetta chagosensis* in Israel, was deemed an ideal target for the application of a sequence of ring closing alkyne metathesis (RCAM), *trans*-hydrostannylation and tin/chloride exchange to install the unique (*Z,Z*)-chlorodiene motif within a highly decorated macrocycle. An additional obstacle to this endeavor was posed by the unsecured structure assignment of the natural product, whose synthesis had not been tackled before.

After the successful preparation of the required building blocks, the original endgame strategy was studied. However, RCAM could not be achieved, presumably due to the highly strained enyne macrocycle. Attempted ring closing diene-ene metathesis to circumvent such macrocyclic enynes did not succeed either. An alternative strategy based on the construction of an acyclic enyne was hampered by inefficient Sonogashira cross coupling and unfeasible hydrometalations.



Despite enormous efforts and catalyst development, conventional approaches such as RCAM, RCM and cross coupling strategies failed in this complex environment with an exceptionally high density of potentially coordinating functional groups. A remedy was found in the functionalization of the alkyne prior to fragment assembly: the intricate chlorodiene-containing macrolactone was finally accessed by bis-metalation of the northern domain followed by selective Stille coupling with the southern sector and subsequent macrolactonization. Thus, the synthesis of the sophisticated intermediate by this forth route sets the stage for the completion of the first total synthesis of chagosensine.



Max-Planck-Institut
für Kohlenforschung

tu technische universität
dortmund

**Enantioinversion in the Gold(I)-catalyzed
Hydroalkoxylation of Allenes**

&

**Studies Toward the Total Synthesis of
Chagosensine**

Table of Contents

1 Enantioinversion in the Gold(I)-catalyzed Hydroalkoxylation of Allenes	1
1.1 Introduction.....	1
1.1.1 Homogeneous Gold Catalysis.....	1
1.1.2 TADDOL-Phosphoramidites as One-point Binding Ligands for Asymmetric Gold Catalysis...	2
1.1.3 Intramolecular Hydrofunctionalizations of Allenes.....	4
1.2 Objectives.....	8
1.3 A Striking Case of Enantioinversion.....	8
1.3.1 The Phenomenon of Enantioinversion.....	8
1.3.2 The Scope of Enantioinversion in the Gold(I)-catalyzed Hydroalkoxylation of Allenes	9
1.3.3 Control Experiments.....	11
1.3.4 Reaction Parameters	16
1.3.4.1 Solvent.....	16
1.3.4.2 Counterion.....	18
1.3.4.3 Temperature.....	20
1.3.5 DFT Calculations ^[42]	25
1.3.5 NMR Studies ^[44]	31
1.3.6 Conclusion	34
2 Studies Toward the Total Synthesis of Chagosensine	36
2.1 Introduction.....	36
2.1.1 Natural Product Total Synthesis.....	36
2.1.2 Ring Closing Alkyne Metathesis and Postmetathetic Transformations	37
2.2 Isolation and Structural Discussion of Chagosensine.....	39
2.3 Objectives.....	41
2.4 The Metathesis Approach	42
2.4.1 Retrosynthetic Analysis	42
2.4.2 Model Studies on the Key Sequence.....	43

TABLE OF CONTENTS

2.4.3 Synthesis of the Northern Alcohol Fragments 48 and 49 ^[102]	50
2.4.4 Synthesis of the Southern Acid Fragment 60	53
2.4.5 Synthesis of the Sidechain 18	63
2.4.6 Fragment Assembly and Attempted Ring Closure	64
2.5 The First Macrolactonization Approach: Hydrostannylation	72
2.5.1 Retrosynthetic Analysis	72
2.5.2 Modification of the Northern Alcohol Fragments	73
2.5.3 Modification of the Southern Sector	79
2.5.4 Fragment Assembly	80
2.5.5 Hydrometalations	84
2.6 The Second Macrolactonization Approach: Bis-Metalation	91
2.6.1 Retrosynthetic Analysis and Strategic Considerations	91
2.6.2 Bis-Stannylation and Stille Coupling	93
2.6.3 Efforts Toward the Macrocycle	96
2.6.4 Outlook	97
3 Summary and Conclusion	99
3.1 Enantioinversion in the Gold(I)-catalyzed Hydroalkoxylation of Allenes	99
3.2 Studies Toward the Total Synthesis of Chagosensine	102
4 Experimental Section	108
4.1 General Experimental Methods	108
4.2 Enantioinversion in the Gold(I)-catalyzed Hydroalkoxylation of Allenes	109
4.3 Studies Toward the Total Synthesis of Chagosensine	118
4.3.1 Model Studies	118
4.3.1.1 Synthesis of the Diyne Model Substrates	118
4.3.1.2 Synthesis of the Enyne Model Substrates	125
4.3.2 Synthesis of the Northern Alcohol Fragments 48 and 49	132
4.3.3 Synthesis of the Southern Acid Fragment 60	141
4.3.4 Synthesis of the Sidechain 18	157

TABLE OF CONTENTS

4.3.5 Fragment Assembly and Attempted RCAM.....	159
4.3.6 Synthesis of the Northern Alcohol Fragments 122 and 123	171
4.3.7 Synthesis of the Southern Vinyl Iodide Fragments 137 and 139	181
4.3.8 Fragment Assembly and Hydrometalations	184
4.3.9 Synthesis of the Macrolactone 174	195
5 Glossary	203
6 Bibliography	206
7 Appendix	216
7.1 Crystallographic Data	216
7.2 Calibration of HPLC-MS for RCAM.....	217

1 Enantioinversion in the Gold(I)-catalyzed Hydroalkoxylation of Allenes

1.1 Introduction

1.1.1 Homogeneous Gold Catalysis

Over the past decade, the activation of an unsaturated carbon–carbon bond by a π -acidic noble-metal catalyst has been exploited for a wide range of new transformations of alkynes, allenes and alkenes.^[1] The discovery of this novel reactivity allowed the construction of diverse carbocyclic and heterocyclic scaffolds with increased molecular complexity from readily available substrates with high atom economy and functional group tolerance.^[2] Thus, numerous applications to target-oriented synthesis have been reported soon after.^[3] Efficient asymmetric variants of such transformations, however, proved challenging due to the favored linear-dicoordination of gold.^[4] This geometrical constraint forces the substrate to approach the reactive gold center *trans* to the chiral ancillary ligand L*, *i.e.* at maximum distance from the chiral information (Figure 1.1). With only single coordination sites, the rotation about the L*–Au bond and the Au–substrate bond remains *per se* unrestricted. Additionally, gold-catalyzed reactions are believed to proceed through outer-sphere pathways. Hence, the nucleophile does not enter the first coordination sphere of the Au⁺ center and therefore attacks the π -system from the opposite side.

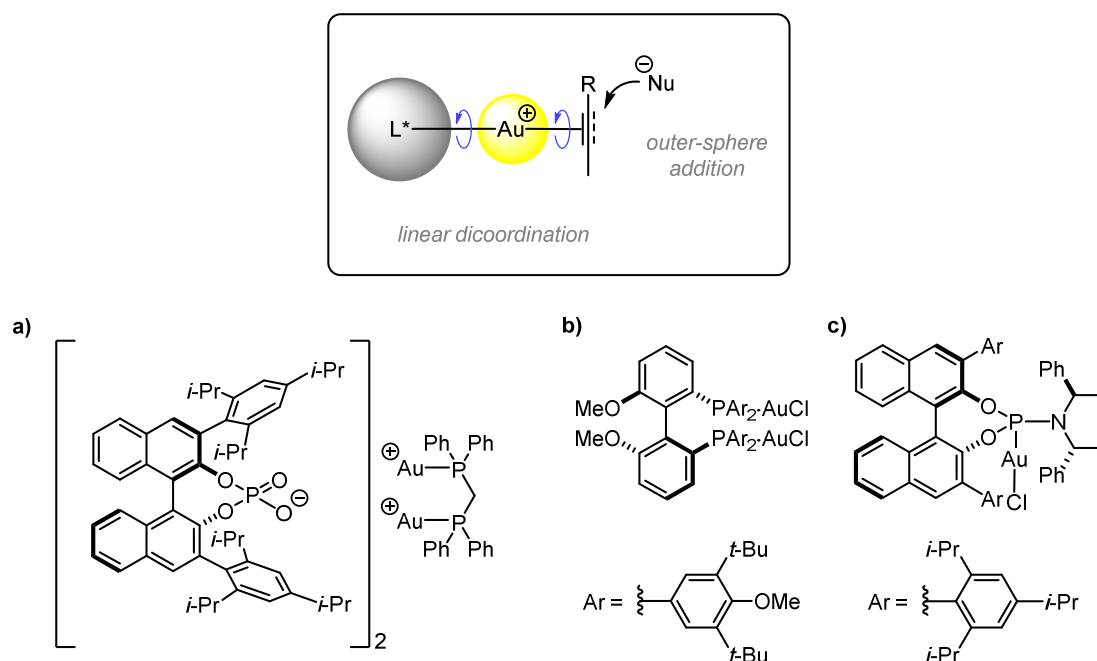


Figure 1.1. Top: intrinsic geometrical constraints to gold catalysis. Bottom: concepts for asymmetric gold catalysis: **a)** chiral counterion strategy; **b)** chiral dinuclear gold-phosphine complex; **c)** chiral phosphoramidite-gold complex.

Three major concepts to tackle the intricate transfer of chiral information from ligand to substrate have been established in homogeneous gold catalysis during the last few years: the use of chiral counterions,^[5] chiral dinuclear gold-phosphine complexes^[6] and the development of chiral one-point binding ligands (Figure 1.1).^[7]

1.1.2 TADDOL-Phosphoramidites as One-point Binding Ligands for Asymmetric Gold Catalysis

In this context, Fürstner and coworkers developed monodentate phosphoramidites featuring a TADDOL-related, yet acyclic backbone as chiral ligands for homogeneous gold catalysis.^[7b,7c,8] A general feature of these ligands is their short and flexible synthesis, providing a fast access to a library of catalysts; a selection is depicted in Figure 1.2.

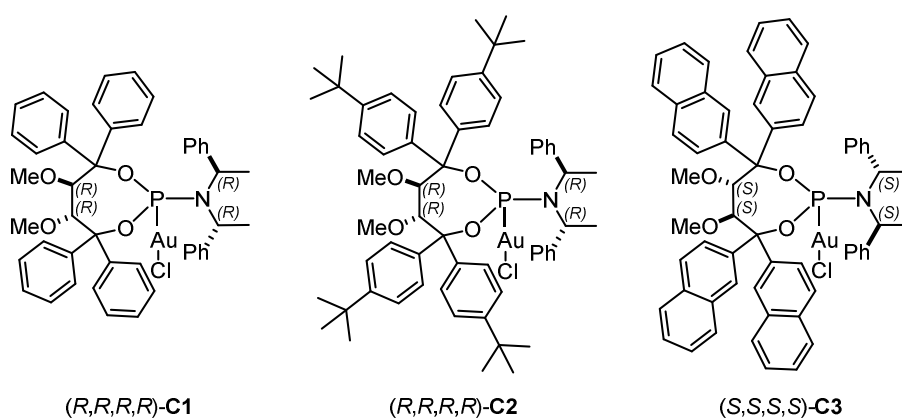
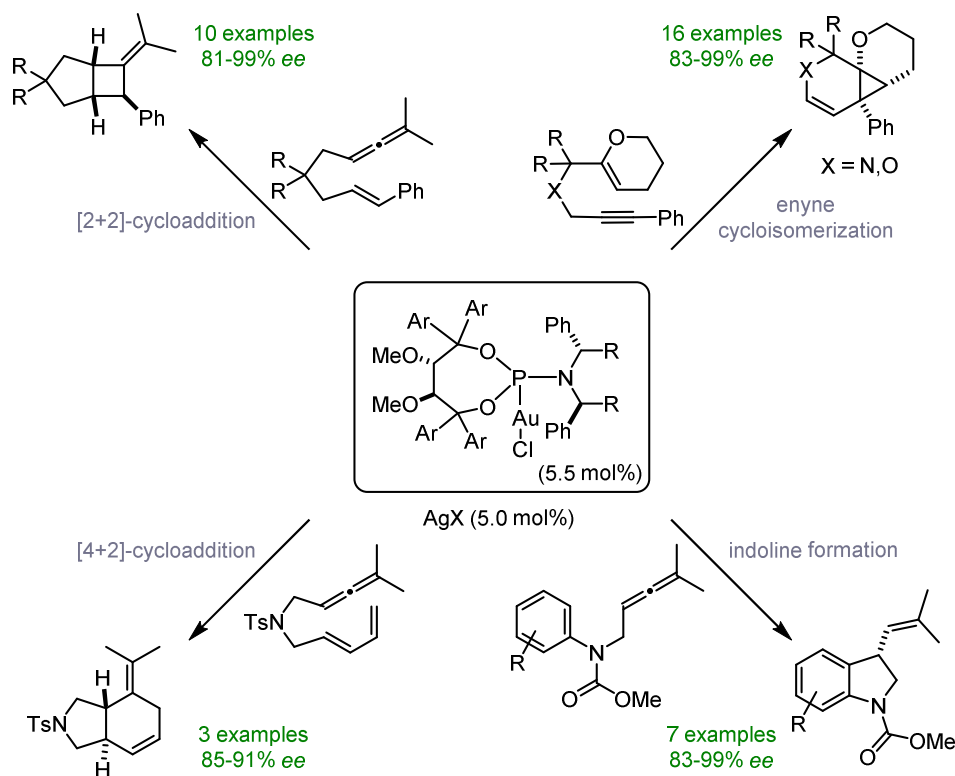


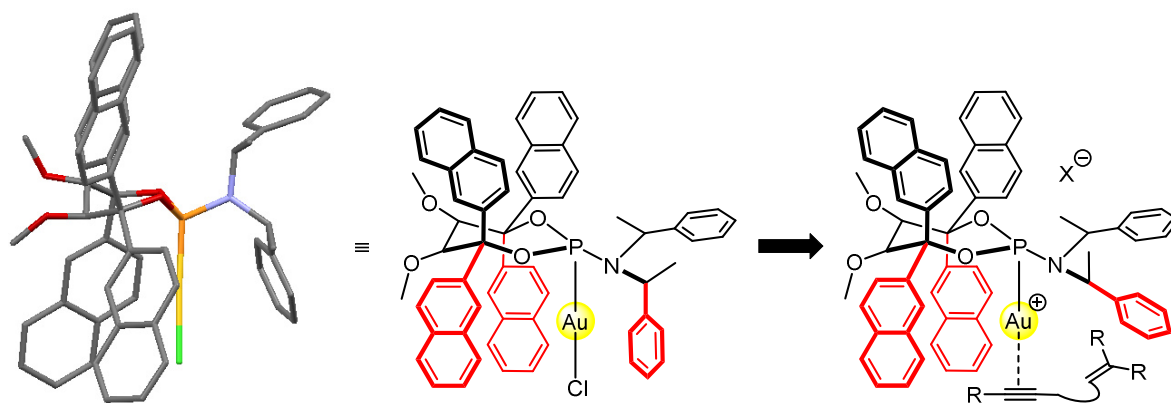
Figure 1.2. Selection of phosphoramidite-gold complexes of either enantiomeric series developed by Fürstner *et al.*^[7b,7c,8]

In contrast to their preceding BINOL-derived congeners (see Figure 1.1 c)),^[9] the TADDOL-based phosphoramidites are easily prepared on large scale from cheap starting materials and amenable to structural editing. As the corresponding gold complexes are air- and moisture-tolerant, they represent a user-friendly tool for organic synthesis. These complexes proved valuable for a broad variety of mechanistically distinct gold-catalyzed enantioselective transformations. One-point binding ligands – if appropriately designed – are beneficial, as the chiral information is closer to the metal center, therefore improving the chirality transfer onto the substrate. In this regard, [2+2]- and [4+2]-cycloadditions, enyne cycloisomerizations and indoline formations were accomplished with good to excellent enantioselectivities (Scheme 1.1).



Scheme 1.1. Variety of transformations successfully catalyzed by TADDOL-based phosphoramidite-gold complexes.

The origin of enantioselection was de-convoluted with the aid of computational studies conducted on the enyne cycloisomerization catalyzed by gold complex (*S,S,S,S*)-**C3**.^[7c] The crystal structure of this precatalyst, which served as a starting point for the calculations, revealed that two of the aryl groups at the TADDOL-moiety and one phenyl group of the amine part form a cavity around the metal center (Scheme 1.2, red). This pseudo- C_3 symmetrical pocket extends well beyond the gold atom only for substituted phenyl rings or larger aromatic systems. Thus, the substrate bound to the gold center will be buried in the chiral environment and enantioselectivity should be improved as compared to analogs bearing smaller substituents at the ligand. DFT calculations suggest that this pseudo- C_3 symmetry converts into C_1 symmetry upon substrate binding, which translates to the absolute stereochemistry of the product by a unidirectional rotation of the substrate in the cavity (Scheme 1.2).

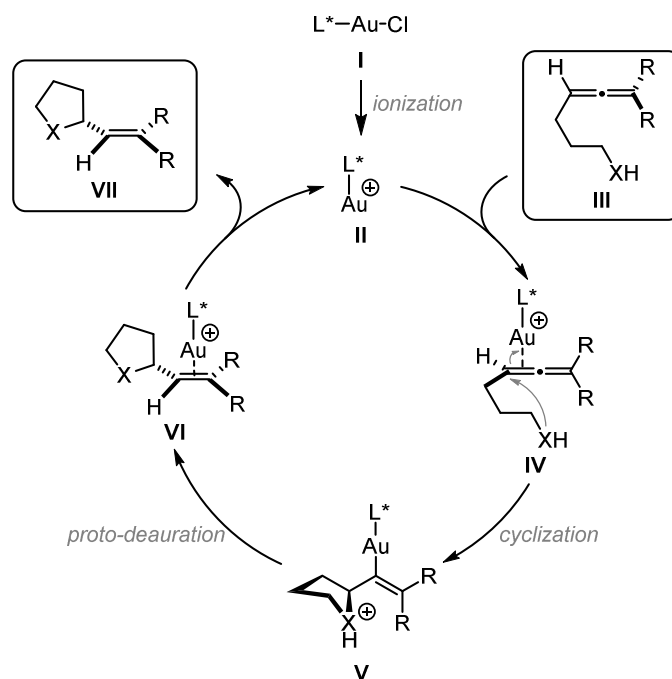


Scheme 1.2. Probable origin of enantioselection in enyne cycloisomerizations. X-ray structure of (*S,S,S,S*)-**C3** (left), schematic illustration with pseudo- C_3 symmetric cavity highlighted in red (middle) and repeal of symmetry upon substrate binding (right).^[7c]

As a result, the architecture of the catalyst and thus the size of the chiral cavity are crucial for the formation of the desired products with high enantioselectivities. In order to ultimately challenge the novel catalytic system, the reaction scope was further expanded.

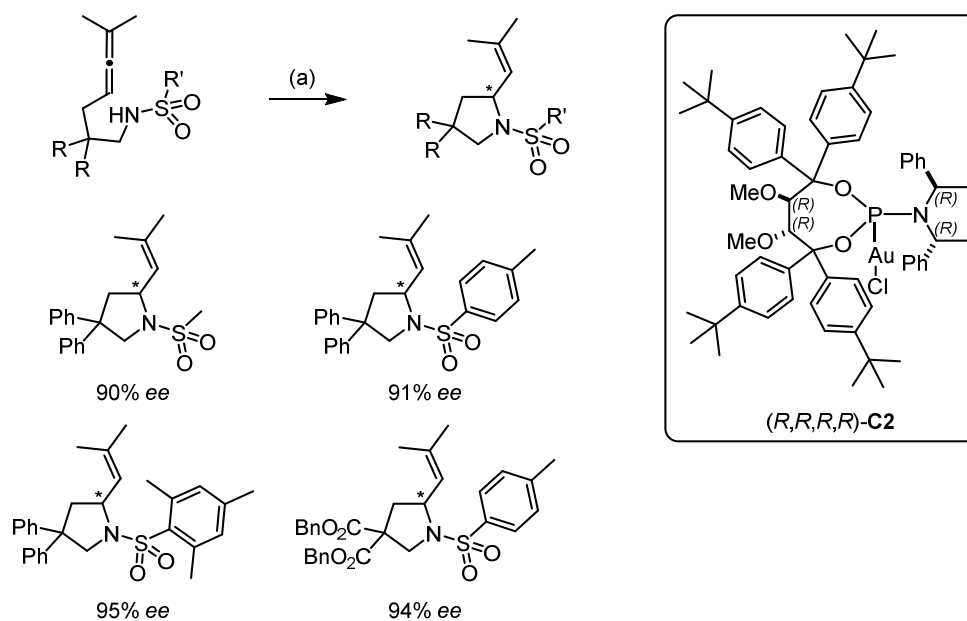
1.1.3 Intramolecular Hydrofunctionalizations of Allenes

Intramolecular hydrofunctionalizations of allenes as highly atom economical processes affording heterocycles^[10] were envisioned to showcase the power of the new single-point binding ligands in asymmetric gold catalysis. These transformations comprising both *endo*- and *exo*-cyclizations of carbon-, sulfur-, nitrogen- or oxygen-nucleophiles onto allenes had been investigated in great detail by different research groups.^[11] Initially, the reaction mechanism was subject to intense debate: Widenhoefer proposed an outer-sphere mechanism^[6d] while Yamamoto suggested coordination of the nucleophile to the gold and an inner-sphere addition to the allene.^[12] Only after the subsequent isolation of a first vinyl gold species during the cyclization of an allenolate,^[13] and other gold intermediates characterized thereafter,^[14] could the former proposals be re-evaluated. Hence, hydrofunctionalizations of allenes are commonly believed to proceed through outer-sphere pathways with the proposed mechanism depicted in Scheme 1.3. After ionization of the precatalyst **I**, the cationic gold species **II** activates the allenic π -system of starting material **III** forming a π -complex **IV**. Nucleophilic attack at the activated carbon leads to the vinyl gold intermediate **V**, which undergoes proto-deauration to give the π -complex **VI**. Decomplexation liberates the product **VII** concomitant with the regeneration of the cationic gold catalyst **II**.



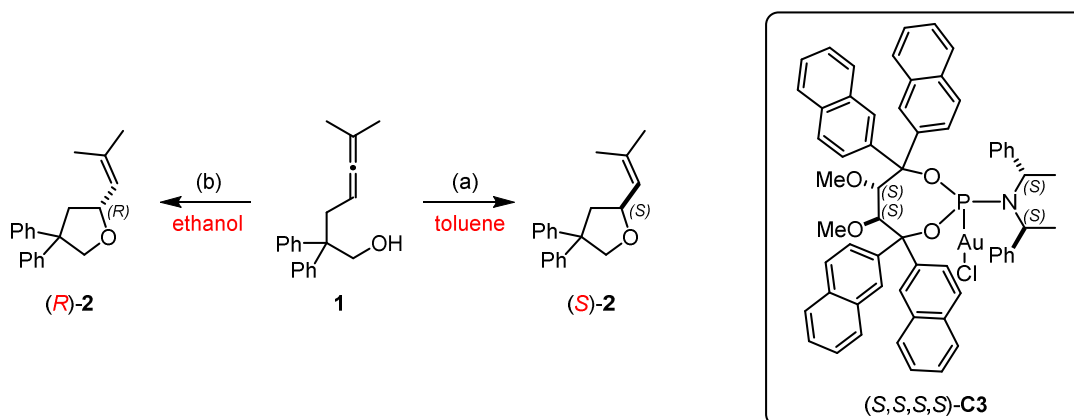
Scheme 1.3. Mechanistic proposal for the intramolecular hydrofunctionalization of allenes.

Despite the advanced studies on this transformation, it was not until 2007 that Widenhoefer *et al.* reported the first enantioselective gold-catalyzed hydroalkoxylation.^[6d] Since then, asymmetric *exo*-hydroaminations and -alkoxylations of allenes have been subject of intense investigations.^[5a,15] As a result, such reactions represent a stringent test for the competence of novel catalysts. Thus, Fürstner and coworkers applied the newly designed TADDOL-related phosphoramidite-gold complexes to aminoallenes, which were cyclized to the corresponding pyrrolidines with 90 to 95% *ee* (Scheme 1.4).^[7c]



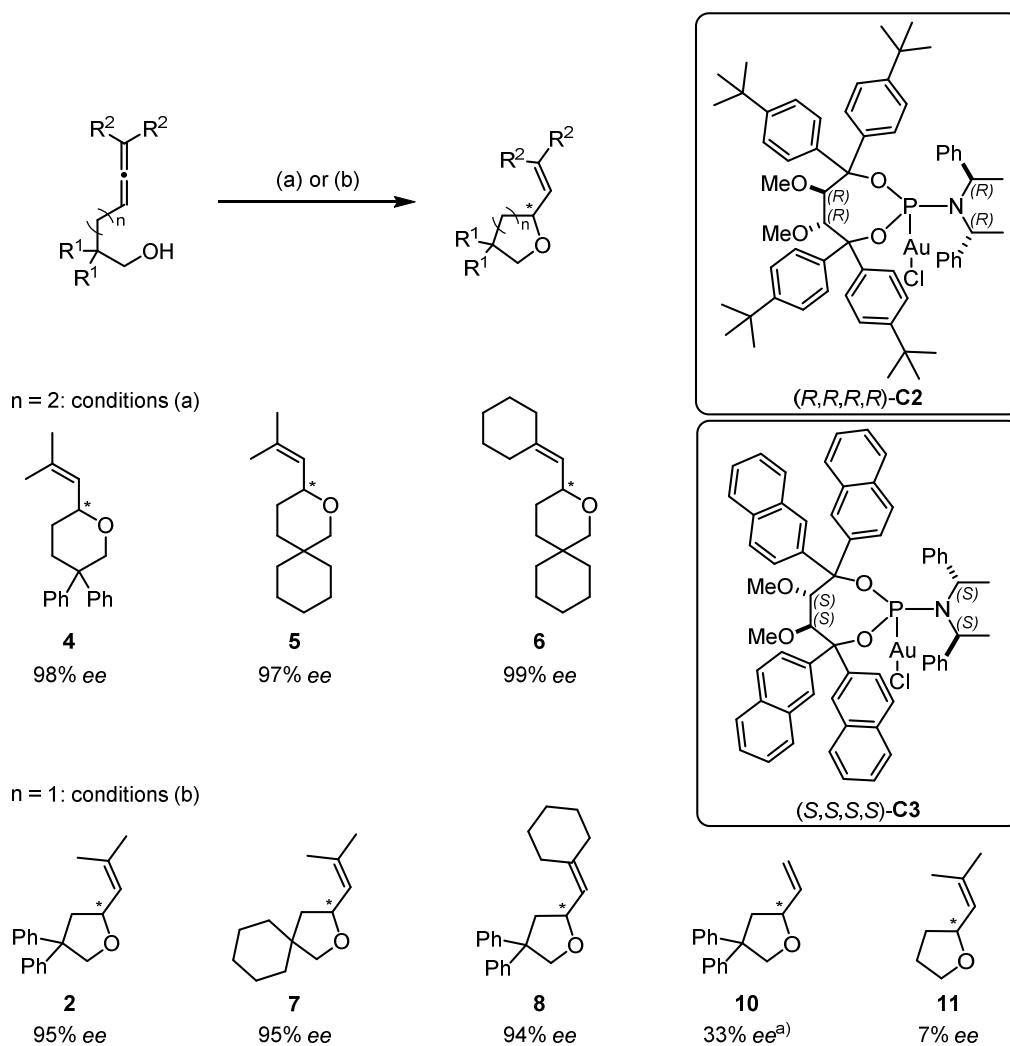
Scheme 1.4. Intramolecular hydroamination of allenes. Reagents and conditions: (a) (R,R,R,R) -C2 (5.5 mol%), $AgBF_4$ (5.0 mol%), toluene/EtOAc, 0 °C.^[7c]

This chemistry was further extended to the related hydroalkoxylation reactions.^[16] Since the enantioselectivities for the former transformation could be enhanced to over 90% *ee* using precatalyst (*R,R,R,R*)-**C2** in toluene/EtOAc mixtures (1:1), the hydroalkoxylation was conducted under similar conditions. However, the 6-*exo* cyclization of δ -allenol **3** in toluene at ambient temperature gave the corresponding tetrahydropyran **4** in only 19% *ee*. The *ee* could not be improved by screening various solvents typically used for this transformation (CH_2Cl_2 , THF, Et_2O , EtOAc, *etc.*). Somewhat surprisingly, ethanol provided the best result with 85% *ee* at ambient temperature that could be increased to 98% *ee* at low temperature (Scheme 1.6), without the detection of intermolecular addition of ethanol. Variation in the substitution pattern was tolerated at the allene terminus as well as at the alkyl chain as demonstrated by the tetrahydropyrans **5** and **6**. Next, the chain length was modified and different γ -allenols were subjected to the optimized reaction conditions. Interestingly, precatalyst (*R,R,R,R*)-**C2** gave only poor enantioselectivities for the 5-*exo*-cyclizations. Therefore, the naphthyl variant (*S,S,S,S*)-**C3** that had proven more effective in previous cycloisomerization reactions was employed. A striking observation was made when this catalyst was first utilized for the hydroalkoxylation of **1** at room temperature: it provided (*S*)-(-)-**2** in 38% *ee* in toluene, but gave the opposite enantiomer (*R*)-(+)-**2** in 78% *ee* when tested in ethanol (Scheme 1.5).



Scheme 1.5. Solvent-dependent enantioinversion. Reagents and conditions: (a) (*S,S,S,S*)-**C3** (5.5 mol%), AgBF_4 (5.0 mol%), toluene, (*S*)-(-)-**2** 87%, (-)-38% *ee*; (b) (*S,S,S,S*)-**C3** (5.5 mol%), AgBF_4 (5.0 mol%), ethanol, (*R*)-(+)-**2** 93%, (+)-78% *ee*.

The enantiomeric excess for (*R*)-(+)-**2** could be improved to 95% by cooling the reaction in ethanol to $-78\text{ }^\circ\text{C}$ (Scheme 1.6). After adopting the same conditions for differently substituted γ -allenols, the corresponding tetrahydrofurans **7** and **8** could be obtained in excellent *ees*. However, submitting the terminal allene **9** to the optimized reaction conditions (at ambient temperature) afforded the desired product **10** in only 33% *ee*. Enantiodiscrimination dropped even more drastically when the geminal disubstitution of the alkyl chain was removed (**11**, 7% *ee*).^[16] Substitution at both the allene and the tether seemed indispensable for high levels of enantioselectivity.



Scheme 1.6. Hydroalkoxylation of allenols. Reagents and conditions: (a) *(R,R,R,R)*-**C2** (5.5 mol%), AgBF_4 (5.0 mol%), EtOH (0.1 M), -78°C ; (b) *(S,S,S,S)*-**C3** (5.5 mol%), AgBF_4 (5.0 mol%), EtOH (0.1 M), -78°C ; ^{a)} experiment conducted at ambient temperature.^[16]

As outlined above, the enantioselection in this particular catalytic system is believed to originate from a unidirectional rotation of the substrate in the catalyst's cavity (see Scheme 1.2). Unsurprisingly, the substrate scope is therefore highly dependent on steric factors. More intriguing, however, is the strong solvent dependence of the enantioselectivity observed for the 5-*exo*-cyclization using *(S,S,S,S)*-**C3** (Scheme 1.5), which was therefore subject to further investigations.

1.2 Objectives

The previously developed TADDOL-based phosphoramidites proved successful as single-point binding ligands in a wide variety of gold-catalyzed transformations. However, the fascinating discovery of a solvent-induced enantioinversion in intramolecular hydroalkoxylations of allenes raised questions on the underlying mechanism for enantioselection. In order to shed light on the stereodiscrimination process and further improve substrate scope and enantioselectivity, a more detailed investigation of this impressive dual stereoselection was planned.

First, the scope of enantioinversion should be determined for the intramolecular hydroalkoxylation of allenes by revisiting previously employed ligands and substrates. Moreover, it was envisaged to correlate and rationalize a link between reaction conditions and stereochemical outcome. Once this has been established, NMR spectroscopy and characterization of possible reaction intermediates could provide further insights. DFT calculations could help to propose a plausible mechanistic scenario accounting for the experimental observations. Thus, a comprehensive mechanistic study was conducted with the results presented below.

1.3 A Striking Case of Enantioinversion

Remark: this project was initiated by former postdoctoral researcher Dr. Luca Mantilli, who observed the solvent-dependent enantioinversion in the hydroalkoxylation reaction. The phenomenon was studied in detail within this PhD research. A collaboration with postdoctoral researcher Dr. Larry M. Wolf at the department of theoretical chemistry and Dr. Christophe Farès, head of the department of NMR-spectroscopy, led to joint publication.^[17]

1.3.1 The Phenomenon of Enantioinversion

Enantioinversion is a process in which both enantiomers of a product are obtained using a single chiral source by solely changing the reaction conditions (Figure 1.3).^[18] In the case of chiral ligands stemming from chiral pool precursors, the antipode of a given catalyst might be inaccessible or expensive, thus enantioinversion can provide an alternative entry to a desired product. Along the same line, the use of only one chiral ligand is beneficial to avoid a second multi-step catalyst synthesis to access the enantiomeric product.



Figure 1.3. Principle of enantioinversion.

The greater concept is not restricted to enantioselectivity but has also been described for regio- and diastereoselective processes using organo- as well as transition metal catalysts in a broad range of transformations.^[18]

Although this phenomenon is not uncommon, it has been rarely used as a result of rational design, due to the difficulties in predicting, manipulating and optimizing a particular reaction. Examples of enantioinversion in homogeneous gold catalysis have only been mentioned on two occasions and the understanding of the origin of this effect at a molecular level is almost non-existent.^[19] Thus, it seemed pertinent to investigate this phenomenon in more detail.

1.3.2 The Scope of Enantioinversion in the Gold(I)-catalyzed Hydroalkoxylation of Allenes

An initial series of experiments was performed in order to evaluate the impact of the solvent-induced enantioinversion in gold-catalyzed hydroalkoxylation. Steric properties of both the ligand and the substrate seemed to play a crucial role. Thus, a first screening taking these factors into account was conducted. Three different catalysts with sterically distinct aryl periphery and amine substitution were investigated (Figure 1.4).

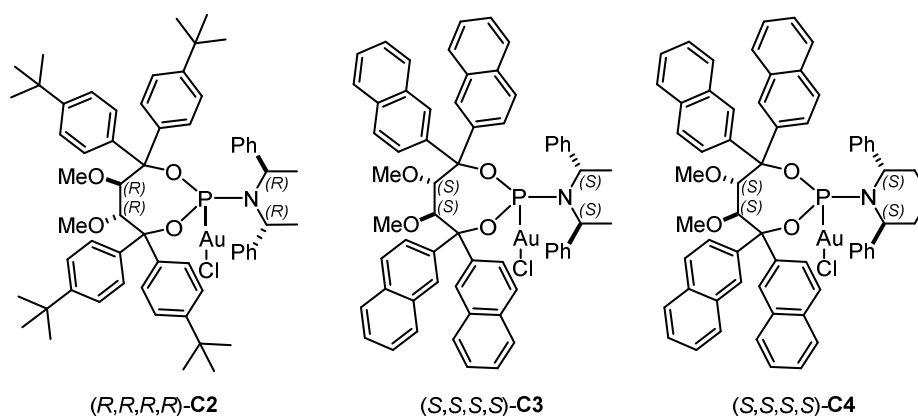
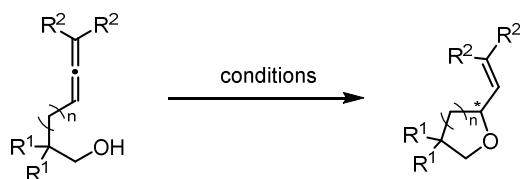


Figure 1.4. Catalysts screened in hydroalkoxylation reactions.

Complex **C2** bears an acyclic amine backbone and 4-*t*-butyl-phenyl groups on the TADDOL-moiety, which is substituted with 2-naphthyl groups in complex **C3**. The cyclic amine scaffold in complex **C4** is expected to reduce the flexibility of the system. These three catalysts were employed in the formation of **2**, **7**, **8** and **4**; the most important results are summarized in Table 1.1.

Table 1.1. Screening of gold complexes carrying different phosphoramidites in the cyclization of different allenols.^{a)}

Entry	Product	Precatalyst	Solvent	T [°C]	(+) [ee, %]	(-) [ee, %]
1		C3	CH ₂ Cl ₂	22		(-)-59
2		C3	CH ₂ Cl ₂	-60	(+)-29	
3		C3	EtOAc	22		(-)-68
4		C3	EtOAc	-60	(+)-77	
5		C3	EtOH	-60	(+)-97	
6		C2	CH ₂ Cl ₂	22	(+)-26	
7		C2	CH ₂ Cl ₂	-60	(+)-51	
8		C4	CH ₂ Cl ₂	22		(-)-50
9		C4	CH ₂ Cl ₂	-60		(-)-12
10		C3	CH ₂ Cl ₂	22	(+)-1	
11		C3	CH ₂ Cl ₂	-60	(+)-55	
12		C3	EtOH	-60	(+)-92	
13		C3	EtOH	-78	(+)-95	
14		C3	CH ₂ Cl ₂	22		(-)-25
15		C3	CH ₂ Cl ₂	-60	(+)-26	
16		C3	EtOAc	22		(-)-35
17		C3	EtOAc	-60	(+)-86	
18		C3	EtOH	-60	(+)-94	
19		C3	CH ₂ Cl ₂	22	(+)-23	
20		C3	CH ₂ Cl ₂	-60		(-)-35
21		C3	EtOH	-60		(-)-72
22		C3	CH ₂ Cl ₂	22	(+)-9	
23		C2	CH ₂ Cl ₂	-60	(+)-77	
24		C2	EtOH	-60	(+)-96	
25		C2	EtOH	-78	(+)-98	

^{a)} Precatalyst (5.5 mol%), AgBF₄ (5.0 mol%), indicated solvent (0.1 M), indicated temperature.

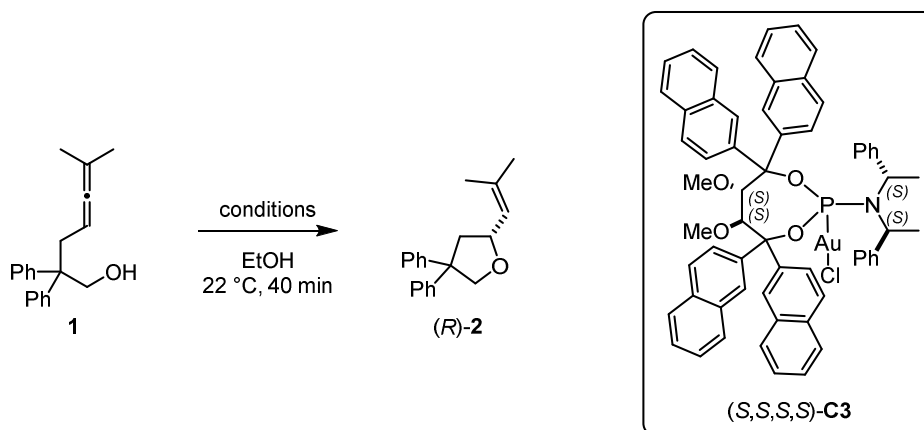
A solvent- or temperature-dependent switch in enantioselectivity was observed employing catalyst **C3** in CH₂Cl₂ or EtOAc with the exception of the cyclohexyl-substituted tetrahydrofuran **7** (Entries 10-13). In contrast, no inversion was observed for reactions conducted in ethanol, while the *ee* increased with decreasing temperature. Catalyst **C2**, which had shown conventional behavior in the 6-*exo* cyclizations before (see Scheme 1.6), also provided **2** with higher *ees* at lower temperatures without a change in enantioselectivity in CH₂Cl₂ (Entries 6 and 7). Enantioinversion, which seemed

unique to the 2-naphthyl substituted ligand, was no longer observed when the rigidity of the system was increased, as evident from the reaction employing complex **C4** (Entries 8 and 9). However, decreasing the temperature to $-60\text{ }^{\circ}\text{C}$ led to an erosion of *ee*, hinting toward a possible flip to the opposite enantiomer at even lower temperatures. Along the same lines, it cannot be excluded that substrate **7** might undergo enantioinversion at a higher temperature. Attempts to evaluate this hypothesis were hampered by decomposition of the catalyst upon heating.

In summary, the enantioinversion seemed to be fairly dependent on the ligand design. The highly symmetrical precatalyst **C2** performed as expected, while inversion of enantioselectivity was only observed for the less symmetrical 2-naphthyl variant **C3**. The phenomenon was also found to be substrate-dependent, especially with respect to the temperature range, in which the switch takes place. Thus, in the studied temperature range, cyclization of allenol **1** to tetrahydrofuran **2** represented the most impressive enantioinversion when the reaction was performed in EtOAc (Entries 3 and 4). At this stage, it was abstained from optimizing the conditions for each substrate; rather, allenol **1** was used as a model in the following mechanistic studies in order to rationalize the outcomes to this unusual phenomenon.

1.3.3 Control Experiments

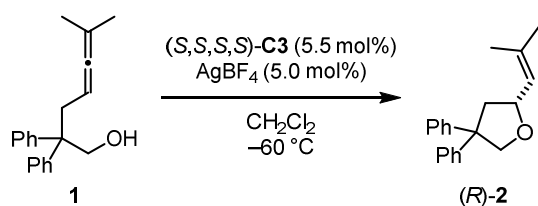
At the outset of this study, a series of control experiments was performed to scrutinize the role of each reaction component under the previously identified standard conditions (*vide supra*). In homogeneous gold catalysis, the catalytically active cationic complex is prepared by a halide abstraction reaction from a precatalyst $\text{L}^*\text{-AuCl}$ with an appropriate silver salt. The catalyst solution is then typically filtered in order to remove silver chloride, before being added to the reaction mixture. Since silver salts alone or in combination with gold catalysts also exhibit catalytic activity,^[20] the cyclization of allenol **1** to tetrahydrofuran **2** was repeated without filtering the catalyst solution consisting of (*S,S,S,S*)-**C3** and AgBF_4 . No difference in enantioselectivity was observed as compared to the standard conditions (Table 1.2, Entries 1 and 2). The reaction was also conducted in the presence of silver chloride and the absence of the chiral gold catalyst. Insoluble silver chloride was unable to catalyze the reaction as almost no conversion of starting material was observed within five days (Entry 3). The use of silver tetrafluoroborate led to the formation of the racemic product in less than 10% yield after 24 hours (Entry 4). Thus compared to the fast gold catalysis, silver-catalyzed racemic background reactions seemed to be too slow to influence the enantiomeric excess of the product. The reaction rate was also reduced when the precatalyst was not ionized by a suitable silver salt (Entry 5). Additionally, enantioselectivity was independent of the concentration of the reaction and the catalyst loading (Entries 6-8).

Table 1.2. Basic control experiments.

Entry	Catalyst (mol %)	Co-catalyst (mol%)	Concentration [M]	Conversion [%]	(R) [ee, %]
1	(S,S,S,S)-C3 (5.5)	AgBF ₄ (5.0)	0.1	> 99	(+)-78
2 ^{a)}	(S,S,S,S)-C3 (5.5)	AgBF ₄ (5.0)	0.1	> 99	(+)-77
3	–	AgCl (5.0)	0.1	< 5 ^{b)}	n.d.
4	–	AgBF ₄ (5.0)	0.1	10 ^{c)}	rac
5	(S,S,S,S)-C3 (5.5)	–	0.1	25 ^{c)}	(+)-65
6	(S,S,S,S)-C3 (5.5)	AgBF ₄ (5.0)	0.2	> 99	(+)-78
7	(S,S,S,S)-C3 (5.5)	AgBF ₄ (5.0)	0.01	> 99	(+)-77
8	(S,S,S,S)-C3 (16)	AgBF ₄ (15)	0.1	> 99	(+)-78

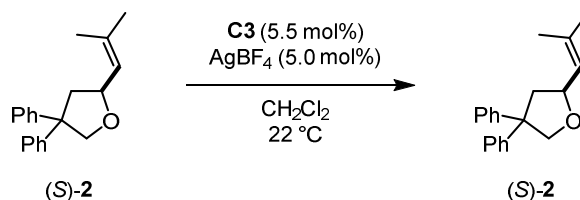
^{a)} no filtration of catalyst solution; ^{b)} after 5 d reaction time; ^{c)} after 24 h reaction time.

In order to rule out an alteration of the catalyst by reaction products, further control experiments were performed. First, the dependence of enantioselectivity on conversion was surveyed. To this end, the *ee* of the product was determined at various time intervals while the reaction was in progress. Since the conversion was very fast in ethanol at ambient temperature (*vide supra*), the solvent was exchanged for CH₂Cl₂ and the mixture cooled to –60 °C. These conditions allowed extracting numerous aliquots before the reaction was completed and further data points were collected beyond full conversion after approx. 16 hours. The enantiomeric excess was found to be constant over the entire timeframe (Table 1.3). In an additional experiment, the stability of the catalyst was verified by NMR spectroscopy, indicating no change within eight hours at ambient temperature.

Table 1.3. Continuous sampling and *ee* determination.

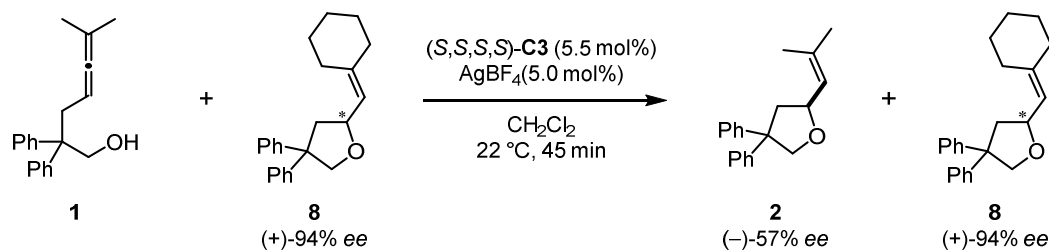
Entry	Time	(<i>R</i>) [<i>ee</i> , %]
1	30 min	(+)-27
2	60 min	(+)-26
3	90 min	(+)-27
4	120 min	(+)-27
5	180 min	(+)-27
6	17.5 h	(+)-25
7	24 h	(+)-26
8	48 h	(+)-26

Likewise, even the prolonged exposure of product (*S*)-2 (54% *ee*) to freshly prepared catalyst of either absolute configuration under the standard reaction conditions in CH_2Cl_2 did not lead to an erosion of enantioselectivity (Table 1.4). Thus, product formation is irreversible.

Table 1.4. Investigation of possible product influence.

Entry	Time [h]	C3	(<i>S</i>) [<i>ee</i> , %]	Entry	Time [h]	C3	(<i>S</i>) [<i>ee</i> , %]
1	12	(<i>S,S,S,S</i>)	(-)-53	7	12	(<i>R,R,R,R</i>)	(-)-50
2	24		(-)-54	8	24		(-)-51
3	36		(-)-50	9	36		(-)-51
4	48		(-)-51	10	48		(-)-54
5	60		(-)-53	11	60		(-)-54
6	72		(-)-53	12	72		(-)-52

The gold-catalyzed hydroalkoxylation of allene **1** to tetrahydrofuran **2** was also carried out in the presence of a different hydroalkoxylation product (+)-**8** (94% *ee*). No significant erosion of *ee* was observed for tetrahydrofuran **2** and the *ee* of the added tetrahydrofuran (+)-**8** remained unchanged (Scheme 1.7). Auto-induction through a change of the catalyst by reaction products can therefore be excluded.^[18c,21]



Scheme 1.7. No product influence on enantioselectivity.

Ideally, stereoselection in asymmetric catalysis should be described by a linear correlation between the *ee* of the product and the *ee* of the precatalyst.^[22] This relationship was studied next in search for deviations from linearity – so-called non-linear effects – that could explain the observed enantioinversion. For this purpose, a series of reactions was set up in CH_2Cl_2 at both $22\text{ }^\circ\text{C}$ and $-60\text{ }^\circ\text{C}$. Accurately defined mixtures of $(S,S,S,S)\text{-C3}$ and $(R,R,R,R)\text{-C3}$ were activated with AgBF_4 at ambient temperature before being added to the substrate solutions at the respective temperatures. The resulting mixtures were stirred at ambient temperature for 45 minutes or at $-60\text{ }^\circ\text{C}$ for 16 hours. The resulting mixtures were stirred at ambient temperature for 45 minutes or at $-60\text{ }^\circ\text{C}$ for 16 hours. The *ee* of the product was determined by HPLC (Table 1.5) and plotted against the *ee* of the precatalyst, resulting in a linear correlation at either temperature (Figure 1.5).

Table 1.5. Correlation between *ee* of precatalyst **C3** and *ee* of product **2**.

Entry	T [°C]	C3 [ee,%]	2 [ee, %]	Entry	T [°C]	C3 [ee, %]	2 [ee, %]
1	22	> (+)-99	(-)-58	10	-60	> (+)-99	(+)-29
2		(+)-60	(-)-28	11		(+)-60	(+)-23
3		(+)-50	(-)-21	12		(+)-50	(+)-17
4		(+)-20	(-)-5	13		(+)-20	(+)-8
5		0	0	14		0	(+)-1
6		(-)-20	(+)-13	15		(-)-20	(-)-8
7		(-)-50	(+)-18	16		(-)-50	(-)-16
8		(-)-60	(+)-27	17		(-)-60	(-)-17
9		> (-)-99	(+)-59	18		> (-)-99	(-)-27

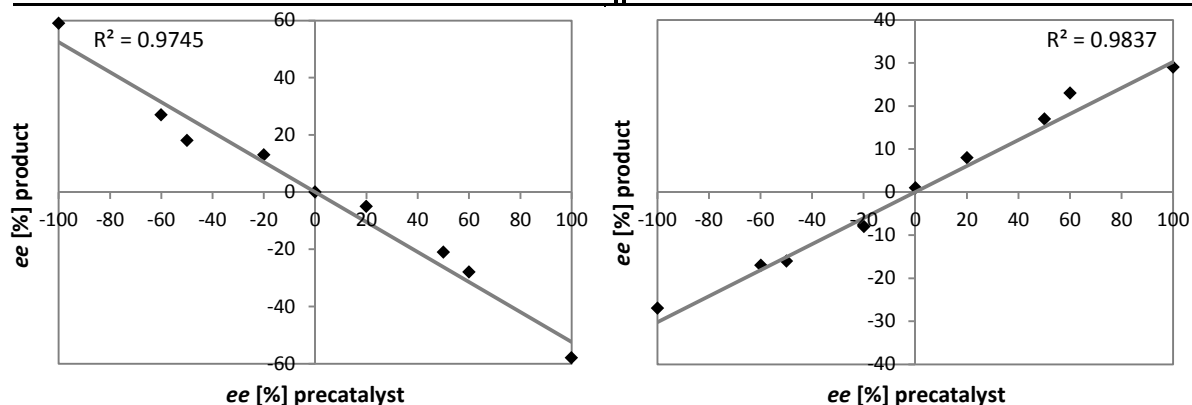
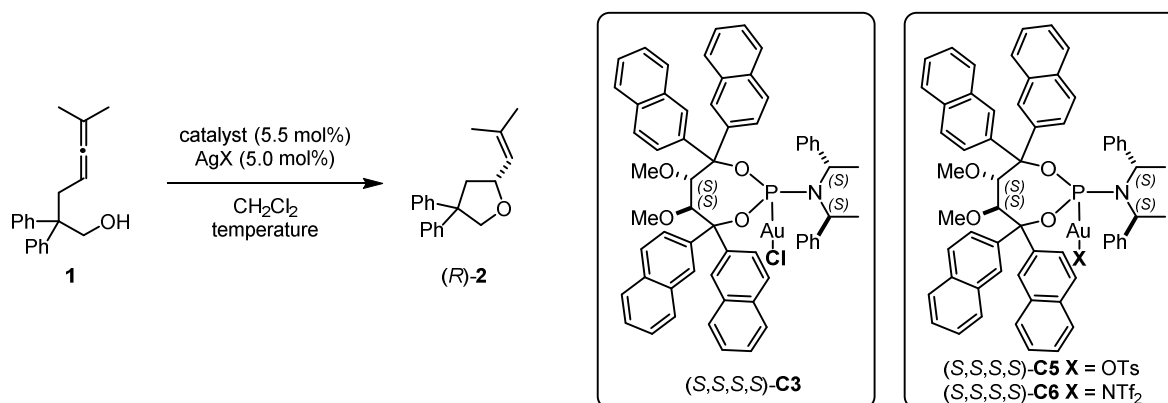


Figure 1.5. Left: correlation between *ee* precatalyst and *ee* product at $22\text{ }^\circ\text{C}$. Right: correlation between *ee* precatalyst and *ee* product at $-60\text{ }^\circ\text{C}$.

Since a linear correlation was observed in both temperature regimes, the formation of aggregates^[23] and even more importantly *gem*-diaurated complexes, previously identified as possible intermediates,^[24] could be excluded. Thus, the enantiodiscrimination process is not controlled by dimeric or oligomeric forms of the catalyst and an *in situ* kinetic resolution can be ruled out.^[25]

In order to exclude the possibility that moisture was condensed in the reaction mixture during the filtration of the catalyst suspension after ionization, an additional control experiment was performed. In contrast to chloride abstraction using AgBF₄, the cationic complexes resulting from ionization with AgOTs or AgNTf₂ could be isolated. Thus, the reaction was repeated in CH₂Cl₂ at both ambient and low temperature using the *in situ* ionization protocol and the results were compared to those employing the pre-isolated cationic complexes (*S,S,S,S*)-**C5** or (*S,S,S,S*)-**C6** (Table 1.6).

Table 1.6. Comparison of catalyst (*S,S,S,S*)-**C3** ionized *in situ* with AgOTs or AgNTf₂ with catalyst (*S,S,S,S*)-**C5** and (*S,S,S,S*)-**C6** prepared *ex situ*.^{a)}



Entry	Catalyst	AgX	Temperature [°C]	(R) [ee, %]
1	(<i>S,S,S,S</i>)- C3	OTs	22	(+)-70
2	(<i>S,S,S,S</i>)- C5	–	22	(+)-73
3	(<i>S,S,S,S</i>)- C3	OTs	–60	(+)-92
4	(<i>S,S,S,S</i>)- C5	–	–60	(+)-94
5	(<i>S,S,S,S</i>)- C3	NTf ₂	22	(–)-36
6	(<i>S,S,S,S</i>)- C6	–	22	(–)-32
7	(<i>S,S,S,S</i>)- C3	NTf ₂	–60	(+)-51
8	(<i>S,S,S,S</i>)- C6	–	–60	(+)-59

^{a)} All reactions were performed in 0.1 M solutions.

At both temperature regimes, comparable enantioselectivities were obtained regardless of the ionization method. Thus, adventitious moisture affecting the enantioselectivity outcome in aprotic solvents could be ruled out. In summary, the observed enantioinversion could not be explained by an irregular behavior of the catalytic system and the underlying mechanism seemed to be a more involved process.

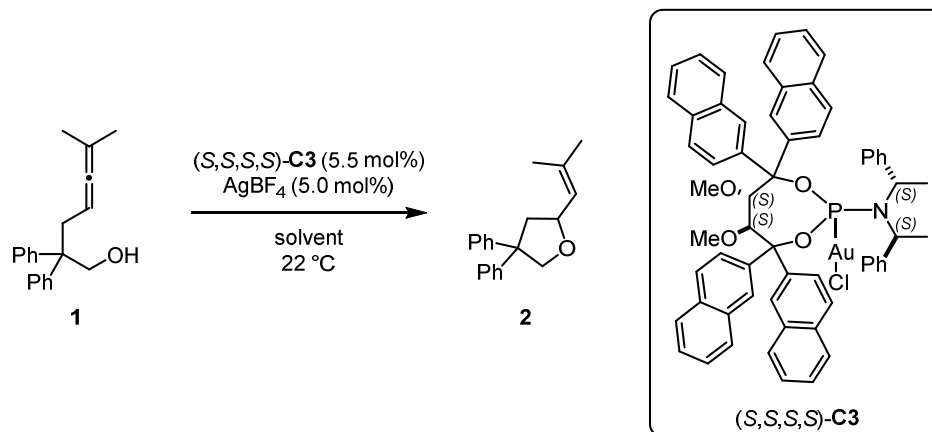
1.3.4 Reaction Parameters

With the insights gained from the first set of control experiments, a combined experimental and computational study to de-convolute the intriguing enantioinversion seemed worthwhile. For a start, thorough screenings of the reaction parameters were conducted.

1.3.4.1 Solvent

During the optimization of the reaction conditions different solvents had been evaluated and the selection was now broadened. When the reaction was carried out at ambient temperature in solvents of low polarity, such as different chlorohydrocarbons, trifluorotoluene and toluene or in acetone, the (–)-product was formed in 21-59% *ee* (Table 1.7, Entries 1-7). More polar solvents like acetonitrile and nitromethane afforded only 7% *ee* (Entries 8 and 9), while the best *ee* for (S)-(–)-**2** was obtained in EtOAc (Entry 10). However, protic co-solvents had a massive influence: conducting the reaction in EtOAc/H₂O mixtures (9:1) afforded the (+)-product in 59% *ee* (Entry 11). Protic solvents, such as methanol and ethanol, favored the formation of (R)-(+)-**2** (Entries 12 and 13). Interestingly, also the aprotic but coordinating solvents THF and DMA provided (R)-(+)-**2** (Entries 14 and 15). Unfortunately, more extreme polarities could not be assessed as catalyst and substrate were insoluble in nonpolar hexane, pentane and HMDSO as well as in the most polar solvent water, preventing the reaction from occurring (Entries 16-19).

The inherent virtue of the TADDOL-based phosphoramidite ligands of low symmetry to provide either antipode of a given product solely by changing the solvent had thus far only been recognized on one occasion.^[26] The authors suggested a modification of the structure of the catalyst through coordination of the solvent. Beyond its role to dissolve substrate and reactant, the solvent is known to influence reactivity and selectivity of a reaction,^[18d,27] which also applied to the present case study. The results summarized above show that either enantiomer of **2** can be obtained with respectable optical purity by solely changing the reaction solvent while using a single enantiomer of catalyst **3**. By this means, (R)-(+)-**2** was obtained in 83% *ee* in DMA while (S)-(–)-**2** was produced in no less than 68% *ee* in EtOAc. Overall, the reversal of enantioselectivity seemed to be governed by solvent properties and the following trend might be deduced from the screening: protic and coordinating solvents favor the formation of (R)-(+)-**2** as opposed to aprotic and non-coordinating solvents favoring (S)-(–)-**2**.

Table 1.7. Enantioinversion induced by the solvent at ambient temperature (22 °C).^{a)}

Entry	Solvent	(R) [ee, %]	(S) [ee, %]	Yield [%]
1	CH ₂ Cl ₂		(-)-59	95
2	CHCl ₃		(-)-50	89
3	CCl ₄		(-)-28	73
4	(CH ₂ Cl) ₂		(-)-53	85
5	toluene		(-)-38	87
6	PhCF ₃		(-)-47	74
7	acetone		(-)-21	86
8	MeCN		(-)-7	72
9	MeNO ₂		(-)-7	81
10	EtOAc		(-)-68	77
11	EtOAc/H ₂ O (9:1)	(+)-59		70
12	MeOH	(+)-72		86
13	EtOH	(+)-78		93
14	THF	(+)-23		86
15	DMA	(+)-83		76
16	hexane	–	–	0 ^{b)}
17	pentane	–	–	0 ^{b)}
18	HMDSO	–	–	0 ^{b)}
19	H ₂ O	–	–	0 ^{b)}

^{a)} All reactions were performed in 0.1 M solutions; ^{b)} insolubility of substrate and gold complex prevents the reaction from occurring.

An equally pronounced enantioinversion triggered by a switch from toluene to methanol had recently been observed in the case of hydroaminations of alkenes using dinuclear gold complexes.^[19b] In this case, the authors suggest that the change in reaction mechanism arises from the ability of methanol to act as a proton transfer agent.^[28] To evaluate such a proposal for the present example, further alcoholic solvents were examined. Methanol, ethanol and *i*-propanol gave similar enantioselectivities (71-78% *ee*) at equal reaction rates (99% conversion in 45 minutes), while the rate was significantly diminished (10% conversion in 45 minutes) in *t*-butanol and the enantioselectivity decreased to 44% *ee*. A similar behavior had been reported by Haddad and coworkers in catalytic asymmetric hydrogenations^[29] and by Tang *et al.* in the alkylation of indoles.^[30] The findings suggest that a combination of proton transfer ability and steric congestion in the chiral cavity is responsible for the disparity in enantioselectivity and reaction rate. Less bulky alcohols could be incorporated in the chiral cavity of the catalyst described above (see Section 1.1.2), altering its conformation and thereby increasing the enantioselectivity. The transformation is accelerated by a possible assistance in the proton transfer step. In contrast, sterically more demanding *t*-butanol might not be included in the chiral pocket, thus proton transfer is not facilitated. Furthermore, if the reaction rate was diffusion controlled, the high viscosity of *t*-butanol could also play an important role. Additionally, rotation of the substrate (*vide supra*) in the more open cavity might be less restricted as reflected in lower enantiomeric excess.

Although EtOAc and DMA gave the highest *ees*, CH₂Cl₂ and ethanol were the solvents of choice for further screenings, since they are more readily dried. As traces of water had shown a massive influence on enantioselectivity, strictly anhydrous conditions were mandatory in all experiments.

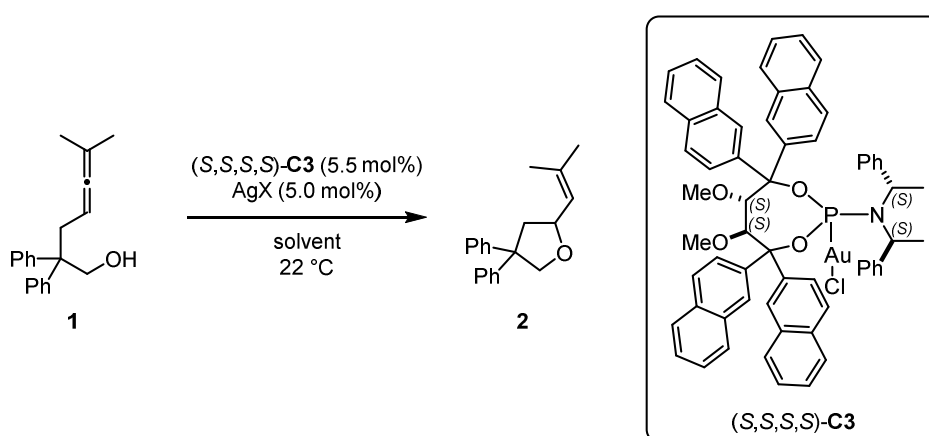
1.3.4.2 Counterion

Next, the escorting counterion as a second reaction parameter was studied in more detail. The nature of the counterion has been identified to play a crucial role in the reactivity and stereoselectivity of cationic metal catalysts in previous asymmetric transformations.^[18d,31] While the use of chiral counterions has attracted increased attention over the past years,^[32] the exploitation of achiral counterions in efficient chirality switching remained rare.^[1b,33] For gold(I)-catalyzed reactions, Bandini *et al.* have previously disclosed an inversion of stereoinduction when applying tosylate or BARF anions in their hydroamination-S_N2'-cascade reactions.^[19a] The counterion appeared to be directly involved in the stereodiscriminating step in the S_N2' reaction, as shown by the same group.^[34] The counterion was also found to affect the regioselectivity in gold-catalyzed pyrrole-synthesis as demonstrated by Davies and coworkers.^[35] It has been proposed that ligation of the counterion to the catalytic metal center can alter the initial catalyst structure or that of a transition state.^[18d]

Additionally, the ability of the counterion to participate in the proton migration event has been recognized before in cycloadditions and hydroaminations.^[28b,36]

It was speculated that the coordination strength of the counteranion was the pivotal characteristic. Therefore, a screening of different counterions in CH₂Cl₂ as well as in ethanol at ambient temperature was performed. Importantly, an alteration of the asymmetric induction was only observed when dichloromethane was used as solvent (Table 1.8, Entries 1-7). Weakly coordinating counterions favored the production of (*S*)-**2** in this solvent, while the more strongly coordinating trifluoroacetate and tosylate led to the preferred formation of (*R*)-**2**. In contrast, the effect of the counterion on the stereochemical course completely vanished in ethanol (Entries 8-12).

Table 1.8. Enantioinversion induced by the counterion at ambient temperature (22 °C).^{a)}



Entry	Solvent	X	(<i>R</i>) [<i>ee</i> , %]	(<i>S</i>) [<i>ee</i> , %]	Yield [%]
1	CH ₂ Cl ₂	BF ₄		(-)-59	95
2		SbF ₆		(-)-32	96
3		ClO ₄		(-)-43	68
4		NTf ₂		(-)-36	79
5		OTf		(-)-14	82
6		CF ₃ COO	(+)-66		87
7		TsO	(+)-70		96
8	EtOH	BF ₄	(+)-78		93
9		SbF ₆	(+)-78		92
10		NTf ₂	(+)-78		90
11		TsO	(+)-77		91
12		CF ₃ COO	(+)-77		95

^{a)} All reactions were performed in 0.1 M solutions.

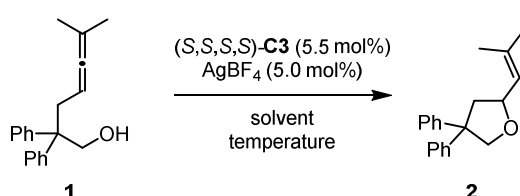
In conclusion, coordinating solvents and coordinating counterions in non-coordinating solvents share the same behavior. However, neither the size of the anion and thus steric interactions nor the coordination strength alone seemed to be responsible for the inversion phenomenon, suggesting that the situation is more complicated. The ability of the counterion to participate in hydrogen

bonding to the substrate and/or the ligand should also be considered, as suggested by Fan and coworkers for a similar finding.^[37] All three factors together – size, coordination strength and hydrogen bonding ability – could play an important role in the underlying mechanism.

1.3.4.3 Temperature

Temperature is known to be an ideal parameter for improving the diastereo- and enantioselectivity of a given transformation. However, only a few examples of dual enantioselectivity controlled by altering the temperature alone have been reported to date.^[18d,21,27,38] Based on the preliminary screenings (see Section 1.3.2), temperature studies were conducted in numerous protic and aprotic solvents (Table 1.9).

Table 1.9. Enantioinversion by changing the reaction temperature.^{a)}



Entry	Solvent	T [°C]	(R) [ee, %]	(S) [ee, %]	Yield [%]
1	EtOAc	22		(-)-68	77
2		-60	(+)-77		80
3	CH ₂ Cl ₂	22		(-)-59	95
4		-60	(+)-29		89
5	toluene	22		(-)-38	71
6		-60	(+)-33		71
7	EtOH	22	(+)-78		93
8		-30	(+)-92		90
9		-60	(+)-97		93
10	MeOH	22	(+)-72		86
11		-60	(+)-96		96
12	Et ₂ O	22	(+)-6		78
13		-60	(+)-74		80
14	THF	22	(+)-23		78
15		-60	(+)-86		88
16	DMA	22	(+)-83		76
17		-20	(+)-91		63

^{a)} All reactions were performed in 0.1 M solutions.

A reversal of enantioselectivity by altering the temperature was observed exclusively for aprotic solvents. In contrast, protic and coordinating solvents predominantly gave (*R*)-**2** in the temperature range studied (Table 1.9, Entries 7-17). Nevertheless, the temperature dependence of the *ee* for these solvents cannot be approximated by the Arrhenius equation. In THF, for instance, the *ee* at 22 °C is (+)-23%. If the Arrhenius activation energy E_a were constant, the equation

$$E_a = RT \cdot \ln \frac{(1+ee)}{(1-ee)} \quad (1)^{[39]}$$

predicts an *ee* of (+)-31% at -60 °C, but (+)-86% was detected. This massive deviation implies that the activation energy must change with temperature, in that it renders the disfavored pathway at room temperature the preferred pathway in the low temperature regime.

The remarkable temperature dependence was further investigated by Eyring studies, which allowed the enthalpic ($\Delta\Delta H^\ddagger$) and entropic contributions ($\Delta\Delta S^\ddagger$) to be derived. Moreover, a switch in mechanism can be detected by a deviation from linearity in modified Eyring plots as these parameters change.

In transition state theory, the temperature-dependent variance of the rate of a chemical reaction is described by the Eyring equation (2):

$$k = \frac{k_B T}{h} e^{\frac{-\Delta G^\ddagger}{RT}} \quad (2)$$

The *ee* of an asymmetric reaction can be expressed as the natural logarithm of the relative rate constant for the formation of two enantiomers (*R*) and (*S*) as follows:

$$\ln \frac{k_R}{k_S} = \ln \frac{100 + \% ee}{100 - \% ee} \quad (3)$$

An alternative representation is provided by the differential Eyring equation (4):^[40]

$$\ln \frac{k_R}{k_S} = - \frac{\Delta\Delta H^\ddagger}{R} \frac{1}{T} + \frac{\Delta\Delta S^\ddagger}{R} \quad (4)$$

Eyring studies were performed in both ethanol and CH₂Cl₂ using the gold precatalyst (*S,S,S*)-**C3** and AgBF₄. Every data point was independently determined three times (Tables 1.10 and 1.11). According to equation (3), the enantioselectivity was expressed as the natural logarithm of the relative rate constants for the formation of (*R*)-**2** and (*S*)-**2** (Table 1.10 and 1.11, data used for Eyring plot highlighted in blue for ethanol and green for CH₂Cl₂). These values were plotted against the

reciprocal temperature and the differential Eyring equation (4) was applied, using at least four data points for each linear regression whilst minimizing the R^2 value (Figure 1.6).

Table 1.10. Data for ethanol.

Entry	T [°C]	T^{-1} [$10^3 \cdot K^{-1}$]	ee [%]	ee [%]	ee [%]	\emptyset ee [%]	$\ln(k_R/k_S)$
1	-85	5.3191	(+)-91	(+)-90	(+)-92	(+)-91	3.0550
2	-78	5.2182	(+)-95	(+)-92	(+)-92	(+)-93	3.3168
3	-70	4.9261	(+)-95	(+)-93	(+)-95	(+)-94	3.4761
4	-60	4.6948	(+)-96	(+)-95	(+)-97	(+)-96	3.8918
5	-50	4.4843	(+)-95	(+)-96	(+)-96	(+)-96	3.8918
6	-40	4.2918	(+)-95	(+)-95	(+)-94	(+)-95	3.6636
7	-21	3.9683	(+)-92	(+)-93	(+)-93	(+)-93	3.3168
8	0	3.6630	(+)-87	(+)-87	(+)-87	(+)-87	2.6662
9	10	3.5336	(+)-85	(+)-85	(+)-84	(+)-85	2.5123
10	22	3.3898	(+)-78	(+)-77	(+)-78	(+)-78	2.0907
11	38	3.2154	(+)-72	(+)-71	(+)-72	(+)-72	1.8153

Table 1.11. Data for CH_2Cl_2 .

Entry	T [°C]	$10^3 T^{-1}$ [K^{-1}]	ee [%]	ee [%]	ee [%]	\emptyset ee [%]	$\ln(k_R/k_S)$
1	-60	4.6948	(+)-29	(+)-28	(+)-29	(+)-29	0.5971
2	-50	4.4843	(+)-26	(+)-27	(+)-24	(+)-26	0.5322
3	-40	4.2918	(+)-24	(+)-26	(+)-22	(+)-24	0.4895
4	-21	3.9683	(+)-14	(+)-21	(+)-25	(+)-20	0.4055
5	-10	3.8023	(-)-14	(-)-26	(-)-17	(-)-19	-0.3847
6	0	3.6630	(-)-31	(-)-29	(-)-32	(-)-31	-0.6411
7	10	3.5336	(-)-41	(-)-41	(-)-43	(-)-42	-0.8954
8	22	3.3898	(-)-57	(-)-59	(-)-57	(-)-58	-1.3249

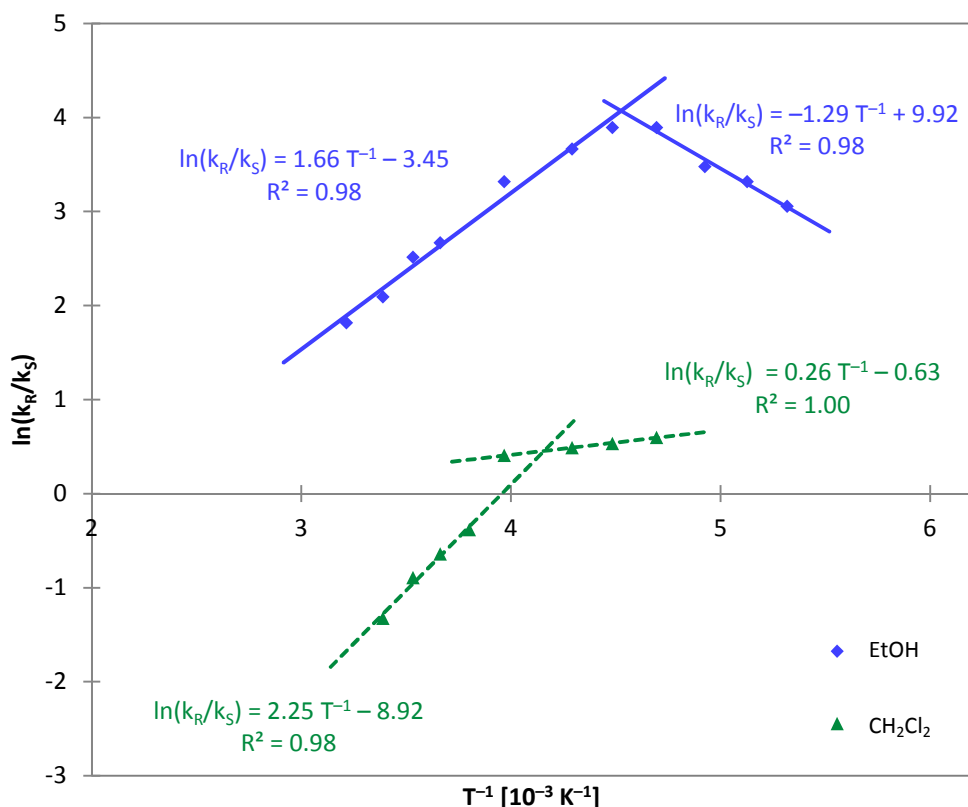


Figure 1.6. Eyring plot for the gold-catalyzed hydroalkoxylation in EtOH (blue squares) and CH₂Cl₂ (green triangles).

Additionally, the thermodynamic parameters were obtained from the linear equations (Table 1.12). The findings point toward a remarkable entropic component.

Table 1.12. Linear regression equations and thermodynamic parameters deduced from the differential Eyring equation (4).

Solvent	Sector	$\ln(k_R/k_S)$	$\Delta\Delta H^\ddagger$ [kcal·mol ⁻¹]	$\Delta\Delta S^\ddagger$ [cal·mol ⁻¹ ·K ⁻¹]
EtOH	left	$1.66 T^{-1} - 3.45$	-3.3	-6.8
	right	$-1.29 T^{-1} + 9.92$	2.6	19.7
CH ₂ Cl ₂	left	$2.25 T^{-1} - 8.92$	-4.5	-17.7
	right	$0.26 T^{-1} - 0.63$	-0.5	-1.2

Due to the presence of two linear regions for each solvent in the Eyring plot, two sets of thermodynamic parameters can be derived. Subtraction of the appropriate parameters provide $\delta\Delta\Delta H^\ddagger = \Delta\Delta H^\ddagger_{(\text{right})} - \Delta\Delta H^\ddagger_{(\text{left})}$ and $\delta\Delta\Delta S^\ddagger = \Delta\Delta S^\ddagger_{(\text{right})} - \Delta\Delta S^\ddagger_{(\text{left})}$, which represent the change in dominance of enthalpy and entropy in the partial steps.^[41] Thus, $\delta\Delta\Delta H^\ddagger(\text{EtOH}) = 5.9 \text{ kcal}\cdot\text{mol}^{-1}$ and $\delta\Delta\Delta S^\ddagger(\text{EtOH}) = 26.5 \text{ cal}\cdot\text{mol}^{-1}\cdot\text{K}^{-1}$ for ethanol as well as $\delta\Delta\Delta H^\ddagger(\text{CH}_2\text{Cl}_2) = 4.0 \text{ kcal}\cdot\text{mol}^{-1}$ and $\delta\Delta\Delta S^\ddagger(\text{CH}_2\text{Cl}_2) = 16.5 \text{ cal}\cdot\text{mol}^{-1}\cdot\text{K}^{-1}$ for dichloromethane are obtained and plotted on an enthalpy/entropy diagram (Figure 1.7). Linear regression through the two data points and the

zeropoint – known as the isoinversion relationship – allows the isoinversion temperature T_i to be determined from the slope. For the present case, T_i is 229 K ($-44\text{ }^\circ\text{C}$), at which temperature the optimal selectivity is to be expected. In theory, selectivity phenomena can be interpreted, assessed and optimized with the isoinversion principle.^[41] However, this needs a large amount of data and the underlying mechanism cannot be deduced from merely thermodynamic parameters.

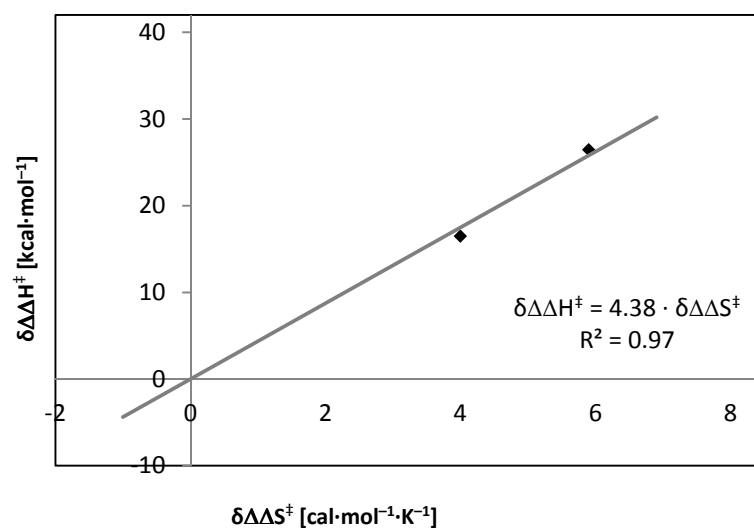


Figure 1.7. Isoinversion diagram.

1.3.5 DFT Calculations^[42]

At this stage it could only be speculated, whether a proton shuttle mechanism was operative or conformational changes of the organogold intermediates triggered the reversal of enantioselectivity. Thus, attempts to improve the understanding of the phenomenon were made with the aid of DFT calculations^[43] at the PBE0-D3//TPSS-D3 level of theory. To this end, the situation at ambient temperature in EtOAc was analyzed first. The resulting energy profile is depicted in Figure 1.8 and the corresponding catalytic cycle illustrated in Scheme 1.8.

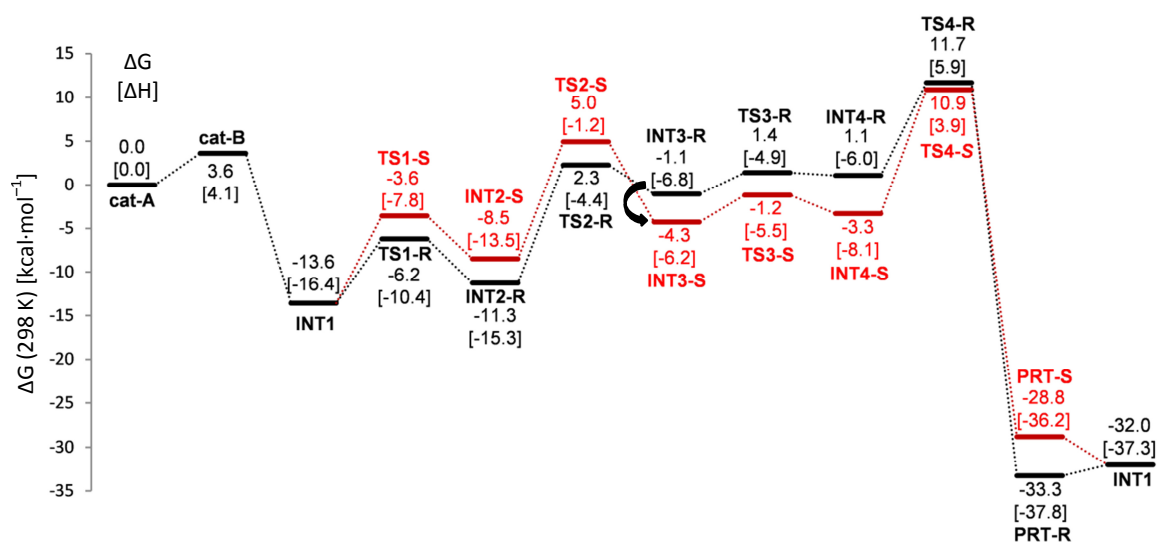
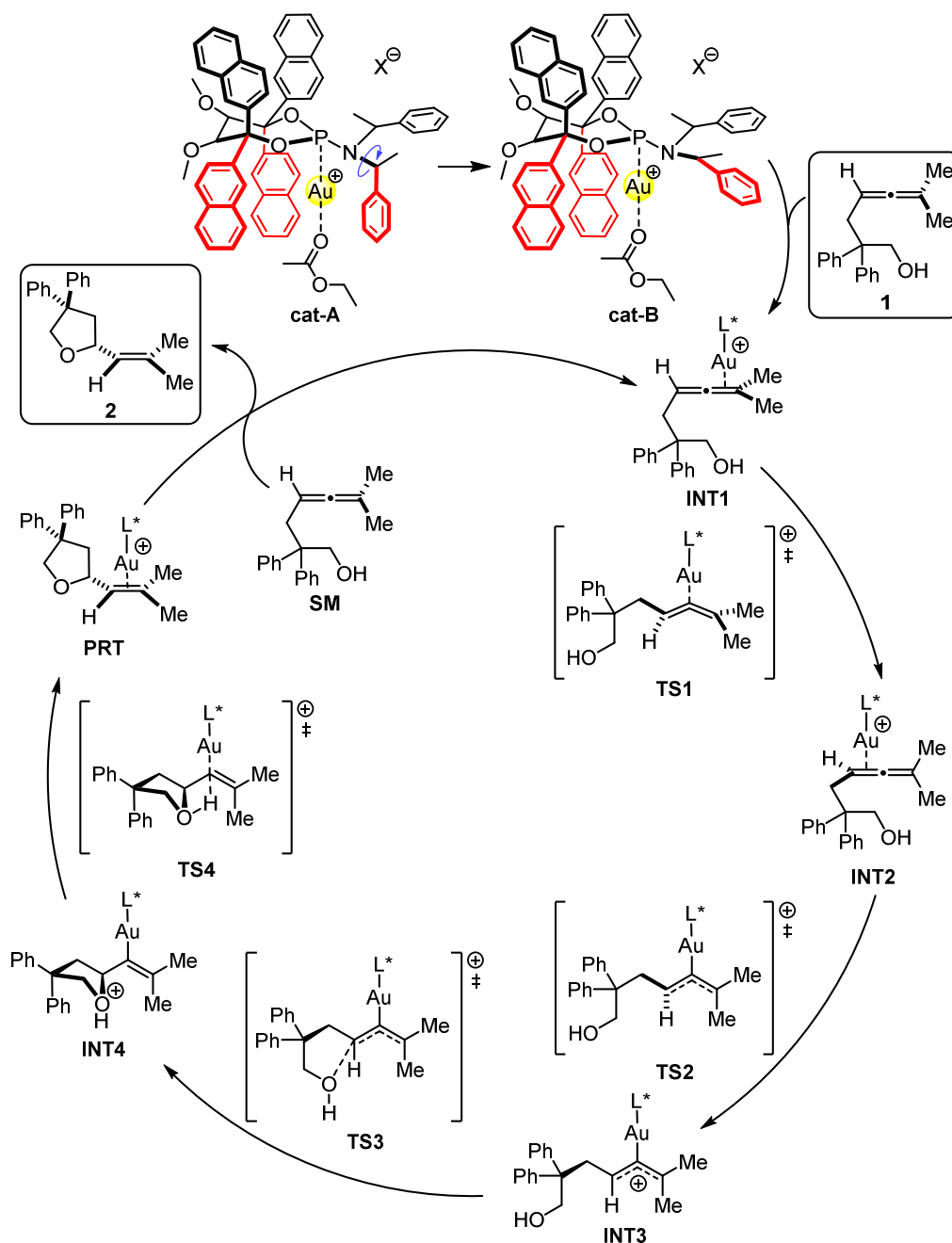


Figure 1.8. Computed Gibbs free energy profile at 298 K in EtOAc (enthalpies are enclosed in brackets); diastereomeric channels for the (*S*)-product (red) and the (*R*)-product (black); possible shortcut (thick arrow).

The cationic complex **cat-A** was used as starting point, representing catalyst (*S,S,S,S*)-**C3** after ionization and formal exchange of chloride by EtOAc. The bulky amino group of this lowest-energy complex must undergo a rotation (indicated by the blue arrow in Scheme 1.8) forming **cat-B** to expose the gold atom and allow substrate binding. Initially, complexation of the substrate **1** occurs preferably at the dimethyl substituted double bond providing π -complex **INT1**. Nonetheless, slippage of gold to the adjacent double bond forming π -complex **INT2** has only a small barrier (**TS1**). The chiral ligand **L*** splits the pathway at this stage into two diastereomeric channels with **INT2-R** being favored. A twist of the gold-associated double bond by 90° leads to two diastereomeric allyl cations **INT3** thermodynamically favoring **INT3-S**. It has to be mentioned, that only a series of facile single bond rotations is necessary to interconvert **INT3-S** into **INT3-R**, representing a possible shortcut between the two diastereomeric channels (Figure 1.8, thick arrow). Direct access from **INT1** to **INT3** has also been investigated, but no stable product could be located. **INT3** needs to overcome only a small barrier (**TS3**) to evolve into the cyclized vinyl gold species **INT4**. The subsequent proto-

deuration *via* 1,3-proton shift exhibits a significant barrier (**TS4**), while the final release of the product **2** with concurrent complexation of a new substrate molecule is almost barrierless.



Scheme 1.8. Plausible catalytic cycle for the hydroalkoxylation in aprotic solvents.

Overall, the energy profile obtained above is consistent with the experimental findings as formation of the (*S*)-product is favored, but interconversion between the two channels is possible accounting for the measured moderate *ees* of approx. 60%.

Next, the pathway in the protic solvent methanol was computed with an explicit molecule of methanol included for each stationary point on the pathway (Figure 1.9). Methanol is coordinated to the gold center in the ionized catalyst **cat-A**, which undergoes the above mentioned conformational

change to **cat-B** to make space for the incoming substrate. Methanol will most likely be associated to the substrate *via* hydrogen bonding prior to complexation. Since the concentration of the associating methanol is large and constant, entropy for the association essentially plays no influential role and complexation to the dimethyl substituted double bond is again preferred (**INT1-p**). The barrier (**TS1-p**) for the catalyst to glide to the adjacent double bond forming π -complex **INT2-p** is low and the pathway is likewise split into two diastereomeric channels at this stage. Due to hydrogen bonding, the pendant hydroxy group becomes more nucleophilic and cyclization to **INT3-p** occurs directly, bypassing a discrete allyl cation intermediate. Assistance from methanol in the 1,3-proton migration step *via* the six-membered transition state **TS3-p** significantly lowers the barrier for proto-deauration. Thus, the one-step twisting/cyclization event becomes rate-limiting in protic media. An inversion of the selectivity similar to the aprotic case is improbable, since a free allyl cation intermediate is never generated and the pathways cross only after the rate-determining step in **INT3-p**.

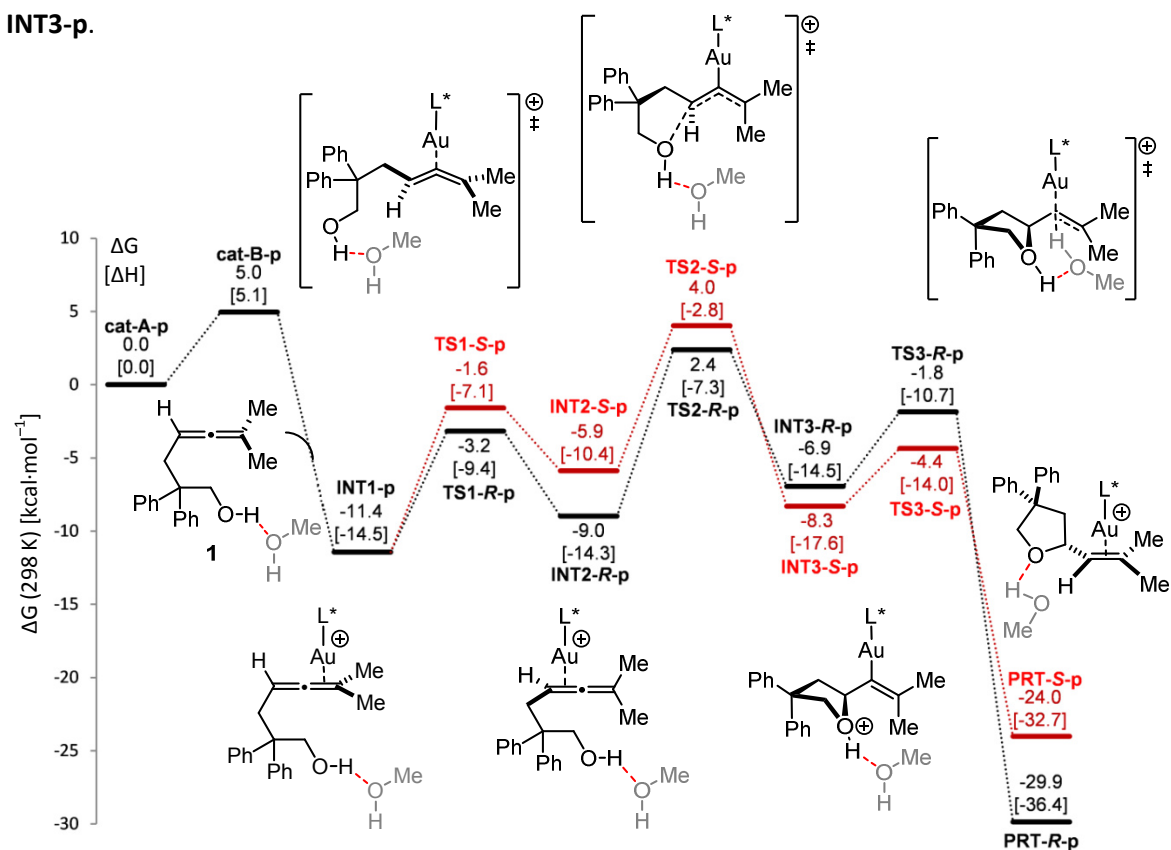


Figure 1.9. Computed Gibbs free energy profile at 298 K in MeOH (enthalpies are enclosed in brackets); diastereomeric channels for the (*S*)-product (red) and the (*R*)-product (black).

The protic solvent was found to act as a proton shuttle facilitating the 1,3-proton shift *via* the six-membered transition state **TS3-p**. Therefore, the formation of the (*R*)-product is always favored in a protic solvent; the overall barrier is reduced by more than 7 kcal·mol⁻¹.

This proposed mechanism conforms reasonably well to the results obtained from the experiments. The calculated activation parameters $\Delta\Delta H_{\text{calc}}^{\ddagger} = -4.5 \text{ kcal}\cdot\text{mol}^{-1}$ and $\Delta\Delta S_{\text{calc}}^{\ddagger} = -9.6 \text{ cal}\cdot\text{mol}^{-1}\cdot\text{K}^{-1}$ are relatively close to the experimentally observed parameters $\Delta\Delta H_{\text{exp}}^{\ddagger} = -3.3 \text{ kcal}\cdot\text{mol}^{-1}$ and $\Delta\Delta S_{\text{exp}}^{\ddagger} = -6.8 \text{ cal}\cdot\text{mol}^{-1}\cdot\text{K}^{-1}$ obtained in ethanol (see Table 1.12). It has to be noted that not only coordinating and especially protic solvents, but also coordinating counterions residing in close proximity to the gold cation (TsO^- or CF_3COO^-) may be able to assist proto-deauration and therefore intrinsically favor the formation of (*R*)-**2**.

As proto-deauration represents the rate-determining step in aprotic media at ambient temperature as depicted above, a more accessible alternative pathway was projected comprising an assisted proto-deauration process resembling the scenario in protic media. First, it was assumed, that a second substrate molecule could be involved in the 1,3-proton shift. The resulting energy profile with neopentyl alcohol mimicking the second substrate is depicted in Figure 1.10 and compared with the previous scenario in aprotic solvent.

The association of a second substrate molecule to **INT2** *via* hydrogen bonding again increases the nucleophilicity of the pendant hydroxy group. Thus, the allyl cation intermediate is bypassed and the formerly two-step process becomes a one-step twisting/cyclization process to form the cyclized vinyl gold species **INT4-a**. The initial association providing **INT2-a** is uphill in energy, yet the activation for the one-step cyclization event (**TS3-a**) is similar to that of the two-step sequence. Most importantly, the assisted proto-deauration *via* a six-membered transition state **TS4-a** is significantly facilitated. In summary, the rate-limiting step is shifted from **TS4** to **TS3-a**, while the overall barrier is reduced by more than $5 \text{ kcal}\cdot\text{mol}^{-1}$. For this mechanistic scenario, the formation of the (*R*)-product is again favored.

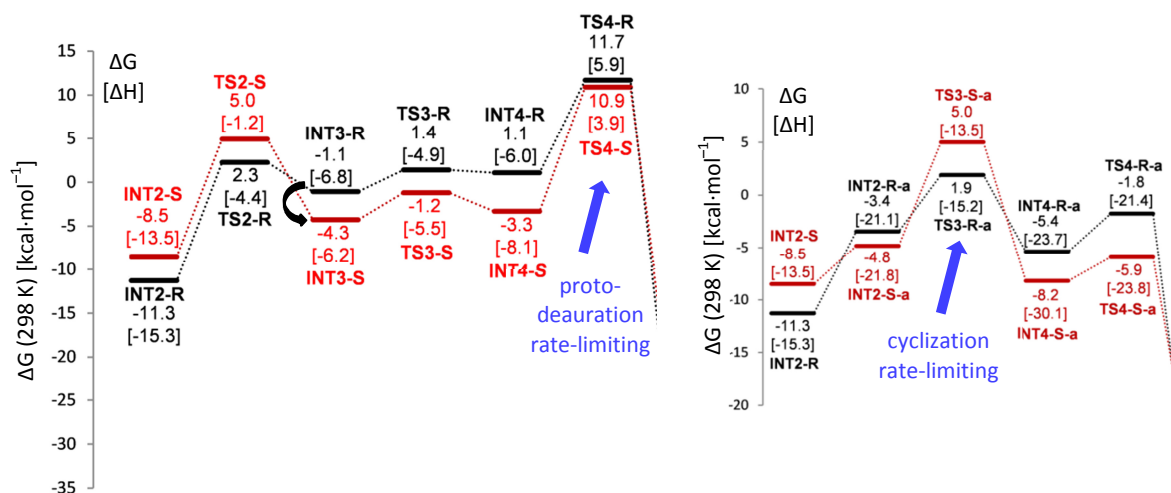
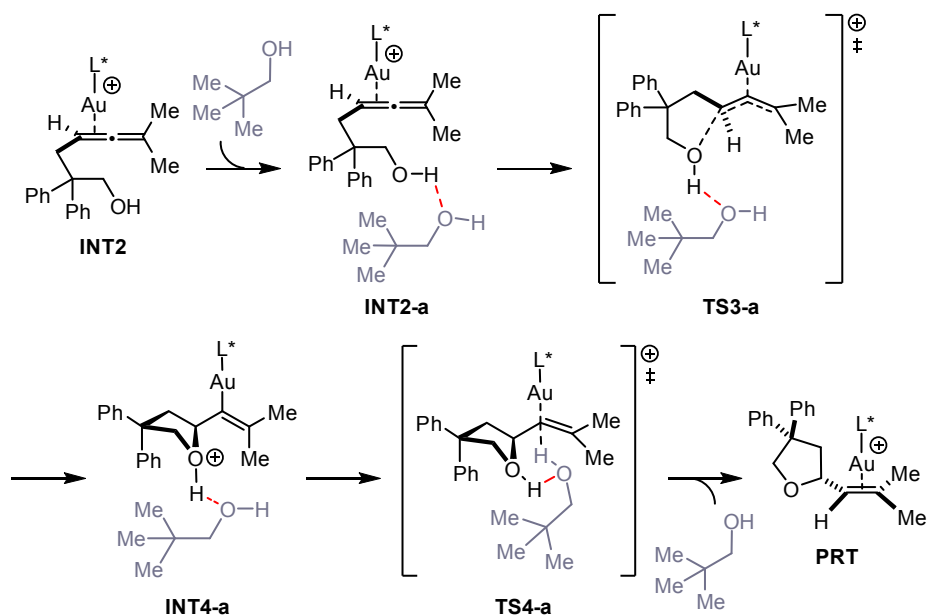


Figure 1.10. Comparison of energy profiles at 298 K in EtOAc (enthalpies are enclosed in brackets) for unassisted proto-deauration (left, excerpt of Figure 1.8) and assisted proto-deauration (right).



Scheme 1.9. Excerpt of the catalytic cycle for the hydroalkoxylation assisted by a second substrate molecule (modelled as neopentyl alcohol for the sake of CPU-time).

The inversion in selectivity with temperature in aprotic media was also studied by means of DFT calculations. For this purpose, the situation was compared with the assisted pathway in EtOAc at 298 K (Figure 1.11, a)). At low temperature, substrate association is less uphill in energy as the entropic cost is reduced. Substrate-assisted cyclization as well as proto-deauration becomes more facile compared to ambient temperature. Furthermore, assisted cyclization is favored over unassisted cyclization and the substrate-assisted pathway always prevails at 213 K (Figure 1.11, b) faded). Once again, no facile possibility for the (*R*)- and (*S*)-pathways to cross is given, since the allyl cation intermediate is bypassed. The formation of (*R*)-(+)-**2** is kinetically preferred in the rate-limiting cyclization step and conforms well to the results observed experimentally.

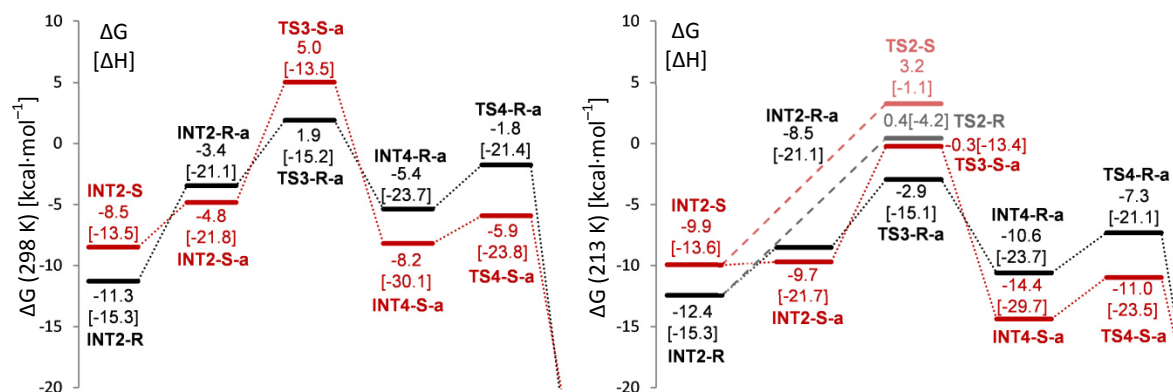


Figure 1.11. Computed Gibbs free energy profiles for the assisted pathways in EtOAc at 298 K (left) and 213 K (right, **TS2** for the unassisted pathway for comparison faded).

Nonetheless, one possibility for interconversion between the two pathways by transformation of **INT4-a** into **INT3** and *vice versa* through a barrierless association/dissociation of a second substrate molecule has to be considered (Figure 1.12). The differential Gibbs free energy ($\Delta\Delta G$) of **TS4-R-a** and **INT3-R** is rather small at ambient temperature so that formation of (*R*)-(+)-**2** via **TS4-R-a** and interchannel crossing through single-bond rotations in **INT3-R** to **INT3-S** are competitive. In turn, **INT3-S** can coordinate an assisting substrate molecule and form (*S*)-(–)-**2** via **TS4-S-a** (Figure 1.12 left). At ambient temperature, both pathways are therefore accessible with the lower-energy pathway producing the (*S*)-product. Under cryogenic conditions, the temperature-dependent entropic penalty for the association is reduced, thus the associative pathway becomes favored by about 4 to 5 kcal·mol^{–1} at 213 K. Since access to allyl cation **INT3** is suppressed, (*R*)-(+)-**2** is the preferentially formed product in this scenario (Figure 1.12, right).

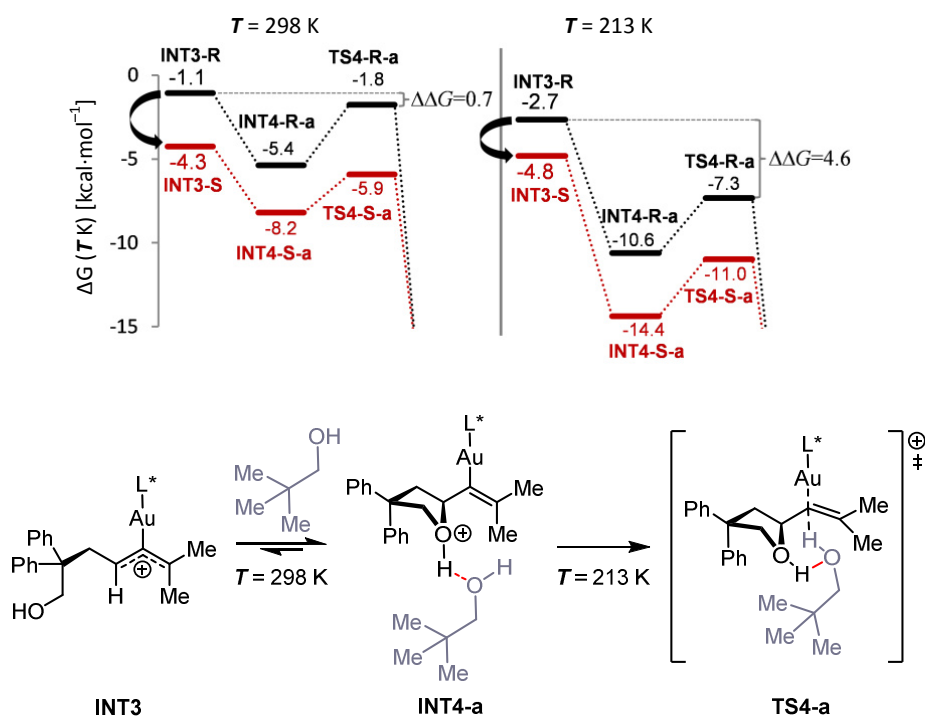
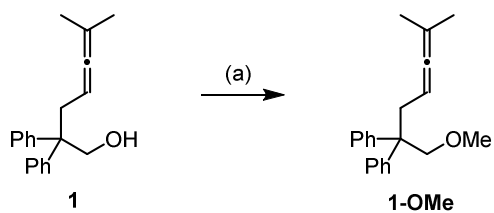


Figure 1.12. Gibbs free energy profiles highlighting the temperature-dependent pathways available to **INT4-a** in EtOAc at 298 K (left) and 213 K (right).

1.3.5 NMR Studies^[44]

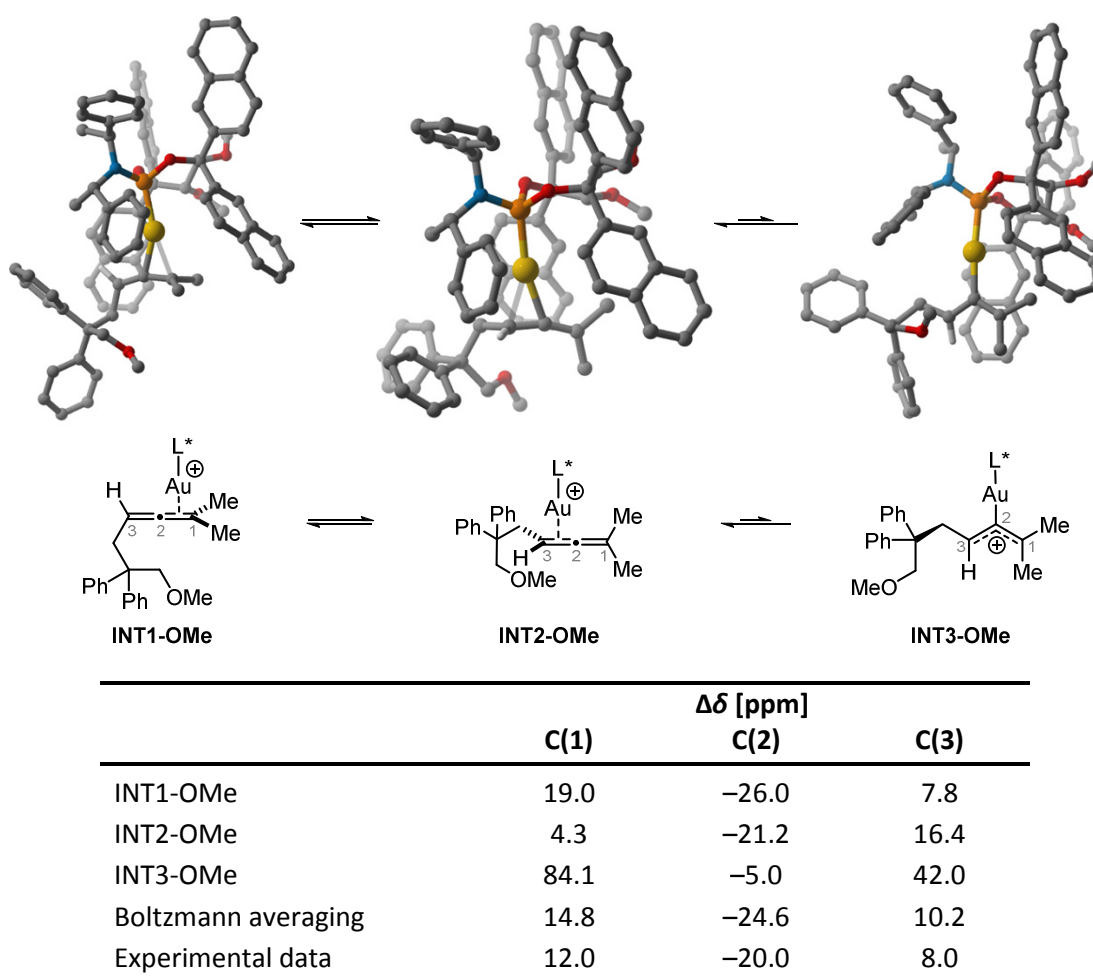
The computational results were also scrutinized against detailed NMR studies, which proved extremely challenging due to the large and conformationally flexible system with numerous overlapping aromatic signals and independent chemical exchange processes. Furthermore, the reaction of substrate **1** was too fast to study initial complexation of the allenol to the gold center. Thus, an unreactive methoxy-allene derivative **1-OMe** was prepared (Scheme 1.10).



Scheme 1.10. Preparation of substrate **1-OMe** for NMR studies. Reagents and conditions: (a) NaH, MeI, THF, 0 °C, 70%.

The ionized catalyst (*S,S,S,S*)-**C3** was mixed with **1-OMe** in stoichiometric ratio in anhydrous CD₂Cl₂ and analyzed over a temperature range of –80 to +50 °C. Although the model substrate **1-OMe** could not undergo hydroalkoxylation, it slowly underwent isomerization to a mixture of 1,3-dienes after several days. Nevertheless, important information could be deduced from the spectral data.

Upon complexation, only the central allene C-atom is significantly shifted upfield by -23 ppm and exhibits a J_{CP} coupling of 14 Hz, indicating either an η^1 coordination mode (**INT3**) or a fast slippage process of the gold center from one double-bond π -face to the other (**INT1** \leftrightarrow **INT2**, Scheme 1.11). The latter is in line with the observation that the exchange is still fast at -50 °C but becomes slower at -80 °C, causing broadening of the resonances corresponding to the two terminal allene C-atoms. This interpretation is consistent with the literature^[45] as well as with the computed Gibbs free energy profiles, in which **INT1** and **INT2** are separated by only a small energetic barrier and are both lower in energy than the allyl cation **INT3** (see Figure 1.8). Additionally, Boltzmann averaging of the computed chemical shifts for each C-atom of the allene moiety is in better agreement with the experimental values than the computed shifts of any individual isomer (Scheme 1.11).



Scheme 1.11. DFT model of the loaded complex using **1-OMe** which matches onto the experimentally observed NOE contacts; experimental and computed ^{13}C NMR shift changes ($\Delta\delta$) upon complexation.

Moreover, NOE contacts between the bound **1-OMe** and the ligand unambiguously revealed that only two out of four possible modes for the coordination of the allene substrate to the gold center are sterically accessible. With the allenic proton showing no NOE contact to the catalyst, the

assumed orientation corresponds to the computed structures of the gold π -complexes **INT1** and **INT2**. Complexation to the other two π -faces has also been calculated but could safely be disregarded as they are much higher in energy. In summary, the experimental results from the NMR study corroborate the conclusions drawn from the DFT calculations.

Another distinctive NMR feature of the π -complex was the presence of two slowly exchanging conformations. The conformer ratio of approx. 3:2 was fairly constant over a wide temperature range. Scrupulous analysis of the spectra indicated a 180° flip of the naphthyl group that is closest to the dimethyl substituted allene terminus. Based on NOE analysis, the position and orientation of the model substrate within the catalyst binding site was found to remain unaffected by this rotatory movement (Figure 1.13).

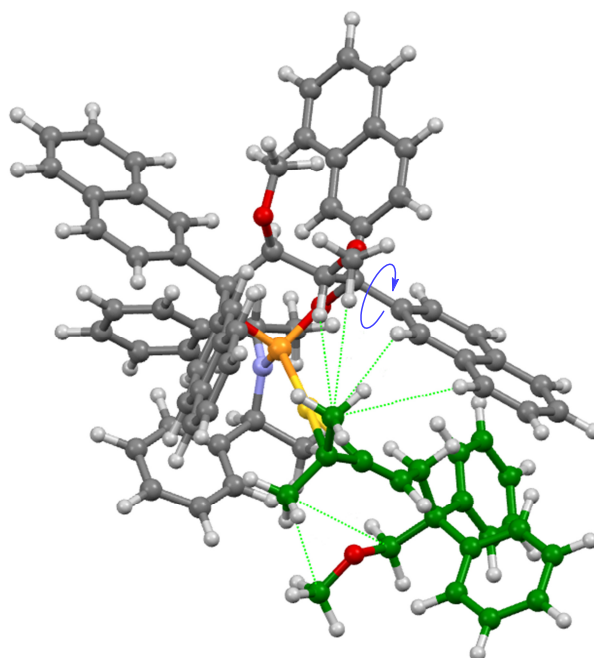


Figure 1.13. Key NOE contacts (green) between model substrate **1-OMe** and catalyst; naphthyl ring flip indicated by the blue arrow.

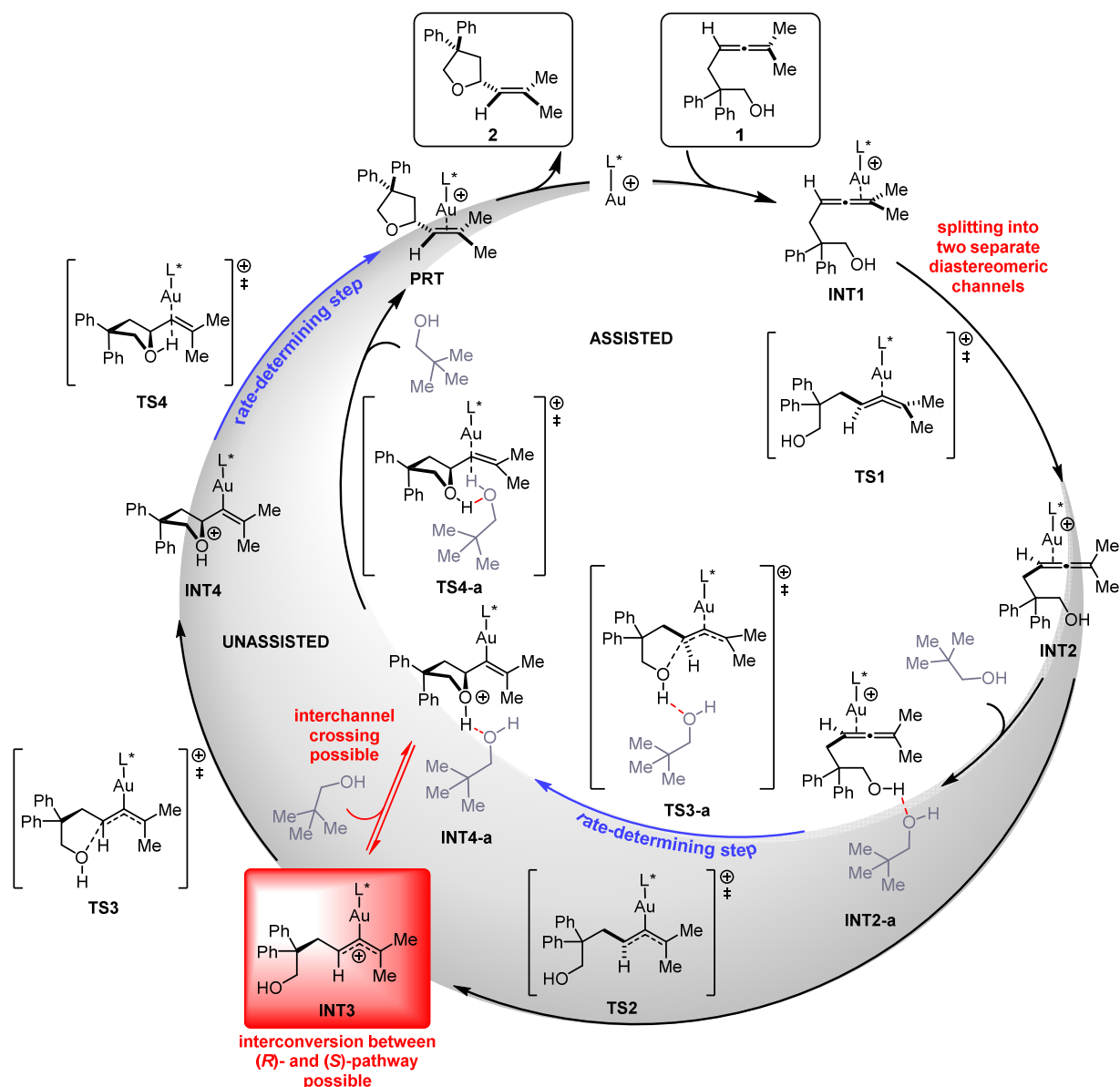
An additional rotameric process independent of the naphthyl flip was observed. Rotation of the symmetric amine moiety of the phosphoramidite about the P–N bond occurs on a much faster time scale both for the minor and the major conformer (millisecond time scale at –20 °C). Consequently, this rotation is relatively unhindered by the bound substrate or the naphthyl groups.

These observations suggest that the amine rotation as well as the naphthyl ring flip have little bearing on the enantioselectivity. Thus, it is not the conformational behavior of the ligand that is primarily responsible for the enantioinversion as proposed on other occasions.^[46] Instead, a more involved mechanism with a strong entropic component as described above is operative.

1.3.6 Conclusion

In summary, the TADDOL-related phosphoramidite-gold complexes previously designed in the Fürstner group can serve as efficient catalysts in hydroalkoxylations of allenes achieving high levels of asymmetric induction. The outstanding character of the reaction studied herein is that either antipode of a given product can be made using a single chiral source but modifying reaction conditions such as solvent, counterion and temperature. The autonomous action of each parameter suffices for switching the stereochemistry, yet these factors can also act in synergy to further increase the selectivities. The effect was observed for the naphthyl substituted one-point binding ligand with different allenols; however, the magnitude of the enantioinversion was dependent on the substitution pattern of the substrate. Nevertheless, the phenomenon of enantioinversion cannot be explained solely by steric interactions. A combination of DFT calculations and experimental investigations including NMR studies allowed to unravel the underlying mechanism in quite some detail.

The major reason for the enantioinversion was found in the existence of two competing pathways: a pathway where proto-deauration is rate-limiting favors the (*S*)-product, whereas an alternative outlet involving assisted proto-deauration preferably produces the (*R*)-product. A plausible mechanistic scenario allowing to rationalize the experimental observations is depicted in Scheme 1.12 on the basis of DFT calculations. The outer catalytic cycle represents the mechanistic scenario in the absence of an efficient proton shuttle, while the inner cycle illustrates the assisted process. In the unassisted pathway, an interconversion between the diastereomeric channels accounting for the (*S*)- and the (*R*)-product is possible at the allyl cation stage **INT3**. In the assisted pathway, this intermediate is bypassed and facile interconversion essentially impossible. A channel crossing between the unassisted and assisted pathway is however feasible, since association of a second substrate molecule at the allyl cation stage **INT3** is energetically accessible, which explains a transition to the assisted pathway at low temperature.



Scheme 1.12. Plausible mechanistic scenario: outer cycle unassisted pathway (grey); inner cycle assisted pathway (white); possible interchannel crossing at the allyl cation intermediate (red).

For the unassisted case interconversions between the two diastereomeric channels as well as to the mechanistically different assisted pathway are possible at the allyl cation intermediate. Thus, high enantiomeric excess for the (*S*)-product is difficult to achieve. In contrast, the assisted pathway is the preferred channel at low temperature and in the presence of proton shuttles (provided by solvent or counterion) delivering the (*R*)-product in excellent *ee*. For this scenario, the entropic component to the reaction free energy profile is significantly increased and can ultimately dictate the stereochemical course. In any event, the analysis of this case study highlights that entropic changes along the reaction coordinate should not be underestimated in asymmetric catalysis.^[47]

2 Studies Toward the Total Synthesis of Chagosensine

2.1 Introduction

2.1.1 Natural Product Total Synthesis

Living organisms produce a wide variety of secondary metabolites, which are not involved in the essential maintenance of the organism.^[48] However, such compounds often contribute to growth, reproduction or defense through interaction with a specific molecular target.^[49] The structures of secondary metabolites have been optimized in the evolutionary process in order to improve the biological activity. As a result, natural products display fascinating architectures and versatile biological profiles.^[50] Sometimes, they show high levels of activity even in completely remote contexts and are therefore a valuable source for drug discovery processes in pharmaceutical and agricultural chemistry – not only by providing novel bioactive compounds, but also by inspiring the design of new structures.^[51]

Polyketides represent a large and structurally diverse class of natural products with a broad spectrum of biological activities. They are constructed by multifunctional protein complexes called polyketide synthases and usually exhibit highly oxygenated and stereochemically enriched scaffolds.^[52] Frequently, only minute amounts of the secondary metabolite are available and the natural supply of the producing organism is typically limited. Semisynthesis or chemical synthesis can overcome this issue, bearing the great advantage of providing access to non-natural derivatives, whose biological activity can also be evaluated.^[53] A striking example is found in the macrocyclic polyketide halichondrin B, which was synthesized in almost 90 steps six years after its isolation from a marine sponge in 1986.^[54] During a drug development program at Eisai Co., Ltd., the simplified synthetic analog eribulin was obtained in 62 steps and showed even increased inhibition of tubulin polymerization compared to the natural product (Figure 2.1).^[55] The highly potent natural product derivative was approved as an anticancer drug in 2010.^[56]

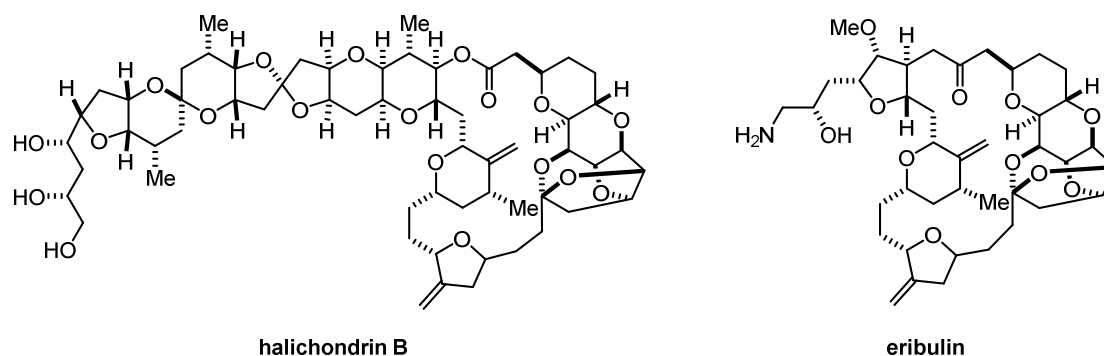


Figure 2.1. Natural product halichondrin B; approved natural product derived drug eribulin.

A huge number of polyketides are found in marine sponges and soft corals.^[57] Among these, macrocyclic lactones (macrolides) such as the above mentioned halichondrin B are the most widespread subclass produced by marine organisms. More than 350 marine macrolides have been characterized since the first report in 1974 of aplysiatoxin, a brominated tumor-promoting natural product (Figure 2.2).^[58] Despite the availability of chloride and bromide ions in seawater, only a limited number of halogenated macrolides have been identified to date.^[59] Interestingly, bromide is more frequently incorporated, although chloride occurs in higher concentrations in seawater.^[60] Nonetheless, chlorinated natural products show important biological activities as exemplified by spongistatin, a highly potent macrolactone currently in preclinical studies as an anticancer drug candidate (Figure 2.2).^[61]

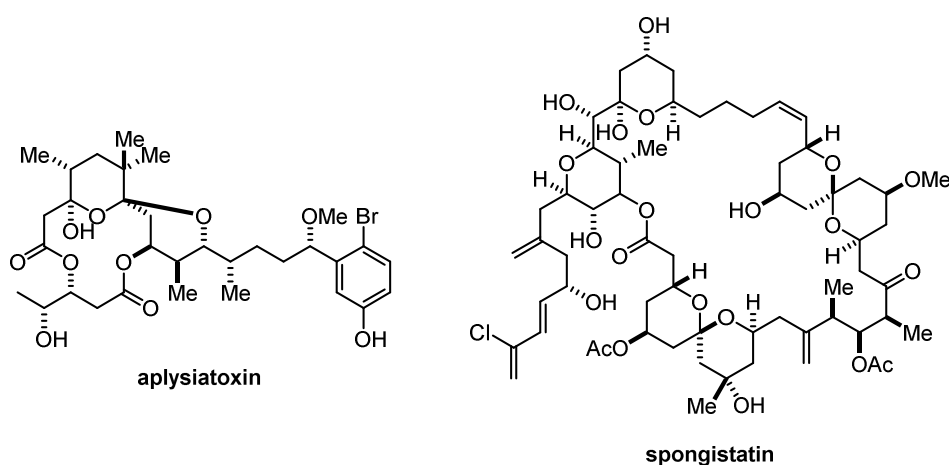


Figure 2.2. Selected halogenated marine macrolides.

More marine polyketides are expected to be discovered and their complex structures will continue to inspire synthetic chemists to develop new methodologies and innovative technologies to access larger quantities for structure–activity relationship studies and eventually medical use.^[61b] Their total synthesis represents an ultimate challenge for established synthetic methods, which must provide high yields and selectivities in the challenging environment of a natural product with a complex architecture and numerous polar functional groups.^[62] Furthermore, total synthesis serves as the ultimate tool to either confirm or reassign a proposed structure.^[63]

2.1.2 Ring Closing Alkyne Metathesis and Postmetathetic Transformations

Over the past decades, different methodologies have been developed to access such macrocyclic natural products, the most prominent representatives being macrolactonization, intramolecular cross coupling and ring closing olefin metathesis. An alternative approach is found in ring closing alkyne metathesis (RCAM), which was first accomplished in 1998^[64] and has experienced significant advancement ever since.^[65] The initially employed tungsten alkylidyne **C7** was soon replaced by

molybdenum complex **C8**,^[66] which had to be activated *in situ* by dichloromethane^[67] or 1,1-dichloropropane^[68] (Figure 2.3). Although the lower Lewis acidity of molybdenum compared to tungsten led to an improved functional group tolerance, the catalytic system suffered from moisture sensitivity and its ability to cleave molecular oxygen as well as nitrogen, which further complicated its use. With the advent of a new generation of molybdenum catalysts, such as **C19** and **C10** endowed with silanolate ligands (Figure 2.3), user-friendliness was combined with high activity and exceptional functional group tolerance.^[69] Consequently, RCAM can now be used to construct highly functionalized cycloalkynes under very mild conditions.^[70]

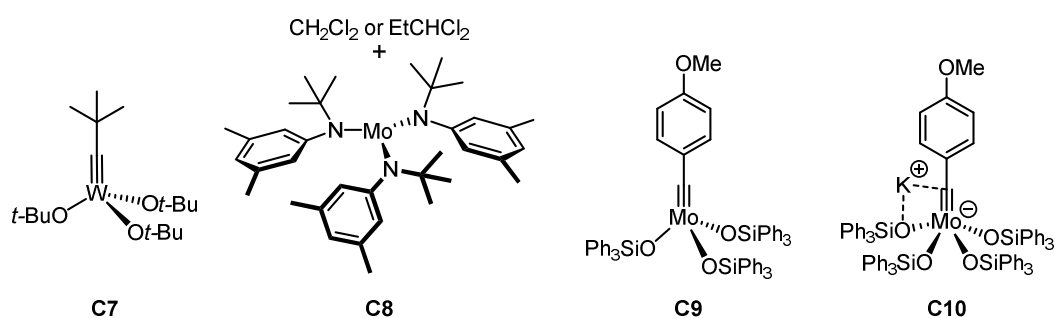
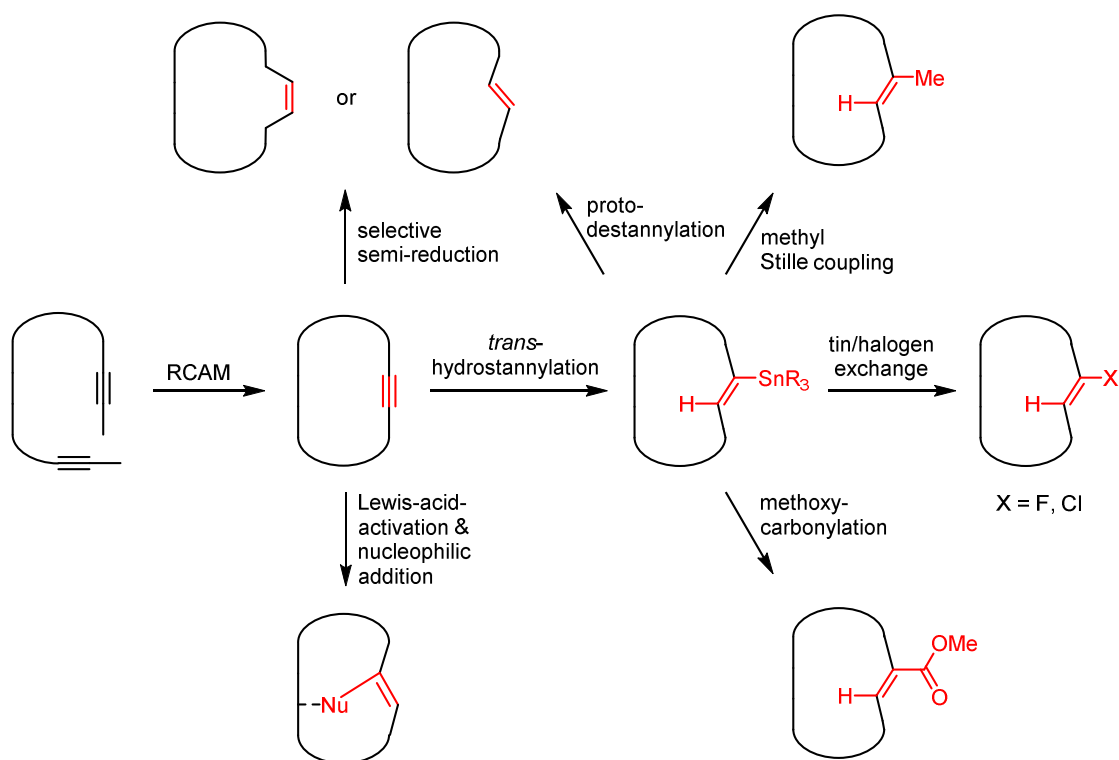


Figure 2.3. Established catalysts for RCAM.

This development has promoted RCAM as a viable C–C bond forming tool for total synthesis, especially since the cycloalkyne constitutes a handle for further postmetathetic derivatizations as depicted in Scheme 2.1. Selective access to (*Z*)- and (*E*)-olefins is provided by semi-reduction^[71] and thus represents an alternative to olefin metathesis, where stereoselectivity often presents a challenge.^[72] Furthermore, π -acid catalysis opens up a route for inter- as well as intramolecular attack of a nucleophile to the activated cyclic alkyne, eventually comprising multiple ring closing events.^[73]

More recently, Fürstner and coworkers have reported on the ruthenium-catalyzed transformation of internal alkynes into *trans*-hydrogenated^[74] or *trans*-hydrometalated olefins.^[75] Among these, *trans*-hydrostannylation has proven outstanding for its high levels of selectivity combined with the possibility to further functionalize the products. Excellent *trans*-selectivity is achieved by employing the bulky and neutral ruthenium catalyst $[\text{Cp}^*\text{RuCl}]_4$. Regioselectivity is determined by the substrate bias: a protic functional group in proximity to the alkyne leads to stannylated products in the proximal position to the functional group.^[76] The alkenylstannanes can subsequently be converted into the corresponding disubstituted (*E*)-alkenes by proto-destannylation or trisubstituted alkenes by Stille cross coupling.^[77] Alternatively, palladium-catalyzed carbonylation gives rise to the respective acrylates^[78] and vinyl chlorides or vinyl fluorides can be obtained by tin/halogen exchange.^[77,79]



Scheme 2.1. RCAM and postmetathetic functionalizations.

This new methodology of RCAM and postmetathetic functionalization not only provides access to new structural motifs within a macrocyclic framework, but also allows for new retrosynthetic analyses of architecturally challenging target molecules. The application of a sequence of ring closing alkyne metathesis, hydrostannylation and tin/chloride exchange to access the (*Z,Z*)-chlorodiene containing macrolide chagosensine will be described in the following chapters.

2.2 Isolation and Structural Discussion of Chagosensine

Chagosensine (**15**) was isolated in 2003 from the widely abundant Red Sea calcareous sponge *Leucetta chagosensis* collected in the Gulf of Aqaba (Eilat, Israel).^[80] The very same sponge, as well as other members of the genus *Leucetta* have previously been identified as sources of imidazole alkaloids with cytotoxic^[81] or antifungal^[82] properties, as well as antimicrobial lipids.^[83] The biological activity of the novel polyketide chagosensine, however, has not yet been evaluated.

The structure of chagosensine was elucidated primarily based on NMR spectroscopic data. The connectivity and relative configuration was assigned by ¹H-¹H coupling constants and two-dimensional NMR techniques, including COSY, HMBC and NOESY correlations. Thus, chagosensine was characterized as a highly decorated 16-membered macrolactone containing two *trans*-configured tetrahydrofuran moieties and an unprecedented (*Z,Z*)-chlorodiene (Figure 2.4). Additional

unsaturation is found in the sidechain, featuring an allylic alcohol and a carboxylic acid. The polyoxygenated macrolide bears a total of nine secondary and two tertiary stereogenic centers.

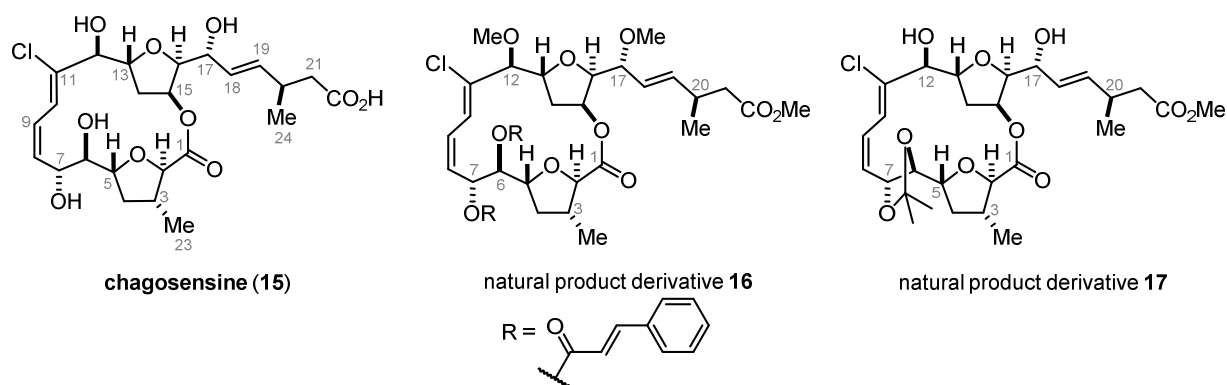


Figure 2.4. Structure of chagosensine (**15**) and its synthetic derivatives **16** and **17**.^[80]

The absolute stereochemistry was evaluated by derivatization of the natural product and degradation studies. Reduction of the macrolactone followed by oxidative cleavage of the C6–C7-diol provided the southern THF-moiety. Upon further degradation and comparison with commercially available material, the C3 stereogenic center was assigned as (*R*), which in turn allowed assignment of the C2 and C5 stereochemistry. The absolute configuration at C6 and C7 was determined by derivatization of the natural product. To this end, the carboxylic acid, the C12- and C17-alcohol were methylated prior to esterification of the diol with *p*-methoxycinnamoyl chloride giving derivative **16**. Both C6 and C7 were found to possess (*R*)-configuration based on the Cotton effect observed during CD spectroscopy.^[84] The configuration at C12 and C17 could be determined *via* modified Mosher analysis^[85] of derivative **17**, which was obtained after acetalization of the southern diol and methylation of the carboxylic acid. The tertiary stereogenic center in the sidechain was elucidated as having (*S*)-configuration by chemical degradation. Ozonolysis of the C18–C19 double bond followed by oxidative work-up and methylation gave rise to the corresponding diester, which was compared with commercially available material. The absolute configuration of the northern THF-ring was not confirmed experimentally and remains therefore in question.

While the conjugated (*Z,Z*)-chlorodiene is unprecedented in the literature, some structural motifs of chagosensine can be found in other polyketides of marine origin (Figure 2.5). For example, the 2,5-*trans*-THF-ring with an adjacent *anti*-diol found in the southern domain is also present in the cytotoxic macrolide amphidinolide F.^[86] While, the 2,5-*trans*-THF-ring in the northern domain resembles the originally proposed structure of the haterumalide family members,^[87] this particular subunit was reassigned after total synthesis^[88] prior to submission of the chagosensine isolation report, which does not cite this critical publication. In fact, Řezanka *et al.* have only determined the relative configuration of this moiety, thus a misassignment at C13, C15 and C16 is possible.

Nevertheless, the stereochemical proposal for the northern segment of chagosensine does appear in the antiproliferative natural product isolaulimalide,^[89] which has been confirmed after total synthesis.^[90]

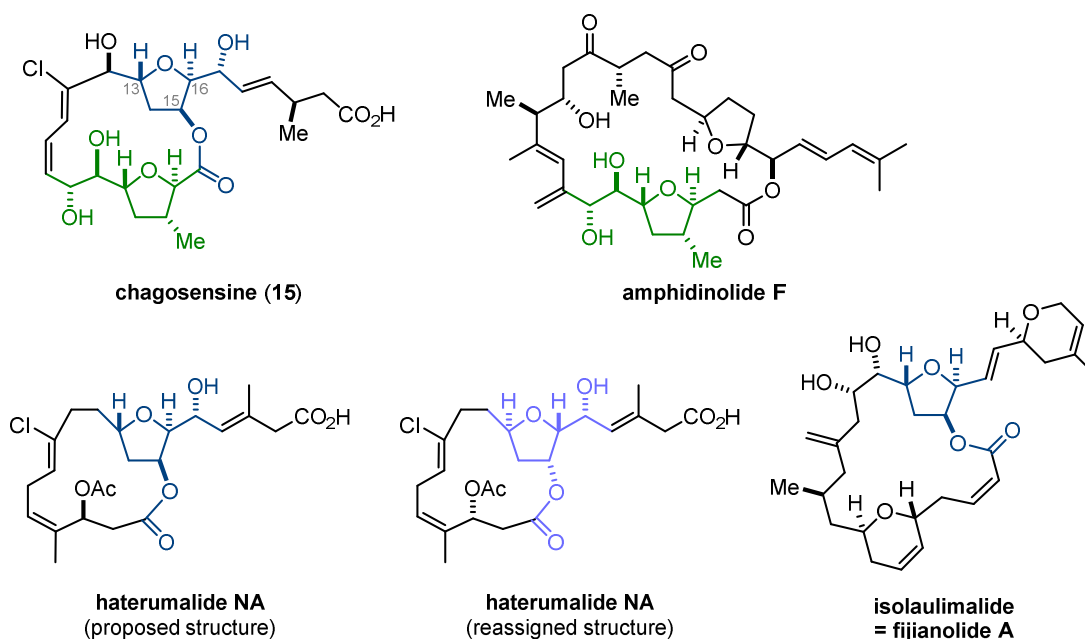


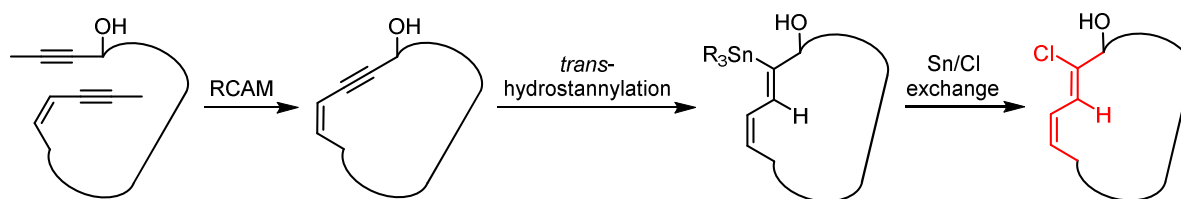
Figure 2.5. Structural relatives of chagosensine in nature.

This comparison with related marine macrolides highlights the unique structural features of chagosensine and points toward potentially promising biological activity. The need for material supply to ultimately assign its configuration and evaluate its pharmacological profile in combination with the apparent lack of synthetic efforts renders this natural product a valuable target for total synthesis.

2.3 Objectives

Chagosensine was chosen as a target for total synthesis in order to unambiguously determine its structure. Therefore, a highly convergent synthetic strategy with late stage fragment assembly was desirable. The stereochemistry should be set as flexible as possible to account for a potential misassignment and hence to allow correction of single stereogenic centers. This is best achieved by relying on asymmetric catalysis and avoiding chiral pool starting materials.

From a synthetic viewpoint, the primary challenge posed by chagosensine is the construction of the unprecedented chlorodiene motif embedded in the macrocyclic framework. With the recently developed postmetathetic functionalization of cycloalkynes at hand, this motif was planned to be accessed *via* a sequence of RCAM, ruthenium-catalyzed *trans*-hydrostannylation and tin/chloride exchange (Scheme 2.2).



Scheme 2.2. Envisaged key sequence for the total synthesis of chagosensine.

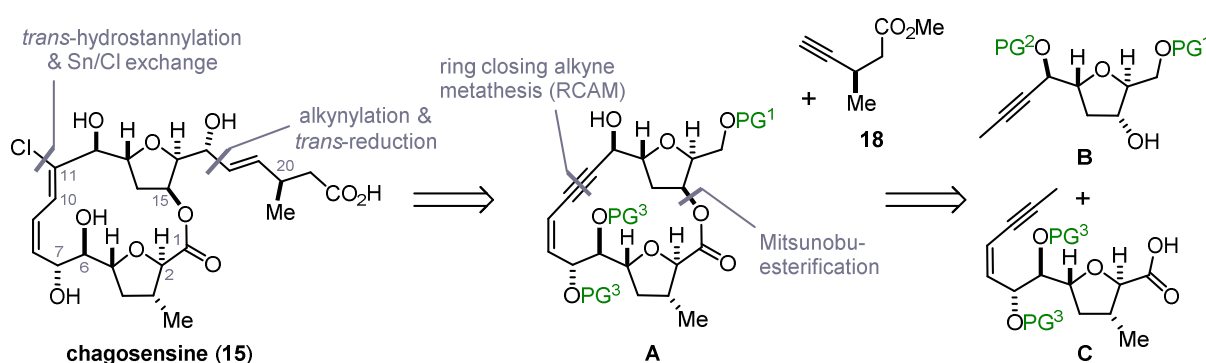
The work reported in this thesis thus aims to further increase the structural scope of RCAM by application to a highly substituted enyne-ynone precursor with exceptionally high density of potentially coordinating groups. Moreover, the novel hydrometalation was thought to be established as synthetically viable postmetathetic transformation, since chagosensine undoubtedly represents the most complex substrate for this methodology so far.

Once a robust synthesis for the true natural product is established, sufficient material for preliminary biological testing should be provided.

2.4 The Metathesis Approach

2.4.1 Retrosynthetic Analysis

As outlined above, the unique (*Z,Z*)-chlorodiene within the macrocyclic scaffold of chagosensine (**15**) was planned to be accessed through a sequence of ring closing alkyne metathesis (RCAM), *trans*-hydrostannylation and tin/chloride exchange. Consequently, a highly convergent synthesis was designed (Scheme 2.3). The sidechain was thought to be installed at a late stage by diastereoselective alkynylation of a macrocyclic aldehyde with alkyne **18** followed by *trans*-hydrostannylation/destannylation. The macrocyclic chlorodiene found in the natural product can be traced back to enyne **A** via tin/chloride exchange and *trans*-hydrostannylation. Fragment assembly prior to ring closure hinged upon a Mitsunobu esterification. Hence, macrocycle **A** was retrosynthetically disassembled into alkyne **B** and carboxylic acid **C** as the key building blocks.



Scheme 2.3. Retrosynthetic analysis of chagosensine; PG = protecting group.

Since modern transition metal catalyzed transformations were thought to be implemented late in the synthesis of a complex target, it seemed advisable to challenge the key sequence first on model systems.

2.4.2 Model Studies on the Key Sequence

Despite the intriguing examples of ring closing alkyne metathesis (RCAM) in macrolide total synthesis,^[71a,71b,73b,73d,91] it was unclear at the outset of this project whether the ring closure between a propargylic alcohol and a (*Z*)-enyne with an allylic alcohol would be feasible. Alkynes bearing potential leaving groups in the propargylic position are known to be problematic in alkyne metathesis, since basically all well-defined catalysts for this transformation are Schrock alkylidynes, which are characterized by high-valence metals and electron-donating ligands.^[65] The inherent Lewis acidity of these complexes endangers fragile substituents, such as propargylic alcohols, due to the resonance stabilization of the resulting carbocations (Figure 2.6, **VIII**). The Lewis acidity, however, can be modulated by the electron-donating ligand set and a productive [2+2]-cycloaddition/-cycloreversion sequence to form an alkylidyne of type **IX** is feasible. The latter, however, is again prone to decomposition by elimination of the propargylic alcohol generating a vinylidene species that is unable to undergo alkyne metathesis.^[92]

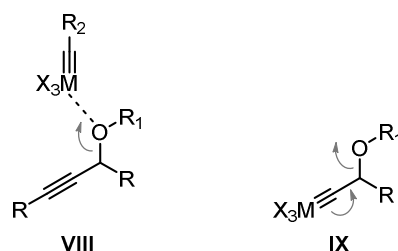
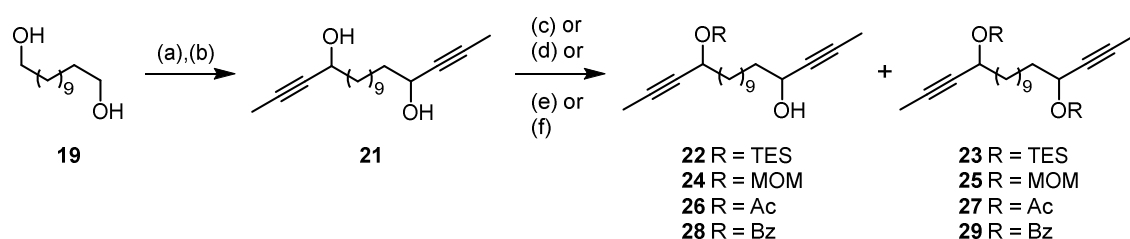


Figure 2.6. Effects of metal alkylidynes on propargylic substituents.

With the development of Mo-complex **C9** (see Figure 2.7) Fürstner *et al.* succeeded in modulating the metal's Lewis acidity and therefore significantly increasing the functional group tolerance.^[69,93] Key to the success was the catalyst design comprising triarylsilanolate ligands. The aryl groups are not too bulky to impede substrate binding, yet bulky enough to disfavor polymerization through an associative mechanism. The stereoelectronic properties of the silanolates are highly beneficial as bending of the Mo–O–Si hinge reduces electron donation of the ligand to the metal. The resulting increased Lewis acidity at the molybdenum center favors substrate binding. In contrast, stretching of the Mo–O–Si bonds leads to increased electron donation downregulating the molybdenum's Lewis acidity and hence facilitating product release.^[65] Due to constant thermal motion, the catalyst is thus expected to meet the opposing electronic requirements within the catalytic cycle and was found to tolerate substrates with protic functional groups in the propargylic position.^[70e,77,91b] Nevertheless,

only substrates comprising one propargylic substitution and one unfunctionalized alkyne had so far been studied in metathesis reactions. Therefore, the merger of two propargylic alcohols represented the next challenge and a series of suitable model substrates was designed.

Starting from 1,12-dodecandiol (**19**), a set of nine differently protected bis-propargylic diols was synthesized. After the copper-catalyzed aerobic oxidation developed by Stahl and coworkers^[94] provided 1,12-dodecandial (**20**), addition of propynyl-Grignard reagent furnished diol **21** as a mixture of spectroscopically and chromatographically indistinguishable *syn/anti*-diastereomers (Scheme 2.4). Since only a limited number of protic functional groups had thus far been tolerated by alkyne metathesis catalysts,^[91b,95] diol **21** was mono-protected as TES-ether **22**, MOM-acetal **24**, acetate **26** and benzoate **28** in moderate yields. The bis-protected alcohols **23**, **25**, **27** and **29** were simultaneously formed and isolated from the reaction mixtures.



Scheme 2.4. Synthesis of diyne model substrates. Reagents and conditions: (a) $\text{Cu}(\text{MeCN})_4(\text{PF}_6)_6$ (5 mol%), bipyridine (5 mol%), TEMPO (5 mol%), NMI (10 mol%), air, MeCN, 86%; (b) CH_3CCMgBr , THF, 90%; (c) TESCl, imidazole, DMAP (cat.), CH_2Cl_2 , **22** 43%, **23** 21%; (d) MOMCl, *i*-Pr₂NEt, DMAP (cat.), CH_2Cl_2 , **24** 41%, **25** 14%; (e) Ac_2O , Et₃N, DMAP (cat.), CH_2Cl_2 , **26** 72%, **27** 21%; (f) BzCl, Et₃N, DMAP (cat.), CH_2Cl_2 , **28** 30%, **29** 48%.

With this set of diynes in hand, the RCAM was first tested under standard conditions. All reactions employing the latest generation of aryl-alkylidyne molybdenum catalysts comprising silanolate ligands, introduced as either the neutral species **C9** or the potassium ate-complex **C10** (Figure 2.7), largely failed to produce the corresponding macrocycles. Solely the bis-MOM-protected derivative **25** could be cyclized in 54% yield (Table 2.1, Entry 3). This result epitomizes that RCAM between bis-propargylic substrates is in general possible and that the problem arises from an incompetence of the chosen catalyst.

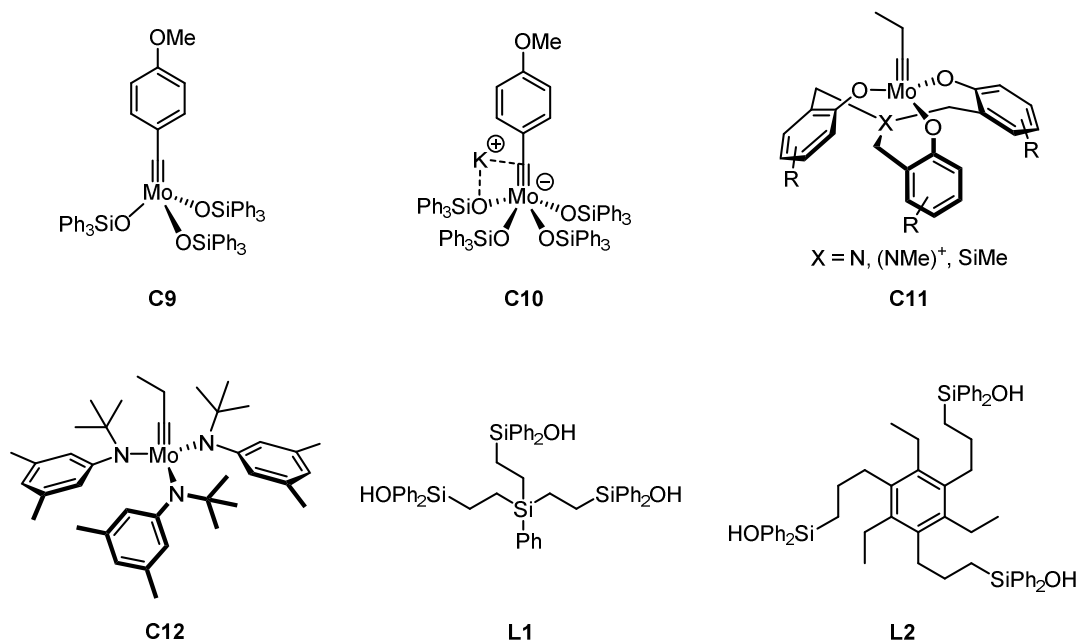


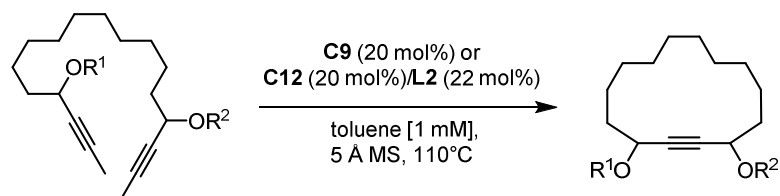
Figure 2.7. Molybdenum catalysts **C9**, **C10**, **C11** and **C12**, as well as recently developed multidentate silanolate ligands **L1** and **L2**.

Parallel to this work, further catalyst development was undertaken in the Fürstner group.^[96] As speculated in the past,^[97] the silanolate ligands of **C9** seem to suffer from partial or even complete ligand exchange by protic functional groups. Therefore, a new generation of catalysts was designed based on multidentate ligands, inspired by the work of Zhang and coworkers, who utilized podand ligands to obtain chelate complexes of the general type **C11** (Figure 2.7).^[98] In order to maintain the above mentioned advantages of the silanol ligands, chelating siloxides were synthesized. Upon complexation of the chelating ligand **L1** or **L2** to the precatalyst **C12**, a mixture of products was formed and the isolation of a defined catalyst species has thus far proven impossible.^[92b] Instead of chelating a single metal center, the trisilanols act as cross-linking agents between multiple metal centers. Nevertheless, application of this new generation of catalysts to the RCAM of the challenging bis-propargylic test substrates seemed worthwhile.

For the absence of a well-defined solid-state structure, an *in situ* protocol for RCAM was developed: a freshly prepared solution of precatalyst **C12** and ligand **L1** or **L2** was stirred prior to its addition to the respective substrate solution. Indeed, this two-component catalyst system **C12/L2** was capable of metathesizing the bis- and mono-MOM substrates as well as the bis- and mono-TES substrates (Table 2.1, Entries 1-4). Also, two protic groups were tolerated as demonstrated by diol **21** (Entry 5). In general, less protic substrates, *i.e.* protected alcohols, gave better results than their more protic analogs. Only mono- and bis-esters **26-29** completely failed to react (Entries 6-9), presumably due to their enhanced leaving group ability increasing the risk of catalyst decomposition *via* formation of a metal-vinylidene species (*vide supra*). In summary, the scope of RCAM has been expanded to bis-

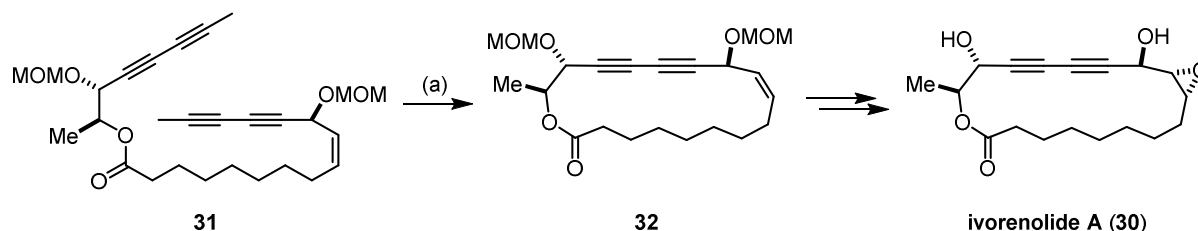
propargylic substrates, provided that the propargylic substituents are only moderate leaving groups. This represents an important progress given the prevalence of bis-functionalized unsaturated systems in macrocyclic natural products.

Table 2.1. RCAM of bis-propargylic substrates.^[96]



Entry	Substrate	R ¹	R ²	Yield [%]	
				C9	C12/L2
1	23	TES	TES	0	71
2	22	TES	H	0	64
3	25	MOM	MOM	54	70
4	24	MOM	H	0	67
5	21	H	H	0	53
6	27	Ac	Ac	0	0
7	26	Ac	H	0	0
8	29	Bz	Bz	0	0
9	28	Bz	H	0	0

These findings ultimately led to the successful completion of the total synthesis of ivorenolide A (**30**), a diyne containing natural product.^[92b] Previous attempts to achieve ring closure to the cyclic diyne flanked by two propargylic alcohols had met with failure, whereas the doubly MOM-protected precursor **31** in combination with the new catalytic system provided macrocycle **32** (Scheme 2.5).



Scheme 2.5. Synthesis of ivorenolide A. Reagents and conditions: (a) **C12** (20 mol%), **L2** (20 mol%), 5 Å MS, toluene, 60 °C, 78%.^[92b]

Next, the attention was paid to further conjugated substitutions. Thus far, substrates with propargylic and conjugated substitution on either side of the newly formed triple bond had only been investigated once. A (*Z*)-enyne displaying a methyl group in the allylic position had been successfully

metathesized with a propargylic alcohol.^[70e,71a] The envisioned chagosensine RCAM precursor, however, possesses an additional alcohol adjacent to the unsaturated system (*vide supra*, Scheme 2.3). Once again, a leaving group in conjugation to the alkyne **X** or alkylidyne **XI** poses the risk of elimination, since stabilization of the resulting cation over the π -system is similarly effective (Figure 2.8).

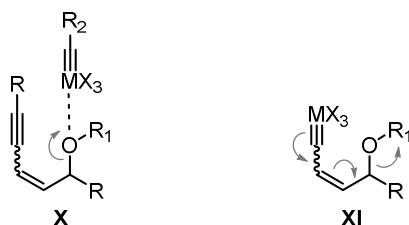
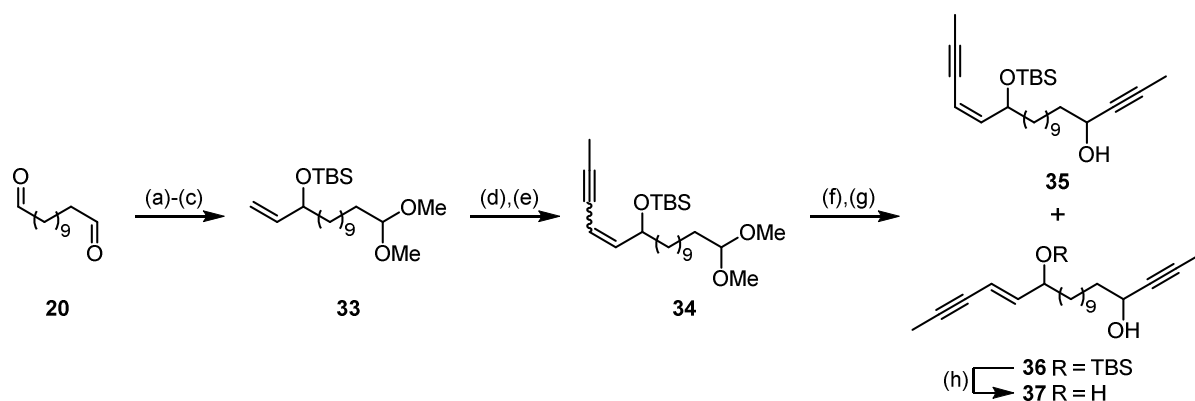


Figure 2.8. Effects of metal alkylidynes on allylic substituents in conjugation to the triple bond.

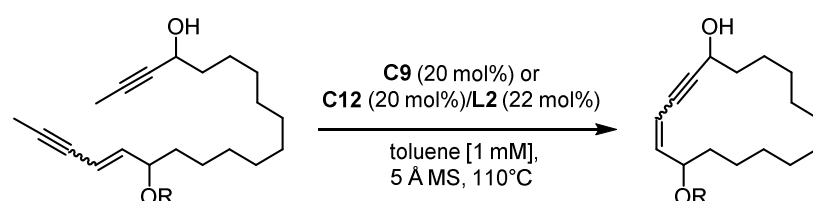
In order to evaluate the enhanced properties of the newly developed catalytic system, a second set of model substrates was synthesized, comprising an enyne flanked by alcoholic groups (Scheme 2.6). The previously obtained dial **20** (*vide supra*, Scheme 2.4) served as starting material and was mono-protected as dimethoxy acetal, which allowed mono-addition of vinyl-Grignard reagent to the remaining aldehyde. The resulting alcohol was protected as TBS-ether **33**. Ozonolysis followed by Wittig olefination provided enyne **34** as an inseparable 1.7:1 mixture of *E/Z* diastereomers. Subsequent acetal cleavage with PPTS and alkylation afforded a mixture of four diastereomers, yet the *syn/anti*-diastereomers were once again indistinguishable by NMR spectroscopy and column chromatography. The *E/Z*-isomers were finally separated by preparative HPLC. The (*Z*)-enyne **35** matching the chagosensine pattern was obviously the more relevant model substrate, but the (*E*)-enyne also represents an interesting compound for comparison. In addition, the TBS-ether of the major (*E*)-diastereomer **36** was cleaved to obtain a third substrate **37** for further RCAM trials.



Scheme 2.6. Synthesis of enyne-yne model substrates. Reagents and conditions: (a) *p*-TsOH, MeOH, toluene, 0 °C, 54%; (b) H₂CCHMgBr, THF, 66%; (c) TBSCl, imidazole, DMAP (cat.), CH₂Cl₂, 92%; (d) O₃, CH₂Cl₂, -78 °C; PPh₃, -78 °C to rt, 89%; (e) but-2-yn-1-yltriphenylphosphonium bromide, *n*-BuLi, THF, -78 °C to rt, 60% (*E/Z* 1.7:1); (f) PPTS, acetone/H₂O, 60 °C; (g) CH₃CCMgBr, THF, **35** 23% over two steps, **36** 38% over two steps; (h) TBAF, THF, 0 °C, 88%.

In accordance with the previous observations and the challenges depicted in Figure 2.8, catalysts **C9** and **C10** were unable to metathesize any of the enyne-yne (Table 2.2). Most of the starting material could be recovered, while only traces of anisol transfer from the catalyst to either alkyne were observed. Using these catalyst, both alkynes can be accessed only in an unproductive fashion. Fortunately, **C12/L2** gave the corresponding macrocyclic enynes **38** and **39** in excellent and good yield (Entries 1 and 2). Subtle differences in reactivity could arise from ring strain, which is assumed to be slightly higher for the (*E*)- than for the (*Z*)-enyne. In addition, **40** could only be obtained in moderate yield (Entry 3), corroborating the trend that multiple protic functional groups harm the catalyst.

Table 2.2. RCAM of enyne-yne substrates.



Entry	Substrate	R	Double Bond Geometry	Product	Yield [%]	
					C9	C12/L2
1	35	TBS	(<i>Z</i>)	38	0	90
2	36	TBS	(<i>E</i>)	39	0	76
3	37	H	(<i>E</i>)	40	0	40

These studies nicely demonstrate that total synthesis can drive methodology development: only after the advent of a new catalytic system was the metathesis of bis-propargylic or allylic-propargylic alcohols possible. With the results obtained from this survey, the first step of the projected key sequence in the envisioned total synthesis of chagosensine seemed feasible. Thus, the second key transformation, *i.e.* the ruthenium-catalyzed *trans*-hydrostannylation of an enyne, had to be investigated.

The *trans*-selective hydroelementation of alkynes to trisubstituted alkenes is attractive for its excellent regioselectivity, provided that the alkyne is endowed with protic functional groups on only one side.^[76] In these cases the α -substituted *trans*-olefins are obtained. Based on single crystal x-ray analysis, the protic group was found to form a hydrogen bond to the chloride ligand of the ruthenium complex **C13** and thus pre-organizes catalyst, substrate and hydroelementation reagent (Figure 2.9).^[76] For alkynes missing protic functional groups, regioselectivity is drastically diminished although electronic and steric properties are operative.

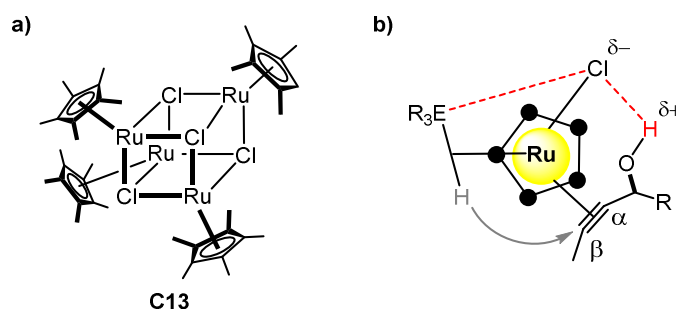


Figure 2.9. a) $[\text{Cp}^*\text{RuCl}]_4$ as efficient catalyst for hydroelementations; b) schematic pre-organization of catalyst, substrate and hydride species (top view model). • = CMe.

Moreover, the absence of a directing group can completely shut down the reactivity in case of competitive binding modes. The latter is true for conjugated systems, e.g. enyne substrates where the ruthenium can be trapped by both triple and double bond.^[99] These substrates can only be converted to the corresponding dienes in the presence of a neighboring protic group. Acyclic enyne substrates had been studied in hydrostannylations before and had shown excellent regioselectivity for the proximal position (Figure 2.10, **41** and **42**).^[76] In contrast to isolated propargylic alcohols, the reaction was significantly slower. Therefore, the tin hydride had to be added *via* syringe pump over the course of 1.5 to 2 hours to prevent catalyst decomposition.^[100] Hydrostannylations can also be directed by a 1,2-diol adjacent to the alkyne as demonstrated by compound **43**. Limitations were found for alkynes flanked with oxygen substitution on either side of the triple bond, causing a significant loss of regioselectivity even if only one is a hydrogen bond donor (see **44**). In this case of electronic equality of both C_{sp} -centers, steric bulk seems to dictate the reaction outcome and hydride delivery from the sterically less hindered side is slightly preferred.

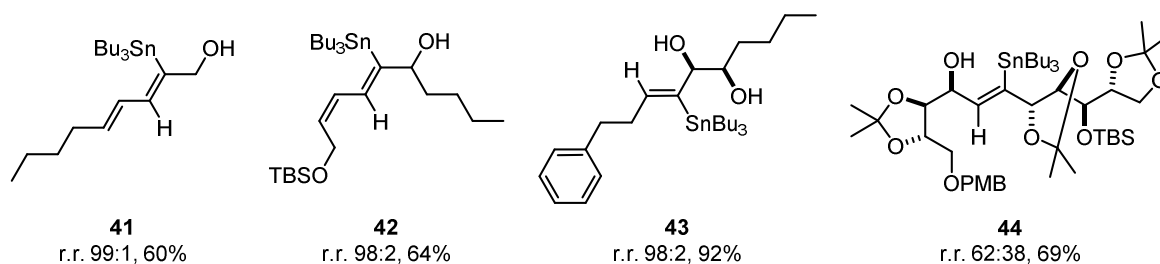
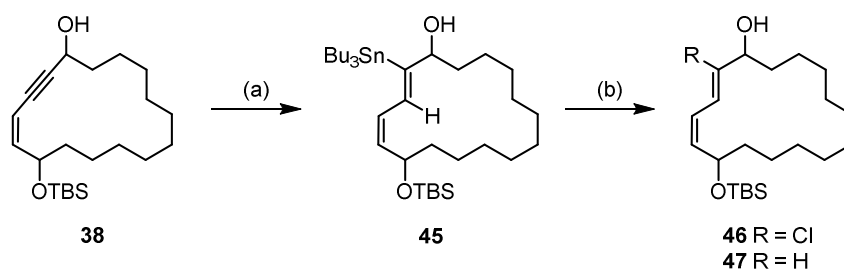


Figure 2.10. Literature-known alkenylstannanes obtained *via trans*-hydrostannylation of the corresponding alkynes; r.r. given as ratio of depicted isomer to opposite regioisomer.^[76]

These observations had to be considered for the projected application of this methodology to the total synthesis of chagosensine. The respective substrate *en route* to the target molecule (Scheme 2.3, **A**) resembles a combination of the species mentioned above: it possesses a concealed 1,2-diol adjacent to the triple bond and a protected allylic alcohol on the other side. However, since the free propargylic alcohol was believed to direct the metal to the adjacent alkyne,^[76] the protected allylic alcohol should not affect reactivity or regioselectivity. To test this expectation, the previously

obtained cyclic enynes were submitted to the standard reaction conditions.^[75b] (*Z*)-Enyne **38** could be transformed into the corresponding α /*trans*-hydrostannylated diene **45** in good yield and excellent selectivity (Scheme 2.7). The obtained dienylstannane was elaborated into (*Z,Z*)-chlorodiene **46** by means of copper-mediated tin/chloride exchange.^[101] The only byproduct observed was the proto-demetalated diene **47**. Dienylstannane **45** had to be isolated, as a one-pot procedure by introduction of CuCl₂ after complete addition of tributyltin hydride gave a complex mixture of products.



Scheme 2.7. Construction of the chlorodiene motif. Reagents and conditions: (a) [Cp*RuCl]₄ (20 mol%), Bu₃SnH, CH₂Cl₂, 90 min, 79%, *Z*/*E* > 20:1, α / β > 95:5; (b) CuCl₂, THF, **46** 67%, **47** 6%.

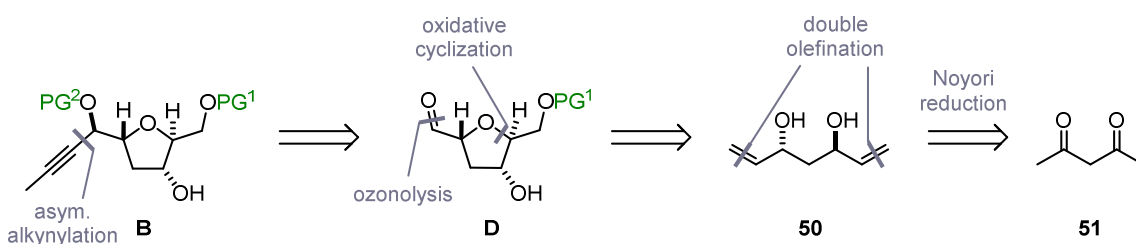
As expected, the double bond geometry of the neighboring olefin within this relatively unstrained macrocycle had no influence on the ruthenium-catalyzed transformation, since the corresponding (*E*)-enyne **39** behaved equally well (see Section 4.3.1).

The successful investigation of the key sequence on suitable model systems encouraged us to embark on the total synthesis of chagosensine pursuing the strategy outlined above (Section 2.4.1).

2.4.3 Synthesis of the Northern Alcohol Fragments **48** and **49**^[102]

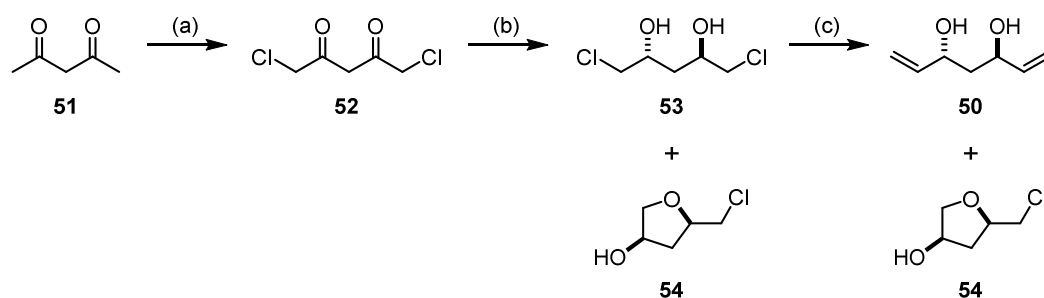
Remark: A first entry to these northern alcohol fragments was developed in close collaboration with postdoctoral researcher Dr. Jakub Flasz.^[103]

The northern fragment possesses four stereogenic centers and a methyl-capped alkyne. The hidden symmetry in this fragment inspired the construction of the THF-moiety prior to asymmetric alkylation of aldehyde **D** (Scheme 2.8). The synthesis of **D** would comprise an ozonolysis of the corresponding olefin and a cobalt-catalyzed oxidative cyclization, thereby leading back to the literature-known C₂-symmetric diol **50**.^[104] The latter can be prepared from acetyl acetone (**51**) in three steps including chlorination, double Noyori reduction and double olefination.



Scheme 2.8. Retrosynthetic analysis of the northern alcohol fragment **B**; PG = protecting group.

The synthetic efforts toward chagosensine commenced with the synthesis of two differently protected northern fragments to provide flexibility for the key sequence. At first, 1,5-dichloropentane-2,4-dione (**52**) was obtained *via* dichlorination of acetyl acetone (**51**) in the presence of excess aluminum trichloride. This reaction was first described by Nojiri *et al.* and later modified by Rychnovsky and coworkers (Scheme 2.9).^[105] The poor but reproducible yield of approx. 22% (literature: approx. 25%) is attributed to the unavoidable formation of structural isomers and partial decomposition. Next, diketone **52** was reduced to the corresponding *anti*-diol **53** by asymmetric hydrogenation, taking advantage of the highly efficient Noyori catalyst.^[105c,106] The *anti*-diol was obtained in consistently high enantio- and diastereoselectivity as evident from initial double Mosher esterification and subsequent NMR analysis thereof (see Section 4.3.2; for further batches, optical rotation values were compared). Dichloride **53** was converted to the diene **50** following a procedure by Hanson and coworkers, which has only been applied on one other occasion.^[104,107] To this end, alkylchloride **53** was attacked by a sulfur ylide generated from trimethyl sulfonium iodide and *n*-BuLi as typically used in Corey-Chaykovsky reactions.^[108] However, the reported results could not be reproduced in our laboratories: formation of 5-(chloromethyl)tetrahydrofuran-3-ol (**54**) resulting from intramolecular S_N2 reaction of **53** could not be prevented and the two products were difficult to separate; therefore a maximum of 65% of pure **50** was obtained. The byproduct had only been mentioned by Rychnovsky and coworkers, who detected its formation during the Noyori hydrogenation, if the temperature exceeded 100 °C.^[105c] Traces of this byproduct were also detected during the hydrogenation even at lower temperatures in our laboratories.

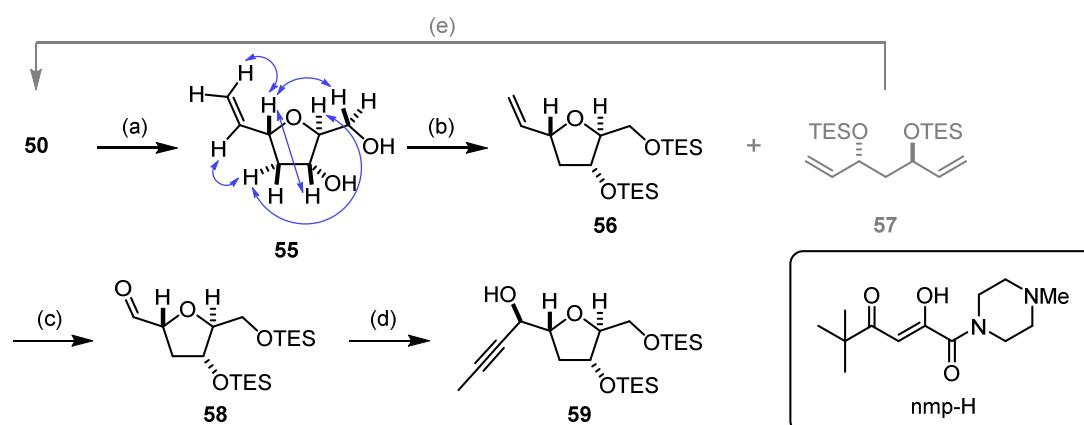


Scheme 2.9. Reagents and conditions: (a) (i) AlCl₃, ClCH₂COCl, PhNO₂, (CH₂Cl)₂, 65 °C, 8 h; (ii) sat. aq. Cu(OAc)₂; (iii) H₂SO₄ (10%), Et₂O, 22%; (b) [RuCl₂((*S*)-BINAP)]₂·Et₃N (0.1 mol%), H₂ (62 bar), 70 °C, **53/54** (crude ¹H NMR) 6:1, **53** 39%, 97% *ee*, *d.r.* > 20:1; (c) Me₃SI, *n*-BuLi, THF, -40 °C to rt, **50/54** (crude ¹H NMR) 9:1 **50** 65%.

The *trans*-tetrahydrofuran was generated *via* a cobalt-catalyzed aerobic oxidative cyclization, initially reported by Mukaiyama and coworkers.^[109] Conditions described by Pagenkopf *et al.*, who had recently developed a more effective water-soluble cobalt catalyst, furnished diol **55** with excellent *trans*-selectivity (Scheme 2.10).^[110] However, the reaction did not always go to completion and addition of a second portion of catalyst to the reaction mixture proved ineffective. When the crude mixture was directly bis-silylated to provide **56**, low and inconsistent yields were observed. One

byproduct was the bis-silylated diol **57**, which arose from unreacted starting material. It could be recovered by cleaving the silyl ethers with TBAF. Traces of the chlorinated byproduct **54** from the previous step mentioned above were found to poison the cobalt catalyst, which caused inefficient cyclization. In contrast to the cyclization precursor **50**, the THF-containing diol **55** turned out to be water soluble, accounting for a further decrease in yield. Hence, scrupulous re-purification of the starting material **50** in combination with a slightly modified non-aqueous work-up led to significant improvement ensuring a reproducible yield of 78%.^[111] Notably, the reaction proved exquisitely selective: although the cyclization precursor **50** bears two π -systems, only oxidative 5-*exo* cyclization to the desired product **55** was detected, leaving the second unsaturation untouched.

After bis-silylation of diol **55** under standard conditions,^[112] ozonolysis of the double bond of **56** was investigated to furnish aldehyde **58**. Initial experiments followed a method employing *N*-methylmorpholine-*N*-oxide (NMO), which is thought to trap the carbonyl oxide after decay of the primary ozonide, thereby avoiding the formation of the secondary ozonide.^[113] Since reproducibility was not assured for this transformation, classical conditions using excess triphenylphosphine to quench the secondary ozonide were applied, which afforded the desired aldehyde in 75% yield (Scheme 2.10).^[114]

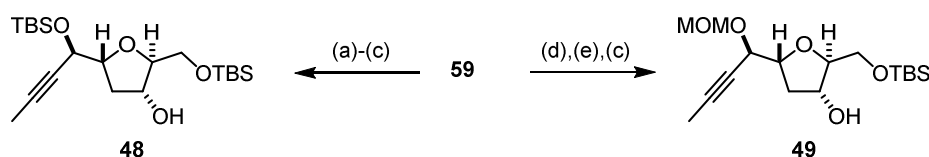


Scheme 2.10. Reagents and conditions: (a) $\text{Co}(\text{nmp})_2$ (10 mol%), *t*-BuOOH (10 mol%), *i*-PrOH, O_2 , 55 °C, 78%; (b) TESCl, imidazole, DMAP (cat.), DMF, 81%; (c) O_3 , CH_2Cl_2 , -78 °C; PPh_3 , -78 °C to rt, 75%; (d) propyne, (-)-NME, Et_3N , $\text{Zn}(\text{OTf})_2$, toluene, -78 °C to rt, 75%, d.r. > 12:1; (e) TBAF, THF, -50 °C, 80%. Key NOE contacts (blue) for *trans*-THF **55**.

Next, a Carreira alkylation introducing the chiral propargylic alcohol for the conceived macrocyclization was envisioned.^[115] In two recent total syntheses by Fürstner and coworkers this methodology had successfully been employed with propyne gas,^[77,116] which had rarely been used before.^[117] The present example represents the only α -oxygenated aldehyde substrate, which was selectively propynylated in good yields using a slightly larger excess of all reagents and prolonged reaction times (Scheme 2.10). After Mosher ester analysis^[118] of the newly formed stereogenic center

at C12 (see Section 4.3.2), the reaction sequence was repeated on large scale providing more than one gram of propargylic alcohol **59** as a preferred storage point.

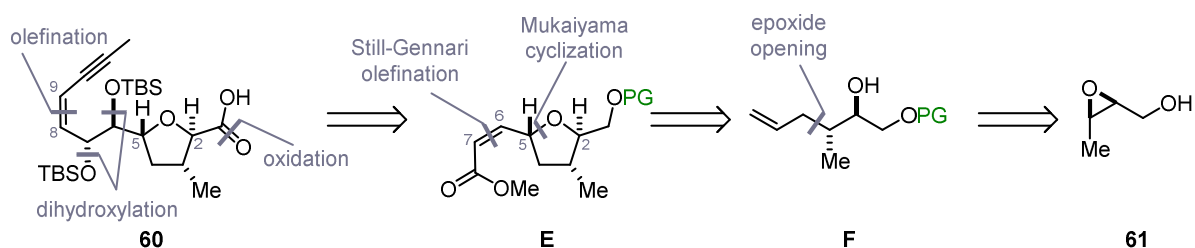
Protecting group manipulations were necessary to liberate the secondary alcohol in the THF-ring for fragment assembly. Initially, two different protecting groups were chosen: a TBS-ether to permit global deprotection after cyclization and a MOM-acetal to ensure orthogonality to the other protecting groups. After preparation of both compounds, TES-cleavage under adequate conditions followed by mono-TBS-protection of the primary alcohol provided the two alcohols **48** and **49** in 10 linear steps each (Scheme 2.11).



Scheme 2.11. Reagents and conditions: (a) TBSCl, imidazole, DMF, 82%; (b) *p*-TsOH, MeOH, $-50\text{ }^{\circ}\text{C}$, 73%; (c) TBSCl, imidazole, DMF, **48** 54%, **49** 76%; (d) MOMCl, *i*-Pr₂NEt, CH₂Cl₂, 91%; (e) TBAF, THF, $0\text{ }^{\circ}\text{C}$, 88%.

2.4.4 Synthesis of the Southern Acid Fragment **60**

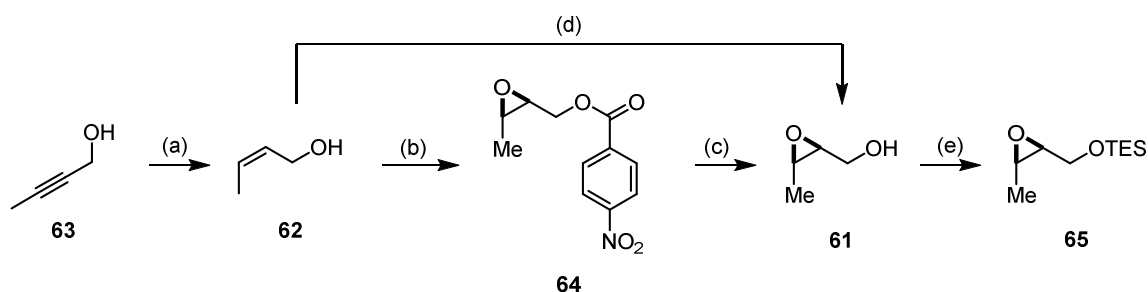
The southern acid segment **60**, which contains five of the eleven stereogenic centers of chagosensine, is structurally unique for its *anti/syn*-triol motif adjacent to a (*Z*)-enyne. Furthermore, the stereogenic center at C2 forms a major obstacle, as its position α to the carboxyl functionality renders it prone to epimerization. In the retrosynthetic analysis, the acid unit was therefore planned to be installed last (Scheme 2.12). Further disconnections centered on a (*Z*)-selective olefination and a Sharpless asymmetric dihydroxylation, simplifying **60** to α,β -unsaturated ester **E**. The latter was thought to be installed *via* Still-Gennari olefination after oxidative Mukaiyama cyclization and oxidation. Thus, scission of the C5–O bond revealed alcohol **F**, which in turn can be obtained by regioselective opening of literature-known epoxide **61**.^[119]



Scheme 2.12. Retrosynthetic analysis of southern acid fragment **60**; PG = protecting group.

Since **61** is accessed by Sharpless asymmetric epoxidation (SAE) of (*Z*)-crotyl alcohol (**62**),^[120] the synthesis of the southern fragment **60** commenced with a semi-hydrogenation of 2-butyne-1-ol (**63**).^[121] The well-precedented reaction worked best using the Rosenmund catalyst with quinoline as

poison for the palladium surface in methanol (Scheme 2.13).^[122] Next, (*Z*)-2-buten-1-ol (**62**) was transformed into epoxide **61** following a standard SAE procedure using (+)-diethyl tartrate as the chiral ligand.^[111] The reaction was highly reproducible and scalable; however, the enantiomeric excess of 89-91% could not be increased. In order to overcome this limit, an *in situ* derivatization of epoxy alcohol **61** to the corresponding 4-nitrobenzoate **64** was investigated.^[123] After two recrystallizations from diethyl ether, the *ee* of the product could be increased to a maximum of 94%. Since this derivatization showed no significant improvement in enantioselectivity but led to an inevitable loss of material, the idea was abandoned. Instead, the slightly volatile epoxide **61** was protected as a triethyl silyl ether **65** in a separate step. The TES-ether was chosen as a protecting group, because of the possibility of direct oxidation to the corresponding aldehyde under Swern conditions,^[124] which would save one step in the longest linear sequence later in the synthesis.

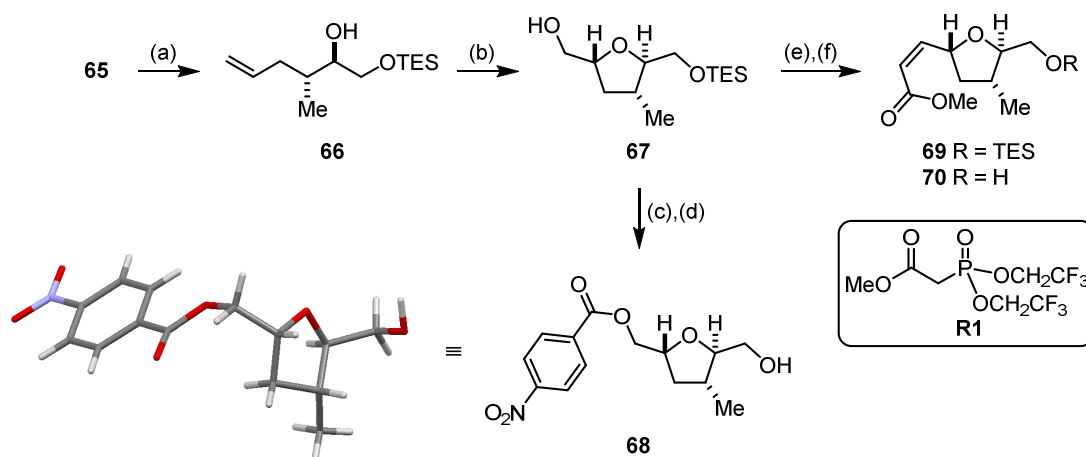


Scheme 2.13. Reagents and conditions: (a) 10 wt% Pd/BaSO₄ (5 mol%), quinoline, MeOH, H₂ (atmospheric pressure), 65%; (b) Ti(O*i*-Pr)₄ (5 mol%), (+)-DET (6 mol%), *t*-BuOOH, 4 Å MS, CH₂Cl₂, -20 °C; P(OMe)₃, Et₃N, 4-nitrobenzoyl chloride, 0 °C, 58%, 94% *ee*; (c) NaOMe, MeOH, 0 °C, 78%; (d) Ti(O*i*-Pr)₄ (5 mol%), (+)-DET (6 mol%), *t*-BuOOH, 4 Å MS, CH₂Cl₂, -20 °C, 74%, 90% *ee*; (e) TESCl, pyridine, DMAP (cat.), CH₂Cl₂, 98%.

Selective epoxide opening was accomplished with allyl-magnesium chloride in the presence of catalytic amounts of copper iodide (Scheme 2.14). The best results were obtained by slow addition of epoxy ether **65** to a chilled suspension of the Grignard-reagent and 20 mol% of CuI in THF, providing the desired bis-homoallylic alcohol **66** in a 10:1 regioisomeric ratio.^[125] In analogy to the northern fragment, an aerobic oxidative Mukaiyama cyclization was envisioned as reliable entry to the southern 2,5-*trans*-THF-moiety. The cobalt catalyst described above^[110] smoothly cyclized the precursor **66** to the desired THF-ring **67**, while formation of the *cis*-diastereomer was not detectable. On small scale, the TES-ether subsisted under the slightly acidic work-up conditions, yet on scale-up desilylation led to a water-soluble diol. Hence, only a half-saturated ammonium chloride solution could be applied without damaging the product, which led to substantial amounts of the nmp-ligand in the organic extracts and complicated chromatographic purification.

A derivative was synthesized to verify the absolute stereochemistry by single crystal x-ray analysis. To this end, the primary alcohol was esterified with 4-nitrobenzoyl chloride and the resulting benzoate

desilylated by treatment with acid. The resulting alcohol **68** was crystallized from dichloromethane by slow evaporation. As just the racemate (approx. 10%) crystallized – a phenomenon described quite well in the literature^[126] – only the relative stereochemistry could be confirmed (see Section 7.1). Attempts to crystallize the enantiomerically pure mother liquor were hampered by slow degradation of the material.



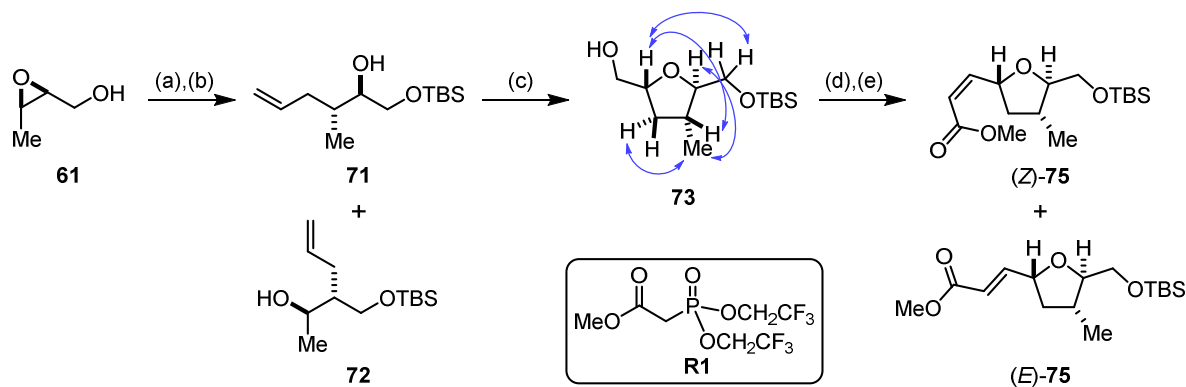
Scheme 2.14. Reagents and conditions: (a) allyl-MgCl, CuI (20 mol%), THF, $-25\text{ }^{\circ}\text{C}$, 67%, r.r. 10:1; (b) $\text{Co}(\text{nmp})_2$ (10 mol%), *t*-BuOOH (20 mol%), *i*-PrOH, O_2 , $55\text{ }^{\circ}\text{C}$, 78%; (c) 4-nitrobenzoyl chloride, pyridine, DMAP (cat.), CH_2Cl_2 ; (d) $\text{AcOH}/\text{H}_2\text{O}/\text{THF}$ (6:3:1), 68% over two steps; (e) DMP, NaHCO_3 , $\text{CH}_2\text{Cl}_2/\text{H}_2\text{O}$, $0\text{ }^{\circ}\text{C}$ to rt; (f) **R1**, KHMDs, 18-crown-6, THF, $-78\text{ }^{\circ}\text{C}$; **69** 28% over two steps, *Z/E* = 8:1.

In parallel, the route toward the southern acid fragment was continued, focusing on the oxidation of the primary alcohol to the corresponding aldehyde using Dess-Martin periodinane.^[127] Although reaction monitoring indicated full conversion of the starting material, the crude yield never exceeded 50%. This outcome could be improved by the sequential addition of one equivalent of water, which helped to enhance the reaction rate and avoid the formation of alkoxyperiodinanes.^[128] Equally beneficial and more convenient is the addition of excess *t*-butanol.^[129] Nevertheless, this mild oxidation method suffered from partial C5-epimerization (approx. 10%) visible in the NMR spectrum of the crude mixture. The reaction was therefore buffered with NaHCO_3 to trap excessive acetic acid. The exact same protocol had been used successfully in Kobayashi's synthesis of the southern fragment of amphidinolide C, which closely resembles the present aldehyde, and the obtained product was even found to be stable on silica gel.^[130] Unfortunately, this modification could not entirely suppress C5-epimerization – depending on the batch of DMP and the amount of residual acid – and the resulting diastereomeric mixture was not stable on silica gel. The crude aldehyde was subjected to the Still-Gennari olefination^[131] to scrutinize the remaining steps toward the enyne motif. Following the standard protocol,^[111,132] the desired α/β -unsaturated ester **69** was isolated as a

8:1 *Z/E* mixture, albeit in low yield (Scheme 2.14). The remaining material was identified as the primary alcohol resulting from TES-cleavage, which could not be separated from the phosphonate.

At this stage, the labile primary TES-ether, which had complicated purification of the Mukaiyama cyclization product and proven unstable in the Still-Gennari olefination, was replaced by a more robust TBS-group. Uneventful protection of epoxy alcohol **61** followed by epoxide opening with 15 mol% copper iodide provided the desired regioisomer **71** as the major product (10:1). After chromatographic separation, the Mukaiyama cyclization gave the 2,5-*trans*-THF product **73** in reproducibly good yields on a multi-gram scale (Scheme 2.15).

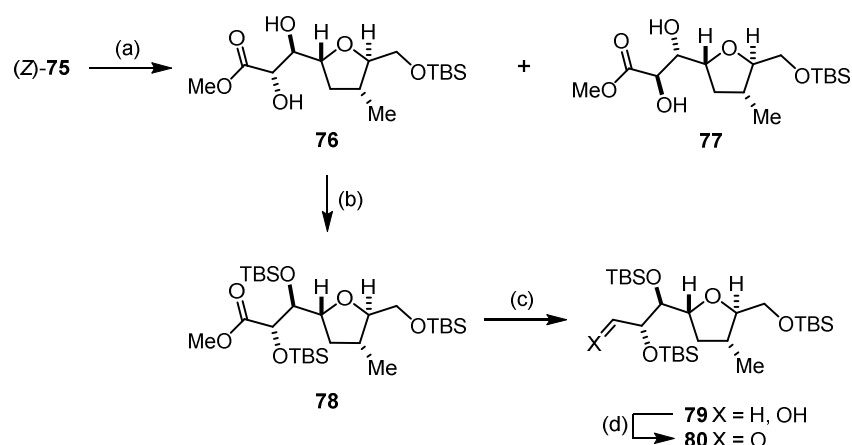
With ample material in hand the cumbersome oxidation was revisited, initially repeating the Dess-Martin conditions. Since no improvement could be asserted compared to the TES-version, a fully catalytic methodology recently introduced by Stahl *et al.* was applied.^[94] Simple filtration to remove the reagents seemed appealing, since purification of this aldehyde by chromatography led to loss of material (30% yield after flash chromatography). In the present case, however, the reaction showed only low conversion of starting material after 24 h (< 10%), which might be attributed to the good chelation ability of the substrate to the copper catalyst. Likewise, an alternative TEMPO oxidation, *i.e.* the Anelli oxidation^[133], as well as the TPAP/NMO oxidation^[134] met with failure: the conversion was incomplete after 24 hours at ambient temperature and NMR spectra of the crude material revealed partial decomposition. Classical Swern conditions were investigated next, providing an epimeric mixture of the product and degraded material. Thus, the Parikh-Doering modification of the Swern oxidation as a milder alternative was studied.^[135] The standard conditions using triethylamine as base at ambient temperature showed partial epimerization (approx. 10%) too. Finally, replacing triethylamine by the more bulky Hünig's base and performing the reaction at -25 °C completely suppressed epimerization. Aldehyde **74** was isolated in excellent yield and purity after work-up with pH 7 phosphate buffer and drying under high vacuum. The crude material was used in the subsequent olefination step, which proceeded without complication (Scheme 2.15). The 12:1 mixture of (*Z*)- and (*E*)-**75** could be separated by flash chromatography on fine silica gel, affording (*Z*)-**75** in 63% over two steps.



Scheme 2.15. Reagents and conditions: (a) TBSCl, imidazole, DMAP (cat.), CH₂Cl₂, 96%; (b) allyl-MgCl, CuI (15 mol%), THF, -25 °C, r.r. 10:1, **71** 67%, **72** 4%; (c) Co(nmp)₂ (10 mol%), *t*-BuOOH (10 mol%), *i*-PrOH, O₂, 55 °C, 79%; (d) SO₃·pyridine, DMSO, *i*-Pr₂NEt, CH₂Cl₂, -25 °C; (e) **R1**, KHMDS, 18-crown-6, THF, -78 °C, (*Z*)-**75** 63% over two steps, (*E*)-**75** 5% over two steps. Key NOE contacts (blue) for the *trans*-THF compound **73**.

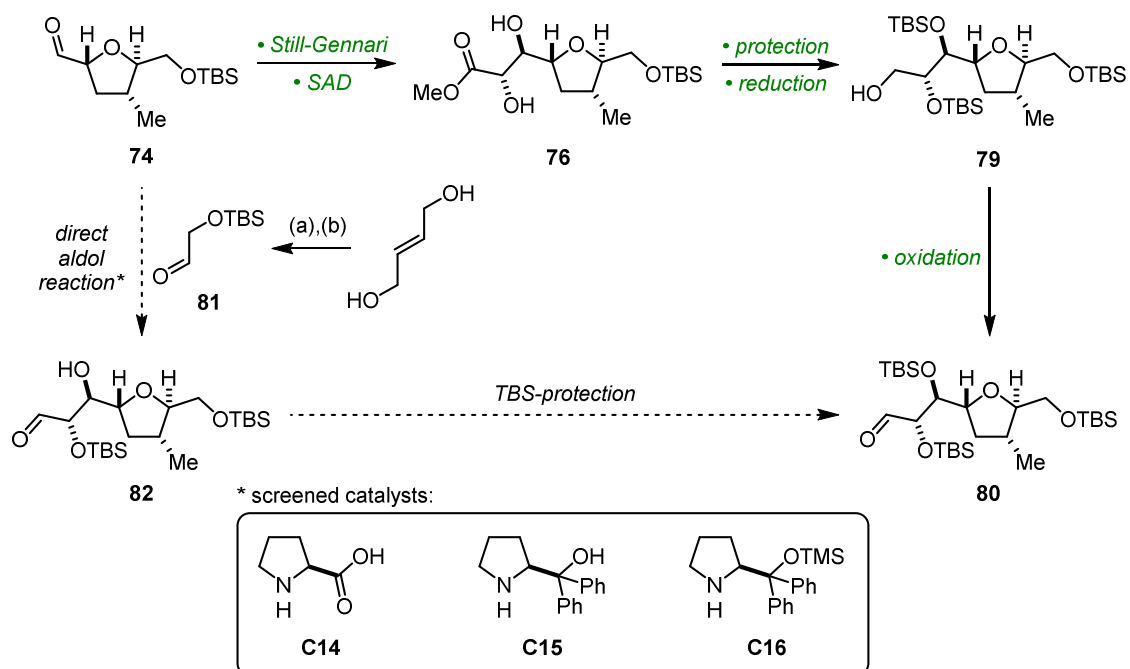
Next, the Sharpless asymmetric dihydroxylation of the (*Z*)-double bond was addressed in order to install the required *anti*-diol.^[136] Only a few aliphatic *cis*-olefins as substrates for this transformation were reported in the literature with diastereoselectivities ranging between 4:1 and 8:1.^[137] Nonetheless, the pyrimidine-based ligand (DHQD)₂PYR^[138] was successfully utilized in a closely related amphidinolide C fragment synthesis to access the *anti*-diol.^[111] This result prompted the application of the reported conditions for the dihydroxylation of olefin (*Z*)-**75**, which could be obtained with a workable diastereomeric ratio of 5:1 (Scheme 2.16). The diastereomers were separated by flash chromatography on fine silica gel providing more than one gram of the diol in a single operation. The vicinal alcohols were then masked as TBS-ethers using a large excess of TBS-triflate.

A selective reduction of methyl ester **78** to aldehyde **80** met with failure, although the feasibility for similarly oxygenated compounds had been reported.^[137c] Treatment with one equivalent of the reducing agent (titration of *i*-Bu₂AlH prior to use)^[139] in aprotic solvent at low temperature ultimately led to a mixture of aldehyde, alcohol and remaining starting material. Presumably, the neighboring coordinating groups instigate the breakdown of the otherwise stable hemiacetal allowing for a second hydride to be delivered. Consequently, an excess of *i*-Bu₂AlH was used affording the alcohol **79** in excellent yield. At this stage, the absolute configuration at C6 and C7 was determined by NMR analysis and comparison with the available data of the fragments of amphidinolides C and F (see Section 4.3.3).^[73b,111,140] Subsequent re-oxidation of the alcohol to the aldehyde **80** was accomplished under the previously established Parikh-Doering conditions (Scheme 2.16).



Scheme 2.16. Reagents and conditions: (a) K_2OsO_4 (6 mol%), $(DHQD)_2Pyr$ (3 mol%), $K_3Fe(CN)_6$, K_2CO_3 , $MeSO_2NH_2$, $t-BuOH/H_2O$, $0\text{ }^\circ\text{C}$, **76** 67%, **77** 11%; (b) TBSOTf, 2,6-lutidine, DMAP (cat.), CH_2Cl_2 , 86%; (c) $i-Bu_2AlH$, toluene, $-78\text{ }^\circ\text{C}$, 98%; (d) $SO_3\cdot$ pyridine, DMSO, $i-Pr_2NEt$, CH_2Cl_2 , $-25\text{ }^\circ\text{C}$, 94%.

Since selective reduction of ester **78** to the aldehyde oxidation state was not feasible and the installation of the *anti*-diol–aldehyde motif *via* olefination/dihydroxylation appeared lengthy and included two laborious separations of diastereomers, a shortcut was investigated. Specifically, a direct cross aldol reaction between aldehyde **74** and protected α -hydroxy aldehyde **81** could give rise to aldehyde **82**, which after protection of the remaining alcohol as a TBS-ether would deliver aldehyde **80**. This alternative route might save three steps in the longest linear sequence (Scheme 2.17).



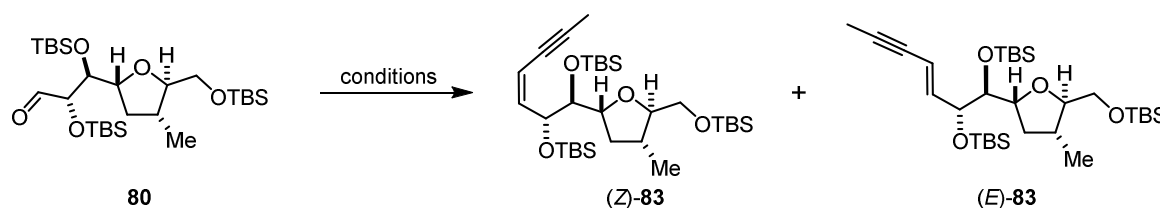
Scheme 2.17. Envisioned Aldol shortcut to aldehyde **80**. Reagents and conditions: (a) TBSCl, imidazole, DMAP (cat.), CH_2Cl_2 , quant.; (b) O_3 , CH_2Cl_2 , $-78\text{ }^\circ\text{C}$; PPH_3 , $-78\text{ }^\circ\text{C}$ to rt, 94%.

Although this type of aldol reaction suffers from possible self-condensation, polyaldolization and other side reactions,^[141] literature evidence for proline-catalyzed enantioselective aldehyde cross aldol reactions legitimated a short screening of conditions using either L-proline or proline-derived catalysts.^[142] After the straightforward preparation of aldehyde **81**,^[143] the aldol reaction was studied using L-proline (**C14**) in various solvents with slow addition of donor aldehyde **81**.^[144] Neither extending the addition time of **81** nor increasing the loading of L-proline (**C14**) to stoichiometric amounts led to the desired C–C bond formation. Diphenylprolinol (**C15**) as well as the Hayashi-Jørgensen catalyst (**C16**) were likewise incapable of inducing the reaction. In summary, all efforts resulted in side reactions with no traces of the desired product detectable. Cross aldol reactions relying on chiral auxiliaries^[145] are expected to provide the required *anti*-diol, yet they were not attractive in the present case due to an increase in step count. Thus, the original route to aldehyde **80** was maintained in spite of its length, as it was manageable on multi-gram scale.

Next, the crucial (*Z*)-selective olefination to furnish the enyne moiety was addressed. (*Z*)-enyne had been successfully installed in two previous total syntheses in the Fürstner group utilizing a Julia-Kocienski reaction.^[70a,71a,146] Yet, the very same conditions led to a strong preference for the (*E*)-isomer when aldehyde **80** was employed (Table 2.3, Entry 1). Reported reactions with propargylic sulfones have predominantly led to (*Z*)-configured double bonds, since the faster Smiles rearrangement of the *syn*-alkoxide intermediate dictates the stereoselectivity.^[147] However, the present case is exceptional, probably due to the sterically demanding α,β -dihydroxylated aldehyde **80**. The initial attack of the nucleophile to the aldehyde is expected to be reversible, yet an irreversible Smiles rearrangement would favor the *cis* double bond. The puzzling result can therefore not be explained according to the general understanding of the olefination mechanism. Instead, either collapse of the *syn*-alkoxides shifts the equilibrium to the unfavored *anti*-alkoxides which undergo Smiles rearrangement, or alternative pathways to form the (*E*) double bond starting from a *syn*-alkoxide become energetically accessible.^[147] To investigate the role of the counterion, which is usually thought to dictate the formation of *syn*-alkoxides *via* closed transition states or *anti*-alkoxides *via* open transition states, 18-crown-6 was added to sequester the potassium cation. In this case, the reactivity was shut down and significant amounts of dimerized sulfone^[148] were detected along with remaining starting material (Entry 2). The influence of the counterion was further tested by replacing potassium with the smaller lithium ion (Entry 3). The preference for the (*E*)-configuration was significantly reduced, which is comparable to the many examples of regular sulfones described in the literature.^[147] Keeping the lithium ion but switching from the polar solvent (THF) to toluene as a less polar solvent again favored the (*E*) double bond, which contradicts the general understanding of the reaction (Entry 4). The latter might be explained by the presence of one equivalent of THF in the

substrate which might act as an internal ligand. Neither replacement of lithium by sodium nor addition of LiCl could invert the selectivity (Entries 5 and 6). Slight improvements were realized by addition of HMPA, which presumably influences the chelation mode (Entry 7). Utilizing the 1-phenyl-1*H*-tetrazol-5-yl sulfone (PT)^[149] instead of the benzothiazol-2-yl sulfone (BT) also favored the (*E*) geometry, although this preference was less profound than in the BT-series. This observation is also opposing the common understanding of the reaction, since the PT is usually known to give better (*E*)-selectivity due to the sterically demanding phenyl substituent, which hints toward an abnormal coordination mode.

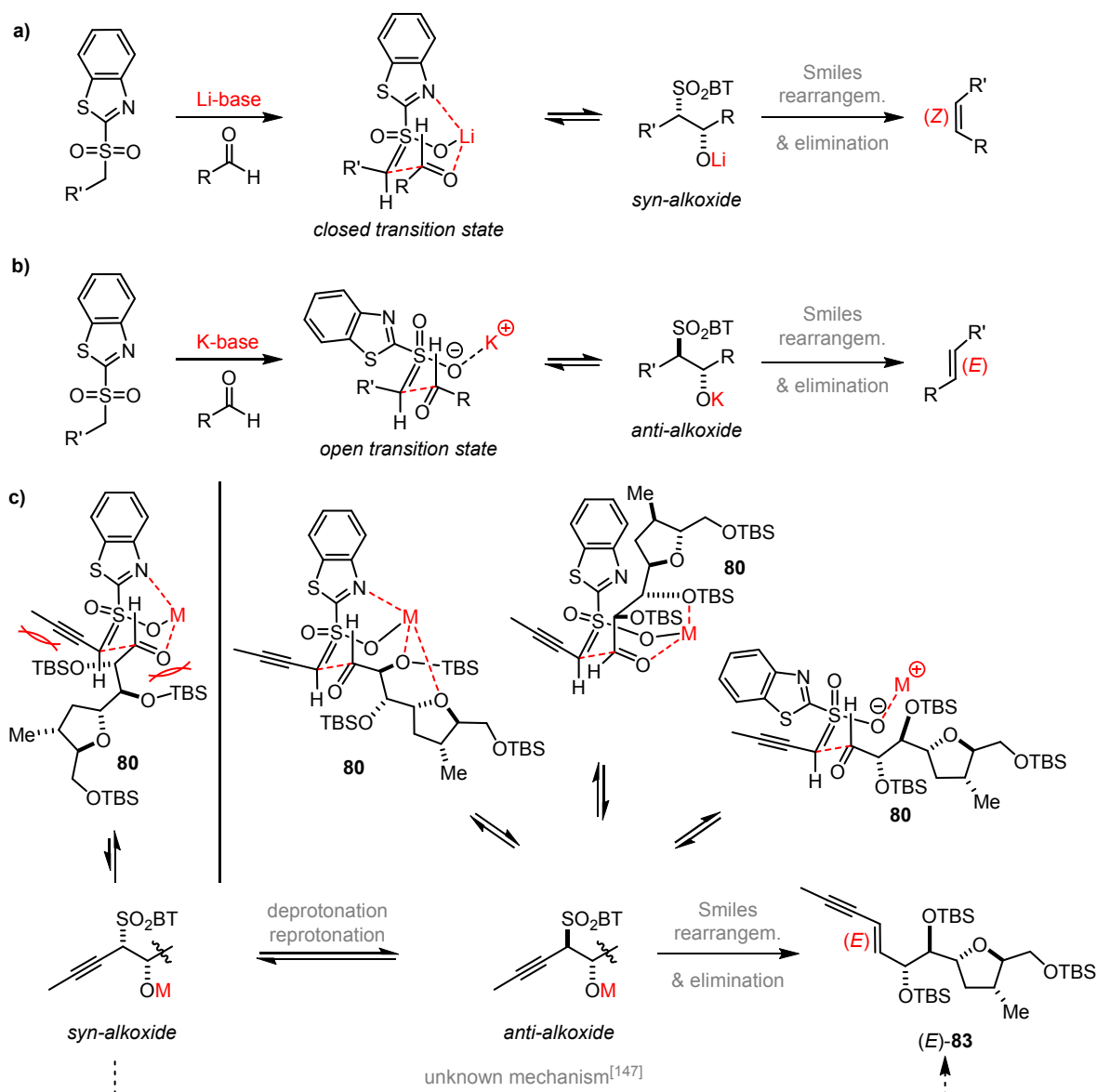
Table 2.3. Attempted (*Z*)-selective olefinations.



Entry	Conditions	Solvent	T [°C]	Z/E
1	BT, KHMDS	THF	-55	1:11
2	BT, KHMDS, 18-crown-6	THF	-55	– ^{a)}
3	BT, LiHMDS	THF	-55	1:1
4	BT, LiHMDS	toluene	-55	1:2
5	BT, NaHMDS	toluene	-55	1:3.4
6	BT, LiHMDS, LiCl	THF	-55	1:1
7	BT, LiHMDS, HMPA	THF	-55	2:1
8	PT, KHMDS	THF	-55	1:7
9	Ph ₃ PCH ₂ CCCH ₃ , BuLi	THF	-78	1.4:1
10	Me ₃ PCH ₂ CCCH ₃ , <i>t</i> -BuOK	THF	23	1:1
11	Me ₃ PCH ₂ CCCH ₃ , LiHMDS	THF	-78	2:1

BT = benzothiazol-2-yl sulfone, PT = 1-phenyl-1*H*-tetrazol-5-yl sulfone. ^{a)} s.m., dimerized sulfone

Collectively, the stereochemical outcome of this operationally simple olefination technology is difficult to predict and the results reported herein are rather exceptional.^[150] A rationale for the findings is given in Scheme 2.18, where possible influences of the sterically demanding and highly oxygenated neighboring groups prohibit a defined pre-organization of sulfone and aldehyde.

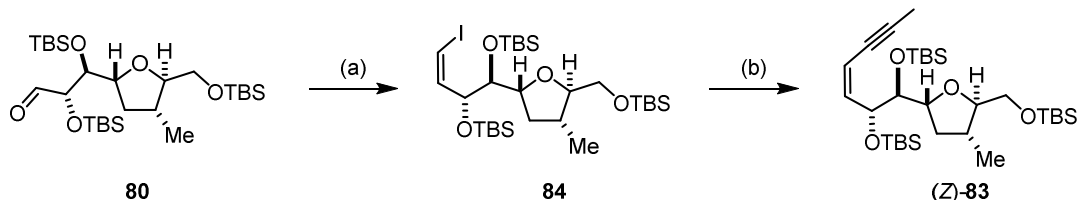


Scheme 2.18. Rationale for diastereoselectivity in Julia-Kocienski olefinations: **a)** commonly accepted mechanistic manifold for (Z)-olefination, **b)** complementary (E)-olefination, **c)** several possible pre-orientations leading to the (E)-olefin under variable conditions.

After having studied the Julia-Kocienski method in detail, an alternative Wittig olefination was investigated (Entries 9-11). Upon variation of the phosphonium salt and the alkali metal base, the best result was again obtained using LiHMDS in THF, providing a Z/E ratio of 2:1 (Entry 11).

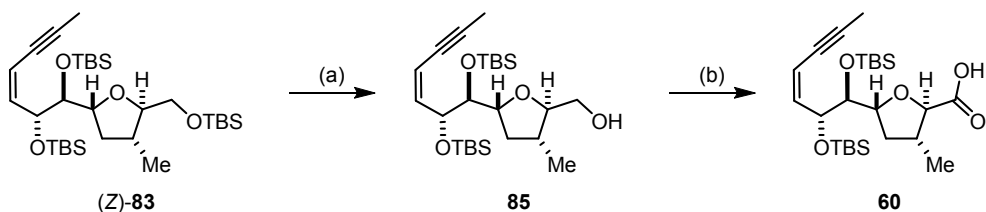
Based on these findings, further methods such as Peterson or Still-Gennari olefinations were not explored due to the necessity of preparing the reagents combined with the presumably little chance of success. Instead, the focus shifted to a two-step sequence *via* the vinyl-iodide (Scheme 2.19). Surprisingly, the well-established Stork-Zhao reaction^[151] was not affected by the surrounding steric bulk and exclusively provided the (Z)-vinyl iodide **84** in high yield. Unfortunately, neither DMPU nor DMSO was able to replace the highly carcinogenic HMPA. A good compromise was found by reducing

the equivalents of HMPA to five, which led to full conversion while only slightly diminishing the reaction rate. In a second step, the vinyl iodide was subjected to a modified Suzuki propynylation protocol reported by Fürstner *et al.*^[152] furnishing the enyne (*Z*)-**83** in 83% over two steps as a single isomer and in more than 400 mg in one batch.



Scheme 2.19. Installation of the (*Z*)-enyne. Reagents and conditions: (a) $\text{PPh}_3\text{CH}_2\text{I}_2$, NaHMDS, THF/HMPA (19:1), $-78\text{ }^\circ\text{C}$, 97%, *Z/E* > 20:1; (b) 1-propynyllithium, $\text{B}(\text{OMe})_3$, $[\text{Pd}(\text{dppf})\text{Cl}_2]\cdot\text{CH}_2\text{Cl}_2$ (15 mol%), THF, $65\text{ }^\circ\text{C}$, 86%.

To complete the synthesis of the southern domain, the primary TBS-ether was selectively cleaved in the presence of the allylic and homoallylic secondary TBS-ethers using a large excess of HF-pyridine buffered with additional pyridine by following a procedure by Curran *et al.* (Scheme 2.20).^[153]



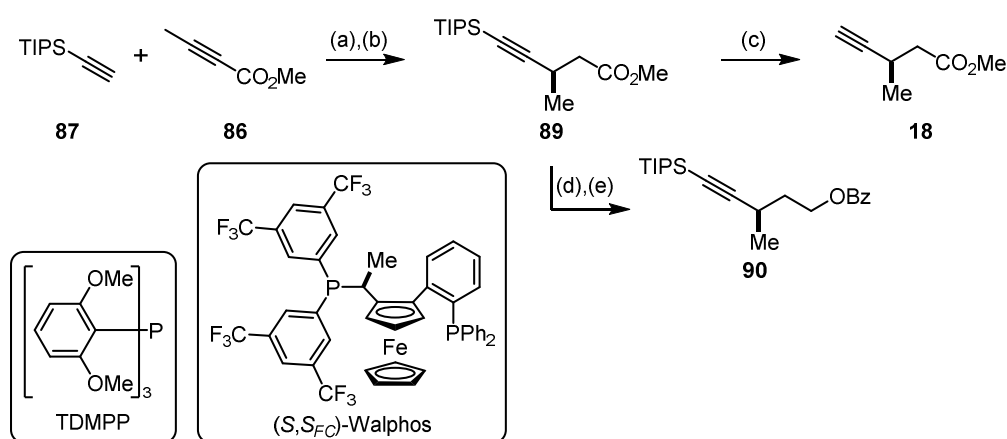
Scheme 2.20. Completion of the synthesis of acid **60**. Reagents and conditions: (a) HF-pyridine, pyridine, THF, rt, 85%; (b) TPAP (10 mol%), $\text{NMO}\cdot\text{H}_2\text{O}$, MeCN, rt, 83%.

The primary alcohol **85** was then oxidized to the carboxylic acid **60** using TPAP in combination with NMO monohydrate in acetonitrile.^[154] Attempts to isolate the carboxylic acid by means of acid/base extraction or by column chromatography with small amounts of acetic acid (1-5%) met with failure: significant epimerization at the α -stereogenic center was observed. The latter could be circumvented by a work-up with pH 5 phosphate buffer and subsequent purification by flash chromatography with hexanes/ethyl acetate. With all transformations optimized, the southern fragment **60** was obtained in 15 linear steps, the preferable storage point being the more stable protected alcohol **83**.

2.4.5 Synthesis of the Sidechain 18

Remark: All experiments in this section were carried out in collaboration with Dr. Jakub Flasz and M. Sc. Marc Heinrich; details can be found elsewhere.^[103,155]

The synthesis of the sidechain **18** was accomplished in three steps comprising an alkyne–alkyne coupling and an asymmetric 1,4-reduction followed by desilylation. Methyl-2-butynoate (**86**) was regioselectively coupled with TIPS-acetylene (**87**) under palladium catalysis^[156] to yield the known enyne **88** (Scheme 2.21).^[157] The tertiary stereogenic center was set by asymmetric 1,4-reduction using conditions described by Trost *et al.*^[158] The enantiomeric excess, which was determined *via* derivatization of the product **89** to the corresponding benzoate **90** and chiral HPLC analysis thereof, was only moderate when using Josiphos as chiral ligand. Fortunately, the *ee* could be enhanced to 98% by switching to (*S,S*_{FC})-WalPhos. As the sidechain **18** proved highly volatile, the TIPS-protecting group was removed using a freshly prepared solution of TBAF in diethyl ether.

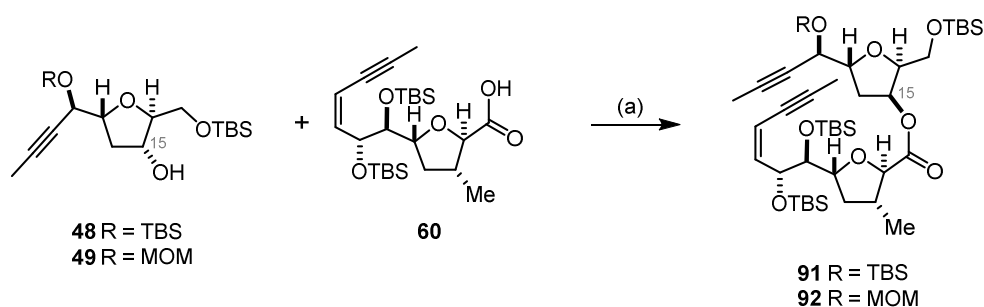


Scheme 2.21. Synthesis of the sidechain **18**. Reagents and conditions: (a) Pd(OAc)₂ (3 mol%), TDMPP (3 mol%), toluene, 91%; (b) Cu(OAc)₂ (5 mol%), (*S,S*_{FC})-WalPhos (5 mol%), Me(EtO)₂SiH, toluene/*t*-BuOH, 4 °C, 79%, 98% *ee*; (c) TBAF, Et₂O, 81%; (d) LiAlH₄, THF, 0 °C, 82%; (e) pyridine, BzCl, CH₂Cl₂, 0 °C, 80%.

Since **18** was planned to be deployed later in the synthesis, the material was stored at the protected stage **89** and the synthesis of the macrocycle from the northern alcohol and the southern acid fragments studied first.

2.4.6 Fragment Assembly and Attempted Ring Closure

With the southern acid fragment **60** and the northern alcohol segment **48** in hand, the stage was set for their assembly. Since the stereogenic center at C15 had to be inverted, a Mitsunobu esterification was envisioned. Initially, low yields (35-38%) were obtained for the desired product **91** when the reaction was carried out in THF.^[71c,159] The result could be improved by changing the solvent to toluene, providing the requisite RCAM precursor **91** in 79% yield (Scheme 2.22).^[160] These conditions were also used for the MOM-protected northern fragment **49** affording 93% of ester **92**.



Scheme 2.22. Fragment assembly. Reagents and conditions: (a) PPh_3 , DIAD, toluene, 0 °C, **91** 79%, **92** 93%.

Next, the crucial ring closure *via* RCAM was tackled. Although the molybdenum alkylidene complex **C9** endowed with bulky triphenylsilylanolate ligands had failed in the model series (see Section 2.4.2), this standard catalyst was tested on the real substrates, which carried protecting groups on the propargylic alcohol. When ester **91** was subjected to RCAM-conditions, no conversion was observed (Table 2.4). Increasing the catalyst loading to 50 mol% and warming the reaction mixture to 80 °C or 120 °C resulted in anisol transfer and traces of an acyclic dimer, while no peak corresponding to the desired product could be detected by HPLC-MS.

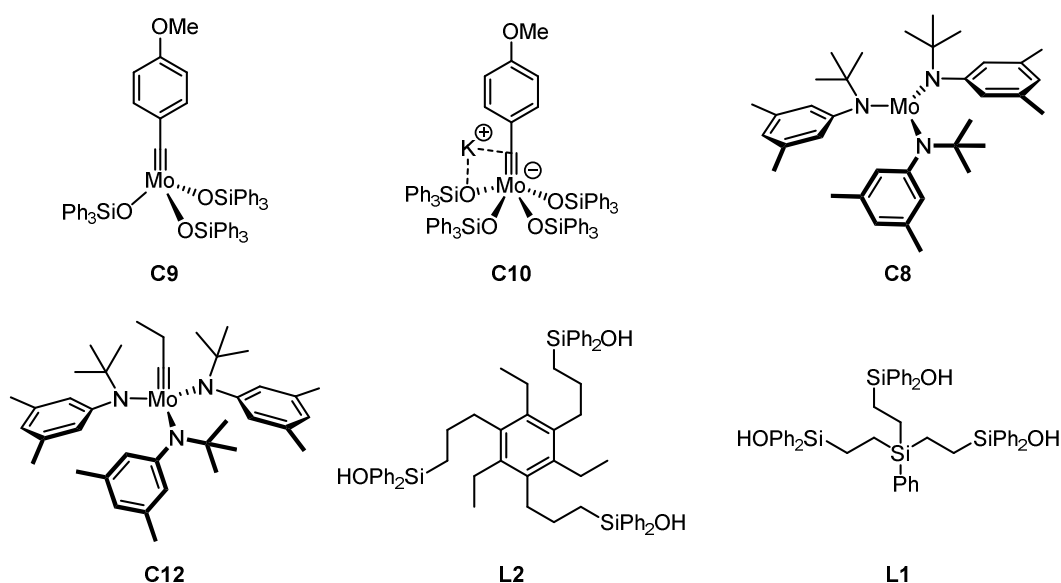
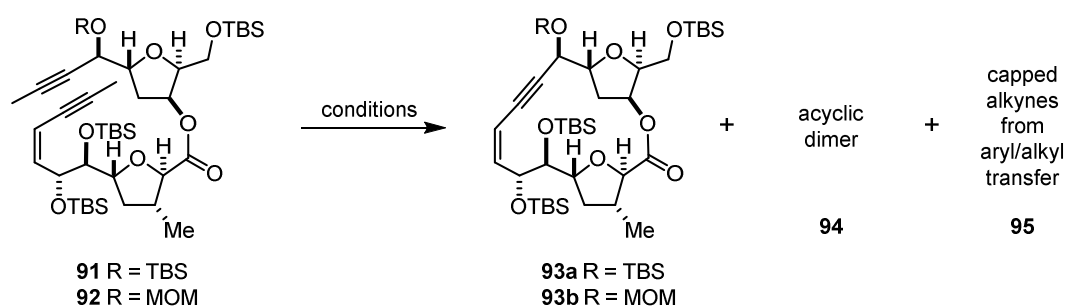


Figure 2.11. Molybdenum catalysts **C9**, **C10**, precatalysts **C8** and **C12**, as well as recently developed multidentate silanolate ligands **L2** and **L1**.

The outcome was independent of whether the neutral catalyst **C9** or the ate-complex **C10** (Figure 2.11) was employed. In a previous total synthesis of the similarly complex natural product leiodermatolide, the Cummins' precatalyst **C8**^[66a,66c,67] in combination with CH₂Cl₂ for *in situ* activation had been identified as the only effective catalyst.^[71a] Therefore, **91** was reacted with the activated complex at 100 and 130 °C, but only traces of product could be detected with slightly increased amounts of open dimer, while the majority of starting material was still unconsumed. While these results were in line with the experience gathered from the model studies, the novel two-component catalyst system also failed to convert enyne-yne **91** to the corresponding cyclic enyne. Since the bulky TBS-group on the propargylic alcohol creates severe steric hindrance about the reacting site, the less bulky MOM-variant **92** was investigated next. At first sight, the new catalytic system seemed to work well, as more than 80% of starting material was consumed within 30 min at 110 °C and HPLC-MS indicated approx. 55% of the desired macrocycle. Upon isolation however, only 15% of **93b** could be obtained along with 5-10% of the ethyl capped open enyne-yne, while dimer formation was hardly observed.

Table 2.4. Attempted RCAM of **91** and **92**.^{a)}



Entry	Substrate	Cat. (mol%)	Conditions	91	93	94	95
1	91	C9 (50)	5 Å MS, toluene (0.002 M), rt	> 90	0	0	traces
2	91	C9 (50)	5 Å MS, toluene (0.002 M), 120 °C	> 90	0	4	traces
3	91	C10 (50)	5 Å MS, toluene (0.002 M), 120 °C	> 90	0	2	traces
4	91	C8 (50)	CH ₂ Cl ₂ , toluene (0.002 M), 130 °C	> 90	traces	1	–
5	91	C12/L2 (20)	5 Å MS, toluene (0.002 M), 110 °C	> 80	traces	0	traces
6	92	C9 (50)	5 Å MS, toluene (0.002 M), 120 °C	> 80	0	traces	13
7	92	C8 (50)	CH ₂ Cl ₂ , toluene (0.001 M), 100 °C	> 90	3	0	–
8	92	C12/L2 (40)	5 Å MS, toluene (0.002 M), 110 °C	20	45	0	25
9	92	C12/L2 (20)	5 Å MS, toluene (0.001 M), 110 °C	25	55	0	10
10	92	C12/L1 (20)	5 Å MS, toluene (0.001 M), 110 °C	30	45	0	15

^{a)} Product distribution given as relative conversion monitored by LCMS.

This result showed that careful calibration of the HPLC-MS was mandatory to properly monitor the reaction and account for polymerization causing weight loss upon filtration (see Section 7.2). Conducting the reaction at a fairly large scale allowed taking aliquots every three minutes and plotting the product distribution as conversion *versus* time (Figure 2.12). As it turned out, most of the material was polymerizing within minutes, while only trace amounts of product were formed. Altering temperature, dilution and catalyst loadings could not prevent the unwanted side reaction from occurring.

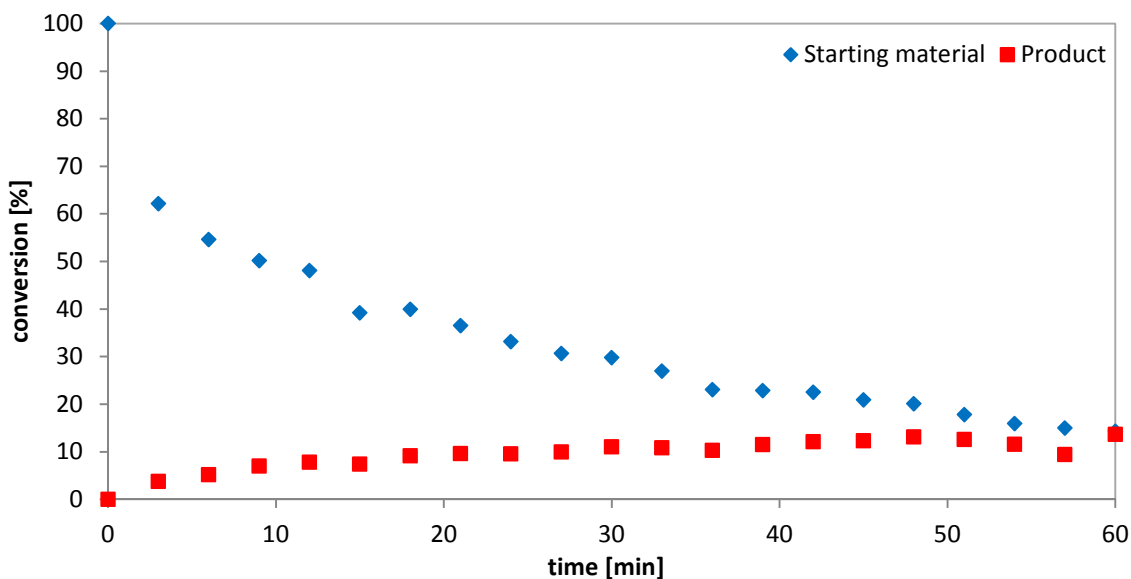
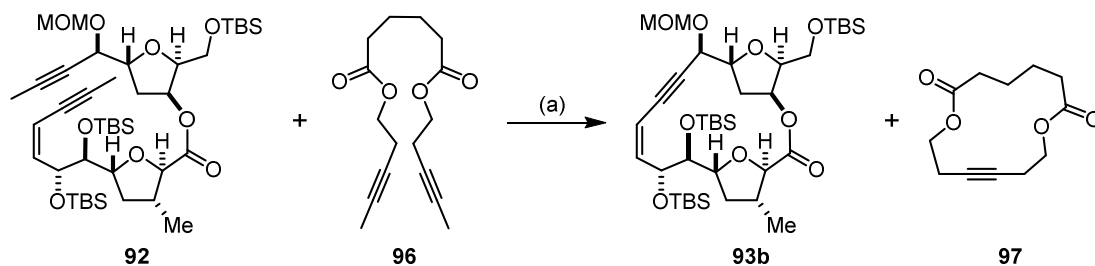


Figure 2.12. Absolute conversion studied by HPLC-MS after calibration with starting material **92** and product **93b**.

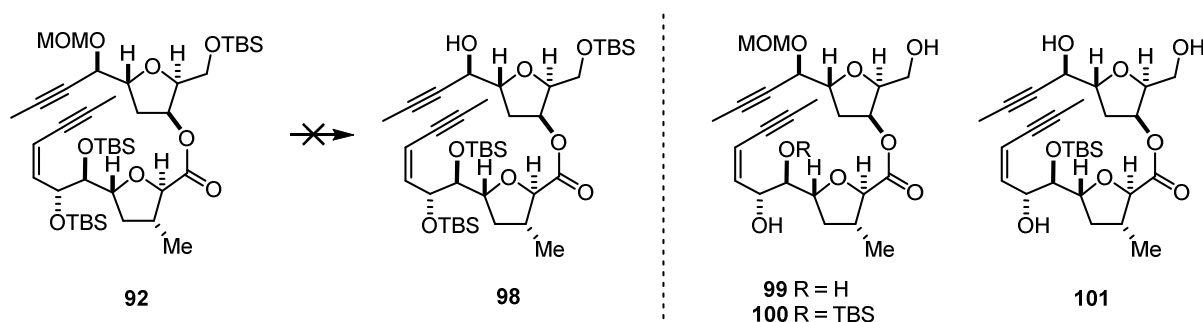
The ratio of cyclic monomer to polymer was found to be 1:5. In order to decrease the extent of polymerization, different modifications to the reaction conditions were made. Unfortunately, sealed tube experiments to enforce depolymerization as well as employing additives, such as Lewis acids or coordinating co-solvents, did not improve the reaction outcome. Increasing the loading of the ligand **L2** while maintaining the loading of the catalyst **C12** shifted the ratio only marginally toward product formation (1:4).

To better understand the mechanism of polymerization, a few control experiments were performed. Interestingly, the closed and fairly strained enyne **93b** was not opened by the catalyst and seemed to be rather stable when re-subjected to the reaction conditions. Furthermore, the activity of the catalyst was studied by addition of the benchmark substrate **96** to the mixture after six hours reaction time (Scheme 2.23).^[92b] The cyclic diester **97** was formed quantitatively, thus the new catalytic system seemed to possess improved stability and was not deactivated by substrate or products.



Scheme 2.23. Catalyst activity study. Reagents and conditions: (a) **C12** (20 mol%), **L2** (25 mol%), 5 Å MS, toluene (0.001 M), 110 °C, 6 h; then **96**. Results: **97** quant, **93b** 15%, **92** 10%, ethyl transfer products and polymer.

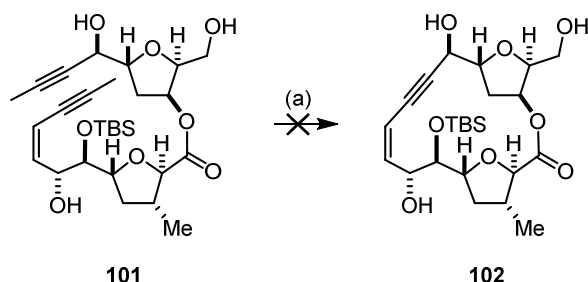
Since all attempts with a MOM-acetal or TBS-ether in the propargylic position basically failed to productively close the macrocycle, deprotection of the propargylic alcohol prior to the metathesis was anticipated. As recent total syntheses by Fürstner and coworkers had demonstrated, a free propargylic alcohol could – in the case of otherwise sterically hindered substrates – even be beneficial for the ring closure using catalyst **C9** or **C12/L2**.^[70e,77,91b,92b] The MOM-acetal **92** served as a starting point to liberate the propargylic alcohol. Since Brønsted acids would endanger the integrity of the silyl ethers, a variety of boron based Lewis acids was screened; all the products detected by NMR and/or ESI-MS of the crude mixtures are depicted in Scheme 2.24.



Scheme 2.24. Attempted MOM-deprotection.

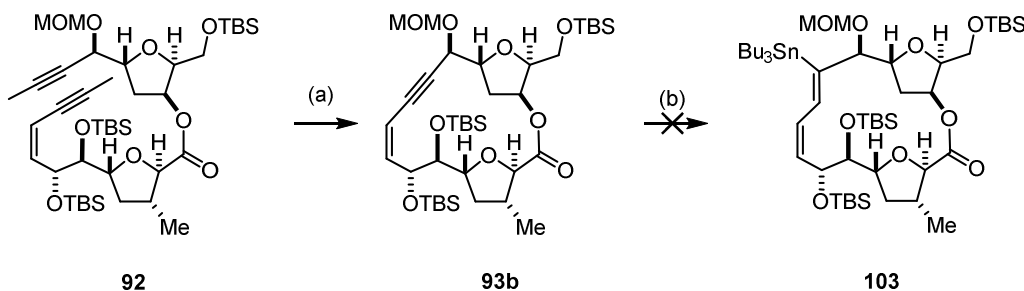
Treatment with catecholchloroborane^[161] at low temperature led to a complex mixture of products, whereas triphenylcarbenium tetrafluoroborate^[162] and lithium tetrafluoroborate at ambient temperature were unable to convert the starting material. Increasing the temperature to 70 °C afforded cleavage of all TBS-ethers leaving the MOM-acetal untouched (**99**), as lithium tetrafluoroborate dissociates to lithium fluoride and boron trifluoride.^[163] Freshly prepared Me_2BBr ^[164] at low temperature could not evoke any reaction; adding up to four equivalents of reagent led to the cleavage of the primary and the allylic TBS-ether without harming the MOM-acetal (**100**). Sequentially adding more equivalents of Me_2BBr (10 equiv.) finally triggered MOM-cleavage, setting free a very polar triol **D**. These findings point toward complexation of the slim but highly Lewis acidic Me_2BBr to multiple coordination sites in the molecule. Thus, selective cleavage *via* preferred complexation to the MOM-acetal was impossible. Nevertheless, the isolated triol **101** was

subjected to the metathesis conditions using the **C12/L2** catalyst system (Scheme 2.25). No consumption of starting material was observed, most likely due to the multiple protic sites in this particular substrate.



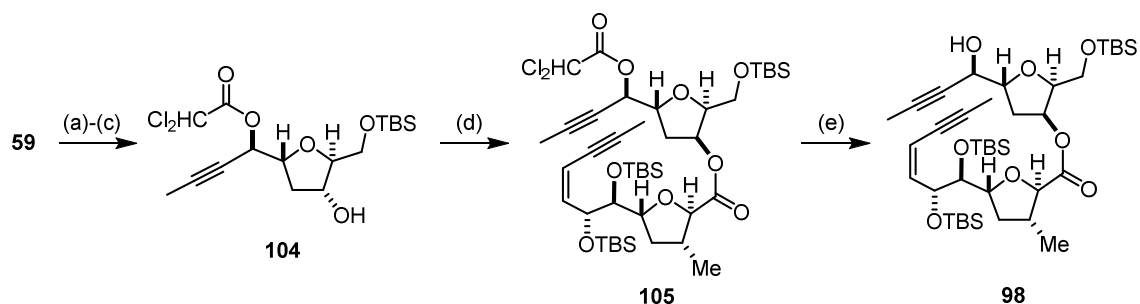
Scheme 2.25. Attempted RCAM of triol **101**. Reagents and conditions: (a) **C12** (20 mol%), **L2** (25 mol%), 5 Å MS, toluene (0.001 M), 110 °C.

As selective MOM-deprotection was to no avail for diyne **92** and cleavage of the MOM-acetal after cyclization to **93b** was expected to be likewise challenging, the ruthenium-catalyzed *trans*-hydrostannylation was tested at this stage. Upon subjecting a small amount of macrocyclic enyne **93b** to the standard conditions with a high ruthenium loading of 200 mol%, no product formation was observed (Scheme 2.26). Presumably, the ruthenium engages in unproductive complexation with the double and the triple bond, preventing the hydrostannylation reaction from occurring. This result highlights the necessity for a free hydroxy group in proximity to the enyne to direct the metal center to the triple bond.



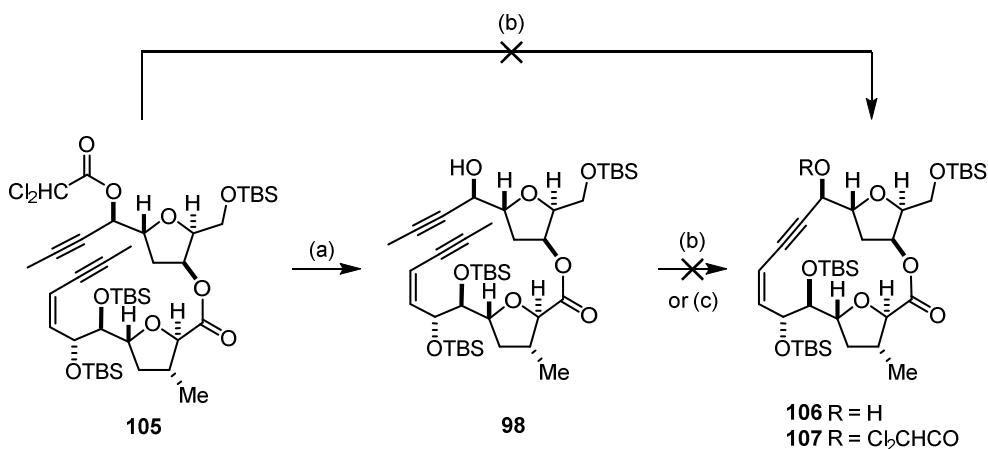
Scheme 2.26. Attempted key sequence with MOM-acetal **92**. Reagents and conditions: (a) **C12** (20 mol%), **L2** (25 mol%), 5 Å MS, toluene (0.001 M), 110 °C, 15%; (b) **C13** (200 mol%), Bu₃SnH, CH₂Cl₂, rt, 2 h.

An alternative route to the free propargylic alcohol **98** was therefore investigated. Esterification of **59** was achieved using dichloroacetic anhydride in dichloromethane. The subsequent TES-cleavage using TBAF had to be buffered with dichloroacetic acid to avoid saponification or transesterification of the dichloroacetate. Silylation and Mitsunobu esterification with carboxylic acid **60** delivered the desired ester **105** in acceptable yield. As anticipated, selective saponification of the dichloroacetate in presence of the ester could be achieved with one equivalent of lithium hydroxide in 1,4-dioxane/water at 4 °C, furnishing propargylic alcohol **98** in readiness for RCAM (Scheme 2.27).



Scheme 2.27. Synthesis of propargylic alcohol **98**. Reagents and conditions: (a) $(\text{CHCl}_2\text{CO})_2\text{O}$, pyridine, CH_2Cl_2 , 0°C , 79%; (b) TBAF, $\text{CHCl}_2\text{CO}_2\text{H}$, THF, -30°C , 97%; (c) TBSCl, imidazole, DMAP (cat.), DMF, 59%; (d) **60**, PPh_3 , DIAD, toluene, 0°C , 65%; (e) LiOH, 1,4-dioxane/ H_2O , 4°C , 87%.

Unfortunately, this precursor also failed to cyclize under the metathesis conditions: only traces of product could be observed by HPLC while the vast majority of the starting material must have formed oligo- and polymers as assumed by the loss of material. The free alcohol seemed to even favor these polymerization events, since half of the starting material was consumed within ten minutes without formation of meaningful amounts of product. After two hours, less than 10% of starting material could be recovered (Scheme 2.28). Although silanolate catalyst **C9** had already failed in model substrates bearing a free propargylic alcohol (*vide supra*), compound **98** was also exposed to this catalyst. The reaction was repeated at ambient as well as at elevated temperature. In both cases, starting material could be recovered almost quantitatively. As a last resort, the dichloroacetate **105** was submitted to the **C12/L2** catalyst system using the standard conditions. After two hours at 110°C no product formation was observed; mostly starting material could be recovered and the free propargylic alcohol **98** was the only other product detected in the reaction mixture. This finding is consistent with the diyne model substrates bearing esters in propargylic positions, which were likewise destroying the catalyst with the remaining material staying integer.



Scheme 2.28. Attempted RCAM of **105** and **98**. Reagents and conditions: (a) LiOH, 1,4-dioxane/ H_2O , 4°C , 87%; (b) **C12** (20 mol%), **L2** (25 mol%), 5 Å MS, toluene (0.001 M), 110°C ; (c) **C9** (20 mol%), 5 Å MS, toluene (0.001 M), 110°C .

After the investigation of four different substrates (**91**, **92**, **105** and **98**) using four different catalytic systems and various conditions, doubts arose as to whether this substrate type was tolerated at all. One might argue that the propargylic alcohol adjacent to a THF-ring as part of a concealed 1,2-diol functionality could pose a challenge to the transition metal catalyst. Such a motif could act as a chelating ligand and propargylic-homopropargylic diols had not been employed in RCAM reactions so far. The RCAM precursors of mandelalide A **109** and amphidinolide F **110** represent the only two substrates bearing α -oxygenated THF-subunits in their skeletons; notwithstanding, the respective ethers/esters were located on the opposite side of the THF-ring, retaining an unsubstituted methylene unit in the propargylic position (Figure 2.13).^[71b,73b]

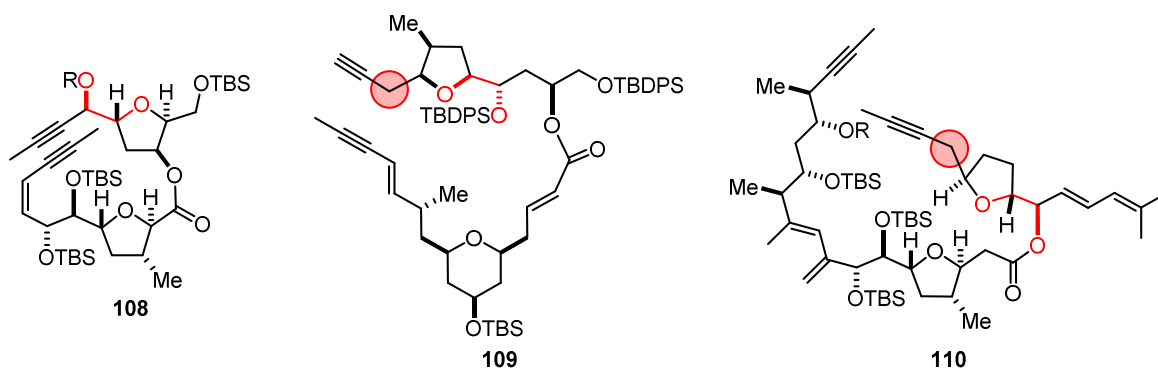
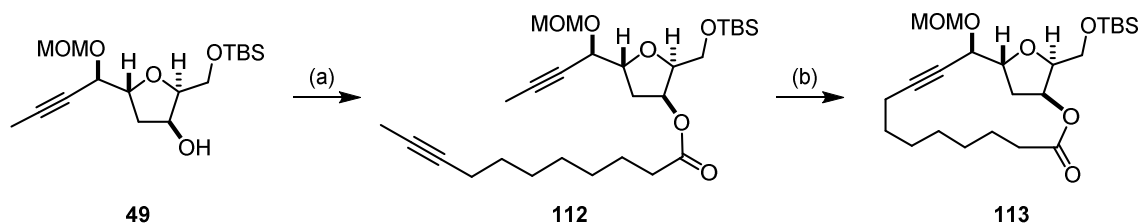


Figure 2.13. RCAM precursors of chagosensine **108**, mandelalide A **109** and amphidinolide F **110**.

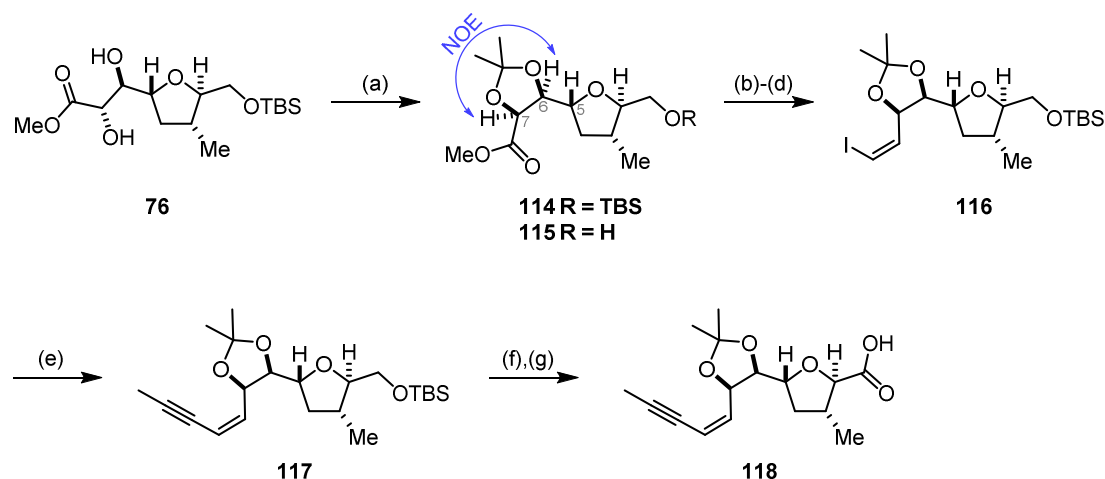
To test this issue, an additional model system was synthesized. Thus, northern alcohol **49** was esterified with 9-undecynoic acid (**111**) under Mitsunobu conditions, affording diyne **112** in unoptimized yield. This time, under the standard RCAM conditions, the expected monocycle **113** was isolated in 87% yield after three hours at 110 °C, ruling out that the hidden diol motif was recalcitrant (Scheme 2.29).



Scheme 2.29. Synthesis of THF-containing macrocycle **113**. Reagents and conditions: (a) 9-undecynoic acid (**111**), PPh_3 , DIAD, toluene, 0 °C, 54%; (b) **C12** (20 mol%), **L2** (25 mol%), 5 Å MS, toluene (0.001 M), 110 °C, 87%.

Combining this observation with the previous results, where modifications were performed centering on the propargylic alcohol unit, steric congestion was thought to be the major hurdle. Hence, the vicinal bulky TBS-ethers at C6 and C7 were replaced by an acetonide protection. Despite the formation of a third five-membered ring in the system, steric bulk in close proximity to the (*Z*)-enyne would be decreased. The synthesis of the southern domain was therefore adjusted as depicted in

Scheme 2.30. Acid-catalyzed acetalization was accompanied by TBS-cleavage, which could be reduced to 4% by using 5 mol% of *p*-TsOH.* Subsequent reduction of methyl ester **114** was more efficient when LiAlH₄ was employed instead of *i*-Bu₂AlH and the Parikh-Doering oxidation translated well to the acetonide system giving constantly high yields. The two-step protocol to install the enyne moiety was maintained, although the (*Z*)-selective olefination of the less hindered aldehyde was expected to show better selectivity. Finishing the sequence in analogy to the previous route, carboxylic acid **118** was delivered uneventfully.

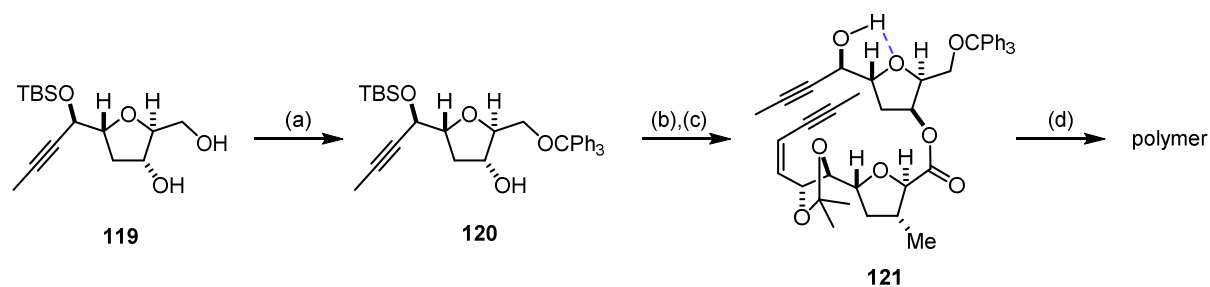


Scheme 2.30. Synthesis of southern acid **118**. Reagents and conditions: (a) 2,2-dimethoxypropane, *p*-TsOH·H₂O (5 mol%), **114** 88%, **115** 4%; (b) LiAlH₄, THF, 0 °C to rt, 95%; (c) SO₃·pyridine, DMSO, *i*-Pr₂NEt, CH₂Cl₂, -25 °C; (d) PPh₃CH₂I₂, NaHMDS, HMPA, THF, 67% over two steps, *Z/E* > 20:1; (e) 1-propynyllithium, B(OMe)₃, [Pd(dppf)Cl₂]·CH₂Cl₂ (10 mol%), THF, 65 °C, 82%; (f) HF·pyridine, pyridine, THF, rt, 90%; (g) TPAP (10 mol%), NMO·H₂O, MeCN, rt, 75%.

In order to provide a compatible northern fragment, diol **119** was mono-protected as a trityl-ether **120**. Mitsunobu esterification preceded TBS-deprotection that furnished ester **121** in readiness for ring closure. Once again, all suitable RCAM-catalysts (Figure 2.11) were screened providing similar results. **C9** and **C10** were unable to convert the starting material, whereas **C12/L2** led to rapid polymerization. The latter was occurring even faster than for propargylic alcohol **98**, since for this particular substrate 85% of starting material was consumed within ten minutes while only traces of product were detected (Scheme 2.31). The free propargylic alcohol presumably forms a hydrogen bond to the neighboring THF rendering the propargylic oxygen more Lewis basic. It was thus speculated, that stronger binding to the Lewis acidic molybdenum center favors polymerization *via* an associative mechanism^[68] with the molybdenum residing at this chelating position. In contrast to the slim aliphatic alkylidene catalyst **C12**, the more bulky aryl-alkylidene catalysts **C9** and **C10** disfavor

* NOE studies of the cyclic acetal **114** allowed to draw a more definite conclusion on the stereochemical assignment of the *anti*-diol. Presence and absence of NOE contacts in combination with the indicative coupling constants (Karplus relation) $J_{5,6} = 6.7$ Hz and $J_{6,7} = 6.8$ Hz provide evidence for the depicted configuration (Scheme 2.30).

substrate association. Ring strain however, seems to play only an inferior role as no formation of closed dimer was observed on any occasion.



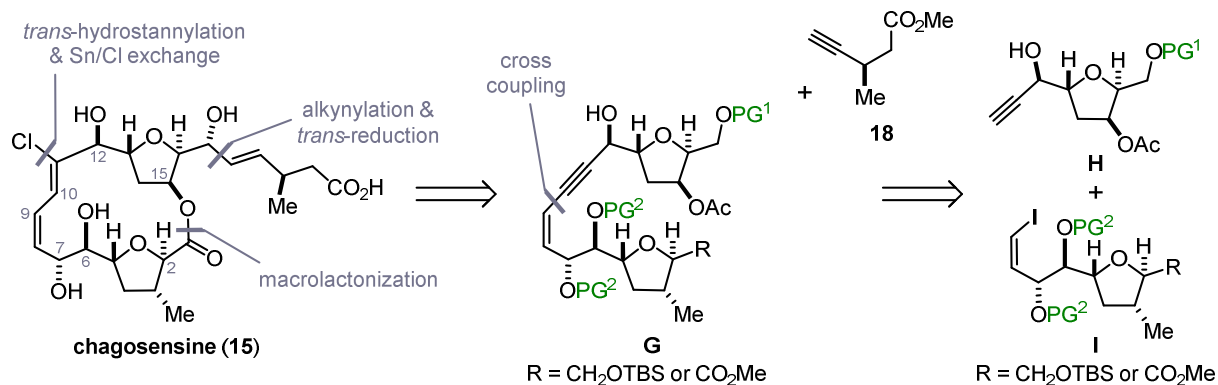
Scheme 2.31. Synthesis of RCAM precursor **121**. Reagents and conditions: (a) Ph₃CCl, Et₃N, CH₂Cl₂, 0 °C to rt, 95%; (b) **118**, PPh₃, DIAD, toluene, 0 °C, 79%; (c) TBAF, THF, -30 °C to rt, 67%; (d) **C12** (20 mol%), **L2** (25 mol%), 5 Å MS, toluene (0.001 M), 110 °C.

Although inspection of hand-held models suggested that RCAM could be feasible, all attempts had basically met with failure. The electronic properties of the triple bonds and their highly oxygenated surroundings in combination with the steric demand hampered a productive ring closure. Since the oxygenation pattern and high density of functional groups are characteristic traits of the target molecule that cannot be omitted, the synthetic strategy had to be re-evaluated. It was clearly desirable to relieve potential strain by avoiding enyne intermediates. One possibility to do so would be ring closing alkene metathesis (RCM). This approach, which posed the challenge of constructing the signature (*Z,Z*)-chlorodiene moiety prior to fragment assembly and ring closure, was comprehensively investigated by M. Sc. Marc Heinrich and will not be discussed within this work.^[155] The acyclic (*Z,Z*)-chlorodiene motif could be synthesized, but ring closure *via* diene-ene metathesis was not feasible although numerous catalysts were studied under a variety of reaction conditions.

2.5 The First Macrolactonization Approach: Hydrostannylation

2.5.1 Retrosynthetic Analysis

An alternative strategy with inverted order of events was conceived to avoid highly strained enyne macrocycles. Installation of the (*Z,Z*)-chlorodiene *via* the hydrostannylation strategy should precede ring closure. As a consequence, the latter had to be realized by means of macrolactonization. Mapping this strategy onto a more complete retrosynthesis of chagosensine, where the sidechain **18** was still thought to be installed last, revealed the acyclic enyne **G** as the key intermediate. Scission of the C9–C10 bond in **G** divided the molecule into a terminal alkyne **H** and a vinyl iodide **I** (Scheme 2.32). Since fragment assembly was sought to occur *via* cross coupling, both building blocks synthesized for the RCAM approach needed to be modified accordingly.

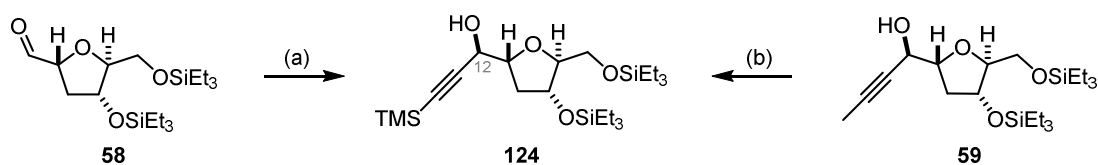


Scheme 2.32. Retrosynthetic analysis of chagosensine; PG = protecting group.

2.5.2 Modification of the Northern Alcohol Fragments

*Remark: The syntheses of the modified alcohol fragments **122** and **123** were established in collaboration with postdoctoral researcher Dr. Aurélien Letort.^[165]*

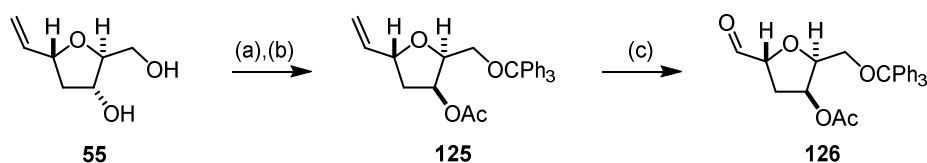
Two major modifications of the northern sector had to be made: a terminal alkyne was required for the cross coupling and the secondary alcohol within the THF-ring needed to be protected orthogonally to all other protecting groups to allow selective deprotection prior to macrolactonization. To this end, it was planned to perform an asymmetric Carreira alkylation of aldehyde **58** with TMS-acetylene instead of propyne (Scheme 2.33, (a)). Surprisingly, the conditions could not be translated onto the TMS-capped alkyne **124**, which was obtained in very poor yield (< 10%). The titanium-mediated alternative described by Pu and coworkers^[166] lacked selectivity, yet the mixture of diastereomers was chromatographically separable providing 31% of the desired (12*R*)-alcohol and 29% of the undesired (12*S*)-alcohol. Interestingly, when switching the chiral ligand from (*R*)- to (*S*)-BINOL, the desired diastereomer was only slightly disfavored, suggesting that the enantiomeric ligand was unable to override the substrate bias. Sole substrate control over the addition of lithium TMS-acetylide at low temperature gave a 1:1 mixture of diastereomers, highlighting the need for an asymmetric methodology. The best result was obtained with the Trost alkylation^[167] using (*R,R*)-ProPhenol and a threefold excess of dimethyl zinc and TMS-acetylene: the desired (12*R*)-alcohol was favored by 5:1 and isolated in moderate yield.



Scheme 2.33. Asymmetric alkylation. Reagents and Conditions: (a) TMS-acetylene, Me_2Zn , (*R,R*)-ProPhenol (20 mol%), TPPO (40 mol%), toluene, 4 °C, 41%, d.r. 5:1; (b) TMS-propyne, **C12** (20 mol%), **L2** (25 mol%), toluene (0.01 M), 110 °C, 39%.

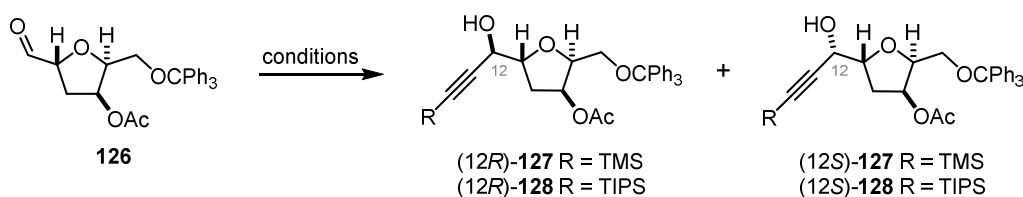
As an alternative entry to alcohol **124**, a cross metathesis between TMS-propyne and methyl-capped alkyne **59** was envisioned (Scheme 2.33, (b)). The latter had been obtained in good yield and diastereoselectivity before (see Section 2.4.3). Both, the well-defined catalyst **C9** and the two-component catalytic system **C12/L2** were capable to deliver **124**, however, the yield did not exceed 40% using a fivefold excess of TMS-propyne.

As alcohol **124** was difficult to access and multi-step protecting group management would be required afterwards, a new protecting group strategy was pursued starting from diol **55**. The primary alcohol was selectively protected as a trityl-ether prior to Mitsunobu esterification of the remaining secondary alcohol with acetic acid (Scheme 2.34).^[168] The artifice of directly inverting the stereogenic center while protecting the secondary alcohol would later broaden the opportunities for macrolactonization. Olefin **125** was dihydroxylated and the resulting glycol immediately cleaved to the corresponding aldehyde **126**.^[165]



Scheme 2.34. New protecting group strategy. Reagents and conditions: (a) Ph₃CCl, Et₃N, CH₂Cl₂, 88%; (b) AcOH, PPh₃, DIAD, toluene, 95%; (c) K₂OsO₄ (2 mol%), NaIO₄, 2,6-lutidine, dioxane/H₂O, 92%.

Next, asymmetric alkynylations of aldehyde **126** were studied in detail with the most meaningful results discussed herein. The standard Carreira alkynylation was investigated first, since there was literature precedence for acetates remaining untouched under these conditions.^[169] In this specific case, however, only 10% of a 5:1 diastereomeric mixture was obtained, along with degradation of the starting material (Table 2.5, Entry 1). An indium-catalyzed Shibasaki alkynylation^[170] led to immediate trityl deprotection (Entry 2). The Trost alkynylation conditions afforded a 6:1 mixture of isomers in 16% yield (Entry 3). In addition to poor yields, the diastereomers could not be separated by column chromatography. Thus, the TMS-acetylene was replaced by the more bulky TIPS-acetylene. Under the same conditions, the Trost alkynylation gave only up to 30% of a separable mixture of diastereomers, accompanied by decomposition of the starting material (Entry 4). The absolute stereochemistry at C12 was determined *via* Mosher ester analysis of the minor diastereomer (see Section 4.3.6).^[118] Lowering the temperature to -10 °C to ensure a more selective addition into the aldehyde over the acetate led to even more degradation. Since decomposition products lacking the trityl group were also detected in the Carreira alkynylation (Entry 6), it was speculated that the zinc species were damaging the starting material.^[165]

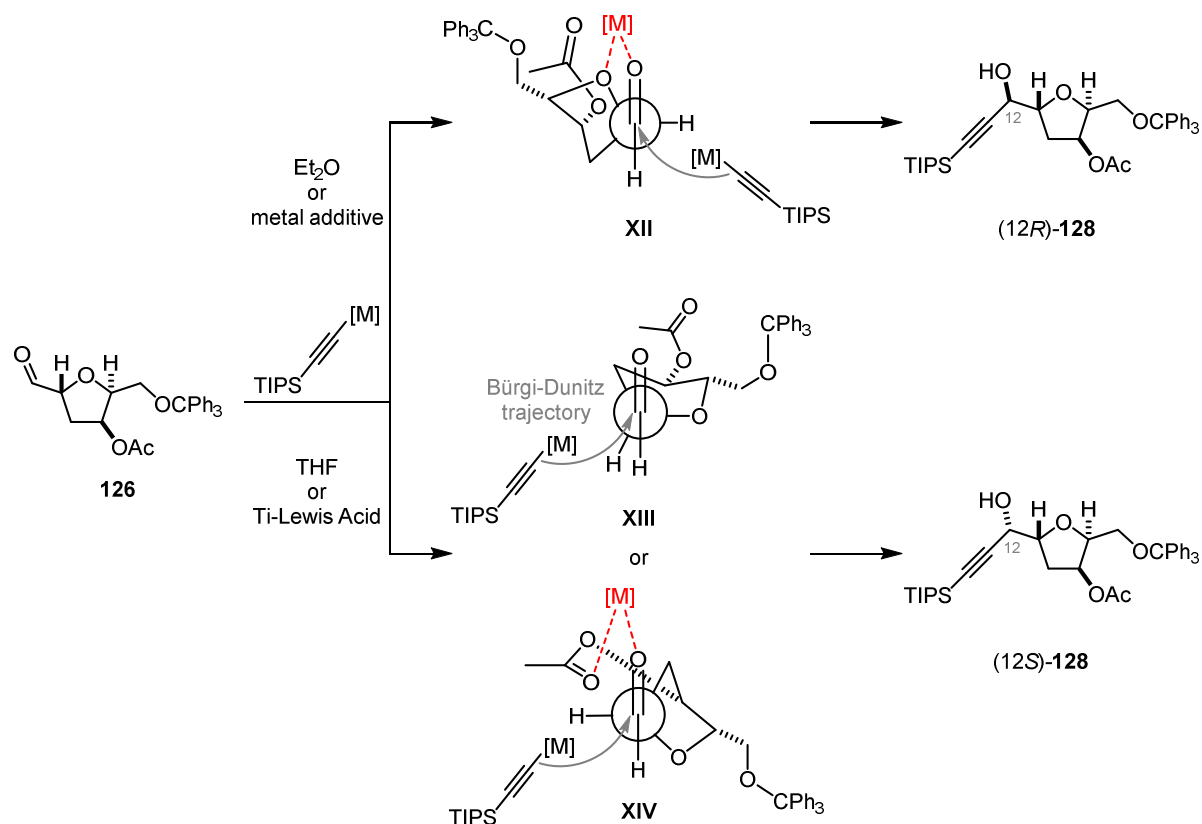
Table 2.5. Alkynylations of **126**.

Entry	Alkyne	Conditions	d.r. (12R)/(12S) ^{a)}	Yield [%] ^{b)}
1	TMSCCH	(-)-NME, Zn(OTf) ₂ , Et ₃ N, toluene, rt	5:1	10
2	TMSCCH	InBr ₃ , (S)-BINOL, Cy ₂ NMe, CH ₂ Cl ₂ , rt	–	decomposition
3	TMSCCH	(R,R)-ProPhenol, Me ₂ Zn, TPPO, toluene, 4 °C	6:1	16
4	TIPSCCH	(R,R)-ProPhenol, Me ₂ Zn, TPPO, toluene, 4 °C	3:1	30
5	TIPSCCH	(R,R)-ProPhenol, Me ₂ Zn, TPPO, toluene, –10 °C	3:1	6
6	TIPSCCH	(-)-NME, Zn(OTf) ₂ , Et ₃ N, toluene, rt	20:1	11
7	TIPSCCH	<i>i</i> -PrMgCl·LiCl, THF, –78 °C	–	deacetylation
8	TIPSCCH	<i>n</i> -BuLi, THF, –78 °C	1:2	67
9	TIPSCCH	<i>n</i> -BuLi, Et ₂ O, –78 °C	1.5:1	42
10	TIPSCCH	<i>n</i> -BuLi, Et ₂ O, ClTi(<i>Oi</i> -Pr) ₃ , –78 °C	1:6	34
11	TIPSCCH	<i>n</i> -BuLi, Et ₂ O, CeCl ₃ , –78 °C	1.2:1	53
12	TIPSCCH	<i>n</i> -BuLi, Et ₂ O, Lil, –40 °C	3:1	65

^{a)} determined by ¹H NMR of crude mixture; ^{b)} yield of diastereomeric mixture.

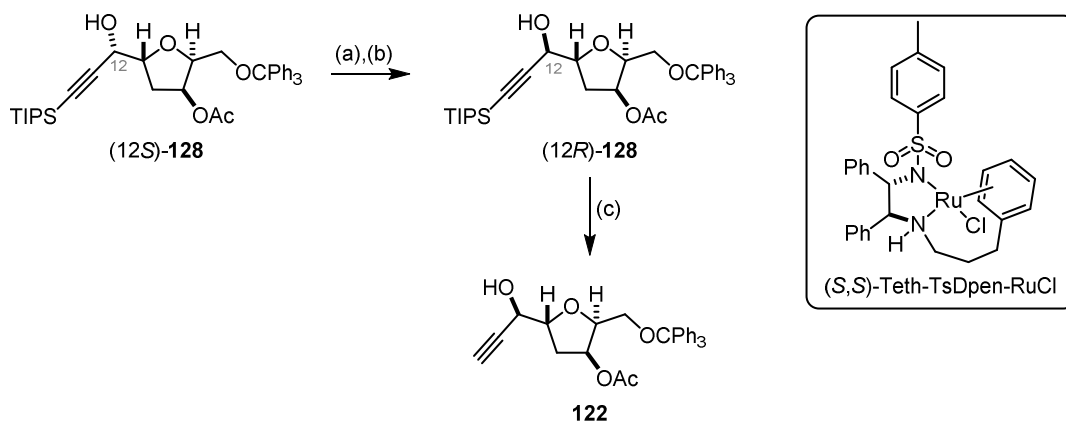
In order to retain the protecting group strategy, a substrate controlled addition into the aldehyde was investigated. Initial experiments using the corresponding Grignard species led to deacetylation, while Li-alkynylides at low temperature in THF and Et₂O gave rise to opposite diastereomers (Entries 7-9). This phenomenon is frequently observed in reactions involving organometallic compounds, due to the stronger coordination of THF as compared to Et₂O.^[171] In the present example, THF seems to prevent the formation of the 1,2-Cram chelate **XII**,^[172] which would favor the required propargylic alcohol (12R)-**128** as illustrated in Scheme 2.35. The attack of the acetylide rather goes through a Felkin-Anh model of type **XIII**.^[173] Therefore, reactions in Et₂O and metal salt additives should preferably deliver the desired product. However, addition of ClTi(*Oi*-Pr)₃ or Ti(*Oi*-Pr)₄ was beneficial for the formation of (12S)-**128** as well (Entry 10), whereas cerium slightly shifted the ratio toward the desired isomer (12R)-**128** (Entry 11). Based on these findings, it was speculated that the highly oxygenated substrate might align in a different fashion, allowing for example the formation of a 1,6-chelate **XIV**, which again favors the undesired product. Clearly, other chelates (e.g. involving the primary alcohol or even multiple chelations that possibly trigger a ring flip) might also be feasible, rendering the situation fairly complicated. As a consequence, lithium salts were added to block the

numerous coordination sites. Indeed, the best result was obtained with a fivefold excess of lithium iodide shown in Entry 12.^[165]



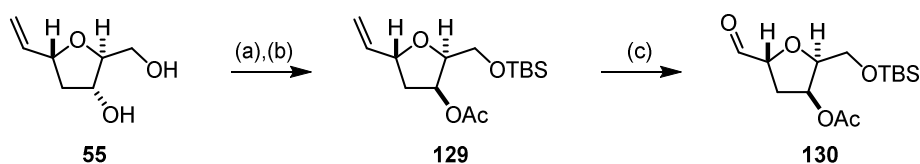
Scheme 2.35. Rationale for the observed diastereoselectivity: **XII** 1,2-Cram-chelate accounting for (12*R*)-**128**; **XIII** Felkin-Anh model and **XIV** 1,6-chelate, both accounting for (12*S*)-**128**; nucleophilic attack along a Bürgi-Dunitz trajectory (grey).

After separation, the undesired alcohol could be converted into the desired isomer by a two-step sequence comprised of an oxidation to the ynone followed by a highly selective Noyori transfer hydrogenation (Scheme 2.36).^[174] Desilylation using TBAF afforded the terminal alkyne **122** in 90% yield.^[165]



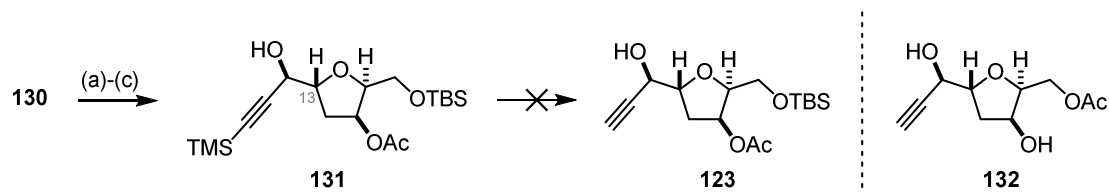
Scheme 2.36. Completion of the northern fragment **122**. Reagents and conditions: (a) DMP, NaHCO₃, CH₂Cl₂; (b) (*S,S*)-Teth-TsDpen-RuCl (10 mol%), HCO₂H·Et₃N, CH₂Cl₂, 80% over two steps, d.r. 12:1; (c) TBAF, AcOH, TBAF, 90%.

To provide flexibility for the endgame studies, a second northern alcohol fragment was synthesized with a different protecting group on the primary alcohol. Since this protecting group needed to survive the majority of steps in the synthesis, yet had to be orthogonal to the protecting groups in the southern fragment, two major mutations were made. As it was known from the southern fragment that selective deprotection of a primary TBS-ether in the presence of allylic and homoallylic TBS-ethers is feasible, the trityl-group in the northern fragment was replaced by a TBS-group. The southern domain had to be adjusted to this new strategy to maintain orthogonality between the two fragments as will be described in the next section. Diol **55** was mono TBS-protected^[175] in 81% yield (Scheme 2.37). Subsequent Mitsunobu esterification threw as expected and ozonolysis under classical conditions provided aldehyde **130** in 87% yield.^[165]



Scheme 2.37. Alternative protecting group strategy. Reagents and conditions: (a) TBSCl, Et₃N, DMAP (cat.), CH₂Cl₂, 81%; (b) AcOH, PPh₃, DIAD, toluene, 84%; (c) O₃, CH₂Cl₂, -78 °C; PPh₃, -78 °C to rt, 87%.

The use of the more labile TMS-alkyne was clearly advisable for this particular compound, since cleavage of the silyl cap in the presence of a primary TBS-ether and an acetate was expected to be challenging. Alkynylation under the previously optimized conditions showed basically no selectivity and gave low yield. This outcome was remedied by the oxidation/reduction sequence described above, providing the desired propargylic alcohol **131** in 19% over three steps (Scheme 2.38). All compounds were rather unstable and the ynone intermediate suffered from epimerization at C13, with the resulting *syn*-THF-moiety rapidly decomposing. Subsequent TMS-cleavage turned out to be cumbersome, leading to decomposition when silver fluoride was used or partial TBS-cleavage accompanied by acetate migration to give **132** when using TBAF at low temperature.

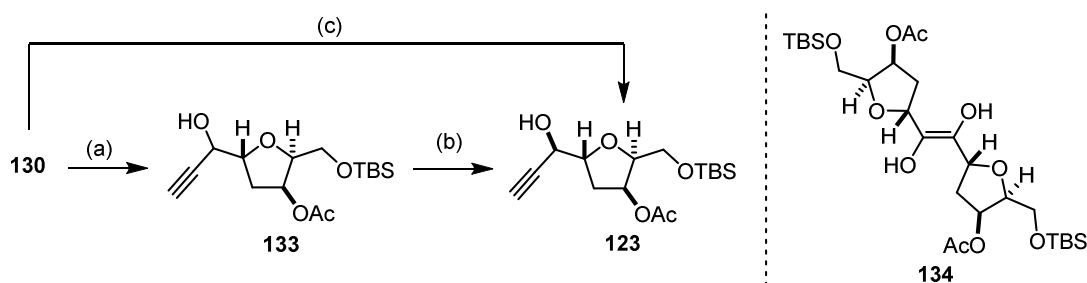


Scheme 2.38. Efforts toward the northern fragment **123**. Reagents and conditions: (a) TMS-C≡C-H, *n*-BuLi, Et₂O, LiI, -40 °C, 37%, d.r. 1:1; (b) DMP, NaHCO₃, CH₂Cl₂, 61%; (c) (*S,S*)-Teth-TsDpen-RuCl (7 mol%), HCO₂H·Et₃N, CH₂Cl₂, 83%, d.r. > 20:1.

An alternative and shorter entry to **123** avoiding the rather difficult desilylation was found in the direct alkynylation using acetylene. In analogy to the former results, addition of Grignard-reagent mostly led to deacetylation. Attempts to oxidize the alcohol and diastereoselectively reduce the

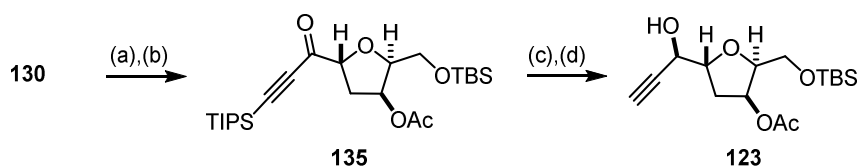
obtained ketone *via* CBS reduction^[176] gave a 1:1 isomeric mixture in poor yield (Scheme 2.39). The ynone itself was again unstable and decomposed during column chromatography or upon storage and thus prohibited further attempts for selective reduction.

In order to circumvent these additional steps, a diastereoselective alkylation with acetylene gas was pursued following a procedure by Carreira and coworkers.^[177] Under these conditions, enolization of the aldehyde proved problematic: along with a small amount of a 2.3:1 diastereomeric mixture of the alcohol, which could only be separated by preparative HPLC, significant decomposition was observed. The major component of the complex mixture was the dimerized aldehyde **134** (Scheme 2.39). Overall, this route to the terminal alkyne **123** was inefficient and therefore abandoned without further analysis.



Scheme 2.39. Alternative routes toward the northern fragment **123**. Reagents and conditions: (a) HCCMgBr, Et₂O, -20 °C, 18%, d.r. 1:1; (b) (i) DMP, NaHCO₃, *t*-BuOH, CH₂Cl₂, rt; (ii) (*S*)-(-)-2-Me-CBS, BH₃·THF, THF, EtOH, -40 °C, **123** 24% over two steps, d.r. 1:1; (c) acetylene, (-)-NME, Zn(OTf)₂, *i*-Pr₂NEt, toluene, -40 °C to rt, **123** 19%, d.r. 2.3:1; **134** verified by ESI-MS.

Instead, the bulkier TIPS-variant was investigated (Scheme 2.40). Alkylation using the lithium acetylide translated well onto the primary TBS-ether providing an even higher d.r. than in the case of the primary trityl-ether. Nonetheless, the diastereomeric mixture was oxidized to the corresponding ynone **135**, which was relatively stable in contrast to the TMS-derivative. Reduction to the alcohol was achieved with excellent yield and diastereoselectivity. Selective cleavage of the TIPS-group with TBAF was difficult, yet the terminal alkyne could finally be obtained in yields ranging between 45% and 65%.^[165]



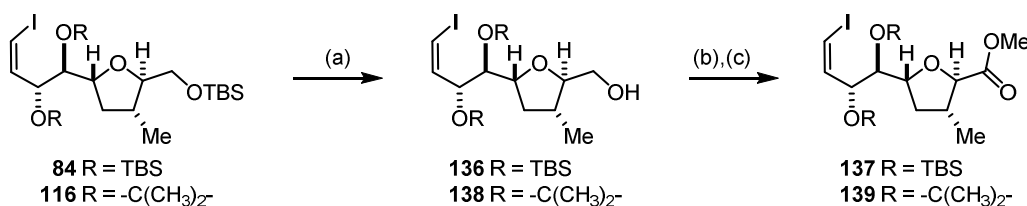
Scheme 2.40. Completion of the synthesis of alcohol **123**. Reagents and conditions: (a) TIPSCCH, *n*-BuLi, Et₂O, Lil, -40 °C, 67%, d.r. 5:1; (b) DMP, NaHCO₃, *t*-BuOH, CH₂Cl₂, 65%; (c) (*S,S*)-Teth-TsDpen-RuCl (7 mol%), HCO₂H·Et₃N, CH₂Cl₂, 96%, d.r. > 20:1; (d) TBAF, THF, -35 °C, 61%.

Overall, access to the northern fragments **122** and **123** was established with 11 steps in the longest linear sequence. The low overall yield of 1-2% pinpoints a severe bottleneck for material supply. A more efficient alternative to the required fragment is therefore desirable once the stereochemical assignment of chagosensine has been confirmed or corrected.

2.5.3 Modification of the Southern Sector

The vinyl iodide intermediate of the previous synthesis of the southern fragment (Section 2.4.4) represented a valuable cross coupling partner. Both, the bis-TBS-ether **84** as well as the acetonide version **116** could be directly engaged in Sonogashira cross couplings. As a supplement, the primary TBS-ether was transformed into the corresponding methyl ester **137** providing a suitable coupling partner for alcohol **123**. As (*Z*)-vinyl iodides tend to isomerize and decompose when exposed to light or heat the subsequent reactions were performed in the dark.

Selective cleavage of the primary TBS-ether **84** was again achieved using the HF-pyridine protocol (Scheme 2.41). The primary alcohol **136** was obtained in excellent yield and further oxidized to the carboxylic acid using TPAP/NMO. TMS-diazomethane effected methylation of the crude carboxylic acid,^[178] but initially low yields were observed. These findings were attributed to impurities in the crude mixture arising from the TPAP/NMO oxidation. Thus, the PIDA/TEMPO oxidation was considered due to a more convenient work-up protocol.^[179] An acetonitrile/hexanes extraction allowed iodobenzene impurities stemming from PIDA to be removed and provided a spectroscopically pure carboxylic acid. The respective methyl ester **137** could be obtained in 66% yield over two steps. The same sequence was applied to the acetonide-protected vinyl iodide **116** giving rise to the methyl ester **139** in similarly good yields.



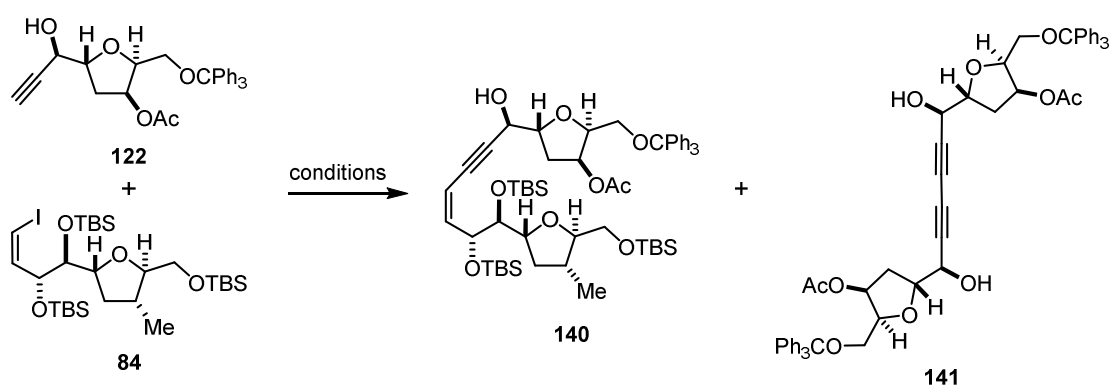
Scheme 2.41. Synthesis of southern iodides **137** and **139**. Reagents and conditions: (a) HF-pyridine, pyridine, THF, **136** 91%, **138** 98%; (b) PIDA, TEMPO (20 mol%), NaHCO₃, MeCN/H₂O; (c) TMSCHN₂, THF, 0 °C, **137** 66%, **139** 72% over two steps.

Overall, the efficient and scalable route to the vinyl iodides **84** and **116** in twelve linear steps was extended by a sequence of three steps to provide methyl esters **137** and **139** to increase flexibility in the endgame studies discussed in the following section.

2.5.4 Fragment Assembly

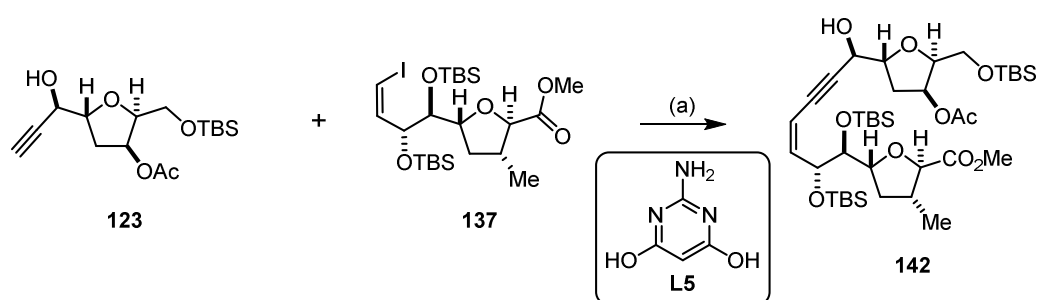
The critical assembly phase of the new building blocks commenced with a Sonogashira cross coupling.^[180] As it turned out, the ostensibly routine cross coupling reaction between trityl-ether **122** and vinyl iodide **84** suffered from low conversions, thus a screening was necessary. Under standard conditions using copper iodide and triethylamine in acetonitrile, Pd(PPh₃)₄ failed to convert the starting materials (Table 2.6, Entry 1),^[181] while Pd(PPh₃)₂Cl₂ provided 7% of the desired enyne **140** along with 31% of the Glaser coupling product **141** (Entry 2).^[182] The vinyl iodide **84** could be recovered from the reaction mixture in 86%, whereas the northern fragment had mainly decomposed. Only a slight improvement was observed by reducing the amount of copper while increasing the palladium loading (Entry 3). Replacing acetonitrile with THF as solvent shut the reactivity down; both starting materials were recovered (Entry 4). The best results were obtained when the reaction was performed in triethylamine as solvent under gentle warming (Entry 5).^[183] Other Pd(II)-sources, e.g. [Pd(dppf)Cl₂].CH₂Cl₂, brought no improvement (Entry 6). The yield of the desired enyne **140** could be increased to 34% by slow addition of a solution of the rather fragile alkyne to the reaction mixture *via* syringe pump (Entry 7). These conditions were originally used by Clark *et al.* to install a structurally very similar enyne motif in the C18-C34 fragment of amphidinolide C in respectable 82% yield.^[184] In the present case, however, the northern alkyne was still decomposing, preventing an efficient cross coupling. Furthermore, traces of the diyne formed *via* Glaser coupling were detected in all instances, although the solvents were carefully degassed prior to use. These observations led to the assumption that degradation products of highly oxygenated **123** could oxidize the copper(I) species and thus trigger homocoupling of any remaining alkyne. It was therefore advisable to investigate a copper-free cross coupling by employing (allylPdCl)₂ and tri-*t*-butylphosphine in acetonitrile with DABCO as base.^[185] Unfortunately, no improvement was recorded as the desired product was isolated in only 19% yield (Entry 8).

Since Suzuki coupling had been successful for the construction of the methyl-capped enyne in the previous synthetic strategy (see Section 2.4.4), fragment assembly was attempted with slightly modified conditions. The terminal alkyne **122** was treated with excess *n*-BuLi and the lithiated species transmetalated to boron before it was subjected to the palladium-catalyzed coupling event with **84** (Entry 9). However, no product was detected and once again the southern fragment was recovered while the northern sector had mainly decomposed. The latter is probably due to the borate ester formed at the propargylic alcohol. Therefore, the corresponding TMS-ether was prepared and the Suzuki coupling repeated with equimolar amounts of lithium base and borate. The desired product was still not formed and the northern alcohol was decomposed, despite protection.

Table 2.6. Cross coupling reactions.

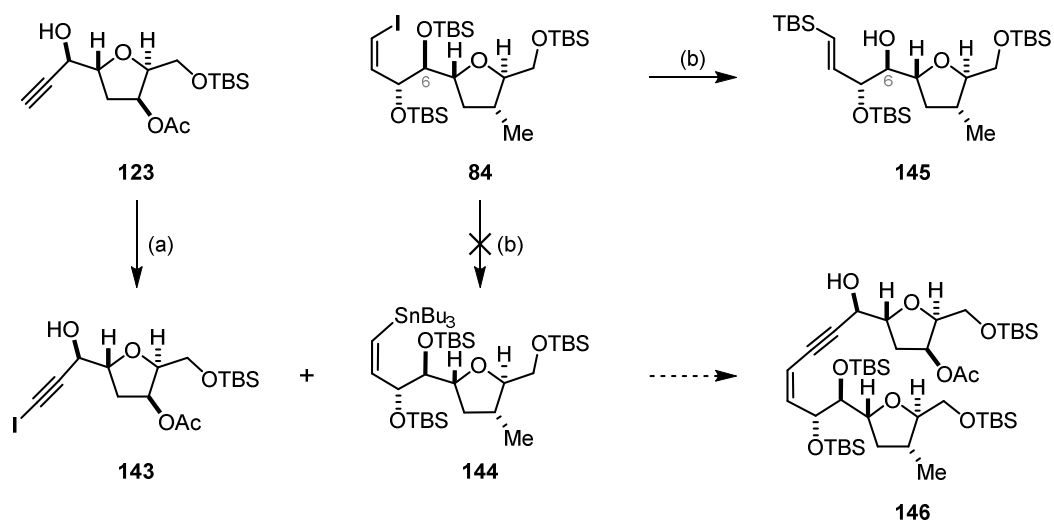
Entry	Conditions	Solvent	Result	Yield [%]
1	Pd(PPh ₃) ₄ (5 mol%), Cul (20 mol%), Et ₃ N	MeCN	no reaction	–
2	Pd(PPh ₃) ₂ Cl ₂ (5 mol%), Cul (20 mol%), Et ₃ N	MeCN	31% 141	7
3	Pd(PPh ₃) ₂ Cl ₂ (10 mol%), Cul (10 mol%), Et ₃ N	MeCN	19% 141	10
4	Pd(PPh ₃) ₂ Cl ₂ (10 mol%), Cul (10 mol%), Et ₃ N	THF	no reaction	–
5	Pd(PPh ₃) ₂ Cl ₂ (10 mol%), Cul (15 mol%), 55 °C	Et ₃ N	traces of 141	28
6	[Pd(dppf)Cl ₂]·CH ₂ Cl ₂ (10 mol%), Cul (15 mol%), 55 °C	Et ₃ N	traces of 141	25
7	Pd(PPh ₃) ₂ Cl ₂ (10 mol%), Cul (15 mol%), 55 °C, 2.5 h	Et ₃ N	traces of 141	34
8	(allylPdCl) ₂ (5 mol%), P(<i>t</i> -Bu) ₃ HBF ₄ (20 mol%), DABCO	DMF	84 recovered	19
9	<i>n</i> -BuLi, B(OMe) ₃ ; [Pd(dppf)Cl ₂]·CH ₂ Cl ₂ (10 mol%), 65 °C	THF	84 recovered	–

A second acyclic enyne was synthesized from **123** and **137** to provide an alternative substrate for the crucial endgame studies. Using the best reaction conditions found for **140** (see Table 2.6, Entry 7), the TBS-analog **142** was also obtained in a maximum yield of 33%. The use of an excess of alkyne did not alter the result. Therefore, a highly reactive copper-free catalytic system was envisioned that has found application in chemical biology employing 2-amino-4,6-dihydropyrimidine **L5** or its sodium salt as a ligand for palladium.^[186] The reaction was performed at 0 °C in DMF without reaching completion providing **142** in moderate, but reproducible yield, while the remaining starting materials could be partially recovered (Scheme 2.42). An increase in temperature enhanced the conversion but did not improve the yield of **142**.



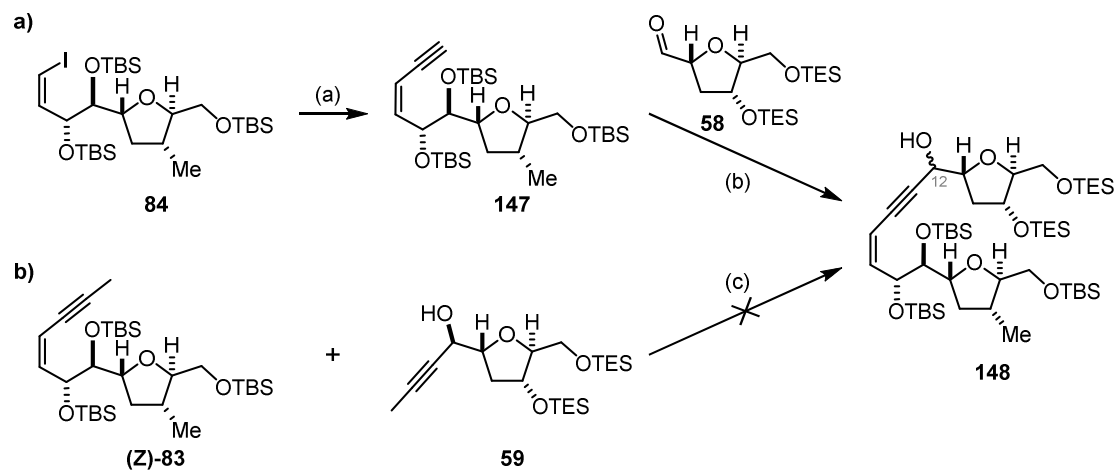
Scheme 2.42. Synthesis of enyne **142**. Reagents and conditions: (a) $\text{Pd}(\text{OAc})_2$ (10 mol%), **L5** (20 mol%), Cs_2CO_3 , DMF , 0°C , 36% (51% b.r.s.m.).

An opportunity to overcome the low reactivity might be found by recourse to Stille cross coupling, which mandated ‘umpolung’ of the coupling partners. To this end, the terminal alkyne of **123** was transformed into iodoalkyne **143** without incident by a silver-catalyzed iodination (Scheme 2.43).^[187] Next, the southern coupling partner had to be metalated to tin. The more readily available primary TBS-ether **84** was the substrate of choice, despite the compatibility issues that one would have to face later. A palladium-catalyzed stannylation with $\text{Pd}_2(\text{dba})_3$ and hexamethylditin in NMP ^[188] failed to proceed. In contrast, lithium/halogen exchange of **84** with $t\text{-BuLi}$ at -78°C followed by addition of tributyltin chloride and warming to ambient temperature^[189] afforded a single product. Evaluation of the analytical data indicated rearrangement of the C6-OTBS-group, providing the (*E*)-configured vinyl silane **145**. Although the desired product had not been formed, the mono-protected diol was isolated to verify the absolute configuration of the C6-alcohol by Mosher ester analysis (see Section 4.3.7).^[118] The decisive factor is that steric bulk seems to be a major drawback in the design of the southern domain. However, the acetonide-containing southern fragment was not contemplated as an alternative at this stage, since consecutive hydroelementations of the respective enyne would most likely lack regioselectivity (see Section 2.4.2).



Scheme 2.43. Anticipated ‘inverted’ cross coupling. Reagents and conditions: (a) AgNO_3 , NCS , DMF , rt, 83%; (b) $t\text{-BuLi}$, Bu_3SnCl , THF , -78°C to rt, **145** 61%.

In parallel, an alternative entry to the (*Z*)-enyne bypassing the cross coupling was investigated. An alkynylation strategy was deemed little promising, taking into account that all previous additions of metal acetylides into aldehydes had been rather unsuccessful. Nonetheless, a few experiments were sampled with the bis-TES-protected northern fragment **58**. At first, construction of the terminal enyne starting from vinyl iodide **84** had to be mastered. Adopting the conditions of the previously successful Suzuki coupling utilizing sodium acetylide furnished **147** (Scheme 2.44, a)). Opting for a Carreira alkynylation,^[190] which had shown the best diastereoselectivities in all alkynylations so far, led to a complex mixture. After re-isolation of enyne **147**, a substrate-controlled addition of the derived lithium acetylide was pursued delivering the product as a 3:1 mixture of C12-epimers. Determination of the absolute configuration at C12 was postponed. Nevertheless, the epimeric mixture of **148** served well as an additional substrate for hydroelementation reactions.



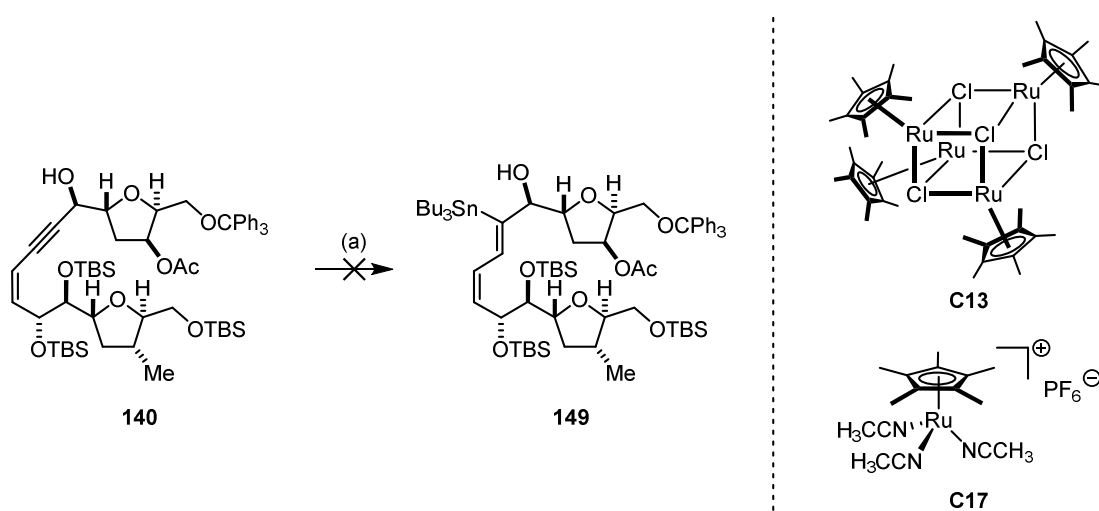
Scheme 2.44. Different approaches to enyne **148**. Reagents and conditions: (a) 1-ethynylsodium, B(OMe)₃, [Pd(dppf)Cl₂]₂·CH₂Cl₂ (15 mol%), 65 °C, 62%; (b) *n*-BuLi, **58**, THF, -78 °C, 42% (3:1 C12-epimeric mixture); (c) 5 Å MS, **C12** (20 mol%), **L2** (22 mol%), toluene (0.01 M), 110 °C.

Last but not least, cross alkyne metathesis between (*Z*)-**83** and **59** represented one more opportunity to construct the same acyclic enyne **148** in a stereochemically defined manner by recycling formerly synthesized fragments (Scheme 2.44, b)). Despite the known hassles for cross metathesis as fragment coupling between two equally valuable alkynes, **83** and **59** were exposed to **C12/L2**. Unfortunately, neither forcing conditions nor excess of the propargylic alcohol **59** could induce product formation.

In summary, construction of the acyclic (*Z*)-enyne motif by cross coupling or alkynylation has proven unexpectedly challenging. Nevertheless, three different substrates **140**, **142** and **148** were obtained in sufficient quantities to test the subsequent *trans*-hydroelementation reaction. Optimization to provide larger quantities of these advanced intermediates was postponed to a later stage. First, the key transformation to install the conspicuous (*Z,Z*)-chlorodiene had to be reduced to practice.

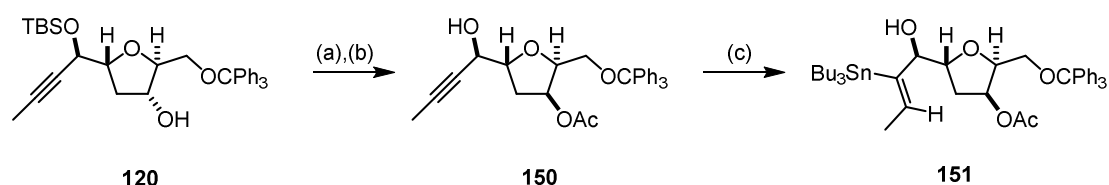
2.5.5 Hydrometalations

As discussed in Section 2.4.2, enynes undergo hydrometalations to the corresponding functionalized dienes; yet, the reaction is significantly slower than that of isolated alkynes. Thus, the optimized conditions from the model studies were adopted for the following series of substrates toward chagosensine. First, the acyclic enyne **140** was exposed to the neutral ruthenium catalyst **C13** at ambient temperature. Usually, a color change to deep purple is indicative for π -complex formation upon deaggregation of the tetrameric **C13** by the alkyne. This conspicuous coloration was also observed in the case of the unadorned model enynes but failed to appear here. A stock solution of tributyltin hydride was added over the course of 90 minutes, but no conversion of the starting material was observed (Scheme 2.45). This result could not be changed by an inverse addition mode, namely adding a solution of starting material and tributyltin hydride to a solution of the catalyst.



Scheme 2.45. Attempted *trans*-hydrostannylation of **140**. Reagents and conditions: (a) **C13** (20 mol%) or **C17** (20 mol%), Bu_3SnH , CH_2Cl_2 .

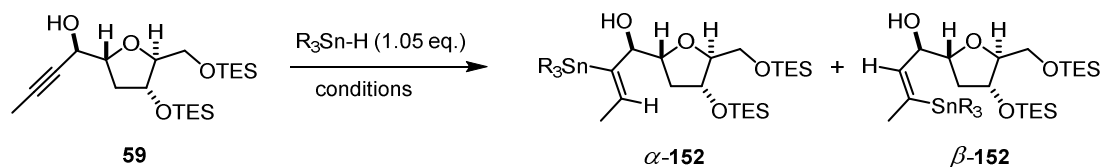
As ruthenium catalysts are known to exhibit a strong affinity to aromatic π -systems,^[191] limitations of this methodology had been observed for substrates bearing such moieties. Solely electron-deficient arenes had been tolerated before and it was speculated that the trityl protecting group was trapping the ruthenium catalyst.^[75b,76] Therefore, an excess of the ruthenium complex was used, but the starting material was still unchanged. Since utilization of the cationic complex **C17** could not alter the result either, a model substrate based on the northern segment was prepared to reduce the degree of complexity (Scheme 2.46). Under the standard conditions using 20 mol% of **C13** and maintaining the slow addition of tributyltin hydride, **150** was fully consumed. The only isolated product was the α /*trans* alkenylstannane **151**, which was obtained in low yield.



Scheme 2.46. Model substrate for *trans*-hydrostannylation. Reagents and conditions: (a) AcOH, PPh₃, DIAD, toluene, 82%; (b) TBAF, THF, 0 °C, 83%; (c) **C13** (20 mol%), Bu₃SnH, CH₂Cl₂, 37%.

For simple methyl-capped alkynes a redox-isomerization could be imagined as a side reaction.^[192] However, no indication for such a product was found in the crude proton NMR, which was surprisingly clean. It was concluded, that byproducts formed in the reaction bind tightly to the ruthenium and were presumably removed together with the catalyst by filtration over a short pad of silica. Since the trityl-group was believed to contribute primarily to such complexation, another test substrate was subjected to the hydrostannylation conditions lacking any aromatic moiety. Propargylic alcohol **59** (see Section 2.4.3) was identified as a suitable model. Initial experiments proved the assumption wrong, as the results obtained from this exercise showed that the two test substrates behaved similar: despite complete conversion, the yield was only moderate in both cases. Nevertheless, a clear preference for the desired α - over the β -isomer was observed (r.r. 97:3) with only the *trans*-products being detectable.

Table 2.7. Hydrostannylation reactions of model alkyne **59**.



Entry	R	Conditions	Time	Result ^{a)}	Yield [%] ^{b)}
1	Bu	C13 (20 mol%), 0.2 M, rt	90 min	α/β 97:3	43
2	Bu	C13 (20 mol%), 0.2 M, rt	10 min	α/β 97:3	49
3	Bu ^{c)}	C13 (20 mol%), 0.2 M, rt	10 min	α/β 97:3	48
4	Bu	C13 (20 mol%), 0.2 M, Sc(OTf) ₃ , rt	10 min	complex mixture	–
5	Bu	C13 (20 mol%), 0.2 M, CuCl ₂ , rt	10 min	complex mixture	6
6	Bu	C13 (20 mol%), 0.2 M, BHT, rt	10 min	α/β 97:3	60
7	Ph	AIBN, toluene, 0.2 M, 80 °C	16 h	α (trans/cis 65:35)	50
8	Ph	BEt ₃ , air, toluene, 0.2 M, rt	16 h	α	68
9	Me	C13 (10 mol%), 6 mM, –50 °C	10 min	α (quant.)	n.d. ^{d)}
10	Me	C17 (10 mol%), 6 mM, –50 °C	10 min	α trans/cis 80:20	n.d. ^{d)}

^{a)} determined by ¹H NMR of the crude mixture and indicative J_{SnH} herein; ^{b)} yield of regioisomeric mixture; ^{c)} s.m. and R₃SnH added to catalyst solution; ^{d)} NMR experiments, products decomposed upon isolation.

Suspecting that the limitation was arising from the THF–propargylic alcohol as a strong chelating motif rather than the aromatic moieties, the hydrostannylation of **59** was studied in more detail (Table 2.7). Adjusting the addition time as well as changing the order of addition had no impact on the reaction outcome (Entries 2 and 3). To perturb the assumed chelation of the oxygen-atoms to ruthenium, coordination sites were tentatively saturated by addition of Lewis acids such as Sc(OTf)₃ or CuCl₂ (Entries 4 and 5). In both cases, the starting material was instantaneously consumed leading to a complex mixture of unidentified products. In order to preclude radical background reactions, BHT was added resulting in a cleaner reaction with only desired product and unreacted starting material detectable (Entry 6). On the other hand, radical alternatives to the envisaged reaction were examined. A thermally initiated hydrostannylation with triphenyltin hydride almost exclusively gave the α -isomer as well,^[193] yet the yield was in the same range than for the transition metal catalyzed reaction and the *E/Z* selectivity was significantly lower (Entry 7). Milder initiation with BEt₃ and air as disclosed by Hale and coworkers^[194] worked extremely well, delivering 68% of the α /*trans*-isomer as the only detectable product (Entry 8), possibly offering an alternative for the envisioned construction of the (*Z,Z*)-chlorodiene in the natural product.

Since no other α -THF–propargylic alcohol had not been subjected to *trans*-hydroelementations in the Fürstner group before, NMR studies were conducted to verify the complexation mode of such substrates.^[195] As depicted in Figure 2.14, the predicted π -complex **XV** was formed when **59** and [Cp**Ru*Cl]₄ were mixed in equimolar amounts and cooled to –30 °C in an NMR tube as indicative by the *sp*-carbon shifts and the proton shift of the hydroxy group. Importantly, no contribution from the THF-ring was recorded under these conditions, but the π -complex proved unstable above –30 °C, where decomposition was observed. Therefore, hydrostannylation was performed at –50 °C; first stoichiometric in ruthenium, then catalytic. For these studies trimethyltin hydride was used for the sake of clarity in the NMR spectra. The hydrostannylation was found to be a clean transformation, yet the product was unstable upon chromatographic purification (Entry 9). Additionally, an α /*trans*: α /*cis* 4:1 mixture was detected when utilizing the cationic catalyst **C17** (Entry 10), and upon prolonged reaction time or at elevated reaction temperature isomerization to the *cis*-isomer occurred. The latter turned out to be rather unstable and decomposed rapidly accounting for the initially observed low yields.

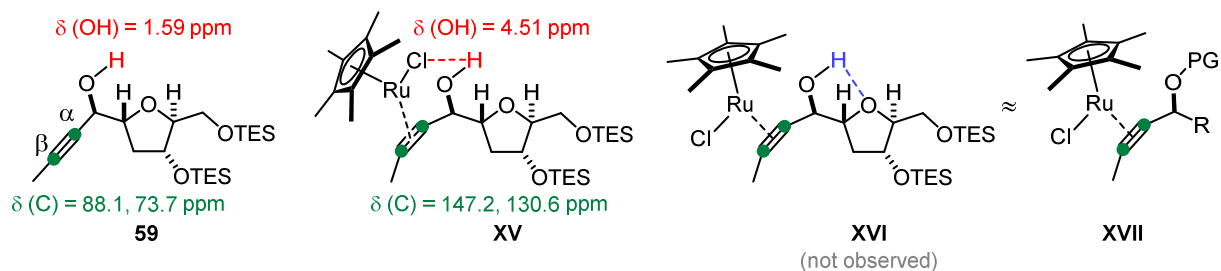
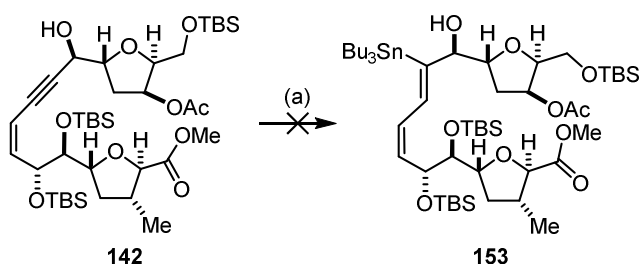


Figure 2.14. Coordination of **C13** to alkyne **59**: **XV** observed π -complex, indicative proton shifts (red) and carbon shifts (green); **XVI** alternative π -complex lacking preorganization *via* intermolecular hydrogen bonding (not observed); **XVII** π -complex as observed for regular protected propargylic alcohols^[195]; PG = protecting group.

In summary, important conclusions can be drawn from these studies: the expected π -complex **XV** between the ruthenium catalyst and the substrate is only stable at low temperature. Thus, the stabilizing contribution through intermolecular hydrogen bonding seems to be rather small. Nevertheless, hydrostannylations of this π -complex at low temperature lead to the expected *α /trans*-products with high conversion and regioselectivity; the products however are not entirely stable. Unfortunately, these findings do not allow drawing conclusions for the enyne case, where the substrate appeared to be inert.

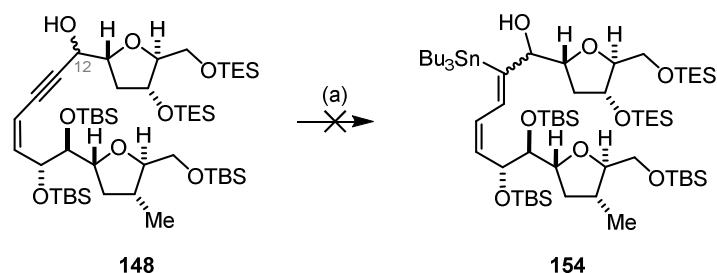
Since the trityl group had not been entirely ruled out as troublemaker, hydrostannylations of TBS-ether **142** were studied next. Catalytic quantities of **C13** again failed to induce conversion of the starting material. Thus, the reaction was conducted with dropwise addition of two separate stock solutions of three equivalents of Ru-complex **C13** and one equivalent tin hydride in CH_2Cl_2 each. The experimental challenge notwithstanding, no product formation could be observed and more than 80% starting material was recovered from the reaction mixture (Scheme 2.47).



Scheme 2.47. Attempted hydrostannylation of **142**. Reagents and conditions: (a) **C13** (20 or 300 mol%), Bu_3SnH , CH_2Cl_2 .

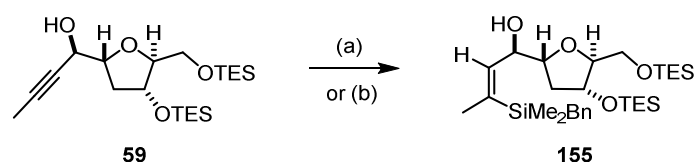
In order to remove further potentially coordinating functional groups, enyne **148** was projected as a more suitable substrate, although it was only available as an undefined C12-epimeric mixture. Using the same experimental setup, this intermediate was not inert, but reacted unspecifically (Scheme 2.48). Along with starting material, the correct high resolution mass was indeed found in the crude mixture, consisting of at least six compounds. However, no evidence for the desired product could be provided by NMR spectroscopy. Although lacking coordinating ester functionalities,

enyne **148** still bears eight oxygenated sites possibly interfering with metal complexation in an unproductive fashion. Thus, this third substrate seemed also unable to meet the criteria to be tolerated by the ruthenium complex.



Scheme 2.48. Attempted hydrostannylation of **148**. Reagents and conditions: (a) **C13** (300 mol%), Bu_3SnH , CH_2Cl_2 , traces by ESI-HRMS (regio- and diastereoselectivity unknown).

Overall, hydrostannylation failed to produce the desired intermediates *en route* to chagosensine for reasons that remain unclear. Hence, ruthenium-catalyzed hydrosilylation experiments were conducted to gain more insight into the recently developed methodology. In preparative terms, hydrosilylation is the more facile reaction compared to hydrostannylation, as catalyst poisoning is obviated and slow addition of the silane unnecessary.^[75b,100] As a first foray, model propargylic alcohol **59** was reacted with BnMe_2SiH under otherwise identical conditions. A very clean and fast reaction was observed providing the corresponding alkenylsilane **155** in 81% isolated yield (Scheme 2.49). Surprisingly, NMR analysis revealed an α/β -ratio of 1:9 as opposed to the hydrostannylation.



Scheme 2.49. Hydrosilylation reactions of model alkyne **59**. Reagents and conditions: (a) **C13** (20 mol%), BnMe_2SiH , CH_2Cl_2 , 81%, r.r. 9:1; (b) **C13** (20 mol%), BnMe_2SiH , LiCl , CH_2Cl_2 , 75%, r.r. 9:1.

The inverted regioselectivity is unexpected and may be explained by different binding modes between substrate and ruthenium. To prove this assumption, lithium chloride was added to interfere with the coordination, but the regioselectivity remained unchanged. This result is more closely in line with the regioselectivity observed for protected alcohols.^[76] Hydrosilylations of substrates missing a protic neighboring group usually favor β /*trans*-products as opposed to hydrostannylations, which preferably produce α /*trans*-products (albeit with decreased selectivity compared to hydroxy-directed versions). The pre-organization of the σ -complex dictating the regioselectivity is not only orchestrated by the substrate itself, but also influenced by the hydride species *via* interligand interactions (Figure 2.15).

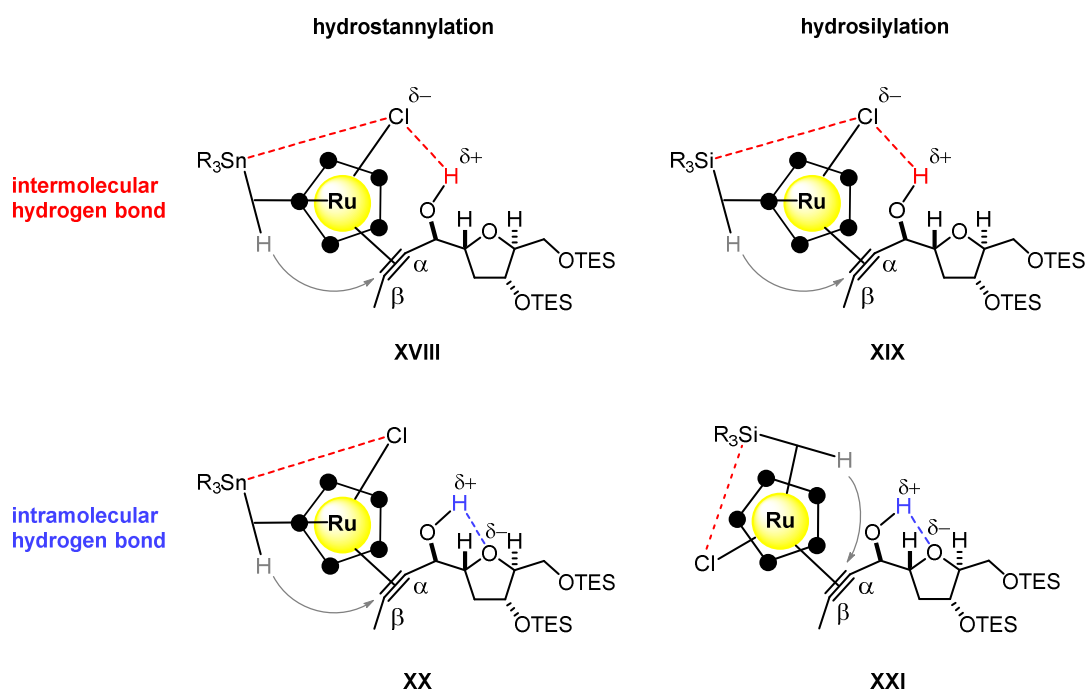
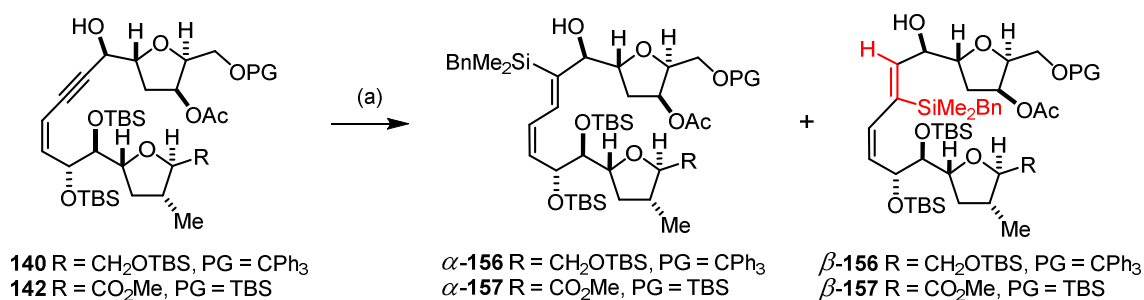


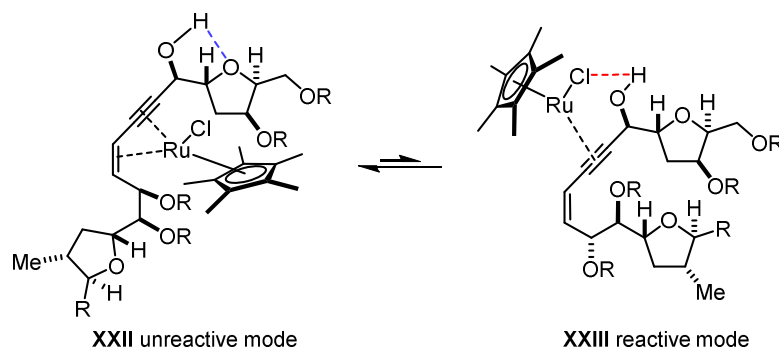
Figure 2.15. Possible pre-organizations of the ligand sphere of the activated catalyst: **XVIII**, **XIX** interligand interactions (red) between substrate, ligand and hydroelementation reagent favoring α /*trans*-products; **XX**, **XXI** interligand interactions (red) only between ligand and hydroelementation reagent, competing intramolecular hydrogen bonding (blue) leading to α /*trans*-alkenylstannanes and β /*trans*-alkenylsilanes respectively. • = CMe.

Refocusing on the enyne substrates, the more robust hydrosilylation was performed as a proof of concept. When dimethylbenzylsilane was added to enyne **140** and **C13** at ambient temperature, the exact product mass could indeed be detected in a complex reaction mixture, from which still more than 60% of unreacted starting material was recovered (Scheme 2.50). Furthermore, the TBS-protected substrate **142** was subjected to the hydrosilylation conditions using catalytic amounts of **C13**. Only traces of product were detected, while most of the starting material remained untouched. More portions of catalyst were added, until full conversion was finally achieved with three equivalents of **C13**. The major product of an isomeric mixture with at least three compounds bearing the same high resolution mass was characterized as the β /*trans* product β -**157**. In this particularly complex environment, the hydride arguably seems to be transferred preferentially from the less hindered position and hydrogen bonding, if available at all, plays a significantly inferior role.



Scheme 2.50. Attempted hydrosilylations. Reagents and conditions: (a) **C13** (300 mol%), BnMe₂SiH, CH₂Cl₂, β -**157** 25%.

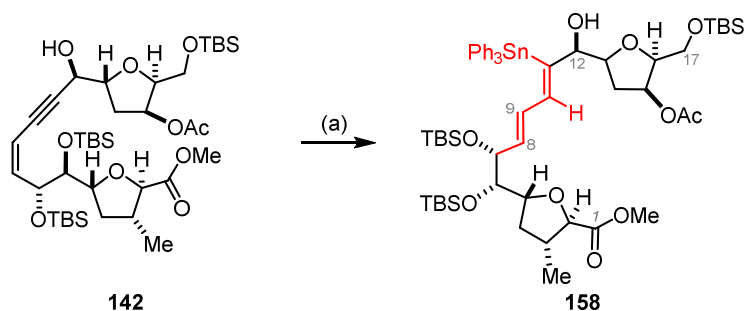
In summary, the results discussed above hint toward complexation of the ruthenium catalyst by the enyne and/or the numerous coordinating groups displayed within the substrate. Presumably due to competitive intramolecular hydrogen bonding with the THF-ring (Scheme 2.51, **XXII**), hydrogen bonding between the hydroxy group and the chloride ligand seems to be too weak to guide the ruthenium catalyst to engage in a productive complexation **XXIII** (Scheme 2.51).^[99] Steric bulk is supposed to play a minor role, since the slim (*Z*)-enyne should be accessible in the flexible acyclic system from one side or the other, which cannot be validated at this point.



Scheme 2.51. Competitive binding modes between ruthenium complex and enyne substrate.

Overall, only small energetic differences seem to be policy makers for both reactivity and regioselectivity. As deduced from the model studies, the intermolecular hydrogen bond of such α -THF-propargylic alcohol motifs to the chloride ligand seems largely unavailable.

A promising alternative surfaced in the radical hydrostannylation. This methodology has previously been applied to advanced intermediates for total syntheses^[174c,196] and has the advantage of using mild initiation conditions. In addition, it had given the best results for converting the test substrate **59** to the desired alkenylstannane (see Table 2.7, Entry 8). Thus, enyne **142** was subjected to the reported conditions and was cleanly transformed into a single product. Upon analysis, all hopes were dashed: the desired α /*trans*-alkenylstannane had indeed formed, yet the C8–C9 (*Z*)-double bond had been isomerized to the (*E*)-isomer **158** (Scheme 2.52). Attempts to prevent radical isomerization by avoiding excess of the tin hydride species met with failure.^[197] Thus far, the thermodynamically more stable products were obtained in all literature examples utilizing this method. The challenging (*Z,Z*)-dienylstannane envisioned herein therefore seems inaccessible by this methodology.



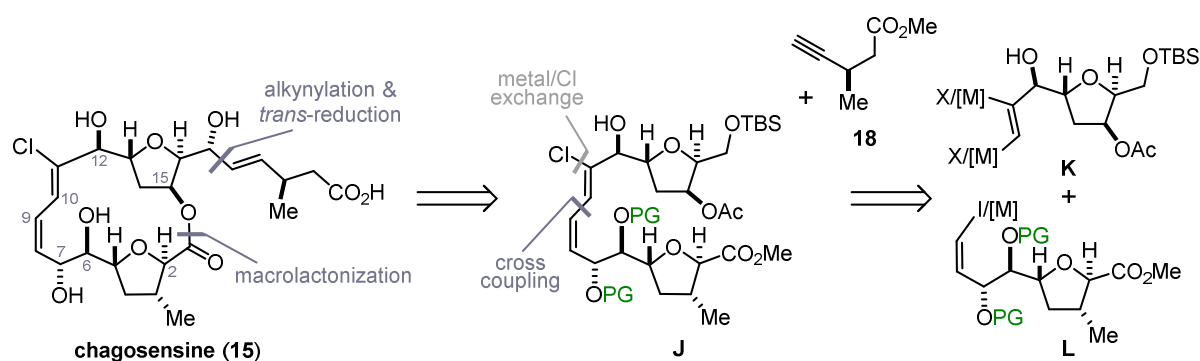
Scheme 2.52. Radical *trans*-hydrostannylation. Reagents and conditions: (a) Ph_3SnH , BEt_3 , toluene, air, 58%.

Since all possible *trans*-hydroelementations largely remained without success and the preparation of the precursors was cumbersome as well, the initial strategy for the formation of the (*Z,Z*)-chlorodiene motif had to be abandoned at this stage.

2.6 The Second Macrolactonization Approach: Bis-Metalation

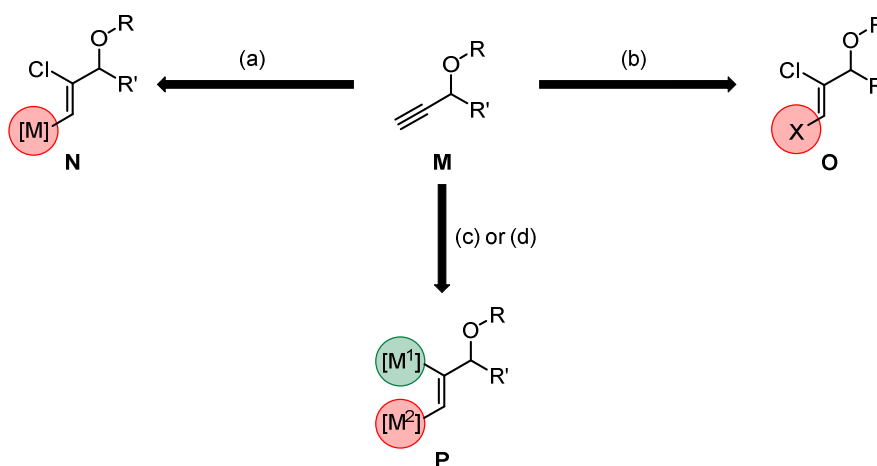
2.6.1 Retrosynthetic Analysis and Strategic Considerations

After the unfruitful efforts with respect to RCAM or cross coupling followed by *trans*-hydrostannylation – eventually dismissing both cornerstones of the original synthesis plan – the tactics had to be changed. The major goal was to retain the THF-rings in both fragments, with the most prominent retrosynthetic cut lying in the ester functionality between the two THF-rings. In analogy to the former approach, macrolactonization as the ring closing manoeuvre would still precede the installation of the sidechain. Thus, the same advanced (*Z,Z*)-chlorodiene **J** needed to be elaborated. However, it was planned to avoid any enyne intermediates that had proven difficult to construct and to functionalize. While scission of the C9–C10 bond remained the most obvious disconnection, the order of steps was inverted compared to the previous blueprint: **J** was thought to be accessed *via* selective cross coupling between the terminal vinyl metal (or halogen) moiety of the northern fragment **K** and a vinyl iodide (or metal) species **L** (Scheme 2.53). If the vinyl chloride was not in place already prior to coupling, it would be obtained by metal/chloride exchange of the remaining vinyl metal species.



Scheme 2.53. Revised retrosynthetic analysis based on cross coupling; PG = protecting group; [M] = metal; X = halide.

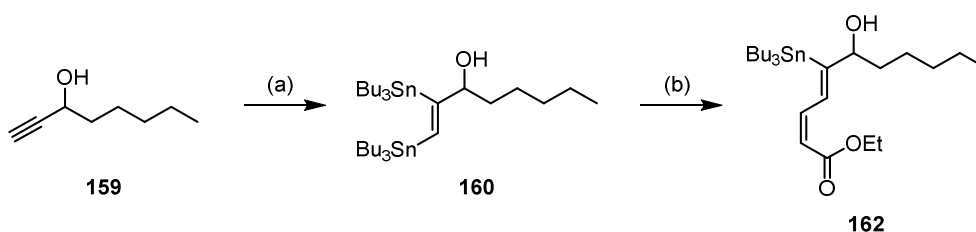
Despite the increasing number of publications on halo- and bis-metalations of alkynes,^[198] there is still little precedence for the selective bis-functionalization of terminal aliphatic alkynes bearing substituents at the propargylic position. The most tantalizing methodology for the facile construction of a chlorodiene is found in a chlorometalation of **M** to give **N** followed by sp^2 - sp^2 cross coupling, provided that the metal is delivered at the terminal position (Scheme 2.54, (a)).^[198c,199] Alternatively, a bis-halogenation could also provide the desired vinyl chloride **O** with a second halide in the terminal position as handle for cross coupling reactions with a suitable southern fragment (Scheme 2.54, (b)).^[200] Since such methods ensuring the required regio- and stereoselectivity were to no avail for (protected) propargylic alcohols,^[201] an alternative scenario was conceived. A *cis*-selective bis-metalation could give rise to a hetero-bis-metalated alkene **P**,^[202] where one metal can be exchanged for chloride (Scheme 2.54, (c) green) while the second metal can engage in cross coupling (red). This concept requires excellent regioselectivity and the possibility to discriminate between the two metals: the internal metal should undergo facile chloride exchange without harming the second metal or – alternatively – stay integer during the cross coupling event of the terminal center and get replaced by chloride afterward. Only a few methods allowing for such a selective reaction sequence were described in the literature; among them there is no oxygenated propargylic substrate. Thus, a forth strategy was contemplated, where bis-metalation would provide a trisubstituted alkene of type **P** ($[M^1] = [M^2]$).^[203] The terminal and thus sterically less hindered metal center should engage in a selective cross coupling and the internal metal could be swapped for chloride in a second step. Based on a thorough literature search and a few preliminary studies on simple propargylic alcohols,^[201] the forth strategy was further investigated.



Scheme 2.54. Concepts for bis-functionalization of terminal alkyne **M**: (a) chlorometalation to vinyl chloride **N**; (b) chlorohalogenation to vinyl chloride **O**; (c) hetero-bis-metalation to alkene **P** ($M^1 \neq M^2$); (d) bis-metalation to alkene **P** ($M^1 = M^2$).

2.6.2 Bis-Stannylation and Stille Coupling

As the tin/chloride exchange is well precedented^[77,101] and had proven successful for the installation of chlorodienes during the model studies performed within this work (see Section 2.4.2), bis-stannylation was identified as the strategy of choice. However, little evidence was found in the literature for the selective cross coupling of 1,2-bis-stannylated alkenes at the outset of this study.^[204] Therefore, the envisioned strategy was tested on commercially available 1-octin-3-ol (**159**). Following a procedure disclosed by Lautens *et al.*,^[203f] palladium-catalyzed bis-stannylation of the alkyne smoothly provided the corresponding *cis*-bis-stannane **160** in respectable yields as long as the sensitive and isomerization-prone products were handled in the dark and silica gel for purification was deactivated with triethylamine (Scheme 2.55). The projected selective Stille coupling was then tested with commercially available ethyl *cis*-3-iodoacrylate (**161**) using a protocol for sensitive substrates reported by Fürstner and coworkers.^[205] This modified procedure uses copper thiophene-2-carboxylate (CuTC) in polar solvents to enhance the reaction rate by transmetalating the stannane precursor to a more reactive copper analog.^[206] In addition, $[\text{Ph}_2\text{PO}_2][\text{NBu}_4]$ acts as a tin scavenger rendering the transmetalation irreversible.^[207] The overall mild and efficient method has found broad application in the synthesis of polyfunctionalized and polyunsaturated compounds,^[140b] and also succeeded in the present case: the desired dienylstannane **162** was obtained in acceptable yields after one hour at ambient temperature.

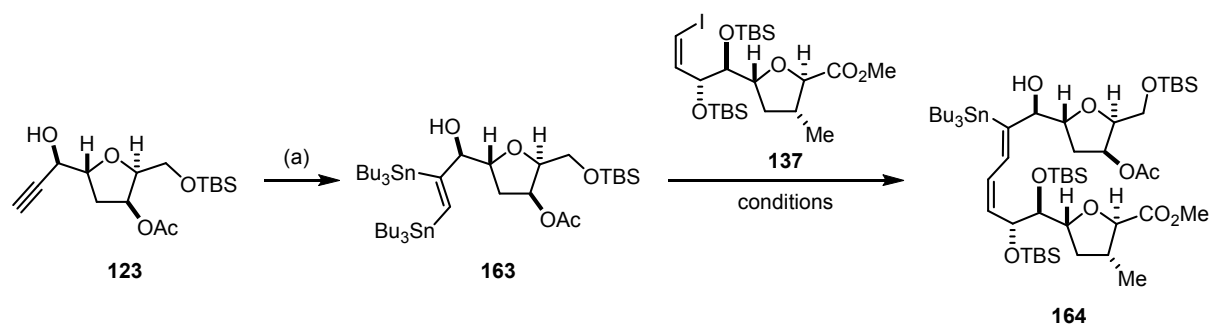


Scheme 2.55. Bis-stannylation and selective Stille coupling. Reagents and conditions: (a) $\text{Pd}(t\text{-BuNC})_2\text{Cl}_2$ (10 mol%), $(\text{Bu}_3\text{Sn})_2$, THF, 85%; (b) ethyl 3-*cis*-iodoacrylate (**161**), $\text{Pd}(\text{PPh}_3)_4$ (20 mol%), CuTC, $[\text{Ph}_2\text{PO}_2][\text{NBu}_4]$, DMF, 59%.

Encouraged by these results, construction of the proper (*Z,Z*)-alkenylstannane was pursued. With the formerly improved protecting group strategy in mind, bis-stannylation of terminal alkyne **123** was performed and the corresponding bis-stannane **163** was isolated in 75% yield. Due to the sensitivity of this product, it was prepared only on demand. The crucial cross coupling reaction was then addressed with vinyl iodide **137** as counterpart. In the event, no coupling occurred between the bis-stannane and the vinyl iodide under the previously successful conditions (Table 2.8, Entry 1). Thus, a variety of other conditions used in cross couplings between vinyl iodides and vinyl stannanes were screened.^[160b,208] In most cases, the fragile bis-stannane decomposed; the vinyl iodide could be

recovered from the reaction mixture, except when forcing conditions were applied, which caused isomerization to the (*E*)-double bond (Entry 5).

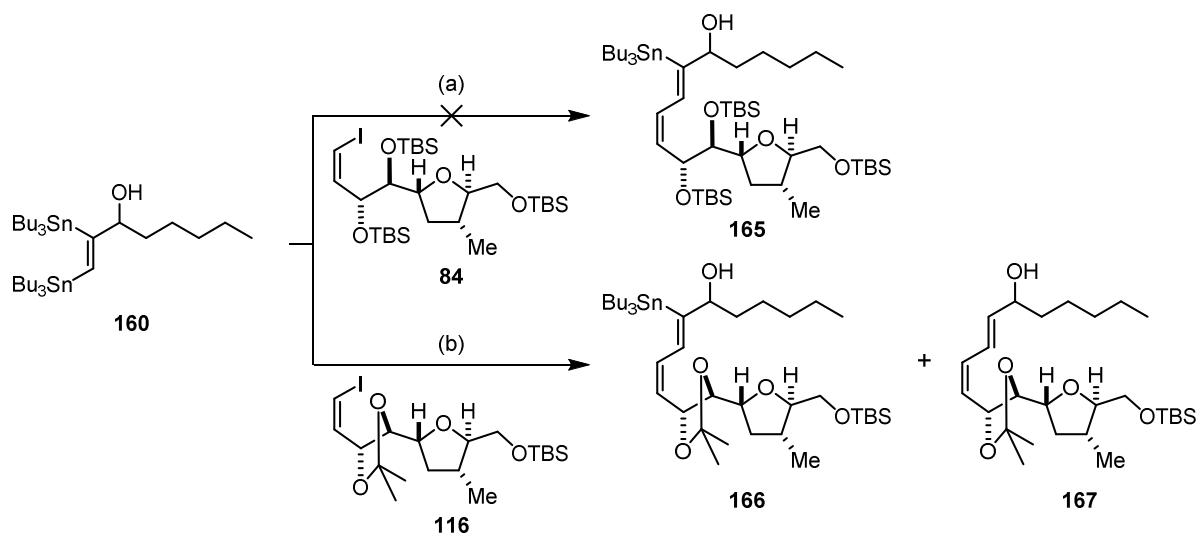
Table 2.8. Stille couplings between **163** and **137**. (a) Pd(*t*-BuNC)₂Cl₂ (20 mol%), (Bu₃Sn)₂, THF, 75%.



Entry	Conditions	Result ^{a)}	164 [%]
1	Pd(PPh ₃) ₄ (20 mol%), [Bu ₄ N][Ph ₂ PO ₂], CuTC, DMF, rt	163 consumed	0
2	Pd(PPh ₃) ₂ Cl ₂ (20 mol%), AsPh ₃ , THF, rt	no reaction	0
3	Pd(MeCN) ₂ Cl ₂ (20 mol%), DMF, rt	no reaction	0
4	Pd(MeCN) ₂ Cl ₂ (10 mol%), <i>i</i> -Pr ₂ NEt, DMF	no reaction	0
5	Pd(MeCN) ₂ Cl ₂ (10 mol%), AsPh ₃ , [Bu ₄ N][Ph ₂ PO ₂], DMF, 65 °C	163 consumed ^{b)}	0
6	Pd ₂ (dba) ₃ (20 mol%), AsPh ₃ , DMF, rt	163 consumed	0

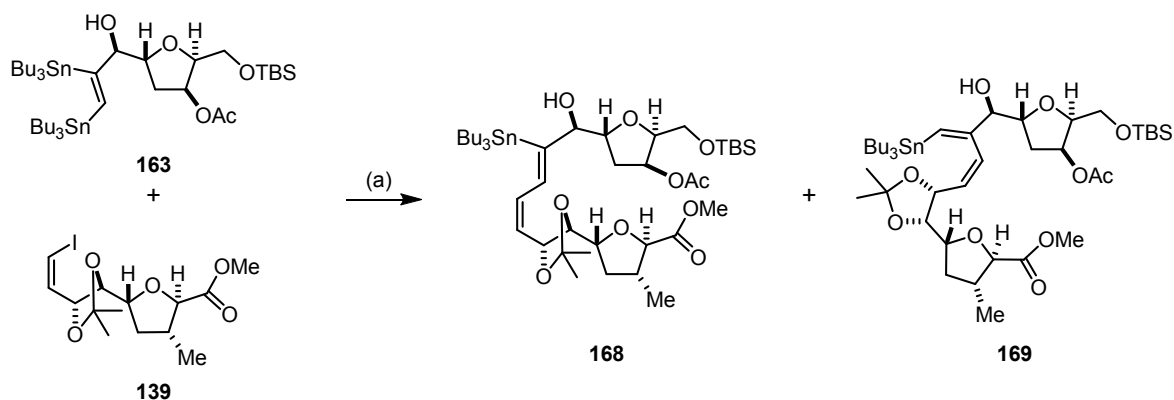
^{a)} determined by TLC analysis and ¹H NMR of crude mixture; ^{b)} **137** isomerized to (*E*)-vinyl iodide.

A control experiment between model bis-stannane **160** and less valuable **84** likewise showed no reaction, indicating that the sterically demanding vicinal TBS-ethers presumably interfered with the cross coupling (Scheme 2.56). In a recent total synthesis, ring closing Stille coupling between a similarly congested (*Z*)-vinyl iodide flanked by a bis-TES-protected diol was reported to be intricate as well; depending on the diol's stereochemistry, the reaction gave only moderate yield or failed completely.^[209] Hence, the southern counterpart was replaced by the acetonide **116**. Selective Stille coupling at the terminal position was feasible in this case, but demetalation of the second tin also occurred to a large extent. A one-pot procedure comprising cross coupling followed by tin/chloride exchange was envisioned. However, the addition of either NCS or CuCl₂ led to a complex reaction mixture with no trace of the desired product.



Scheme 2.56. Attempted selective Stille couplings. Reagents and conditions: (a) **84**, Pd(PPh₃)₄ (20 mol%), CuTC, [Ph₂PO₂][NBu₄], DMF; (b) **116**, Pd(PPh₃)₄ (20 mol%), CuTC, [Ph₂PO₂][NBu₄], DMF, **166/167** (1.2:1) approx. 50%.

Next, bis-stannane **163** and vinyl iodide **139** were subjected to the Fürstner conditions and the desired dienylstannane **168** was formed within less than one hour. In the initial attempt, the product was isolated in 44%, but when the reaction was repeated on a slightly larger scale, the regioisomer **169** was obtained in 24% yield along with **168** in 40% yield (Scheme 2.57). Although far from perfection, this result was promising as Stille couplings with similarly complex substrates had shown even worse results than this yet unoptimized process.^[160b,209]



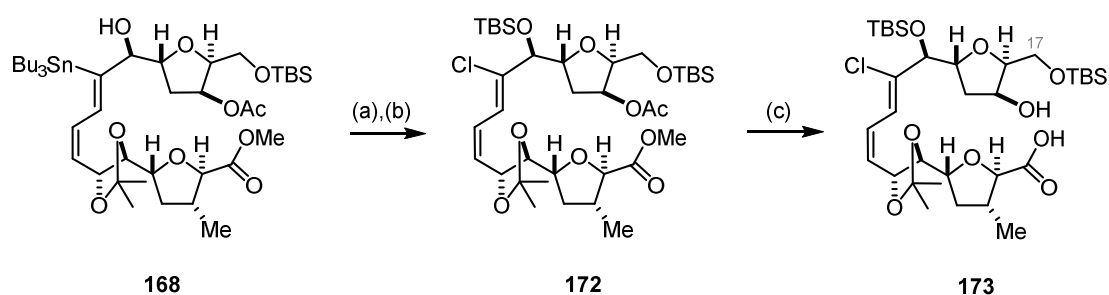
Scheme 2.57. Stille coupling. Reagents and conditions: (a) Pd(PPh₃)₄ (40 mol%), CuTC, [Ph₂PO₂][NBu₄], DMF, **168** 40%, **169** 24%.

However, the reaction proved rather capricious: besides the formation of regioisomers proto-demetalated products were observed from time to time. The latter are expected to arise from transmetalation of tin to copper followed by proto-decupration. Since these products were obtained using exactly one equivalent of CuTC, it was assumed that CuTC can hardly distinguish between the internal and the terminal stannane leading to random transmetalations. While the terminal stannane is sterically less hindered, transmetalation of the internal stannane could be facilitated by hydrogen

bonding of the neighboring hydroxy group to the thiophene-2-carboxylate. The subsequent cross coupling occurs more readily *via* the cuprate than the stannane, thus purely steric effects might be circumstantial. Moreover, hydroxy-directed selective Suzuki cross couplings of diboranes have been reported by Morken and coworkers,^[210] suggesting that a putative Pd-O interaction might account for the formation of **169**. Hence, optimization of the conditions for this transformation is required, preferably omitting CuTC or protecting the allylic alcohol prior to the coupling process. Nevertheless, the material obtained *via* this route was used to elaborate the dienylstannane into the sophisticated macrocycle.

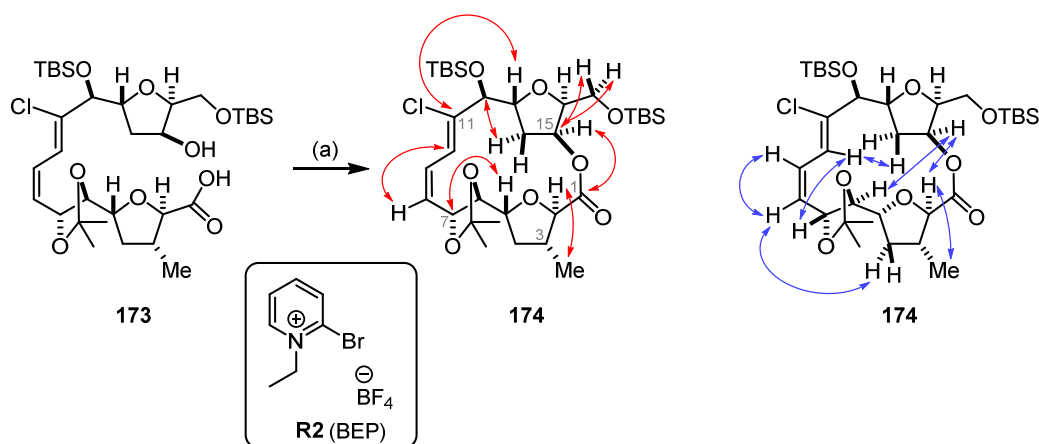
2.6.3 Efforts Toward the Macrocycle

Since bis-stannylation and Stille coupling allowed for the first time the isolation of the (*Z,Z*)-dienylstannane **168**, the delicate chlorodiene was finally within reach. The use of five equivalents of anhydrous copper(II) chloride provided the desired chlorodiene in good yield (Scheme 2.58). 2,6-Lutidine was employed as a proton scavenger to avoid intramolecular protodemetalation through the neighboring hydroxy group. Subsequently, the allylic alcohol was protected as a TBS-ether using TBSOTf and 2,6-lutidine giving rise to **172**. A priori, protection of this secondary alcohol might not be necessary for the construction of the macrocycle; nevertheless, the protected and thus less polar compound was expected to reduce hassle. A short screening was required for the concomitant saponification of the acetate and the methyl ester of **172**. A first trial employing lithium hydroxide in a THF/water mixture at ambient temperature gave substantial amounts of the primary alcohol at C17 as a very polar byproduct resulting from TBS-cleavage. Interestingly, lowering the temperature to 0 °C showed that cleavage of the methyl ester occurred readily, while saponification of the acetate could not be achieved without damaging the primary TBS-ether. A switch to potassium hydroxide did not improve the outcome. Finally, concurrent saponification was accomplished using potassium carbonate in a CH₂Cl₂/MeOH mixture (6:1) affording the secoacid **173** in 79% yield. The solvent ratio was crucial as more methanol led to decomposition of the compounds for reasons that remain unclear.



Scheme 2.58. Elaboration to the secoacid. Reagents and conditions: (a) CuCl₂, 2,6-lutidine, THF, 70%; (b) TBSOTf, 2,6-lutidine, CH₂Cl₂, 83%; (c) K₂CO₃, CH₂Cl₂/aq. MeOH 6:1, 79%.

The stage was now set for the challenging macrolactonization.^[211] In preliminary studies, Yamaguchi^[181a,212] and Shiina^[213] macrolactonizations under different reaction conditions showed no promising results.^[214] Hence, an Evans-modified Mukaiyama macrolactonization^[215] employing 2-bromo-1-ethylpyridinium tetrafluoroborate (BEP) was performed. At first, the reaction was conducted in CH_2Cl_2 , but only very little conversion was detected. Therefore, the mixture was swiftly concentrated and the residue diluted with dichloroethane. Stirring of the reaction mixture at reflux temperature was beneficial for the cyclization; despite the small scale, isolation and scrupulous characterization of macrolactone **174** was achieved (Scheme 2.59). High resolution mass spectrometry confirmed the macrocyclic monomer and NMR spectroscopy provided further structural information. HMBC correlations specifically between H-15 and C1 unambiguously proved the ring closure. Furthermore, transannular NOE contacts between the two THF-rings as well as to the diene motif highlight the complex architecture of the macrolactone of chagosensine. As only contacts between protons are being measured, it is readily understood that the high density of functional groups certainly creates ring strain. In combination with the experiment, where also starting material was recovered from the unoptimized reaction, an important conclusion can be drawn: the highly decorated macrocycle is only formed under forcing conditions, yet its synthesis is feasible following this forth strategy.

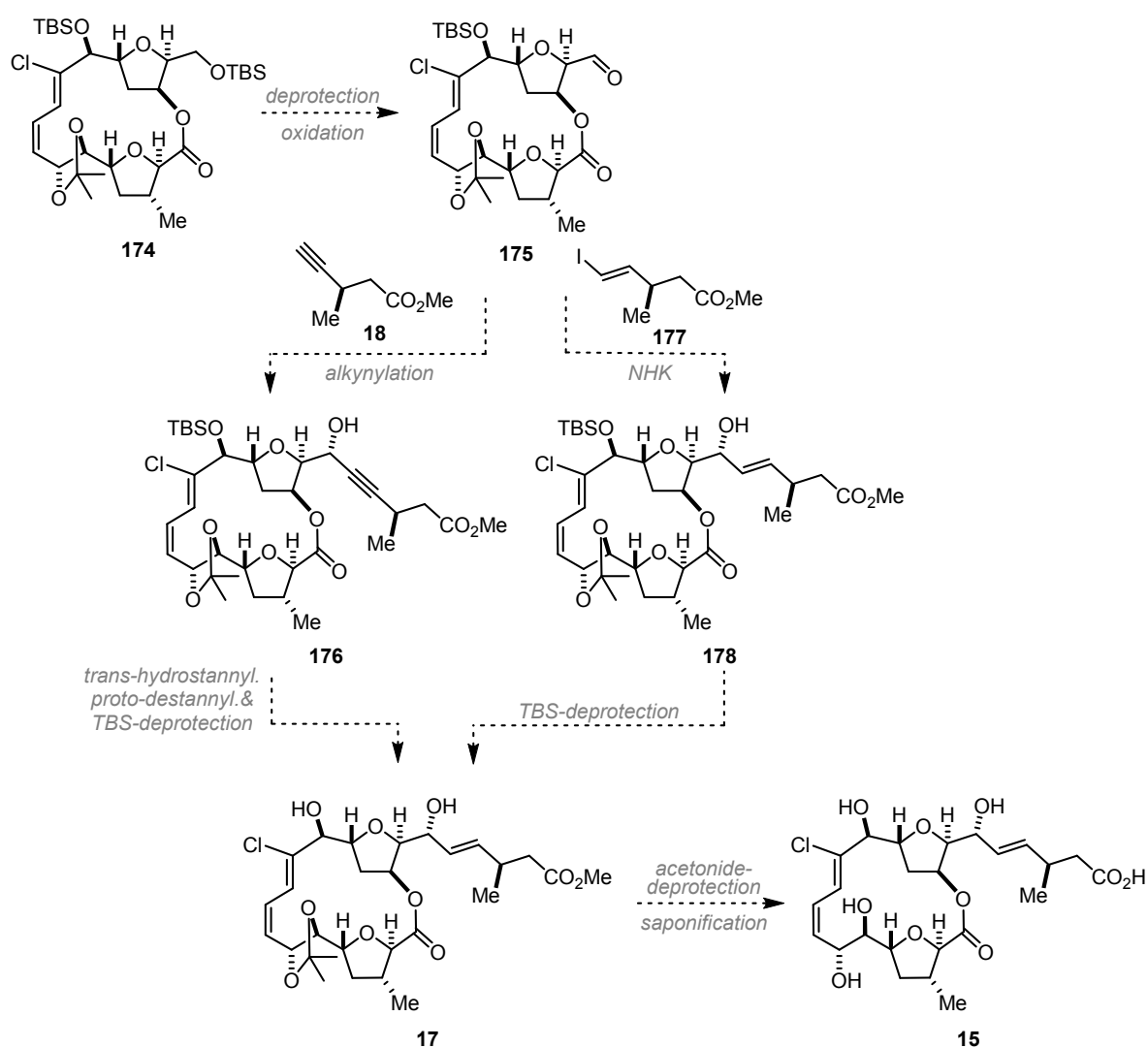


Scheme 2.59. Macrolactonization and characterization of the macrocycle **174**. Reagents and conditions: (a) **R2**, NaHCO_3 , $(\text{CH}_2\text{Cl}_2)_2$ (0.0005 M), 80 °C, approx. 25%; decisive HMBC correlations (red) and NOE contacts (blue).

2.6.4 Outlook

After detailed evaluation of four different strategies leaving no stone unturned, a route to this highly sophisticated intermediate was finally found. Future work will focus on optimization of the two key steps of the endgame, *i.e.* Stille cross coupling for fragment assembly and macrolactonization for ring closure, in order to provide sufficient material for completing the total synthesis of chagosensine. To this end, a few unknown steps remain to be investigated (Scheme 2.60). The primary TBS-ether

needs to be cleaved selectively and the resulting alcohol oxidized to the aldehyde **175**. The sidechain **18** can then be attached by diastereoselective alkynylation before reducing the triple bond *via* a *trans*-hydrostannylation/destannylation sequence. Alternatively, the terminal alkyne of the sidechain can be converted into a vinyl iodide **177** and a Nozaki-Hiyama-Kishi reaction with aldehyde **175** could give rise to the allylic alcohol **178**.^[216] The configuration of the alcohol at C17 must be determined by Mosher ester analysis. Cleavage of the allylic TBS-ether would provide a derivative **17** synthesized by the isolation team^[80] and comparison of the synthetic material with the reported compound could already allow to draw conclusions on the structure at this point. Acetonide deprotection would finally precede cleavage of the methyl ester to arrive at the natural product in 26 to 27 steps in the longest linear sequence.



Scheme 2.60. Future work to complete the total synthesis of chagosensine (**15**).

3 Summary and Conclusion

During the course of this thesis, the catalytic activation of π -systems was explored in two different research topics. The first project placed in the field of physical organic chemistry dealt with the detailed mechanistic study of a π -acid-catalyzed transformation. The investigated gold(I)-catalyzed hydroalkoxylation of allenes showed an impressive enantioinversion solely caused by reaction conditions. In the second part of this thesis, a total synthesis program toward chagosensine with an emphasis on ring closing alkyne metathesis (RCAM), cross coupling reactions and *trans*-hydrometalations addressed the selective functionalization of alkynes. Both projects have led to significant progress in methodology development through enhanced mechanistic understanding at the molecular level.

3.1 Enantioinversion in the Gold(I)-catalyzed Hydroalkoxylation of Allenes

Since the turn of the millennium, homogeneous π -acid catalysis has become an important research area.^[2] Intensive efforts have advanced the discovery of novel reactivities as well as the development of numerous ligands and catalysts.^[1] In sharp contrast, asymmetric gold catalysis is still underexplored, mainly due to the challenge posed by the intrinsic geometrical properties of this noble metal.^[4a] The favored linear dicoordination renders chirality transfer from the ligand to the substrate in an outer-sphere mechanism exceptionally difficult (Figure 3.1). Only a limited number of concepts to overcome this issue have been developed to date.

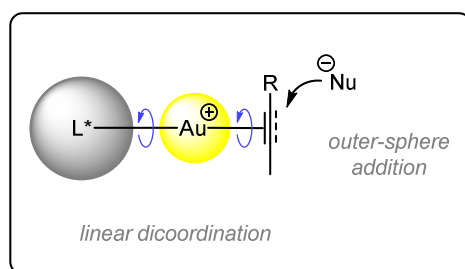
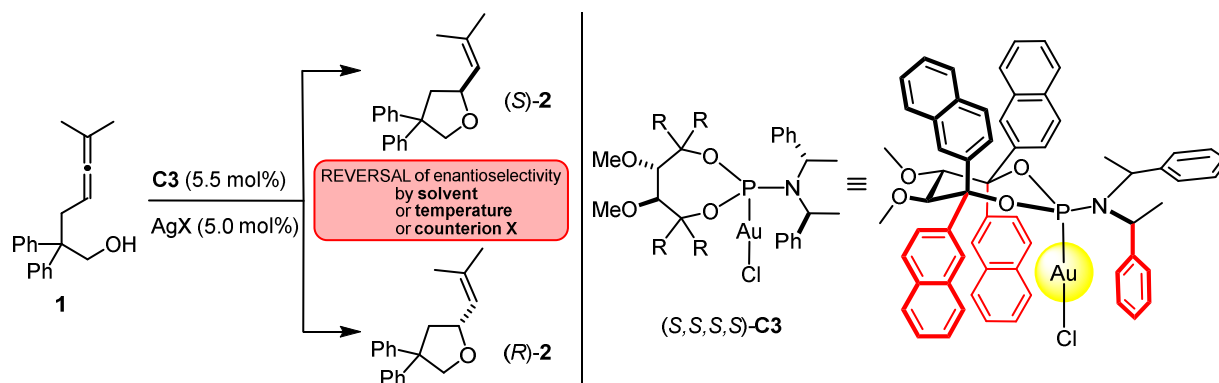


Figure 3.1. Geometrical constraints to asymmetric gold catalysis.

In 2010, Fürstner and coworkers reported a new type of phosphoramidites, featuring a TADDOL-related but acyclic backbone, as one-point binding ligands for asymmetric gold catalysis.^[7b] The derived complexes, for instance **C3**, proved successful in various transformations such as cycloadditions, enyne cycloisomerizations, indoline syntheses and hydroaminations of allenes.^[7c,8] During the application to the intramolecular hydroalkoxylation, a striking case of enantioinversion was observed: the sense of induction in the cyclization of allenol **1** to tetrahydrofuran **2** could be

swapped from (*S*) to (*R*) solely by changing either the solvent or the temperature or the escorting counterion, while using the very same chiral gold complex **C3** (Scheme 3.1).



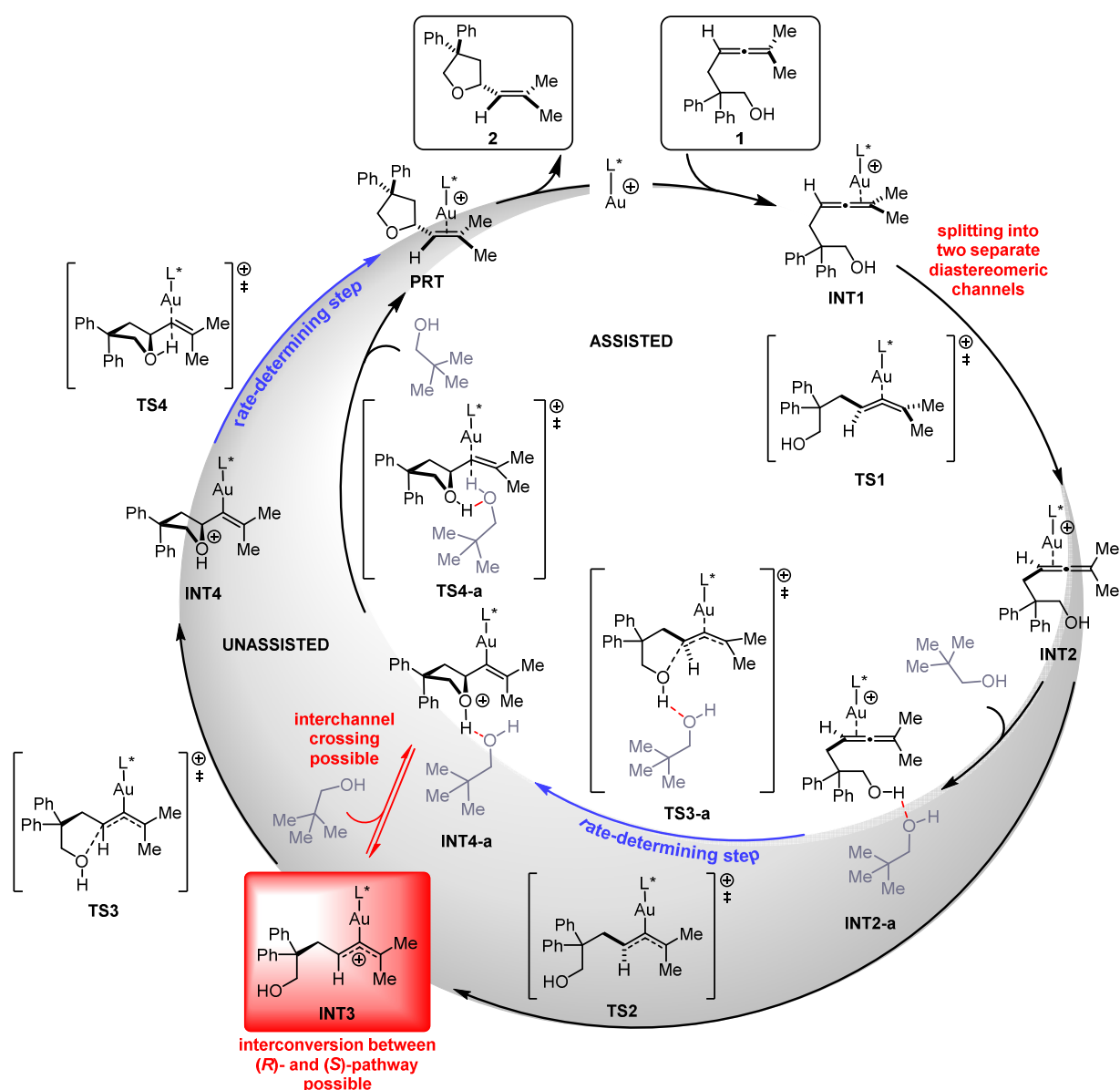
Scheme 3.1. Gold-catalyzed hydroalkoxylation subject to immense enantioinversion; R = 2-naphthyl.

The perplexing phenomenon of enantioinversion, in which a single chiral source delivers either enantiomer of a given product, is not uncommon.^[18d,41,217] However, the understanding of its origins at the molecular level is quite limited. Moreover, the present case seemed particularly remarkable, since it represents the first reported example in which three different parameters are able to trigger a significant switch. Therefore, a detailed mechanistic study was conducted to unravel the underlying secrets.

Thorough screenings of solvent, temperature and counterion indicated that these three parameters can also act in synergy providing either antipode of product **2** in meaningful to outstanding optical purity: (*R*)-**2** was obtained in 97% *ee* in EtOH at $-60\text{ }^{\circ}\text{C}$ and (*S*)-**2** in 68% *ee* in EtOAc at $22\text{ }^{\circ}\text{C}$, both using complex (*S,S,S,S*)-**C3** as precatalyst and AgBF_4 for its activation. Substrates with different substitution pattern and ring size behaved similarly, but showed a less pronounced switch. Thus, allenol **1** was used as a model for further mechanistic studies. Control experiments confirmed that the *ee* changed neither with conversion nor on prolonged exposure of the product to the catalyst, and that *ee* of the precatalyst and *ee* of the product show a linear correlation at both high and low temperature. The temperature dependence of the enantioselectivity was further investigated by Eyring studies, which allowed the enthalpic and entropic contributions to the differential activation free energies to be derived. The findings point toward a remarkable entropic component which was analyzed in more detail by means of DFT calculations.^[42]

The major reason for the enantioinversion was found in the existence of two competing pathways: a pathway where proto-deauration is rate-determining favors the (*S*)-product, whereas an alternative outlet involving assisted proto-deauration preferably produces the (*R*)-product.^[17] Such assistance can be provided either by a protic solvent, a coordinating counterion or a second substrate molecule

and accounts for the observed entropic component. In the unassisted pathway, an interconversion between the diastereomeric channels accounting for the (*S*)- and the (*R*)-product is possible at the allyl cation stage **INT3**. In the assisted pathway, this intermediate is bypassed and facile interconversion essentially impossible. A channel crossing between the unassisted and assisted pathway is however feasible, since association of a second substrate molecule at the allyl cation stage **INT3** is energetically accessible. This explains a transition to the assisted pathway at low temperature, for which the entropic component to the reaction free energy profile is significantly increased and can ultimately dictate the stereochemical course. In summary, the computational results, which were also calibrated against NMR spectroscopic data,^[44] provide a plausible mechanistic scenario and allow rationalizing the experimental observations (Scheme 3.2).^[17]



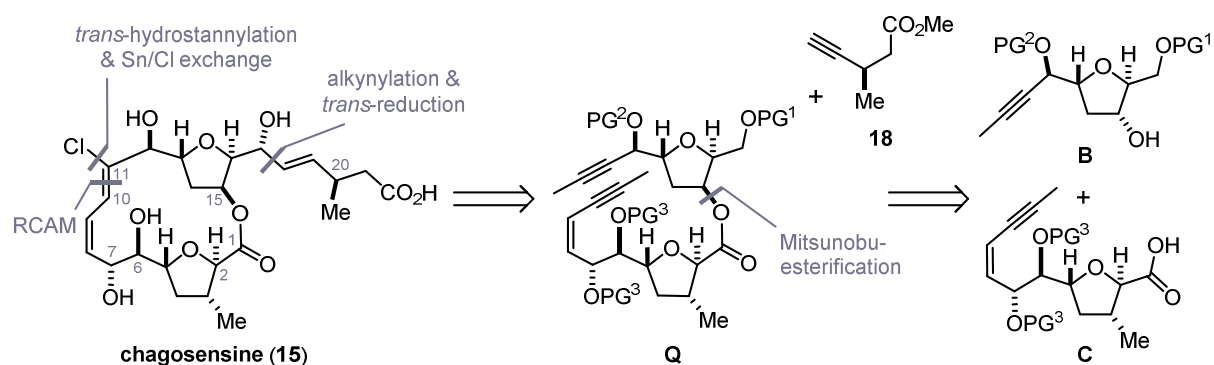
Scheme 3.2. Plausible mechanistic scenario: outer cycle unassisted pathway (grey); inner cycle assisted pathway (white); possible interchannel crossing at the allyl cation intermediate (red).

This case study represents the first example that explains the unusual effect of enantioinversion at the molecular level *via* a combined experimental and theoretical approach. Although the present case is fairly specific, an important lesson can be learned: for the understanding of a multi-step mechanism, one has to consider the whole reaction coordinate rather than merely sterics in the transition state, where the critical parameter of entropy is often underestimated.

3.2 Studies Toward the Total Synthesis of Chagosensine

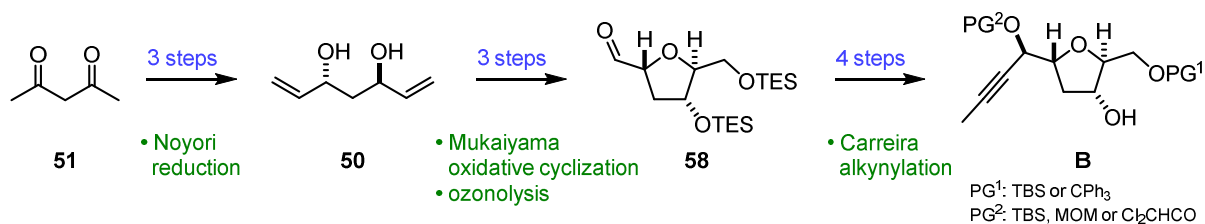
During the course of this thesis, ring closing alkyne metathesis (RCAM)^[65] and postmetathetic *trans*-selective hydrometalations^[75c] were investigated in the context of a challenging total synthesis campaign. The marine polyketide chagosensine (**15**) was deemed an ideal target for this sequence of transformations in order to access the unique (*Z,Z*)-chlorodiene motif within a highly substituted macrocycle.^[80] An additional obstacle to this endeavor was posed by the unsecured structure assignment of the natural product, whose synthesis had not been tackled before.

The original synthetic strategy was based on a key sequence comprising RCAM, *trans*-hydrostannylation and tin/chloride exchange. A convergent synthesis with late stage fragment assembly was designed, which would also provide access to other diastereomers, if necessary. The envisioned key sequence should precede the installation of the sidechain **18**. Further disconnections of the advanced intermediate **Q** divide the molecule into a northern alcohol **B** and a southern carboxylic acid fragment **C** as the key building blocks (Scheme 3.3).



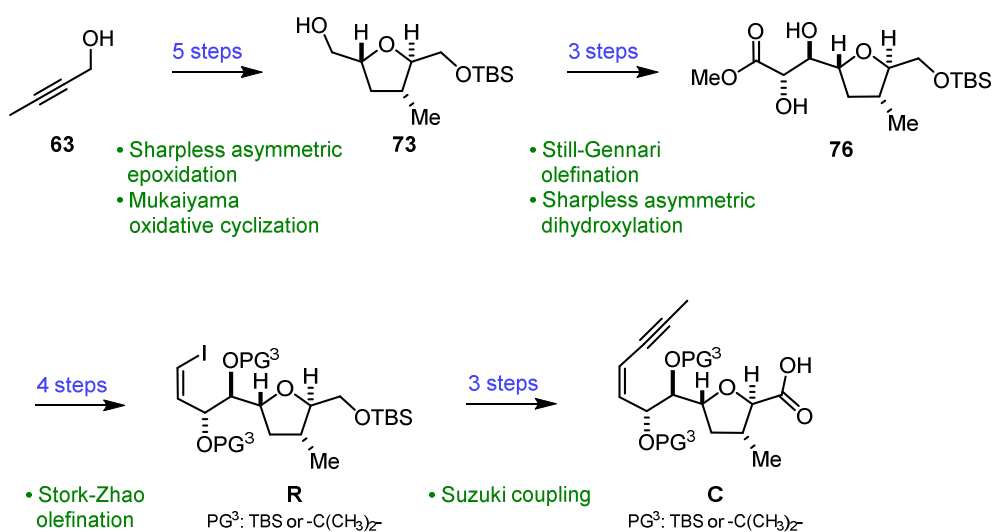
Scheme 3.3. Initially proposed retrosynthetic analysis of chagosensine; PG = protecting group.

The northern alcohol fragment **B** was prepared from the literature-known *anti*-diol **50**, which can be obtained in three steps from commercial acetyl acetone (**51**).^[104,105c] The *trans*-THF moiety was installed *via* cobalt-catalyzed Mukaiyama aerobic oxidative cyclization.^[110] After protection of the resulting diol, ozonolysis of the remaining double bond gave rise to aldehyde **58**. The methyl-capped alkyne was introduced by Carreira alkylation using propyne.^[77] Protecting group manipulations provided a library of secondary alcohols in ten steps (Scheme 3.4).



Scheme 3.4. Synthesis of the northern alcohol fragment **B**; PG = protecting group.

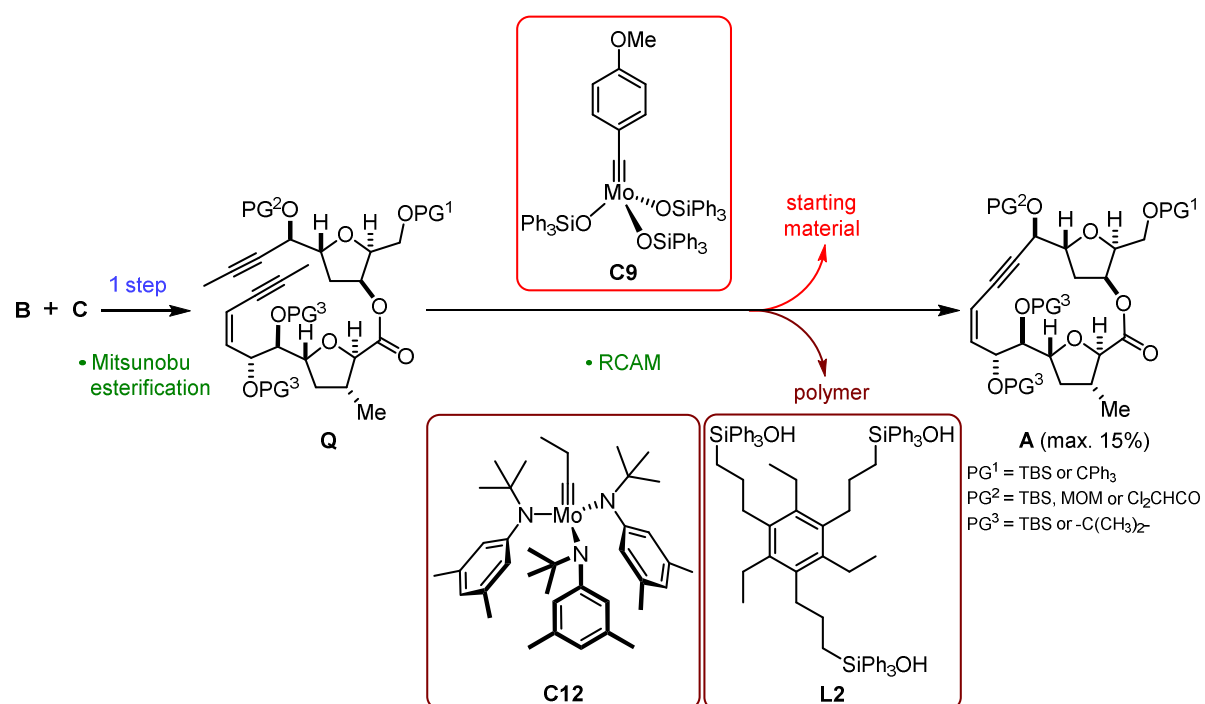
The synthesis of the southern fragment started with the semi-hydrogenation of 2-butyne-1-ol (**63**) followed by Sharpless asymmetric epoxidation.^[111,122] After TBS-protection of the primary alcohol, regioselective epoxide opening and subsequent Mukaiyama oxidative cyclization afforded *trans*-THF-ring **73**. A sequence comprising oxidation of the primary alcohol, Still-Gennari olefination and Sharpless asymmetric dihydroxylation provided *anti*-diol **76**.^[111] Protection of the diol as either TBS-ethers or cyclic acetal preceded adjustment of the oxidation state and Stork-Zhao olefination to produce (*Z*)-vinyl iodide **R**. Suzuki coupling^[152] gave rise to the corresponding enyne, before cleavage of the TBS-ether and oxidation to the carboxylic acid completed the 15-step synthesis of fragment **C** with an overall yield of 6% (Scheme 3.5).



Scheme 3.5. Synthesis of the southern fragment **C**; PG = protecting group.

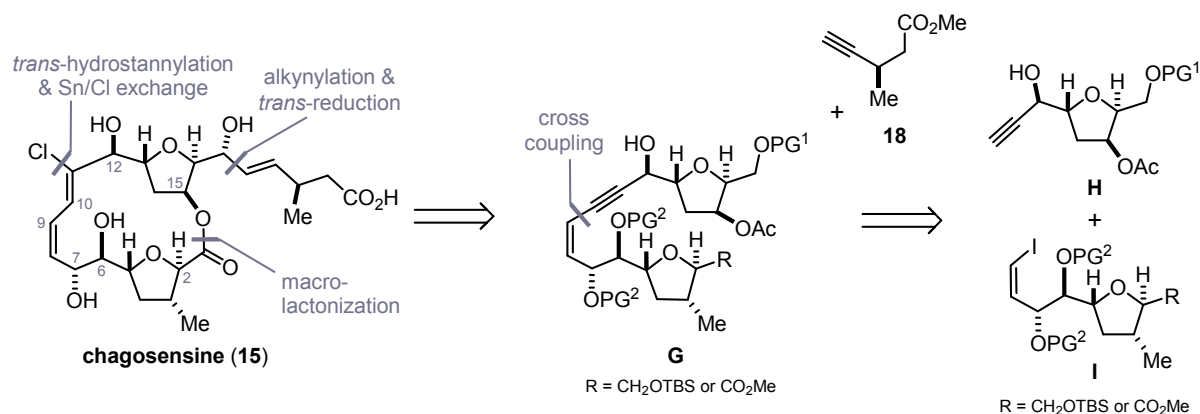
The two fragments were assembled by Mitsunobu esterification, setting the stage for the projected enyne-yne metathesis of **Q**, which exhibits oxygen functionalities adjacent to both π -systems. Such motifs proved particularly challenging and the latest generation of molybdenum catalysts endowed with silanolate ligands such as **C9**^[69b] was found incompetent to induce ring closure on appropriate model substrates. This issue has inspired further catalyst development, which was advanced in parallel to this work.^[96] Key to success was a new catalyst design based on multidentate silanolate ligands. Despite lacking a well-defined solid-state structure, precatalyst **C12** and ligand **L2** could be used for alkyne metathesis, efficiently cyclizing model substrates for the chagosensine

macrolactone.^[92b] However, the novel two-component catalyst system failed in the attempted ring closing events of the highly complex enyne-yne **Q** (Scheme 3.6). In contrast to the previous catalyst generation, the substrates were not unreactive but underwent rapid polymerization. Solely for a MOM-protected propargylic alcohol, the macrocyclic monomer could be isolated in 15% yield. Screening of other available RCAM catalysts under various reaction conditions did not improve this result. Neither switching or removing the protecting group on the propargylic alcohol nor replacing the bulky TBS-ethers of the southern diol by an acetonide could assist the cyclization. At this stage, it seems likely that the highly strained enyne macrocycle as well as the unusual density of potentially coordinating functional groups prevent a productive macrocyclization.



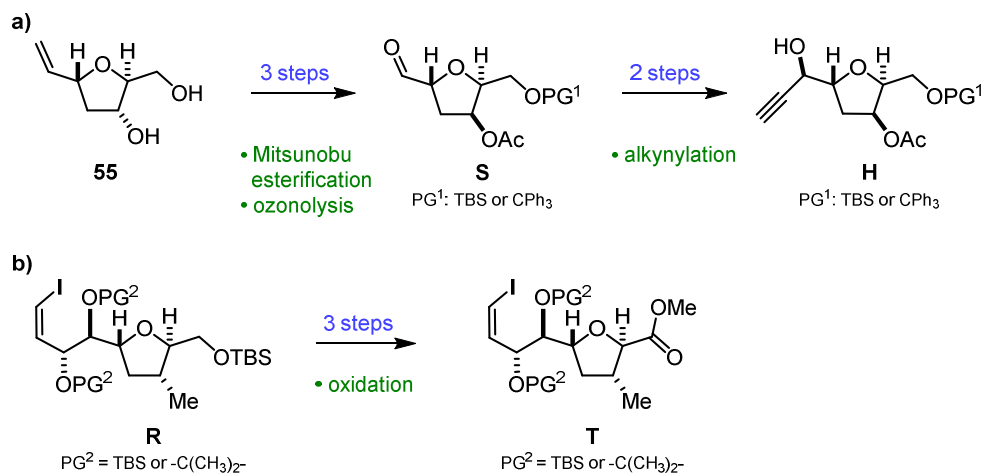
Scheme 3.6. Fragment assembly and attempted RCAM; PG = protecting group.

Consequently, an alternative strategy was conceived in order to avoid strained intermediates. The installation of the (*Z,Z*)-chlorodiene should precede ring closure, which had to be accomplished by macrolactonization.^[211] The convergent design of the initial synthetic plan provided flexibility for the endgame tactics, largely maintaining the individual building blocks and the late stage introduction of the sidechain **18**. The acyclic enyne **G** was planned to be accessed through cross coupling between terminal alkyne **H** and vinyl iodide **I** (Scheme 3.7).



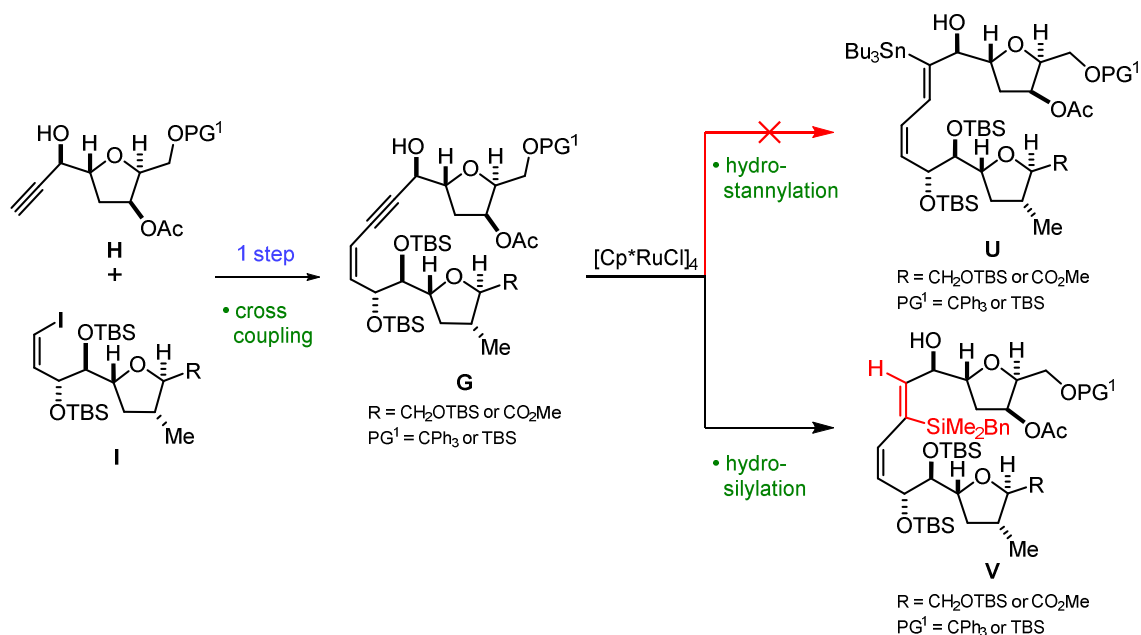
Scheme 3.7. Revised retrosynthetic analysis of chagosensine; PG = protecting group.

The required modifications at the northern fragment **H** were achieved starting from *trans*-THF **55**. Mono-protection and Mitsunobu esterification of the secondary alcohol with acetic acid followed by ozonolysis afforded aldehyde **S**. Substrate-controlled alkylation and desilylation provided the terminal alkyne **H** in nine steps (Scheme 3.8, a)). Vinyl iodide **R** could serve as coupling partner before or after elaboration to the methyl ester **T** by deprotection, oxidation and methylation (Scheme 3.8, b)).



Scheme 3.8. Synthesis of a) the modified northern fragment **H** and b) the southern fragment **T**; PG = protecting group.

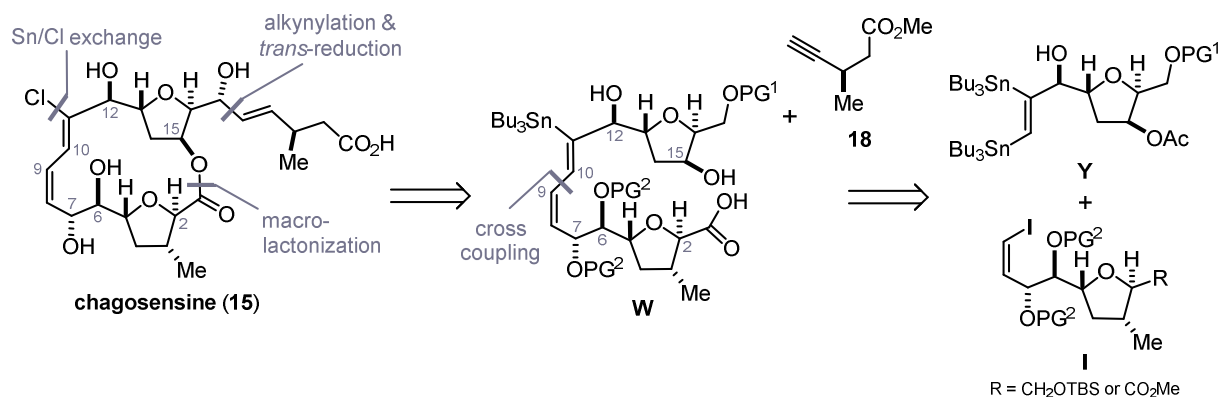
Subsequent fragment assembly by means of Sonogashira cross coupling was cumbersome, even under conditions avoiding copper co-catalysis. Moreover, the obtained acyclic enynes failed to succumb to ruthenium-catalyzed *trans*-hydrostannylations, while hydrosilylations gave rise to the undesired regioisomer (Scheme 3.9).



Scheme 3.9. Fragment assembly and attempted *trans*-hydrometalations; PG = protecting group.

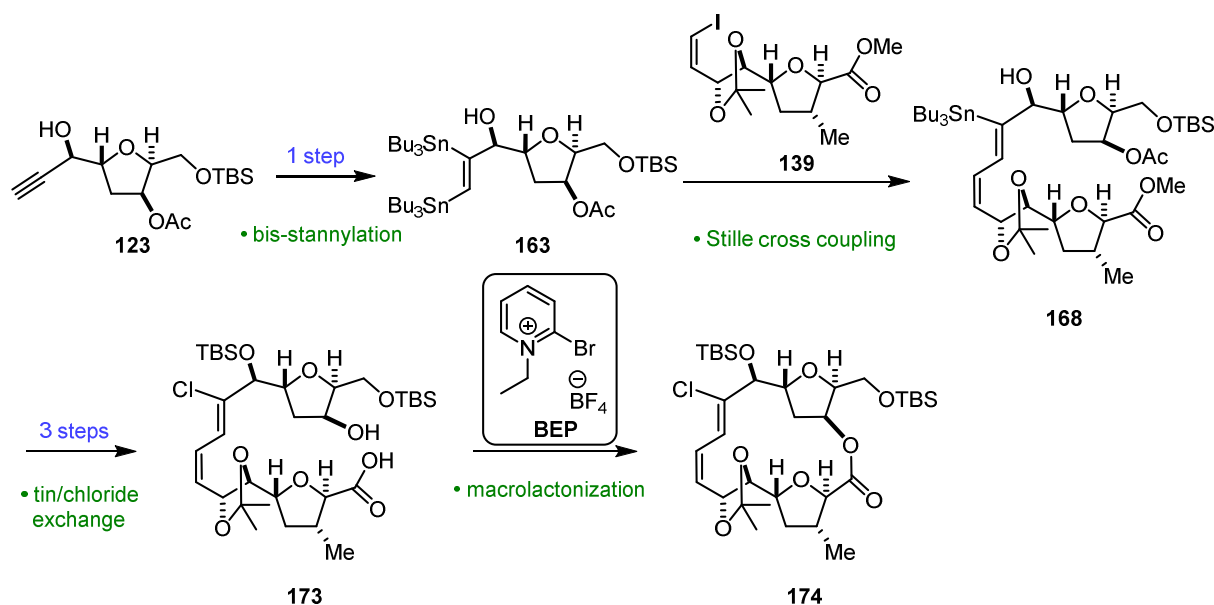
This result can be rationalized based on the numerous potentially coordinating functional groups that trap and therefore inactivate the ruthenium catalyst. Furthermore, the crucial intermolecular hydrogen bonding between the propargylic hydroxy group and the chloride ligand of the ruthenium catalyst seems to be unavailable due to competitive intramolecular hydrogen bonding. Thus far, conditions to influence the unfavorable setting were only found for α -THF-propargylic alcohols, a structural motif frequently displayed in marine macrolides.

Since both enyne-based approaches to construct the intricate chlorodiene had failed, another route was investigated (Scheme 3.10). The chlorodiene should be obtained by tin/chloride exchange prior to macrolactonization and installation of the sidechain. Scission of the C9–C10 bond divided the crucial acyclic dienylstannane **W** into bis-stannane **Y** and southern vinyl iodide **I**.



Scheme 3.10. Ultimately successful retrosynthetic analysis of chagosensine; PG = protecting group.

Palladium-catalyzed bis-stannylation^[203f] of **123** followed by a selective Stille cross coupling with **139** furnished dienylstannane **168**. Tin/chloride exchange gave rise to the (*Z,Z*)-chlorodiene, which was elaborated to the secoacid **173** by protection and saponification. Preliminary studies on the challenging cyclization provided the desired macrolactone **174** under forcing conditions following the Evans-modified Mukaiyama procedure^[215] (Scheme 3.11).



Scheme 3.11. Successful route to macrolactone **174**.

This strategy has finally given access to the key macrocyclic (*Z,Z*)-chlorodiene, which was unambiguously characterized by HRMS and NMR spectroscopy. The observation of transannular NOE contacts highlights the crowded and strained nature of the 16-membered macrolactone. Future work will focus on the optimization and the elaboration of the remaining steps to complete the total synthesis, which will ultimately allow for structure validation and preliminary biological testing.

The synthetic studies toward the challenging macrolide chagosensine have pushed the boundaries of two recent methodologies. For both RCAM and ruthenium-catalyzed hydrometalations, new substrate classes have been made available through catalyst development or adjustment of reaction conditions. During the course of this thesis, however, it was not possible to successfully apply these transformations *en route* to chagosensine. The highly decorated and complex framework found in this specific natural product prohibited the use of conventional approaches, such as RCAM, RCM^[155] and Sonogashira reactions, which all failed despite enormous efforts. Only the design of a route employing a bis-metalated northern domain in the cross coupling event for fragment assembly followed by macrolactonization resulted in the successful synthesis of the macrocycle of chagosensine. The work reported herein has overcome the major obstacles and provides a promising perspective for the total synthesis of chagosensine, which seems now within reach.

4 Experimental Section

4.1 General Experimental Methods

All reactions were carried out under Ar in flame-dried glassware, unless H₂O was used as solvent or otherwise noted. The following solvents and organic bases were purified by distillation over the drying agents indicated and were transferred under Ar: THF, Et₂O (Mg/anthracene); hexanes, toluene (Na/K); triethylamine, diisopropylamine, diisopropylethylamine, HMPA, DMSO, CH₂Cl₂, DMA (CaH₂); MeOH, EtOH, *i*-PrOH (Mg, stored over 3 Å MS). DMF, 1,4-dioxane, MeCN and pyridine were dried by an adsorption solvent purification system based on molecular sieves. All other commercially available compounds (ABCR, Acros, Alfa Aesar, Aldrich, Fluka, STREM, TCI) were used as received unless otherwise noted. The following compounds were prepared according to the cited protocol by myself or within the department of Prof. Fürstner: **C9**,^[69a] **C10**,^[69a] **C8**,^[66a] **C12**,^[68] **L1**,^[92b] **L2**,^[92b] Co(nmp)₂,^[110] PPh₃CH₂I₂,^[218] Me₂BBr,^[219] Pd(PPh₃)₄,^[220] [Cp**Ru*Cl]₄, [RuCl₂((*S*)-BINAP)]₂·Et₃N,^[106a] Pd(*t*-BuNC)₂Cl₂.^[221]

Thin layer chromatography (TLC) was performed on Macherey-Nagel precoated plates (POLYGRAM® SIL/UV254). Detection was achieved under UV light (254 nm) and by staining with acidic *p*-anisaldehyde, acidic cerium-ammonium-molybdenate or basic KMnO₄ solutions.

Flash chromatography was performed with Merck silica gel 60 (40-63 μm pore size) using pre-distilled or HPLC-grade solvents. In some cases, fine Merck silica gel 60 (15-40 μm pore size) was necessary as indicated within the experimental procedures.

NMR spectra were recorded on Bruker DPX 300, AMX 300, AV 400, AV 500 or AVIII 600 spectrometers in the solvents indicated. Chemical shifts (δ) are reported in ppm relative to TMS; coupling constants (*J*) are given in Hz. The solvent signals were used as references and the chemical shifts converted to the TMS scale (CDCl₃: δ_H ≡ 7.26 ppm, δ_C ≡ 77.16 ppm; CD₂Cl₂: δ_H ≡ 5.32 ppm, δ_C ≡ 53.84 ppm; C₆D₆: δ_H ≡ 7.16 ppm, δ_C ≡ 128.06 ppm). Multiplets are indicated by the following abbreviations: s: singlet, d: doublet, t: triplet, q: quartet, quint: quintet, hept: heptet, m: multiplet. The abbreviation br indicates a broad signal. ¹³C spectra were recorded in [¹H]-decoupled mode and the values of the chemical shifts are rounded to one decimal point. All spectra from 500 MHz and 600 MHz spectrometers were acquired by the NMR department under the guidance of Dr. Christophe Farès at the Max-Planck-Institut für Kohlenforschung.

IR spectra were recorded on Alpha Platinum ATR (Bruker) at room temperature, wavenumbers (ν̃) are given in cm⁻¹.

Mass spectrometric samples were measured by the department for mass spectrometry at the Max-Planck-Institut für Kohlenforschung using the following devices: MS (EI): Finnigan MAT 8200 (70 eV), ESI-MS: Bruker ESQ3000, accurate mass determinations: Bruker APEX III FT-MS (7 T magnet) or MAT 95 (Finnigan).

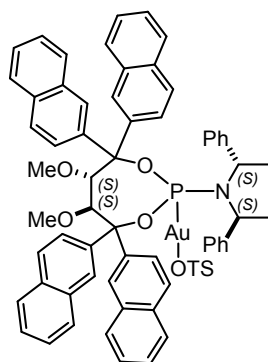
Optical rotations were measured with a Perkin-Elmer model 343 or an A-Krüß Optronic Model P8000-t polarimeter at a wavelength of 589 nm. The values are given as specific optical rotation with exact temperature, concentration ($c/(10 \text{ mg/mL})$) and solvent.

Melting points (m.p.) were measured on a Büchi Melting Point B-540 and are uncorrected.

4.2 Enantioinversion in the Gold(I)-catalyzed Hydroalkoxylation of Allenes

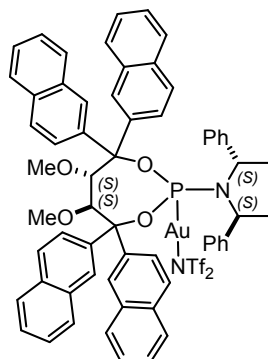
The catalysts were prepared as previously reported by our group;^[7b,7c,8] the preparation of (*S,S,S,S*)-**C5** and (*S,S,S,S*)-**C6** is described below:

Pre-activated catalyst (*S,S,S,S*)-C5. Silver tosylate (7.6 mg, 27 μmol) was added to a solution of gold



catalyst (*S,S,S,S*)-**C3** (31 mg, 27 μmol) in anhydrous CH_2Cl_2 (0.3 mL) at room temperature. The resulting pale yellow solution was stirred at ambient temperature for 15 min, then filtered over a pad of Celite® eluting with CH_2Cl_2 (10 mL). The solvent was removed under reduced pressure affording the catalyst as an amorphous yellow solid (34 mg, 98%). ^1H NMR (400 MHz, CD_2Cl_2): δ = 8.47 (s, 1H), 8.28 (s, 1H), 8.01 (s, 1H), 7.97–7.73 (m, 14H), 7.73–7.64 (m, 4H), 7.58–7.45 (m, 12H), 7.44–7.34 (m, 2H), 7.21–7.15 (m, 3H), 7.03–6.93 (m, 4H), 5.65 (d, J = 7.3 Hz, 1H), 5.18–5.06 (m, 2H), 4.87 (d, J = 7.3 Hz, 1H), 3.39 (s, 3H), 2.55 (s, 3H), 2.37 (s, 3H), 1.91 ppm (d, J = 7.1 Hz, 6H). ^{31}P NMR (162 MHz, CD_2Cl_2): δ = 95.8 ppm.[†]

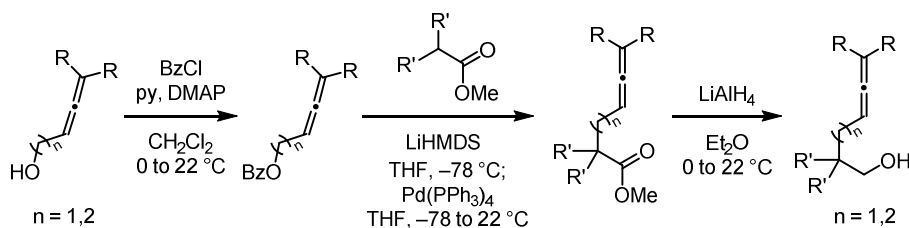
Pre-activated catalyst (*S,S,S,S*)-C6. To a solution of gold catalyst (*S,S,S,S*)-**C3** (31 mg, 27 μmol) in



anhydrous CH_2Cl_2 (0.3 mL) at room temperature was added silver tosylate (10 mg, 27 μmol). The resulting pale yellow solution was stirred at ambient temperature for 15 min, then filtered over a pad of Celite® eluting with CH_2Cl_2 (10 mL). The solvent was removed under reduced pressure affording the catalyst as an amorphous yellow solid (35 mg, 92%). ^1H NMR (400 MHz, CD_2Cl_2): δ = 8.26 (s, 1H), 8.09 (s, 1H), 7.94–7.73 (m, 14H), 7.59–7.39 (m, 12H), 7.18–7.13 (m, 2H), 7.13–7.03 (m, 8H), 5.44 (d, J = 6.8 Hz, 1H), 5.20–5.08 (m, 2H), 5.05 (d, J = 6.7 Hz, 1H), 3.50 (s, 3H), 2.59 (s, 3H), 1.92 ppm (d, J = 7.1 Hz, 6H). ^{31}P NMR (162 MHz, CD_2Cl_2): δ = 103.8 ppm.[†]

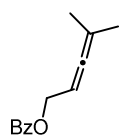
[†] For comparison: ^{31}P NMR of (*S,S,S,S*)-**C3** (162 MHz, CD_2Cl_2): δ = 113.8 ppm.

All substrates were prepared by a three-step protocol starting from commercial 5-methyl-3,4-hexadien-1-ol or literature-known 4-cyclo-hexylidenebut-3-en-1-ol,^[222] 3-cyclohexylidene-prop-2-en-1-ol^[223] or 4-methylpenta-2,3-dien-1-ol^[224] (Scheme 4.1).



Scheme 4.1 Preparation of the hydroxy-allene substrates.

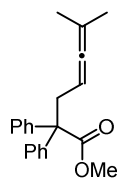
4-Methylpenta-2,3-dien-1-yl benzoate (S1). Pyridine (1.00 mL, 12.2. mmol) and DMAP (125 mg,



1.02 mmol, 10 mol%) were added to a solution of 4-methylpenta-2,3-dien-1-ol (1.00 g, 10.2 mmol) in CH₂Cl₂ (10 mL) at 0 °C. Finally, benzoyl chloride (1.78 mL, 15.3 mmol) was added dropwise and the resulting yellow suspension was stirred at ambient temperature for 15 h. The reaction was quenched with aq. sat. NH₄Cl solution (10 mL) and the aqueous layer extracted with CH₂Cl₂ (3 x 15 mL). The combined extracts were washed with HCl (1 M, 10 mL), NaOH (1 M, 10 mL) and brine (25 mL), dried over Na₂SO₄, filtered and concentrated. The residue was purified by flash chromatography (hexanes/*t*-butyl methyl ether 50:1) to yield benzoate **S1** as a pale yellow oil (1.59 g, 77%).

¹H NMR (400 MHz, CDCl₃): δ = 8.07–8.03 (m, 2H), 7.57–7.53 (m, 1H), 7.45–7.42 (m, 2H), 5.22 (tsept, *J* = 6.4, 2.8 Hz, 1H), 4.76 (d, *J* = 6.4 Hz, 2H), 1.70 ppm (d, *J* = 2.8 Hz, 6H). ¹³C NMR (100 MHz, CDCl₃): δ = 203.5, 166.5, 133.0, 130.6, 129.7, 129.7, 128.6, 128.4, 97.6, 85.0, 63.8, 20.4 ppm. IR (film): $\tilde{\nu}$ = 2938, 1715, 1602, 1584, 1451, 1362, 1315, 1268, 1176, 1108, 1068, 1025, 939, 804, 707, 686, 581, 543 cm⁻¹. MS (EI) *m/z* (%): 105 (100), 77 (28). HRMS (EI): *m/z* calcd for C₁₃H₁₄O₂: 202.0994, found: 202.0992. The analytical and spectroscopic data are in agreement with those reported in the literature.^[225]

Allene ester S2. A solution of LiHMDS (1.24 g, 7.42 mmol) in THF (10 mL) was added dropwise over



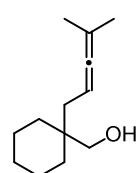
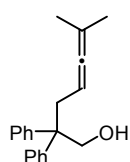
15 min to a solution of methyl diphenylacetate (1.68 g, 7.42 mmol) in THF (20 mL) at –78 °C and the resulting mixture was stirred at this temperature for 1.5 h. In a second flask, Pd(PPh₃)₄ (214 mg, 0.19 mmol, 5 mol%) was dissolved in THF (5 mL) and a solution of allene benzoate **S1** (750 mg, 3.71 mmol) in THF (5 mL) was added. The resulting mixture was stirred for 30 min at ambient temperature, before it was added to the enolate solution at –78 °C *via* syringe. The mixture was warmed to room temperature and stirred overnight. The reaction was quenched with aq. sat. NH₄Cl solution (20 mL) and the aqueous layer extracted with *t*-butyl methyl ether (3 x 25 mL). The combined extracts were washed with brine (50 mL), dried over

Na_2SO_4 , filtered and concentrated. The residue was purified by flash chromatography (hexanes/*t*-butyl methyl ether 40:1) to furnish the title compound as a colorless oil (715 mg, 63%). ^1H NMR (400 MHz, CDCl_3): δ = 7.30–7.27 (m, 5H), 7.25–7.20 (m, 5H), 4.72–4.65 (m, 1H), 3.68 (s, 3H), 3.06 (d, J = 7.5 Hz, 2H), 1.46 ppm (d, J = 2.8 Hz, 6H). ^{13}C NMR (100 MHz, CDCl_3): δ = 203.8, 174.7, 142.5, 129.2, 127.9, 126.9, 94.6, 84.6, 60.6, 52.6, 39.2, 20.3 ppm. IR (film): $\tilde{\nu}$ = 2958, 2853, 1730, 1599, 1495, 1446, 1362, 1275, 1218, 1036, 859, 813, 788, 750, 729, 697, 662, 612, 575, 501 cm^{-1} . MS (EI) m/z (%): 306 (33), 275 (12), 274 (27), 263 (15), 248 (21), 247 (100), 246 (20), 232 (19), 231 (36), 225 (39), 205 (37), 203 (10), 197 (44), 166 (15), 165 (52), 157 (11), 105 (26), 91 (25), 77 (12). HRMS (ESIpos): m/z calcd for $\text{C}_{21}\text{H}_{22}\text{O}_2\text{Na}$: 329.1512, found: 329.1511.

Hydroxy-allene 1. A solution of ester **S2** (840 mg, 2.74 mmol) in Et_2O (4 mL) was added dropwise to a suspension of LiAlH_4 (520 mg, 13.7 mmol) in Et_2O (8 mL) at 0 °C. The resulting mixture was allowed to warm to ambient temperature and stirred overnight. After cooling to 0 °C, the reaction was carefully quenched with H_2O (0.52 mL) followed by NaOH (10%, 0.52 mL) and H_2O (1.56 mL). The resulting suspension was stirred for 1 h before it was filtered through a pad of Celite®, eluting with *t*-butyl methyl ether (20 mL). The combined filtrates were concentrated and the residue purified by flash chromatography (hexanes/*t*-butyl methyl ether 19:1) to give alcohol **1** as a colorless oil that solidified upon standing (735 mg, 96%). m.p. [*t*-butyl methyl ether] = 49–50 °C. ^1H NMR (400 MHz, CDCl_3): δ = 7.35–7.31 (m, 4H), 7.28–7.24 (m, 6H), 4.68–4.64 (m, 1H), 4.24 (s, 2H), 2.91 (d, J = 7.1, 2H), 1.61 (d, J = 2.5, 6H), 1.43 ppm (brs, 1H). ^{13}C NMR (100 MHz, CDCl_3): δ = 203.6, 145.3, 128.4, 128.3, 126.4, 94.5, 84.5, 68.4, 52.3, 37.4, 20.5 ppm. IR (film): $\tilde{\nu}$ = 3581, 3475, 3083, 3055, 2974, 2921, 2880, 1971, 1952, 1884, 1807, 1598, 1577, 1493, 1443, 1377, 1363, 1308, 1227, 1189, 1154, 1121, 1105, 1072, 1035, 1017, 1004, 951, 907, 885, 818, 771, 755, 732, 691 cm^{-1} . MS (EI) m/z (%): 278 (23), 263 (34), 248 (34), 233 (63), 205 (100), 179 (28), 178 (32), 165 (31), 157 (24), 115 (41), 103 (25), 91 (61), 83 (34), 77 (22), 69 (80). HRMS (ESIpos): m/z calcd for $\text{C}_{20}\text{H}_{22}\text{ONa}$: 301.1568, found: 301.1570. The analytical and spectroscopic data are in agreement with those reported in the literature.^[15c,226]

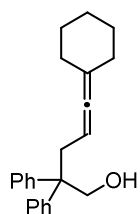
All other hydroxy-allenes were prepared analogously. Their spectral and analytical data are summarized below.

Hydroxy-allene S3. The crude material was purified by flash chromatography (pentane/*t*-butyl methyl ether 10:1) to give hydroxy-allene **S3** (87%) as a colorless oil. ^1H NMR (400 MHz, CD_2Cl_2): δ = 4.91 (thept, J = 10.9, 2.8, 1H), 3.41 (d, J = 3.7, 2H), 1.99 (d, J = 8.1, 2H), 1.67 (d, J = 3.2, 6H), 1.54 (brs, 1H), 1.46–1.42 (m, 5H), 1.36–1.28 ppm (m, 6H). ^{13}C NMR (100 MHz, CD_2Cl_2): δ = 203.3, 94.2, 84.8, 68.9, 38.3, 35.5, 32.5, 26.8, 21.8, 20.7 ppm. IR (film): $\tilde{\nu}$ = 3356, 2977, 2924, 2851, 1972, 1965, 1451, 1403, 1362, 1237, 1214, 1188, 1134, 1112,



1034, 1027, 1008, 975, 923, 894, 847, 829, 805, 704, 655 cm^{-1} . MS (EI) m/z (%): 180 (12), 179 (100), 95 (13), 85 (11), 83 (11), 81 (16), 69 (89), 67 (21), 55 (14), 41 (20). HRMS (ESIpos): m/z calcd for $\text{C}_{13}\text{H}_{22}\text{O}$: 194.1669, found: 194.1671.

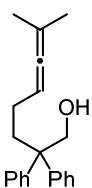
Hydroxy-allene S4. The crude material was purified by flash chromatography (hexanes/EtOAc 10:1)



to give the title compound as a white solid (93%). m.p. [EtOAc] = 78–79 °C. ^1H NMR (400 MHz, CDCl_3): δ = 7.32–7.27 (m, 4H), 7.23–7.19 (m, 6H), 4.62 (tt, J = 7.6, 2.1 Hz, 1H), 4.20 (d, J = 6.7, 2H), 2.88 (d, J = 7.6 Hz, 2H), 1.98–1.95 (m, 4H), 1.54–1.46 (m, 6H), 1.30 ppm (t, J = 6.7 Hz, 1H). ^{13}C NMR (100 MHz, CDCl_3): δ = 200.5, 145.9, 128.6, 128.4, 126.5, 102.1, 84.5, 68.4, 52.4, 37.8, 31.7, 27.8, 26.5 ppm. IR (film): $\tilde{\nu}$ = 3558, 3470,

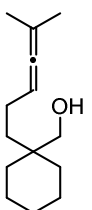
3059, 3021, 2921, 2880, 2851, 2832, 1963, 1597, 1575, 1494, 1470, 1443, 1323, 1260, 1234, 1104, 1069, 1045, 1024, 977, 919, 897, 845, 834, 805, 769, 755, 695 cm^{-1} . MS (EI) m/z (%): 288 (20), 287 (81), 227 (37), 205 (33), 201 (27), 197 (59), 196 (35), 179 (18), 178 (19), 167 (23), 165 (35), 141 (23), 105 (91), 91 (100), 79 (20), 77 (34), 67 (15). HRMS (ESIpos) m/z calcd for $\text{C}_{23}\text{H}_{26}\text{O}$: 318.1982, found: 318.1984. The analytical and spectroscopic data are in agreement with those reported in the literature.^[227]

Hydroxy-allene 3. The crude material was purified by filtration through a short plug of SiO_2 (*t*-butyl



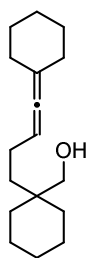
methyl ether) to give the title compound as a colorless oil (99%). ^1H NMR (400 MHz, CDCl_3): δ = 7.33–7.29 (m, 4H), 7.24–7.19 (m, 6H), 4.94–4.89 (m, 1H), 4.16 (brs, 2H), 2.28–2.23 (m, 2H), 1.75–1.69 (m, 2H), 1.68 (d, J = 2.9 Hz, 6H), 1.17 ppm (brs, 1H). ^{13}C NMR (100 MHz, CDCl_3): δ = 201.5, 145.6, 128.4, 128.3, 126.5, 95.6, 89.0, 68.5, 52.2, 36.0, 24.5, 20.9 ppm. IR (film): $\tilde{\nu}$ = 3553, 3411, 3087, 3057, 3024, 2976, 2930, 2907, 2861, 1970, 1958, 1950, 1878, 1807, 1598, 1579, 1495, 1444, 1386, 1361, 1232, 1188, 1157, 1039, 1023, 1003, 908, 847, 801, 755, 697 cm^{-1} . MS (EI) m/z (%): 205 (10), 183 (23), 180 (10), 179 (12), 178 (14), 167 (13), 165 (21), 158 (14), 157 (15), 143 (14), 105 (21), 98 (100), 91 (38), 81 (16), 79 (24), 77 (15), 41 (14). HRMS (ESIpos) m/z calcd for $\text{C}_{21}\text{H}_{24}\text{O}$: 292.1830, found: 292.1827. The analytical and spectroscopic data are in agreement with those reported in the literature.^[223]

Hydroxy-allene S5. The crude material was purified by flash chromatography (pentane/ Et_2O 5:1) to

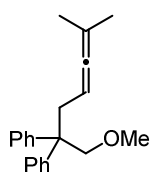


afford the title compound as a colorless oil (79%). ^1H NMR (400 MHz, CD_2Cl_2): δ = 4.99–4.93 (m, 1H), 3.39 (d, J = 5.8 Hz, 2H), 1.92–1.86 (m, 2H), 1.67 (d, J = 2.9 Hz, 6H), 1.45–1.39 (m, 8H), 1.31–1.28 (m, 4H), 1.25–1.22 ppm (m, 1H). ^{13}C NMR (100 MHz, CD_2Cl_2): δ = 201.7, 95.5, 89.9, 68.4, 37.3, 34.8, 32.8, 26.8, 23.5, 21.9, 20.9 ppm. IR (film): $\tilde{\nu}$ = 3395, 2924, 2851, 1969, 1728, 1451, 1375, 1361, 1262, 1230, 1189, 1135, 1044, 1034, 1022, 976, 848, 797, 713 cm^{-1} . MS (EI) m/z (%): 121 (19), 98 (100), 96 (19), 95 (35), 93 (16), 82 (31), 81 (31), 79 (29), 67 (53), 55 (22), 41 (26). HRMS (ESIpos) m/z calcd for $\text{C}_{14}\text{H}_{24}\text{OH}$: 209.1903, found: 209.1905.

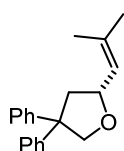
Hydroxy-allene S6. The crude material was purified by flash chromatography (pentane/Et₂O 4:1) to afford the title compound as a colorless oil (82%). ¹H NMR (400 MHz, CD₂Cl₂): δ = 5.00–4.96 (m, 1H), 3.39 (s, 2H), 2.14–2.05 (m, 4H), 1.92–1.86 (m, 2H), 1.60–1.50 (m, 6H), 1.45–1.40 (m, 7H), 1.31–1.29 ppm (m, 5H). ¹³C NMR (100 MHz, CD₂Cl₂): δ = 198.3, 103.2, 89.8, 68.6, 37.3, 34.6, 32.9, 32.2, 28.0, 26.9, 26.6, 23.5, 21.9 ppm. IR (film): $\tilde{\nu}$ = 3382, 2924, 2851, 2358, 1996, 1967, 1714, 1446, 1344, 1264, 1238, 1130, 1034, 979, 931, 895, 850, 797, 737, 704 cm⁻¹. MS (EI) *m/z* (%): 248 (31), 205 (71), 187 (20), 167 (20), 166 (100), 109 (36), 108 (37), 107 (27), 97 (16), 96 (18), 95 (34), 93 (28), 911 (23), 81 (62), 80 (16), 79 (48), 67 (57), 55 (27), 41 (18). HRMS (ESIpos) *m/z* calcd for C₁₇H₂₈O: 248.2141, found: 248.2140.



Allene ether 1-OMe. A solution of hydroxy-allene **1** (175 mg, 0.63 mmol) in THF (1 mL) was added dropwise to a suspension of NaH (18.1 mg, 0.76 mmol) in THF (1 mL) at 0 °C. The mixture was stirred at ambient temperature for 2 h before methyl iodide (78.0 μL, 1.26 mmol) was introduced at 0 °C. The resulting solution was stirred at ambient temperature for another 2 h before it was diluted with *t*-butyl methyl ether (5 mL) and the reaction was quenched with water (5 mL). The aqueous layer was extracted with *t*-butyl methyl ether (3 × 10 mL), and the combined extracts were washed with brine (25 mL), dried over Na₂SO₄, filtered and concentrated. The residue was purified by flash chromatography (hexanes/*t*-butyl methyl ether 50:1) to afford the title compound as a colorless oil that solidified upon standing (128 mg, 70%). m.p. [CHCl₃] = 54–55 °C. ¹H NMR (400 MHz, CD₂Cl₂): δ = 7.29–7.25 (m, 4H), 7.20–7.16 (m, 6H), 4.64–4.58 (m, 1H), 3.99 (s, 2H), 3.31 (s, 3H), 2.87 (d, *J* = 7.6 Hz, 2H), 1.57 ppm (d, *J* = 2.9 Hz, 6H). ¹³C NMR (100 MHz, CD₂Cl₂): δ = 203.9, 146.8, 128.4, 128.2, 126.3, 94.5, 85.0, 78.3, 59.4, 50.9, 37.7, 20.5 ppm. IR (film): $\tilde{\nu}$ = 2979, 2879, 2019, 1597, 1496, 1473, 1443, 1360, 1192, 1135, 1110, 1071, 1029, 985, 940, 795, 775, 754, 739, 698, 629, 615, 571, 504, 423 cm⁻¹. MS (EI) *m/z* (%): 248 (20), 247 (100), 245 (14), 212 (11), 211 (74), 210 (33), 205 (23), 201 (14), 180 (11), 179 (41), 178 (37), 175 (30), 169 (27), 167 (18), 165 (31), 152 (13), 115 (10), 105 (33), 91 (62), 77 (18), 41 (13). HRMS (EI): *m/z* calcd for C₂₁H₂₄O: 292.1827, found: 292.1825.



Representative Procedure for Gold Catalysis. Preparation of Tetrahydrofuran 2. A mixture containing gold(I)-complex (*S,S,S,S*)-**C3** (2.6 mg, 2.0 μmol, 5.5 mol%) and AgBF₄ (0.4 mg, 1.8 μmol, 5.0 mol%) in EtOH (0.2 mL) was stirred for 15 min at ambient temperature before it was transferred to a solution of hydroxy-allene **1** (10 mg, 36 μmol) in EtOH (0.2 mL) at the indicated temperature *via* a cannula equipped with a PTFE filter (Perfect-Flow®, 0.45 μm pore size, Ø 13 mm) to retain the precipitates. The resulting solution was stirred until TLC showed complete conversion. At this point, the solution was filtered through a plug of silica, the filtrate was concentrated and the residue purified by flash chromatography (hexane/*t*-butyl methyl

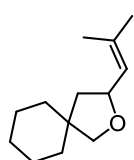


ether 19:1) to afford the title compound as a colorless oil (9.3 mg, 93%, 97% *ee*). Reactions performed in non-polar solvents were directly submitted to flash chromatography (hexane/*t*-butyl methyl ether 19:1) to yield the title compound. $[\alpha]_{\text{D}}^{20} = +146.9$ ($c = 1.0$, CHCl_3). ^1H NMR (400 MHz, CDCl_3): $\delta = 7.41\text{--}7.30$ (m, 6H), 7.27–7.22 (m, 4H), 5.32 (dt, $J = 8.7, 1.4$ Hz, 1H), 4.76 (td, $J = 9.2, 5.9$ Hz, 1H), 4.65 (dd, $J = 8.7, 1.1$ Hz, 1H), 4.20 (d, $J = 8.7$ Hz, 1H), 2.67 (ddd, $J = 12.2, 5.9, 1.1$ Hz, 1H), 2.41 (dd, $J = 12.2, 9.6$ Hz, 1H), 1.76 (d, $J = 1.3$ Hz, 3H), 1.68 ppm (d, $J = 1.3$ Hz, 3H). ^{13}C NMR (100 MHz, CDCl_3): $\delta = 146.4, 146.3, 136.5, 128.5, 128.5, 127.3, 127.3, 126.5, 126.4, 125.9, 77.0, 75.3, 56.5, 45.6, 26.0, 18.4$ ppm. IR (film): $\tilde{\nu} = 3459, 3058, 3026, 2976, 2924, 1784, 1730, 1598, 1579, 1494, 1446, 1378, 1316, 1275, 1157, 1028, 1001, 972, 912, 868, 841, 754, 731, 697, 660$ cm^{-1} . MS (EI) m/z (%): 278 (69), 263 (38), 248 (46), 233 (70), 205 (100), 180 (21), 179 (35), 178 (29), 165 (41), 157 (31), 116 (23), 115 (32), 103 (29), 91 (71), 83 (32), 77 (20), 69 (81). HRMS (ESIpos): m/z calcd for $\text{C}_{20}\text{H}_{22}\text{O}$: 278.1670, found: 278.1671. The *ee* was determined by HPLC (250 mm, Chiralcel IA (IA00CE-LH-028), 5 μm , \varnothing 4.6 mm, *n*-heptane/2-propanol 98:2, flow rate = 1.0 mL/min 4.0 MPa, 298 K, UV, 220 nm): major enantiomer $t_{\text{R}} = 6.0$ min; minor enantiomer $t_{\text{R}} = 6.9$ min.

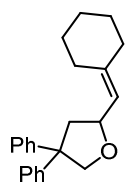
The absolute configuration was assigned to be (*R*) by comparison of the optical rotation of the sample ($[\alpha]_{\text{D}}^{20} = +146.9$ ($c = 1.0$, CHCl_3) (97% *ee*)) with that of the (*S*)-enantiomer reported in the literature, which had the opposite sign ($[\alpha]_{\text{D}}^{20} = -74.9$ ($c = 0.36$, CHCl_3) (70% *ee*)).^[15c,226]

All other tetrahydrofurans were prepared analogously. Their spectral and analytical data are summarized below.

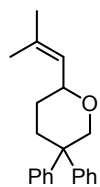
Tetrahydrofuran 7. Colorless oil (89%, 95% *ee*). $[\alpha]_{\text{D}}^{20} = +6.2$ ($c = 1.0$, CHCl_3). ^1H NMR (400 MHz, CDCl_3): $\delta = 5.21$ (dt, $J = 8.5, 1.4$ Hz, 1H), 4.59 (td, $J = 8.8, 6.6$ Hz, 1H), 3.63 (d, $J = 8.4$ Hz, 1H), 3.50 (d, $J = 8.4$ Hz, 1H), 1.88 (dd, $J = 12.4, 6.6$ Hz, 1H), 1.72 (d, $J = 1.4$ Hz, 3H), 1.68 (d, $J = 1.3$ Hz, 3H), 1.47–1.39 (m, 10H), 1.34 ppm (dd, $J = 12.4, 9.0$ Hz, 1H). ^{13}C NMR (100 MHz, CDCl_3): $\delta = 135.7, 126.6, 78.5, 75.4, 45.6, 44.3, 37.2, 35.8, 26.2, 25.9, 24.2, 23.8, 18.3$ ppm. IR (film): $\tilde{\nu} = 2922, 2851, 1676, 1447, 1376, 1316, 1258, 1106, 1050, 1006, 979, 946, 891, 866, 849, 820, 668$ cm^{-1} . MS (EI) m/z (%): 112 (48), 98 (15), 95 (25), 83 (26), 82 (100), 81 (23), 79 (28), 69 (20), 67 (62), 55 (22), 41 (36); HRMS (ESIpos): m/z calcd for $\text{C}_{13}\text{H}_{22}\text{O}$: 194.1669, found: 194.1671. The *ee* was determined by HPLC (150 mm, Chiralcel OJ-3R (OJ3RCD-QD007), 3 μm , \varnothing 4.6 mm, acetonitrile/ H_2O 60:40, flow rate = 0.5 mL/min 10.6 MPa, 288 K, UV, 210 nm): major enantiomer $t_{\text{R}} = 16.6$ min; minor enantiomer $t_{\text{R}} = 17.9$ min.



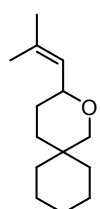
Tetrahydrofuran 8. Colorless oil (91%, 94% *ee*). $[\alpha]_{\text{D}}^{20} = +87.8$ ($c = 1.0$, CHCl_3). ^1H NMR (400 MHz, CDCl_3): $\delta = 7.35\text{--}7.27$ (m, 6H), 7.23–7.18 (m, 4H), 5.23 (dt, $J = 8.7, 1.2$ Hz, 1H), 4.77 (ddd, $J = 9.7, 8.7, 5.9$ Hz, 1H), 4.62 (dd, $J = 8.7, 1.1$ Hz, 1H), 4.16 (d, $J = 8.7$ Hz, 1H), 2.62 (ddd, $J = 12.2, 5.9, 1.1$ Hz, 1H), 2.38 (dd, $J = 12.2, 9.7$ Hz, 1H), 2.18–2.14 (m, 1H), 2.11–2.04 (m, 3H), 1.58–1.45 ppm (m, 7H). ^{13}C NMR (100 MHz, CDCl_3): $\delta = 146.5, 146.3, 144.2, 128.5, 128.5, 127.3, 127.3, 126.5, 126.3, 122.7, 77.0, 74.4, 56.6, 46.0, 37.2, 29.4, 28.5, 28.0, 26.8$ ppm. IR (film): $\tilde{\nu} = 3089, 3058, 3026, 2925, 2853, 1789, 1668, 1598, 1493, 1446, 1324, 1268, 1131, 1051, 1030, 1001, 970, 933, 909, 863, 756, 730, 697, 658$ cm^{-1} . MS (EI) m/z (%): 318 (100), 288 (52), 241 (24), 206 (26), 205 (62), 197 (46), 194 (29), 193 (22), 180 (48), 179 (38), 178 (29), 167 (65), 165 (44), 125 (15), 124 (48), 123 (25), 116 (22), 115 (30), 103 (26), 91 (54), 81 (30), 77 (16). HRMS (ESIpos): m/z calcd for $\text{C}_{23}\text{H}_{26}\text{O}$: 318.1980, found: 318.1984. The *ee* was determined by HPLC (250 mm, Chiralcel IA (IA00CE-LH-028), 5 μm , \varnothing 4.6 mm, *n*-heptane/2-propanol 98:2, flow rate = 1.0 mL/min 4.0 MPa, 298 K, UV, 220 nm): major enantiomer $t_{\text{R}} = 5.9$ min; minor enantiomer $t_{\text{R}} = 6.6$ min.



Tetrahydrofuran 4. Colorless oil (93%, 98% *ee*). $[\alpha]_{\text{D}}^{20} = +6.2$ ($c = 1.0$, CHCl_3). ^1H NMR (400 MHz, CDCl_3): $\delta = 7.45\text{--}7.42$ (m, 2H), 7.30–7.23 (m, 4H), 7.19–7.16 (m, 4H), 5.15 (dt, $J = 8.2, 1.4$ Hz, 1H), 4.64 (dd, $J = 12.1, 2.3$ Hz, 1H), 4.14 (ddd, $J = 10.9, 8.2, 2.5$ Hz, 1H), 3.61 (d, $J = 12.1$ Hz, 1H), 2.50–2.45 (m, 2H), 1.70 (s, 6H), 1.53–1.49 (m, 1H), 1.39–1.32 ppm (m, 1H). ^{13}C NMR (100 MHz, CDCl_3): $\delta = 146.9, 145.9, 136.1, 129.1, 128.4, 128.1, 127.1, 126.4, 126.0, 125.8, 75.1, 75.0, 45.8, 34.8, 28.4, 25.9, 18.5$ ppm. IR (film): $\tilde{\nu} = 3087, 3058, 3023, 2936, 2916, 2848, 1678, 1598, 1579, 1494, 1445, 1375, 1319, 1243, 1195, 1139, 1090, 1076, 1032, 1011, 972, 910, 870, 821, 764, 752, 731, 695, 661$ cm^{-1} . MS (EI) m/z (%): 214 (12), 201 (14), 194 (11), 181 (16), 180 (100), 179 (33), 178 (25), 165 (35), 115 (12), 91 (14), 82 (19), 67 (10). HRMS (ESIpos): m/z calcd for $\text{C}_{21}\text{H}_{24}\text{O}$: 292.1828, found: 292.1827. The *ee* was determined by HPLC (250 mm, Chiralcel IA (IA00CE-LH-028), 5 μm , \varnothing 4.6 mm, *n*-heptane/2-propanol 98:2, flow rate = 1.0 mL/min 4.0 MPa, 298 K, UV, 220 nm): major enantiomer $t_{\text{R}} = 4.2$ min; minor enantiomer $t_{\text{R}} = 4.6$ min.

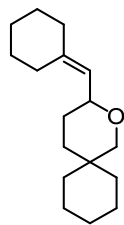


Tetrahydrofuran 5. Colorless oil (89%, 97% *ee*). $[\alpha]_{\text{D}}^{20} = -14.2$ ($c = 1.3$, CHCl_3). ^1H NMR (400 MHz, CD_2Cl_2): $\delta = 5.15$ (d, $J = 7.9$ Hz, 1H), 3.89 (ddd, $J = 10.8, 7.8, 2.6$ Hz, 1H), 3.69 (dd, $J = 11.3, 2.6$ Hz, 1H), 3.09 (d, $J = 11.2$ Hz, 1H), 1.76–1.72 (m, 1H), 1.70 (s, 3H), 1.65 (s, 3H), 1.56–1.53 (m, 1H), 1.49–1.32 (m, 9H), 1.23–1.19 (m, 1H), 1.14–1.11 ppm (m, 2H). ^{13}C NMR (100 MHz, CD_2Cl_2): $\delta = 134.8, 127.0, 76.6, 75.8, 37.0, 34.5, 32.1, 31.6, 28.2, 27.3, 25.7, 21.9, 21.9, 18.4$ ppm. IR (film): $\tilde{\nu} = 2923, 2848, 2162, 2024, 1736, 1678, 1450, 1375, 1345, 1326, 1270, 1259, 1222, 1184, 1157, 1129, 1080, 1071, 1054, 1007, 987, 952, 930, 906, 865, 846, 819, 713, 668$ cm^{-1} . MS (EI) m/z (%): 208 (17), 193 (100), 175 (23), 109 (25), 95 (26), 85 (32), 82 (31), 81 (43), 69 (21), 67 (64), 55 (25), 41 (27). HRMS (ESIpos): m/z calcd for $\text{C}_{14}\text{H}_{24}\text{O}$: 208.1827, found: 208.1827. The



ee was determined by GC (30 m, BGB-176/SE-52 G/510, 220/80 1/min 150 12/min 220 5min iso/320, flow rate 0.50 bar H₂: minor enantiomer *t_R* = 62.5 min; major enantiomer *t_R* = 63.1 min).

Tetrahydrofuran 6. Colorless oil (84%, 99% *ee*). $[\alpha]_{\text{D}}^{20} = -0.8$ (*c* = 1.3, CHCl₃). ¹H NMR (400 MHz,



CD₂Cl₂): δ = 5.09 (dt, *J* = 7.9, 1.2 Hz, 1H), 3.93 (ddd, *J* = 10.8, 7.8, 2.8 Hz, 1H), 3.69 (dd, *J* = 11.2, 2.7 Hz, 1H), 3.08 (d, *J* = 11.3 Hz, 1H), 2.18–2.12 (m, 2H), 2.09–2.04 (m, 2H), 1.74 (dq, *J* = 13.1, 2.9 Hz, 1H), 1.61–1.53 (m, 4H), 1.52–1.29 (m, 12H), 1.26–1.18 (m, 1H), 1.15–1.10 (m, 2H). ¹³C NMR (100 MHz, CD₂Cl₂): δ = 142.6, 123.8, 76.6, 75.1, 37.2, 37.0, 34.5, 32.1, 31.6, 29.8, 28.7, 28.3, 27.3, 27.1, 21.9, 21.9 ppm. IR (film): $\tilde{\nu}$ = 3391, 2924,

2851, 1729, 1449, 1258, 1187, 1157, 1071, 1050, 1011, 952, 905, 866, 846, 802, 736 cm⁻¹. MS (EI) *m/z* (%): 248 (18), 207 (19), 205 (56), 187 (18), 167 (19), 166 (98), 133 (15), 123 (17), 109 (49), 108 (53), 107 (38), 97 (27), 96 (33), 95 (54), 94 (17), 93 (43), 91 (40), 83 (17), 82 (17), 81 (100), 80 (25), 79 (79), 77 (28), 68 (20), 67 (97), 57 (22), 55 (47), 53 (18). HRMS (ESI): *m/z* calcd for C₁₇H₂₈ONa: 271.2030, found: 271.2032. The *ee* was determined by HPLC (150 mm, Chiralcel OJ-3R (OJ3RCD-QD007), 3 μm, Ø 4.6 mm, Acetonitrile, flow rate = 0.5 mL/min, 3.8 MPa, 298 K, UV, 210 nm): minor enantiomer *t_R* = 6.7 min; major enantiomer *t_R* = 18.1 min.

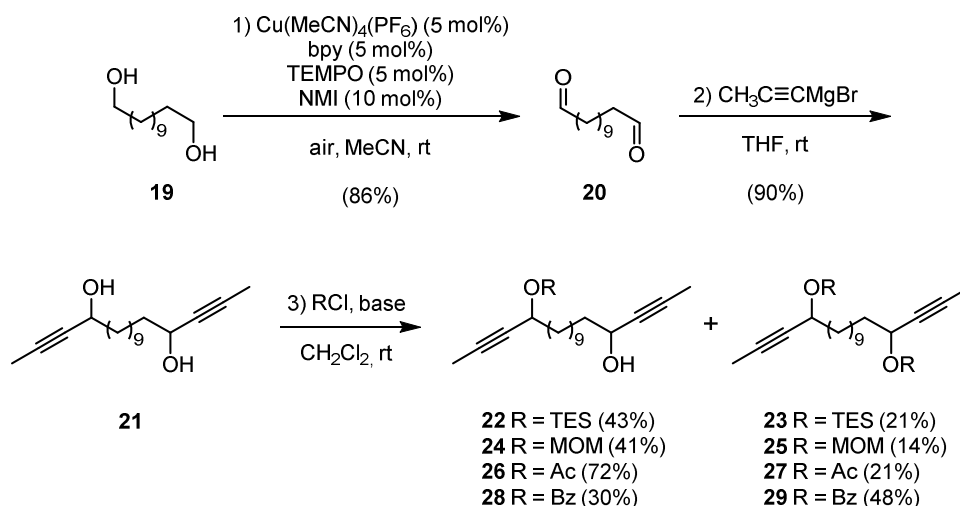
Search for Any Non-Linear Effects. Each flame-dried finger-Schlenk was loaded with allenol **1** (11 mg, 40 μmol) in anhydrous CH_2Cl_2 (0.2 mL) and stirred at the respective temperature. Accurately defined mixtures of (*S,S,S,S*)-**C3** and (*R,R,R,R*)-**C3** (total mass 2.25 mg, 2.19 μmol) were activated with AgBF_4 (0.40 mg, 2.05 μmol) in anhydrous CH_2Cl_2 (0.2 mL) at ambient temperature for 15 min. These activated catalyst solutions were transferred into the reaction vessels *via* cannula equipped with a PTFE filter (Perfect-Flow[®], 0.45 μm pore size, \varnothing 13 mm) to retain the precipitates. The resulting solutions were stirred at ambient temperature for 45 min or at -60 $^\circ\text{C}$ for 16 h. The mixtures were submitted to flash chromatography (hexane/*t*-butyl methyl ether 19:1) and the *ee* of the products determined by HPLC (*vide supra*).

Eyring Studies. Eyring studies were performed in both EtOH and CH_2Cl_2 using the gold precatalyst (*S,S,S,S*)-**C3** and AgBF_4 . Every data point was independently determined three times. For each reaction, complex (*S,S,S,S*)-**C3** (1.58 mg, 1.40 μmol , 5.5 mol%) and AgBF_4 (0.24 mg, 1.30 μmol , 5.0 mol%) were dissolved in anhydrous EtOH or CH_2Cl_2 (0.1 mL) at ambient temperature and the resulting mixture was stirred for 15 min. In parallel, a solution of allenol **1** (7.00 mg, 25.1 μmol) in anhydrous EtOH or CH_2Cl_2 (0.15 mL) was placed in a flame-dried finger-Schlenk flask and equilibrated at the indicated temperature. The solution of the activated catalyst was then introduced *via* a cannula equipped with a PTFE filter (Perfect-Flow[®], 0.45 μm pore size, \varnothing 13 mm) and the resulting mixture was stirred until complete conversion was achieved. In the case of EtOH, the reaction mixtures were then quickly filtered through a plug of silica, the filtrate was concentrated and the residue submitted to flash chromatography (hexane/*t*-butyl methyl ether 19:1). For CH_2Cl_2 , the reaction mixtures were directly submitted to flash chromatography (hexane/*t*-butyl methyl ether 19:1). The enantiomeric excess of the resulting products was determined by HPLC (*vide supra*).

4.3 Studies Toward the Total Synthesis of Chagosensine

4.3.1 Model Studies

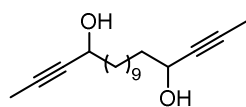
4.3.1.1 Synthesis of the Diyne Model Substrates



Scheme 4.2 Preparation of the diyne model substrates.

Dodecan-1,12-dial (20). $[\text{Cu}(\text{MeCN})_4]\text{BF}_4$ (622 mg, 1.98 mmol, 5 mol%), 2,2'-bipyridine (309 mg, 1.98 mmol, 5 mol%), TEMPO (309 mg, 1.98 mmol, 5 mol%) and *N*-methyl-imidazole (406 mg, 4.94 mmol, 10 mol%) were added sequentially to a solution of dodecan-1,12-diol (10.0 g, 49.4 mmol) in CH_3CN (50 mL) in an open flask. The resulting dark red mixture was vigorously stirred open to air for 72 h, after which time the solution had turned blue. The mixture was diluted with CH_2Cl_2 /hexanes 1:1 (250 mL) and filtered through a plug of silica. Removal of the solvent under reduced pressure furnished the title compound **20** as a white solid, which was pure enough for further use (8.40 g, 86%). m.p. $[\text{CHCl}_3] = 49\text{--}51\text{ }^\circ\text{C}$. ^1H NMR (400 MHz, CDCl_3): $\delta = 9.77$ (t, $J = 1.9$ Hz, 2H), 2.42 (td, $J = 7.3, 1.9$ Hz, 4H), 1.63 (quint, $J = 7.1$ Hz, 4H), 1.29 ppm (brs, 12H). ^{13}C NMR (100 MHz, CDCl_3): $\delta = 203.1$ (2C), 44.0 (2C), 29.4 (4C), 29.2 (2C), 22.2 ppm (2C). IR (film): $\tilde{\nu} = 2924, 2853, 1721, 1464, 1391, 723, 521\text{ cm}^{-1}$. MS (EI) m/z (%): 136 (10), 121 (15), 111 (14), 110 (12), 109 (10), 107 (13), 98 (34), 97 (21), 96 (21), 95 (100), 94 (23), 93 (17), 85 (12), 84 (20), 83 (29), 82 (41), 81 (99), 80 (18), 79 (25), 71 (21), 70 (20), 69 (58), 68 (42), 67 (86), 57 (65), 56 (18), 55 (91), 54 (23), 53 (11), 44 (29), 43 (43), 42 (14), 41 (75), 39 (20), 29 (13). HRMS (CI): m/z calcd for $\text{C}_{12}\text{H}_{22}\text{O}_2$: 199.1698, found: 199.1696. The analytical and spectroscopic data are in agreement with those reported in the literature.^[228]

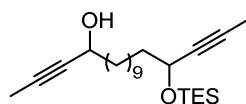
Octadeca-2,16-diyne-4,15-diol (21). A solution of 1-propynylmagnesium bromide in THF (0.5 M,



41.9 mL, 20.9 mmol) was added to a solution of dial **20** (1.66 g, 8.37 mmol) in THF (15 mL) and the resulting mixture was stirred at ambient temperature for 5 h. The reaction was quenched with aq. sat. NH_4Cl (20 mL) and the aqueous

layer extracted with *t*-butyl methyl ether (3×30 mL). The combined extracts were washed with brine (50 mL), dried over Na_2SO_4 , filtered and concentrated. The residue was purified by flash chromatography (hexanes/*t*-butyl methyl ether 6:1 to 3:1) to afford diol **21** as an amorphous white solid (2.10 g, 90%). ^1H NMR (400 MHz, CDCl_3): δ = 4.25 (tq, J = 6.3, 2.0 Hz, 2H), 1.78 (d, J = 2.1 Hz, 6H), 1.65 (quint, J = 7.3 Hz, 4H), 1.46–1.37 (m, 4H), 1.22 ppm (brs, 12H). ^{13}C NMR (100 MHz, CDCl_3): δ = 81.1 (2C), 80.6 (2C), 62.9 (2C), 38.3 (2C), 29.7 (4C), 29.4 (2C), 25.3 (2C), 3.7 ppm (2C). IR (film): $\tilde{\nu}$ = 3364, 2923, 2854, 1453, 1023 cm^{-1} . MS (ESIpos) m/z (%): 301.1 (100 (M+Na)). HRMS (ESIpos): m/z calcd for $\text{C}_{18}\text{H}_{30}\text{O}_2\text{Na}$: 301.2138, found: 301.2138.

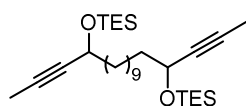
Silyl ethers 22 and 23. Imidazole (91.7 mg, 1.35 mmol) and DMAP (11.0 mg, 0.09 mmol, 10 mol%)



were added to a solution of diol **21** (250 mg, 0.90 mmol) in CH_2Cl_2 (90 mL) at 0 °C, followed by TESCl (0.15 mL, 0.90 mmol). The resulting mixture was stirred at ambient temperature for 16 h. The reaction was quenched with aq.

sat. NH_4Cl solution (40 mL) and the aqueous layer extracted with CH_2Cl_2 (3×40 mL). The combined extracts were dried over Na_2SO_4 , filtered and concentrated. The residue was purified by flash chromatography (hexanes) to afford the mono-silyl ether **22** (150 mg, 43%) and the bis-silyl ether **23** (97.3 mg, 21%) as colorless oil each. Analytical data for **22**: ^1H NMR (400 MHz, CDCl_3): δ = 4.35–4.26 (m, 2H), 1.85 (d, J = 2.1 Hz, 3H), 1.82 (d, J = 2.1 Hz, 3H), 1.68–1.58 (m, 4H), 1.46–1.35 (m, 4H), 1.27 (brs, 12H), 0.97 (t, J = 7.9 Hz, 9H), 0.64 ppm (qd, J = 7.9, 3.5 Hz, 6H). ^{13}C NMR (100 MHz, CDCl_3): δ = 81.2, 81.1, 80.6, 79.9, 63.1, 62.9, 39.2, 38.3, 29.7 (4C), 29.5, 29.4, 25.4, 25.3, 7.0 (3C), 4.9 (3C), 3.7 ppm (2C). IR (film): $\tilde{\nu}$ = 3360, 2921, 2854, 1459, 1238, 1078, 1004, 726 cm^{-1} . MS (EI) m/z (%): 364 (14), 363 (46), 323 (15), 243 (16), 184 (17), 183 (100), 171 (11), 161 (12), 159 (11), 147 (23), 145 (13), 135 (17), 133 (28), 127 (18), 125 (44), 121 (28), 119 (30), 115 (36), 113 (22), 109 (31), 107 (34), 105 (31), 103 (69), 97 (65), 95 (73), 93 (39), 91 (18), 87 (31), 81 (50), 79 (26), 75(45), 69 (74), 67 (32), 59 (11), 55 (23), 41 (12). HRMS (ESIpos): m/z calcd for $\text{C}_{24}\text{H}_{44}\text{O}_2\text{SiNa}$: 415.3003, found: 415.3002.

Analytical data for **23**: ^1H NMR (400 MHz, CDCl_3): δ = 4.29 (tq, J = 6.5, 2.1 Hz, 2H), 1.82 (d, J = 2.1 Hz,

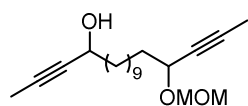


6H), 1.65–1.58 (m, 4H), 1.42–1.36 (m, 4H), 1.26 (brs, 12H), 0.97 (t, J = 7.9 Hz, 18H), 0.64 (q, J = 7.9 Hz, 6H), 0.63 ppm (q, J = 7.9 Hz, 6H). ^{13}C NMR (100 MHz, CDCl_3): δ = 81.2 (2C), 79.9 (2C), 63.1 (2C), 39.2 (2C), 29.7 (4C), 29.5 (2C), 25.4

(2C), 7.0 (6C), 4.9 (6C), 3.7 ppm (2C). IR (film): $\tilde{\nu}$ = 2922, 2876, 2855, 1460, 1340, 1239, 1084, 1005, 743 cm^{-1} . MS (EI) m/z (%): 479 (11), 478 (31), 477 (74), 346 (15), 345 (50), 336 (17), 335 (61), 243

(24), 217 (38), 205 (30), 203 (10), 190 (11), 189 (54), 184 (17), 183 (100), 177 (10), 161 (22), 159 (12), 155 (37), 154 (12), 153 (10), 149 (19), 147 (22), 145 (14), 135 (18), 133 (27), 131 (13), 127 (38), 125 (51), 121 (29), 119 (27), 117 (15), 115 (72), 113 (11), 109 (25), 107 (33), 105 (34), 103 (86), 97 (69), 95 (50), 93 (32), 91 (59), 90 (10), 89 (10), 87 (66), 83 (13), 81 (41), 79 (23), 77 (16), 75 (46), 69 (18), 67 (29), 65 (16), 59 (34), 57 (10), 55 (20), 47 (10), 45 (16), 43 (12), 41 (16), 39 (17), 29 (13). HRMS (ESIpos): m/z calcd for $C_{30}H_{58}O_2Si_2Na$: 529.3868, found: 529.3874.

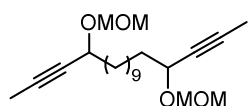
Methoxymethyl acetals **24 and **25**.** Hünig's base (0.17 mL, 1.00 mmol) and DMAP (11.0 mg,



0.09 mmol, 10 mol%) were added to a solution of diol **21** (250 mg, 0.90 mmol) in CH_2Cl_2 (9 mL) at 0 °C, followed by MOMCl (68.2 μ L, 0.90 mmol). The resulting mixture was stirred at ambient temperature for 16 h. The reaction

was quenched with aq. sat. NH_4Cl solution (8 mL) and the aqueous layer extracted with CH_2Cl_2 (3×10 mL). The combined extracts were dried over Na_2SO_4 , filtered and concentrated. The residue was purified by flash chromatography (hexanes/*t*-butyl methyl ether 9:1) to afford the mono-MOM-derivative **24** (119 mg, 41%) and the bis-MOM-protected compound **25** (44.8 mg, 14%) as colorless oil each. Analytical data for **24**: 1H NMR (400 MHz, $CDCl_3$): δ = 4.94 (d, J = 6.7 Hz, 1H), 4.56 (d, J = 6.7 Hz, 1H), 4.29 (dtq, J = 17.3, 6.5, 2.1 Hz, 2H), 3.36 (s, 3H), 1.84 (d, J = 2.1 Hz, 6H), 1.71–1.60 (m, 4H), 1.47–1.37 (m, 4H), 1.27 ppm (brs, 12H). ^{13}C NMR (100 MHz, $CDCl_3$): δ = 93.9, 81.6, 81.0, 80.7, 78.0, 66.0, 62.9, 55.7, 38.3, 36.1, 29.7 (4C), 29.5, 29.4, 25.5, 25.3, 3.71, 3.69 ppm. IR (film): $\tilde{\nu}$ = 3457, 2922, 2854, 1465, 1343, 1148, 1097, 1033, 921, 723 cm^{-1} . MS (EI) m/z (%): 113 (36), 95 (19), 93 (14), 85 (16), 83 (12), 81 (18), 79 (11), 69 (41), 68 (17), 67 (17), 55 (16), 53 (11), 45 (100), 41 (10). HRMS (ESIpos): m/z calcd for $C_{20}H_{34}O_3Na$: 345.2400, found: 345.2403.

Analytical data for **25**: 1H NMR (400 MHz, $CDCl_3$): δ = 4.95 (d, J = 6.8 Hz, 2H), 4.57 (d, J = 6.6 Hz, 2H),



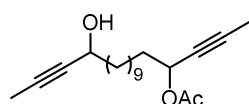
4.27 (tq, J = 6.5, 2.1 Hz, 2H), 3.37 (s, 6H), 1.84 (d, J = 2.1 Hz, 6H), 1.74–1.62 (m, 4H), 1.48–1.39 (m, 4H), 1.28 (brs, 12H). ^{13}C NMR (100 MHz, $CDCl_3$): δ = 94.0 (2C), 81.7 (2C), 78.0 (2C), 66.0 (2C), 55.7 (2C), 36.2 (2C), 29.71 (2C), 29.69 (2C),

29.5 (2C), 25.5 (2C), 3.7 ppm (2C). IR (film): $\tilde{\nu}$ = 2923, 2854, 1466, 1344, 1148, 1097, 1034, 920 cm^{-1} .

MS (EI) m/z (%): 149 (13), 147 (10), 135 (21), 133 (12), 123 (13), 121 (21), 119 (13), 113 (77), 112 (11), 111 (11), 109 (18), 108 (13), 107 (26), 105 (13), 98 (20), 96 (11), 95 (35), 94 (16), 93 (31), 91 (13), 85 (31), 83 (28), 82 (17), 81 (31), 79 (22), 77 (11), 69 (12), 68 (15), 67 (24), 55 (15), 53 (14), 45 (100).

HRMS (ESIpos): m/z calcd for $C_{22}H_{38}O_4Na$: 389.2662, found: 389.2660.

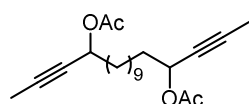
Acetates 26 and 27. Triethylamine (0.19 mL, 1.35 mmol) and DMAP (11.0 mg, 0.09 mmol, 10 mol%)



were added to a solution of diol **21** (250 mg, 0.90 mmol) in CH₂Cl₂ (90 mL) at 0 °C, followed by acetic anhydride (84.9 μL, 0.90 mmol). The resulting mixture was stirred at ambient temperature for 16 h. The reaction was quenched with

aq. sat. NH₄Cl solution (40 mL) and the aqueous layer extracted with CH₂Cl₂ (3 × 40 mL). The combined extracts were dried over Na₂SO₄, filtered and concentrated. The residue was purified by flash chromatography (hexanes/*t*-butyl methyl ether 10:1) to afford the mono-acetate **26** (209 mg, 72%) and the bis-acetate **27** (67.0 mg, 21%) as pale yellow oil each. Analytical data for **26**: ¹H NMR (400 MHz, CDCl₃): δ = 5.31 (tq, *J* = 6.6, 2.1 Hz, 1H), 4.32 (tq, *J* = 6.5, 2.1 Hz, 1H), 2.07 (s, 3H), 1.85 (d, *J* = 2.1 Hz, 3H), 1.84 (d, *J* = 2.1 Hz, 3H), 1.73–1.61 (m, 4H), 1.46–1.36 (m, 4H), 1.27 ppm (brs, 12H). ¹³C NMR (100 MHz, CDCl₃): δ = 170.4, 81.8, 81.0, 80.6, 77.0, 64.8, 62.9, 38.3, 35.2, 29.7 (2C), 29.6 (2C), 29.4, 29.3, 25.3, 25.2, 21.3, 3.8, 3.7 ppm. IR (film): $\tilde{\nu}$ = 3459, 2923, 2854, 1738, 1371, 1232, 1019, 957, 722 cm⁻¹. MS (EI) *m/z* (%): 175 (10), 163 (14), 161 (18), 149 (27), 147 (19), 145 (12), 137 (11), 136 (15), 135 (37), 133 (19), 131 (11), 129 (26), 126 (15), 125 (12), 123 (23), 122 (15), 121 (34), 119 (20), 111 (23), 110 (20), 109 (36), 108 (21), 107 (43), 105 (25), 97 (13), 96 (15), 95 (60), 94 (23), 93 (61), 91 (31), 84 (71), 83 (13), 82 (20), 81 (54), 80 (15), 79 (53), 77 (16), 69 (100), 68 (40), 67 (51), 66 (17), 55 (30), 43 (64), 41 (21), 39 (14). HRMS (ESIpos): *m/z* calcd for C₂₀H₃₂O₃Na: 343.2244, found: 343.2242.

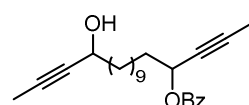
Analytical data for **27**: ¹H NMR (400 MHz, CDCl₃): δ = 5.31 (tq, *J* = 6.7, 2.1 Hz, 2H), 2.07 (s, 6H), 1.84 (d, *J* = 2.1 Hz, 6H), 1.74–1.67 (m, 4H), 1.44–1.36 (m, 4H), 1.27 ppm (brs, 12H).



¹³C NMR (100 MHz, CDCl₃): δ = 170.3 (2C), 81.8 (2C), 77.0 (2C), 64.8 (2C), 35.2 (2C), 29.64 (2C), 29.59 (2C), 29.3 (2C), 25.2 (2C), 21.3 (2C), 3.8 ppm (2C).

IR (film): $\tilde{\nu}$ = 2924, 2855, 1738, 1371, 1232, 1019, 955, 605 cm⁻¹. MS (EI) *m/z* (%): 287 (12), 260 (23), 259 (18), 245 (11), 175 (13), 163 (13), 161 (21), 159 (12), 149 (25), 147 (21), 145 (18), 143 (10), 137 (14), 136 (16), 135 (27), 133 (22), 131 (16), 126 (27), 125 (18), 124 (11), 123 (25), 122 (13), 121 (25), 119 (24), 117 (10), 111 (27), 110 (22), 109 (39), 108 (14), 107 (32), 105 (28), 95 (48), 94 (14), 93 (42), 91 (31), 84 (79), 83 (10), 81 (38), 79 (41), 77 (15), 69 (23), 68 (28), 67 (37), 66 (13), 55 (23), 43 (100), 41 (14). HRMS (ESIpos): *m/z* calcd for C₂₂H₃₄O₄Na: 385.2349, found: 385.22348.

Benzoates 28 and 29. Triethylamine (0.19 mL, 1.35 mmol) and DMAP (11.0 mg, 0.09 mmol, 10 mol%) were added to a solution of diol **21** (250 mg, 0.90 mmol) in CH₂Cl₂ (30 mL) at 0 °C, followed by

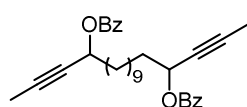


benzoyl chloride (115 μL, 0.99 mmol). The resulting mixture was stirred at ambient temperature for 16 h. The reaction was quenched with aq. sat. NH₄Cl solution (10 mL) and the aqueous layer extracted with CH₂Cl₂ (3 × 15 mL). The

combined extracts were dried over Na₂SO₄, filtered and concentrated. The residue was purified by

flash chromatography (hexanes/*t*-butyl methyl ether 10:1) to afford the mono-benzoate **28** (102 mg, 30%) and the bis-protected compound **29** (210 mg, 48%) as pale yellow oil each. Analytical data for **28**: ^1H NMR (400 MHz, CDCl_3): δ = 8.07 (d, J = 7.1 Hz, 2H), 7.56 (t, J = 7.4 Hz, 1H), 7.44 (t, J = 7.6 Hz, 2H), 5.56 (tq, J = 6.6, 2.1 Hz, 1H), 4.32 (tq, J = 6.5, 2.1 Hz, 1H), 1.85 (d, J = 2.1 Hz, 3H), 1.84 (d, J = 2.1 Hz, 3H), 1.69–1.61 (m, 4H), 1.52–1.45 (m, 2H), 1.45–1.38 (m, 2H), 1.28 ppm (brs, 12H). ^{13}C NMR (100 MHz, CDCl_3): δ = 165.9, 133.1, 130.3, 129.9 (2C), 128.5 (2C), 81.9, 81.0, 80.6, 77.1, 65.3, 62.9, 38.3, 35.3, 29.7 (2C), 29.6 (2C), 29.4, 29.3, 25.33, 25.26, 3.8, 3.7 ppm. IR (film): $\tilde{\nu}$ = 3473, 2924, 2855, 1721, 1452, 1315, 1268, 1108, 1026, 712 cm^{-1} . MS (EI) m/z (%): 105 (100), 69 (12). HRMS (ESIpos): m/z calcd for $\text{C}_{25}\text{H}_{24}\text{O}_3\text{Na}$: 405.2400, found: 405.2403.

Analytical data for **29**: ^1H NMR (400 MHz, CDCl_3): δ = 8.07 (d, J = 7.1 Hz, 4H), 7.56 (t, J = 7.4 Hz, 2H),



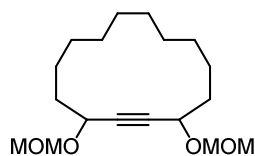
7.44 (t, J = 7.7 Hz, 4H), 5.56 (tq, J = 6.5, 2.1 Hz, 2H), 1.94–1.87 (m, 2H), 1.85 (d, J = 2.1 Hz, 6H), 1.84–1.77 (m, 2H), 1.54–1.44 (m, 4H), 1.27 ppm (brs, 12H).

^{13}C NMR (100 MHz, CDCl_3): δ = 165.8 (2C), 133.1 (2C), 130.3 (2C), 129.9 (4C), 128.5 (4C), 81.9 (2C), 77.1 (2C), 65.3 (2C), 35.3 (2C), 29.7 (2C), 29.6 (2C), 29.3 (2C), 25.3 (2C), 3.8 ppm (2C). IR (film): $\tilde{\nu}$ = 2923, 2854, 1717, 1451, 1314, 1263, 1097, 1026, 709 cm^{-1} . MS (EI) m/z (%): 105 (100). HRMS (ESIpos): m/z calcd for $\text{C}_{32}\text{H}_{38}\text{O}_4\text{Na}$: 509.2662, found: 509.2661.

RCAM Reactions

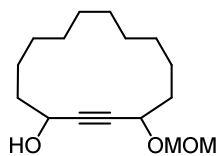
Representative Procedure for RCAM Reactions using $[\text{Mo}(\equiv\text{CC}_6\text{H}_4\text{OMe})(\text{OSiPh}_3)_3]$ as Catalyst.

Preparation of 3,14-bis(methoxymethoxy)-cyclotetradec-1-yne (S7). 5 Å MS (200 mg) was added to



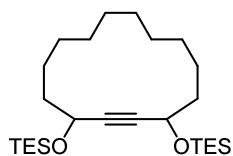
a solution of diyne **25** (36.7 mg, 100 μmol) in toluene (50 mL) and the resulting suspension was stirred for 30 min at room temperature. The mixture was then heated to 110 $^\circ\text{C}$ before complex **C9** (20.8 mg, 20.0 μmol , 20 mol%) was added. Stirring was continued for 90 min, and the mixture was filtered

through a pad of Celite[®], which was carefully rinsed with EtOAc. The combined filtrates were concentrated and the residue purified by flash chromatography (hexanes/EtOAc 20:1 to 4:1) to afford the title compound as a colorless oil (16.9 mg, 54%, *syn/anti*-mixture). ^1H NMR (400 MHz, CDCl_3): δ = 4.91 (dd, J = 6.8, 3.4 Hz, 2H), 4.59 (dd, J = 6.8, 3.0 Hz, 2H), 4.49–4.39 (m, 2H), 3.37 (s, 6H), 1.81–1.62 (m, 4H), 1.55–1.21 ppm (m, 16H). ^{13}C NMR (100 MHz, CDCl_3): δ = 94.3, 84.8, 84.6, 66.3, 66.2, 55.7, 35.1, 34.9, 26.6, 26.5, 25.9, 25.8, 23.82, 23.79, 22.44, 22.38 ppm. IR (film): $\tilde{\nu}$ = 2929, 2860, 2822, 2776, 1459, 1400, 1338, 1213, 1148, 1097, 1026, 919, 848, 792, 724, 704, 554, 441, 415 cm^{-1} . MS (EI) m/z (%): 133 (11), 121 (18), 119 (11), 109 (17), 108 (12), 107 (20), 105 (13), 97 (15), 95 (30), 94 (17), 93 (25), 92 (11), 91 (28), 82 (12), 81 (34), 80 (25), 79 (38), 77 (13), 69 (11), 67 (32), 55 (20), 45 (100), 41 (16). HRMS (ESIpos): m/z calcd for $\text{C}_{18}\text{H}_{32}\text{O}_4\text{Na}$: 355.2189, found: 335.2193.

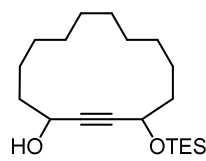
Representative Procedure for RCAM Reactions using the Two-Component Catalyst System.**Preparation of 4-(methoxymethoxy)cyclotetradec-2-yne-1-ol (S8).**

5 Å MS (200 mg) was added to a solution of diyne **24** (32.2 mg, 100 μmol) in toluene (50 mL) at room temperature and stirred for 30 min. The mixture was then heated to 110 °C before a freshly prepared solution of trisilanol **L2** (19.4 mg, 22.0 μmol, 22 mol%) and complex **C12** (13.3 mg, 20.0 μmol, 20 mol%) in toluene (1 mL) was added, which had been stirred for 5 min prior to use. Stirring was continued at 110 °C for 30 min. The mixture was cooled to ambient temperature, the molecular sieves were filtered off through a pad of Celite®, which was carefully rinsed with EtOAc, and the combined filtrates were concentrated. The residue was purified by flash chromatography (hexanes/EtOAc 20:1 to 4:1) to afford the title compound as a colorless oil (18.0 mg, 67%, *syn/anti*-mixture). ¹H NMR (400 MHz, CDCl₃): δ = 4.92 (dd, *J* = 6.8, 5.5 Hz, 1H), 4.60 (dd, *J* = 6.8, 1.8 Hz, 1H), 4.56–4.40 (m, 2H), 3.38 (s, 3H), 1.89–1.82 (m, 1H), 1.78–1.63 (m, 4H), 1.56–1.22 ppm (m, 16H). ¹³C NMR (100 MHz, CDCl₃): δ = 94.3, 87.11, 87.06, 84.1, 83.9, 66.3, 66.1, 63.0, 55.8, 37.2, 37.1, 35.0, 34.9, 26.6, 26.5, 25.9, 25.81, 25.77, 25.7, 23.9, 23.8, 22.5, 22.4, 22.32, 22.30 ppm. IR (film): $\tilde{\nu}$ = 3400, 2928, 2859, 1459, 1429, 1338, 1260, 1213, 1150, 1097, 1026, 918, 865, 801, 731, 700, 509 cm⁻¹. MS (EI) *m/z* (%): 149 (11), 147 (12), 135 (19), 133 (18), 131 (13), 123 (13), 122 (11), 121 (30), 119 (21), 117 (14), 111 (17), 110 (16), 109 (33), 108 (23), 107 (42), 105 (28), 98 (20), 97 (29), 96 (32), 95 (66), 94 (43), 93 (56), 92 (26), 91 (68), 84 (17), 83 (32), 82 (37), 81 (88), 80 (61), 79 (100), 78 (19), 77 (35), 71 (13), 70 (14), 69 (35), 68 (37), 67 (93), 66 (17), 65 (19), 57 (14), 56 (11), 55 (74), 54 (25), 53 (21), 45 (79), 43 (21), 41 (59), 39 (23), 31 (26), 30 (18). HRMS (ESIpos): *m/z* calcd for C₁₆H₂₈O₃Na: 291.1928, found: 291.1931.

The following compounds were prepared analogously:

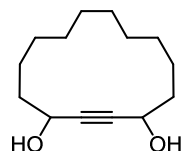
3,14-Bis((triethylsilyl)oxy)cyclotetradec-1-yne (S9).

hexanes/EtOAc 100:1) afforded the title compound as a colorless oil (32.0 mg, 71%, *syn/anti*-mixture). ¹H NMR (400 MHz, CDCl₃) δ = 4.51–4.39 (m, 2H), 1.73–1.21 (m, 20H), 0.97 (t, *J* = 7.9 Hz, 18H), 0.71–0.56 ppm (m, 12H). ¹³C NMR (100 MHz, CDCl₃): δ = 85.9, 85.6, 63.4, 63.2, 38.7, 38.4, 26.7, 26.4, 26.1, 25.8, 24.0, 23.8, 22.4, 22.3, 7.0, 4.94, 4.88 ppm. IR (film): $\tilde{\nu}$ = 2949, 2935, 2875, 1732, 1459, 1414, 1378, 1348, 1334, 1260, 1239, 1074, 1006, 975, 843, 803, 726, 675, 533, 458 cm⁻¹. MS (EI) *m/z* (%): 425 (11), 424 (29), 423 (81), 291 (28), 217 (45), 205 (10), 190 (18), 189 (100), 161 (17), 133 (11), 121 (14), 115 (23), 107 (17), 103 (31), 95 (12), 93 (13), 87 (41), 81 (10), 75 (18), 59 (11). HRMS (ESIpos): *m/z* calcd for C₂₆H₅₂O₂Si₂Na: 475.3404, found: 475.3398.

4-((Triethylsilyl)oxy)cyclotetradec-2-yn-1-ol (S10). Purification by flash chromatography (hexanes/

EtOAc 10:1 to 4:1) afforded the title compound as a colorless oil (21.8 mg, 64%, *syn/anti*-mixture). ^1H NMR (400 MHz, CDCl_3) δ = 4.53–4.41 (m, 2H), 1.74–1.60 (m, 5H), 1.49–1.25 (m, 16H), 0.98 (t, J = 7.9 Hz, 9H), 0.70–0.59 ppm (m, 6H). ^{13}C NMR (100 MHz, CDCl_3): δ = 87.1, 86.9, 85.4, 85.1, 63.3, 63.2, 63.1, 63.0, 38.4, 38.3,

37.2, 26.60, 26.56, 26.53, 26.47, 25.84, 25.82, 25.78, 25.7, 23.89, 23.85, 23.8, 22.4, 22.3, 7.0, 4.92, 4.90 ppm. IR (film): $\tilde{\nu}$ = 3359, 2931, 2874, 2859, 1458, 1413, 1378, 1334, 1259, 1239, 1151, 1072, 1006, 802, 726, 549, 427 cm^{-1} . MS (EI) m/z (%): 121 (11), 107 (16), 105 (12), 103 (100), 95 (16), 93 (18), 91 (16), 87 (14), 81 (18), 79 (20), 75 (89), 67 (20), 55 (12), 47 (13). HRMS (ESIpos): m/z calcd for $\text{C}_{20}\text{H}_{38}\text{O}_2\text{SiNa}$: 361.2521, found: 361.2533.

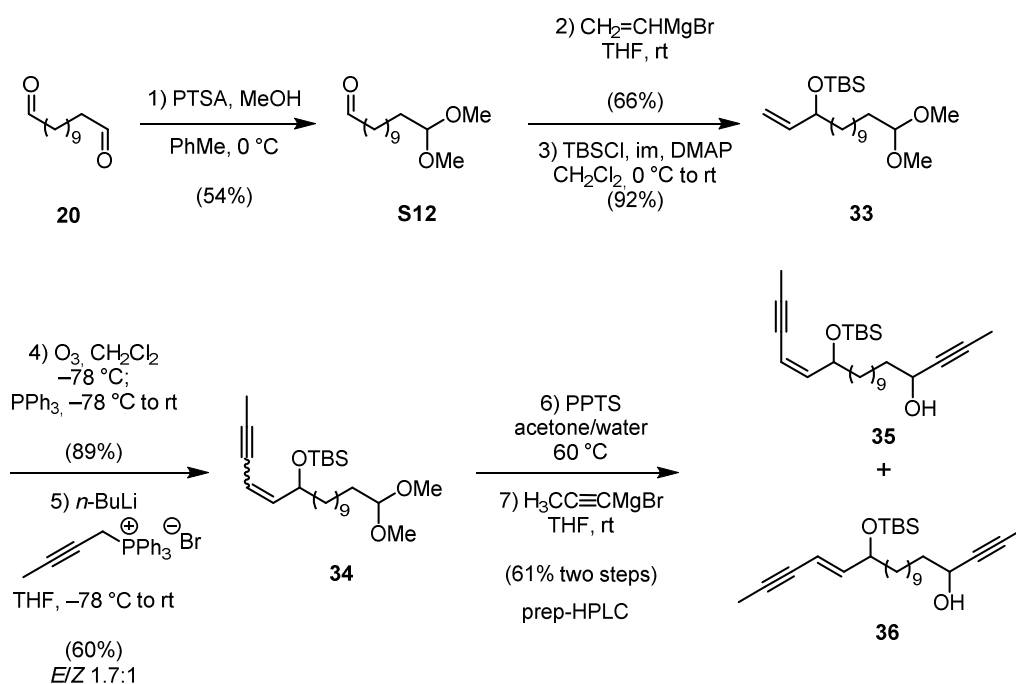
Cyclotetradec-2-yne-1,4-diol (S11). Purification by flash chromatography (hexanes/EtOAc 4:1 to 1:1)

afforded the title compound as a colorless solid (11.8 mg, 53%, *syn/anti*-mixture).

m.p. [EtOAc] = 110–111 °C. ^1H NMR (400 MHz, CDCl_3): δ = 4.58–4.44 (m, 2H), 1.98–1.89 (m, 2H), 1.79–1.62 (m, 4H), 1.52–1.26 ppm (m, 16H). ^{13}C NMR (100 MHz, CDCl_3): δ = 86.5, 86.2, 63.04, 62.96, 37.2, 37.1, 26.53, 26.50, 25.74, 25.71, 23.8, 22.4, 22.3 ppm.

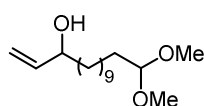
IR (film): $\tilde{\nu}$ = 3273, 2923, 2856, 1729, 1457, 1443, 1341, 1297, 1146, 1107, 1020, 945, 723, 702, 590, 533, 512, 440 cm^{-1} . MS (EI) m/z (%): 149 (12), 135 (19), 133 (14), 131 (13), 123 (11), 122 (10), 121 (29), 119 (18), 117 (14), 111 (19), 110 (15), 109 (28), 108 (24), 107 (48), 106 (12), 105 (24), 98 (21), 97 (30), 96 (35), 95 (67), 94 (49), 93 (57), 92 (25), 91 (62), 84 (26), 83 (44), 82 (39), 81 (91), 80 (60), 79 (100), 78 (18), 77 (34), 71 (21), 70 (30), 69 (40), 68 (37), 67 (93), 66 (17), 65 (19), 57 (26), 56 (14), 55 (92), 54 (25), 53 (23), 43 (33), 42 (12), 41 (68), 39 (27). HRMS (ESIpos): m/z calcd for $\text{C}_{14}\text{H}_{24}\text{O}_2\text{Na}$: 247.1667, found: 247.1668.

4.3.1.2 Synthesis of the Enyne Model Substrates



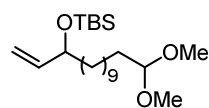
Scheme 4.3 Preparation of the enyne model substrates.

12,12-Dimethoxydodecanal (S12). *p*-TsOH·H₂O (288 mg, 1.51 mmol) was added to a solution of dodecan-1,12-dial (**20**) (3.00 g, 15.1 mmol) and MeOH (1.29 mL, 31.8 mmol) in toluene (100 mL) at 0 °C. The solution was stirred for 1 h before it was poured into aq. sat. NaHCO₃ (60 mL). The aqueous layer was extracted with EtOAc (3 × 60 mL), and the combined extracts were dried over Na₂SO₄, filtered and concentrated. The residue was purified by flash chromatography (hexanes/EtOAc 40:1) to furnish the title compound as a colorless oil (2.01 g, 54%). ¹H NMR (400 MHz, CDCl₃): δ = 9.75 (t, *J* = 1.6 Hz, 1H), 4.35 (t, *J* = 5.7 Hz, 1H), 3.30 (s, 6H), 2.41 (td, *J* = 7.3, 1.6 Hz, 2H), 1.65–1.55 (m, 4H), 1.26 ppm (brs, 14H). ¹³C NMR (100 MHz, CDCl₃): δ = 203.1, 104.7, 52.7 (2C), 44.1, 32.6, 29.7, 29.6, 29.5, 29.4, 29.28, 29.26, 24.7, 22.2 ppm. IR (film): $\tilde{\nu}$ = 2925, 2854, 1726, 1464, 1387, 1191, 1128, 1055, 953, 723 cm⁻¹. MS (EI) *m/z* (%): 75 (22), 71 (100), 41 (22). HRMS (ESIpos): *m/z* calcd for C₁₄H₂₈O₃Na: 267.1931, found: 267.1931. The analytical and spectroscopic data are in agreement with those reported in the literature.^[229] The byproduct 1,1,12,12-tetramethoxydodecane could be recovered and converted to aldehyde **S12** by treatment with HCl (1 M) in THF at ambient temperature for 6 h.

14,14-Dimethoxytetradec-1-en-3-ol (S13).

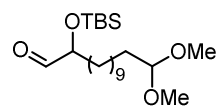
A solution of vinyl magnesium bromide (1.0 M in THF, 6.87 mL, 6.87 mmol) was added to a solution of aldehyde **S12** (1.40 g, 5.73 mmol) in anhydrous THF (50 mL). The resulting mixture was stirred at ambient temperature for 1 h. The reaction was quenched with aq. sat. NH_4Cl (20 mL) and

the aqueous layer extracted with *t*-butyl methyl ether (3 × 25 mL). The combined extracts were dried over Na_2SO_4 , filtered and concentrated. The residue was purified by flash chromatography (hexanes/*t*-butyl methyl ether 12:1 to 3:1) to afford the allylic alcohol **S13** as a colorless oil (1.03 g, 3.78 mmol, 66%). ^1H NMR (400 MHz, CDCl_3): δ = 5.86 (ddd, J = 16.9, 10.4, 6.3 Hz, 1H), 5.21 (dt, J = 17.2, 1.4 Hz, 1H), 5.09 (dt, J = 10.4, 1.3 Hz, 1H), 4.35 (t, J = 5.8 Hz, 1H), 4.08 (q, J = 6.5 Hz, 1H), 3.30 (s, 6H), 1.70 (brs, 1H), 1.61–1.48 (m, 4H), 1.26 ppm (brs, 16H). ^{13}C NMR (100 MHz, CDCl_3): δ = 141.5, 114.6, 104.7, 73.4, 52.7 (2C), 37.2, 32.6, 29.7 (4C), 29.64, 29.59, 25.5, 24.7 ppm. IR (film): $\tilde{\nu}$ = 3445, 2925, 2854, 1464, 1386, 1192, 1126, 1054, 991, 919 cm^{-1} . MS (EI) m/z (%): 97 (11), 95 (16), 94 (11), 93 (13), 82 (11), 81 (22), 80 (13), 79 (20), 75 (25), 71 (100), 68 (12), 67 (25), 57 (17), 55 (17), 41 (27), 31 (12). HRMS (ESIpos): m/z calcd for $\text{C}_{16}\text{H}_{32}\text{O}_3\text{Na}$: 295.2244, found: 295.2243. The analytical and spectroscopic data are in agreement with those reported in the literature.^[230]

Silyl ether 33.

(Imidazole (250 mg, 3.67 mmol), DMAP (22.4 mg, 0.18 mmol, 10 mol%) and TBSCl (415 mg, 2.75 mmol) were successively added to a solution of alcohol **S13** (500 mg, 1.84 mmol) in CH_2Cl_2 (18 mL) at 0 °C. The resulting mixture was allowed to warm to ambient temperature and stirred for 16 h. The reaction was quenched

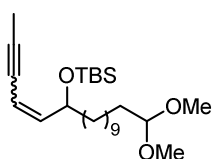
with aq. sat. NaHCO_3 (10 mL) and the aqueous layer extracted with CH_2Cl_2 (3 × 15 mL). The combined extracts were dried over Na_2SO_4 , filtered and concentrated. The residue was purified by flash chromatography (hexanes/*t*-butyl methyl ether 50:1) to yield silyl ether **33** as a colorless oil (653 mg, 92%). ^1H NMR (400 MHz, CDCl_3): δ = 5.79 (ddd, J = 17.1, 10.4, 6.0 Hz, 1H), 5.12 (ddd, J = 17.1, 1.9, 1.3 Hz, 1H), 5.00 (ddd, J = 10.4, 1.9, 1.2 Hz, 1H), 4.36 (t, J = 5.7 Hz, 1H), 4.06 (dtt, J = 7.2, 6.0, 1.3 Hz, 1H), 3.31 (s, 6H), 1.62–1.55 (m, 2H), 1.50–1.39 (m, 2H), 1.26 (brs, 16H), 0.89 (s, 9H), 0.05 (s, 3H), 0.03 ppm (s, 3H). ^{13}C NMR (100 MHz, CDCl_3): δ = 142.1, 113.5, 104.7, 74.0, 52.7 (2C), 38.3, 32.6, 29.77, 29.75, 29.72, 29.70, 29.69, 29.6, 26.0 (3C), 25.4, 24.8, 18.4, -4.2, -4.7 ppm. IR (film): $\tilde{\nu}$ = 2926, 2855, 1463, 1361, 1252, 1126, 1076, 920, 835, 775 cm^{-1} . MS (EI) m/z (%): 297 (10), 223 (32), 171 (38), 135 (10), 109 (32), 107 (22), 95 (37), 94 (11), 89 (12), 81 (20), 75 (100), 73 (16), 71 (28), 67 (17). HRMS (ESIpos): m/z calcd for $\text{C}_{22}\text{H}_{46}\text{O}_3\text{SiNa}$: 409.3108, found: 409.3108.

Aldehyde S14.

silyl ether **33** (650 mg, 1.68 mmol) was dissolved in CH_2Cl_2 (17 mL) and the resulting solution was cooled to -78 °C. Ozone was bubbled through the solution until the blue color persisted (approx. 30 min). After purging the reaction mixture with O_2 and Ar, PPh_3 (573 mg, 2.19 mmol) was added in one portion, the cooling bath was

removed and the colorless solution stirred at ambient temperature for 6 h. The mixture was concentrated and the residue purified by flash chromatography (hexanes/*t*-butyl methyl ether 40:1 to 20:1) to afford aldehyde **S14** as a colorless oil (582 mg, 89%). ^1H NMR (400 MHz, CDCl_3): δ = 9.59 (d, J = 1.7 Hz, 1H), 4.35 (t, J = 5.8 Hz, 1H), 3.95 (ddd, J = 7.1, 5.5, 1.8 Hz, 1H), 3.31 (s, 6H), 1.64–1.54 (m, 4H), 1.26 (brs, 16H), 0.92 (s, 9H), 0.08 (s, 3H), 0.07 ppm (s, 3H). ^{13}C NMR (100 MHz, CDCl_3): δ = 204.7, 104.7, 77.8, 52.7 (2C), 32.8, 32.6, 29.7, 29.64 (2C), 29.62, 29.58, 29.55, 25.9 (3C), 24.7 (2C), 18.4, -4.5, -4.8 ppm. IR (film): $\tilde{\nu}$ = 2927, 2855, 1736, 1464, 1362, 1253, 1123, 1076, 838, 778 cm^{-1} . MS (EI) m/z (%): 357 (12), 327 (20), 300 (11), 299 (49), 267 (23), 175 (21), 95 (10), 89 (10), 81 (11), 75 (100), 73 (21). HRMS (ESIpos): m/z calcd for $\text{C}_{21}\text{H}_{44}\text{O}_4\text{SiNa}$: 411.2901, found: 411.2903.

Enyne 34. A solution of *n*-BuLi (1.6 M in hexanes, 1.37 mL, 2.20 mmol) was added to a solution of



2-butynyltriphenylphosphonium bromide (869 mg, 2.20 mmol) in THF (10 mL) at

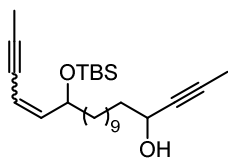
0 °C. The resulting orange mixture was stirred at ambient temperature for 30 min

before it was cooled to -78 °C. A solution of aldehyde **S14** (428 mg, 1.10 mmol) in

THF (2 mL) was added, the cooling bath removed and the resulting mixture

stirred for 12 h at ambient temperature. The reaction was quenched with H_2O (10 mL) and the aqueous layer extracted with EtOAc (3 \times 15 mL). The combined extracts were washed with brine (20 mL), dried over Na_2SO_4 , filtered and concentrated. The residue was purified by flash chromatography (hexanes/*t*-butyl methyl ether 100:0 to 50:1) to afford an inseparable mixture of (*E*)- and (*Z*)-enyne **34** as a yellow oil (279 mg, 60%, *E/Z* 1.7:1). ^1H NMR (400 MHz, CDCl_3): (*E*)-enyne: δ = 6.01 (ddd, J = 15.8, 5.7, 0.8 Hz, 1H), 5.58 (dq, J = 15.8, 2.3, 1.4 Hz, 1H), 4.36 (t, J = 5.8 Hz, 1H), 4.10 (tdd, J = 6.3, 5.7, 1.4 Hz, 1H), 3.31 (s, 6H), 1.94 (d, J = 2.3 Hz, 3H), 1.62–1.57 (m, 2H), 1.49–1.42 (m, 2H), 1.25 (brs, 16H), 0.89 (s, 9H), 0.04 (s, 3H), 0.02 ppm (s, 3H); (*Z*)-enyne: δ = 5.73 (ddd, J = 10.7, 8.7, 0.8 Hz, 1H), 5.38 (dq, J = 10.7, 2.4, 0.9 Hz, 1H), 4.59 (dtd, J = 8.7, 6.3, 0.9 Hz, 1H), 4.36 (t, J = 5.8 Hz, 1H), 3.31 (s, 6H), 1.97 (d, J = 2.4 Hz, 3H), 1.62–1.57 (m, 2H), 1.49–1.42 (m, 2H), 1.25 (brs, 16H), 0.88 (s, 9H), 0.04 (s, 3H), 0.02 ppm (s, 3H). ^{13}C NMR (100 MHz, CDCl_3): (*E*)-enyne: δ = 145.4, 109.0, 104.7, 86.0, 78.1, 72.8, 52.7 (2C), 38.1, 32.6, 29.8, 29.72 (2C), 29.70, 29.69, 29.6, 26.0 (3C), 25.2, 24.8, 18.4, 4.5, -4.3, -4.7 ppm; (*Z*)-enyne: δ = 145.7, 108.6, 104.7, 90.7, 76.2, 70.8, 52.7 (2C), 37.8, 32.6, 29.8, 29.72 (2C), 29.70, 29.69, 29.6, 26.1 (3C), 25.3, 24.8, 18.4, 4.5, -4.2, -4.8 ppm. IR (film): $\tilde{\nu}$ = 2926, 2855, 1463, 1361, 1253, 1126, 1074, 836, 776 cm^{-1} . MS (EI) m/z (%): 392 (11), 335 (15), 261 (21), 229 (12), 209 (30), 105 (12), 89 (16), 75 (100), 73 (22). HRMS (ESIpos): m/z calcd for $\text{C}_{25}\text{H}_{48}\text{O}_3\text{SiNa}$: 447.3265, found: 447.3269.

Enynes 35 and 36. Pyridinium *p*-toluenesulfonate (40.5 mg, 0.16 mmol) was added to a solution of



(*E,Z*)-**34** (228 mg, 0.54 mmol) in acetone (50 mL) and water (1.4 mL), and the resulting mixture was stirred at 60 °C for 4 h. After cooling to ambient temperature, the mixture was concentrated, the residue was partitioned between CH₂Cl₂ (5 mL) and H₂O (5 mL), and the aqueous layer was extracted

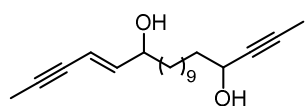
with CH₂Cl₂ (2 × 5 mL). The combined extracts were dried over Na₂SO₄, filtered and concentrated to furnish the crude aldehyde, which was used in the next step without further purification.

A solution of 1-propynylmagnesium bromide in THF (0.5 M, 1.62 mL, 0.81 mmol) was added to a solution of the crude aldehyde in THF (5 mL) and the resulting mixture stirred at ambient temperature for 4 h. The reaction was quenched with aq. sat. NH₄Cl solution (5 mL) and the aqueous layer was extracted with *t*-butyl methyl ether (3 × 10 mL). The combined extracts were washed with brine (50 mL), dried over Na₂SO₄, filtered and concentrated. The residue was purified by flash chromatography (hexanes/EtOAc 15:1) to afford a mixture of (*E*)- and (*Z*)-enynes **36** and **35**. The diastereomers were separated by preparative HPLC (Kromasil C18, 5 μm, 150×30 mm, MeCN/H₂O = 95:5, 35 °C, 25 bar, 35 mL/min, *t_R* (*E*) = 11.6 min, *t_R* (*Z*) = 13.4 min) to yield (*E*)-enyne **36** (87.9 mg, 38% over two steps) and (*Z*)-enyne **35** (50.2 mg, 23% over two steps) as a yellow oil each.

Analytical data for (*E*)-enyne **36**: ¹H NMR (400 MHz, CDCl₃): δ = 6.00 (ddd, *J* = 15.8, 5.7, 0.8 Hz, 1H), 5.57 (dq, *J* = 15.8, 2.3, 1.4 Hz, 1H), 4.31 (tq, *J* = 6.6, 2.1 Hz, 1H), 4.10 (tdd, *J* = 6.3, 5.7, 1.5 Hz, 1H), 1.93 (d, *J* = 2.3 Hz, 3H), 1.84 (d, *J* = 2.1 Hz, 3H), 1.69–1.59 (m, 2H), 1.49–1.36 (m, 4H), 1.24 (brs, 14H), 0.88 (s, 9H), 0.03 (s, 3H), 0.02 ppm (s, 3H). ¹³C NMR (100 MHz, CDCl₃): δ = 145.4, 109.0, 86.0, 81.0, 80.7, 78.1, 72.8, 62.9, 38.3, 38.1, 29.74, 29.70 (2C), 29.67 (2C), 29.4, 26.0 (3C), 25.3, 25.1, 18.4, 4.4, 3.7, –4.3, –4.7 ppm.

Analytical data for (*Z*)-enyne **35**: ¹H NMR (400 MHz, CDCl₃): δ = 5.73 (dd, *J* = 10.6, 8.9 Hz, 1H), 5.38 (dq, *J* = 10.8, 2.4, 0.9 Hz, 1H), 4.59 (dtd, *J* = 8.9, 7.1, 0.9 Hz, 1H), 4.32 (tq, *J* = 6.5, 2.1 Hz, 1H), 1.97 (d, *J* = 2.4 Hz, 3H), 1.84 (d, *J* = 2.1 Hz, 3H), 1.69–1.60 (m, 2H), 1.47–1.36 (m, 4H), 1.27 (brs, 14H), 0.88 (s, 9H), 0.07 (s, 3H), 0.04 ppm (s, 3H). ¹³C NMR (100 MHz, CDCl₃): δ = 145.7, 108.7, 90.7, 81.0, 80.7, 76.2, 70.8, 62.9, 38.3, 37.8, 29.77, 29.75, 29.72, 29.71, 29.70, 29.5, 26.1 (3C), 25.4, 25.3, 18.3, 4.5, 3.7, –4.2, –4.8 ppm. IR (film): $\tilde{\nu}$ = 3361, 2925, 2854, 1463, 1361, 1254, 1085, 955, 835, 775 cm⁻¹. MS (EI) *m/z* (%): 362 (10), 361 (35), 269 (24), 210 (16), 209 (87), 173 (10), 171 (14), 169 (21), 159 (22), 157 (22), 149 (18), 147 (10), 145 (35), 143 (15), 133 (18), 131 (23), 121 (13), 119 (29), 109 (15), 107 (22), 105 (35), 95 (38), 93 (29), 91 (23), 81 (33), 79 (28), 77 (13), 75 (100), 73 (58), 69 (23), 67 (23), 578 (12), 55 (21). HRMS (ESIpos): *m/z* calcd for C₂₆H₄₆O₂SiNa: 441.3159, found: 441.3159.

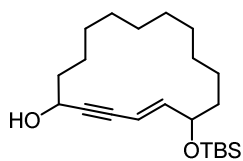
Diol 37. A solution of TBAF (1 M in THF, 80 μ L, 80 μ mol) was added to a solution of (*E*)-enyne **36**



(28 mg, 67 μ mol) in THF (0.6 mL) at 0 $^{\circ}$ C. The resulting mixture was stirred at ambient temperature for 1 h. The reaction was quenched with aq. sat. NH_4Cl solution (1 mL) and the aqueous layer extracted with

t-butyl methyl ether (3 \times 3 mL). The combined extracts were washed with brine (5 mL), dried over Na_2SO_4 , filtered and concentrated. The residue was purified by flash chromatography (hexanes/EtOAc 8:1) to afford diol **37** as a pale yellow oil (18 mg, 88%). ^1H NMR (400 MHz, CDCl_3): δ = 6.03 (dd, J = 15.9, 6.4 Hz, 1H), 5.64 (dq, J = 15.9, 2.3, 1.4 Hz, 1H), 4.31 (tq, J = 6.7, 2.1 Hz, 1H), 4.11 (qd, J = 6.2, 1.4 Hz, 1H), 1.93 (d, J = 2.3 Hz, 3H), 1.84 (d, J = 2.1 Hz, 3H), 1.69–1.60 (m, 2H), 1.60–1.47 (m, 2H), 1.45–1.37 (m, 2H), 1.27 ppm (brs, 14H). ^{13}C NMR (100 MHz, CDCl_3): δ = 144.5, 110.5, 86.7, 81.0, 80.7, 77.8, 72.6, 62.9, 38.3, 37.2, 29.6 (5C), 29.4, 25.4, 25.3, 4.4, 3.7 ppm. IR (film): $\tilde{\nu}$ = 3335, 2921, 2853, 1464, 1081, 956, 722 cm^{-1} . MS (ESIpos) m/z (%): 327.2 (100 (M+Na)). HRMS (ESIpos): m/z calcd for $\text{C}_{20}\text{H}_{32}\text{O}_2\text{Na}$: 327.2294, found: 327.2296.

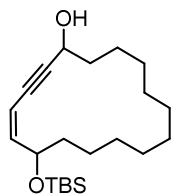
(*E*)-6-((*t*-Dimethylsilyl)oxy)cyclohexadec-4-en-2-yn-1-ol (39). This compound was prepared



according to the representative procedure for RCAM reactions using the two-component catalyst system (*vide supra*). Purification by flash chromatography (hexanes/*t*-butyl methyl ether 20:1) provided enyne **39** as a colorless oil (19.8 mg, 76%, *syn/anti*-mixture). ^1H NMR (400 MHz, CDCl_3): δ = 6.15 (dd,

J = 15.8, 5.2 Hz, 1H), 6.14 (dd, J = 15.8, 5.2 Hz, 1H), 5.72–5.62 (m, 2H), 4.55–4.48 (m, 2H), 4.28–4.23 (m, 2H), 1.84–1.65 (m, 8H), 1.48–1.38 (m, 8H), 1.35–1.19 (m, 24H), 0.89 (s, 18H), 0.04 (s, 6H), 0.03 ppm (s, 6H). ^{13}C NMR (100 MHz, CDCl_3): δ = 148.1, 147.8, 108.1, 108.0, 90.59, 90.55, 84.5, 84.4, 72.33, 72.27, 63.43, 63.37, 37.3, 37.2, 36.1 (2C), 28.41, 28.38, 27.9 (4C), 27.8 (2C), 27.62 (2C), 27.57, 27.5, 26.0 (6C), 23.7, 23.5, 21.92, 21.86, 18.4 (2C), –4.6 (2C), –4.8 ppm (2C). IR (film): $\tilde{\nu}$ = 3348, 2926, 2855, 1462, 1361, 1255, 1073, 956, 836, 776 cm^{-1} . MS (ESIpos) m/z (%): 387.3 (100 (M+Na)). HRMS (ESIpos): m/z calcd for $\text{C}_{22}\text{H}_{40}\text{O}_2\text{SiNa}$: 387.2690, found: 387.2691.

(*Z*)-6-((*t*-Dimethylsilyl)oxy)cyclohexadec-4-en-2-yn-1-ol (38). This compound was prepared



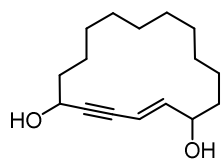
according to the representative procedure for RCAM reactions using the two-component catalyst system (*vide supra*). Colorless oil (22.3 mg, 90%); the diastereomers could be separated by flash chromatography (hexanes/*t*-butyl methyl ether 20:1).

Analytical data for the faster eluting diastereomer: ^1H NMR (300 MHz, CDCl_3): δ = 5.84 (dd, J = 10.9, 8.8 Hz, 1H), 5.48 (ddd, J = 10.8, 2.1, 0.8 Hz, 1H), 4.63 (td, J = 8.2, 4.9 Hz, 1H), 4.55 (ddd, J = 7.8, 5.1, 2.0 Hz, 1H), 1.79–1.66 (m, 2H), 1.53 (brs, 1H), 1.44–1.28 (m, 18H), 0.89 (s, 9H), 0.10 (s, 3H), 0.06 ppm

(s, 3H). ^{13}C NMR (75 MHz, CDCl_3): δ = 147.6, 107.7, 95.2, 81.5, 71.2, 63.6, 37.9, 36.9, 27.1 (2C), 26.9, 26.7, 26.1 (3C), 25.63, 25.60, 23.74, 23.71, 18.4, -4.1, -4.6 ppm.

Analytical data for the slower eluting diastereomer: ^1H NMR (300 MHz, CDCl_3): δ = 5.82 (dd, J = 10.9, 8.9 Hz, 1H), 5.48 (d, J = 10.9 Hz, 1H), 4.66–4.52 (m, 2H), 1.89–1.65 (m, 4H), 1.47–1.28 (m, 17H), 0.89 (s, 9H), 0.08 (s, 3H), 0.04 ppm (s, 3H). ^{13}C NMR (75 MHz, CDCl_3): δ = 147.1, 107.7, 95.0, 81.8, 71.2, 63.2, 37.7, 36.7, 27.3, 27.1, 26.72, 26.71, 26.1, 26.0 (3C), 25.7, 23.8, 23.7, 18.3, -4.1, -4.7 ppm. IR (film): $\tilde{\nu}$ = 3432, 2927, 2856, 1461, 1361, 1071, 1018, 907, 835, 776, 732 cm^{-1} . MS (ESIpos) m/z (%): 387.3 (100 (M+Na)). HRMS (ESIpos): m/z calcd for $\text{C}_{22}\text{H}_{40}\text{O}_2\text{SiNa}$: 387.2690, found: 387.2692.

(E)-Cyclohexadec-2-en-4-yne-1,6-diol (40). This compound was prepared according to the

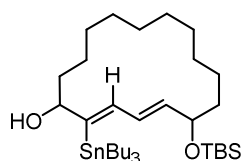


representative procedure for RCAM reactions using the two-component catalyst system (*vide supra*). Purification by flash chromatography (hexanes/EtOAc 4:1) provided enyne **40** as a colorless solid (3.3 mg, 40%, *syn/anti*-mixture). m.p. [EtOAc] = 92–93 °C. ^1H NMR (300 MHz, CDCl_3): δ = 6.16 (ddd, J = 15.9, 6.5, 3.4 Hz,

1H), 5.71 (dt, J = 15.9, 1.6 Hz, 1H), 4.59–4.46 (m, 1H), 4.30–4.18 (m, 1H), 1.85–1.65 (m, 4H), 1.61–1.19 ppm (m, 18H). ^{13}C NMR (100 MHz, CDCl_3): δ = 146.9, 146.8, 109.70, 109.68, 91.3, 91.2, 83.99, 83.96, 72.63, 72.58, 63.37, 63.36, 37.14, 37.12, 35.54, 35.51, 28.4, 28.3, 27.9 (2C), 27.8, 27.74 (2C), 27.72, 27.69, 27.64, 27.62, 27.61, 23.6, 23.5, 22.5 ppm (2C). IR (film): $\tilde{\nu}$ = 3670, 3309, 2923, 2852, 2219, 1633, 1459, 1407, 1342, 1292, 1168, 1115, 1015, 955, 871, 798, 710, 553, 507, 469 cm^{-1} . MS (ESIpos) m/z (%): 273.2 (100 (M+Na)). HRMS (ESIpos): m/z calcd for $\text{C}_{16}\text{H}_{26}\text{O}_2\text{Na}$: 273.1824, found: 273.1825.

Representative Procedure for *trans*-Hydrostannylation Reactions with Enyne Substrates.

Preparation of (2Z,4E)-6-((*t*-dimethylsilyloxy)-2-(tristannyl)cyclohexadeca-2,4-dien-1-ol (S15). A

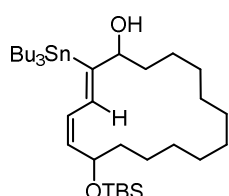


solution of Bu_3SnH (9.3 μL , 35 μmol) in CH_2Cl_2 (0.15 mL) was added dropwise over 90 min *via* syringe pump to a solution of enyne **39** (12 mg, 33 μmol) and $[\text{Cp}^*\text{RuCl}]_4$ (1.8 mg, 6.6 μmol , 20 mol%) in CH_2Cl_2 (0.2 mL). All volatiles were evaporated and the residue was purified by flash chromatography (hexanes/

t-butyl methyl ether 19:1) to afford stannane **S15** as a pale yellow oil (17.9 mg, 83%, Z/E > 20:1, α/β > 95:5, *syn/anti*-mixture with regard to diol). ^1H NMR (400 MHz, CDCl_3): δ = 6.75 (d, J = 10.9 Hz, J_{SnH} = 119 Hz, 1H), 6.68 (d, J = 10.7 Hz, J_{SnH} = 117 Hz, 1H), 6.29 (ddd, J = 14.7, 10.9, 1.7 Hz, 1H), 6.08 (dd, J = 14.9, 10.7 Hz, 1H), 5.68 (dd, J = 14.7, 4.3 Hz, 1H), 5.59 (dd, J = 14.9, 8.4 Hz, 1H), 4.40 (dt, J = 4.9, 2.4 Hz, 1H), 4.31–4.20 (m, 2H), 4.07 (td, J = 9.0, 3.7 Hz, 1H), 1.78–1.57 (m, 5H), 1.56–1.42 (m, 18H), 1.38–1.28 (m, 20H), 1.27–1.10 (m, 32H), 1.04–0.98 (m, 10H), 0.92 (s, 9H), 0.90–0.89 (m, 9H), 0.88 (s, 9H), 0.06 (s, 9H), 0.04 ppm (s, 3H). ^{13}C NMR (100 MHz, CDCl_3): δ = 153.4, 151.2, 140.2, 140.0, 139.4, 139.3, 130.7, 128.8, 81.0, 80.4, 74.9, 71.8, 37.5, 36.9, 36.8, 36.6, 29.40 (3C), 29.39 (3C), 29.0,

28.9, 28.5, 28.2 (2C), 28.0 (2C), 27.9, 27.74, 27.72, 27.70, 27.6 (6C), 27.5, 26.2 (3C), 26.1 (3C), 24.2, 23.8, 23.5, 21.8, 18.5, 18.4, 13.8 (6C), 11.5 (3C), 11.2 (3C), -4.1, -4.4, -4.6, -4.8 ppm. ^{119}Sn NMR (150 MHz, CDCl_3): $\delta = -55.1, -56.2$ ppm. IR (film): $\tilde{\nu} = 3373, 2926, 2854, 1461, 1253, 1070, 967, 835, 775, 667$ cm^{-1} . MS (ESIpos) m/z (%): 679.4 (55 (M+Na)). HRMS (ESIpos): m/z calcd for $\text{C}_{34}\text{H}_{68}\text{O}_2\text{SiSnNa}$: 679.3902, found: 679.3903.

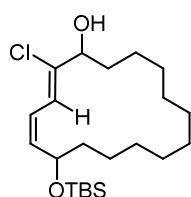
(2Z,4Z)-6-((*t*-Dimethylsilyl)oxy)-2-(tristannyl)cyclohexadeca-2,4-dien-1-ol (45). A solution of Bu_3SnH



(5.5 μL , 20 μmol) in CH_2Cl_2 (0.1 mL) was added dropwise over 90 min *via* syringe pump to a solution of enyne **38** (7.1 mg, 19 μmol) and $[\text{Cp}^*\text{RuCl}]_4$ (1.0 mg, 3.7 μmol , 19 mol%) in CH_2Cl_2 (0.1 mL). All volatiles were evaporated and the residue was purified by flash chromatography (hexanes/*t*-butyl methyl ether

19:1) to afford stannane **45** as a pale yellow oil (10 mg, 79%, $Z/E > 20:1$, $\alpha/\beta > 95:5$). ^1H NMR (400 MHz, CDCl_3): $\delta = 6.84$ (d, $J = 11.4$ Hz, $J_{\text{SnH}} = 115$ Hz, 1H), 5.93 (dt, $J = 11.2, 1.2$ Hz, 1H), 5.42 (ddd, $J = 11.2, 8.6, 1.1$ Hz, 1H), 4.62 (q, $J = 7.0$ Hz, 1H), 4.24 (ddd, $J = 9.6, 4.7, 2.9$ Hz, 1H), 1.54–1.38 (m, 12H), 1.36–1.25 (m, 20H), 1.03–0.96 (m, 5H), 0.91–0.86 (m, 10H), 0.88 (s, 9H), 0.05 (s, 3H), 0.03 ppm (s, 3H). ^{13}C NMR (100 MHz, CDCl_3): $\delta = 155.4, 137.3, 135.1, 127.2, 81.1, 68.5, 37.23, 37.18, 29.4$ (3C), 27.6, 27.5 (3C), 27.4, 27.2, 27.0, 26.6, 26.3, 26.1 (3C), 25.3, 24.3, 18.4, 13.9 (3C), 11.7 (3C), -4.0, -4.5 ppm. ^{119}Sn NMR (150 MHz, CDCl_3): $\delta = -53.5$ ppm. IR (film): $\tilde{\nu} = 3481, 2954, 2926, 2855, 1462, 1251, 1071, 1005, 836, 775, 676$ cm^{-1} . MS (EI) m/z (%): 599 (13), 597 (12), 468 (14), 467 (57), 466 (25), 265 (45), 464 (19), 463 (25), 365 (47), 364 (19), 363 (35), 362 (14), 361 (19), 281 (11), 251 (16), 249 (13), 218 (18), 217 (100), 195 (12), 193 (11), 179 (12), 177 (17), 175 (12), 135 (35), 121 (34), 107 (12), 95 (16), 93 (21), 91 (12), 81 (16), 79 (16), 75 (24), 73 (13), 67 (17). HRMS (ESIneg): m/z calcd for $\text{C}_{34}\text{H}_{67}\text{O}_2\text{SiSn}$: 655.3937, found: 655.3946.

(Z,Z)-Chlorodiene 46. A solution of dienylstannane **45** (9.7 mg, 15 μmol) in THF (0.2 mL) was added to

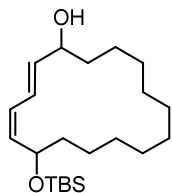


a suspension of CuCl_2 (5.0 mg, 37 μmol) in THF (0.15 mL). The resulting mixture was stirred at ambient temperature for 24 h. The mixture was diluted with *t*-butyl methyl ether (2.5 mL) and the reaction quenched with aq. sat. NaHCO_3 (3 mL). The aqueous layer was extracted with *t*-butyl methyl ether (3 \times 4 mL). The combined

extracts were washed with brine (5 mL), dried over Na_2SO_4 , filtered and concentrated. The residue was purified by flash chromatography (hexanes/*t*-butyl methyl ether 15:1 to 10:1) to afford chlorodiene **46** (4.0 mg, 67%) along with diene **47** (0.3 mg, 6%) as a colorless oil each. ^1H NMR (400 MHz, CDCl_3): $\delta = 6.41$ (dd, $J = 11.0, 0.9$ Hz, 1H), 6.30 (td, $J = 11.0, 1.3$ Hz, 1H), 5.64 (ddd, $J = 11.0, 8.4, 0.9$ Hz, 1H), 4.49 (dddd, $J = 8.3, 7.2, 5.6, 1.3$ Hz, 1H), 4.33 (dd, $J = 10.2, 4.6$ Hz, 1H), 1.93–1.78 (m, 2H), 1.71–1.65 (m, 1H), 1.53–1.49 (m, 1H), 1.45–1.40 (m, 1H), 1.38–1.30 (m, 11H), 1.23–1.07 (m, 4H), 0.88 (s, 9H), 0.05 (s, 3H), 0.03 ppm (s, 3H). ^{13}C NMR (100 MHz, CDCl_3): $\delta = 140.6, 137.4, 122.0, 121.1, 75.4,$

69.2, 37.1, 34.7, 27.6, 27.5, 27.1, 26.9, 26.3, 26.0 (3C), 25.9, 25.2, 24.2, 18.3, -4.1, -4.6 ppm. IR (film): $\tilde{\nu}$ = 3368, 2927, 2856, 1727, 1461, 1360, 1251, 1074, 835, 775, 734, 663, 584 cm^{-1} . MS (ESIpos) m/z (%): 423.2 (100 (M+Na)). HRMS (ESIpos): m/z calcd for $\text{C}_{22}\text{H}_{41}\text{O}_2\text{ClSiNa}$: 423.2457, found: 423.2453.

Analytical data for **47**: ^1H NMR (400 MHz, CDCl_3): δ = 6.31 (dd, J = 15.3, 11.2 Hz, 1H), 5.94 (t, J = 11.1

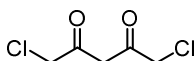


Hz, 1H), 5.54 (dd, J = 15.1, 8.9 Hz, 1H), 5.42 (dd, J = 11.0, 8.5 Hz, 1H), 4.55 (q, J = 7.4 Hz, 1H), 4.19 (td, J = 9.4, 4.2 Hz, 1H), 1.77–1.69 (m, 2H), 1.46–1.40 (m, 2H), 1.36–1.29 (m, 12H), 1.17–1.06 (m, 4H), 0.88 (s, 9H), 0.06 (s, 3H), 0.03 ppm (s, 3H). IR (film): $\tilde{\nu}$ = 3433, 2926, 2855, 1729, 1461, 1257, 1074, 948, 835, 775, 670 cm^{-1} . MS (ESIpos)

m/z (%): 389.3 (100 (M+Na)). HRMS (ESIpos): m/z calcd for $\text{C}_{22}\text{H}_{42}\text{O}_2\text{SiNa}$: 389.2846, found: 389.2845.

4.3.2 Synthesis of the Northern Alcohol Fragments **48** and **49**

1,5-Dichloropentane-2,4-dione (52). An oven-dried 3-necked flask equipped with a 250 ml dropping

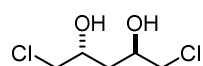


funnel and a reflux condenser, which was connected to two Drechsel bottles filled with 1 M NaOH solution, was charged with AlCl_3 (60.0 g, 450 mmol). Nitrobenzene

(76.0 mL, 738 mmol) was added dropwise over 30 min, followed by the dropwise addition of 1,2-dichloroethane (90.0 mL, 1.14 mol) over 30 min. The mixture was stirred vigorously for 30 min before it was cooled to 0 °C. Next, acetyl acetone (46.2 mL, 450 mmol) was added dropwise over 30 min, followed by chloroacetyl chloride (79.2 mL, 994 mmol), which was added dropwise over 40 min. The resulting mixture was allowed to warm to rt, the reflux condenser was replaced by an internal thermometer, and the addition funnel was replaced by a distillation head, which was attached to the set of Drechsel bottles. The mixture was then gently heated to 65 °C over the course of 2 hours. Distillation of acetyl chloride (38–39 °C) was continued for 6 h, before the mixture was cooled to rt and poured into a mixture of ice and conc. HCl (65 mL). The resulting suspension was stirred vigorously at rt for 17 h before the phases were separated. The aqueous phase was extracted with Et_2O (4 × 200 mL) and the combined extracts were poured into sat. aq. $\text{Cu}(\text{OAc})_2$ solution (800 mL). The resulting biphasic mixture was stirred vigorously at rt for 24 h before it was filtered with suction. The collected precipitate was washed with Et_2O (200 mL) and triturated with Et_2O (250 mL). Filtration with suction afforded the copper complex as green powdery solid, which was then suspended in a mixture of Et_2O (400 mL) and 10% H_2SO_4 (250 mL). The mixture was stirred at rt for 24 h, the phases were separated and the aqueous phase was further extracted with Et_2O (250 mL). The combined organic extracts were dried over Na_2SO_4 , filtered and concentrated. Purification by Kugelrohr distillation afforded **52** (16.8 g, 22%) as a yellow oil that darkened over time. The product was detected as a mixture of keto-enol tautomers in the NMR: Enol: ^1H NMR (400 MHz, CDCl_3): δ = 14.49 (s, 1H), 6.18 (s, 1H), 4.09 ppm (s, 4H). ^{13}C NMR (100 MHz, CDCl_3): δ = 196.5,

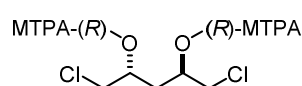
187.4, 96.9, 44.2 ppm (2C). Ketone: ^1H NMR (400 MHz, CDCl_3): δ = 4.18 (s, 4H), 3.98 ppm (s, 2H). ^{13}C NMR (100 MHz, CDCl_3): δ = 196.4 (2C), 50.6, 48.4 ppm (2C). IR (film): $\tilde{\nu}$ = 2937, 1727, 1604, 1397, 1321, 1227, 1191, 1123, 903, 723, 650, 574 cm^{-1} . MS (EI) m/z (%): 132 (14), 121 (33), 119 (100), 79 (10), 77 (32), 68 (12), 67 (19), 49 (12), 43 (26), 39 (16), 37 (13), 36 (17). HRMS (ESIpos): m/z calcd for $\text{C}_5\text{H}_6\text{O}_2\text{Cl}_2\text{Na}$: 190.9637; found: 190.9638.

(2R,4R)-1,5-Dichloropentane-2,4-diol (53). Freshly distilled **52** (8.50 g, 50.3 mmol) was dissolved in



MeOH (23 mL) and the resulting solution was degassed with an Ar stream for 20 min. $[\text{RuCl}_2((S)\text{-BINAP})_2]\cdot\text{Et}_3\text{N}$ (45.1 mg, 0.05 mmol, 0.1 mol%) was added and the resulting mixture was cannulated into an oven-dried 100 mL autoclave, which was then sealed and pressurized with H_2 (62 bar). The reaction mixture was stirred at 70 °C (external temperature) for 16 h before it was cooled to rt and concentrated. The residue was taken up in hexanes/EtOAc (1:1, 100 mL) and passed through a plug of silica. The filter cake was washed with hexanes/EtOAc (1:1, 250 mL) and the combined filtrates were concentrated. Recrystallization from CH_2Cl_2 /hexanes (3:2, 70 mL) afforded diol **53** (3.4 g, 39%, 97% *ee*, d.r. > 20:1) as colorless needles. m.p. [hexanes] = 86–88 °C. $[\alpha]_{\text{D}}^{20} = +21.1$ ($c = 1.0$, CHCl_3). ^1H NMR (400 MHz, CDCl_3): δ = 4.14 (tdd, $J = 6.8, 5.4, 4.1$ Hz, 2H), 3.65 (dd, $J = 11.1, 4.0$ Hz, 2H), 3.53 (dd, $J = 11.1, 6.9$ Hz, 2H), 2.77 (brs, 2H), 1.75 ppm (dd, $J = 6.7, 5.3$ Hz, 2H). ^{13}C NMR (100 MHz, CDCl_3): δ = 68.7 (2C), 50.1 (2C), 37.6 ppm. IR (film): $\tilde{\nu}$ = 3361, 3285, 2959, 2890, 1433, 1402, 1326, 1294, 1215, 1186, 1102, 1072, 1052, 911, 709, 571 cm^{-1} . MS (ESI_{neg}) m/z (%): 171.0 (100 (M–H)). HRMS (ESI_{neg}): m/z calcd for $\text{C}_5\text{H}_9\text{O}_2\text{Cl}_2$: 170.9985; found: 170.9987.

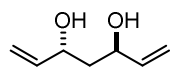
The enantiomeric excess of diol **53** was initially determined by a modified Mosher analysis as



described by Rychnovsky and coworkers^[105b] and for further batches of material by comparison of optical rotation values. To a solution of diol **53** (5.0 mg, 31 μmol) in CH_2Cl_2 (3 mL) was added triethylamine (26 μL , 0.19 mmol) followed by (*S*)-(+)- α -methoxy- α -trifluoromethyl-phenylacetyl chloride ((*S*)-MTPA-Cl) (25 μL , 0.13 mmol) and DMAP (0.5 mg, 4.1 μmol , 13 mol%). The reaction was stirred at rt for 2 h, before it was quenched with sat. aq. NaHCO_3 (3 mL) and extracted with CH_2Cl_2 (3 \times 5 mL). The combined extracts were dried over Na_2SO_4 , filtered and concentrated. The crude diastereomeric mixture of (*R*)-MTPA-**53** was obtained as a colorless oil (17.5 mg, 47%). $[\alpha]_{\text{D}}^{20} = +82.5$ ($c = 2.02$, CHCl_3). ^1H NMR (400 MHz, CDCl_3): δ = 7.62–7.55 (m, 4H), 7.47–7.41 (m, 6H), 5.05 (ddt, $J = 7.6, 5.3, 4.1$ Hz, 2H), 3.73 (dd, $J = 12.3, 4.0$ Hz, 2H), 3.633 (s, 3H), 3.630 (s, 3H), 3.49 (dd, $J = 12.3, 4.2$ Hz, 2H), 2.08 ppm (dd, $J = 7.3, 5.2$ Hz, 2H). ^{13}C NMR (100 MHz, CDCl_3): δ = 166.1 (2C), 132.2 (2C), 130.0 (2C), 128.8 (4C), 127.25 (2C), 127.24 (2C), 124.8 (2C), 121.9 (2C), 71.5 (2C), 56.0, 55.9, 45.2 (2C), 34.5 ppm. IR (film): $\tilde{\nu}$ = 2956, 2851, 1753, 1452, 1242, 1170, 1122, 1082, 1017, 819, 765, 719, 699 cm^{-1} . MS (ESIpos) m/z (%): 627.1 (100 (M+Na)). HRMS (ESIpos): m/z calcd for $\text{C}_{25}\text{H}_{24}\text{O}_6\text{F}_6\text{Cl}_2\text{Na}$: 327.0746; found: 627.0750. The enantiomeric excess

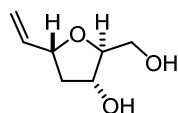
was determined based on ^1H NMR by integration of the central CH_2 signal of each derivative at 400 MHz in CDCl_3 . The signal for the (*R,R*)-diol derivative appears at 2.08 ppm (dd, $J = 7.3, 5.2$ Hz, 2H) whereas the signal for the (*S,S*)-diol derivative appears at 2.20 ppm (dd, $J = 7.3, 5.5$ Hz, 0.03H). Hence, 98.5% of the (*R,R*)-diol and 1.5% of the (*S,S*)-diol were detected in the diastereomeric mixture, resulting in approx. 97% *ee* of diol **53**.

(3*R*,5*R*)-Hepta-1,6-diene-3,5-diol (50). A solution of *n*-BuLi (1.59 M in hexanes, 158.4 mL, 232 mmol)



was added dropwise over 10 min to a -40 °C cold solution of Me_3SI (47.2 g, 232 mmol) in THF (140 mL). The resulting mixture was stirred for 15 min before a freshly prepared solution of diol **53** (4.00 g, 23.2 mmol) in THF (20 mL) was added dropwise over 5 min. The mixture was allowed to warm to rt over the course of 6 h and stirred for 12 h before it was poured into sat. aq. NH_4Cl (200 mL). The aqueous layer was extracted with *t*-butyl methyl ether (3×250 mL). The combined organic extracts were dried over Na_2SO_4 , filtered and concentrated. The residue was purified by flash chromatography (hexanes/EtOAc 10:1) to give the desired product as a colorless oil (1.91 g, 65%). $[\alpha]_{\text{D}}^{20} = -27.8$ ($c = 1.0, \text{CHCl}_3$). ^1H NMR (400 MHz, CDCl_3): $\delta = 5.92$ (ddd, $J = 17.2, 10.5, 5.5$ Hz, 2H), 5.29 (dt, $J = 17.2, 1.5$ Hz, 2H), 5.15 (dt, $J = 10.5, 1.4$ Hz, 2H), 4.46 (tdd, $J = 6.9, 5.4, 1.5$ Hz, 2H), 2.42 (brs, 2H), 1.78 ppm (dd, $J = 6.1, 5.3$ Hz, 2H). ^{13}C NMR (100 MHz, CDCl_3): $\delta = 140.5$ (2C), 114.8 (2C), 70.6 (2C), 42.0 ppm. IR (film): $\tilde{\nu} = 3328, 3082, 2983, 2915, 1645, 1422, 1315, 1114, 1054, 991, 921, 824, 656$ cm^{-1} . MS (EI) m/z (%): 57 (40), 56 (16), 55 (36), 54 (100), 43 (11), 39 (20), 29 (19), 27 (13). HRMS (ESIpos): m/z calcd for $\text{C}_7\text{H}_{12}\text{O}_2\text{Na}$: 151.0729; found: 151.0731.

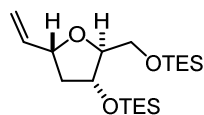
(2*S*,3*R*,5*R*)-2-(Hydroxymethyl)-5-vinyltetrahydrofuran-3-ol (55). Diol **50** (1.81 g, 14.1 mmol) in



2-propanol (147 mL) was added to a flask charged with $\text{Co}(\text{nmp})_2$ (798 mg, 1.41 mmol, 10 mol%). The pale red solution was purged with O_2 for 15 min before *t*-BuOOH (5.5 M in decane, 0.26 mL, 1.41 mmol, 10 mol%) was added in one portion; the solution slowly turned green. The reaction mixture was stirred at 55 °C under an oxygen atmosphere (balloon) for 5 h. After cooling to rt, the oxygen atmosphere was replaced by argon. The solvent was removed under reduced pressure, the residue was re-dissolved in EtOAc (10 mL) and the solution was filtered through a pad of silica (1 cm) over packed Celite[®] (3 cm), eluting with EtOAc (100 mL). The solvent was removed under reduced pressure and the residue purified by flash chromatography (hexanes/EtOAc 2:1 to 1:2) to yield the desired diol **55** as a pale yellow oil (1.59 g, 78%). $[\alpha]_{\text{D}}^{20} = -37.3$ ($c = 1.0, \text{CHCl}_3$). ^1H NMR (400 MHz, CDCl_3): $\delta = 5.97$ (ddd, $J = 17.0, 10.3, 6.4$ Hz, 1H), 5.28 (dt, $J = 17.2, 1.4$ Hz, 1H), 5.14 (dt, $J = 10.3, 1.3$ Hz, 1H), 4.52 (ddd, $J = 7.0, 6.4, 1.0$ Hz, 1H), 4.32 (q, $J = 6.1$ Hz, 1H), 3.92 (td, $J = 5.0, 4.0$ Hz, 1H), 3.74 (dd, $J = 11.7, 4.0$ Hz, 1H), 3.64 (dd, $J = 11.7, 4.9$ Hz, 1H), 2.41 (ddd, $J = 12.8, 6.8, 6.7$ Hz, 1H), 2.32 (brs, 1H), 2.26 (brs, 1H), 1.84 ppm (ddd, $J = 13.2, 7.2, 6.2$ Hz, 1H). ^{13}C NMR (100 MHz, CDCl_3): $\delta = 139.3, 115.8, 85.3, 79.3, 73.2, 62.8, 41.2$ ppm.

IR (film): $\tilde{\nu}$ = 3359, 2930, 2877, 1645, 1427, 1338, 1329, 1088, 1035, 989, 928, 887, 857, 670 cm^{-1} . MS (EI) m/z (%): 113 (43), 95 (32), 83 (27), 71 (11), 70 (19), 69 (10), 67 (53), 60 (11), 57 (29), 56 (28), 55 (100), 54 (16), 53 (11), 43 (30), 42 (12), 41 (37), 39 (23), 31 (20), 29 (24), 27 (14). HRMS (ESIpos): m/z calcd for $\text{C}_7\text{H}_{12}\text{O}_3\text{Na}$: 167.0679, found: 167.0680.

Bis-TES-ether 56. A solution of diol **55** (1.00 g, 6.94 mmol) in anhydrous DMF (20 mL) was cooled to 0 °C. Imidazole (1.89 g, 27.7 mmol) and DMAP (84.7 mg, 0.69 mmol, 10 mol%) were added followed by TESCl (3.14 g, 20.8 mmol). The resulting solution was stirred at ambient temperature for 3 h. The reaction was quenched with sat. aq.



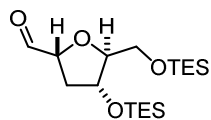
NaHCO₃ (30 mL) and the mixture was extracted with *t*-butyl methyl ether (3 × 50 mL). The combined extracts were dried over Na₂SO₄, filtered and concentrated. The residue was purified by flash chromatography (hexanes/*t*-butyl methyl ether 300:1) to yield the title compound as a colorless oil (2.09 g, 81%). $[\alpha]_{\text{D}}^{20}$ = -22.7 (*c* = 1.0, CHCl₃). ¹H NMR (500 MHz, CDCl₃): δ = 6.00 (ddd, *J* = 17.2, 10.2, 7.5 Hz, 1H), 5.17 (ddd, *J* = 17.2, 1.6, 1.0 Hz, 1H), 5.05 (ddd, *J* = 10.2, 1.6, 1.0 Hz, 1H), 4.44 (dtt, *J* = 8.0, 6.6, 1.0 Hz, 1H), 4.38 (ddd, *J* = 6.3, 5.3, 3.9 Hz, 1H), 3.88 (q, *J* = 4.3 Hz, 1H), 3.64 (dd, *J* = 10.9, 4.2 Hz, 1H), 3.59 (dd, *J* = 10.9, 4.9 Hz, 1H), 2.30 (ddd, *J* = 12.6, 7.0, 6.6 Hz, 1H), 1.74 (ddd, *J* = 12.6, 6.6, 5.2 Hz, 1H), 0.958 (t, *J* = 7.9 Hz, 9H), 0.955 (t, *J* = 7.9 Hz, 9H), 0.602 (q, *J* = 7.9 Hz, 6H), 0.600 ppm (q, *J* = 7.9 Hz, 6H). ¹³C NMR (125 MHz, CDCl₃): δ = 140.1, 115.3, 86.6, 80.3, 73.4, 63.4, 41.6, 6.9 (6C), 4.9 (3C), 4.5 (3C) ppm. IR (film): $\tilde{\nu}$ = 2954, 2911, 2876, 1458, 1415, 1238, 1110, 1077, 1004, 918, 835, 785, 726 cm^{-1} . MS (EI) m/z (%): 343 (14), 190 (24), 289 (100), 259 (27), 240 (10), 217 (12), 211 (25), 145 (10), 117 (69), 115 (25), 87 (21). HRMS (ESIpos): m/z calcd for $\text{C}_{19}\text{H}_{40}\text{O}_3\text{Si}_2\text{Na}$: 395.2408, found: 395.2411.

Bis-TES-ether 57. In case of instant silyl protection of the crude mixture of diol **55**, a second compound was isolated after flash chromatography, which appeared to be the bis-silylated starting material of the Mukaiyama oxidative cyclization **57**. This undesired byproduct was isolated only once (302 mg, 12%) and characterized as follows: $[\alpha]_{\text{D}}^{20}$ = -5.4 (*c* = 1.0, CHCl₃). ¹H NMR (400 MHz, CDCl₃): δ = 5.81 (ddd, *J* = 17.3, 10.3, 7.1 Hz, 2H), 5.13 (ddd, *J* = 17.2, 1.8 Hz, 2H), 5.04 (ddd, *J* = 10.2, 1.7, 0.9 Hz, 2H), 4.16 (tdd, *J* = 7.5, 6.0, 1.0 Hz, 2H), 1.70 (t, *J* = 6.6 Hz, 2H), 0.94 (t, *J* = 7.9 Hz, 18H), 0.59 ppm (q, *J* = 7.6 Hz, 12H). ¹³C NMR (100 MHz, CDCl₃): δ = 141.8 (2C), 114.5 (2C), 71.2 (2C), 47.2, 7.0 (6C), 5.2 ppm (6C). IR (film): $\tilde{\nu}$ = 2982, 2913, 1427, 1115, 1051, 903, 723, 650 cm^{-1} . MS (ESIpos) m/z (%): 379.2 (100 (M+Na)). HRMS (ESIpos): m/z calcd for $\text{C}_{19}\text{H}_{40}\text{O}_2\text{Si}_2\text{Na}$: 379.2459, found: 379.2460.

The bis-silyl ether **57** could be cleaved to diol **50** as follows: A solution of TBAF (1 M in THF, 3.31 mL, 3.31 mmol) was added to a solution of bis-silyl ether **57** (295 mg, 0.83 mmol) in THF (8 mL) at -50 °C. The resulting reaction mixture was stirred at this temperature for 3.5 h. The reaction was quenched

with sat. aq. NH_4Cl (10 mL) and the mixture was extracted with *t*-butyl methyl ether (3×15 mL). The combined organic extracts were dried over Na_2SO_4 , filtered and concentrated. The residue was purified by flash chromatography (hexanes/EtOAc 10:1) to give the desired product **50** (85 mg, 80%) as a colorless oil (analytical data *vide supra*).

Tetrahydrofuran-carbaldehyde 58. Ozone was bubbled through a solution of olefin **56** (2.75 g,

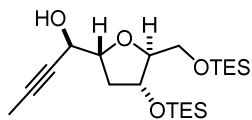


7.38 mmol) in CH_2Cl_2 (500 mL) at -78 °C for 90 min, until the blue color persisted.

Oxygen was then bubbled through the mixture for approx. one minute followed by argon until the solution was colorless. PPh_3 (2.90 g, 11.1 mmol) was added in

one portion and the mixture was allowed to reach rt overnight. The mixture was washed with sat. aq. NaHCO_3 (100 mL) and brine (100 mL), dried over Na_2SO_4 , filtered and concentrated. The residue was purified by flash chromatography (hexanes/*t*-butyl methyl ether 100:1 to 20:1) to afford the title compound as a colorless oil (2.07 g, 75%). $[\alpha]_D^{20} = -5.7$ ($c = 1.0$, CHCl_3). ^1H NMR (400 MHz, CDCl_3): $\delta = 9.72$ (d, $J = 1.5$ Hz, 1H), 4.34 (m, 2H), 4.07 (dd, $J = 6.8, 4.1$ Hz, 1H), 3.64 (dd, $J = 10.7, 4.1$ Hz, 1H), 3.42 (dd, $J = 10.7, 6.7$ Hz, 1H), 2.30 (ddd, $J = 13.4, 9.4, 4.3$ Hz, 1H), 2.02 (ddd, $J = 13.0, 1.8, 1.8$ Hz, 1H), 0.95 (t, $J = 7.9$ Hz, 9H), 0.92 (t, $J = 7.9$ Hz, 9H), 0.60 (q, $J = 7.9$ Hz, 6H), 0.57 ppm (q, $J = 7.9$ Hz, 6H). ^{13}C NMR (100 MHz, CDCl_3): $\delta = 205.7, 89.0, 83.0, 72.8, 63.5, 38.9, 6.9$ (3C), 6.8 (3C), 4.8 (3C), 4.4 ppm (3C). IR (film): $\tilde{\nu} = 2954, 2912, 2877, 1735, 1459, 1415, 1239, 1177, 1091, 1042, 1005, 977, 863, 797, 726$ cm^{-1} . MS (EI) m/z (%): 346 (15), 345 (52), 317 (25), 289 (20), 259 (15), 213 (14), 189 (13), 188 (13), 187 (96), 171 (12), 159 (17), 157 (10), 145 (37), 131 (16), 118 (10), 117 (100), 115 (54), 103 (23), 101 (10), 87 (47), 75 (10), 59 (21). HRMS (ESIpos): m/z calcd for $\text{C}_{18}\text{H}_{38}\text{O}_4\text{Si}_2\text{Na}$: 397.2201, found: 397.2200.

Propargylic alcohol 59. A Schlenk flask was charged with $\text{Zn}(\text{OTf})_2$ (3.82 g, 10.5 mmol) and (1*R*, 2*S*)-



(-)-*N*-methylephedrine (1.88 g, 10.5 mmol) before toluene (25 mL) and Et_3N

(1.46 mL, 10.5 mmol) were added. The mixture was stirred at rt for 2 h before

being cooled to -78 °C. Next, condensed propyne (excess, approx. 1 mL) was

cannulated from a Schlenk tube at -78 °C into the cold solution. The reaction mixture was taken out of the cooling bath and stirred at rt for 1 h before a freshly prepared solution of aldehyde **58** (1.75 g, 4.67 mmol) in toluene (25 mL) was added. After 48 h, the reaction was quenched by addition of sat. aq. NH_4Cl (30 mL). The aqueous phase was extracted with *t*-butyl methyl ether (3×50 mL) and the combined extracts were dried over Na_2SO_4 , filtered and concentrated. The residue was purified by flash chromatography (hexanes/*t*-butyl methyl ether 19:1 to 10:1) to give propargylic alcohol **59** as a colorless oil (1.45 g, 75%, d.r. > 12:1). $[\alpha]_D^{20} = -12.5$ ($c = 1.0$, CHCl_3). ^1H NMR (400 MHz, CDCl_3): $\delta = 4.41$ (dt, $J = 6.4, 2.4$ Hz, 1H), 4.35 (dt, $J = 5.9, 2.3$ Hz, 1H), 4.15 (ddd, $J = 8.5, 6.3, 3.5$ Hz, 1H), 3.97 (ddd, $J = 6.2, 4.1, 2.0$ Hz, 1H), 3.63 (dd, $J = 10.7, 4.2$ Hz, 1H), 3.45 (dd, $J = 10.7, 6.3$ Hz, 1H), 3.20 (d,

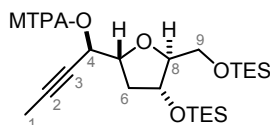
$J = 2.9$ Hz, 1H), 2.29 (ddd, $J = 13.6, 8.6, 5.9$ Hz, 1H), 1.87 (m, 1H), 1.85 (d, $J = 2.2$ Hz, 3H), 0.953 (t, $J = 7.9$ Hz, 9H), 0.948 (t, $J = 7.9$ Hz, 9H), 0.61 (q, $J = 7.9$ Hz, 6H), 0.58 ppm (q, $J = 7.9$ Hz, 6H). ^{13}C NMR (100 MHz, CDCl_3): $\delta = 87.9, 82.8, 81.6, 77.8, 73.4, 65.8, 63.3, 37.2, 6.9$ (3C), 6.8 (3C), 4.7 (3C), 4.5 (3C), 3.9 ppm. IR (film): $\tilde{\nu} = 3450, 2953, 2912, 2876, 1458, 1414, 1238, 1109, 1035, 1003, 831, 794, 726$ cm^{-1} . MS (EI) m/z (%): 385 (23), 253 (11), 213 (32), 146 (11), 145 (84), 133 (13), 131 (17), 118 (11), 117 (100), 115 (43), 103 (21), 87 (29). HRMS (ESIpos): m/z calcd for $\text{C}_{21}\text{H}_{42}\text{O}_4\text{Si}_2\text{Na}$: 437.2514, found: 437.2515.

Mosher ester analysis of alcohol 59. Triethylamine (10 μL , 72 μmol) and DMAP (3.0 mg, 24 μmol) were added to a solution of alcohol **59** (10 mg, 24 μmol) in CH_2Cl_2 (0.25 mL) followed by (*R*)-(-)- α -methoxy- α -trifluoromethyl-phenylacetyl chloride ((*R*)-MTPA-Cl) (9.0 μL , 48 μmol). The reaction was stirred at rt for 4 h, before it was quenched with sat. aq. NaHCO_3 (3 mL). The aqueous layer was extracted with CH_2Cl_2 (3 \times 5 mL), the combined extracts were dried over Na_2SO_4 , filtered and concentrated. The residue was purified by flash chromatography (hexanes/*t*-butyl methyl ether 19:1) to give the corresponding (*S*)-Mosher ester (*S*)-MTPA-**59** (11 mg, 72%), which analyzed as follows: ^1H NMR (400 MHz, CDCl_3): $\delta = 7.63\text{--}7.58$ (m, 2H), 7.41–7.35 (m, 3H), 5.91 (dq, $J = 8.5, 2.2$ Hz, 1H), 4.32 (dt, $J = 6.0, 3.0$ Hz, 1H), 4.17 (ddd, $J = 8.5, 7.8, 3.7$ Hz, 1H), 3.89 (ddd, $J = 5.2, 3.8, 2.8$ Hz, 1H), 3.59 (d, $J = 1.1$ Hz, 3H), 3.59 (dd, $J = 10.9, 3.8$ Hz, 1H), 3.46 (dd, $J = 10.9, 5.3$ Hz, 1H), 2.17 (ddd, $J = 13.6, 7.8, 6.0$ Hz, 1H), 2.00 (dt, $J = 13.3, 3.4$ Hz, 1H), 1.85 (d, $J = 2.2$ Hz, 3H), 0.97 (t, $J = 7.9$ Hz, 9H), 0.93 (t, $J = 8.0$ Hz, 9H), 0.61 (q, $J = 7.7$ Hz, 6H), 0.57 ppm (q, $J = 7.9$ Hz, 6H). ^{19}F NMR (282 MHz, CDCl_3): $\delta = -72.0$ ppm. MS (ESIpos) m/z (%): 653.3 (100 (M+Na)). HRMS (ESI): m/z calcd for $\text{C}_{31}\text{H}_{49}\text{O}_6\text{F}_3\text{Si}_2\text{Na}$: 653.2912, found: 653.2921.

The same procedure was followed for the preparation of (*R*)-MTPA-**59** (5.0 mg, 33%), which analyzed as follows: ^1H NMR (400 MHz, CDCl_3): $\delta = 7.64\text{--}7.59$ (m, 2H), 7.40–7.35 (m, 3H), 5.84 (dq, $J = 8.9, 2.1$ Hz, 1H), 4.34 (dt, $J = 5.8, 2.8$ Hz, 1H), 4.23 (ddd, $J = 8.9, 8.0, 3.4$ Hz, 1H), 3.91 (ddd, $J = 5.3, 3.8, 2.6$ Hz, 1H), 3.64 (d, $J = 1.2$ Hz, 3H), 3.60 (dd, $J = 10.9, 3.8$ Hz, 1H), 3.48 (dd, $J = 10.9, 5.3$ Hz, 1H), 2.22 (ddd, $J = 13.7, 8.1, 5.9$ Hz, 1H), 2.00 (dt, $J = 13.3, 3.2$ Hz, 1H), 1.80 (d, $J = 2.2$ Hz, 3H), 0.97 (t, $J = 7.9$ Hz, 9H), 0.94 (t, $J = 7.9$ Hz, 9H), 0.62 (q, $J = 7.7$ Hz, 6H), 0.58 ppm (q, $J = 7.8$ Hz, 6H). ^{19}F NMR (282 MHz, CDCl_3): $\delta = -71.8$ ppm. MS (ESIpos) m/z (%): 653.3 (100 (M+Na)). HRMS (ESI): m/z calcd for $\text{C}_{31}\text{H}_{49}\text{O}_6\text{F}_3\text{Si}_2\text{Na}$: 653.2912, found: 653.2920.

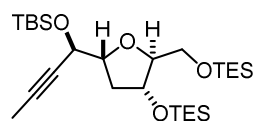
Both products were analyzed according to Hoyer and co-workers.^[118]

Table 4.1. Mosher ester analysis for the assignment of the C(4) stereocenter; arbitrary numbering as shown in the insert.



Assignment	59 [ppm]	(S)-MTPA-59 [ppm]	(R)-MTPA-59 [ppm]	Δ (δ (S-R)) [ppm]
1	1.85	1.85	1.80	+0.05
4	4.41	5.91	5.84	-0.07
5	4.15	4.17	4.23	-0.06
6a	2.29	2.17	2.22	-0.05
6b	1.87	2.00	2.00	0.00
7	4.35	4.32	4.34	-0.02
8	3.97	3.89	3.91	-0.02
9a	3.63	3.59	3.60	-0.01
9b	3.45	3.46	3.48	-0.02
TES	0.95	0.97	0.97	0.00
	0.95	0.93	0.94	-0.01
TES	0.61	0.61	0.62	-0.01
	0.58	0.57	0.58	-0.01

***t*-Butyl-dimethyl silyl ether **S16**.** Imidazole (102 mg, 1.50 mmol) was added to a solution of



propargylic alcohol **59** (250 mg, 0.60 mmol) in DMF (4 mL) and the solution was cooled to 0 °C before TBSCl (109 mg, 0.72 mmol) was added. The resulting mixture was stirred at rt for 4 h, before the reaction was quenched

with sat. aq. NaHCO₃ (10 mL) and the aqueous layer extracted with *t*-butyl methyl ether (3 × 15 mL).

The combined extracts were washed with water (50 mL) and brine (50 mL), dried over Na₂SO₄,

filtered and concentrated. The residue was purified by flash chromatography (hexanes/EtOAc 40:1)

to give the desired *t*-butyl-dimethyl silyl ether **S16** as a colorless oil (260 mg, 82%). $[\alpha]_D^{20} = -31.3$

(*c* = 1.0, CHCl₃). ¹H NMR (400 MHz, CDCl₃): δ = 4.50 (dq, *J* = 7.3, 2.1 Hz, 1H), 4.27 (ddd, *J* = 6.2, 4.5,

3.7 Hz, 1H), 4.00 (td, *J* = 7.5, 5.1 Hz, 1H), 3.81 (dt, *J* = 5.5, 4.1 Hz, 1H), 3.61 (dd, *J* = 10.8, 4.2 Hz, 1H),

3.51 (dd, *J* = 10.8, 5.4 Hz, 1H), 2.16 (ddd, *J* = 13.5, 7.6, 6.2 Hz, 1H), 1.96 (dt, *J* = 13.0, 4.9, 1H), 1.81 (d,

J = 2.1 Hz, 3H), 0.96 (t, *J* = 7.9 Hz, 9H), 0.94 (t, *J* = 7.9 Hz, 9H), 0.91 (s, 9H), 0.60 (q, *J* = 7.9 Hz, 6H), 0.58

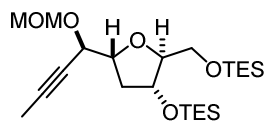
(q, $J = 7.9$ Hz, 6H), 0.11 (s, 3H), 0.10 ppm (s, 3H). ^{13}C NMR (100 MHz, CDCl_3): $\delta = 86.6, 82.4, 81.2, 78.7, 72.7, 67.0, 63.2, 37.0, 26.1$ (3C), 18.7, 6.9 (6C), 4.8 (3C), 4.5 (3C), 3.8, $-4.6, -4.7$ ppm. IR (film): $\tilde{\nu} = 2954, 2877, 1461, 1414, 1247, 1114, 1079, 1041, 1005, 940, 837, 778, 743, 670$ cm^{-1} . MS (EI) m/z (%): 499 (12), 173 (12), 472 (26), 471 (63), 339 (30), 313 (24), 213 (18), 212 (18), 211 (96), 209 (31), 207 (16), 189 (12), 183 (11), 181 (42), 161 (11), 155 (41), 147 (16), 146 (13), 145 (100), 133 (14), 131 (14), 117 (63), 115 (51), 97 (10), 89 (50), 87 (33), 75 (12), 73 (50). HRMS (ESIpos): m/z calcd for $\text{C}_{27}\text{H}_{56}\text{O}_4\text{Si}_3\text{Na}$: 551.3379, found: 551.3383.

Diol 119. A solution of *t*-butyl-dimethyl silyl ether **S16** (250 mg, 0.47 mmol) in MeOH (5 mL) was cooled to -50 °C before *p*-toluenesulfonic acid monohydrate (PTSA, 9.00 mg, 0.05 mmol) was added. The resulting mixture was stirred at -50 °C for 5 h. The reaction was quenched with sat. aq. NaHCO_3 (5 mL) and the mixture was extracted with EtOAc (3×10 mL). The combined extracts were dried over Na_2SO_4 , filtered and concentrated. The residue was purified by flash chromatography (hexanes/*t*-butyl methyl ether 10:1 to 2:1) to afford the title compound **119** as a colorless oil (103 mg, 73%). $[\alpha]_{\text{D}}^{20} = -76.6$ ($c = 1.0, \text{CHCl}_3$). ^1H NMR (400 MHz, CDCl_3): $\delta = 4.42$ (dq, $J = 4.3, 2.1$ Hz, 1H), 4.18 (dt, $J = 8.7, 4.5$ Hz, 2H), 4.04 (dt, $J = 5.4, 3.9$ Hz, 1H), 3.65 (dt, $J = 11.6, 4.7$ Hz, 1H), 3.54 (dt, $J = 11.1, 4.9$ Hz, 1H), 3.20 (d, $J = 8.7$ Hz, 1H), 2.37 (ddd, $J = 13.8, 8.6, 6.8$ Hz, 1H), 2.10 (t, $J = 6.1$ Hz, 1H), 1.97 (dt, $J = 13.8, 4.2$, 1H), 1.86 (d, $J = 2.2$ Hz, 3H), 0.91 (s, 9H), 0.16 (s, 3H), 0.14 ppm (s, 3H). ^{13}C NMR (100 MHz, CDCl_3): $\delta = 87.2, 82.5, 81.6, 78.6, 72.6, 66.3, 62.8, 36.7, 26.0$ (3C), 18.5, 3.8, $-4.5, -4.7$ ppm. IR (film): $\tilde{\nu} = 3393, 2928, 2857, 1472, 1361, 1252, 1088, 1004, 939, 837, 778, 670$ cm^{-1} . MS (ESIpos) m/z (%): 323.2 (100 (M+Na)). HRMS (ESIpos): m/z calcd for $\text{C}_{15}\text{H}_{28}\text{O}_4\text{SiNa}$: 323.1649, found: 323.1652.

Bis-*t*-butyl-dimethyl silyl ether 48. Imidazole (23.1 mg, 0.34 mmol) was added to a solution of diol **119** (50.0 mg, 0.17 mmol) in DMF (3 mL) and the solution was cooled to 0 °C before TBSCl (28.2 mg, 0.19 mmol) was added. The resulting mixture was stirred at rt for 8 h, before the reaction was quenched with sat. aq. NaHCO_3 (10 mL). The aqueous layer was extracted with *t*-butyl methyl ether (3×15 mL), the combined extracts were washed with water (40 mL) and brine (40 mL), dried over Na_2SO_4 , filtered and concentrated. The residue was purified by flash chromatography (hexanes/EtOAc 10:1) to yield the title compound **48** as a colorless oil (38 mg, 54%). $[\alpha]_{\text{D}}^{20} = -42.6$ ($c = 0.69, \text{CHCl}_3$). ^1H NMR (400 MHz, CDCl_3): $\delta = 4.40$ (dq, $J = 4.3, 2.2$ Hz, 1H), 4.02 (dt, $J = 8.9, 4.2$ Hz, 2H), 4.02 (ddt, $J = 5.9, 3.8, 2.3$ Hz, 1H), 3.70 (dd, $J = 10.5, 3.8$ Hz, 1H), 3.52 (dd, $J = 10.5, 6.2$ Hz, 1H), 3.27 (d, $J = 8.9$ Hz, 1H), 2.41 (ddd, $J = 13.7, 9.0, 6.5$ Hz, 1H), 1.92 (dddd, $J = 13.7, 4.3, 2.9, 0.7$ Hz, 1H), 1.86 (d, $J = 2.2$ Hz, 3H), 0.92 (s, 9H), 0.88 (s, 9H), 0.16 (s, 3H), 0.14 (s, 3H), 0.04 ppm (s, 6H). ^{13}C NMR (100 MHz, CDCl_3): $\delta = 87.3, 82.3, 82.1, 78.8, 73.9, 66.2, 64.4, 36.3, 26.0$ (6C), 18.5, 18.4, 3.9, $-4.4, -4.7, -5.3$ ppm (2C). IR (film):

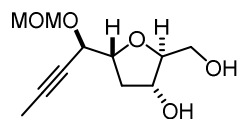
$\tilde{\nu}$ = 3445, 2954, 2929, 2857, 1472, 1361, 1254, 1088, 1005, 937, 836, 777, 670 cm^{-1} . MS (ESIpos) m/z (%): 437.3 (100 (M+Na)). HRMS (ESIpos): m/z calcd for $\text{C}_{21}\text{H}_{42}\text{O}_4\text{Si}_2\text{Na}$: 437.2514, found: 437.2510.

Methoxymethyl acetal **S17.** A solution of propargylic alcohol **59** (160 mg, 0.39 mmol) in CH_2Cl_2 (5 mL) was cooled to 0 °C before Hünig's base (0.27 mL, 1.54 mmol) followed by MOMCl (58.6 μL , 0.77 mmol) was added. The resulting mixture was stirred at rt for 16 h, before the reaction was quenched with sat. aq. NaHCO_3 (10 mL).



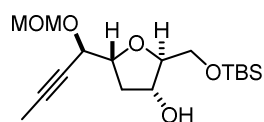
The aqueous layer was extracted with CH_2Cl_2 (3 \times 15 mL), the combined extracts were dried over Na_2SO_4 , filtered and concentrated. The residue was purified by flash chromatography (hexanes/*t*-butyl methyl ether 30:1 to 20:1) to afford the title compound **S17** as a colorless oil (160 mg, 91%). $[\alpha]_{\text{D}}^{20}$ = -64.0 (c = 1.0, CHCl_3). ^1H NMR (400 MHz, CDCl_3): δ = 4.94 (dd, J = 6.6, 1.4 Hz, 1H), 4.67 (dd, J = 6.6, 1.6 Hz, 1H), 4.51 (dq, J = 8.3, 2.1 Hz, 1H), 4.33 (dt, J = 6.2, 3.4 Hz, 1H), 4.14 (tdd, J = 8.3, 4.4, 1.4 Hz, 1H), 3.90 (dt, J = 5.8, 3.9 Hz, 1H), 3.63 (ddd, J = 10.8, 4.1, 1.4 Hz, 1H), 3.49 (ddd, J = 10.6, 5.7, 1.3 Hz, 1H), 3.40 (s, 3H), 2.23 (ddd, J = 13.2, 7.9, 6.0 Hz, 1H), 2.01 (dt, J = 13.2, 4.2, 1H), 1.84 (d, J = 2.1 Hz, 3H), 0.96 (t, J = 7.9 Hz, 9H), 0.94 (t, J = 7.9 Hz, 9H), 0.60 (q, J = 7.9 Hz, 6H), 0.58 ppm (q, J = 7.9 Hz, 6H). ^{13}C NMR (100 MHz, CDCl_3): δ = 94.3, 87.4, 82.9, 81.1, 75.8, 73.0, 69.3, 63.2, 55.5, 37.5, 6.9 (6C), 4.9 (3C), 4.5 (3C), 3.8 ppm. IR (film): $\tilde{\nu}$ = 2953, 2877, 1459, 1415, 1239, 1150, 1089, 1053, 1031, 1007, 942, 840, 796, 726 cm^{-1} . MS (EI) m/z (%): 399 (17), 362 (15), 213 (17), 146 (10), 145 (80), 131 (15), 118 (11), 117 (100), 115 (38), 87 (19). HRMS (ESIpos): m/z calcd for $\text{C}_{23}\text{H}_{46}\text{O}_5\text{Si}_2\text{Na}$: 481.2776, found: 481.2780.

Diol **S18.** A solution of methoxymethyl acetal **S17** (160 mg, 0.35 mmol) in THF (5 mL) was cooled to 0 °C before a solution of TBAF (1 M in THF, 0.77 mL, 0.77 mmol) was added and the resulting mixture was stirred for 10 min. The reaction was quenched with sat. aq. NH_4Cl (5 mL) and the aqueous layer was extracted with EtOAc



(3 \times 10 mL). The combined extracts were dried over Na_2SO_4 , filtered and concentrated. The yellow residue was purified by flash chromatography (hexanes/EtOAc 1:1 to 0:1 to EtOAc/MeOH 95:5) to yield the title compound **S18** as a colorless oil (71 mg, 88%). $[\alpha]_{\text{D}}^{20}$ = -170.8 (c = 1.0, CHCl_3). ^1H NMR (400 MHz, CDCl_3): δ = 5.05 (d, J = 6.7 Hz, 1H), 4.66 (d, J = 6.8 Hz, 1H), 4.41 (dq, J = 4.2, 2.1 Hz, 1H), 4.35 (dt, J = 8.7, 4.3 Hz, 1H), 4.26 (ddd, J = 7.6, 7.1, 3.3 Hz, 1H), 4.08 (ddd, J = 5.1, 4.0, 3.0 Hz, 1H), 3.69 (dd, J = 12.0, 3.9 Hz, 1H), 3.58 (dd, J = 11.8, 5.0 Hz, 1H), 3.41 (s, 3H), 3.11 (d, J = 8.5 Hz, 1H), 2.45 (ddd, J = 13.8, 8.7, 6.8 Hz, 1H), 1.97 (dt, J = 13.8, 3.8, 1H), 1.89 ppm (d, J = 2.1 Hz, 3H). ^{13}C NMR (100 MHz, CDCl_3): δ = 94.0, 87.6, 83.9, 80.6, 74.9, 72.9, 68.5, 63.0, 56.2, 37.5, 3.89 ppm. IR (film): $\tilde{\nu}$ = 3401, 2922, 2892, 1443, 1331, 1215, 1149, 1096, 1030, 930 cm^{-1} . MS (EI) m/z (%): 117 (17), 45 (23), 36 (10), 29 (100). HRMS (ESIpos): m/z calcd for $\text{C}_{11}\text{H}_{18}\text{O}_5\text{Na}$: 253.1046, found: 253.1045.

Alcohol 49. Imidazole (41.4 mg, 0.61 mmol) was added to a solution of diol **S18** (70.0 mg, 0.30 mmol)



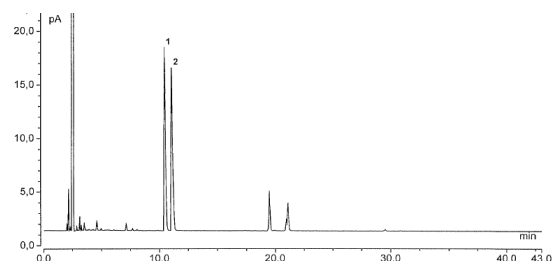
in CH₂Cl₂ (6 mL) and the solution was cooled to 0 °C before TBSCl (50.4 mg, 0.33 mmol) was added followed by DMAP (3.71 mg, 0.03 mmol, 10 mol%).

The resulting mixture was stirred at rt for 16 h, before the reaction was quenched with half-sat. aq. NH₄Cl (5 mL). The aqueous layer was extracted with CH₂Cl₂ (3 × 8 mL), the combined extracts were dried over Na₂SO₄, filtered and concentrated. The residue was purified by flash chromatography (hexanes/EtOAc 10:1) to afford the desired alcohol **49** as a colorless oil (80 mg, 76%). [α]_D²⁰ = -108.6 (c = 0.88, CHCl₃). ¹H NMR (400 MHz, CDCl₃): δ = 5.04 (d, *J* = 6.8 Hz, 1H), 4.65 (d, *J* = 6.8 Hz, 1H), 4.38 (dq, *J* = 4.3, 2.1 Hz, 1H), 4.34 (dt, *J* = 9.0, 4.0 Hz, 1H), 4.26 (ddt, *J* = 8.8, 6.4, 2.5 Hz, 1H), 4.04 (ddd, *J* = 6.0, 3.6, 2.3 Hz, 1H), 3.71 (dd, *J* = 10.5, 3.7 Hz, 1H), 3.54 (dd, *J* = 10.6, 6.0 Hz, 1H), 3.40 (s, 3H), 3.28 (d, *J* = 8.7 Hz, 1H), 2.48 (ddd, *J* = 13.7, 8.9, 6.5 Hz, 1H), 1.91 (dddd, *J* = 13.8, 4.3, 3.0, 0.7 Hz, 1H), 1.88 (d, *J* = 2.1 Hz, 3H), 0.88 (s, 9H), 0.05 ppm (s, 6H). ¹³C NMR (100 MHz, CDCl₃): δ = 94.0, 87.6, 83.7, 80.9, 75.2, 74.1, 68.4, 64.5, 56.2, 37.1, 26.0 (3C), 18.4, 4.0, -5.3, -5.4 ppm. IR (film): $\tilde{\nu}$ = 3442, 2928, 2857, 1472, 1361, 1254, 1149, 1097, 1034, 935, 835, 778, 669 cm⁻¹. MS (ESIpos) *m/z* (%): 367.2 (100 (M+Na)). HRMS (ESIpos): *m/z* calcd for C₁₇H₃₂O₅SiNa: 367.1911, found: 367.1908.

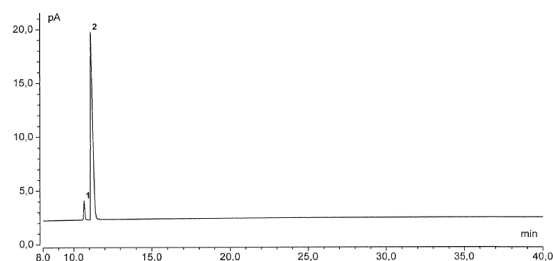
4.3.3 Synthesis of the Southern Acid Fragment 60

(Z)-But-2-en-1-ol (62). Quinoline (4.21 mL, 35.7 mmol, 0.1 equiv) was added to a suspension of 10 wt% Pd/BaSO₄ (1.90 g, 17.8 mmol, 5 mol%) in MeOH (125 mL) and the resulting mixture was stirred for 20 min at ambient temperature. Subsequently, 2-butyne-1-ol (25.0 g, 357 mmol) was added and seven balloons of hydrogen were slowly bubbled through the suspension over 12 h. The reaction progress was monitored by GC-MS/FID (method 50:10, *t_R* (s.m.) = 2.74 min, *t_R* (product) = 2.23 min) and the reaction immediately stopped by replacing the H₂ atmosphere with Ar as soon as the starting material was fully consumed (this was crucial to avoid overreduction or isomerization of the double bond). The reaction mixture was filtered through a pad of Celite[®], eluting with CH₂Cl₂ (40 mL). The resulting yellow solution was carefully concentrated *via* distillation (vigreux, 400 mbar, 30 °C) and the residue finally distilled (75 mbar, 75–80 °C) to afford the title compound **62** as a pale yellow liquid (16.8 g, 232 mmol, 65%). ¹H NMR (400 MHz, CDCl₃): δ = 5.64–5.59 (m, 2H), 4.21 (d, *J* = 3.1 Hz, 1H), 4.20 (d, *J* = 4.6 Hz, 1H), 1.67 ppm (d, *J* = 5.3 Hz, 3H). ¹³C NMR (100 MHz, CDCl₃): δ = 129.3, 127.4, 58.4, 13.1 ppm. IR (film): $\tilde{\nu}$ = 3407, 3024, 2932, 1738, 1657, 1446, 1378, 1260, 1040, 813, 696 cm⁻¹. MS (EI) *m/z* (%): 72 (29), 57 (100), 54 (12), 43 (30), 41 (20), 39 (30), 31 (12), 29 (25), 27 (12). HRMS (EI): *m/z* calcd for C₄H₈O: 72.0575, found: 72.0575. The analytical and spectroscopic data are in agreement with those reported in the literature.^[231]

((2*S*,3*R*)-3-Methyloxiran-2-yl)methanol (61**).** A 500 mL jacketed Schlenk flask was charged with activated powdered 4 Å MS (14 g) and CH₂Cl₂ (500 mL) and cooled to –20 °C. Subsequently, (+)-diethyl (L)-tartrate (2.03 mL, 11.9 mmol, 6 mol%) and Ti(*Oi*-Pr)₄ (2.94 mL, 9.92 mmol, 5 mol%) were added, followed by allylic alcohol **62** (14.3 g, 198 mmol). The reaction mixture was stirred for 45 min at the same temperature, before *t*-BuOOH (5.5 M in decane, 54.0 mL, 297 mmol) was added *via* a dropping funnel over 60 min, and the resulting mixture was stirred for 40 h at –20 °C. The septum was removed, dimethyl sulfide (21.8 mL, 297 mmol) was added and the resulting mixture stirred open to atmosphere at ambient temperature for 24 h. The reaction mixture was filtered through a pad of Celite® and rinsed with CH₂Cl₂ (300 mL). The solvent was evaporated and the residue purified by flash chromatography (pentane/Et₂O 4:1) followed by distillation (12 mbar, 59–64 °C) to yield epoxide **61** as a colorless oil (12.9 g, 74%, 90% *ee*). $[\alpha]_{\text{D}}^{20} = -4.8$ (*c* = 1.0, CHCl₃). ¹H NMR (400 MHz, CDCl₃): δ = 3.85 (dq, *J* = 11.3, 3.6 Hz, 1H), 3.68 (ddd, *J* = 11.6, 6.2, 3.7 Hz, 1H), 3.19–3.11 (m, 2H), 2.09 (brs, 1H), 1.31 ppm (d, *J* = 5.5 Hz, 3H). ¹³C NMR (100 MHz, CDCl₃): δ = 60.8, 56.9, 53.0, 13.5 ppm. IR (film): $\tilde{\nu}$ = 3397, 2930, 1451, 1040, 986, 877, 829, 783, 731 cm⁻¹. MS (EI) *m/z* (%): 45 (100), 44 (43), 43 (48), 31 (32), 29 (26), 27 (16). HRMS (ESIpos): *m/z* calcd for C₄H₈O₂Na: 111.0416, found: 111.0416. The *ee* was determined by GC (30 m, BGB-176/BGB-15 G/618, 80 1/min 120 8/min 220 3/min iso, flow rate 0.50 bar H₂: minor enantiomer *t_R* = 10.7 min; major enantiomer *t_R* = 11.1 min). The analytical and spectroscopic data are in agreement with those reported in the literature.^[119]



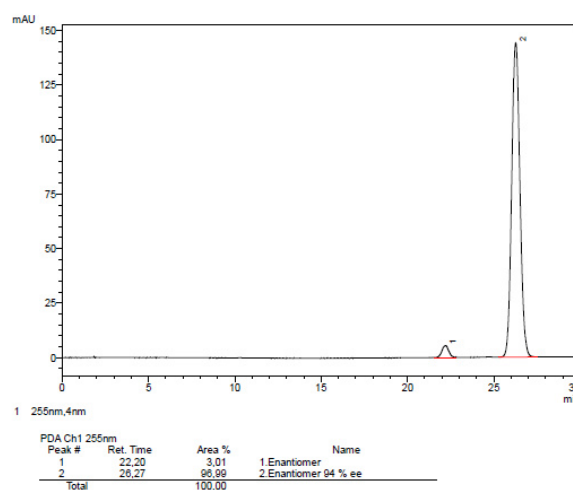
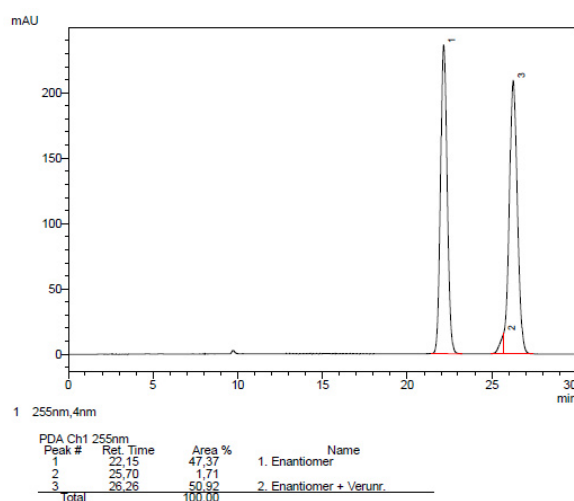
No.	Ret.Time min	area-% %
1	10.42	50,10
2	11.05	49,90



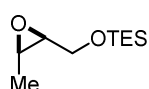
No.	Ret.Time min	area-% %
1	10.67	4,77
2	11.10	95,23

((2*S*,3*R*)-3-Methyloxiran-2-yl)methyl 4-nitrobenzoate (64**).** A 100 mL jacketed Schlenk flask was charged with activated powdered 4 Å MS (320 mg) and CH₂Cl₂ (20 mL) and cooled to –20 °C. Subsequently, (+)-diethyl (L)-tartrate (71.9 μL, 0.42 mmol, 6 mol%) and Ti(*Oi*-Pr)₄ (103 μL, 0.35 mmol, 5 mol%) were added, followed by allylic alcohol **62** (500 mg, 6.93 mmol). The reaction mixture was stirred for 45 min at the same temperature, before *t*-BuOOH (5.5 M in decane, 1.89 mL, 10.4 mmol) was added *via* syringe pump over 20 min, and the resulting mixture was stirred for 20 h at –20 °C. Afterward, trimethyl phosphite (1.23 mL, 10.4 mmol) was slowly added *via* syringe pump. Next, Et₃N (1.16 mL, 8.32 mmol) was

added followed by a solution of 4-nitrobenzoyl chloride (1.29 g, 6.93 mmol) in CH_2Cl_2 (1.8 mL). The resulting mixture was warmed to 0 °C and stirred for 1 h. The reaction mixture was filtered through a pad of Celite® and rinsed with CH_2Cl_2 (10 mL). The filtrate was washed with aq. tartaric acid (10%, 3 × 5 mL), aq. sat. NaHCO_3 (3 × 5 mL) and brine (2 × 5 mL), dried over Na_2SO_4 , filtered and concentrated. The residue solidified upon standing and was recrystallized twice from Et_2O to afford the title compound **64** as pale yellow crystals (953 mg, 58%, 94% *ee*). m.p. [Et_2O] = 69–71 °C. $[\alpha]_{\text{D}}^{20} = -26.3$ ($c = 1.2$, CHCl_3). ^1H NMR (400 MHz, CDCl_3): $\delta = 8.32$ – 8.28 (m, 2H), 8.27 – 8.23 (m, 2H), 4.65 (dd, $J = 12.1$, 4.0 Hz, 1H), 4.33 (dd, $J = 12.1$, 7.2 Hz, 1H), 3.32 (dt, $J = 7.1$, 4.1 Hz, 1H), 3.22 (qd, $J = 5.6$, 4.3 Hz, 1H), 1.40 ppm (d, $J = 5.6$ Hz, 3H). ^{13}C NMR (100 MHz, CDCl_3): $\delta = 164.7$, 150.8, 135.2, 131.0 (2C), 123.7 (2C), 64.4, 53.6, 52.3, 13.6 ppm. IR (film): $\tilde{\nu} = 3111$, 1731, 1523, 1336, 1271, 1119, 1066, 949, 807, 718 cm^{-1} . MS (EI) m/z (%): 150 (100), 104 (15). HRMS (ESIpos): m/z calcd for $\text{C}_{11}\text{H}_{11}\text{NO}_5\text{Na}$: 260.0529, found: 260.0529. The *ee* was determined by HPLC (150 mm, Chiralpak IC-3, \varnothing 4.6 mm, *n*-heptane/2-propanol 95:5, flow rate = 1.0 mL/min, 56 bar, 293 K, UV, 255 nm): minor enantiomer $t_R = 22.2$ min; major enantiomer $t_R = 26.3$ min.

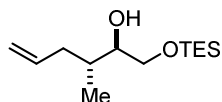


Triethyl(((2S,3R)-3-methyloxiran-2-yl)methoxy)silane (65). Pyridine (1.98 mL, 25.6 mmol), DMAP (444 mg, 3.63 mmol, 20 mol%) and TESCl (3.96 mL, 23.6 mmol) were sequentially added to a solution of epoxy alcohol **61** (1.60 g, 18.2 mmol) in CH_2Cl_2 (80 mL) at 0 °C. The resulting mixture was stirred at ambient temperature for 2 h. The reaction was quenched with aq. half-sat. NH_4Cl (60 mL) and the aqueous layer extracted with CH_2Cl_2 (3 × 50 mL). The combined extracts were dried over Na_2SO_4 , filtered and concentrated. The residue was purified by flash chromatography (pentane) to yield the title compound as a colorless oil (3.60 g, 98%). $[\alpha]_{\text{D}}^{20} = +6.2$ ($c = 1.0$, CHCl_3). ^1H NMR (400 MHz, CDCl_3): $\delta = 3.73$ (d, $J = 5.3$ Hz, 2H), 3.14 – 3.09 (m, 2H), 1.29 (d, $J = 5.4$ Hz, 3H), 0.97 (t, $J = 7.9$ Hz, 9H), 0.63 ppm (q, $J = 8.1$ Hz, 6H). ^{13}C NMR (100 MHz, CDCl_3): $\delta = 61.1$, 57.0, 52.5, 13.4, 6.8 (3C), 4.5 ppm (3C). IR (film): $\tilde{\nu} = 2955$, 2913, 2877, 1459, 1415, 1339,



1240, 1091, 1006, 975, 783, 742, 728, 673 cm^{-1} . MS (EI) m/z (%): 173 (18), 146 (11), 145 (100), 143 (54), 129 (31), 117 (14), 115 (81), 101 (24), 87 (44), 75 (13), 59 (19), 45 (13). HRMS (ESIpos): m/z calcd for $\text{C}_{10}\text{H}_{22}\text{O}_2\text{SiNa}$: 225.1281, found: 225.1283.

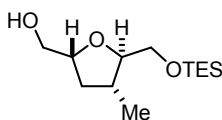
(2R,3R)-3-Methyl-1-((triethylsilyloxy)hex-5-en-2-ol (66). A solution of allyl-MgCl (2 M in THF,



17.3 mL, 34.6 mmol) was added to a suspension of CuI (659 mg, 3.46 mmol, 20 mol%) in THF (70 mL) at $-25\text{ }^{\circ}\text{C}$. The resulting mixture was stirred for 5 min, before a solution of epoxy silyl ether **65** (3.50 g, 17.3 mmol) in THF (40 mL) was

added dropwise over 30 min. The resulting mixture was stirred at $-25\text{ }^{\circ}\text{C}$ for 6 h. The reaction was quenched with aq. half-sat. NH_4Cl (30 mL) and the aqueous layer extracted with *t*-butyl methyl ether (3 \times 40 mL). The combined extracts were dried over Na_2SO_4 , filtered and concentrated. The residue was purified by flash chromatography (hexanes/*t*-butyl methyl ether 99:1) to afford the title compound **66** as a pale yellow oil (2.82 g, 67%, r.r. 10:1). $[\alpha]_{\text{D}}^{20} = -8.7$ ($c = 1.0$, CHCl_3). ^1H NMR (400 MHz, CDCl_3): $\delta = 5.80$ (dddd, $J = 16.8, 10.1, 7.9, 6.5$ Hz, 1H), 5.10–4.97 (m, 2H), 3.70 (dd, $J = 9.3, 2.7$ Hz, 1H), 3.70 (dd, $J = 9.3, 8.0$ Hz, 1H), 3.42 (ddd, $J = 8.0, 6.8, 2.5$ Hz, 1H), 2.42–2.34 (m, 1H), 2.00–1.91 (m, 1H), 1.65 (dqt, $J = 11.4, 4.5, 2.2$ Hz, 1H), 0.96 (t, $J = 7.9$ Hz, 9H), 0.85 (d, $J = 6.9$ Hz, 3H), 0.62 ppm (q, $J = 8.0$ Hz, 6H). ^{13}C NMR (100 MHz, CDCl_3): $\delta = 137.3, 116.2, 75.2, 64.9, 37.3, 35.7, 15.2, 6.9$ (3C), 4.5 ppm (3C). IR (film): $\tilde{\nu} = 3440, 2956, 2913, 2877, 1459, 1414, 1239, 1092, 1005, 910, 789, 743$ cm^{-1} . MS (EI) m/z (%): 215 (14), 117 (29), 115 (19), 105 (71), 104 (10), 103 (88), 95 (100), 87 (22), 75 (53), 67 (22), 59 (18), 47 (12). HRMS (ESIpos): m/z calcd for $\text{C}_{13}\text{H}_{28}\text{O}_2\text{SiNa}$: 267.1751, found: 267.1751.

((2R,4R,5R)-4-Methyl-5-(((triethylsilyloxy)methyl)tetrahydrofuran-2-yl)methanol (67). A solution of



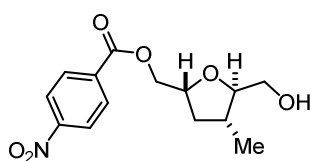
alcohol **66** (1.40 g, 5.73 mmol) in *i*-PrOH (10 mL) was added to a solution of $\text{Co}(\text{nmp})_2$ (323 mg, 0.57 mmol, 10 mol%) in *i*-PrOH (40 mL). The pale red solution was purged with O_2 for 15 min before *t*-BuOOH (5.5 M in decane,

0.21 mL, 1.15 mmol, 20 mol%) was added in one portion. The reaction mixture was stirred at $55\text{ }^{\circ}\text{C}$ under oxygen atmosphere (balloon) for 5 h; the solution turned green. After cooling to ambient temperature, the atmosphere was replaced by Ar and the solvent was evaporated. The crude oil was partitioned between aq. half-sat. NH_4Cl (25 mL) and *t*-butyl methyl ether (25 mL) and the aqueous layer extracted with *t*-butyl methyl ether (2 \times 30 mL). The combined extracts were washed with water (3 \times 20 mL) and brine (20 mL), dried over Na_2SO_4 , filtered and concentrated. The residue was purified by flash chromatography (hexanes/*t*-butyl methyl ether 4:1) to yield the title compound **67** as a pale yellow oil (1.16 g, 78%). $[\alpha]_{\text{D}}^{20} = -20.8$ ($c = 1.0$, CHCl_3). ^1H NMR (400 MHz, CDCl_3): $\delta = 4.08$ (dtd, $J = 9.6, 5.6, 3.1$ Hz, 1H), 3.70 (dd, $J = 10.7, 1.8$ Hz, 1H), 3.69 (dd, $J = 12.0, 5.0$ Hz, 1H), 3.64 (dd, $J = 11.0, 5.0$ Hz, 1H), 3.56–3.52 (m, 1H), 3.49 (dd, $J = 11.0, 5.0$ Hz, 1H), 3.67–3.52 (m, 2H), 1.84 (brs,

1H), 1.42 (dt, $J = 11.7, 10.1$ Hz, 1H), 1.07 (d, $J = 6.3$ Hz, 3H), 0.96 (t, $J = 7.9$ Hz, 9H), 0.61 ppm (q, $J = 8.0$ Hz, 6H). ^{13}C NMR (100 MHz, CDCl_3): $\delta = 86.3, 79.3, 65.0, 64.7, 36.7, 36.5, 17.4, 6.9$ (3C), 4.5 ppm (3C). IR (film): $\tilde{\nu} = 3395, 2955, 2913, 2875, 1458, 1414, 1381, 1239, 1086, 1052, 1016, 911, 741, 671$ cm^{-1} . MS (EI) m/z (%): 232 (17), 231 (100), 229 (20), 214 (12), 213 (76), 185 (14), 170 (20), 145 (16), 115 (32), 105 (29), 103 (57), 93 (28), 87 (14), 81 (11), 77 (15), 75 (26), 73 (13), 69 (23), 67 (25). HRMS (ESIpos): m/z calcd for $\text{C}_{13}\text{H}_{28}\text{O}_3\text{SiNa}$: 283.1700, found: 283.1699.

The relative stereochemistry was confirmed by single crystal x-ray analysis of a *p*-nitrobenzoate derivative, which was prepared in analytical quantities by the following two-step protocol:

Nitrobenzoate 68. Pyridine (7.5 μL , 92 μmol), 4-nitrobenzoyl chloride (17.5 mg, 92.1 μmol) and

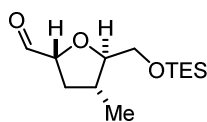


DMAP (1.9 mg, 15 μmol , 20 mol%) were sequentially added to a solution of alcohol **67** (20.0 mg, 76.8 μmol) in CH_2Cl_2 (0.5 mL) at 0 °C. The resulting solution was stirred at rt for 3.5 h. The reaction was quenched with aq. half-sat. NH_4Cl (2 mL) and the aqueous layer extracted with

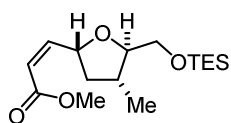
CH_2Cl_2 (3 \times 5 mL). The combined extracts were dried over Na_2SO_4 , filtered and concentrated to yield the crude benzoate (26 mg), which was used in the next step without further purification.

A mixture of acetic acid/ H_2O /THF (6:3:1, 1 mL) was added to the crude benzoate (26 mg, 64 μmol) and the resulting mixture was vigorously stirred at rt for 20 min. The layers were separated and the aqueous layer was extracted with EtOAc (3 \times 5 mL). The combined extracts were dried over Na_2SO_4 , filtered and concentrated. The residue was purified by flash chromatography (hexanes/EtOAc 4:1 to 1:1) to yield the title compound **68** as a yellow oil (16 mg, 68% over two steps). $[\alpha]_{\text{D}}^{20} = -35.4$ ($c = 0.24$, CHCl_3). ^1H NMR (400 MHz, CDCl_3): $\delta = 8.29$ (dt, $J = 9.0, 1.9$ Hz, 2H) 8.23 (dd, $J = 9.1, 2.1$ Hz, 2H), 4.45 (dd, $J = 10.8, 2.6$ Hz, 1H), 4.42–4.36 (m, 1H), 4.33 (dd, $J = 10.8, 6.4$ Hz, 1H), 3.79 (dd, $J = 11.7, 2.6$ Hz, 1H), 3.62 (ddd, $J = 8.8, 4.8, 2.5$ Hz, 1H), 3.56 (dd, $J = 11.7, 4.8$ Hz, 1H), 2.29 (ddd, $J = 11.5, 7.1, 5.7$ Hz, 1H), 2.21 (ddt, $J = 10.7, 9.0, 6.5$ Hz, 1H), 1.93 (brs, 1H), 1.46 (ddd, $J = 11.5, 10.5, 9.2$ Hz, 1H), 1.08 ppm (d, $J = 6.4$ Hz, 3H). ^{13}C NMR (100 MHz, CDCl_3): $\delta = 164.8, 150.7, 135.5, 131.0$ (2C), 123.7 (2C), 86.3, 76.4, 68.1, 62.9, 37.7, 34.9, 16.5 ppm. IR (film): $\tilde{\nu} = 3433, 2928, 2875, 1722, 1606, 1526, 1456, 1346, 1320, 1271, 1108, 1049, 1014, 973, 913, 873, 842, 784, 719$ cm^{-1} . MS (EI) m/z (%): 265 (15), 264 (94), 150 (100), 128 (11), 115 (51), 104 (21), 97 (40), 71 (50), 69 (23), 41 (13). HRMS (ESIpos): m/z calcd for $\text{C}_{14}\text{H}_{17}\text{NO}_6\text{Na}$: 318.0948, found: 318.0949. Single crystals were grown by slow evaporation from CH_2Cl_2 . Only the racemate (10%) was crystallizing (see Appendix).

Aldehyde 74. NaHCO₃ (197 mg, 2.34 mmol) was added to a solution of DMP (250 mg, 0.59 mmol) in CH₂Cl₂ (2 mL) at 0 °C. Next, a solution of alcohol **67** (97.5 mg, 0.39 mmol) in CH₂Cl₂ (2 mL) was added. The resulting mixture was allowed to reach ambient temperature and stirred for 90 min. Aqueous CH₂Cl₂ (10 μL H₂O in 2 mL CH₂Cl₂) was added over 1 h *via* syringe pump. After the addition was completed, the mixture was diluted with hexanes (5 mL), filtered through cotton and rinsed with additional hexanes. Removal of the solvent afforded the crude aldehyde **74** as a pale yellow oil (65 mg). The crude aldehyde was used in the next step without further purification.

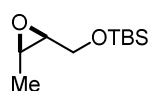


(Z)-Olefin 69. 18-Crown-6 (286 mg, 1.08 mmol) was added to a solution of KHMDS (80.3 mg, 0.40 mmol) in THF (1.3 mL). After cooling to -78 °C methyl O,O'-bis(2,2,2-trifluoroethyl)-phosphono-



acetate (85.1 μL, 0.40 mmol) was added dropwise and the resulting solution stirred for 20 min. Next, a solution of crude aldehyde **74** (65.0 mg, 0.25 mmol) in THF (1 mL) was added dropwise over 10 min. The resulting mixture was stirred for 3 h at -78 °C before it was poured into aq. half-sat. NH₄Cl (50 mL). The aqueous layer was extracted with EtOAc (3 × 50 mL). The combined extracts were washed with brine (50 mL), dried over Na₂SO₄, filtered and concentrated. The residue was purified by flash chromatography (fine SiO₂, hexanes/*t*-butyl methyl ether 99:1) to yield the title compound as a pale yellow oil (22 mg, 28% over two steps, *Z/E* 8:1). The major byproduct was the desilylated alcohol, which was co-eluting with the phosphonate and thus not pure enough for full characterization. $[\alpha]_D^{20} = +31.8$ (*c* = 1.0, CHCl₃). ¹H NMR (400 MHz, CDCl₃): δ = 6.34 (dd, *J* = 11.7, 7.2 Hz, 1H), 5.74 (dd, *J* = 11.7, 1.6 Hz, 1H), 5.37 (dddd, *J* = 9.7, 7.4, 5.9, 1.6 Hz, 1H), 3.69 (s, 3H), 3.67–3.65 (m, 2H), 3.61 (ddd, *J* = 8.0, 5.2, 4.1 Hz, 1H), 2.49 (ddd, *J* = 12.5, 6.9, 5.9 Hz, 1H), 2.22–2.11 (m, 1H), 1.30 (ddd, *J* = 12.2, 10.6, 9.8 Hz, 1H), 1.07 (d, *J* = 6.6 Hz, 3H), 0.95 (t, *J* = 7.9 Hz, 9H), 0.61 ppm (q, *J* = 7.7 Hz, 6H). ¹³C NMR (100 MHz, CDCl₃): δ = 166.4, 152.3, 118.5, 86.6, 75.8, 64.7, 51.4, 41.4, 36.7, 17.5, 6.9 (3C), 4.5 ppm (3C). IR (film): $\tilde{\nu} = 2954, 2875, 1723, 1649, 1458, 1438, 1405, 1196, 1179, 1081, 1037, 1004, 819, 773, 726$ cm⁻¹. MS (EI) *m/z* (%): 285 (13), 153 (16), 225 (32), 207 (12), 185 (21), 169 (20), 165 (20), 165 (17), 151 (14), 145 (26), 139 (23), 137 (36), 133 (46), 123 (12), 121 (50), 117 (78), 115 (47), 113 (15), 111 (69), 109 (28), 108 (10), 107 (45), 106 (11), 105 (100), 103 (73), 101 (12), 99 (21), 98 (12), 97 (10), 95 (27), 93 (25), 91 (23), 89 (36), 88 (12), 87 (80), 85 (31), 83 (14), 81 (45), 80 (12), 79 (68), 77 (33), 75 (87), 73 (13), 71 (11), 69 (11), 68 (11), 67 (15), 61 (17), 59 (93), 58 (15), 57 (17), 55 (41), 53 (25), 47 (30), 45 (29), 43 (24), 41 (21), 40 (23), 39 (16), 29 (15). HRMS (ESIpos): *m/z* calcd for C₁₆H₃₀O₄SiNa: 337.1806, found: 337.1804.

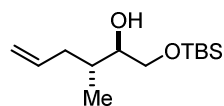
***t*-Dimethyl(((2*S*,3*R*)-3-methyloxiran-2-yl)methoxy)silane (S19).** Imidazole (12.9 g, 190 mmol), DMAP



(892 mg, 7.30 mmol, 5 mol%) and TBSCl (26.5 g, 176 mmol) were sequentially added

to a solution of epoxy alcohol **61** (12.9 g, 146 mmol) in CH₂Cl₂ (280 mL) at 0 °C. The resulting mixture was stirred at ambient temperature for 3.5 h. The reaction was quenched with aq. half-sat. NH₄Cl (200 mL) and the aqueous layer extracted with CH₂Cl₂ (3 × 200 mL). The combined extracts were dried over Na₂SO₄, filtered and concentrated. The residue was purified by flash chromatography (pentane/Et₂O 99:1) to yield the title compound as a colorless oil (28.4 g, 96%). $[\alpha]_D^{20} = +7.1$ (c = 1.0, CHCl₃). ¹H NMR (400 MHz, CD₂Cl₂): δ = 3.76 (d, *J* = 11.5, 4.8 Hz, 1H), 3.67 (ddd, *J* = 11.6, 6.0 Hz, 1H), 3.05 (qd, *J* = 5.5, 4.3 Hz, 1H), 2.99 (dt, *J* = 6.0, 4.6 Hz, 1H), 1.25 (d, *J* = 5.5 Hz, 3H), 0.90 (s, 9H), 0.082 (s, 3H), 0.076 ppm (s, 3H). ¹³C NMR (100 MHz, CD₂Cl₂): δ = 61.9, 57.1, 52.4, 25.9 (3C), 18.5, 13.5, -5.2, -5.3 ppm. IR (film): $\tilde{\nu}$ = 2955, 2930, 2857, 1472, 1391, 1361, 1254, 1091, 1006, 975, 939, 886, 834, 775, 666 cm⁻¹. MS (EI) *m/z* (%): 145 (46), 116 (11), 115 (100), 101 (65), 85 (25), 75 (38), 73 (20), 59 (30). HRMS (ESIpos): *m/z* calcd for C₁₀H₂₂O₂SiNa: 225.1281, found: 225.1281.

(2*R*,3*R*)-1-((*t*-Dimethylsilyl)oxy)-3-methylhex-5-en-2-ol (71). A solution of allyl-MgCl (2 M in THF,

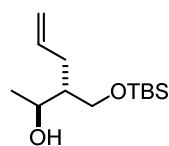


22.2 mL, 44.5 mmol) was added to a suspension of CuI (847 mg, 4.45 mmol, 15 mol%) in THF (70 mL) at -25 °C. The resulting mixture was stirred for 10 min,

before a solution of epoxy silyl ether **S19** (6.00 g, 29.6 mmol) in THF (20 mL) was

added dropwise over 30 min. The resulting mixture was stirred at -25 °C for 6 h. The reaction was quenched with aq. half-sat. NH₄Cl (50 mL) and the aqueous layer extracted with *t*-butyl methyl ether (3 × 50 mL). The combined extracts were dried over Na₂SO₄, filtered and concentrated. The residue was purified by flash chromatography (hexanes/*t*-butyl methyl ether 300:1) to afford the title compound **71** as a pale yellow oil (5.57 g, 77%, r.r. 10:1) and its regioisomer **72** as a colorless oil (310 mg, 4%). $[\alpha]_D^{20} = -13.4$ (c = 1.0, CHCl₃). ¹H NMR (400 MHz, CDCl₃): δ = 5.80 (dddd, *J* = 16.8, 10.1, 7.9, 6.4 Hz, 1H), 5.09–4.97 (m, 2H), 3.70 (dd, *J* = 9.6, 3.0 Hz, 1H), 3.48 (dd, *J* = 9.6, 7.7 Hz, 1H), 3.41 (td, *J* = 7.4, 3.0 Hz, 1H), 2.54 (brs, 1H), 2.43–2.34 (m, 1H), 1.95 (dddt, *J* = 13.9, 8.9, 7.9, 1.1 Hz, 1H), 1.66 (dddd, *J* = 12.9, 11.0, 5.8, 2.8 Hz, 1H), 0.90 (s, 9H), 0.85 (d, *J* = 6.9 Hz, 3H), 0.08 ppm (s, 6H). ¹³C NMR (100 MHz, CDCl₃): δ = 137.3, 116.2, 75.2, 65.2, 37.3, 35.7, 26.0 (3C), 18.4, 15.2, -5.2, -5.3 ppm. IR (film): $\tilde{\nu}$ = 3484, 2955, 2929, 2858, 1463, 1362, 1254, 1093, 993, 911, 835, 777, 670 cm⁻¹. MS (EI) *m/z* (%): 187 (15), 145 (13), 105 (57), 95 (100), 89 (13), 75 (82), 73 (25), 67 (11). HRMS (ESIpos): *m/z* calcd for C₁₃H₂₈O₂SiNa: 267.1751, found: 267.1751.

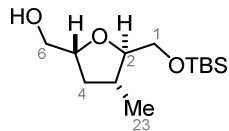
Regioisomer **72**: $[\alpha]_D^{20} = +2.1$ (c = 0.7, CHCl₃). ¹H NMR (400 MHz, CDCl₃): δ = 5.77 (ddt, *J* = 17.0, 10.1,



7.1 Hz, 1H), 5.09–4.97 (m, 2H), 4.02 (qd, *J* = 6.5, 2.7 Hz, 1H), 3.76 (dd, *J* = 10.0, 5.9 Hz, 1H), 3.72 (dd, *J* = 10.0, 4.0 Hz, 1H), 2.15–2.06 (m, 2H), 1.69 (dddd, *J* = 10.2, 8.7, 4.0, 2.7 Hz, 1H), 1.19 (d, *J* = 6.5 Hz, 3H), 0.90 (s, 9H), 0.07 ppm (s, 6H). ¹³C NMR (100 MHz,

CDCl₃): δ = 137.3, 116.4, 70.8, 65.1, 44.9, 30.1, 26.0 (3C), 19.5, 18.2, -5.5 ppm (2C). IR (film): $\tilde{\nu}$ = 3443, 2956, 2929, 2858, 1472, 1362, 1254, 1094, 992, 911, 836, 776, 670 cm⁻¹. MS (EI) m/z (%): 105 (63), 95 (34), 75 (100), 73 (16). HRMS (ESIpos): m/z calcd for C₁₃H₂₈O₂SiNa: 267.1751, found: 267.1749.

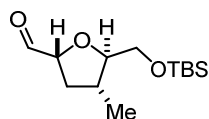
Alcohol 73. A solution of alcohol **71** (4.00 g, 16.4 mmol) in *i*-PrOH (10 mL) was added to a solution of



Co(nmp)₂ (925 mg, 1.64 mmol, 10 mol%) in *i*-PrOH (90 mL). The pale red solution was purged with O₂ for 15 min before *t*-BuOOH (5.5 M in decane, 0.29 mL, 1.64 mmol, 10 mol%) was added in one portion. The reaction mixture

was stirred at 55 °C under oxygen atmosphere (balloon) for 5 h; the solution turned green. After cooling to ambient temperature, the atmosphere was replaced by Ar and the solvent evaporated. The crude oil was partitioned between aq. half-sat. NH₄Cl (50 mL) and *t*-butyl methyl ether (50 mL) and the aqueous layer extracted with *t*-butyl methyl ether (2 × 80 mL). The combined extracts were washed with water (3 × 50 mL) and brine (50 mL), dried over Na₂SO₄, filtered and concentrated. The residue was purified by flash chromatography (hexanes/*t*-butyl methyl ether 25:1 to 20:1) to yield the title compound **73** as a pale yellow oil (3.36 g, 79%). $[\alpha]_D^{20}$ = -16.4 (*c* = 1.0, CHCl₃). ¹H NMR (500 MHz, CDCl₃): δ = 4.52 (dtd, *J* = 9.8, 5.7, 3.2 Hz, 1H, H-5), 3.69 (ddd, *J* = 11.6, 6.4, 3.2 Hz, 1H, H-6), 3.69 (dd, *J* = 11.0, 4.5 Hz, 1H, H-1), 3.66 (dd, *J* = 11.0, 4.5 Hz, 1H, H-1), 3.58 (dt, *J* = 8.4, 4.5 Hz, 1H, H-2), 3.49 (dt, *J* = 11.9, 5.8 Hz, 1H, H-6), 2.15 (dddq, *J* = 10.8, 8.2, 7.0, 6.6 Hz, 1H, H-3), 2.06 (ddd, *J* = 12.0, 7.1, 5.8 Hz, 1H, H-4), 1.95 (t, *J* = 6.2 Hz, 1H, 6-OH), 1.41 (ddd, *J* = 11.9, 10.5, 9.8 Hz, 1H, H-4), 1.07 (d, *J* = 6.6 Hz, 3H, H-23), 0.90 (s, 9H, TBS), 0.07 ppm (s, 6H, TBS). ¹³C NMR (125 MHz, CDCl₃): δ = 86.2 (C2), 79.3 (C5), 65.1 (C6), 65.0 (C1), 36.8 (C4), 36.5 (C3), 26.1 (3C, TBS), 18.6 (TBS), 17.5 (C23), -5.1 (TBS), -5.2 ppm (TBS). IR (film): $\tilde{\nu}$ = 3432, 2955, 2929, 2857, 1729, 1462, 1388, 1361, 1253, 1128, 1085, 1054, 1005, 906, 834, 775, 729, 649 cm⁻¹. MS (EI) m/z (%): 229 (15), 203 (49), 185 (29), 117 (28), 115 (17), 111 (12), 105 (28), 103 (10), 101 (11), 93 (33), 89 (10), 83 (12), 81 (22), 75 (100), 73 (48), 69 (21), 59 (17), 57 (21), 55 (22), 43 (12), 41 (18). HRMS (ESIpos): m/z calcd for C₁₃H₂₈O₃SiNa: 283.1700, found: 283.1700.

Aldehyde 74. Hünig's base (11.0 mL, 63.4 mmol) was added to a solution of alcohol **73** (3.30 g,

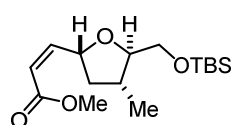


12.7 mmol) in CH₂Cl₂ (110 mL) at -25 °C. In a second flask, SO₃·pyridine (5.04 g, 31.7 mmol) was suspended in DMSO (9.00 mL, 126 mmol) and stirred for 10 min at rt, before it was added to the alcohol solution at -25 °C and the flask was

rinsed with CH₂Cl₂ (5 mL). The resulting mixture was stirred for 30 min at -25 °C. The mixture was poured into pH 7 phosphate buffer (50 mL) and *t*-butyl methyl ether (50 mL), and the aqueous layer was extracted with *t*-butyl methyl ether (3 × 100 mL). The combined extracts were washed with pH 7 phosphate buffer (100 mL), and brine (100 mL), dried over Na₂SO₄, filtered and concentrated

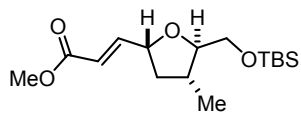
under high vacuum to yield the crude aldehyde **74** as a yellow oil. An analytical sample was purified by flash chromatography (hexanes/*t*-butyl methyl ether 9:1) for characterization. The crude aldehyde was used in the next step without further purification. $[\alpha]_{\text{D}}^{20} = +3.4$ ($c = 1.0$, CHCl_3). $^1\text{H NMR}$ (400 MHz, CDCl_3): $\delta = 9.66$ (d, $J = 2.2$ Hz, 1H), 4.28 (ddd, $J = 8.8, 7.4, 2.2$ Hz, 1H), 3.77–3.71 (m, 1H), 3.68 (d, $J = 4.1$ Hz, 1H), 3.64 (dd, $J = 7.9, 4.0$ Hz, 1H), 2.35 (dt, $J = 12.2, 7.4$ Hz, 1H), 2.22 (dtd, $J = 14.2, 7.4, 2.4$ Hz, 1H), 1.58 (dt, $J = 12.2, 9.0$ Hz, 1H), 1.06 (d, $J = 6.6$ Hz, 3H), 0.89 (s, 9H), 0.059 (s, 3H), 0.057 ppm (s, 3H). $^{13}\text{C NMR}$ (100 MHz, CDCl_3): $\delta = 203.1, 87.8, 82.8, 64.3, 36.5, 35.4, 26.1$ (3C), 18.5, 17.3, $-5.19, -5.25$ ppm. IR (film): $\tilde{\nu} = 2956, 2929, 2857, 1734, 1462, 1388, 1361, 1254, 1130, 1087, 1058, 1004, 939, 834, 776, 671$ cm^{-1} . MS (EI) m/z (%): 229 (25), 201 (34), 185 (13), 145 (12), 143 (11), 129 (13), 117 (11), 115 (18), 105 (11), 103 (19), 101 (20), 89 (13), 75 (100), 73 (72), 59 (23), 57 (12), 55 (12), 41 (14). HRMS (ESIpos): m/z calcd for $\text{C}_{13}\text{H}_{26}\text{O}_3\text{SiNa}$: 281.1543, found: 281.1545.

Olefin (Z)-75. 18-Crown-6 (7.37 g, 27.9 mmol) was added to a solution of KHMDS (3.03 g, 15.2 mmol) in THF (60 mL). After cooling to -78 °C methyl O,O'-bis(2,2,2-trifluoroethyl)phosphono-acetate (3.22 mL, 15.2 mmol) was added dropwise and the resulting mixture was stirred for 20 min. Next, a solution of aldehyde **74** (3.27 g, 12.7 mmol) in THF (15 mL) was added dropwise over 10 min. The resulting mixture was stirred for 3 h at -78 °C before it was poured into aq. half-sat. NH_4Cl (70 mL). The aqueous layer was extracted with EtOAc (3×70 mL). The combined extracts were washed with brine (100 mL), dried over Na_2SO_4 , filtered and concentrated. The residue was purified by flash chromatography (fine SiO_2 , hexanes/*t*-butyl methyl ether 99:1) to yield the title compound (*Z*)-**75** as a pale yellow oil (2.50 g, 63% over two steps, *Z/E* 12:1); the undesired (*E*)-**75** (190 mg, 5% over two steps) could also be isolated in high purity.

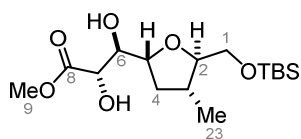


Analytical data for (*Z*)-**75**: $[\alpha]_{\text{D}}^{20} = +40.8$ ($c = 1.0$, CHCl_3). $^1\text{H NMR}$ (400 MHz, CDCl_3): $\delta = 6.33$ (dd, $J = 11.7, 7.3$ Hz, 1H), 5.75 (dd, $J = 11.7, 1.6$ Hz, 1H), 5.37 (dddd, $J = 9.8, 7.4, 5.9, 1.6$ Hz, 1H), 3.69 (s, 3H), 3.68–3.65 (m, 2H), 3.61 (ddd, $J = 8.2, 5.0, 4.1$ Hz, 1H), 2.48 (ddd, $J = 12.4, 7.0, 5.9$ Hz, 1H), 2.24–2.13 (m, 1H), 1.30 (ddd, $J = 12.1, 10.6, 9.8$ Hz, 1H), 1.07 (d, $J = 6.6$ Hz, 3H), 0.89 (s, 9H), 0.06 ppm (s, 6H). $^{13}\text{C NMR}$ (100 MHz, CDCl_3): $\delta = 166.4, 152.3, 118.5, 86.5, 75.8, 65.0, 51.5, 41.4, 36.7, 26.1$ (3C), 18.6, 17.5, $-5.16, -5.17$ ppm. IR (film): $\tilde{\nu} = 2954, 2929, 2857, 1724, 1648, 1462, 1438, 1404, 1254, 1198, 1180, 1083, 1038, 1005, 837, 777, 674$ cm^{-1} . MS (EI) m/z (%): 258 (18), 257 (100), 227 (16), 225 (30), 197 (28), 169 (15), 165 (13), 139 (28), 137 (15), 133 (39), 121 (35), 117 (58), 111 (35), 107 (20), 105 (33), 89 (23), 81 (11), 79 (18), 75 (45), 73 (37), 59 (13). HRMS (ESIpos): m/z calcd for $\text{C}_{16}\text{H}_{30}\text{O}_4\text{SiNa}$: 337.1806, found: 337.1806.

Analytical data for (*E*)-**75**: $[\alpha]_D^{20} = +17.3$ ($c = 0.93$, CHCl_3). $^1\text{H NMR}$ (400 MHz, CDCl_3): $\delta = 6.94$ (dd, $J = 15.6, 5.2$ Hz, 1H), 6.04 (dd, $J = 15.6, 1.6$ Hz, 1H), 4.54 (dddd, $J = 9.9, 6.0, 5.2, 1.6$ Hz, 1H), 3.73 (s, 3H), 3.70 (d, $J = 4.4$ Hz, 1H), 3.68 (d, $J = 4.2$ Hz, 1H), 3.60 (dd, $J = 8.1, 4.1$ Hz, 1H), 2.30 (ddd, $J = 11.5, 7.0, 5.9$ Hz, 1H), 2.22 (ddq, $J = 10.4, 8.1, 6.5$ Hz, 1H), 1.39 (dt, $J = 11.6, 10.0$ Hz, 1H), 1.07 (d, $J = 6.5$ Hz, 3H), 0.89 (s, 9H), 0.062 (s, 3H), 0.058 ppm (s, 3H). $^{13}\text{C NMR}$ (100 MHz, CDCl_3): $\delta = 167.2, 149.0, 119.5, 86.5, 77.7, 64.6, 51.7, 41.7, 36.5, 26.1$ (3C), 18.5, 17.4, $-5.15, -5.19$ ppm. IR (film): $\tilde{\nu} = 2955, 2930, 2857, 1728, 1662, 1462, 1436, 1361, 1300, 1258, 1166, 1125, 1089, 1006, 837, 777, 675$ cm^{-1} . MS (ESIpos) m/z (%): 337.2 (100 (M+Na)). HRMS (ESIpos): m/z calcd for $\text{C}_{16}\text{H}_{30}\text{O}_4\text{SiNa}$: 337.1806, found: 337.1807.

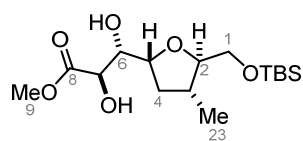


Diol 76 and 77. $\text{K}_3\text{Fe}(\text{CN})_6$ (5.61 g, 17.0 mmol), K_2CO_3 (2.36 g, 17.0 mmol), K_2OsO_4 (126 mg, 0.34 mmol, 6 mol%), $(\text{DHQD})_2\text{PYR}$ (150 mg, 0.17 mmol, 3 mol%) and MeSO_2NH_2 (540 mg, 5.68 mmol) were sequentially added to a mixture of (*Z*)-**75** (1.79 g, 5.68 mmol) in *t*-BuOH/ H_2O (1:1, 100 mL) at 0 °C. The resulting mixture was stirred at 0 °C for 48 h before it was poured into a solution of NH_4Cl , $\text{Na}_2\text{S}_2\text{O}_3$ and water (1:1:2, 100 mL). The mixture was vigorously stirred for 10 min at rt, diluted with EtOAc and the aqueous layer extracted with EtOAc (3 × 100 mL). The combined extracts were washed with brine (200 mL), dried over Na_2SO_4 , filtered and concentrated. The residue was purified by flash chromatography (fine SiO_2 , hexanes/EtOAc 19:1 to 8:1) to yield the desired diol **76** (1.33 g, 67%, d.r. 5:1) and its undesired diastereomer **77** (215 mg, 11%) as colorless oil each.



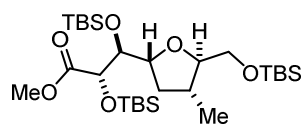
Analytical data for **76**: $[\alpha]_D^{20} = -8.0$ ($c = 1.0$, CHCl_3). $^1\text{H NMR}$ (500 MHz, CDCl_3): $\delta = 4.29$ (dd, $J = 9.2, 4.3$ Hz, 1H, H-7), 4.05 (ddd, $J = 10.0, 5.6, 3.4$ Hz, 1H, H-5), 3.78 (s, 3H, H-9), 3.74 (ddd, $J = 8.4, 4.4, 3.6$ Hz, 1H, H-6), 3.67 (dd, $J = 10.9, 4.0$ Hz, 1H, H-1), 3.62 (dd, $J = 10.9, 4.6$ Hz, 1H, H-1), 3.54 (ddd, $J = 8.6, 4.6, 4.0$ Hz, 1H, H-2), 3.39 (d, $J = 9.6$ Hz, 1H, 7-OH), 2.75 (d, $J = 8.5$ Hz, 1H, 6-OH), 2.12 (ddqd, $J = 10.6, 8.6, 6.8, 6.6$ Hz, 1H, H-3), 2.07 (ddd, $J = 11.8, 6.8, 5.6$ Hz, 1H, H-4), 1.64 (dt, $J = 11.4, 10.6$ Hz, 1H, H-4), 1.07 (d, $J = 6.4$ Hz, 3H, H-23), 0.89 (s, 9H, TBS), 0.06 ppm (s, 6H, TBS). $^{13}\text{C NMR}$ (125 MHz, CDCl_3): $\delta = 172.9$ (C8), 87.0 (C2), 78.7 (C5), 73.7 (C7), 73.4 (C6), 64.6 (C1), 52.5 (C9), 37.4 (C4), 36.0 (C3), 26.0 (3C, TBS), 18.5 (TBS), 17.0 (C23), -5.19 (TBS), -5.23 ppm (TBS). IR (film): $\tilde{\nu} = 3458, 2954, 2929, 2857, 1740, 1461, 1440, 1388, 1253, 1128, 1080, 1004, 836, 777, 647$ cm^{-1} . MS (EI) m/z (%): 292 (14), 291 (77), 259 (25), 155 (11), 231 (39), 230 (15), 229 (82), 213 (11), 186 (12), 185 (80), 181 (17), 171 (24), 167 (11), 157 (12), 153 (11), 149 (15), 145 (13), 143 (14), 139 (27), 129 (11), 127 (13), 126 (12), 121 (19), 117 (48), 115 (66), 113 (11), 109 (23), 107 (11), 105 (24), 103 (12), 101 (14), 97 (19), 93 (23), 89 (22), 85 (12), 81 (23), 75 (88), 73 (100), 69 (12), 59 (16), 55 (14), 43 (12), 41 (11). HRMS (ESIpos): m/z calcd for $\text{C}_{16}\text{H}_{32}\text{O}_6\text{SiNa}$: 371.1860, found: 371.1863.

Analytical data for **77**: $[\alpha]_D^{20} = -17.6$ ($c = 1.4$, CHCl_3). $^1\text{H NMR}$ (500 MHz, CDCl_3): $\delta = 4.32$ (t, $J = 4.4$ Hz,



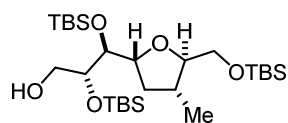
1H, H-7), 4.03 (ddd, $J = 9.2, 7.4, 6.0$ Hz, 1H, H-5), 3.80 (s, 3H, H-9), 3.81 (ddd, $J = 9.2, 7.4, 6.0$ Hz, 1H, H-6), 3.64 (dd, $J = 11.7, 4.3$ Hz, 1H, H-1), 3.60 (dd, $J = 11.0, 4.6$ Hz, 1H, H-1), 3.48 (dt, $J = 8.6, 4.4$ Hz, 1H, H-2), 3.31 (d, $J = 4.8$ Hz, 1H, 7-OH), 2.53 (d, $J = 6.0$ Hz, 1H, 6-OH), 2.28 (ddd, $J = 12.4, 6.8, 6.0$ Hz, 1H, H-4), 2.10 (dddq, $J = 10.8, 8.5, 7.0, 6.6$ Hz, 1H, H-3), 1.55 (ddd, $J = 12.4, 10.6, 9.2$ Hz, 1H, H-4), 1.07 (d, $J = 6.6$ Hz, 3H, H-23), 0.89 (s, 9H, TBS), 0.05 ppm (s, 6H, TBS). $^{13}\text{C NMR}$ (125 MHz, CDCl_3): $\delta = 173.2$ (C8), 86.6 (C2), 78.4 (C5), 75.2 (C6), 72.7 (C7), 64.8 (C1), 52.7 (C9), 38.4 (C4), 36.2 (C3), 26.1 (3C, TBS), 18.5 (TBS), 17.3 (C23), -5.19 (TBS), -5.21 ppm (TBS). IR (film): $\tilde{\nu} = 3439, 2954, 2929, 2857, 1741, 1462, 1388, 1254, 1129, 1087, 1004, 837, 777, 671$ cm^{-1} . MS (ESIpos) m/z (%): 371.2 (100 (M+Na)). HRMS (ESIpos): m/z calcd for $\text{C}_{16}\text{H}_{32}\text{O}_6\text{SiNa}$: 371.1860, found: 371.1858.

Methyl ester 78. 2,6-Lutidine (1.75 mL, 15.0 mmol), DMAP (51.0 mg, 0.42 mmol, 20 mol%) and TBSOTf (2.88 mL, 12.5 mmol) were sequentially added to a solution of diol **76** (728 mg, 2.09 mmol) in CH_2Cl_2 (10 mL) at 0 °C. The resulting mixture was stirred at rt for 24 h. The reaction was quenched with aq.



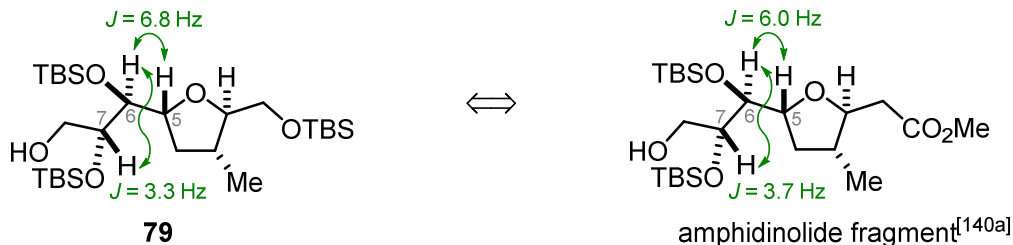
half-sat. NH_4Cl (10 mL) and the aqueous layer extracted with CH_2Cl_2 (3×10 mL). The combined extracts were dried over Na_2SO_4 , filtered and concentrated. The residue was purified by flash chromatography (hexanes/*t*-butyl methyl ether 99:1) to afford the title compound **78** as a colorless oil (1.12 g, 86%). $[\alpha]_D^{20} = -4.9$ ($c = 1.0$, CHCl_3). $^1\text{H NMR}$ (400 MHz, CDCl_3): $\delta = 4.22$ (d, $J = 3.4$ Hz, 1H), 4.04 (ddd, $J = 10.0, 6.6, 5.2$ Hz, 1H), 3.84 (dd, $J = 6.7, 3.4$ Hz, 1H), 3.69 (s, 3H), 3.64 (dd, $J = 10.7, 4.8$ Hz, 1H), 3.60 (dd, $J = 10.7, 4.6$ Hz, 1H), 3.43 (dt, $J = 8.8, 4.6$ Hz, 1H), 2.14–2.00 (m, 2H), 1.47–1.36 (m, 1H), 1.04 (d, $J = 6.1$ Hz, 3H), 0.89 (s, 9H), 0.88 (s, 9H), 0.87 (s, 9H), 0.08 (s, 3H), 0.06 (s, 3H), 0.05 (s, 3H), 0.04 (s, 3H), 0.039 ppm (s, 6H). $^{13}\text{C NMR}$ (100 MHz, CDCl_3): $\delta = 172.5, 85.1, 79.3, 78.1, 75.2, 65.0, 51.7, 37.5, 37.0, 26.09$ (3C), 26.08 (3C), 25.8 (3C), 18.5, 18.43, 18.42, 17.0, -4.1, -4.7, -5.0, -5.17, -5.23 ppm (2C). IR (film): $\tilde{\nu} = 2954, 2927, 2856, 1736, 1462, 1388, 1361, 1253, 1129, 1091, 1005, 836, 778, 673$ cm^{-1} . MS (EI) m/z (%): 521 (16), 520 (35), 519 (83), 388 (10), 387 (34), 355 (11), 295 (15), 256 (11), 255 (57), 229 (42), 223 (18), 185 (50), 163 (14), 149 (21), 147 (18), 117 (20), 115 (18), 89 (24), 75 (18), 73 (100). HRMS (ESIpos): m/z calcd for $\text{C}_{28}\text{H}_{60}\text{O}_6\text{Si}_3\text{Na}$: 599.3590, found: 599.3596.

Alcohol 79. Diisobutylaluminum hydride (1.2 M in toluene, 2.86 mL, 3.43 mmol) was added to a solution of ester **78** (900 mg, 1.56 mmol) in toluene (18 mL) at -78 °C. The resulting mixture was stirred at -78 °C for 1 h. The mixture was then poured *via* cannula into aq. sat. Rochelle salt (15 mL) and the emulsion was vigorously stirred at rt for 2 h. The layers were separated and the aqueous layer was extracted with *t*-butyl methyl ether (3×20 mL). The combined extracts were washed with brine (25 mL), dried over



Na_2SO_4 , filtered and concentrated. The residue was purified by flash chromatography (hexanes/*t*-butyl methyl ether 19:1) to afford the title compound **79** as a colorless oil (838 mg, 98%). $[\alpha]_{\text{D}}^{20} = -4.3$ ($c = 1.0$, CHCl_3). ^1H NMR (400 MHz, CDCl_3): $\delta = 4.00$ (ddd, $J = 10.2, 5.7, 3.3$ Hz, 1H), 3.78 (ddd, $J = 10.5, 6.9, 3.6$ Hz, 1H), 3.73 (ddd, $J = 6.8, 3.4, 1.9$ Hz, 1H), 3.67–3.59 (m, 3H), 3.57–3.53 (m, 1H), 3.53–3.49 (m, 1H), 3.45 (ddd, $J = 10.4, 8.9, 3.3$ Hz, 1H), 2.09 (ddt, $J = 11.3, 8.9, 6.6$ Hz, 1H), 2.00 (dt, $J = 12.4, 6.2$ Hz, 1H), 1.66–1.56 (m, 1H), 1.05 (d, $J = 6.4$ Hz, 3H), 0.91 (s, 9H), 0.89 (s, 9H), 0.88 (s, 9H), 0.12 (s, 3H), 0.08 (s, 3H), 0.07 (s, 6H), 0.04 ppm (s, 6H). ^{13}C NMR (100 MHz, CDCl_3): $\delta = 86.1, 79.9, 78.3, 75.9, 64.6, 62.8, 37.6, 36.5, 26.3$ (3C), 26.1 (3C), 26.0 (3C), 18.6, 18.44, 18.39, 16.5, $-3.9, -4.47, -4.53, -4.8, -5.3$ ppm (2C). IR (film): $\tilde{\nu} = 3461, 2954, 2929, 2886, 2857, 1472, 1462, 1388, 1361, 1252, 1129, 1075, 1004, 832, 773, 672$ cm^{-1} . MS (EI) m/z (%): 493 (14), 492 (30), 491 (72), 360 (18), 359 (63), 267 (47), 231 (12), 229 (54), 228 (12), 227 (71), 209 (24), 199 (11), 197 (11), 186 (13), 185 (83), 171 (22), 159 (10), 149 (20), 147 (15), 135 (33), 117 (39), 115 (24), 107 (13), 103 (15), 89 (25), 75 (29), 73 (100). HRMS (ESIpos): m/z calcd for $\text{C}_{27}\text{H}_{60}\text{O}_5\text{Si}_3\text{Na}$: 571.3641, found: 571.3642.

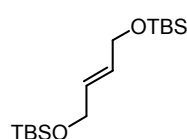
The absolute configuration at C6 and C7 was assigned by NMR analysis and comparison of indicative coupling constants $J_{5,6}$ and $J_{6,7}$ (green) with the available data of the fragments of amphidinolides C and F (right).^[140a] The diol was later unambiguously assigned by preparation of the cyclic acetal and NOE studies as well as by Mosher ester analysis at C6 of a derivative.



Aldehyde 80. Hünig's base (1.60 mL, 9.21 mmol) was added to a solution of alcohol **79** (722 mg, 1.32 mmol) in CH_2Cl_2 (10 mL) at -25 °C. In a second flask, SO_3 ·pyridine (523 mg, 3.29 mmol) was suspended in DMSO (0.93 mL, 13.2 mmol) and the suspension was stirred for 10 min at rt, before it was added to the alcohol solution at -25 °C and the flask was rinsed with CH_2Cl_2 (2 mL). The resulting mixture was stirred for 45 min at -25 °C. The mixture was poured into pH 7 phosphate buffer (15 mL) and *t*-butyl methyl ether (15 mL), the layers were separated and the aqueous layer was extracted with *t*-butyl methyl ether (3 × 20 mL). The combined extracts were washed with pH 7 phosphate buffer (20 mL), followed by brine (20 mL), dried over Na_2SO_4 , filtered and concentrated. The residue was purified by flash chromatography (hexanes/*t*-butyl methyl ether 50:1 to 30:1) to yield aldehyde **80** as a colorless oil (678 mg, 94%). $[\alpha]_{\text{D}}^{20} = +12.6$ ($c = 1.0$, CHCl_3). ^1H NMR (400 MHz, CDCl_3): $\delta = 9.62$ (d, $J = 1.0$ Hz, 1H), 4.08–3.99 (m, 2H), 3.90 (dd, $J = 6.2, 1.9$ Hz, 1H), 3.65–3.61 (m, 2H), 3.47 (dt, $J = 8.7, 4.4$ Hz, 1H),

2.16–1.99 (m, 2H), 1.58–1.48 (m, 1H), 1.05 (d, $J = 6.2$ Hz, 3H), 0.92 (s, 9H), 0.89 (s, 9H), 0.88 (s, 9H), 0.09 (s, 6H), 0.08 (s, 3H), 0.07 (s, 3H), 0.05 ppm (s, 6H). ^{13}C NMR (100 MHz, CDCl_3): $\delta = 202.8, 85.8, 81.0, 79.6, 78.7, 64.8, 37.5, 36.6, 26.11$ (3C), 26.09 (3C), 26.0 (3C), $18.50, 18.47, 18.4, 16.8, -4.4, -4.5, -4.6, -4.8, -5.18, -5.21$ ppm. IR (film): $\tilde{\nu} = 2954, 2929, 2886, 2857, 1736, 1472, 1463, 1388, 1361, 1252, 1131, 1084, 1005, 832, 774, 672$ cm^{-1} . MS (EI) m/z (%): 505 (12), 490 (13), 489 (33), 475 (10), 373 (13), 357 (24), 231 (17), 230 (18), 229 (100), 289 (13), 186 (12), 185 (71), 183 (10), 171 (15), 149 (14), 147 (14), 115 (21), 103 (14), 75 (31), 73 (83), 57 (12). HRMS (ESIpos): m/z calcd for $\text{C}_{27}\text{H}_{58}\text{O}_5\text{Si}_3\text{Na}$: 569.3484, found: 569.3485.

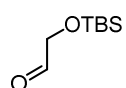
1,4-Di-(*t*-butyldimethylsilyloxy)but-2-ene (S20). Imidazole (1.85 g, 27.2 mmol), DMAP (139 mg,



1.13 mmol, 10 mol%) and TBSCl (3.76 g, 25.0 mmol) were sequentially added to a solution of *trans*-2-butene-1,4-diol (1.00 g, 11.3 mmol) in CH_2Cl_2 (100 mL) at 0°C .

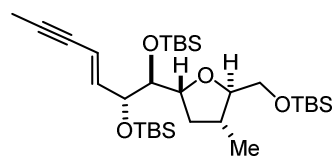
The resulting mixture was stirred at rt for 5 h. The reaction was quenched with water (30 mL) and the aqueous layer was extracted with CH_2Cl_2 (3×40 mL). The combined organic extracts were dried over Na_2SO_4 , filtered and concentrated. The residue was purified by flash chromatography (hexanes/*t*-butyl methyl ether 50:1) to yield the title compound **S20** as a colorless oil (3.58 mg, quant.). ^1H NMR (400 MHz, CDCl_3): $\delta = 5.55$ (td, $J = 2.9, 0.7$ Hz, 2H), 4.23 (dd, $J = 2.9, 0.7$ Hz, 4H), 0.90 (s, 18H), 0.07 ppm (s, 12H). ^{13}C NMR (100 MHz, CDCl_3): $\delta = 130.3$ (2C), 59.8 (2C), 26.1 (6C), 18.5 (2C), -5.0 ppm (4C). IR (film): $\tilde{\nu} = 2955, 2929, 2886, 2857, 1463, 1389, 1253, 1079, 1006, 834, 774, 669$ cm^{-1} . MS (EI) m/z (%): 259 (13), 189 (13), 148 (16), 147 (100), 75 (13), 73 (53). HRMS (ESI_{neg}): m/z calcd for $\text{C}_{16}\text{H}_{36}\text{O}_2\text{Si}_2\text{Na}$: 339.2146, found: 339.2148. The analytical and spectroscopic data are in agreement with those reported in the literature.^[232]

Aldehyde 81. Ozone was bubbled through a solution of olefin **S20** (1.00 g, 3.16 mmol) in CH_2Cl_2

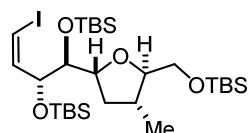


(20 mL) at -78°C until the solution turned blue. Argon was then bubbled through the solution until the reaction mixture turned colorless. Triphenylphosphine (994 mg, 3.79 mmol) was added, and the mixture was warmed to room temperature and stirred for 3 h. The solvent was removed in vacuo, and the residue was purified by flash chromatography (hexanes/*t*-butyl methyl ether 20:1) to yield the title compound as a colorless oil (1.04 g, 94%). ^1H NMR (400 MHz, CDCl_3): $\delta = 9.70$ (t, $J = 0.9$ Hz, 1H), 4.22 (d, $J = 0.8$ Hz, 2H), 0.93 (s, 9H), 0.10 ppm (s, 6H). ^{13}C NMR (100 MHz, CDCl_3): $\delta = 202.5, 69.8, 25.9$ (3C), 18.5, -5.3 ppm (2C). IR (film): $\tilde{\nu} = 2953, 2930, 2885, 2858, 1741, 1472, 1362, 1255, 1104, 1006, 939, 836, 778, 669$ cm^{-1} . MS (EI) m/z (%): 117 (100), 89 (59), 73 (26), 59 (31). HRMS (ESI_{neg}): m/z calcd for $\text{C}_8\text{H}_{18}\text{O}_2\text{SiNa}$: 197.0968, found: 197.0968. The analytical and spectroscopic data are in agreement with those reported in the literature.^[143]

(E)-Enyne (E)-83. A solution of KHMDS (58.1 mg, 0.29 mmol) in THF (0.4 mL) was added to a solution of 2-(but-2-yn-1-ylsulfonyl)benzo[*d*]thiazole (77.5 mg, 0.29 mmol) in THF (0.4 mL) at $-55\text{ }^{\circ}\text{C}$. The dark red solution was stirred for 30 min at this temperature before a solution of aldehyde **80** (53.0 mg, 96.9 μmol) in THF (0.2 mL) was added dropwise. The resulting mixture was stirred at $-55\text{ }^{\circ}\text{C}$ for 13 h before it was poured into brine (1 mL) and warmed to ambient temperature. The mixture was diluted with H_2O (2 mL) and *t*-butyl methyl ether (2 mL), the layers separated and the aqueous layer extracted with *t*-butyl methyl ether ($3 \times 5\text{ mL}$). The combined extracts were dried over Na_2SO_4 , filtered and concentrated. The residue was purified by flash chromatography (hexanes) to afford the title compound **(E)-83** as a colorless oil (15.7 mg, 28%, *E/Z* 7:1). $[\alpha]_{\text{D}}^{20} = -1.6$ ($c = 1.0$, CHCl_3). ^1H NMR (400 MHz, CDCl_3): $\delta = 6.07$ (dd, $J = 16.0, 6.7\text{ Hz}$, 1H), 5.54 (dq, $J = 16.0, 2.4, 1.3\text{ Hz}$, 1H), 4.13 (ddd, $J = 6.7, 3.4, 1.3\text{ Hz}$, 1H), 3.87 (dt, $J = 10.1, 5.8\text{ Hz}$, 1H), 3.66 (dd, $J = 10.6, 4.9\text{ Hz}$, 1H), 3.60 (dd, $J = 10.6, 4.7\text{ Hz}$, 1H), 3.50 (dd, $J = 6.0, 3.4\text{ Hz}$, 1H), 3.42 (dt, $J = 9.0, 4.7\text{ Hz}$, 1H), 2.15–1.97 (m, 2H), 1.94 (d, $J = 2.4\text{ Hz}$, 3H), 1.36 (ddd, $J = 11.3, 10.9, 6.2\text{ Hz}$, 1H), 1.05 (d, $J = 6.4\text{ Hz}$, 3H), 0.90 (s, 9H), 0.891 (s, 9H), 0.886 (s, 9H), 0.07 (s, 6H), 0.06 (s, 3H), 0.05 (s, 6H), 0.03 ppm (s, 3H). ^{13}C NMR (100 MHz, CDCl_3): $\delta = 142.6, 111.2, 86.2, 85.2, 79.7, 79.5, 78.3, 75.3, 65.2, 37.9, 37.2, 26.3$, (3C), 26.2 (3C), 26.1 (3C), 18.6, 18.5, 18.4, 17.2, 4.5, $-4.0, -4.1, -4.2, -4.5, -5.2$ ppm (2C). IR (film): $\tilde{\nu} = 2954, 2929, 2856, 1462, 1388, 1361, 1252, 1084, 1005, 960, 832, 774, 675\text{ cm}^{-1}$. MS (EI) m/z (%): 583 (10), 582 (21), 525 (11), 373 (13), 229 (26), 209 (41), 186 (16), 185 (100), 149 (12), 147 (13), 115 (13), 89 (16), 75 (16), 73 (91). HRMS (ESIpos): m/z calcd for $\text{C}_{31}\text{H}_{62}\text{O}_4\text{Si}_3\text{Na}$: 605.3848, found: 605.3847.

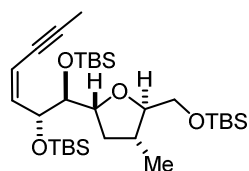


(Z)-Vinyl iodide 84. Iodomethyltriphenylphosphonium iodide (997 mg, 2.29 mmol) was added in portions to a solution of NaHMDS (386 mg, 2.10 mmol) in THF (15 mL). The resulting yellow mixture was stirred at rt for 30 min before it was cooled to $-78\text{ }^{\circ}\text{C}$. HMPA (0.80 mL, 4.57 mmol) was added, followed by a solution of aldehyde **80** (500 mg, 0.91 mmol) in THF (3 mL). The resulting mixture was stirred at $-78\text{ }^{\circ}\text{C}$ for 7 h. The reaction was quenched with H_2O (8 mL) and the aqueous layer was extracted with *t*-butyl methyl ether ($3 \times 10\text{ mL}$). The combined extracts were dried over Na_2SO_4 , filtered and concentrated. The residue was purified by flash chromatography (hexanes/*t*-butyl methyl ether 300:1) to afford the title compound **84** as a colorless oil (596 mg, 97%, *Z/E* > 20:1). $[\alpha]_{\text{D}}^{20} = +6.9$ ($c = 1.0$, CHCl_3). ^1H NMR (400 MHz, CDCl_3): $\delta = 6.40$ (dd, $J = 8.2, 7.7\text{ Hz}$, 1H), 6.27 (dd, $J = 7.7, 0.5\text{ Hz}$, 1H), 4.31 (ddd, $J = 8.3, 1.9, 0.8\text{ Hz}$, 1H), 3.75 (ddd, $J = 9.8, 8.0, 5.7\text{ Hz}$, 1H), 3.67–3.59 (m, 3H), 3.46 (dt, $J = 9.2, 4.7\text{ Hz}$, 1H), 2.29 (ddd, $J = 12.3, 7.0, 5.7\text{ Hz}$, 1H), 2.06 (ddt, $J = 11.0, 8.8, 6.7\text{ Hz}$, 1H), 1.31 (td, $J = 11.6, 10.0\text{ Hz}$, 1H), 1.07 (d, $J = 6.6\text{ Hz}$, 3H), 0.90 (s, 9H), 0.882 (s, 9H), 0.875 (s, 9H), 0.11 (s, 3H), 0.09 (s, 6H), 0.07 (s, 3H), 0.04 ppm (s, 6H). ^{13}C NMR (100 MHz, CDCl_3): $\delta = 141.9, 84.9, 81.8, 80.7, 79.3, 76.7, 65.2, 38.7, 37.2$.



26.3 (3C), 26.10 (3C), 26.05 (3C), 18.6, 18.5, 18.3, 17.2, -3.9, -4.0, -4.2, -4.5, -5.2 ppm (2C). IR (film): $\tilde{\nu}$ = 2954, 2928, 2886, 2856, 1471, 1462, 1388, 1361, 1252, 1131, 1075, 1005, 959, 832, 774, 672, 594 cm^{-1} . MS (EI) m/z (%): 615 (13), 614 (28), 413 (69), 543 (13), 481 (15), 375 (17), 374 (25), 371 (27), 349 (12), 298 (15), 297 (100), 230 (13), 229 (73), 186 (16), 185 (97), 147 (12), 115 (12), 89 (13), 75 (16), 73 (91). HRMS (ESIpos): m/z calcd for $\text{C}_{28}\text{H}_{59}\text{O}_4\text{Si}_3\text{Na}$: 693.2658, found: 693.2657.

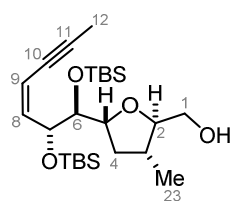
(Z)-Enyne (Z)-83. THF was degassed by three freeze-pump-thaw cycles prior to use. A flame-dried



two-necked round-bottom flask equipped with a reflux condenser was charged with 1-propynyllithium (87.0 mg, 1.89 mmol), which was suspended in degassed THF (12 mL). Trimethyl borate (0.21 mL, 1.89 mmol) was added dropwise *via* syringe at rt. After stirring for 20 min, $[\text{Pd}(\text{dppf})\text{Cl}_2]\cdot\text{CH}_2\text{Cl}_2$

(108 mg, 0.13 mmol, 15 mol%) was added, causing the reaction mixture to turn bright red. Next, a solution of (Z)-vinyl iodide **84** (590 mg, 0.88 mmol) in degassed THF (3 mL + 1 mL rinse) was added and the mixture was stirred at 65°C for 7 h. The pale orange mixture was cooled to ambient temperature; the reaction was quenched with aq. half-sat. NH_4Cl (15 mL) and the aqueous layer extracted with EtOAc (3 × 20 mL). The combined extracts were dried over Na_2SO_4 , filtered and concentrated. The residue was purified by flash chromatography (hexanes/*t*-butyl methyl ether 100:1) to afford the title compound (Z)-**83** as a colorless oil (440 mg, 86%). $[\alpha]_{\text{D}}^{20} = +3.2$ ($c = 1.0$, CHCl_3). ^1H NMR (400 MHz, CDCl_3): $\delta = 5.95$ (ddd, $J = 10.8, 9.1, 0.8$ Hz, 1H), 5.45 (dq, $J = 10.9, 2.4, 0.7$ Hz, 1H), 4.59 (ddd, $J = 9.1, 1.8, 0.8$ Hz, 1H), 3.73 (ddd, $J = 9.9, 8.0, 5.6$ Hz, 1H), 3.67–3.58 (m, 3H), 3.43 (dt, $J = 9.3, 4.7$ Hz, 1H), 2.16 (ddd, $J = 12.1, 7.0, 5.6$ Hz, 1H), 2.03 (ddt, $J = 11.1, 8.6, 6.7$ Hz, 1H), 1.96 (dd, $J = 2.4, 0.6$ Hz, 3H), 1.34–1.26 (m, 1H), 1.05 (d, $J = 6.5$ Hz, 3H), 0.89 (s, 9H), 0.882 (s, 9H), 0.875 (s, 9H), 0.08 (s, 9H), 0.042 (s, 6H), 0.036 ppm (s, 3H). ^{13}C NMR (100 MHz, CDCl_3): $\delta = 142.0, 109.9, 90.6, 84.8, 80.9, 79.8, 77.0, 72.0, 65.3, 38.3, 37.2, 26.2$ (3C), 26.12 (3C), 26.09 (3C), 18.6, 18.5, 18.4, 17.2, 4.5, -4.1, -4.3, -4.6, -4.6, -5.2 ppm (2C). IR (film): $\tilde{\nu}$ = 2954, 2928, 2887, 2856, 1472, 1462, 1388, 1361, 1252, 1131, 1065, 1005, 967, 834, 775, 679 cm^{-1} . MS (ESIpos) m/z (%): 605.4 (100 (M+Na)). HRMS (ESIpos): m/z calcd for $\text{C}_{31}\text{H}_{62}\text{O}_4\text{Si}_3\text{Na}$: 605.3848, found: 605.3843.

Alcohol 85. Pyridine (2.40 mL, 29.6 mmol) was slowly added to a Teflon® vial charged with

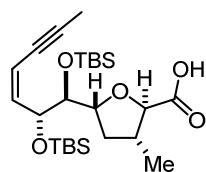


HF·pyridine (0.58 mL, 6.43 mmol) and the resulting mixture diluted with THF (5 mL). This solution was added dropwise to a solution of silyl ether (Z)-**83** (150 mg, 0.26 mmol) in THF (2 mL) in a second Teflon® vial. The resulting mixture was stirred at ambient temperature for 11 h. The mixture was diluted with EtOAc (5 mL) and the reaction was carefully quenched with aq. sat.

NaHCO_3 (10 mL). The layers were separated and the aqueous layer was extracted with EtOAc (4 × 15 mL). The combined organic extracts were dried over Na_2SO_4 , filtered and concentrated. The

residue was purified by flash chromatography (hexanes/EtOAc 50:1) to afford the title compound **85** as a colorless oil (104 mg, 85%). $[\alpha]_D^{20} = +1.8$ ($c = 1.0$, CHCl_3). $^1\text{H NMR}$ (500 MHz, CDCl_3): $\delta = 5.93$ (ddd, $J = 10.9, 9.1, 0.7$ Hz, 1H, H-8), 5.47 (dq, $J = 10.9, 2.4, 0.7$ Hz, 1H, H-9), 4.60 (ddd, $J = 9.2, 1.9, 0.8$ Hz, 1H, H-7), 3.78 (ddd, $J = 10.1, 7.9, 5.6$ Hz, 1H, H-5), 3.69 (ddd, $J = 8.6, 5.2, 3.3$ Hz, 1H, H-1), 3.64 (dd, $J = 7.9, 1.9$ Hz, 1H, H-6), 3.52–3.47 (m, 2H, H-1 and H-2), 2.22 (ddd, $J = 12.0, 7.2, 6.0$ Hz, 1H, H-4), 2.07 (dddq, $J = 11.3, 8.8, 6.8, 6.6$ Hz, 1H, H-3), 1.96 (d, $J = 2.4$ Hz, 3H, H-12), 1.92 (t, $J = 6.1$ Hz, 1H, 1-OH), 1.34 (ddd, $J = 12.0, 11.2, 10.2$ Hz, 1H, H-4), 1.03 (d, $J = 6.5$ Hz, 3H, H-23), 0.91 (s, 9H, 6-TBS), 0.89 (s, 9H, 7-TBS), 0.094 (s, 3H, 6-TBS), 0.089 (s, 3H, 7-TBS), 0.08 (s, 3H, 6-TBS), 0.04 ppm (s, 3H, 7-TBS). $^{13}\text{C NMR}$ (125 MHz, CDCl_3): $\delta = 141.8$ (C8), 110.2 (C9), 90.8 (C11), 84.8 (C2), 81.0 (C6), 80.1 (C5), 76.9 (C10), 72.3 (C7), 63.4 (C1), 38.3 (C4), 35.4 (C3), 26.2 (3C, 6-TBS), 26.1 (3C, 7-TBS), 18.6 (6-TBS), 18.4 (7-TBS), 16.5 (C23), 4.5 (C12), -4.1 (6-TBS), -4.2 (7-TBS), -4.3 (6-TBS), -4.6 ppm (7-TBS). IR (film): $\tilde{\nu} = 3457, 2954, 2928, 2885, 2856, 1472, 1462, 1388, 1361, 1250, 1150, 1107, 1079, 1060, 1005, 964, 834, 775, 679$ cm^{-1} . MS (EI) m/z (%): 469 (11), 468 (28), 411 (25), 260 (13), 259 (68), 209 (27), 189 (13), 185 (24), 171 (30), 159 (10), 147 (17), 144 (12), 133 (12), 127 (48), 115 (62), 109 (11), 97 (15), 75 (34), 73 (100), 71 (38). HRMS (ESIpos): m/z calcd for $\text{C}_{25}\text{H}_{48}\text{O}_4\text{Si}_2\text{Na}$: 491.2983, found: 491.2984.

Carboxylic acid 60. NMO·H₂O (242 mg, 2.07 mmol) and TPAP (7.27 mg, 0.02 mmol, 10 mol%) were



sequentially added to a solution of alcohol **85** (97 mg, 0.21 mmol) in MeCN (1 mL).

The resulting mixture was stirred at rt for 7 h. The reaction was quenched with aq. pH 5 phosphate buffer (2 mL), the layers were separated and the aqueous layer extracted with EtOAc (4 × 5 mL). The combined organic extracts were dried over

Na_2SO_4 , filtered and concentrated. The residue was purified by flash chromatography (hexanes/EtOAc 6:1 to 2:1) affording the title compound **60** as a colorless oil (82.5 mg, 83%). $[\alpha]_D^{20} = +18.4$ ($c = 1.0$, CHCl_3). $^1\text{H NMR}$ (400 MHz, CDCl_3): $\delta = 5.88$ (ddd, $J = 10.9, 9.0, 0.8$ Hz, 1H), 5.50 (dq, $J = 10.9, 2.4, 0.8$ Hz, 1H), 4.61 (ddd, $J = 9.0, 2.0, 0.8$ Hz, 1H), 4.01 (ddd, $J = 10.7, 7.0, 5.0$ Hz, 1H), 3.93 (d, $J = 9.3$ Hz, 1H), 3.70 (dd, $J = 7.0, 2.0$ Hz, 1H), 2.34 (dddq, $J = 10.9, 9.3, 6.6, 6.4$ Hz, 1H), 2.27 (ddd, $J = 11.8, 6.6, 5.0$ Hz, 1H), 1.97 (d, $J = 2.4$ Hz, 3H), 1.48 (ddd, $J = 11.8, 10.9, 10.7$ Hz, 1H), 1.28 (d, $J = 6.4$ Hz, 3H), 0.91 (s, 9H), 0.88 (s, 9H), 0.11 (s, 3H), 0.09 (s, 3H), 0.08 (s, 3H), 0.05 ppm (s, 3H). $^{13}\text{C NMR}$ (100 MHz, CDCl_3): $\delta = 173.1, 141.4, 110.7, 91.5, 82.6, 81.8, 79.9, 76.7, 72.7, 39.9, 38.1, 26.12$ (3C), 26.10 (3C), 18.5, 18.5, 17.3, 4.5, $-4.0, -4.2, -4.4, -4.7$ ppm. IR (film): $\tilde{\nu} = 2954, 2928, 2856, 1722, 1462, 1388, 1361, 1251, 1152, 1080, 1006, 966, 835, 777, 681$ cm^{-1} . MS (ESI^{neg}) m/z (%): 481.3 (100 (M⁻H)). HRMS (ESI^{neg}): m/z calcd for $\text{C}_{25}\text{H}_{45}\text{O}_5\text{Si}_2$: 481.2811, found: 481.2814.

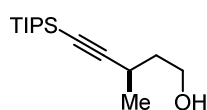
4.3.4 Synthesis of the Sidechain 18

Methyl-(E)-3-methyl-5-(triisopropylsilyl)pent-2-en-4-ynoate (88). Methyl-2-butynoate (980 mg, 10.0 mmol) and TIPS-acetylene (2.80 mL, 12.5 mmol) were added to a solution of Pd(OAc)₂ (67.3 mg, 0.30 mmol, 3 mol%) and TDMPP (133 mg, 0.30 mmol, 3 mol%) in toluene. The resulting mixture was stirred at rt for 20 h before it was diluted with CH₂Cl₂/Et₂O (1:1, 10 mL) and filtered through a plug of Florisil®. The filter cake was washed with CH₂Cl₂/Et₂O (1:1, 30 mL) and Et₂O (50 mL). The filtrates were concentrated and the residue purified by flash chromatography (pentane/Et₂O 20:1) to afford the title compound **88** as a pale yellow oil (2.56 g, 91%). ¹H NMR (400 MHz, CDCl₃): δ = 6.10 (q, *J* = 1.5 Hz, 1H), 3.71 (s, 3H), 2.30 (d, *J* = 1.5 Hz, 3H), 1.10–1.07 ppm (m, 21H). ¹³C NMR (100 MHz, CDCl₃): δ = 166.7, 138.3, 124.3, 108.7, 96.5, 51.4, 20.1, 18.7 (6C), 11.3 ppm (3C). IR (film): $\tilde{\nu}$ = 2945, 2866, 1721, 1615, 1463, 1341, 1240, 1150, 999, 882, 678, 624 cm⁻¹. MS (EI) *m/z* (%): 280 (10), 238 (22), 237 (100), 209 (21), 195 (14), 181 (14), 167 (21), 89 (12). HRMS (ESIpos): *m/z* calcd for C₁₆H₂₈O₂SiNa: 303.1751, found: 303.1752. The analytical and spectroscopic data are in agreement with those reported in the literature.^[157]

Methyl-(R)-3-methyl-5-(triisopropylsilyl)pent-4-ynoate (89). A solution of Cu(OAc)₂ (14.0 mg, 70.0 μmol, 5 mol%) and (*S,S*_{FC})-WalPhos (65.0 mg, 70.0 μmol, 5 mol%) in toluene (1 mL) was stirred at rt for 30 min. Methyl-diethoxysilane (375 mg, 2.80 mmol) was added and the resulting mixture stirred at rt for 30 min before the mixture was cooled to 0 °C. Next, a solution of enyne **88** (392 mg, 1.40 mmol) in toluene (0.8 mL) was added followed by *t*-BuOH (0.27 mL, 2.80 mmol). The resulting mixture was stirred at 4 °C for 4 d. The mixture was filtered through a pad of silica, the filter cake was washed with Et₂O (20 mL) and the filtrates were concentrated. The residue was purified by flash chromatography (pentane/Et₂O 50:1) to afford the title compound **89** as a pale yellow oil (364 mg, 79%, 98% *ee*). $[\alpha]_{\text{D}}^{20} = -25.6$ (*c* = 1.54, CHCl₃). ¹H NMR (400 MHz, CDCl₃): δ = 3.68 (s, 3H), 2.99 (tq, *J* = 7.4, 6.9 Hz, 1H), 2.55 (dd, *J* = 15.2, 7.4 Hz, 1H), 2.41 (dd, *J* = 15.2, 7.4 Hz, 1H), 1.23 (d, *J* = 6.9 Hz, 3H), 1.07–1.00 ppm (m, 21H). ¹³C NMR (100 MHz, CDCl₃): δ = 172.1, 111.6, 80.7, 51.8, 41.9, 24.1, 21.1, 18.7 (6C), 11.3 ppm (3C). IR (film): $\tilde{\nu}$ = 2943, 2865, 2166, 1743, 1463, 1437, 1356, 1249, 1169, 1065, 997, 882, 675, 660, 627 cm⁻¹. MS (EI) *m/z* (%): 240 (11), 239 (63), 209 (22), 198 (15), 197 (100), 169 (64), 167 (13), 155 (15), 145 (26), 141 (58), 127 (17), 117 (17), 99 (13), 95 (11), 91 (15), 89 (30), 75 (29), 59 (23). HRMS (ESIpos): *m/z* calcd for C₁₆H₃₀O₂SiNa: 305.1907, found: 305.1909.

The enantiomeric excess was determined by chiral HPLC of the benzoate derivative, which was prepared in analytical quantities by the following two-step protocol:

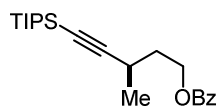
(R)-3-Methyl-5-(triisopropylsilyl)pent-4-yn-1-ol (S21). LiAlH₄ (7.86 mg, 0.21 mmol) was added to a



solution of methyl ester **89** (27.2 mg, 0.10 mmol) in THF (10 mL) at 0 °C. The suspension was stirred at 0 °C for 20 min, then at rt for 1 h. The mixture was diluted with *t*-butyl methyl ether (10 mL) and the reaction was quenched with aq.

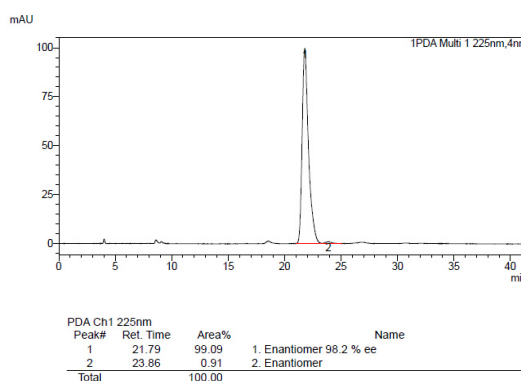
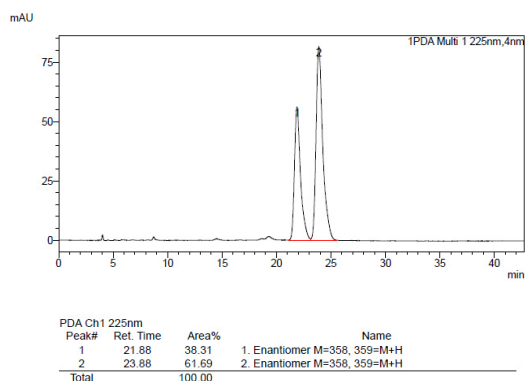
sat. Rochelle salt solution (10 mL). The biphasic mixture was stirred for 16 h, the layers were separated and the aqueous layer was extracted with *t*-butyl methyl ether (3 × 10 mL). The combined extracts were washed with brine (15 mL), dried over Na₂SO₄, filtered and concentrated. The residue was purified by flash chromatography (hexanes/*t*-butyl methyl ether 20:1 to 10:1) to afford alcohol **S21** as a colorless oil (20.2 mg, 82%). $[\alpha]_D^{20} = -57.5$ (*c* = 1.09, CHCl₃). ¹H NMR (400 MHz, CDCl₃): δ = 3.86–3.77 (m, 2H), 2.66 (dq, *J* = 9.4, 6.9, 5.1 Hz, 1H), 1.81 (brs, 1H), 1.79–1.61 (m, 2H), 1.22 (d, *J* = 7.0 Hz, 3H), 1.08–1.02 ppm (m, 21H). ¹³C NMR (100 MHz, CDCl₃): δ = 113.2, 81.1, 61.6, 39.7, 24.2, 21.7, 18.8 (6C), 11.3 ppm (3C). IR (film): $\tilde{\nu} = 3318, 2941, 2891, 2865, 2165, 1463, 1382, 1326, 1243, 1134, 1078, 1052, 996, 883, 675, 660, 620$ cm⁻¹. MS (EI) *m/z* (%): 211 (55), 169 (58), 167 (13), 157 (19), 155 (37), 141 (33), 139 (28), 131 (28), 129 (16), 127 (44), 125 (21), 123 (12), 115 (55), 114 (13), 113 (37), 111 (23), 109 (16), 103 (53), 101 (21), 99 (18), 97 (20), 95 (16), 87 (56), 85 (26), 83 (18), 81 (11), 79 (14), 77 (14), 75 (85), 73 (82), 71 (14), 69 (18), 67 (13), 61 (43), 59 (100), 55 (16), 53 (14), 45 (40), 43 (29), 42 (27), 41 (58), 40 (12), 39 (33), 29 (89), 27 (11). HRMS (ESIpos): *m/z* calcd for C₁₅H₃₀OSiNa: 277.1958, found: 277.1956.

(R)-3-Methyl-5-(triisopropylsilyl)pent-4-yn-1-yl benzoate (90). Pyridine (19.5 μL, 0.24 mmol) and

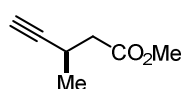


benzoyl chloride (27.9 μL, 0.24 mmol) were sequentially added to a solution of alcohol **S21** (20.2 mg, 0.08 mmol) in CH₂Cl₂ (0.8 mL) at 0 °C. The resulting mixture was stirred at rt for 1.5 h. The reaction was quenched with H₂O (1.5 mL) and the

aqueous layer was extracted with CH₂Cl₂ (3 × 5 mL). The combined extracts were washed with HCl (2 M, 10 mL), aq. sat. NaHCO₃ (10 mL) and aq. half-sat. brine (10 mL), dried over Na₂SO₄, filtered and concentrated. The residue was purified by flash chromatography (hexanes/*t*-butyl methyl ether 25:1) to afford benzoate **90** as a colorless oil (22.6 mg, 80%). $[\alpha]_D^{20} = -29.3$ (*c* = 0.97, CHCl₃). ¹H NMR (400 MHz, CDCl₃): δ = 8.07–8.00 (m, 2H), 7.58–7.53 (m, 1H), 7.46–7.41 (m, 2H), 4.57–4.42 (m, 2H), 2.74 (dddd, *J* = 12.5, 9.1, 6.9, 5.5 Hz, 1H), 1.99–1.81 (m, 2H), 1.27 (d, *J* = 6.9 Hz, 3H), 1.10–0.99 ppm (m, 21H). ¹³C NMR (100 MHz, CDCl₃): δ = 166.6, 133.0, 130.5, 129.7 (2C), 128.5 (2C), 112.2, 81.0, 63.3, 36.0, 24.2, 21.5, 18.8 (6C), 11.4 ppm (3C). IR (film): $\tilde{\nu} = 2942, 2865, 2164, 1723, 1452, 1384, 1272, 1115, 1070, 921, 771, 676, 661, 619$ cm⁻¹. MS (EI) *m/z* (%): 316 (10), 315 (41), 236 (19), 235 (100), 105 (31), 77 (11). HRMS (ESIpos): *m/z* calcd for C₂₂H₃₄O₂SiNa: 381.2220, found: 381.2220. The *ee* was determined by HPLC (150 mm, Chiralcel OJ-3R, Ø 4.6 mm, MeOH/H₂O 85:15, flow rate = 0.5 mL/min, 132 bar, 298 K, UV, 225 nm): major enantiomer *t_R* = 21.8 min; minor enantiomer *t_R* = 23.9 min.



Methyl-(R)-3-methylpent-4-ynoate (18). TBAF (1 M in Et₂O, 1.06 mL, 1.06 mmol) was added to a

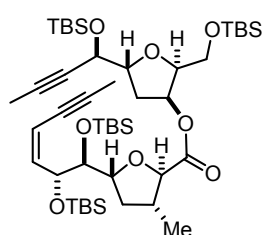


solution of TIPS-alkyne **89** (250 mg, 0.89 mmol) in Et₂O (9 mL). The resulting mixture was stirred at ambient temperature for 17 h. The reaction was quenched with aq.

sat. NH₄Cl (15 mL) and the aqueous layer extracted with Et₂O (3 × 20 mL). The combined extracts were dried over Na₂SO₄, filtered and concentrated. The residue was purified by flash chromatography (pentane/Et₂O 25:1) to afford the title compound as a colorless liquid (90.9 mg, 81%). ¹H NMR (400 MHz, CDCl₃): δ = 3.70 (s, 3H), 2.96 (hd, *J* = 7.1, 2.4 Hz, 1H), 2.57 (dd, *J* = 15.6, 7.3 Hz, 1H), 2.42 (dd, *J* = 15.6, 7.4 Hz, 1H), 2.07 (d, *J* = 2.4 Hz, 1H), 1.24 ppm (d, *J* = 6.9 Hz, 3H). ¹³C NMR (100 MHz, CDCl₃): δ = 171.9, 87.2, 68.9, 51.9, 41.3, 22.7, 20.7 ppm.

4.3.5 Fragment Assembly and Attempted RCAM

Representative Procedure for Mitsunobu Esterification of Northern Alcohol with Southern Acid Fragments. Preparation of Diyne 91. PPh₃ (18 mg, 70 μmol) was added to a solution of alcohol **48**

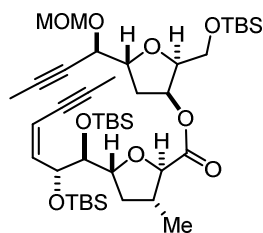


(5.0 mg, 12 μmol) and carboxylic acid **60** (7.0 mg, 14 μmol) in toluene (0.5 mL) at 0 °C. The resulting mixture was stirred for 5 min before DIAD (13.8 μL, 70.0 μmol) was added dropwise and the stirring continued at rt for 3 h. The mixture was diluted with hexanes (2 mL), washed with water (3 mL) and brine (3 mL). The combined extracts were dried over Na₂SO₄, filtered and concentrated.

The residue was purified by flash chromatography (hexanes/*t*-butyl methyl ether 19:1 to 10:1) to yield diyne **91** as a colorless oil (8.3 mg, 79%). [α]_D²⁰ = +12.4 (c = 0.5, CHCl₃). ¹H NMR (400 MHz, CDCl₃): δ = 5.95 (dd, *J* = 10.5, 9.6 Hz, 1H), 5.54–5.39 (m, 2H), 4.61 (dd, *J* = 9.3, 1.4 Hz, 1H), 4.40 (dq, *J* = 4.3, 2.0 Hz, 1H), 4.21–4.14 (m, 1H), 4.12 (dd, *J* = 5.9, 3.5 Hz, 1H), 4.01–3.95 (m, 1H), 3.94 (d, *J* = 8.8 Hz, 1H), 3.78–3.72 (m, 1H), 3.74 (dd, *J* = 6.4, 3.0 Hz, 1H), 3.71 (dd, *J* = 7.6, 1.9 Hz, 1H), 2.36–2.24 (m, 2H), 2.20 (ddd, *J* = 11.9, 6.9, 5.2 Hz, 1H), 2.05 (ddd, *J* = 14.2, 6.7, 1.3 Hz, 1H), 1.96 (d, *J* = 2.3 Hz, 3H), 1.83 (d, *J* = 2.1 Hz, 3H), 1.38 (q, *J* = 11.2 Hz, 1H), 1.19 (d, *J* = 6.4 Hz, 3H), 0.889 (s, 9H), 0.885 (s, 9H), 0.88 (s, 9H), 0.86 (s, 9H), 0.12 (s, 3H), 0.09 (s, 6H), 0.08 (s, 3H), 0.07 (s, 3H), 0.04 (s, 3H),

0.03 (s, 3H), 0.02 ppm (s, 3H). ^{13}C NMR (100 MHz, CDCl_3): δ = 172.6, 141.9, 110.2, 90.9, 82.6, 82.3, 81.9, 81.7, 80.8, 80.2, 78.0, 77.0, 74.5, 72.2, 65.9, 61.0, 40.3, 37.5, 35.0, 26.2 (3C), 26.1 (3C), 26.0 (6C), 18.6, 18.42, 18.36, 18.3, 17.6, 4.5, 3.8, -4.27, -4.32, -4.48, -4.49, -4.6, -4.9, -5.2, -5.3 ppm. IR (film): $\tilde{\nu}$ = 2955, 2929, 2885, 2857, 1761, 1734, 1472, 1463, 1361, 1253, 1091, 1006, 837, 777 cm^{-1} . MS (ESIpos) m/z (%): 901.5 (100 (M+Na)). HRMS (ESIpos): m/z calcd for $\text{C}_{46}\text{H}_{86}\text{O}_8\text{Si}_4\text{Na}$: 901.5292, found: 901.5290.

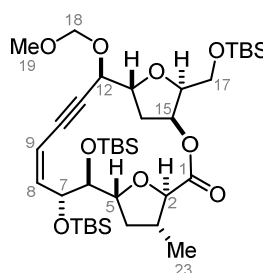
Diyne 92. This compound was prepared according to the representative procedure for Mitsunobu



esterification (*vide supra*) from alcohol **49** and carboxylic acid **60**. Purification by flash chromatography (hexanes/*t*-butyl methyl ether 30:1 to 20:1) provided diyne **92** as a colorless oil (34.9 mg, 93%). $[\alpha]_{\text{D}}^{20}$ = -9.7 (c = 1.0, CHCl_3). ^1H NMR (400 MHz, CDCl_3): δ = 5.95 (dd, J = 10.7, 9.5 Hz, 1H), 5.50–5.44 (m, 2H), 4.94 (d, J = 6.7 Hz, 1H), 4.62 (d, J = 6.7 Hz, 1H), 4.65–4.59

(m, 1H), 4.35 (ddq, J = 6.9, 4.9, 2.4 Hz, 1H), 4.32–4.26 (m, 1H), 4.15 (ddd, J = 7.5, 5.7, 3.5 Hz, 1H), 4.00–3.94 (m, 1H), 3.94 (d, J = 8.8 Hz, 1H), 3.80–3.73 (m, 2H), 3.71 (dd, J = 7.6, 1.8 Hz, 1H), 3.38 (s, 3H), 2.39–2.30 (m, 1H), 2.29–2.19 (m, 2H), 2.14 (ddd, J = 14.1, 6.3, 1.0 Hz, 1H), 1.96 (d, J = 2.3 Hz, 3H), 1.85 (d, J = 2.0 Hz, 3H), 1.38 (q, J = 11.1 Hz, 1H), 1.19 (d, J = 6.5 Hz, 3H), 0.89 (s, 9H), 0.88 (s, 9H), 0.86 (s, 9H), 0.089 (s, 3H), 0.085 (s, 3H), 0.08 (s, 3H), 0.04 (s, 3H), 0.03 (s, 3H), 0.02 ppm (s, 3H). ^{13}C NMR (100 MHz, CDCl_3): δ = 172.5, 141.9, 110.2, 94.1, 90.9, 83.5, 82.6, 82.3, 81.9, 80.2, 79.6, 77.0, 74.7, 74.2, 72.2, 68.4, 60.9, 55.8, 40.3, 37.5, 35.7, 26.2 (3C), 26.1 (3C), 25.9 (3C), 18.6, 18.4, 18.3, 17.7, 4.5, 3.8, -4.3, -4.4, -4.5, -4.6, -5.2, -5.3 ppm. IR (film): $\tilde{\nu}$ = 2954, 2927, 2855, 1733, 1463, 1379, 1255, 1151, 1098, 1033, 965, 837, 778 cm^{-1} . MS (ESIpos) m/z (%): 826.5 (100 (M+NH₄)). HRMS (ESIpos): m/z calcd for $\text{C}_{42}\text{H}_{76}\text{O}_9\text{Si}_3\text{Na}$: 831.4689, found: 831.4690.

Enyne 93b. 5 Å MS (200 mg) was added to a solution of diyne **92** (10.0 mg, 12.4 μmol) in toluene



(5.2 mL) at room temperature and the suspension was stirred for 30 min. The mixture was then heated to 110 °C before a freshly prepared solution of trisilanol **L2** (2.4 mg, 3.1 μmol , 25 mol%) and complex **C12** (1.9 mg, 2.8 μmol , 23 mol%) in toluene (1 mL) was added, which had been stirred for 20 min prior to use. Stirring was continued at 110 °C for 30 min. The mixture was cooled to ambient temperature, the molecular sieves were filtered off

through a pad of Celite®, which was carefully rinsed with EtOAc, and the combined filtrates were concentrated. The residue was purified by flash chromatography (hexanes/EtOAc 30:1) to afford the title compound as a colorless oil (1.4 mg, 15%). $[\alpha]_{\text{D}}^{20}$ = +26.7 (c = 0.03, CHCl_3). ^1H NMR (600 MHz, CDCl_3): *see Table 4.2*. ^{13}C NMR (150 MHz, CDCl_3): *see Table 4.2*. IR (film): $\tilde{\nu}$ = 2956, 2929, 2897, 2857,

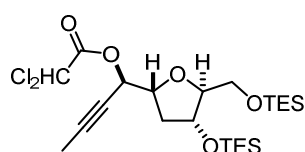
1747, 1471, 1463, 1255, 1154, 1097, 1074, 1034, 837, 778 cm^{-1} . MS (ESIpos) m/z (%): 777.4 (100 (M+Na)). HRMS (ESIpos): m/z calcd for $\text{C}_{38}\text{H}_{70}\text{O}_9\text{Si}_3\text{Na}$: 777.4220, found: 777.4222.

Table 4.2. ^1H and ^{13}C NMR data of enyne **93b** (0.5 mg in 0.25 mL CDCl_3); chagosensine numbering.*

atom n°	^1H NMR (600 MHz, CDCl_3)					^{13}C NMR (150 MHz, CDCl_3)	
	δ [ppm]	m	J [Hz]	COSY	NOESY	δ [ppm]	HMBC
1	-	-	-	-	-	170.5	2, 3, (15)
2	3.97	d	8.4	3	3, 4b, 15, (16), 23	84.0	3, 4a, 23
3	2.62	m	-	2, 4(a)b, 23	2, 4a, (5), 23	36.94	2, 4, 23
4a	2.13	ddd	12.0, 7.8, 6.0	(3), 4b, 5	3, 4b, 5	36.2	(2), 3, 5, 23
4b	1.66	ddd	12.0, 10.6, 9.8	3, 4a, 5	2, 4a, 6, 23		
5	4.29	ddd	9.8, 6.5, 2.1	4ab, (6)	3, 4a, 7, 13	80.17	(2), 4, 7
6	3.56	dd	4.8, 2.1	(5), 7	4b, 5, 7, 8	78.6	4b, 5, (8)
7	4.82	dd	9.7, 4.8	6,8	5, 6, (9), 15	73.2	6, 9
8	5.95	dd	10.8, 9.6	7,9	6, 6-TBS, 7-TBS	145.3	6, (7), 9
9	5.58	dd	10.8, 2.6	8, (12)	(7), 6-TBS, 7-TBS	110.2	7,8
10	-	-	-	-	-	84.7	8, 12
11	-	-	-	-	-	91.0	9, 12, 13
12	4.47	dd	7.3, 2.6	13, (9)	14b, 18ab, 19	69.3	13, 14b, 18
13	4.39	td	7.6, 5.9	12, 14ab	5, 14a	80.20	12, 14b, 15
14a	2.36	ddd	13.1, 6.0, 4.2	13, 14b, 15	13, 14b	36.85	12, (16)
14b	2.17	ddd	13.0, 8.0, 6.0	13, 14a, 15	12, 14a, 15		
15	5.69	dt	5.6, 4.1	14(a)b, 16	2, 7, 14b, (16)	75.9	14a, 16, 17
16	4.26	dt	6.6, 5.2	15,17ab	(2), (14b), 15, 17	81.4	14(a)b, 17
17a	3.82	dd	10.3, 6.9	16	13, 15, 17-TBS	61.5	(16)
17b	3.78	dd	10.3, 5.2	16			
18a	4.92	d	6.7	18b	12, 19, 18b	94.3	12, 19
18b	4.64	d	6.7	18a	12, 19, 18a		
19	3.39	s	-	-	12, (13), 18ab	55.8	18
23	1.10	d	6.6	3	2, 4(a)b, 6-TBS	16.5	2, 4b

* The signals of the TBS groups are not listed and appear as follows: ^1H NMR (600 MHz, CDCl_3): δ = 0.91 (s, 9H), 0.87 (s, 9H), 0.86 (s, 9H), 0.10 (s, 3H), 0.080 (s, 3H), 0.078 (s, 3H), 0.06 (s, 3H), 0.04 (s, 3H), 0.03 ppm (s, 3H). ^{13}C NMR (150 MHz, CDCl_3): δ = 26.4 (3C), 26.0 (6C), 18.4, 18.3, 18.2, -2.9, -3.9, -4.1, -4.7, -5.2, -5.3 ppm.

Dichloroacetate S22. A solution of propargylic alcohol **59** (200 mg, 0.48 mmol) in CH_2Cl_2 (10 mL) was

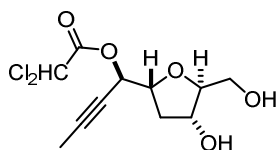


cooled to 0 °C before pyridine (1.00 mL, 12.4 mmol) and dichloroacetic anhydride (0.13 mL, 0.89 mmol) were added. The resulting mixture was stirred for 20 min, concentrated and the residue purified by flash

chromatography (hexanes/*t*-butyl methyl ether 100:1) to provide the desired dichloroacetate **S22** as a colorless oil (200 mg, 79%). $[\alpha]_D^{20}$ = -52.1 (c = 1.0, CHCl_3). ^1H NMR (400 MHz, CDCl_3): δ = 5.99 (s, 1H), 5.73 (dq, J = 8.7, 2.2 Hz, 1H), 4.34 (dt, J = 5.5, 2.6 Hz, 1H), 4.25 (ddd, J = 8.7, 8.1, 3.3 Hz, 1H), 3.90

(ddd, $J = 6.1, 3.9, 2.4$ Hz, 1H), 3.60 (dd, $J = 10.8, 3.9$ Hz, 1H), 3.46 (dd, $J = 10.8, 5.7$ Hz, 1H), 2.24 (ddd, $J = 13.6, 8.0, 5.7$ Hz, 1H), 2.02 (dt, $J = 13.4, 3.0$, 1H), 1.86 (d, $J = 2.2$ Hz, 3H), 0.97 (t, $J = 7.9$ Hz, 9H), 0.94 (t, $J = 7.9$ Hz, 9H), 0.61 (q, $J = 7.9$ Hz, 6H), 0.58 ppm (q, $J = 7.9$ Hz, 6H). ^{13}C NMR (100 MHz, CDCl_3): $\delta = 163.8, 87.9, 84.6, 80.3, 73.4, 73.0, 70.7, 64.5, 63.2, 37.6, 6.88$ (3C), 6.86 (3C), 4.8 (3C), 4.5 (3C), 3.9 ppm. IR (film): $\tilde{\nu} = 2954, 2912, 2877, 1772, 1750, 1459, 1415, 1293, 1239, 1155, 1114, 1092, 1045, 1005, 988, 812, 741, 729$ cm^{-1} . MS (ESIpos) m/z (%): 547.2 (100 (M+Na)). HRMS (ESIpos): m/z calcd for $\text{C}_{23}\text{H}_{42}\text{O}_5\text{Cl}_2\text{Si}_2\text{Na}$: 547.1840, found: 547.1841.

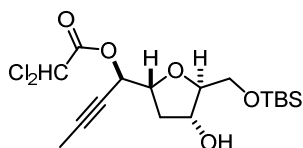
Diol S23. A solution of dichloroacetate **S22** (200 mg, 0.38 mmol) in THF (6 mL) was cooled to -30 $^\circ\text{C}$.



Dichloroacetic acid (104 μL , 1.26 mmol) was added, followed by a solution of TBAF (1 M in THF, 0.84 mL, 0.84 mmol) and the reaction mixture was stirred at -30 $^\circ\text{C}$ for 75 min. The reaction was quenched with sat. aq. NH_4Cl

(5 mL) and the aqueous layer was extracted with EtOAc (3×10 mL). The combined extracts were dried over Na_2SO_4 , filtered and concentrated. The residue was purified by flash chromatography (hexanes/EtOAc 1:1 to 0:1 to EtOAc/MeOH 95:5) to yield the title compound as a colorless oil (110 mg, 97%). $[\alpha]_{\text{D}}^{20} = -92.8$ ($c = 1.0$, CHCl_3). ^1H NMR (400 MHz, CDCl_3): $\delta = 6.02$ (s, 1H), 5.64 (dq, $J = 8.7, 2.2$ Hz, 1H), 4.35 (dt, $J = 6.8, 4.4$ Hz, 1H), 4.29 (td, $J = 7.8, 4.9$ Hz, 1H), 3.94 (q, $J = 4.3$ Hz, 1H), 3.69 (dd, $J = 11.8, 4.2$ Hz, 1H), 3.62 (dd, $J = 11.8, 4.5$ Hz, 1H), 2.52 (brs, 2H), 2.41 (ddd, $J = 13.7, 7.9, 6.8$ Hz, 1H), 2.05 (dt, $J = 13.6, 4.7$, 1H), 1.87 ppm (d, $J = 2.2$ Hz, 3H). ^{13}C NMR (100 MHz, CDCl_3): $\delta = 163.9, 86.1, 85.4, 79.5, 72.8, 72.7, 69.9, 64.4, 62.6, 37.3, 3.9$ ppm. IR (film): $\tilde{\nu} = 3391, 2924, 1764, 1439, 1337, 1296, 1159, 1093, 1058, 977, 919, 812, 668$ cm^{-1} . MS (ESIpos) m/z (%): 319.0 (100 (M+Na)). HRMS (ESIpos): m/z calcd for $\text{C}_{11}\text{H}_{14}\text{O}_5\text{Cl}_2\text{Na}$: 319.0111, found: 319.0109.

Alcohol 104. Imidazole (30.2 mg, 0.44 mmol) was added to a solution of diol **S23** (110 mg,

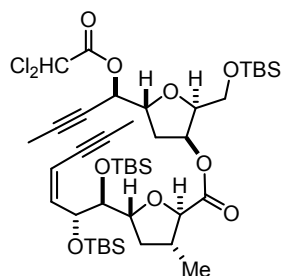


0.37 mmol) in DMF (5.5 mL) and the solution was cooled to 0 $^\circ\text{C}$ before TBSCl (58.6 mg, 0.39 mmol) was added. The resulting mixture was stirred at rt for 6 h, the reaction was quenched with half-sat. aq. NH_4Cl (5 mL)

and the aqueous layer was extracted with EtOAc (3×8 mL). The combined extracts were washed with brine (20 mL), dried over Na_2SO_4 , filtered and concentrated. The residue was purified by flash chromatography (hexanes/EtOAc 6:1 to 0:1) to afford the desired alcohol **104** as a colorless oil (90.1 mg, 59%). $[\alpha]_{\text{D}}^{20} = -41.6$ ($c = 1.0$, CHCl_3). ^1H NMR (400 MHz, CDCl_3): $\delta = 5.99$ (s, 1H), 5.61 (dq, $J = 7.6, 2.2$ Hz, 1H), 4.35 (dq, $J = 6.6, 4.1$ Hz, 1H), 4.28 (td, $J = 7.8, 4.9$ Hz, 1H), 3.90 (dt, $J = 6.0, 3.7$ Hz, 1H), 3.74 (dd, $J = 10.5, 3.8$ Hz, 1H), 3.54 (dd, $J = 10.5, 6.1$ Hz, 1H), 2.42 (ddd, $J = 13.5, 8.0, 6.7$ Hz, 1H), 2.13 (d, $J = 4.1$ Hz, 1H), 2.01 (dt, $J = 13.5, 4.6$ Hz, 1H), 1.87 (d, $J = 2.2$ Hz, 3H), 0.88 (s, 9H), 0.05 ppm (s, 6H). ^{13}C NMR (100 MHz, CDCl_3): $\delta = 163.8, 86.1, 85.1, 79.6, 73.1, 74.1, 70.1, 64.4, 64.2, 36.9, 26.0$ (3C), 18.4, 3.9, $-5.34, -5.31$ ppm. IR (film): $\tilde{\nu} = 3444, 2928, 2857, 1769, 1471, 1294, 1256, 1156, 1088,$

983, 929, 835, 778, 668 cm^{-1} . MS (ESIpos) m/z (%): 433.1 (100 (M+Na)). HRMS (ESIpos): m/z calcd for $\text{C}_{17}\text{H}_{28}\text{O}_5\text{Cl}_2\text{SiNa}$: 433.0975, found: 433.0979.

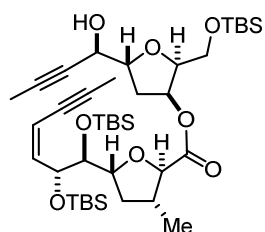
Diyne 105. This compound was prepared according to the representative procedure for Mitsunobu esterification (*vide supra*) from alcohol **104** and carboxylic acid **60**.



Purification by flash chromatography (hexanes/*t*-butyl methyl ether 19:1 to 10:1) provided diene **92** as a colorless oil (37.6 mg, 65%). $[\alpha]_{\text{D}}^{20} = +8.1$ ($c = 0.5$, CHCl_3). $^1\text{H NMR}$ (400 MHz, CDCl_3): $\delta = 5.96$ (s, 1H), 5.93 (dd, $J = 10.0, 0.8$ Hz, 1H), 5.52–5.44 (m, 2H), 5.40 (dq, $J = 6.6, 2.1$ Hz, 1H), 4.61 (dd, $J = 9.3, 1.8$ Hz, 1H), 4.37 (q, $J = 7.6$ Hz, 1H), 4.13 (td, $J = 6.5, 3.5$ Hz, 1H),

4.00–3.90 (m, 1H), 3.94 (d, $J = 8.8$ Hz, 1H), 3.76–3.72 (m, 1H), 3.74 (d, $J = 6.4$ Hz, 1H), 3.70 (dd, $J = 7.6, 1.9$ Hz, 1H), 2.33 (ddt, $J = 10.8, 8.8, 6.6$ Hz, 1H), 2.25–2.17 (m, 3H), 1.96 (d, $J = 2.3$ Hz, 3H), 1.86 (d, $J = 2.1$ Hz, 3H), 1.42–1.32 (m, 1H), 1.19 (d, $J = 6.5$ Hz, 3H), 0.89 (s, 9H), 0.88 (s, 9H), 0.86 (s, 9H), 0.09 (s, 3H), 0.08 (s, 6H), 0.04 (s, 3H), 0.03 (s, 3H), 0.02 ppm (s, 3H). $^{13}\text{C NMR}$ (100 MHz, CDCl_3): $\delta = 172.5, 163.6, 141.9, 110.3, 90.9, 85.3, 82.6, 82.4, 82.1, 80.3, 78.2, 73.9, 72.30, 72.25, 69.7, 64.2, 60.8, 55.8, 40.3, 37.6, 35.8, 26.2$ (3C), 26.1 (3C), 25.9 (3C), 18.6, 18.4, 18.3, 17.7, 4.5, 3.9, $-4.3, -4.36, -4.40, -4.6, -5.2, -5.3$ ppm. IR (film): $\tilde{\nu} = 2955, 2928, 2856, 1737, 1471, 1389, 1361, 1252, 1153, 1082, 1006, 967, 834, 814, 776, 681$ cm^{-1} . MS (ESIpos) m/z (%): 897.4 (100 (M+Na)). HRMS (ESIpos): m/z calcd for $\text{C}_{42}\text{H}_{72}\text{O}_9\text{Cl}_2\text{Si}_3\text{Na}$: 897.3753, found: 897.3761.

Diyne 98. A solution of LiOH (0.5 M in H_2O , 5.7 μmol , 11 μL) was added to a solution of diene **105**

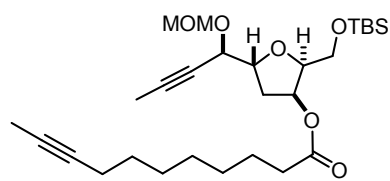


(5.0 mg, 5.7 μmol) in 1,4-dioxane (50 μL). The resulting mixture was stirred at 4–10 $^{\circ}\text{C}$ for 1 h, before it was diluted with EtOAc (2 mL). The reaction was quenched with NH_4Cl (1 mL), the layers were separated and the aqueous layer was extracted with EtOAc (3 \times 2 mL). The combined extracts were washed with brine (5 mL), dried over Na_2SO_4 , filtered and concentrated. The

residue was purified by flash chromatography (hexanes/*t*-butyl methyl ether 10:1 to 2:1) to afford diene **98** as a colorless oil (3.8 mg, 87%). $[\alpha]_{\text{D}}^{20} = +23.4$ ($c = 1.0$, CHCl_3). $^1\text{H NMR}$ (400 MHz, CDCl_3): $\delta = 5.95$ (dd, $J = 10.8, 9.5$ Hz, 1H), 5.50–5.43 (m, 2H), 4.61 (ddd, $J = 9.0, 2.0, 0.8$ Hz, 1H), 4.25–4.18 (m, 2H), 4.11 (ddd, $J = 7.1, 5.9, 3.5$ Hz, 1H), 4.00–3.92 (m, 1H), 3.94 (d, $J = 8.8$ Hz, 1H), 3.79–3.74 (m, 2H), 3.70 (dd, $J = 7.6, 1.9$ Hz, 1H), 2.37–2.30 (m, 1H), 2.28 (d, $J = 4.4$ Hz, 1H), 2.21 (ddd, $J = 11.8, 6.8, 5.1$ Hz, 1H), 2.16–2.10 (m, 2H), 1.97 (d, $J = 2.4$ Hz, 3H), 1.84 (d, $J = 1.8$ Hz, 3H), 1.38 (q, $J = 11.1$ Hz, 1H), 1.20 (d, $J = 6.5$ Hz, 3H), 0.90 (s, 9H), 0.88 (s, 9H), 0.86 (s, 9H), 0.092 (s, 3H), 0.087 (s, 3H), 0.08 (s, 3H), 0.05 (s, 3H), 0.04 (s, 3H), 0.03 ppm (s, 3H). $^{13}\text{C NMR}$ (100 MHz, CDCl_3): $\delta = 172.5, 141.9, 110.3, 90.9, 82.7, 82.6, 82.4, 81.9, 81.2, 80.3, 77.4, 77.0, 74.4, 72.3, 65.5, 61.0, 40.3, 37.6, 35.6, 26.2$ (3C), 26.1 (3C), 26.0 (3C), 18.6, 18.4, 18.3, 17.7, 4.5, 3.8, $-4.3, -4.4, -4.5, -4.6, -5.2, -5.3$ ppm. IR (film):

$\tilde{\nu}$ = 3452, 2954, 2928, 2886, 2856, 1734, 1472, 1389, 1361, 1252, 1081, 1007, 965, 836, 777, 682 cm^{-1} . MS (ESIpos) m/z (%): 787.4 (100 (M+Na)). HRMS (ESIpos): m/z calcd for $\text{C}_{40}\text{H}_{72}\text{O}_8\text{Si}_3\text{Na}$: 787.4427, found: 787.4433.

Diyne 112. This compound was prepared according to the representative procedure for Mitsunobu

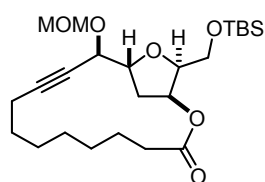


esterification (*vide supra*) from alcohol **49** and 9-undecynoic acid.

Purification by flash chromatography (hexanes/*t*-butyl methyl ether 30:1) provided diyne **112** as a colorless oil (24.0 mg, 54%).

$[\alpha]_{\text{D}}^{20} = -32.1$ ($c = 1.0$, CHCl_3). $^1\text{H NMR}$ (400 MHz, CDCl_3): $\delta = 5.42$ (ddd, $J = 5.0, 3.5, 1.6$ Hz, 1H), 4.94 (d, $J = 6.7$ Hz, 1H), 4.62 (d, $J = 6.7$ Hz, 1H), 4.35 (dq, $J = 6.0, 2.0$ Hz, 1H), 4.30 (dt, $J = 8.6, 6.2$ Hz, 1H), 4.12 (ddd, $J = 7.3, 5.6, 3.6$ Hz, 1H), 3.77 (dd, $J = 10.1, 5.6$ Hz, 1H), 3.74 (dd, $J = 10.1, 7.3$ Hz, 1H), 3.38 (s, 3H), 2.30 (t, $J = 7.6$ Hz, 2H), 2.24 (ddd, $J = 13.6, 8.5, 5.0$ Hz, 1H), 2.18–2.07 (m, 3H), 1.84 (d, $J = 2.0$ Hz, 3H), 1.77 (t, $J = 2.6$ Hz, 3H), 1.64–1.59 (m, 2H), 1.49–1.42 (m, 2H), 1.38–1.29 (m, 6H), 0.86 (s, 9H), 0.03 (s, 3H), 0.02 ppm (s, 3H). $^{13}\text{C NMR}$ (100 MHz, CDCl_3): $\delta = 173.1, 94.1, 83.4, 81.8, 79.6, 79.4, 75.6, 74.8, 73.8, 68.4, 60.9, 55.8, 35.6, 34.6, 29.2, 29.1, 29.0, 28.8, 25.9$ (3C), 25.0, 18.8, 18.3, 3.8, 3.6, $-5.3, -5.4$ ppm. IR (film): $\tilde{\nu} = 2929, 2857, 1737, 1464, 1251, 1150, 1093, 1030, 903, 837, 777, 650$ cm^{-1} . MS (ESIpos) m/z (%): 531.3 (100 (M+Na)). HRMS (ESIpos): m/z calcd for $\text{C}_{28}\text{H}_{48}\text{O}_6\text{SiNa}$: 531.3112, found: 531.3118.

Macrolactone 113. 5 Å MS (100 mg) was added to a solution of diyne **112** (5.0 mg, 10 μmol) in

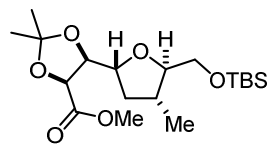


toluene (9 mL) at room temperature and the suspension was stirred for 30 min. The mixture was then heated to 110 $^{\circ}\text{C}$ before a freshly prepared solution of trisilanol **L2** (2.2 mg, 2.5 μmol , 25 mol%) and complex **C12** (1.3 mg, 2.0 μmol , 20 mol%) in toluene (1 mL) was added, which had been

stirred for 20 min prior to use. Stirring was continued at 110 $^{\circ}\text{C}$ for 3 h. The mixture was cooled to ambient temperature, the molecular sieves were filtered off through a pad of Celite[®], which was carefully rinsed with EtOAc, and the combined filtrates were concentrated. The residue was purified by flash chromatography (hexanes/*t*-butyl methyl ether 20:1) to afford the title compound as a colorless oil (3.9 mg, 87%). $[\alpha]_{\text{D}}^{20} = +11.3$ ($c = 0.75$, CHCl_3). $^1\text{H NMR}$ (400 MHz, CDCl_3): $\delta = 5.44$ (t, $J = 3.6$ Hz, 1H), 4.90 (d, $J = 6.6$ Hz, 1H), 4.73 (d, $J = 6.6$ Hz, 1H), 4.33–4.24 (m, 2H), 4.14 (dd, $J = 9.3, 2.7$ Hz, 1H), 3.81 (dd, $J = 9.8, 6.1$ Hz, 1H), 3.77 (dd, $J = 9.8, 8.3$ Hz, 1H), 3.41 (s, 3H), 2.51–2.43 (m, 1H), 2.33–2.23 (m, 1H), 2.23–2.06 (m, 3H), 1.84 (ddd, $J = 13.4, 11.6, 3.6$ Hz, 1H), 1.71–1.65 (m, 2H), 1.46–1.40 (m, 4H), 1.39–1.31 (m, 4H), 0.85 (s, 9H), 0.03 (s, 3H), 0.02 ppm (s, 3H). $^{13}\text{C NMR}$ (100 MHz, CDCl_3): $\delta = 173.4, 94.5, 88.5, 82.4, 81.6, 77.4, 73.3, 69.6, 60.8, 55.7, 39.2, 35.5, 28.4, 28.01, 27.99, 27.6, 26.2, 25.9$ (3C), 19.1, 18.4, $-5.2, -5.4$ ppm. IR (film): $\tilde{\nu} = 2929, 2857, 1738, 1462, 1361, 1247,$

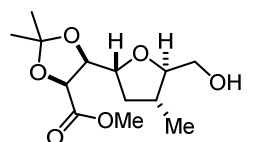
1127, 1081, 1030, 918, 838, 778 cm^{-1} . MS (ESIpos) m/z (%): 477.3 (100 (M+Na)). HRMS (ESIpos): m/z calcd for $\text{C}_{24}\text{H}_{42}\text{O}_6\text{SiNa}$: 477.2643, found: 477.2647.

Ester 114. *p*-TsOH·H₂O (15.3 mg, 0.08 mmol, 5 mol%) was added to a solution of diol **76** (561 mg, 1.61 mmol) in 2,2-dimethoxypropane (16 mL). The resulting mixture was stirred at rt for 5 h. The reaction was quenched with aq. sat. NaHCO₃ (10 mL), the layers were separated and the aqueous layer extracted with EtOAc (3 × 15 mL). The combined extracts were dried over Na₂SO₄, filtered and concentrated. The residue was purified by flash chromatography (hexanes/EtOAc 20:1) to afford the title compound **114** as a colorless oil (552 mg, 88%).



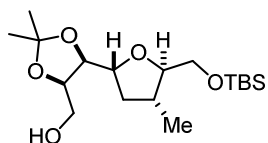
$[\alpha]_{\text{D}}^{20} = +10.3$ ($c = 1.0$, CHCl₃). ¹H NMR (400 MHz, CDCl₃): $\delta = 4.55$ (d, $J = 6.8$ Hz, 1H), 4.24 (t, $J = 6.8$ Hz, 1H), 3.97 (ddd, $J = 9.4, 6.7, 5.7$ Hz, 1H), 3.73 (s, 3H), 3.71 (dd, $J = 10.7, 3.9$ Hz, 1H), 3.63 (dd, $J = 10.5, 5.3$ Hz, 1H), 3.56 (ddd, $J = 7.3, 5.2, 3.6$ Hz, 1H), 2.26–2.17 (m, 2H), 1.62 (s, 3H), 1.46–1.36 (m, 1H), 1.40 (s, 3H), 1.09 (d, $J = 6.1$ Hz, 3H), 0.87 (s, 9H), 0.03 ppm (s, 6H). ¹³C NMR (100 MHz, CDCl₃): $\delta = 170.9, 111.5, 85.9, 81.3, 75.7, 64.7, 52.3, 38.1, 36.8, 26.9, 26.0$ (C3), 25.8, 18.4, 17.8, –5.2, –5.3 ppm. IR (film): $\tilde{\nu} = 2954, 2930, 2858, 1765, 1734, 1461, 1380, 1253, 1202, 1166, 1091, 1005, 871, 838, 777$ cm^{-1} . MS (EI) m/z (%): 331 (25), 241 (19), 230 (11), 229 (57), 185 (39), 171 (10), 159 (16), 157 (14), 139 (51), 117 (95), 115 (14), 107 (12), 101 (10), 89 (22), 75 (54), 73 (100), 59 (24), 55 (10), 43 (26), 41 (12), 40 (42). HRMS (ESIpos): m/z calcd for $\text{C}_{19}\text{H}_{36}\text{O}_6\text{SiNa}$: 411.2173, found: 411.2174.

The desilylated byproduct **115** was also isolated from the crude mixture as a colorless oil (17 mg, 4%).



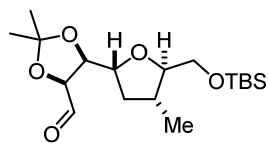
$[\alpha]_{\text{D}}^{20} = -2.9$ ($c = 0.5$, CHCl₃). ¹H NMR (400 MHz, CDCl₃): $\delta = 4.56$ (d, $J = 6.9$ Hz, 1H), 4.27 (dd, $J = 6.9, 6.1$ Hz, 1H), 4.04 (dt, $J = 9.5, 6.1$ Hz, 1H), 3.77 (dd, $J = 11.9, 2.8$ Hz, 1H), 3.74 (s, 3H), 3.58 (ddd, $J = 9.1, 4.2, 2.8$ Hz, 1H), 3.48 (dd, $J = 11.9, 4.2$ Hz, 1H), 2.25 (ddd, $J = 11.5, 7.3, 6.0$ Hz, 1H), 2.17 (dddq, $J = 10.5, 9.1, 7.9, 6.4$ Hz, 1H), 1.97 (brs, 1H), 1.62 (s, 3H), 1.49 (ddd, $J = 11.6, 10.5, 9.3$ Hz, 1H), 1.40 (s, 3H), 1.04 ppm (d, $J = 6.4$ Hz, 3H). ¹³C NMR (100 MHz, CDCl₃): $\delta = 171.0, 111.5, 86.3, 81.2, 76.5, 75.6, 62.4, 52.3, 37.8, 34.8, 26.8, 25.8, 16.2$ ppm. IR (film): $\tilde{\nu} = 3485, 2984, 2954, 2935, 2874, 1757, 1733, 1457, 1438, 1371, 1244, 1204, 1088, 1042, 920, 871, 788$ cm^{-1} . MS (ESIpos) m/z (%): 297.1 (100 (M+Na)). HRMS (ESIpos): m/z calcd for $\text{C}_{13}\text{H}_{22}\text{O}_6\text{Na}$: 297.1309, found: 297.1306.

Alcohol S24. A solution of LiAlH₄ (1 M in THF, 2.83 mL, 2.83 mmol) was added to a solution of ester **114** (550 mg, 1.42 mmol) in THF (14 mL) at 0 °C. The resulting mixture was stirred at ambient temperature for 1 h. The reaction was cooled to 0 °C and carefully quenched with MeOH until gas evolution ceased. The mixture was then poured *via* cannula into aq. sat. Rochelle salt (15 mL), the flask rinsed was rinsed with *t*-butyl methyl ether (5 mL) and the emulsion was vigorously stirred at rt overnight. The layers were



separated and the aqueous layer was extracted with *t*-butyl methyl ether (3 × 20 mL). The combined extracts were washed with brine (25 mL), dried over Na₂SO₄, filtered and concentrated. The residue was purified by flash chromatography (hexanes/*t*-butyl methyl ether 19:1) to afford the title compound **S24** as a colorless oil (487 mg, 95%). $[\alpha]_{\text{D}}^{20} = +2.8$ (*c* = 1.0, CHCl₃). ¹H NMR (400 MHz, CDCl₃): δ = 3.72–3.65 (m, 2H), 4.08 (dd, *J* = 6.3, 3.8 Hz, 1H), 3.72–3.65 (m, 3H), 3.65–3.59 (m, 2H), 3.12 (t, *J* = 6.5 Hz, 1H), 2.24–2.12 (m, 2H), 1.63 (ddd, *J* = 14.0, 13.8, 9.7 Hz, 1H) 1.50 (s, 3H), 1.37 (s, 3H), 1.08 (d, *J* = 6.1 Hz, 3H), 0.88 (s, 9H), 0.04 ppm (s, 6H). ¹³C NMR (100 MHz, CDCl₃): δ = 108.7, 86.5, 78.9, 77.5, 76.0, 64.4, 61.6, 38.3, 36.0, 27.6, 26.0 (3C), 25.8, 18.4, 17.1, –5.28, –5.31 ppm. IR (film): $\tilde{\nu}$ = 3475, 2955, 2930, 2857, 1462, 1378, 1251, 1216, 1168, 1124, 1078, 1040, 1005, 836, 777, 668 cm⁻¹. MS (EI) *m/z* (%): 303 (28), 245 (30), 229 (43), 227 (35), 215 (14), 197 (14), 185 (38), 171 (11), 157 (18), 153 (18), 145 (21), 143 (12), 135 (57), 131 (17), 129 (10), 127 (12), 117 (47), 115 (15), 113 (12), 109 (20), 107 (13), 105 (29), 103 (13), 101 (15), 97 (16), 95 (19), 93 (15), 89 (18), 85 (14), 81 (28), 75 (98), 73 (100), 69 (14), 59 (73), 57 (22), 55 (24), 43 (52), 41 (25), 31 (10), 29 (12). HRMS (ESIpos): *m/z* calcd for C₁₈H₃₆O₅SiNa: 383.2224, found: 383.2226.

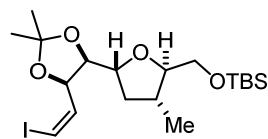
Aldehyde S25. Hünig's base (1.40 mL, 8.03 mmol) was added to a solution of alcohol **S24** (579 mg,



1.61 mmol) in CH₂Cl₂ (8 mL) at –25 °C. In a second flask, SO₃·pyridine (639 mg, 4.01 mmol) was suspended in DMSO (1.15 mL, 16.1 mmol) and the suspension was stirred for 10 min at rt, before it was added to the alcohol

solution at –25 °C and the flask was rinsed with CH₂Cl₂ (2 mL). The resulting mixture was stirred at –25 °C for 45 min. The reaction mixture was poured into pH 7 phosphate buffer (15 mL) and *t*-butyl methyl ether (15 mL), the layers were separated and the aqueous layer was extracted with *t*-butyl methyl ether (3 × 20 mL). The combined extracts were washed with pH 7 phosphate buffer (20 mL), followed by brine (20 mL), dried over Na₂SO₄, filtered and concentrated under high vacuum to yield crude aldehyde **S25** as a pale yellow oil, which was pure by NMR spectroscopy. $[\alpha]_{\text{D}}^{20} = -30.9$ (*c* = 1.0, CHCl₃). ¹H NMR (400 MHz, CDCl₃): δ = 9.66–9.59 (m, 1H), 4.34–4.29 (m, 2H), 4.01 (dtd, *J* = 8.0, 3.8, 2.0 Hz, 1H), 3.65–3.59 (m, 2H), 3.55 (dt, *J* = 8.7, 4.4 Hz, 1H), 2.17–2.06 (m, 2H), 1.57 (s, 3H), 2.52 (ddd, *J* = 14.8, 5.2, 1.5 Hz, 1H), 1.40 (s, 3H), 1.05 (d, *J* = 6.1 Hz, 3H), 0.86 (s, 9H), 0.023 (s, 3H), 0.020 ppm (s, 3H). ¹³C NMR (100 MHz, CDCl₃): δ = 201.6, 111.3, 86.7, 81.6, 81.3, 75.6, 64.6, 37.0, 36.7, 27.1, 26.0 (3C), 25.5, 18.4, 17.1, –5.3 ppm (2C). IR (film): $\tilde{\nu}$ = 2956, 2930, 2857, 1732, 1461, 1381, 1361, 1252, 1214, 1164, 1075, 1004, 835, 776, 667 cm⁻¹. MS (EI) *m/z* (%): 302 (12), 301 (59), 243 (24), 230 (18), 229 (100), 225 (11), 213 (15), 201 (38), 197 (13), 187 (11), 185 (57), 183 (27), 171 (38), 157 (29), 155 (11), 151 (11), 145 (15), 143 (16), 129 (22), 123 (11), 117 (40), 115 (15), 113 (18), 105 (17), 103 (20), 101 (22), 97 (10), 95 (12), 89 (13), 85 (14), 81 (14), 75 (59), 73 (63), 59 (18), 55 (14), 43 (15). HRMS (ESIpos): *m/z* calcd for C₁₈H₃₄O₅SiNa: 381.2068, found: 381.2068.

(Z)-Vinyl iodide 116. Iodomethyltriphenylphosphonium iodide (1.82 g, 4.17 mmol) was added in portions to a solution of NaHMDS (753 mg, 4.11 mmol) in THF (25 mL). The

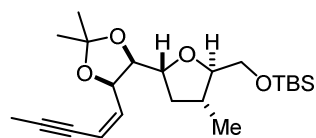


resulting yellow mixture was stirred at rt for 30 min before it was cooled to $-78\text{ }^{\circ}\text{C}$. HMPA (1.40 mL, 8.02 mmol) was added, followed by a solution of

aldehyde **S25** (575 mg, 1.60 mmol) in THF (6 mL). The resulting mixture was stirred at $-78\text{ }^{\circ}\text{C}$ for 4 h. The reaction was quenched with H_2O (15 mL) and the aqueous layer was extracted with *t*-butyl methyl ether (3 \times 20 mL). The combined extracts were dried over Na_2SO_4 , filtered and concentrated.

The residue was purified by flash chromatography (hexanes/*t*-butyl methyl ether 70:1 to 40:1) to afford the title compound **116** as a colorless oil (517 mg, 67% two steps, *Z/E* > 20:1). $[\alpha]_{\text{D}}^{20} = -53.2$ ($c = 0.875$, CHCl_3). $^1\text{H NMR}$ (400 MHz, CDCl_3): $\delta = 6.47$ (dd, $J = 7.7, 0.9$ Hz, 1H), 6.36 (dd, $J = 8.6, 7.7$ Hz, 1H), 4.82 (ddd, $J = 8.6, 6.3, 0.6$ Hz, 1H), 4.14 (t, $J = 6.6$ Hz, 1H), 3.89 (dt, $J = 9.8, 6.3$ Hz, 1H), 3.72 (dd, $J = 10.6, 3.9$ Hz, 1H), 3.65 (dd, $J = 10.6, 5.1$ Hz, 1H), 3.56 (ddd, $J = 8.9, 5.1, 3.9$ Hz, 1H), 2.18 (ddq, $J = 13.9, 10.1, 6.5$ Hz, 1H), 2.07 (ddd, $J = 13.0, 7.2, 5.9$ Hz, 1H), 1.50 (s, 3H), 1.41 (s, 3H), 1.33 (dt, $J = 11.9, 10.1$ Hz, 1H), 1.09 (d, $J = 6.5$ Hz, 3H), 0.88 (s, 9H), 0.04 ppm (s, 6H). $^{13}\text{C NMR}$ (100 MHz, CDCl_3): $\delta = 137.6, 110.0, 86.0, 85.6, 81.1, 79.8, 77.2, 64.9, 38.1, 36.7, 27.8, 26.0$ (3C), 25.8, 18.4, 17.8, -5.2 ppm (2C). IR (film): $\tilde{\nu} = 2955, 2929, 2857, 1461, 1378, 1252, 1214, 1164, 1125, 1085, 1059, 999, 837, 777, 677\text{ cm}^{-1}$. MS (EI) m/z (%): 483 (11), 482 (24), 467 (12), 426 (19), 425 (87), 367 (22), 337 (12), 293 (11), 243 (21), 230 (19), 229 (100), 186 (12), 185 (61), 171 (28), 157 (34), 149 (17), 117 (18), 93 (11), 75 (31), 73 (43). HRMS (ESIpos): m/z calcd for $\text{C}_{19}\text{H}_{35}\text{O}_4\text{SiNa}$: 505.1242, found: 505.1244.

(Z)-Enyne 117. THF was degassed by three freeze-pump-thaw cycles prior to use. A flame-dried Young

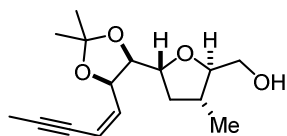


Schlenk was charged with 1-propynyllithium (17.3 mg, 0.65 mmol), which was suspended in degassed THF (1.4 mL). Trimethyl borate (72.0 μL , 0.65 mmol) was added dropwise *via* syringe at rt. After stirring

for 20 min, $[\text{Pd}(\text{dppf})\text{Cl}_2] \cdot \text{CH}_2\text{Cl}_2$ (17.3 mg, 21.1 μmol , 10 mol%) was added, causing the reaction mixture to turn bright red. Next, a solution of (*Z*)-vinyl iodide **116** (102 mg, 0.21 mmol) in degassed THF (0.4 mL + 0.2 mL rinse) was added and the mixture stirred at $65\text{ }^{\circ}\text{C}$ for 7 h. The pale orange mixture was cooled to ambient temperature; the reaction was quenched with aq. half-sat. NH_4Cl (3 mL) and the aqueous layer extracted with EtOAc (3 \times 5 mL). The combined extracts were dried over Na_2SO_4 , filtered and concentrated. The residue was purified by flash chromatography (hexanes/*t*-butyl methyl ether 19:1 to 15:1) to yield the title compound **117** as a colorless oil (68 mg, 82%). $[\alpha]_{\text{D}}^{20} = -67.1$ ($c = 1.0$, CHCl_3). $^1\text{H NMR}$ (400 MHz, CDCl_3): $\delta = 5.87$ (ddd, $J = 10.7, 9.8, 0.8$ Hz, 1H), 5.61 (dq, $J = 10.7, 2.4, 0.8$ Hz, 1H), 5.09 (ddd, $J = 9.8, 6.3, 0.9$ Hz, 1H), 4.11 (dd, $J = 7.4, 6.3$ Hz, 1H), 3.89 (ddd, $J = 9.7, 7.4, 5.6$ Hz, 1H), 3.74 (dd, $J = 10.4, 3.7$ Hz, 1H), 3.64 (dd, $J = 10.4, 5.5$ Hz, 1H), 3.56 (ddd, $J = 7.6, 5.5, 3.7$ Hz, 1H), 2.18 (ddd, $J = 10.2, 5.2, 2.1$ Hz, 1H), 2.10 (ddd, $J = 11.8, 7.2, 5.5$ Hz,

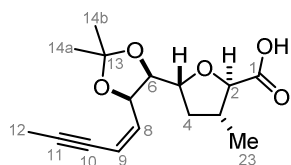
1H), 1.98 (dd, $J = 2.4, 0.7$ Hz, 3H), 1.50 (s, 3H), 1.40 (s, 3H), 1.32–1.23 (m, 1H), 1.08 (d, $J = 6.4$ Hz, 3H), 0.87 (s, 9H), 0.03 ppm (s, 6H). ^{13}C NMR (100 MHz, CDCl_3): $\delta = 137.2, 113.4, 109.7, 92.4, 85.8, 81.6, 77.6, 75.4, 74.9, 65.0, 37.9, 36.9, 28.1, 26.0$ (3C), 25.9, 18.4, 17.9, 4.7, $-5.2, -5.3$ ppm. IR (film): $\tilde{\nu} = 2955, 2929, 2857, 1461, 1378, 1251, 1214, 1165, 1125, 1088, 1058, 1021, 999, 868, 836, 777, 673$ cm^{-1} . MS (EI) m/z (%): 338 (11), 337 (45), 279 (38), 243 (32), 230 (17), 229 (95), 187 (23), 186 (16), 185 (100), 171 (13), 159 (14), 157 (45), 145 (18), 136 (57), 135 (19), 133 (11), 129 (11), 121 (60), 117 (21), 115 (15), 108 (23), 107 (30), 105 (16), 93 (21), 91 (10), 79 (16), 77 (14), 75 (49), 73 (63), 59 (10), 43 (13). HRMS (ESIpos): m/z calcd for $\text{C}_{22}\text{H}_{38}\text{O}_4\text{SiNa}$: 417.2432, found: 417.2435.

Alcohol S26. Pyridine (1.00 mL, 12.4 mmol) was slowly added to a Teflon[®] vial charged with HF-pyridine (0.20 mL, 2.22 mmol) and the resulting mixture was diluted with THF (2 mL). An aliquot of this solution (1.6 mL) was added dropwise to a solution of silyl ether **117** (68.0 mg, 0.17 mmol) in THF (0.4 mL) in a



second Teflon[®] vial. The resulting mixture was stirred at ambient temperature for 18 h. The mixture was diluted with EtOAc (3 mL) and the reaction was carefully quenched with aq. sat. NaHCO_3 (5 mL). The layers were separated and the aqueous layer was extracted with EtOAc (4×8 mL). The combined organic extracts were dried over Na_2SO_4 , filtered and concentrated. The residue was purified by flash chromatography (hexanes/EtOAc 12:1 to 4:1) to afford the title compound **S26** as a colorless oil (43.3 mg, 90%). $[\alpha]_D^{20} = -64.2$ ($c = 1.0, \text{CHCl}_3$). ^1H NMR (400 MHz, CDCl_3): $\delta = 5.93$ (ddd, $J = 10.8, 9.8, 0.6$ Hz, 1H), 5.63 (dq, $J = 10.8, 2.4, 0.6$ Hz, 1H), 5.09 (ddd, $J = 9.8, 6.2, 0.8$ Hz, 1H), 4.14 (dd, $J = 7.7, 6.2$ Hz, 1H), 3.95 (ddd, $J = 9.6, 7.6, 5.4$ Hz, 1H), 3.82 (dd, $J = 12.0, 2.7$ Hz, 1H), 3.58 (ddd, $J = 8.8, 3.8, 2.7$ Hz, 1H), 3.51 (dd, $J = 11.9, 3.8$ Hz, 1H), 2.23–2.11 (m, 2H), 1.98 (d, $J = 2.4$ Hz, 3H), 1.51 (s, 3H), 1.42 (s, 3H), 1.33–1.27 (m, 1H), 1.04 ppm (d, $J = 6.1$ Hz, 3H). ^{13}C NMR (100 MHz, CDCl_3): $\delta = 136.9, 113.8, 109.8, 92.7, 86.2, 81.8, 77.7, 75.3, 74.8, 62.2, 37.6, 34.5, 28.2, 25.9, 16.3, 4.7$ ppm. IR (film): $\tilde{\nu} = 3457, 2954, 2928, 2885, 2856, 1472, 1462, 1388, 1361, 1250, 1150, 1107, 1079, 1060, 1005, 964, 834, 775, 679$ cm^{-1} . MS (EI) m/z (%): 136 (100), 135 (19), 121 (75), 115 (47), 108 (34), 107 (49), 97 (10), 93 (17), 79 (19), 77 (14), 71 (69), 69 (13), 43 (14), 41 (10). HRMS (ESIpos): m/z calcd for $\text{C}_{16}\text{H}_{24}\text{O}_4\text{Na}$: 303.1567, found: 303.1565.

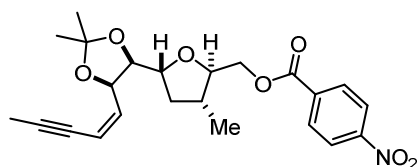
Carboxylic acid 118. NMO· H_2O (104 mg, 0.89 mmol) and TPAP (3.1 mg, 8.9 μmol , 10 mol%) were sequentially added to a solution of alcohol **S26** (25 mg, 89 μmol) in MeCN (0.4 mL). The resulting mixture was stirred at rt for 7 h. The reaction was quenched with aq. pH 5 phosphate buffer (1 mL), the layers were separated and the aqueous layer extracted with EtOAc (4×3 mL). The



combined organic extracts were dried over Na_2SO_4 , filtered and concentrated. The residue was purified by flash chromatography (hexanes/EtOAc 4:1 to 0:1) to yield the title compound **118** as a

colorless oil (19.6 mg, 75%). $[\alpha]_D^{20} = -59.9$ ($c = 0.5$, CHCl_3). $^1\text{H NMR}$ (400 MHz, CDCl_3): $\delta = 8.45$ (brs, 1H, 1-OH), 5.90 (ddd, $J = 10.7, 9.5, 0.8$ Hz, 1H, H-8), 5.65 (dq, $J = 10.7, 2.4, 0.9$ Hz, 1H, H-9), 5.13 (ddd, $J = 9.5, 6.3, 0.9$ Hz, 1H, H-7), 4.16 (dd, $J = 6.3, 5.7$ Hz, 1H, H-6), 4.11 (ddd, $J = 9.5, 6.1, 5.7$ Hz, 1H, H-5), 4.02 (d, $J = 8.5$ Hz, 1H, H-2), 2.37 (dddq, $J = 10.0, 8.5, 7.3, 6.5$ Hz, 1H, H-3), 2.18 (ddd, $J = 12.4, 7.3, 6.1$ Hz, 1H, H-4), 1.97 (d, $J = 2.4$ Hz, 3H, H-12), 1.50 (s, 3H, H-14), 1.40 (s, 3H, H-14), 1.39 (ddd, $J = 12.4, 10.0, 9.5$ Hz, 1H, H-4), 1.24 ppm (d, $J = 6.5$ Hz, 3H, H-23). $^{13}\text{C NMR}$ (100 MHz, CDCl_3): $\delta = 175.6$ (C1), 136.9 (C8), 113.9 (C9), 109.8 (C13), 92.9 (C11), 83.2 (C2), 80.7 (C6), 79.3 (C5), 75.3 (C10), 75.0 (C7), 39.7 (C3), 37.3 (C4), 27.9 (C14), 25.7 (C14), 17.9 (C23), 4.6 ppm (C12). IR (film): $\tilde{\nu} = 2983, 2933, 1731, 1456, 1372, 1250, 1216, 1164, 1130, 1096, 1054, 914, 868, 809, 733$ cm^{-1} . MS (ESI^{neg}) m/z (%): 293.1 (100 (M-H)). HRMS (ESI^{neg}): m/z calcd for $\text{C}_{16}\text{H}_{21}\text{O}_5$: 293.1396, found: 293.1398.

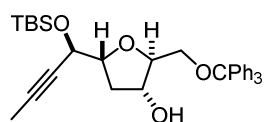
Nitrobenzoate S27. Pyridine (3.8 μL , 46 μmol), 4-nitrobenzoyl chloride (8.1 mg, 43 μmol) and DMAP



(0.9 mg, 7.1 μmol , 20 mol%) were sequentially added to a solution of alcohol **S26** (10 mg, 36 μmol) in CH_2Cl_2 (0.4 mL) at 0 °C. The resulting solution was stirred at rt for 3.5 h. The reaction was quenched with aq. half-sat. NH_4Cl (1 mL) and the

aqueous layer extracted with CH_2Cl_2 (3 \times 3 mL). The combined extracts were dried over Na_2SO_4 , filtered and concentrated. The residue was purified by flash chromatography (hexanes/ EtOAc 9:1) to afford the title compound **S27** (12.2 mg, 80%). $[\alpha]_D^{20} = -64.9$ ($c = 1.0$, CHCl_3). $^1\text{H NMR}$ (400 MHz, CDCl_3): $\delta = 8.29$ (dd, $J = 8.9, 2.2$ Hz, 2H), 8.21 (dd, $J = 8.9, 2.2$ Hz, 2H), 5.90 (dd, $J = 10.8, 9.7$ Hz, 1H), 5.63 (dq, $J = 10.8, 2.4$ Hz, 1H), 5.12 (dd, $J = 9.7, 6.3$ Hz, 1H), 4.49 (dd, $J = 11.8, 3.4$ Hz, 1H), 4.40 (dd, $J = 11.8, 5.1$ Hz, 1H), 4.16 (dd, $J = 7.0, 6.3$ Hz, 1H), 4.00 (ddd, $J = 10.1, 7.0, 5.5$ Hz, 1H), 3.88 (ddd, $J = 8.5, 5.1, 3.4$ Hz, 1H), 2.20 (dt, $J = 11.1, 6.0$ Hz, 1H), 2.14 (tdq, $J = 10.7, 8.5, 6.2$ Hz, 1H), 1.98 (d, $J = 2.4$ Hz, 3H), 1.51 (s, 3H), 1.42 (s, 3H), 1.44–1.37 (m, 1H), 1.14 ppm (d, $J = 6.2$ Hz, 3H). $^{13}\text{C NMR}$ (100 MHz, CDCl_3): $\delta = 164.8, 150.6, 137.0, 135.5, 130.9$ (2C), 123.7 (2C), 113.7, 109.8, 92.7, 83.3, 81.4, 77.8, 75.3, 74.9, 66.4, 37.4, 36.5, 28.1, 25.9, 16.8, 4.7 ppm. IR (film): $\tilde{\nu} = 2960, 2933, 1726, 1608, 1528, 1456, 1369, 1347, 1275, 1216, 1164, 1101, 1057, 1015, 872, 720$ cm^{-1} . MS (EI) m/z (%): 371 (12), 264 (33), 140 (43), 137 (10), 136 (100), 135 (20), 121 (86), 108 (46), 107 (44), 97 (41), 93 (17), 79 (17), 69 (15). HRMS (ESI^{pos}): m/z calcd for $\text{C}_{23}\text{H}_{27}\text{NO}_7\text{Na}$: 452.1680, found: 452.1681. Attempts to obtain single crystals suitable for x-ray crystallography have thus far met with failure.

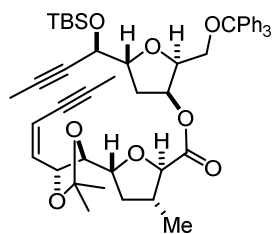
Alcohol 120. Triethylamine (20 μL , 0.1 mmol) was added to a solution of diol **119** (28 mg, 90 μmol) in



CH_2Cl_2 (1 mL) at 0 °C. Trityl chloride (28.6 mg, 0.10 mmol) was added in portions and the reaction mixture stirred at rt for 4 h. The reaction was quenched with H_2O (5 mL) and extracted with CH_2Cl_2 (3 \times 8 mL). The

combined extracts were dried over Na_2SO_4 , filtered and concentrated. The residue was purified by flash chromatography (hexanes/EtOAc 19:1 to 9:1) to afford the desired alcohol **120** as a colorless oil (48.3 mg, 95%). $[\alpha]_{\text{D}}^{20} = -20.4$ ($c = 1.0$, CHCl_3). ^1H NMR (400 MHz, CDCl_3): $\delta = 7.46\text{--}7.40$ (m, 6H), 7.32–7.19 (m, 9H), 4.42 (dq, $J = 4.3, 2.2$ Hz, 1H), 4.26–4.17 (m, 3H), 3.35 (brd, $J = 9.1$ Hz, 1H), 3.18 (dd, $J = 9.6, 4.5$ Hz, 1H), 3.00 (dd, $J = 9.6, 6.3$ Hz, 1H), 2.34 (ddd, $J = 13.9, 9.2, 6.2$ Hz, 1H), 1.90 (dt, $J = 13.9, 3.2$ Hz, 1H), 1.87 (d, $J = 2.2$ Hz, 3H), 0.93 (s, 9H), 0.18 (s, 3H), 0.16 ppm (s, 3H). ^{13}C NMR (100 MHz, CDCl_3): $\delta = 144.0$ (3C), 128.8 (6C), 128.0 (6C), 127.2 (3C), 87.0, 86.5, 82.4, 81.8, 78.8, 73.9, 66.1, 64.4, 36.1, 26.0 (3C), 18.5, 3.9, -4.4 , -4.7 ppm. IR (film): $\tilde{\nu} = 3457, 3059, 2927, 2856, 1491, 1471, 1448, 1251, 1076, 837, 776, 705, 633$ cm^{-1} . MS (ESIpos) m/z (%): 565.3 (100 (M+Na)). HRMS (ESIpos): m/z calcd for $\text{C}_{34}\text{H}_{42}\text{O}_4\text{SiNa}$: 565.2745, found: 565.2744.

Diyne S28. This compound was prepared according to the representative procedure for Mitsunobu



esterification (*vide supra*) from alcohol **120** and carboxylic acid **118**.

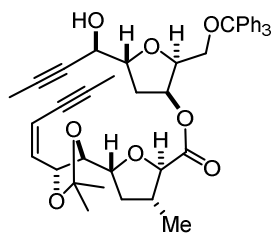
Purification by flash chromatography (hexanes/EtOAc 19:1) provided

diyne **S28** as a colorless oil (18.4 mg, 79%). $[\alpha]_{\text{D}}^{20} = -22.2$ ($c = 1.0$, CHCl_3).

^1H NMR (400 MHz, CDCl_3): $\delta = 7.41\text{--}7.37$ (m, 6H), 7.31–7.27 (m, 6H), 7.26–7.19 (m, 3H), 5.90 (dd, $J = 10.8, 9.5$ Hz, 1H), 5.62 (ddt, $J = 10.8, 2.8, 2.0$

Hz, 1H), 5.52 (t, $J = 3.6$ Hz, 1H), 5.11 (ddd, $J = 9.5, 6.5, 0.9$ Hz, 1H), 4.37 (dq, $J = 4.3, 2.0$ Hz, 1H), 4.30 (td, $J = 6.3, 3.4$ Hz, 1H), 4.20–4.14 (m, 1H), 4.05 (t, $J = 6.2$ Hz, 1H), 3.88–3.81 (m, 2H), 3.43 (dd, $J = 9.2, 6.0$ Hz, 1H), 3.11 (dd, $J = 9.2, 6.7$ Hz, 1H), 2.27 (ddd, $J = 13.9, 8.8, 5.0$ Hz, 1H), 2.08 (ddd, $J = 14.4, 6.7, 1.3$ Hz, 1H), 2.04–2.00 (m, 1H), 1.99 (d, $J = 2.4$ Hz, 3H), 1.93–1.87 (m, 1H), 1.84 (d, $J = 2.1$ Hz, 3H), 1.48 (s, 3H), 1.40 (s, 3H), 1.30–1.24 (m, 1H), 1.03 (d, $J = 6.6$ Hz, 3H), 0.91 (s, 9H), 0.14 (s, 3H), 0.11 ppm (s, 3H). ^{13}C NMR (100 MHz, CDCl_3): $\delta = 172.4, 143.9$ (3C), 136.9, 128.8 (6C), 127.9 (6C), 127.1 (3C), 114.0, 109.7, 92.4, 86.9, 83.5, 81.8, 80.9, 80.4, 80.2, 79.4, 78.0, 75.5, 75.1, 75.0, 65.9, 62.0, 39.7, 36.9, 35.1, 27.8, 26.0 (3C), 25.9, 18.6, 18.5, 4.7, 3.8, -4.5 , -4.8 ppm. IR (film): $\tilde{\nu} = 2928, 2856, 1733, 1491, 1449, 1378, 1252, 1216, 1077, 909, 837, 776, 731, 705, 648, 633$ cm^{-1} . MS (ESIpos) m/z (%): 841.4 (100 (M+Na)). HRMS (ESIpos): m/z calcd for $\text{C}_{50}\text{H}_{62}\text{O}_8\text{SiNa}$: 841.4106, found: 841.4112.

Diyne 121. A solution of TBAF (1 M in THF, 7.3 μL , 7.3 μmol) was added to a solution of diyne **S28**



(5 mg, 6.1 μmol) in THF (0.1 mL) at -30 $^{\circ}\text{C}$ and the resulting mixture was stirred for 4 h slowly warming to rt. The reaction was quenched with aq. sat.

NH_4Cl (1 mL), the layers were separated and the aqueous layer was extracted with EtOAc (3×2 mL). The combined extracts were washed with brine (5 mL), dried over Na_2SO_4 , filtered and concentrated. The residue was

purified by flash chromatography (hexanes/EtOAc 8:1) to afford diyne **121** as a colorless oil (2.9 mg, 67%). $[\alpha]_{\text{D}}^{20} = -13.7$ ($c = 0.35$, CHCl_3). ^1H NMR (400 MHz, CDCl_3): $\delta = 7.39\text{--}7.34$ (m, 6H), 7.31–7.27 (m,

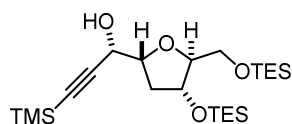
6H), 7.25–7.21 (m, 3H), 5.90 (dd, $J = 10.7, 9.4$ Hz, 1H), 5.62 (ddd, $J = 10.7, 2.5, 0.8$ Hz, 1H), 5.57–5.49 (m, 1H), 5.11 (ddd, $J = 9.4, 6.4, 0.8$ Hz, 1H), 4.28–4.20 (m, 2H), 4.17 (dt, $J = 8.7, 6.5$ Hz, 1H), 4.06 (dd, $J = 5.9, 6.5$ Hz, 1H), 3.85 (d, $J = 7.4$ Hz, 1H), 3.87–3.80 (m, 1H), 3.45 (dd, $J = 9.2, 5.9$ Hz, 1H), 3.16 (dd, $J = 9.2, 6.9$ Hz, 1H), 2.31 (brd, $J = 2.7$ Hz, 1H) 2.19–2.08 (m, 2H), 2.04–1.97 (m, 1H), 1.99 (d, $J = 2.2$ Hz, 3H), 1.90 (ddd, $J = 12.6, 7.3, 5.5$ Hz, 1H), 1.84 (d, $J = 2.1$ Hz, 3H), 1.49 (s, 3H), 1.40 (s, 3H), 1.32–1.24 (m, 1H), 1.04 ppm (d, $J = 6.6$ Hz, 3H). ^{13}C NMR (100 MHz, CDCl_3): $\delta = 172.3, 143.8$ (3C), 136.9, 128.8 (6C), 128.0 (6C), 127.2 (3C), 114.0, 109.7, 92.5, 87.0, 83.5, 82.8, 81.2, 80.5, 80.1, 79.4, 76.8, 75.5, 75.1, 74.7, 65.4, 61.9, 39.7, 36.9, 35.6, 27.8, 25.9, 18.5, 4.7, 3.8 ppm. IR (film): $\tilde{\nu} = 3444, 2931, 2856, 1733, 1492, 1449, 1379, 1256, 1216, 1078, 869, 765, 707, 633$ cm^{-1} . MS (ESIpos) m/z (%): 727.3 (100 (M+Na)). HRMS (ESIpos): m/z calcd for $\text{C}_{44}\text{H}_{48}\text{O}_8\text{Na}$: 727.3241, found: 727.3242.

4.3.6 Synthesis of the Northern Alcohol Fragments **122** and **123**

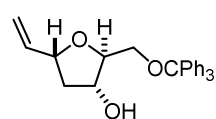
Alcohol (12R)-124. TMS-acetylene (0.23 mL, 1.61 mmol) was added to a solution of (*R,R*)-ProPhenol (68.5 mg, 0.11 mmol, 20 mol%) and TPPO (59.7 mg, 0.54 mmol) in toluene (0.6 mL), followed by Me_2Zn (1.34 mL, 1.61 mmol). The resulting mixture was stirred at 4 °C for 45 min, before a solution of aldehyde **58** (201 mg, 0.54 mmol) in toluene (0.4 mL) was added. The resulting mixture was stirred at 4 °C for 72 h. The reaction was quenched aq. sat. NH_4Cl (2 mL) and the aqueous layer extracted with *t*-butyl methyl ether (3 × 5 mL). The combined extracts were washed with brine (10 mL), dried over Na_2SO_4 , filtered and concentrated. The residue was purified by flash chromatography (hexanes/EtOAc 20:1) to afford alcohol (*12R*)-**124** (104 mg, 41%, d.r. 5:1) and its diastereomer (*12S*)-**124** (16.7 mg, 7%) as a colorless oil each.

Analytical data for (*12R*)-**124**: $[\alpha]_{\text{D}}^{20} = -6.3$ ($c = 1.0, \text{CHCl}_3$). ^1H NMR (400 MHz, CDCl_3): $\delta = 4.51$ (d, $J = 7.0$ Hz, 1H), 4.34 (dt, $J = 5.8, 2.3$ Hz, 1H), 4.15 (ddd, $J = 8.3, 7.0, 3.3$ Hz, 1H), 3.96 (ddd, $J = 6.2, 4.2, 2.1$ Hz, 1H), 3.62 (dd, $J = 10.8, 4.1$ Hz, 1H), 3.46 (dd, $J = 10.7, 6.1$ Hz, 1H), 2.96 (d, $J = 2.5$ Hz, 1H), 2.27 (ddd, $J = 14.0, 8.4, 5.9$ Hz, 1H), 1.91 (dt, $J = 13.5, 2.9$ Hz, 1H), 0.96 (t, $J = 7.9$ Hz, 9H), 0.95 (t, $J = 7.9$ Hz, 9H), 0.60 (q, $J = 7.8$ Hz, 6H), 0.59 (q, $J = 7.9$ Hz, 6H), 0.16 ppm (s, 9H). ^{13}C NMR (100 MHz, CDCl_3): $\delta = 104.0, 90.3, 88.0, 82.7, 73.3, 66.2, 63.3, 37.9, 6.88$ (3C), 6.86 (3C), 4.8 (3C), 4.5 (3C), 0.0 ppm (3C). IR (film): $\tilde{\nu} = 3432, 2954, 2911, 2877, 1459, 1414, 1378, 1249, 1111, 1065, 1003, 841, 741, 725, 660$ cm^{-1} . MS (EI) m/z (%): 443 (20), 213 (26), 147 (13), 146 (12), 145 (95), 131 (10), 118 (11), 117 (100), 115 (44), 103 (12), 87 (43), 75 (13), 73 (18), 59 (13). HRMS (ESIpos): m/z calcd for $\text{C}_{23}\text{H}_{48}\text{O}_4\text{Si}_3\text{Na}$: 495.2753, found: 495.2755.

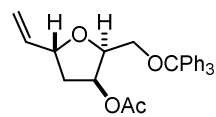
Analytical data for (12*S*)-**124**: ^1H NMR (500 MHz, CDCl_3): δ = 4.48 (dd, J = 6.8, 3.5 Hz, 1H), 4.37 (dt, J = 5.8, 1.8 Hz, 1H), 4.35 (dt, J = 9.0, 3.4 Hz, 1H), 4.24 (d, J = 7.1 Hz, 1H), 4.05 (ddd, J = 6.4, 4.3, 1.6 Hz, 1H), 3.59 (dd, J = 10.6, 4.2 Hz, 1H), 3.41 (dd, J = 10.6, 6.7 Hz, 1H), 2.30 (ddd, J = 14.0, 9.0, 5.7 Hz, 1H), 2.16 (ddd, J = 13.9, 3.0, 1.9 Hz, 1H), 0.98 (t, J = 7.9 Hz, 9H), 0.95 (t, J = 8.0 Hz, 9H), 0.64 (q, J = 8.0 Hz, 6H), 0.59 (q, J = 8.0 Hz, 6H), 0.15 ppm (s, 9H). ^{13}C NMR (125 MHz, CDCl_3): δ = 105.0, 90.4, 88.6, 81.9, 73.2, 64.9, 63.3, 35.1, 6.8 (3C), 6.7 (3C), 4.6 (3C), 4.4 (3C), 0.0 ppm (3C).



(2*S*,3*R*,5*R*)-2-((Trityloxy)methyl)-5-vinyltetrahydrofuran-3-ol (S29). Et_3N (0.65 mL, 4.68 mmol) and trityl chloride (958 mg, 3.43 mmol) were sequentially added to a solution of diol **55** (450 mg, 3.12 mmol) in CH_2Cl_2 (30 mL) at 0 °C. The resulting mixture was stirred at rt overnight. The reaction was quenched with H_2O (25 mL) and the aqueous layer extracted with EtOAc (3 \times 20 mL). The combined extracts were washed with brine (50 mL), dried over Na_2SO_4 , filtered and concentrated. The residue was purified by flash chromatography (hexanes/EtOAc 6:1) to afford alcohol **S29** as a pale yellow oil (1.06 g, 88%). $[\alpha]_{\text{D}}^{20} = -1.9$ ($c = 0.5$, CHCl_3). ^1H NMR (400 MHz, CDCl_3): δ = 7.47–7.40 (m, 6H), 7.34–7.27 (m, 6H), 7.26–7.21 (m, 3H), 5.98 (ddd, J = 17.2, 10.3, 6.3 Hz, 1H), 5.28 (ddd, J = 17.2, 1.5, 1.4 Hz, 1H), 5.13 (dt, J = 10.3, 1.3 Hz, 1H), 4.55 (dtt, J = 7.6, 6.5, 1.3 Hz, 1H), 4.30 (dtd, J = 6.6, 5.4, 4.2 Hz, 1H), 4.05 (dt, J = 6.3, 4.4 Hz, 1H), 3.30 (dd, J = 9.5, 4.6 Hz, 1H), 3.13 (dd, J = 9.5, 6.2 Hz, 1H), 2.42 (dt, J = 12.9, 6.9 Hz, 1H), 1.91 (d, J = 5.2 Hz, 1H), 1.82 ppm (ddd, J = 12.6, 6.7, 5.5 Hz, 1H). ^{13}C NMR (100 MHz, CDCl_3): δ = 143.9 (3C), 139.8, 128.8 (6C), 128.0 (6C), 127.2 (3C), 115.5, 87.0, 84.3, 79.4, 75.4, 65.0, 40.7 ppm. IR (film): $\tilde{\nu}$ = 3424, 3085, 3060, 3023, 2958, 2928, 2871, 1491, 1448, 1220, 1079, 987, 764, 699, 633 cm^{-1} . MS (EI) m/z (%): 244 (20), 243 (100), 165 (24), 143 (13). HRMS (ESIpos): m/z calcd for $\text{C}_{26}\text{H}_{26}\text{O}_3\text{Na}$: 409.1774, found: 409.1777.

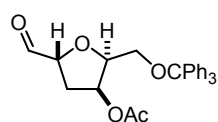


Acetate 125. PPh_3 (1.70 g, 6.47 mmol) was added to a solution of alcohol **S29** (1.00 g, 2.59 mmol) and acetic acid (0.30 mL, 5.17 mmol) in toluene (30 mL). The resulting mixture was stirred for 5 min and then cooled to 0 °C. DIAD (1.27 mL, 6.47 mmol) was added dropwise and the resulting mixture stirred at rt for 1 h. The reaction mixture was diluted with hexanes (30 mL), washed with water (30 mL) and brine (30 mL). The combined extracts were dried over Na_2SO_4 , filtered and concentrated. The residue was purified by flash chromatography (hexanes/*t*-butyl methyl ether 19:1) to yield acetate **125** as a colorless oil (1.05 g, 95%). $[\alpha]_{\text{D}}^{25} = +41.0$ ($c = 1.0$, CHCl_3). ^1H NMR (600 MHz, CDCl_3): δ = 7.45–7.41 (m, 6H), 7.32–7.28 (m, 6H), 7.26–7.22 (m, 3H), 5.86 (ddd, J = 17.0, 10.3, 6.7 Hz, 1H), 5.58 (ddd, J = 5.0, 3.8, 1.5 Hz, 1H), 5.28 (dt, J = 17.1, 1.3 Hz, 1H), 5.15 (dt, J = 10.3, 1.3 Hz, 1H), 4.54 (dt, J = 9.5, 6.4 Hz, 1H), 4.34 (ddd, J = 7.4, 5.4, 3.8 Hz, 1H), 3.40 (dd, J = 9.0, 5.4 Hz, 1H), 3.16 (dd, J = 9.0, 7.4 Hz, 1H), 2.19 (ddd, J = 13.8, 6.1,



1.5 Hz, 1H), 2.00 (ddd, $J = 13.8, 9.5, 5.0$ Hz, 1H), 1.85 ppm (s, 3H). ^{13}C NMR (150 MHz, CDCl_3): $\delta = 170.2, 143.9$ (3C), 138.3, 128.8 (6C), 127.9 (6C), 127.1 (3C), 116.4, 86.8, 79.8, 78.8, 74.4, 61.6, 39.6, 21.0 ppm. IR (film): $\tilde{\nu} = 3086, 3058, 3023, 2984, 2937, 2880, 1742, 1491, 1448, 1373, 1233, 1075, 930, 748, 706, 633$ cm^{-1} . MS (EI) m/z (%): 244 (21), 243 (100), 165 (29), 155 (25), 125 (12). HRMS (ESIpos): m/z calcd for $\text{C}_{28}\text{H}_{28}\text{O}_4\text{Na}$: 451.1880, found: 451.1884.

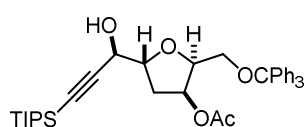
Aldehyde 126. 2,6-lutidine (0.11 mL, 0.93 mmol), potassium osmate (3.44 mg, 9.30 μmol , 2 mol%)



and sodium periodate (400 mg, 1.87 mmol) were sequentially added to a solution of olefin **125** (200 mg, 0.47 mmol) in 1,4-dioxane/water (3:1, 16 mL).

The resulting mixture was stirred at rt for 16 h. The reaction mixture was diluted with CH_2Cl_2 (10 mL) and the aqueous layer was extracted with CH_2Cl_2 (3×10 mL). The combined extracts were dried over Na_2SO_4 , filtered and concentrated. The residue was purified by flash chromatography (hexanes/EtOAc 3:1 to 2:1) to afford the title compound as a colorless oil (185 mg, 92%). $[\alpha]_{\text{D}}^{25} = +57.8$ ($c = 0.5, \text{CHCl}_3$). ^1H NMR (400 MHz, CDCl_3): $\delta = 9.72$ (d, $J = 1.8$ Hz, 1H), 7.43–7.40 (m, 6H), 7.32–7.28 (m, 6H), 7.25–7.21 (m, 3H), 5.51 (q, $J = 3.6$ Hz, 1H), 4.46 (td, $J = 8.2, 1.4$ Hz, 1H), 4.28 (ddd, $J = 6.7, 5.4, 3.7$ Hz, 1H), 3.42 (dd, $J = 9.2, 5.4$ Hz, 1H), 3.22 (dd, $J = 9.3, 6.8$ Hz, 1H), 2.29 (d, $J = 3.5$ Hz, 1H), 2.27 (d, $J = 3.5$ Hz, 1H), 1.85 ppm (s, 3H). ^{13}C NMR (100 MHz, CDCl_3): $\delta = 201.6, 170.1, 143.7$ (3C), 128.8 (6C), 128.0 (6C), 127.3 (3C), 87.0, 81.5, 81.4, 73.2, 61.3, 34.5, 20.9 ppm. IR (film): $\tilde{\nu} = 3086, 3058, 3023, 2951, 2925, 1742, 1491, 1448, 1373, 1231, 1076, 749, 699$ cm^{-1} . MS (EI) m/z (%): 259 (11), 244 (22), 243 (100), 171 (24), 165 (27), 105 (10). HRMS (ESIpos): m/z calcd for $\text{C}_{27}\text{H}_{26}\text{O}_5\text{Na}$: 453.1672, found: 453.1675.

Alkynol 128. A solution of *n*-BuLi (1.6 M in hexane, 0.29 mL, 0.45 mmol) was added to a solution of

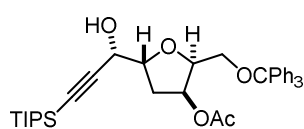


TIPS-acetylene (139 μL , 0.61 mmol) in Et_2O (4 mL) at -78 $^\circ\text{C}$ and the resulting mixture was stirred at that temperature for 30 min. Next, a solution of LiI (207 mg, 1.55 mmol) in Et_2O (1 mL) was added and the

resulting mixture stirred for 30 min at -40 $^\circ\text{C}$. In a second flask, a solution of aldehyde **126** (134 mg, 0.31 mmol) in Et_2O (3 mL) was cooled to -25 $^\circ\text{C}$. The lithium-acetylene solution was added dropwise to the aldehyde solution and stirring was continued overnight. The reaction was quenched with aq. sat. NH_4Cl (8 mL) and the aqueous layer extracted with EtOAc (3×10 mL). The combined extracts were dried over Na_2SO_4 , filtered and concentrated. The residue was purified by flash chromatography (hexanes/EtOAc 4:1) to afford alkynol **128** as a colorless oil (125 mg, 65%, diastereomeric mixture, d.r. 3:1). The diastereomeric mixture could be separated by flash chromatography (fine SiO_2 , hexanes/EtOAc 19:1) to yield the desired diastereomer (12*R*)-**128** (88 mg, 46%) and the undesired diastereomer (12*S*)-**128** (29 mg, 15%).

Analytical data for alcohol (12R)-**128**: $[\alpha]_{\text{D}}^{25} = +40.9$ ($c = 1.0$, CHCl_3). $^1\text{H NMR}$ (600 MHz, CDCl_3): $\delta = 7.41\text{--}7.39$ (m, 6H), $7.30\text{--}7.27$ (m, 6H), $7.25\text{--}7.22$ (m, 3H), 5.54 (ddd, $J = 5.1, 3.5, 1.8$ Hz, 1H), 4.36 (dd, $J = 6.8, 3.9$ Hz, 1H), 4.30 (ddd, $J = 7.3, 5.1, 3.6$ Hz, 1H), 4.22 (ddd, $J = 8.3, 6.8, 0.5$ Hz, 1H), 3.36 (dd, $J = 9.1, 5.1$ Hz, 1H), 3.17 (dd, $J = 9.0, 7.3$ Hz, 1H), 2.26–2.16 (m, 3H), 1.83 (s, 3H), 1.08–1.06 ppm (m, 21H). $^{13}\text{C NMR}$ (150 MHz, CDCl_3): $\delta = 170.2, 143.8$ (3C), 128.8 (6C), 127.9 (6C), 127.2 (3C), 104.9, 87.9, 86.8, 80.7, 80.3, 74.1, 66.1, 61.3, 35.5, 21.0, 18.7 (6C), 11.3 ppm (3C). IR (film): $\tilde{\nu} = 3440, 3058, 2942, 2891, 2865, 1743, 1491, 1449, 1374, 1237, 1077, 883, 705, 678, 633$ cm^{-1} . MS (EI) m/z (%): 244 (21), 243 (100), 165 (14). HRMS (ESIpos): m/z calcd for $\text{C}_{38}\text{H}_{48}\text{O}_5\text{SiNa}$: 635.3163, found: 635.3164.

Analytical data for alcohol (12S)-**128**: $[\alpha]_{\text{D}}^{25} = +33$ ($c = 0.5$, CHCl_3). $^1\text{H NMR}$ (600 MHz, CDCl_3): $\delta = 7.41\text{--}7.37$ (m, 6H), $7.29\text{--}7.26$ (m, 6H), $7.24\text{--}7.20$ (m, 3H), 5.56 (ddd, $J = 5.3, 3.6, 1.6$ Hz, 1H), 4.47 (dd, $J = 6.7, 2.9$ Hz, 1H), 4.45 (ddd, $J = 7.2, 5.1, 3.6$ Hz, 1H), 4.30 (ddd, $J = 9.2, 6.7, 2.9$ Hz, 1H), 3.33 (dd, $J = 9.0, 5.1$ Hz, 1H), 3.14 (dd, $J = 9.0, 7.2$ Hz, 1H), 2.41 (ddd, $J = 14.1, 8.9, 5.3$ Hz, 1H), 2.32 (d, $J = 6.7$ Hz, 1H), 2.10 (ddd, $J = 14.0, 6.8, 1.6$ Hz, 1H), 1.81 (s, 3H), 1.10–1.05 ppm (m, 21H). $^{13}\text{C NMR}$ (150 MHz, CDCl_3): $\delta = 170.2, 143.9$ (3C), 128.8 (6C), 127.9 (6C), 127.2 (3C), 104.7, 87.9, 86.8, 81.2, 80.3, 74.3, 65.2, 61.4, 34.0, 21.0, 18.7 (6C), 11.3 ppm (3C). IR (film): $\tilde{\nu} = 3440, 3059, 2942, 2891, 2865, 1742, 1491, 1449, 1374, 1236, 1076, 883, 705, 678, 633$ cm^{-1} .



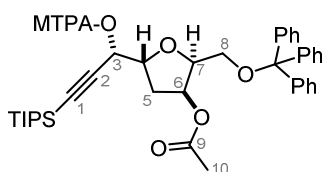
Mosher ester analysis of alcohol (12S)-128. Triethylamine (7.3 μL , 52 μmol) was added to a solution of alcohol (12S)-**128** (8.0 mg, 13 μmol) in CH_2Cl_2 (1 mL) followed by (*R*)-(-)- α -methoxy- α -trifluoromethyl-phenylacetyl chloride ((*R*)-MTPA-Cl) (4.9 μL , 26 μmol). The reaction was stirred at rt for 16 h, then quenched with sat. aq. NaHCO_3 (2 mL) and the mixture was extracted with CH_2Cl_2 (3 \times 5 mL). The combined extracts were dried over Na_2SO_4 , filtered and concentrated. The residue was purified by flash chromatography (hexanes/EtOAc 19:1 to 9:1) to give the corresponding (*S*)-Mosher ester (**S**)-MTPA-**128** (9.5 mg, 87%), which analyzed as follows: $^1\text{H NMR}$ (600 MHz, CDCl_3): $\delta = 7.59\text{--}7.53$ (m, 2H), $7.40\text{--}7.34$ (m, 9H), $7.30\text{--}7.27$ (m, 6H), $7.25\text{--}7.22$ (m, 3H), 5.70 (d, $J = 2.9$ Hz, 1H), 5.42 (ddd, $J = 5.4, 3.6, 1.8$ Hz, 1H), 4.48 (ddd, $J = 8.8, 6.9, 3.0$ Hz, 1H), 4.23 (ddd, $J = 6.7, 5.3, 3.6$ Hz, 1H), 3.55 (d, $J = 1.0$ Hz, 3H), 3.27 (dd, $J = 9.1, 5.3$ Hz, 1H), 3.12 (dd, $J = 9.1, 6.7$ Hz, 1H), 2.35 (ddd, $J = 14.0, 8.7, 5.3$ Hz, 1H), 2.17 (ddd, $J = 14.0, 7.0, 1.9$ Hz, 1H), 1.82 (s, 3H), 1.14–0.96 ppm (m, 21H). MS (ESIpos) m/z (%): 851.4 (100 (M+Na)). HRMS (ESI): m/z calcd for $\text{C}_{48}\text{H}_{55}\text{O}_7\text{F}_3\text{SiNa}$: 851.3561, found: 851.3565.

The same procedure was followed for the preparation of (*R*)-MTPA-**128** (15 mg, 49%), which analyzed as follows: $^1\text{H NMR}$ (600 MHz, CDCl_3): $\delta = 7.56\text{--}7.55$ (m, 2H), $7.39\text{--}7.37$ (m, 6H), $7.36\text{--}7.32$ (m, 3H), $7.30\text{--}7.27$ (m, 6H), $7.24\text{--}7.22$ (m, 3H), 5.75 (d, $J = 2.9$ Hz, 1H), 5.35 (ddd, $J = 5.6, 3.8, 2.0$ Hz,

1H), 4.44 (ddd, $J = 8.5, 6.9, 2.9$ Hz, 1H), 4.02 (ddd, $J = 6.8, 5.1, 3.8$ Hz, 1H), 3.61 (d, $J = 1.1$ Hz, 3H), 3.18 (dd, $J = 9.1, 5.1$ Hz, 1H), 3.06 (dd, $J = 9.1, 6.8$ Hz, 1H), 2.35 (ddd, $J = 13.9, 8.6, 5.4$ Hz, 1H), 2.16 (ddd, $J = 13.9, 7.0, 2.0$ Hz, 1H), 1.80 (s, 3H), 1.08–1.05 ppm (m, 21H). MS (ESIpos) m/z (%): 851.4 (100 (M+Na)). HRMS (ESI): m/z calcd for $C_{48}H_{55}O_7F_3Si_7Na$: 851.3561, found: 851.3564.

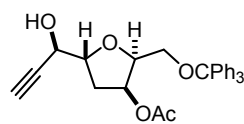
Both products were analyzed according to Hoyer and co-workers:^[118]

Table 4.3. Mosher ester analysis for the assignment of the C(3) stereocenter; arbitrary numbering as shown in the insert.



Assignment	(12 <i>S</i>)-128 [ppm]	(<i>S</i>)-MTPA-128 [ppm]	(<i>R</i>)-MTPA-128 [ppm]	Δ (δ (<i>S</i> - <i>R</i>)) [ppm]
3	4.47	5.70	5.75	-0.05
4	4.45	4.48	4.44	+0.04
5a	2.41	2.35	2.35	0.00
5b	2.10	2.17	2.16	+0.01
6	5.56	5.42	5.35	+0.07
7	4.30	4.23	4.02	+0.21
8a	3.33	3.27	3.18	+0.09
8b	3.14	3.12	3.06	+0.06
10	1.81	1.82	1.80	+0.02
TIPS-Me	1.07	1.03	1.06	-0.03

Alcohol 122. A solution of TBAF (1 M in THF, 61.2 μ L, 61.2 μ mol) was added to a solution of



alkynol (**12*R***)-**128** (30.0 mg, 48.9 μ mol) in THF (3 mL). The resulting mixture was stirred at rt for 20 min. The reaction was quenched with aq. sat. NH_4Cl (5 mL) and the aqueous layer extracted with EtOAc (5 \times 5 mL). The combined

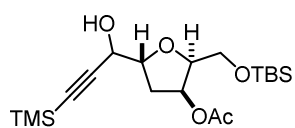
extracts were washed with brine (10 mL), dried over Na_2SO_4 , filtered and concentrated. The residue was purified by flash chromatography (hexanes/EtOAc 3:1 to 2:1) to yield the terminal alkyne **122** as a colorless oil (20.0 mg, 90%). $[\alpha]_D^{25} = +51.0$ ($c = 1.0$, $CHCl_3$). 1H NMR (400 MHz, $CDCl_3$): $\delta = 7.42$ – 7.39 (m, 6H), 7.32 – 7.27 (m, 6H), 7.26 – 7.21 (m, 3H), 5.55 (dt, $J = 3.7, 3.4$ Hz, 1H), 4.33–4.20 (m, 3H), 3.39 (dd, $J = 9.1, 5.2$ Hz, 1H), 3.18 (dd, $J = 9.0, 7.4$ Hz, 1H), 2.47 (d, $J = 2.1$ Hz, 1H), 2.38 (brs, 1H), 2.23–2.14 (m, 2H), 1.83 ppm (s, 3H). ^{13}C NMR (100 MHz, $CDCl_3$): $\delta = 170.2, 143.8$ (3C), 128.8 (6C), 127.9 (6C), 127.2 (3C), 86.9, 81.6, 80.60, 80.57, 74.4, 74.1, 64.9, 61.3, 35.2, 21.0 ppm. IR (film):

$\tilde{\nu}$ = 3435, 3284, 3058, 3022, 2929, 2889, 1737, 1491, 1448, 1374, 1236, 1075, 749, 705, 633 cm^{-1} . MS (EI) m/z (%): 244 (21), 243 (100), 183 (19), 165 (21). HRMS (ESIpos): m/z calcd for $\text{C}_{29}\text{H}_{28}\text{O}_5\text{Na}$: 479.1829, found: 479.1832.

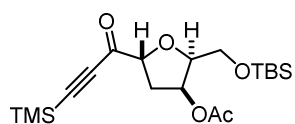
Alcohol **S30.** Et_3N (1.36 mL, 9.73 mmol), TBSCl (1.03 g, 6.81 mmol) and DMAP (39.6 mg, 0.32 mmol, 5 mol%) were sequentially added to a solution of diol **55** (935 mg, 6.49 mmol) in CH_2Cl_2 (40 mL) at 0 °C. The resulting mixture was stirred at rt for 7 h. The reaction was quenched with sat. aq. NaHCO_3 (25 mL) and the aqueous layer extracted with CH_2Cl_2 (3 \times 30 mL). The combined extracts were dried over Na_2SO_4 , filtered and concentrated. The residue was purified by flash chromatography (hexanes/ EtOAc 15:1 to 9:1) to afford alcohol **S30** as a colorless oil (1.35 g, 81%). $[\alpha]_{\text{D}}^{20} = -10.7$ ($c = 1.0$, CHCl_3). ^1H NMR (400 MHz, CDCl_3): $\delta = 5.97$ (ddd, $J = 16.9, 10.3, 6.3$ Hz, 1H), 5.27 (ddd, $J = 17.1, 1.5, 1.4$ Hz, 1H), 5.11 (ddd, $J = 10.3, 1.4, 1.2$ Hz, 1H), 4.52 (tdt, $J = 7.2, 6.2, 1.3$ Hz, 1H), 4.34 (ddd, $J = 6.6, 5.9, 4.4$ Hz, 1H), 3.89 (dt, $J = 6.5, 4.3$ Hz, 1H), 3.81 (dd, $J = 10.2, 4.1$ Hz, 1H), 3.58 (dd, $J = 10.2, 6.6$ Hz, 1H), 2.42 (ddd, $J = 12.7, 6.9, 6.7$ Hz, 1H), 1.82 (ddd, $J = 12.8, 6.9, 5.9$ Hz, 1H), 1.79 (brs, 1H), 0.90 (s, 9H), 0.07 ppm (s, 6H). ^{13}C NMR (100 MHz, CDCl_3): $\delta = 139.9, 115.4, 85.0, 79.5, 75.3, 64.7, 40.7, 26.0$ (3C), 18.4, -5.3 ppm (2C). IR (film): $\tilde{\nu} = 3431, 2954, 2929, 2857, 1472, 1361, 1255, 1131, 1091, 1005, 919, 836, 778, 673$ cm^{-1} . MS (EI) m/z (%): 193 (17), 147 (14), 117 (52), 109 (11), 89 (14), 77 (10), 75 (100), 73 (20), 67 (13), 59 (14), 55 (18), 45 (10), 41 (14), 39 (13). HRMS (ESIpos): m/z calcd for $\text{C}_{13}\text{H}_{26}\text{O}_3\text{SiNa}$: 281.1543, found: 281.1542.

Acetate **129.** PPh_3 (2.70 g, 10.3 mmol) was added to a solution of alcohol **S30** (1.33 g, 5.15 mmol) and acetic acid (0.59 mL, 10.3 mmol) in toluene (40 mL). The resulting mixture was stirred for 5 min and then cooled to 0 °C. DIAD (2.03 mL, 10.3 mmol) was added dropwise and the resulting mixture stirred at rt for 1 h. The reaction mixture was diluted with hexanes (40 mL), washed with water (50 mL) and brine (50 mL), dried over Na_2SO_4 , filtered and concentrated. The residue was purified by flash chromatography (hexanes/ t -butyl methyl ether 19:1) to yield acetate **129** as a colorless oil (1.30 g, 84%). $[\alpha]_{\text{D}}^{25} = +51.0$ ($c = 0.5$, CHCl_3). ^1H NMR (400 MHz, CDCl_3): $\delta = 5.84$ (ddd, $J = 17.0, 10.3, 6.6$ Hz, 1H), 5.47–5.41 (m, 1H), 5.27 (ddd, $J = 17.1, 1.4, 1.3$ Hz, 1H), 5.11 (ddd, $J = 10.1, 1.2, 1.0$ Hz, 1H), 4.58 (dt, $J = 9.4, 6.5$ Hz, 1H), 4.11 (ddd, $J = 7.1, 5.8, 3.8$ Hz, 1H), 3.80–3.72 (m, 2H), 2.19 (ddd, $J = 13.8, 6.2, 1.4$ Hz, 1H), 2.08 (s, 3H), 1.96 (ddd, $J = 14.1, 9.4, 5.0$ Hz, 1H), 0.87 (s, 9H), 0.05 (s, 3H), 0.04 ppm (s, 3H). ^{13}C NMR (100 MHz, CDCl_3): $\delta = 170.3, 138.4, 116.1, 81.1, 79.0, 74.4, 61.1, 39.6, 25.9$ (3C), 21.3, 18.4, $-5.2, -5.4$ ppm. IR (film): $\tilde{\nu} = 3083, 2954, 2930, 2884, 2857, 1743, 1472, 1426, 1373, 1232, 1186, 1088, 1017, 987, 932, 836, 776, 726, 666, 624, 602$ cm^{-1} . MS (ESIpos) m/z (%): 323.2 (100 (M+Na)). HRMS (ESIpos): m/z calcd for $\text{C}_{15}\text{H}_{28}\text{O}_4\text{SiNa}$: 323.1649, found: 323.1646.

Aldehyde 130. Ozone was bubbled through a solution of olefin **129** (250 mg, 0.83 mmol) in CH₂Cl₂ (55 mL) at -78 °C for 30 min, until the blue color persisted. Oxygen was then bubbled through the mixture for approx. one minute followed by argon until the solution was colorless. PPh₃ (327 mg, 1.25 mmol) was added in one portion and the mixture was allowed to reach rt overnight. The mixture was washed with sat. aq. NaHCO₃ (30 mL) and brine (30 mL). The organic layer was dried over Na₂SO₄, filtered and concentrated. The residue was purified by flash chromatography (hexanes/*t*-butyl methyl ether 10:1 to 2:1) to afford the title compound as a colorless oil (220 mg, 87%). $[\alpha]_D^{25} = +37.5$ (*c* = 0.4, CHCl₃). ¹H NMR (400 MHz, CDCl₃): δ = 9.71 (d, *J* = 1.8 Hz, 1H), 5.42 (td, *J* = 4.2, 3.0 Hz, 1H), 4.49 (td, *J* = 8.2, 1.8 Hz, 1H), 4.11 (ddd, *J* = 6.7, 5.6, 3.8 Hz, 1H), 3.83 (dd, *J* = 10.4, 5.5 Hz, 1H), 3.79 (dd, *J* = 10.2, 6.4 Hz, 1H), 2.28 (dd, *J* = 3.6, 1.8 Hz, 1H), 2.26 (dd, *J* = 3.6, 2.2 Hz, 1H), 2.08 (s, 3H), 0.88 (s, 9H), 0.06 (s, 3H), 0.05 ppm (s, 3H). ¹³C NMR (100 MHz, CDCl₃): δ = 201.8, 170.2, 82.7, 81.6, 73.2, 61.0, 34.5, 25.9 (3C), 21.1, 18.4, -5.3, -5.4 ppm. IR (film): $\tilde{\nu}$ = 2955, 2930, 2885, 2857, 1738, 1472, 1443, 1374, 1237, 1092, 837, 777 cm⁻¹. MS (ESIpos) *m/z* (%): 325.1 (100 (M+Na)). HRMS (ESIpos): *m/z* calcd for C₁₄H₂₆O₅SiNa: 325.1442, found: 325.1440.



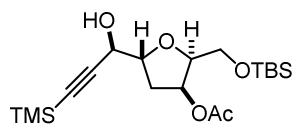
Alkynol 131. A solution of *n*-BuLi (1.6 M in hexane, 93.6 μL, 0.15 mmol) was added to a solution of TMS-acetylene (28.0 μL, 0.20 mmol) in Et₂O (1 mL) at -78 °C and the resulting mixture was stirred at that temperature for 30 min. Next, a solution of Lil (66.8 mg, 0.50 mmol) in Et₂O (1 mL) was added and the resulting mixture was stirred for 30 min at -40 °C. In a second flask, a solution of aldehyde **130** (30 mg, 0.10 mmol) in Et₂O (1 mL) was cooled to -25 °C. The lithium-acetylene solution was added dropwise to the aldehyde solution and stirring was continued overnight. The reaction was quenched with aq. sat. NH₄Cl (4 mL) and the aqueous layer extracted with EtOAc (3 × 8 mL). The combined extracts were dried over Na₂SO₄, filtered and concentrated. The residue was purified by flash chromatography (hexanes/EtOAc 9:1) to afford alkynol **131** as a colorless oil (15.0 mg, 37%, diastereomeric mixture, d.r. 1:1). The diastereomeric mixture was oxidized to the ynone **S31**.



Ynone S31. NaHCO₃ (25.2 mg, 56.2 μmol) was added to a solution of alkynol **131** (15 mg, 37.4 μmol) in CH₂Cl₂ (1 mL). DMP (23.8 mg, 56.2 μmol) was added in one portion and the resulting mixture was stirred at rt for 3 h. The reaction was quenched with aq. sat. NaHCO₃ (1 mL) and the aqueous layer extracted with CH₂Cl₂ (3 × 4 mL). The combined extracts were dried over Na₂SO₄, filtered and concentrated. The residue was purified by flash chromatography (hexanes/*t*-butyl methyl ether 9:1) to afford ynone **S31** as a colorless oil (9.1 mg, 61%). $[\alpha]_D^{20} = +30.2$ (*c* = 0.42, CHCl₃). ¹H NMR (400 MHz, CDCl₃): δ = 5.47–5.41 (m, 1H), 4.63 (td, *J* = 8.2, 0.7 Hz, 1H), 4.21 (ddd, *J* = 7.2, 5.3, 3.7 Hz, 1H), 3.84 (dd, *J* = 10.2, 5.3 Hz, 1H), 3.78 (dd, *J* = 10.1, 7.2 Hz, 1H), 2.39 (dd, *J* = 8.0, 2.3 Hz, 1H), 2.37 (dd, *J* = 8.4, 4.9 Hz, 1H), 2.08 (s, 3H),

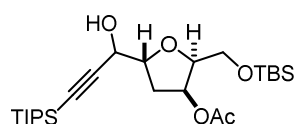
0.87 (s, 9H), 0.25 (s, 9H), 0.054 (s, 3H), 0.045 ppm (s, 3H). ^{13}C NMR (100 MHz, CDCl_3): δ = 187.1, 170.2, 102.7, 99.8, 82.7, 82.6, 73.3, 60.7, 36.5, 25.9 (3C), 21.1, 18.3, -0.7 (3C), -5.3 , -5.4 ppm. IR (film): $\tilde{\nu}$ = 2957, 2930, 2857, 1745, 1683, 1472, 1374, 1252, 1231, 1091, 846, 778 cm^{-1} . MS (ESIpos) m/z (%): 421.2 (100 (M+Na)). HRMS (ESIpos): m/z calcd for $\text{C}_{19}\text{H}_{34}\text{O}_5\text{Si}_2\text{Na}$: 421.1837, found: 421.1837.

Alkynol (12R)-131. A solution of ynone **S31** (9.0 mg, 23 μmol) in CH_2Cl_2 (0.5 mL) was added to a solution of (*S,S*)-Teth-TsDpen-RuCl (1.0 mg, 1.6 μmol , 7 mol%) in $\text{HCO}_2\text{H}/\text{Et}_3\text{N}$ (38 μL) and the resulting mixture was stirred at rt for 45 min. The reaction was quenched with aq. half-sat. NH_4Cl (1 mL) and the

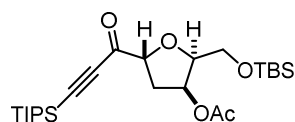


aqueous layer extracted with EtOAc (3×2 mL). The combined extracts were dried over Na_2SO_4 , filtered and concentrated. The residue was purified by flash chromatography (fine SiO_2 , hexanes/EtOAc 10:1) to afford alkynol (12R)-**131** as a colorless oil (7.5 mg, 83%, d.r. > 20:1). $[\alpha]_{\text{D}}^{20}$ = +37.8 (c = 0.5, CHCl_3). ^1H NMR (400 MHz, CDCl_3): δ = 5.42 (ddd, J = 3.5, 3.5, 3.4 Hz, 1H), 4.31–4.21 (m, 2H), 4.09 (ddd, J = 7.1, 5.3, 3.6 Hz, 1H), 3.80–3.72 (m, 2H), 2.39 (brs, 1H), 2.22–2.14 (m, 2H), 2.08 (s, 3H), 0.87 (s, 9H), 0.16 (s, 9H), 0.05 (s, 3H), 0.04 ppm (s, 3H). ^{13}C NMR (100 MHz, CDCl_3): δ = 170.3, 102.9, 91.4, 81.8, 80.8, 74.2, 65.8, 61.0, 35.4, 25.9 (3C), 21.2, 18.4, -0.1 (3C), -5.2 , -5.3 ppm. IR (film): $\tilde{\nu}$ = 3435, 2956, 2930, 2886, 2858, 1745, 1374, 1251, 1095, 842, 778 cm^{-1} . MS (EI) m/z (%): 343 (17), 283 (25), 213 (18), 193 (14), 153 (13), 149 (12), 147 (42), 146 (10), 145 (80), 143 (26), 129 (16), 119 (15), 117 (43), 115 (119, 91 (13), 89 (87), 75 (46), 73 (100), 43 (21). HRMS (ESIpos): m/z calcd for $\text{C}_{19}\text{H}_{36}\text{O}_5\text{Si}_2\text{Na}$: 423.1994, found: 423.1995.

Alkynol S32. A solution of *n*-BuLi (1.6 M in hexane, 0.66 mL, 1.01 mmol) was added to a solution of TIPS-acetylene (0.35 mL, 1.57 mmol) in Et_2O (4 mL) at -78 $^\circ\text{C}$ and the resulting mixture was stirred at that temperature for 30 min. Next, a solution of Lil (420 mg, 3.14 mmol) in Et_2O (1 mL) was added and the resulting mixture stirred for 30 min at -40 $^\circ\text{C}$. In a second flask, a solution of aldehyde **130** (190 mg, 0.63 mmol) in Et_2O (3 mL) was cooled to -25 $^\circ\text{C}$. The lithium-acetylene solution was added dropwise to the aldehyde solution and stirring was continued overnight. The reaction was quenched with aq. sat. NH_4Cl (8 mL) and the aqueous layer extracted with EtOAc (3×10 mL). The combined extracts were dried over Na_2SO_4 , filtered and concentrated. The residue was purified by flash chromatography (hexanes/*t*-butyl methyl ether 9:1) to afford alkynol **S32** as a colorless oil (171 mg, 67%, diastereomeric mixture, d.r. 5:1). The diastereomeric mixture was oxidized to the ynone **135**.

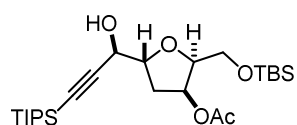


Ynone 135. NaHCO_3 (25.2 mg, 1.65 mmol) was added to a solution of alkynol **S32** (100 mg, 0.21 mmol) in CH_2Cl_2 (5 mL). DMP (131 mg, 0.31 mmol) was added in one portion and the resulting mixture was stirred at rt for 3 h. The reaction



was quenched with aq. sat. NaHCO₃ (5 mL) and the aqueous layer extracted with CH₂Cl₂ (3 × 5 mL). The combined extracts were dried over Na₂SO₄, filtered and concentrated. The residue was purified by flash chromatography (hexanes/*t*-butyl methyl ether 19:1) to afford ynone **135** as a colorless oil (65 mg, 65%). $[\alpha]_D^{20} = +36.7$ (*c* = 1.0, CHCl₃). ¹H NMR (400 MHz, CDCl₃): δ = 5.45 (ddd, *J* = 4.9, 3.6, 2.5 Hz, 1H), 4.63 (td, *J* = 8.2, 0.7 Hz, 1H), 4.23 (ddd, *J* = 7.5, 5.2, 3.7 Hz, 1H), 3.83 (dd, *J* = 10.0, 5.2 Hz, 1H), 3.77 (dd, *J* = 10.0, 7.5 Hz, 1H), 2.39 (dd, *J* = 6.2, 1.8 Hz, 1H), 2.38 (dd, *J* = 8.0, 3.9 Hz, 1H), 2.08 (s, 3H), 1.19–1.08 (m, 21H), 0.87 (s, 9H), 0.044 (s, 3H), 0.035 ppm (s, 3H). ¹³C NMR (100 MHz, CDCl₃): δ = 187.1, 170.2, 101.9, 100.5, 82.8, 82.7, 73.3, 60.5, 36.7, 25.9 (3C), 21.1, 18.6 (3C), 18.3, 11.1 (6C), –5.3, –5.4 ppm. IR (film): $\tilde{\nu}$ = 2946, 2867, 1747, 1682, 1464, 1373, 1230, 1097, 1069, 838, 778, 608 cm⁻¹. MS (EI) *m/z* (%): 427 (12), 426 (31), 425 (95), 366 (20), 365 (65), 213 (19), 209 (19), 173 (18), 163 (10), 159 (17), 157 (12), 146 (13), 145 (100), 133 (13), 131 (11), 130 (11), 129 (84), 119 (10), 117 (53), 115 (29), 103 (16), 91 (10), 89 (100), 87 (11), 75 (42), 73 (74), 59 (15), 43 (21). HRMS (ESIpos): *m/z* calcd for C₂₅H₄₆O₅Si₂Na: 505.2776, found: 505.2778.

Alkynol (12R)-S32. A solution of ynone **135** (63.2 mg, 0.13 mmol) in CH₂Cl₂ (2.4 mL) was added to a



solution of (*S,S*)-Teth-TsDpen-RuCl (5.7 mg, 9.2 μmol, 7 mol%) in HCO₂H/Et₃N (0.22 mL) and the resulting mixture was stirred at rt for 45 min. The reaction was quenched with aq. half-sat. NH₄Cl (2 mL) and the

aqueous layer extracted with EtOAc (3 × 5 mL). The combined extracts were dried over Na₂SO₄, filtered and concentrated. The residue was purified by flash chromatography (fine SiO₂, hexanes/*t*-butyl methyl ester 9:1) to afford alkynol (12R)-**S32** as a colorless oil (58.0 mg, 96%, d.r. > 20:1). $[\alpha]_D^{20} = +40.7$ (*c* = 1.0, CHCl₃). ¹H NMR (400 MHz, CDCl₃): δ = 5.43 (ddd, *J* = 4.1, 3.9, 2.9 Hz, 1H), 4.34 (d, *J* = 6.7 Hz, 1H), 4.26 (dt, *J* = 7.7, 7.0 Hz, 1H), 4.10 (ddd, *J* = 6.6, 5.8, 3.6 Hz, 1H), 3.78–3.72 (m, 2H), 2.21–2.14 (m, 2H), 2.08 (s, 3H), 1.10–1.02 (m, 21H), 0.87 (s, 9H), 0.044 (s, 3H), 0.037 ppm (s, 3H). ¹³C NMR (100 MHz, CDCl₃): δ = 170.3, 104.9, 87.7, 81.7, 81.0, 74.1, 66.0, 61.0, 35.5, 25.9 (3C), 21.2, 18.7 (3C), 18.3, 11.2 (6C), –5.3, –5.4 ppm. IR (film): $\tilde{\nu}$ = 3425, 2930, 2891, 2865, 1745, 1463, 1374, 1238, 1094, 1074, 837, 777, 678 cm⁻¹. MS (EI) *m/z* (%): 441 (12), 427 (25), 367 (23), 273 (14), 213 (22), 173 (14), 157 (24), 146 (13), 145 (100), 143 (22), 129 (15), 119 (17), 117 (24), 115 (32), 103 (10), 91 (13), 89 (66), 87 (15), 75 (33), 73 (46), 59 (15), 43 (11). HRMS (ESIpos): *m/z* calcd for C₂₅H₄₈O₅Si₂Na: 507.2933, found: 507.2935.

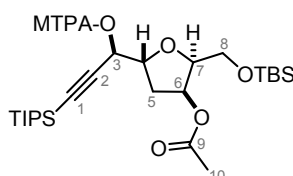
Mosher ester analysis of alcohol (12R)-S32. Triethylamine (5.8 μL, 41 μmol) was added to a solution of alcohol (12R)-**S32** (5.0 mg, 10 μmol) in CH₂Cl₂ (0.5 mL) followed by (*R*)-(-)- α -methoxy- α -trifluoromethyl-phenylacetyl chloride ((*R*)-MTPA-Cl) (3.9 μL, 21 μmol). The reaction was stirred at rt for 16 h, then quenched with sat. aq. NaHCO₃ (3 mL) and the mixture was extracted with CH₂Cl₂ (3 × 5 mL). The combined extracts were dried over Na₂SO₄, filtered and concentrated. The residue

was purified by flash chromatography (hexanes/EtOAc 19:1 to 9:1) to give the corresponding (*S*)-Mosher ester (**(S)-MTPA-S32** (5.5 mg, 76%), which analyzed as follows: ^1H NMR (400 MHz, CDCl_3): δ = 7.59–7.52 (m, 2H), 7.41–7.36 (m, 3H), 5.68 (d, J = 6.3 Hz, 1H), 5.38 (ddd, J = 5.1, 3.5, 1.3 Hz, 1H), 4.34 (dt, J = 8.2, 6.6 Hz, 1H), 4.10 (ddd, J = 6.3, 6.1, 3.5 Hz, 1H), 3.74–3.70 (m, 1H), 3.70–3.67 (m, 1H), 3.57 (d, J = 1.2 Hz, 3H), 2.28 (ddd, J = 13.9, 8.3, 5.3 Hz, 1H), 2.10 (ddd, J = 14.4, 7.0, 1.4 Hz, 1H), 2.05 (s, 3H), 1.09–1.03 (m, 21H), 0.85 (s, 9H), 0.03 (s, 3H), 0.02 ppm (s, 3H). MS (EI) m/z (%): 657 (11), 276 (24), 275 (100), 233 (14), 189 (62), 183 (12), 173 (10), 145 (37), 117 (13), 115 (11), 89 (55), 73 (28). HRMS (ESIpos): m/z calcd for $\text{C}_{35}\text{H}_{55}\text{O}_7\text{F}_3\text{Si}_2\text{Na}$: 723.3331, found: 723.3336.

The same procedure was followed for the preparation of (**R**)-MTPA-S32 (4.6 mg, 63%), which analyzed as follows: ^1H NMR (400 MHz, CDCl_3): δ = 7.57–7.53 (m, 2H), 7.40–7.34 (m, 3H), 5.59 (d, J = 7.5 Hz, 1H), 5.42 (ddd, J = 5.0, 3.5, 1.6 Hz, 1H), 4.41 (dt, J = 8.4, 7.3 Hz, 1H), 4.12 (ddd, J = 6.7, 5.8, 3.5 Hz, 1H), 3.74 (dd, J = 10.2, 6.8 Hz, 1H), 3.70 (dd, J = 10.2, 5.9 Hz, 1H), 3.58 (d, J = 1.2 Hz, 3H), 2.27 (ddd, J = 13.5, 8.3, 5.1 Hz, 1H), 2.19 (ddd, J = 14.4, 7.0, 1.5 Hz, 1H), 2.07 (s, 3H), 1.04–1.01 (m, 21H), 0.86 (s, 9H), 0.03 (s, 3H), 0.02 ppm (s, 3H). MS (EI) m/z (%): 657 (11), 276 (24), 275 (100), 233 (14), 189 (62), 183 (12), 173 (10), 145 (37), 117 (13), 115 (11), 89 (55), 73 (28). HRMS (ESIpos): m/z calcd for $\text{C}_{35}\text{H}_{55}\text{O}_7\text{F}_3\text{Si}_2\text{Na}$: 723.3331, found: 723.3336.

Both products were analyzed according to Hoye and co-workers.^[118]

Table 4.4. Mosher ester analysis for the assignment of the C(3) stereocenter; arbitrary numbering as shown in the insert.



Assignment	(12 <i>R</i>)-S32 [ppm]	(<i>S</i>)-MTPA-S32 [ppm]	(<i>R</i>)-MTPA-S32 [ppm]	Δ (δ (<i>S</i> - <i>R</i>)) [ppm]
3	4.34	5.68	5.59	+0.09
4	4.26	4.34	4.41	-0.07
5a	2.19	2.28	2.27	+0.01
5b	2.16	2.10	2.19	-0.09
6	5.43	5.38	5.42	-0.04
7	4.10	4.10	4.12	-0.02
8a	3.76	3.72	3.74	-0.02
8b	3.74	3.69	3.70	-0.01
10	2.08	2.05	2.07	-0.02
TIPS-Me	1.05	1.06	1.02	+0.04

Alcohol 123. A solution of TBAF (0.5 M in THF, 0.24 mL, 0.12 mmol) was added to a solution of alkynol (12*R*)-**S32** (58 mg, 0.12 mmol) in THF (22 mL) at -35°C . The resulting mixture was stirred at this temperature for 30 h. The reaction was quenched with aq. half-sat. NH_4Cl (10 mL) and the aqueous layer extracted with EtOAc (5 \times 15 mL). The combined extracts were washed with brine (50 mL), dried over Na_2SO_4 , filtered and concentrated. The residue was purified by flash chromatography (hexanes/EtOAc 9:1) to yield the terminal alkyne **123** as a colorless oil (24.0 mg, 61%) along with the desilylated alcohol as a byproduct. $[\alpha]_{\text{D}}^{20} = +46.9$ ($c = 1.0$, CHCl_3). $^1\text{H NMR}$ (400 MHz, CDCl_3): $\delta = 5.43$ (ddd, $J = 4.1, 4.0, 2.8$ Hz, 1H), 4.32–4.25 (m, 2H), 4.11 (ddd, $J = 6.8, 5.7, 3.7$ Hz, 1H), 3.81–3.74 (m, 2H), 2.46 (d, $J = 2.1$ Hz, 1H), 2.21–2.15 (m, 2H), 2.07 (s, 3H), 0.87 (s, 9H), 0.05 (s, 3H), 0.04 ppm (s, 3H). $^{13}\text{C NMR}$ (100 MHz, CDCl_3): $\delta = 170.3, 81.9, 81.6, 80.7, 74.3, 74.1, 65.0, 61.0, 35.2, 25.9$ (3C), 21.2, 18.4, $-5.3, -5.4$ ppm. IR (film): $\tilde{\nu} = 3454, 2929, 2857, 1742, 1472, 1375, 1250, 1093, 838, 778$ cm^{-1} . MS (EI) m/z (%): 271 (16), 213 (12), 212 (13), 211 (79), 193 (19), 169 (11), 167 (17), 159 (11), 145 (44), 143 (29), 129 (47), 119 (15), 117 (74), 91 (16), 89 (55), 81 (119), 75 (100), 73 (58), 43 (38). HRMS (ESIpos): m/z calcd for $\text{C}_{16}\text{H}_{28}\text{O}_5\text{SiNa}$: 351.1598, found: 351.1599.

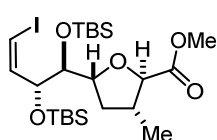
Diol 132. Obtained as a byproduct from the reaction described above *via* TBS-deprotection followed by acetate migration as a colorless oil (5.7 mg, 22%). $[\alpha]_{\text{D}}^{20} = +33.0$ ($c = 0.33$, CHCl_3). $^1\text{H NMR}$ (400 MHz, CDCl_3): $\delta = 4.43$ (dd, $J = 11.6, 7.2$ Hz, 1H), 4.32–4.25 (m, 2H), 4.23 (dd, $J = 5.8, 2.2$ Hz, 1H), 4.10 (dd, $J = 11.6, 5.3$ Hz, 1H), 3.98 (ddd, $J = 7.2, 5.3, 3.0$ Hz, 1H), 2.41 (d, $J = 2.2$ Hz, 1H), 2.12 (ddd, $J = 13.5, 6.3, 1.1$ Hz, 1H), 2.04 (s, 3H), 2.02 ppm (m, 1H). $^{13}\text{C NMR}$ (100 MHz, CDCl_3): $\delta = 171.9, 81.7, 81.1, 80.7, 74.3, 72.0, 65.1, 62.2, 37.1, 21.1$ ppm. IR (film): $\tilde{\nu} = 3436, 3310, 2930, 2886, 2858, 1742, 1472, 1375, 1250, 1095, 838, 778$ cm^{-1} . MS (ESIpos) m/z (%): 237.1 (100 (M+Na)). HRMS (ESIpos): m/z calcd for $\text{C}_{10}\text{H}_{14}\text{O}_5\text{Na}$: 237.0733, found: 237.0731.

4.3.7 Synthesis of the Southern Vinyl Iodide Fragments 137 and 139

Alcohol 136. Pyridine (2.78 mL, 34.4 mmol) was slowly added to a Teflon[®] vial charged with HF-pyridine (0.49 mL, 5.43 mmol) and the resulting mixture diluted with THF (3 mL). This solution was added dropwise to a solution of silyl ether **84** (140 mg, 0.21 mmol) in THF (1 mL) in a second Teflon[®] vial. The resulting mixture was stirred at ambient temperature for 9 h. The mixture was diluted with EtOAc (5 mL) and the reaction was carefully quenched with aq. sat. NaHCO_3 (10 mL). The layers were separated and the aqueous layer was extracted with EtOAc (4 \times 15 mL). The combined organic extracts were dried over Na_2SO_4 , filtered and concentrated. The residue was purified by flash chromatography (hexanes/EtOAc 30:1)

to afford the title compound **136** as a colorless oil (105 mg, 91%). $[\alpha]_D^{20} = +5.8$ ($c = 1.0$, CHCl_3). $^1\text{H NMR}$ (400 MHz, CDCl_3): $\delta = 6.38$ (ddd, $J = 8.2, 7.7$ Hz, 1H), 6.30 (d, $J = 7.7$ Hz, 1H), 4.32 (dd, $J = 8.2, 2.0$ Hz, 1H), 3.81 (ddd, $J = 10.0, 7.7, 5.6$ Hz, 1H), 3.74–3.70 (m, 1H), 3.63 (dd, $J = 7.7, 2.1$ Hz, 1H), 3.54–3.47 (m, 2H), 2.33 (ddd, $J = 12.1, 7.2, 6.2$ Hz, 1H), 2.10 (ddqd, $J = 13.3, 9.0, 6.5, 4.4$ Hz, 1H), 1.91 (brt, $J = 6.1$ Hz, 1H), 1.37 (td, $J = 12.1, 11.2, 10.0$ Hz, 1H), 1.04 (d, $J = 6.5$ Hz, 3H), 0.91 (s, 9H), 0.88 (s, 9H), 0.12 (s, 3H), 0.10 (s, 3H), 0.09 (s, 3H), 0.07 ppm (s, 3H). $^{13}\text{C NMR}$ (100 MHz, CDCl_3): $\delta = 141.8, 84.9, 82.0, 80.7, 79.6, 76.9, 63.2, 38.6, 35.4, 26.2$ (3C), 26.1 (3C), 18.6, 18.3, 16.4, $-3.9, -4.1, -4.17, -4.20$ ppm. IR (film): $\tilde{\nu} = 3447, 2954, 2928, 2856, 1462, 1388, 1361, 1252, 1145, 1077, 1055, 1005, 959, 833, 776, 674$ cm^{-1} . MS (ESIpos) m/z (%): 579.2 (100 (M+Na)). HRMS (ESIpos): m/z calcd for $\text{C}_{22}\text{H}_{45}\text{O}_4\text{Si}_2\text{Na}$: 579.1793, found: 579.1794.

Ester 137. NaHCO_3 (38.0 mg, 0.45 mmol), PIDA (107 mg, 0.33 mmol) and TEMPO (4.7 mg, 30 μmol)



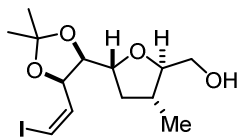
were sequentially added to a solution of alcohol **136** (84.0 mg, 0.15 mmol) in $\text{MeCN}/\text{H}_2\text{O}$ (1:1, 1.5 mL). The resulting mixture was stirred at rt for 20 h. The mixture was diluted with MeCN (5 mL) and the reaction was quenched with pH 5

phosphate buffer (0.5 mL). After filtration through a short pad of Na_2SO_4 , the solvent was removed under reduced pressure. The residue was partitioned between MeCN (5 mL) and cyclohexane (5 mL). The cyclohexane layer was extracted with MeCN (3×8 mL). The combined MeCN-extracts were dried over Na_2SO_4 , filtered and concentrated. The crude acid was used in the next step without further purification.

A solution of TMSCHN_2 (2 M in Et_2O , 0.14 mL, 0.27 mmol) was added to a solution of the crude acid (86 mg, 0.15 mmol) in THF (1.5 mL) at 0 $^\circ\text{C}$. The resulting yellow mixture was stirred at 0 $^\circ\text{C}$ for 30 min before the reaction was carefully quenched with pH 5 phosphate buffer (2 mL). The layers were separated and the aqueous layer was extracted with *t*-butyl methyl ether (3×5 mL). The combined organic extracts were dried over Na_2SO_4 , filtered and concentrated. The residue was purified by flash chromatography (hexanes/*t*-butyl methyl ether 49:1) to yield the title compound **137** as a colorless oil (58.0 mg, 66%, two steps). $[\alpha]_D^{20} = +16.7$ ($c = 1.0$, CHCl_3). $^1\text{H NMR}$ (400 MHz, CDCl_3): $\delta = 6.39$ (dd, $J = 8.3, 7.6$ Hz, 1H), 6.29 (dd, $J = 7.6, 0.7$ Hz, 1H), 4.37 (ddd, $J = 8.2, 2.3, 0.8$ Hz, 1H), 4.03 (ddd, $J = 10.3, 7.2, 5.3$ Hz, 1H), 3.98 (d, $J = 8.6$ Hz, 1H), 3.74 (s, 3H), 3.71 (dd, $J = 7.2, 2.3$ Hz, 1H), 2.36 (dddq, $J = 10.5, 8.5, 6.6, 6.5$ Hz, 1H), 2.27 (ddd, $J = 12.1, 6.9, 5.3$ Hz, 1H), 1.44 (dt, $J = 11.8, 10.5$ Hz, 1H), 1.20 (d, $J = 6.5$ Hz, 3H), 0.90 (s, 9H), 0.88 (s, 9H), 0.13 (s, 3H), 0.09 (s, 6H), 0.08 ppm (s, 3H). $^{13}\text{C NMR}$ (100 MHz, CDCl_3): $\delta = 173.6, 141.9, 82.7, 82.3, 81.4, 79.5, 76.8, 52.0, 39.9, 37.7, 26.2$ (3C), 26.1 (3C), 18.5, 18.3, 17.5, $-3.9, -4.2$ (2C), -4.3 ppm. IR (film): $\tilde{\nu} = 2954, 2928, 2888, 2956, 1759, 1738, 1611, 1472, 1462, 1389, 1361, 1253, 1201, 1146, 1078, 1005, 962, 835, 777, 674$ cm^{-1} . MS (EI) m/z (%): 528 (18), 527 (59), 457 (12), 371 (22), 331 (35), 325 (20), 321 (12), 297 (38), 288 (13), 287 (60), 241 (12),

186 (12), 185 (73), 175 (36), 171 (23), 159 (10), 155 (77), 143 (39), 133 (15), 127 (19), 115 (87), 113 (10), 95 (14), 89 (149), 83 (13), 75 (21), 73 (100), 59 (10). HRMS (ESIpos): m/z calcd for $C_{23}H_{45}O_5Si_2Na$: 607.1742, found: 607.1746.

Alcohol 138. Pyridine (3.46 mL, 42.7 mmol) was slowly added to a Teflon® vial charged with HF-pyridine (0.61 mL, 6.74 mmol) and the resulting mixture was diluted with THF (3.5 mL). This solution was added dropwise to a solution of silyl ether **116** (125 mg, 0.26 mmol) in THF (1.5 mL) in a second Teflon® vial. The resulting



mixture was stirred at ambient temperature for 4 h. The mixture was diluted with EtOAc (5 mL) and the reaction was carefully quenched with aq. sat. $NaHCO_3$ (5 mL). The layers were separated and the aqueous layer was extracted with EtOAc (4 × 10 mL). The combined organic extracts were dried over Na_2SO_4 , filtered and concentrated. The residue was purified by flash chromatography (hexanes/EtOAc 4:1 to 2:1) to afford the title compound **138** as a colorless oil (94.0 mg, 98%). $[\alpha]_D^{20} = -50.7$ ($c = 1.0$, $CHCl_3$). 1H NMR (400 MHz, $CDCl_3$): $\delta = 6.50$ (dd, $J = 7.7, 1.0$ Hz, 1H), 6.34 (dd, $J = 8.7, 7.7$ Hz, 1H), 4.82 (ddd, $J = 8.6, 6.3, 1.0$ Hz, 1H), 4.16 (t, $J = 6.6$ Hz, 1H), 3.94 (ddd, $J = 9.7, 7.0, 5.7$ Hz, 1H), 3.80 (dd, $J = 11.9, 2.7$ Hz, 1H), 3.58 (ddd, $J = 8.9, 3.9, 2.7$ Hz, 1H), 3.50 (dd, $J = 11.9, 4.0$ Hz, 1H), 2.21–2.12 (m, 1H), 2.12–2.06 (m, 1H), 1.98 (brs, 1H), 1.51 (s, 3H), 1.42 (s, 3H), 1.42–1.32 (m, 1H), 1.05 ppm (d, $J = 6.2$ Hz, 3H). ^{13}C NMR (100 MHz, $CDCl_3$): $\delta = 137.3, 110.1, 86.3, 85.8, 81.2, 79.7, 77.3, 62.4, 37.9, 34.7, 27.9, 25.7, 16.3$ ppm. IR (film): $\tilde{\nu} = 3442, 2983, 2957, 2930, 2872, 1455, 1372, 1249, 1251, 1160, 1088, 1053, 926, 866, 816$ cm^{-1} . MS (ESIpos) m/z (%): 391.0 (100 (M+Na)). HRMS (ESIpos): m/z calcd for $C_{13}H_{21}O_4INa$: 391.0377, found: 391.0375.

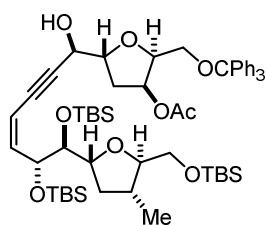
Ester 139. $NaHCO_3$ (65.9 mg, 0.78 mmol), PIDA (185 mg, 0.57 mmol) and TEMPO (8.1 mg, 52 μ mol) were sequentially added to a solution of alcohol **138** (94.0 mg, 0.26 mmol) in MeCN/ H_2O (1:1, 3 mL). The resulting mixture was stirred at rt for 20 h. The mixture was diluted with MeCN (5 mL) and the reaction was quenched with pH 5 phosphate buffer sat. with NaCl (1 mL). After filtration through a short pad of Na_2SO_4 , the solvent was removed under reduced pressure. The residue was partitioned between MeCN (5 mL) and cyclohexane (5 mL). The cyclohexane layer was extracted with MeCN (3 × 8 mL). The combined MeCN-extracts were dried over Na_2SO_4 , filtered and concentrated. The crude acid was used in the next step without further purification.

A solution of $TMSCHN_2$ (2 M in Et_2O , 0.23 mL, 0.46 mmol) was added to a solution of the crude acid (97.6 mg, 0.26 mmol) in THF (2.5 mL) at 0 °C. The resulting yellow mixture was stirred at 0 °C for 1 h before the reaction was carefully quenched with pH 5 phosphate buffer (3 mL). The layers were separated and the aqueous layer was extracted with *t*-butyl methyl ether (3 × 5 mL). The combined organic extracts were dried over Na_2SO_4 , filtered and concentrated. The residue was purified by flash

chromatography (hexanes/*t*-butyl methyl ether 6:1) to yield the title compound **139** as a colorless oil (73.2 mg, 72%, two steps). $[\alpha]_D^{20} = -62.5$ ($c = 0.8$, CHCl_3). $^1\text{H NMR}$ (500 MHz, CDCl_3): $\delta = 6.51$ (dd, $J = 7.7, 1.0$ Hz, 1H), 6.45 (dd, $J = 8.3, 7.7$ Hz, 1H), 4.86 (ddd, $J = 8.3, 6.3, 0.9$ Hz, 1H), 4.18 (t, $J = 6.3$ Hz, 1H), 4.12 (dt, $J = 9.4, 6.0$ Hz, 1H), 4.06 (d, $J = 7.7$ Hz, 1H), 3.72 (s, 3H), 2.43–2.31 (m, 1H), 2.12 (ddd, $J = 12.1, 7.4, 5.8$ Hz, 1H), 1.51 (s, 3H), 1.41 (s, 3H), 1.44 – 1.36 (m, 1H), 1.20 ppm (d, $J = 6.6$ Hz, 3H). $^{13}\text{C NMR}$ (125 MHz, CDCl_3): $\delta = 173.3, 137.5, 110.1, 85.8, 83.8, 80.1, 79.9, 78.9, 52.1, 39.6, 37.2, 27.6, 25.7, 18.2$ ppm. IR (film): $\tilde{\nu} = 2981, 2961, 2933, 2875, 1753, 1615, 1437, 1379, 1274, 1249, 1212, 1164, 1130, 1086, 1057, 867$ cm^{-1} . MS (ESIpos) m/z (%): 419.0 (100 (M+Na)). HRMS (ESIpos): m/z calcd for $\text{C}_{14}\text{H}_{21}\text{O}_5\text{INa}$: 419.0326, found: 419.0322.

4.3.8 Fragment Assembly and Hydrometalations

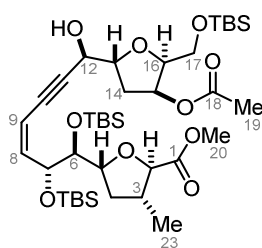
Enyne 140. Et_3N was degassed by three freeze-pump-thaw cycles prior to use. CuI (0.8 mg, 4.5 μmol ,



20 mol%) and $\text{Pd}(\text{dppf})\text{Cl}_2 \cdot \text{CH}_2\text{Cl}_2$ (0.9 mg, 1.1 μmol , 5 mol%) were added to a solution of vinyl iodide **84** (15 mg, 22 μmol) in Et_3N (0.3 mL) and the resulting mixture was warmed to 55 °C. A solution of alkyne **122** (10 mg, 22 μmol) in Et_3N (0.3 mL) was added *via* syringe over 2.5 h. The dark brown suspension was stirred for additional 1.5 h at 55 °C. All volatiles were removed in vacuo

and the residue was purified by flash chromatography (pentane/*t*-butyl methyl ether 15:1 to 5:1) to yield the title compound **140** as a colorless oil (7.7 mg, 34%). $[\alpha]_D^{20} = +21.1$ ($c = 1.0$, CHCl_3). $^1\text{H NMR}$ (400 MHz, CDCl_3): $\delta = 7.41$ –7.38 (m, 6H), 7.32–7.27 (m, 6H), 7.26–7.20 (m, 3H), 6.08 (dd, $J = 11.0, 9.4$ Hz, 1H), 5.58 (td, $J = 3.8, 2.4$ Hz, 1H), 5.51 (dd, $J = 11.0, 1.9$ Hz, 1H), 4.56 (dd, $J = 9.5, 2.3$ Hz, 1H), 4.38 (dd, $J = 5.7, 1.9$ Hz, 1H), 4.29 (ddd, $J = 8.3, 5.0, 3.4$ Hz, 1H), 4.20 (dt, $J = 8.2, 6.5$ Hz, 1H), 3.71 (ddd, $J = 10.0, 7.6, 5.6$ Hz, 1H), 3.63–3.58 (m, 3H), 3.45 (dt, $J = 9.1, 4.7$ Hz, 1H), 3.39 (dd, $J = 8.9, 5.1$ Hz, 1H), 3.17 (dd, $J = 8.9, 7.8$ Hz, 1H), 2.58 (d, $J = 5.7$ Hz, 1H), 2.22–2.12 (m, 3H), 1.99 (ddqd, $J = 11.0, 8.7, 6.5, 4.3$ Hz, 1H), 1.82 (s, 3H), 1.32–1.23 (m, 1H), 0.99 (d, $J = 6.5$ Hz, 3H), 0.89 (s, 9H), 0.88 (s, 9H), 0.86 (s, 9H), 0.08 (s, 3H), 0.07 (s, 3), 0.05 (s, 3H), 0.04 (s, 6H), 0.02 ppm (s, 3H). $^{13}\text{C NMR}$ (100 MHz, CDCl_3): $\delta = 170.1, 144.5, 143.8$ (3C), 128.8 (6C), 127.9 (6C), 127.2 (3C), 108.8, 91.6, 86.8, 84.9, 83.0, 80.7, 80.5, 80.4, 79.6, 74.1, 71.7, 65.5, 65.4, 61.2, 38.2, 37.1, 35.5, 26.2 (3C), 26.1 (6C), 21.0, 18.6, 18.5, 18.3, 17.1, –4.0, –4.2, –4.4, –4.5, –5.20, –5.22 ppm. IR (film): $\tilde{\nu} = 3465, 2953, 2927, 2855, 1744, 1491, 1462, 1449, 1375, 1250, 1076, 965, 938, 836, 776, 705, 633$ cm^{-1} . MS (ESIpos) m/z (%): 1021.5 (100 (M+Na)). HRMS (ESIpos): m/z calcd for $\text{C}_{57}\text{H}_{86}\text{O}_9\text{Si}_3\text{Na}$: 1021.5472, found: 1021.5482.

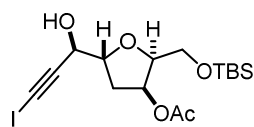
Enyne 142. A flame-dried Schlenk flask was charged with Cs₂CO₃ (8.9 mg, 27 μmol), Pd(OAc)₂ (0.4 mg,



1.7 μmol, 10 mol%) and 2-amino-4,6-dihydropyrimidine (0.4 mg, 3.4 μmol, 20 mol%), evacuated and backfilled with argon three times. A solution of vinyl iodide **137** (10 mg, 17 μmol) in DMF (0.2 mL) was added and the resulting mixture stirred at rt. Next, a solution of alkyne **123** (6.7 mg, 21 μmol) in DMF (0.2 mL) was added *via* syringe over 10 min. The resulting

mixture was stirred at rt for 1h. All volatiles were removed in vacuo and the residue was purified by flash chromatography (hexanes/*t*-butyl methyl ether 15:1 to 4:1) to yield the title compound **142** as a colorless oil (4.8 mg, 36%, 51% b.r.s.m). $[\alpha]_D^{20} = +29.5$ ($c = 0.5$, CHCl₃). ¹H NMR (600 MHz, CDCl₃): $\delta = 6.07$ (dd, $J = 11.0, 9.4$ Hz, 1H, H-8), 5.54 (ddd, $J = 11.1, 2.0, 0.6$ Hz, 1H, H-9), 5.43 (ddd, $J = 4.4, 3.8, 2.0$ Hz, 1H, H-15), 4.62 (ddd, $J = 9.4, 2.5, 0.6$ Hz, 1H, H-7), 4.39 (td, $J = 5.7, 1.9$ Hz, 1H, H-12), 4.26 (ddd, $J = 8.8, 6.6, 6.0$ Hz, 1H, H-13), 4.11 (ddd, $J = 7.2, 5.6, 3.8$ Hz, 1H, H-16), 4.02 (ddd, $J = 10.4, 6.8, 5.2$ Hz, 1H, H-5), 3.99 (d, $J = 8.7$ Hz, 1H, H-2), 3.76 (dd, $J = 10.0, 5.8$ Hz, 1H, H-17), 3.74 (dd, $J = 10.0, 7.2$ Hz, 1H, H-17), 3.73 (s, 3H), 3.72 (dd, $J = 6.6, 2.6$ Hz, 1H, H-6), 2.57 (d, $J = 5.6$ Hz, 1H, 12-OH), 2.34 (ddq, $J = 10.8, 8.8, 6.8$ Hz, 1H, H-3), 2.21 (ddd, $J = 11.9, 6.8, 5.6$ Hz, 1H, H-4), 2.18 (ddd, $J = 14.0, 6.8, 2.0$ Hz, 1H, H-14), 2.14 (ddd, $J = 14.0, 8.8, 4.8$ Hz, 1H, H-14), 2.07 (s, 3H, H-19), 1.43 (dt, $J = 11.9, 10.6$ Hz, 1H, H-4), 1.18 (d, $J = 6.6$ Hz, 3H, H-23), 0.89 (s, 9H, 6-TBS), 0.88 (s, 9H, 7-TBS), 0.87 (s, 9H, 17-TBS), 0.09 (s, 3H, 7-TBS), 0.079 (s, 3H, 6-TBS), 0.077 (s, 3H, 6-TBS), 0.048 (s, 3H, 7-TBS), 0.046 (s, 3H, 17-TBS), 0.04 ppm (s, 3H, 17-TBS). ¹³C NMR (150 MHz, CDCl₃): $\delta = 173.7$ (C1), 170.2 (C18), 144.3 (C8), 109.1 (C9), 92.0 (C11), 82.9 (C10), 82.8 (C2), 81.8 (C16), 81.6 (C5), 80.9 (C13), 79.6 (C6), 74.1 (C15), 71.9 (C7), 65.7 (C12), 60.9 (C17), 52.0 (C20), 39.8 (C3), 37.4 (C4), 35.4 (C14), 26.2 (3C, 6-TBS), 26.1 (3C, 7-TBS), 25.9 (3C, 17-TBS), 21.2 (C19), 18.5 (6-TBS), 18.4 (17-TBS), 18.3 (7-TBS), 17.5 (C23), -4.1 (6-TBS), -4.2 (7-TBS), -4.4 (6-TBS), -4.6 (7-TBS), -5.3 (17-TBS), -5.4 ppm (17-TBS). IR (film): $\tilde{\nu} = 3471, 2954, 2928, 2856, 1743, 1463, 1374, 1250, 1147, 1078, 967, 938, 836, 777, 668$ cm⁻¹. MS (ESIpos) m/z (%): 807.4 (100 (M+Na)). HRMS (ESIpos): m/z calcd for C₃₉H₇₂O₁₀Si₃Na: 807.4326, found: 807.4337.

Iodoalkyne 143. A solution of AgNO₃ (1.6 mg, 9.1 μmol, 15 mol%) in DMF (0.2 mL) was added to a

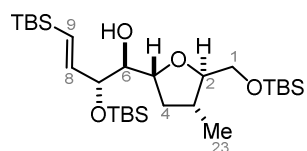


solution of alkyne **123** (20.0 mg, 60.9 μmol) and NIS (20.5 mg, 91.3 μmol) in DMF (0.4 mL). The resulting mixture was stirred for 90 min at rt. The reaction was quenched with of water (5 mL) and the aqueous layer extracted with

EtOAc (5 × 10 mL). The combined extracts were washed with brine (20 mL), dried over Na₂SO₄, filtered and concentrated. The residue was purified by flash chromatography (hexanes/*t*-butyl methyl ether 19:1) to yield the title compound as a yellow oil (23.0 mg, 83%). $[\alpha]_D^{20} = +27.6$ ($c = 1.0$, CHCl₃). ¹H NMR (400 MHz, CDCl₃): $\delta = 5.42$ (td, $J = 4.0, 2.4$ Hz, 1H), 4.41 (t, $J = 5.1$ Hz, 1H), 4.31–4.20 (m, 1H), 4.09 (ddd, $J = 6.8, 5.8, 3.7$ Hz, 1H), 3.82–3.71 (m, 2H), 2.46 (brd, $J = 5.3$ Hz, 1H), 2.19–2.12 (m,

2H), 2.07 (s, 3H), 0.87 (s, 9H), 0.05 (s, 3H), 0.04 ppm (s, 3H). ^{13}C NMR (100 MHz, CDCl_3): δ = 170.3, 92.3, 81.9, 80.9, 74.1, 66.6, 61.0, 53.6, 35.3, 25.9 (3C), 21.2, 18.4, -5.3, -5.4 ppm. IR (film): $\tilde{\nu}$ = 3422, 2928, 2884, 2856, 1727, 1471, 1374, 1249, 1182, 1092, 939, 836, 777, 667 cm^{-1} . MS (ESIpos) m/z (%): 477.1 (100 (M+Na)). HRMS (ESIpos): m/z calcd for $\text{C}_{16}\text{H}_{27}\text{O}_5\text{SiNa}$: 477.0565, found: 477.0563.

Vinyl silane 145. A solution of *t*-BuLi (1.7 M in pentane, 48 μL , 82 μmol) was slowly added to a



solution of vinyl iodide **84** (25.0 mg, 37.3 μmol) in THF (0.4 mL) at $-78\text{ }^\circ\text{C}$ and the resulting mixture was stirred for 20 min. Bu_3SnCl (11 μL , 41 μmol) was added, the reaction mixture warmed to ambient temperature and

stirred for 20 min. The reaction was cooled to $-78\text{ }^\circ\text{C}$, quenched with H_2O (1 mL) followed by NaOH (1 M, 2 mL) and the resulting mixture was vigorously stirred for 1 h at rt. The biphasic mixture was diluted with Et_2O (4 mL), the layers were separated and the aqueous layer was extracted with EtOAc (4 \times 10 mL). The combined organic extracts were dried over Na_2SO_4 , filtered and concentrated. The residue was purified by flash chromatography (hexanes/*t*-butyl methyl ether 100:1) to afford the title compound **145** as a colorless oil (12.3 mg, 61%). $[\alpha]_{\text{D}}^{20} = -6.1$ ($c = 1.0$, CHCl_3). ^1H NMR (600 MHz, CDCl_3): δ = 6.26 (ddd, $J = 14.9, 9.0, 1.0$ Hz, 1H, H-8), 5.72 (d, $J = 14.9$ Hz, 1H, H-9), 4.32 (dd, $J = 9.0, 6.4$ Hz, 1H, H-7), 4.17 (ddd, $J = 9.5, 5.6, 3.5$ Hz, 1H, H-5), 3.65 (dd, $J = 11.0, 4.6$ Hz, 1H, H-1), 3.64 (dd, $J = 11.0, 4.3$ Hz, 1H, H-1), 3.51 (dt, $J = 8.8, 4.6$ Hz, 1H, H-2), 3.20 (td, $J = 6.5, 3.2$ Hz, 1H, H-6), 2.22 (d, $J = 6.7$ Hz, 1H, 6-OH), 2.11 (ddd, $J = 9.9, 5.3, 2.7$ Hz, 1H, H-3), 2.06 (dt, $J = 12.5, 6.2$ Hz, 1H, H-4), 1.57 (q, $J = 10.8$ Hz, 1H, H-4), 1.07 (d, $J = 6.3$ Hz, 3H, H-23), 0.90 (s, 18H, TBS), 0.87 (s, 9H, TBS), 0.14 (s, 3H, TBS), 0.12 (s, 3H, TBS), 0.07 (s, 3H, TBS), 0.06 (s, 6H, TBS), 0.05 ppm (s, 3H, TBS). ^{13}C NMR (150 MHz, CDCl_3): δ = 150.2 (C8), 128.4 (C9), 86.3 (C2), 77.1 (C5), 76.0 (C6), 74.2 (C7), 65.1 (C1), 38.2 (C4), 36.8 (C3), 26.7 (3C, TBS), 26.1 (3C, TBS), 26.0 (3C, TBS), 18.5 (TBS), 18.3 (TBS), 17.2 (C23), 16.8 (TBS), -3.6 (TBS), -3.7 (TBS), -4.15 (TBS), -4.24 (TBS), -5.12 (TBS), -5.14 ppm (TBS). IR (film): $\tilde{\nu}$ = 3515, 2954, 2928, 2856, 1462, 1389, 1361, 1251, 1084, 1006, 938, 834, 810, 774, 729 cm^{-1} . MS (ESIpos) m/z (%): 567.4 (100 (M+Na)). HRMS (ESIpos): m/z calcd for $\text{C}_{28}\text{H}_{60}\text{O}_4\text{Si}_3\text{Na}$: 567.3692, found: 567.3697.

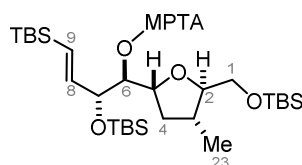
Mosher ester analysis of alcohol 145. Triethylamine (4.6 μL , 33 μmol) and DMAP (0.3 mg, 2.2 μmol , 20 mol%) were added to a solution of alcohol **145** (6.0 mg, 11 μmol) in CH_2Cl_2 (0.3 mL) followed by (*R*)-(-)- α -methoxy- α -trifluoromethyl-phenylacetyl chloride ((*R*)-MTPA-Cl) (4.1 μL , 22 μmol). The resulting mixture was stirred at rt for 48 h, before the reaction was quenched with aq. sat. NaHCO_3 (3 mL). The aqueous layer was extracted with CH_2Cl_2 (3 \times 5 mL), the combined extracts were dried over Na_2SO_4 , filtered and concentrated. The residue was purified by flash chromatography (hexanes/*t*-butyl methyl ether 19:1) to give the corresponding (*S*)-Mosher ester (**S**)-MTPA-**145** (1.6 mg, 19%), which analyzed as follows: $[\alpha]_{\text{D}}^{20} = -43.4$ ($c = 0.25$, CHCl_3). ^1H NMR (400 MHz, CDCl_3): δ = 7.68–7.62 (m, 2H), 7.39–7.34 (m, 3H), 6.32 (dd, $J = 15.0, 9.2$ Hz, 1H), 5.70 (dd, $J = 15.0, 1.0$ Hz,

1H), 5.10 (dd, $J = 7.7, 3.1$ Hz, 1H), 4.52 (ddd, $J = 9.1, 3.2, 1.0$ Hz, 1H), 4.15 (ddd, $J = 9.0, 7.7, 5.5$ Hz, 1H), 3.60 (dd, $J = 10.7, 3.9$ Hz, 1H), 3.55 (dd, $J = 10.8, 4.5$ Hz, 1H), 3.52 (s, 3H), 3.43 (dt, $J = 8.3, 4.2$ Hz, 1H), 2.25–2.17 (m, 1H), 2.17–2.09 (m, 1H), 1.34–1.31 (m, 1H), 1.03 (d, $J = 6.1$ Hz, 3H), 0.89 (s, 9H), 0.85 (s, 18H), 0.12 (s, 3H), 0.09 (s, 3H), 0.05 (s, 3H), 0.04 (s, 3H), –0.01 (s, 3H), –0.02 ppm (s, 3H). MS (ESIpos) m/z (%): 778.5 (100 (M+NH₄)). HRMS (ESIpos): m/z calcd for C₃₈H₆₇O₆F₃Si₃Na: 783.4090, found: 783.4089.

The same procedure was followed for the preparation of (**R**)-MTPA-145 (1.1 mg, 13%), which analyzed as follows: $[\alpha]_D^{20} = +55.0$ ($c = 0.11$, CHCl₃). ¹H NMR (400 MHz, CDCl₃): $\delta = 7.67$ – 7.60 (m, 2H), 7.39–7.31 (m, 3H), 6.16 (dd, $J = 15.0, 8.9$ Hz, 1H), 5.58 (dd, $J = 15.0, 1.1$ Hz, 1H), 5.02 (dd, $J = 8.2, 2.7$ Hz, 1H), 4.33 (ddd, $J = 8.9, 2.8, 1.1$ Hz, 1H), 4.25 (ddd, $J = 9.4, 8.2, 5.5$ Hz, 1H), 3.66 (s, 3H), 3.63–3.60 (m, 2H), 3.49 (dt, $J = 8.1, 3.9$ Hz, 1H), 2.25–2.20 (m, 1H), 2.20–2.16 (m, 1H), 1.38–1.34 (m, 1H), 1.07 (d, $J = 6.2$ Hz, 3H), 0.89 (s, 9H), 0.87 (s, 18H), 0.06 (s, 3H), 0.04 (s, 3H), 0.02 (s, 3H), 0.01 (s, 3H), –0.16 (s, 3H), –0.18 ppm (s, 3H). MS (ESIpos) m/z (%): 783.4 (100 (M+Na)). HRMS (ESIpos): m/z calcd for C₃₈H₆₇O₆F₃Si₃Na: 783.4090, found: 783.4087.

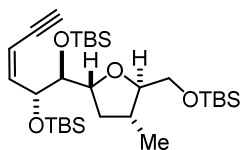
Both products were analyzed according to Hoyer and co-workers.^[118]

Table 4.5. Mosher ester analysis for the assignment of the C(6) stereocenter; chagosensine numbering as shown in the insert.



Assignment	145 [ppm]	(S)-MTPA-145 [ppm]	(R)-MTPA-145 [ppm]	Δ (δ (S–R)) [ppm]
1a	3.65	3.60	3.62	–0.02
1b	3.64	3.55	3.61	–0.06
2	3.51	3.43	3.49	–0.06
3	2.11	2.21	2.22	–0.01
4a	2.06	2.13	2.19	–0.06
4b	1.57	1.33	1.36	–0.03
5	4.17	4.15	4.25	–0.10
6	3.20	5.10	5.02	+0.08
7	4.32	4.52	4.33	+0.19
8	6.26	6.32	6.16	+0.16
9	5.72	5.70	5.58	+0.12
23	1.07	1.03	1.07	–0.04

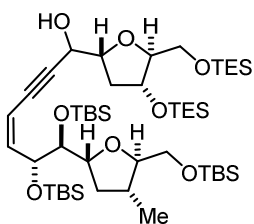
Enyne 147. THF was degassed by three freeze-pump-thaw cycles prior to use. A flame-dried Young



Schlenk was charged with 1-ethynylsodium (4.2 mg, 88 μmol), which was suspended in degassed THF (0.2 mL). Trimethyl borate (10 μL , 88 μmol) was added dropwise *via* syringe at rt. After stirring for 20 min, [Pd(dppf)Cl₂] \cdot CH₂Cl₂

(2.0 mg, 2.4 μmol , 15 mol%) was added, causing the reaction mixture to turn bright red. Next, a solution of (*Z*)-vinyl iodide **84** (10 mg, 16 μmol) in degassed THF (0.1 mL + 0.1 mL rinse) was added and the mixture stirred at 65°C for 2 h. The pale orange mixture was cooled to ambient temperature; the reaction was quenched with aq. half-sat. NH₄Cl (3 mL) and the aqueous layer extracted with EtOAc (3 \times 5 mL). The combined extracts were dried over Na₂SO₄, filtered and concentrated. The residue was purified by flash chromatography (hexanes/*t*-butyl methyl ether 100:1) to afford the title compound **147** as a colorless oil (5.6 mg, 62%). $[\alpha]_{\text{D}}^{20} = +8.8$ ($c = 0.5$, CHCl₃). ¹H NMR (400 MHz, CDCl₃): $\delta = 6.14$ (ddd, $J = 11.1, 9.3, 0.9$ Hz, 1H), 5.49 (dd, $J = 11.3, 2.4$ Hz, 1H), 4.60 (dd, $J = 9.3, 1.8$ Hz, 1H), 3.71 (ddd, $J = 9.8, 8.0, 5.6$ Hz, 1H), 3.67–3.58 (m, 3H), 3.43 (dt, $J = 9.2, 4.7$ Hz, 1H), 3.09 (dd, $J = 2.4, 1.0$ Hz, 1H), 2.21 (ddd, $J = 12.2, 7.0, 5.6$ Hz, 1H), 2.04 (dddd, $J = 13.3, 8.7, 6.7, 4.4$ Hz, 1H), 1.33–1.25 (m, 1H), 1.05 (d, $J = 6.5$ Hz, 3H), 0.89 (s, 9H), 0.882 (s, 9H), 0.877 (s, 9H), 0.10–0.07 (m, 9H), 0.04 ppm (s, 9H). ¹³C NMR (100 MHz, CDCl₃): $\delta = 145.4, 108.4, 84.9, 82.2, 81.0, 80.7, 79.7, 71.9, 65.2, 38.4, 37.2, 26.2$ (3C), 26.1 (6C), 18.6, 18.5, 18.3, 17.3, –4.0, –4.2, –4.58, –4.59, –5.2 ppm (2C). IR (film): $\tilde{\nu} = 2955, 2928, 2856, 1472, 1388, 1361, 1252, 1132, 1070, 1005, 977, 939, 834, 775, 679, 640, 611$ cm⁻¹. MS (ESIpos) m/z (%): 591.4 (100 (M+Na)). HRMS (ESIpos): m/z calcd for C₃₀H₆₀O₄Si₃Na: 591.3692, found: 591.3690.

Enyne 148. A solution of *n*-BuLi (1.6 M in hexane, 5.5 μL , 8.8 μmol) was added to a solution of

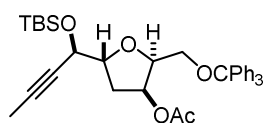


enyne **147** (5.0 mg, 8.8 μmol) in THF (0.2 mL) at –78 °C. After stirring for 30 min, a solution of aldehyde **58** (3.1 mg, 8.4 μmol) in THF (0.2 mL) was added over 2 h *via* syringe pump. The resulting solution was stirred overnight.

The reaction was diluted with *t*-butyl methyl ether (2 mL) and quenched with water (2 mL). The aqueous phase was extracted with *t*-butyl methyl ether (3 \times 4 mL), the combined extracts were dried over Na₂SO₄, filtered and concentrated. The residue was purified by flash chromatography (hexanes/*t*-butyl methyl ether 19:1) to yield the title compound **148** as a colorless oil (2.3 mg, 29% C12-epimeric mixture). ¹H NMR (400 MHz, CDCl₃): $\delta = 6.03$ (dd, $J = 11.1, 9.3$ Hz, 1H), 5.56–5.50 (m, 1H), 4.67 (dd, $J = 6.3, 3.1$ Hz, 1H), 4.52 (dd, $J = 9.3, 1.9$ Hz, 1H), 4.41 (d, $J = 5.4$ Hz, 1H), 4.39–4.33 (m, 1H), 4.15–4.09 (m, 2H), 4.08–4.03 (m, 1H), 3.64–3.57 (m, 3H) 3.45–3.39 (m, 2H), 2.39–2.20 (m, 3H), 2.17–2.07 (m, 1H), 1.24–1.19 (m, 1H), 1.05 (d, $J = 6.5$ Hz, 3H), 0.99–0.92 (m, 18H), 0.89 (s, 9H), 0.884 (s, 9H), 0.876 (s, 9H), 0.65 (q, $J = 8.0$ Hz, 6H),

0.60 (q, $J = 7.7$ Hz, 6H), 0.09 (s, 6H), 0.08 (s, 3H), 0.04 ppm (s, 9H). MS (ESIpos) m/z (%): 965.6 (100 (M+Na)). HRMS (ESIpos): m/z calcd for $C_{48}H_{98}O_8Si_5Na$: 965.6000, found: 965.6002.

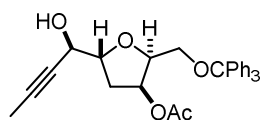
Acetate **S33.** PPh_3 (24.2 mg, 92.1 μ mol) was added to a solution of alcohol **120** (25.0 mg, 46.1 μ mol)



and acetic acid (5.3 μ L, 92.1 μ mol) in toluene (0.5 mL). The resulting mixture was stirred for 5 min and then cooled to 0 °C. DIAD (18.1 μ L, 92.1 μ mol) was added dropwise and the resulting mixture stirred at rt for 1 h. The mixture

was diluted with hexanes (2 mL), washed with water (3 mL) and brine (3 mL), dried over Na_2SO_4 , filtered and concentrated. The residue was purified by flash chromatography (hexanes/*t*-butyl methyl ether 19:1 to 9:1) to afford acetate **S33** as a colorless oil (22.1 mg, 82%). $[\alpha]_D^{20} = +28.4$ ($c = 1.0$, $CHCl_3$). 1H NMR (400 MHz, $CDCl_3$): $\delta = 7.44$ – 7.37 (m, 6H), 7.31 – 7.26 (m, 6H), 7.24 – 7.19 (m, 3H), 5.52 (ddd, $J = 5.1, 3.5, 1.5$ Hz, 1H), 4.39 (dq, $J = 4.4, 2.1$ Hz, 1H), 4.31 (ddd, $J = 7.4, 5.2, 3.4$ Hz, 1H), 4.15 (ddd, $J = 8.6, 6.7, 5.0$ Hz, 1H), 3.38 (dd, $J = 8.9, 5.2$ Hz, 1H), 3.14 (dd, $J = 8.9, 7.5$ Hz, 1H), 2.30 (ddd, $J = 13.9, 8.5, 5.1$ Hz, 1H), 2.09 (ddd, $J = 14.2, 6.7, 1.5$ Hz, 1H), 1.84 (d, $J = 2.2$ Hz, 3H), 1.81 (s, 3H), 0.90 (s, 9H), 0.13 (s, 3H), 0.10 ppm (s, 3H). ^{13}C NMR (100 MHz, $CDCl_3$): $\delta = 170.4, 143.9$ (3C), 128.8 (6C), 127.9 (6C), 127.1 (3C), 86.7, 81.8, 80.8, 80.3, 78.0, 74.4, 65.8, 61.4, 34.9, 26.0 (3C), 21.1, 18.5, 3.8, $-4.5, -4.8$ ppm. IR (film): $\tilde{\nu} = 2927, 2855, 1741, 1491, 1448, 1373, 1242, 1183, 1076, 939, 899, 837, 777, 747, 705, 650, 633$ cm^{-1} . MS (EI) m/z (%): 244 (20), 243 (100), 165 (19). HRMS (ESIpos): m/z calcd for $C_{36}H_{44}O_5SiNa$: 607.2850, found: 607.2857.

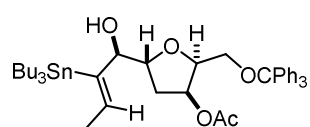
Propargylic alcohol **150.** TBAF (1.0 M in THF, 20.5 μ L, 20.5 μ mol) was added to a solution of



acetate **S33** (10.0 mg, 17.1 μ mol) in THF (0.5 mL) at 0 °C. The resulting mixture was stirred for 60 min. The reaction was diluted with *t*-butyl methyl ether (2 mL), quenched with aq. sat. NH_4Cl (2 mL) and the aqueous layer was

extracted with *t*-butyl methyl ether (3×4 mL). The combined extracts were washed with brine (5 mL), dried over Na_2SO_4 , filtered and concentrated. The residue was purified by flash chromatography (hexanes/*t*-butyl methyl ether 12:1 to 2:1) to afford the title compound **150** as a colorless oil (6.7 mg, 83%). $[\alpha]_D^{20} = +58.1$ ($c = 1.0$, $CHCl_3$). 1H NMR (400 MHz, $CDCl_3$): $\delta = 7.43$ – 7.37 (m, 6H), 7.32 – 7.27 (m, 6H), 7.26 – 7.21 (m, 3H), 5.54 (td, $J = 4.0, 2.3$ Hz, 1H), 4.27 (ddd, $J = 7.7, 5.2, 3.5$ Hz, 1H), 4.22 (tq, $J = 4.4, 2.2$ Hz, 1H), 4.17 (dt, $J = 8.5, 6.6$ Hz, 1H), 3.39 (dd, $J = 9.0, 5.2$ Hz, 1H), 3.18 (dd, $J = 9.0, 7.6$ Hz, 1H), 2.30 (d, $J = 4.8$ Hz, 1H), 2.20–2.09 (m, 2H), 1.84 (d, $J = 2.1$ Hz, 3H), 1.83 ppm (s, 3H). ^{13}C NMR (100 MHz, $CDCl_3$): $\delta = 170.2, 143.8$ (3C), 128.8 (6C), 127.9 (6C), 127.2 (3C), 86.8, 82.7, 81.1, 80.4, 76.8, 74.2, 65.4, 61.2, 35.4, 21.0, 3.8 ppm. IR (film): $\tilde{\nu} = 3467, 3059, 3023, 2922, 2886, 1739, 1491, 1448, 1374, 1239, 1076, 1022, 749, 706, 649, 633$ cm^{-1} . MS (EI) m/z (%): 244 (21), 243 (100), 165 (27). HRMS (ESIpos): m/z calcd for $C_{30}H_{30}O_5Na$: 493.1985, found: 493.1989.

Alkenylstannane 151. An aliquot of a stock solution of tributyltin hydride (0.07 M in CH₂Cl₂, 0.15 mL,



10.0 μmol) was added dropwise over 2 h to a solution of [Cp*RuCl]₄

(0.5 mg, 2.0 μmol, 20 mol%) and propargylic alcohol **150** (4.5 mg,

9.6 μmol) in CH₂Cl₂ (0.2 mL). The brown reaction mixture was

immediately filtered through a short pad of silica, which was rinsed with CH₂Cl₂ (5 mL). All volatiles

were removed in vacuo and the residue was purified by flash chromatography (hexanes/*t*-butyl

methyl ether 19:1) to give the title compound **151** as a pale yellow oil (2.7 mg, 37%, r.r. > 20:1).

$[\alpha]_D^{20} = +69.4$ (*c* = 0.25, CHCl₃). ¹H NMR (400 MHz, CDCl₃): δ = 7.44–7.38 (m, 6H), 7.32–7.27 (m, 6H),

7.26–7.21 (m, 3H), 6.32 (q, *J* = 6.6 Hz, *J*_{SnH} = 122 Hz, 1H), 5.51–5.44 (m, 1H), 4.22 (ddd, *J* = 7.2, 5.2, 3.6

Hz, 1H), 4.05–3.83 (m, 2H), 3.37 (dd, *J* = 9.0, 5.3 Hz, 1H), 3.16 (dd, *J* = 9.0, 7.3 Hz, 1H), 2.46 (d, *J* = 1.5

Hz, 1H), 1.99–1.85 (m, 2H), 1.82 (s, 3H), 1.74 (d, *J* = 6.5 Hz, 3H), 1.51–1.39 (m, 6H), 1.36–1.23 (m, 6H),

1.00–0.89 (m, 6H), 0.86 ppm (t, *J* = 7.3 Hz, 9H). ¹³C NMR (100 MHz, CDCl₃): δ = 170.2, 144.5, 143.9

(3C), 138.4, 128.8 (6C), 127.9 (6C), 127.2 (3C), 86.8, 83.6, 81.1, 79.7, 74.5, 61.4, 35.9, 29.3 (3C), 27.5

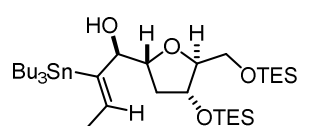
(3C), 21.0, 19.6, 13.8 (3C), 11.3 ppm (3C). ¹¹⁹Sn NMR (150 MHz, CDCl₃): δ = –52.7 ppm. IR (film):

$\tilde{\nu}$ = 3481, 2954, 2925, 2870, 2853, 1743, 1491, 1449, 1374, 1232, 1076, 1021, 937, 746, 705,

633 cm⁻¹. MS (EI) *m/z* (%): 244 (20), 243 (100), 165 (10). HRMS (ESIpos): *m/z* calcd for C₄₂H₅₈O₅SnNa:

785.3198, found: 785.3206.

Alkenylstannane 152. An aliquot of a stock solution of tributyltin hydride (0.07 M in CH₂Cl₂, 0.57 mL,



38.0 μmol) was added dropwise over 2 h to a solution of [Cp*RuCl]₄

(1.8 mg, 7.2 μmol, 20 mol%) and propargylic alcohol **59** (15 mg, 36.2 μmol)

in CH₂Cl₂ (0.5 mL). The brown reaction mixture was immediately filtered

through a short pad of silica, which was rinsed with CH₂Cl₂ (5 mL). All volatiles were removed in

vacuo and the residue was purified by flash chromatography (hexanes/*t*-butyl methyl ether 25:1) to

give the title compound **152** as a pale yellow oil (11 mg, 43%, r.r. 97:3). $[\alpha]_D^{20} = -10.2$ (*c* = 1.0, CHCl₃).

¹H NMR (400 MHz, CDCl₃): δ = 6.32 (q, *J* = 6.6 Hz, *J*_{SnH} = 126 Hz, 1H), 4.30 (dt, *J* = 6.4, 3.3 Hz, 1H), 4.14

(d, *J* = 7.2 Hz, 1H), 3.93–3.85 (m, 2H), 3.61 (dd, *J* = 10.8, 4.2 Hz, 1H), 3.51 (dd, *J* = 10.8, 5.5 Hz, 1H),

3.00 (d, *J* = 1.5 Hz, 1H), 2.09 (ddd, *J* = 13.1, 8.2, 6.3 Hz, 1H), 1.74 (d, *J* = 6.6 Hz, 3H), 1.78–1.67 (m, 1H),

1.56–1.40 (m, 6H), 1.36–1.28 (m, 6H), 1.00–0.92 (m, 24H), 0.89 (t, *J* = 7.3 Hz, 9H), 0.60 (q, *J* = 7.9 Hz,

6H), 0.59 ppm (q, *J* = 7.9 Hz, 6H). ¹³C NMR (100 MHz, CDCl₃): δ = 145.9, 137.6, 87.0, 83.2, 82.8, 73.5,

63.4, 37.2, 29.4 (3C), 27.6 (3C), 19.5, 13.9 (3C), 11.5 (3C), 6.89 (3C), 6.88 (3C), 4.8 (3C), 4.6 ppm (3C).

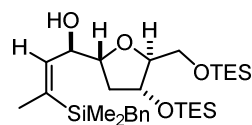
¹¹⁹Sn NMR (150 MHz, CDCl₃): δ = –54.4 ppm. IR (film): $\tilde{\nu}$ = 3446, 2955, 2914, 2876, 1622, 1459, 1415,

1376, 1239, 1111, 1076, 1004, 831, 744, 671, 593 cm⁻¹. MS (EI) *m/z* (%): 653 (17), 651 (26), 650 (40),

649 (100), 648 (51), 647 (75), 646 (35), 645 (37), 517 (11), 407 (24), 405 (18), 403 (11), 355 (12), 251

(15), 249 (11), 177 (11), 117 (20), 115 (21), 87 (17). HRMS (ESIpos): m/z calcd for $C_{33}H_{70}O_4Si_2SnNa$: 729.3726, found: 729.3727.

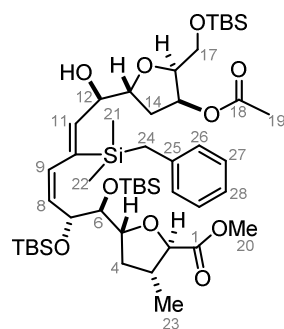
Alkenylsilane 155. Benzyl dimethyl silane (4.6 μ L, 29 μ mol) was added to a solution of $[Cp^*RuCl]_4$ (0.7 mg, 2.4 μ mol, 10 mol%) and propargylic alcohol **59** (10.0 mg, 24.1 μ mol)



in CH_2Cl_2 (0.15 mL). The resulting solution was stirred at rt for 10 min before all volatiles were removed in vacuo. The residue was purified by flash

chromatography (hexanes/*t*-butyl methyl ether 15:1) to yield the title compound **155** as a pale yellow oil (11 mg, 81%, r.r. 9:1). $[\alpha]_D^{20} = -32.4$ ($c = 0.5$, $CHCl_3$). 1H NMR (500 MHz, $CDCl_3$): $\delta = 7.22$ – 7.17 (m, 2H), 7.09–7.04 (m, 1H), 7.03–6.99 (m, 2H), 6.07 (dq, $J = 9.4, 1.6$ Hz, 1H), 4.36 (dt, $J = 6.1, 3.0$ Hz, 1H), 4.10 (ddd, $J = 9.4, 4.7, 2.6$ Hz, 1H), 3.98–3.89 (m, 2H), 3.62 (dd, $J = 10.7, 4.3$ Hz, 1H), 3.48 (dd, $J = 10.8, 6.1$ Hz, 1H), 3.30 (d, $J = 2.6$ Hz, 1H), 2.28–2.19 (m, 3H), 1.77 (d, $J = 1.6$ Hz, 3H), 1.71 (ddd, $J = 13.3, 4.9, 3.3$ Hz, 1H), 0.96 (t, $J = 7.9$ Hz, 9H), 0.95 (t, $J = 7.9$ Hz, 9H), 0.62 (q, $J = 9.5, 8.7$ Hz, 6H), 0.60 (q, $J = 7.8$ Hz, 6H), 0.15 (s, 3H), 0.12 ppm (s, 3H). ^{13}C NMR (125 MHz, $CDCl_3$): $\delta = 142.0, 140.1, 139.0, 128.4$ (2C), 128.2 (2C), 124.2, 87.3, 82.5, 73.4, 72.9, 63.2, 37.5, 26.3, 25.3, 6.88 (3C), 6.85 (3C), 4.7 (3C), 4.5 (3C), $-1.6, -1.7$ ppm. IR (film): $\tilde{\nu} = 3443, 2954, 2911, 2877, 1601, 1493, 1456, 1414, 1248, 1110, 1005, 831, 792, 744, 699$ cm^{-1} . MS (EI) m/z (%): 473 (21), 323 (19), 213 (14), 209 (18), 191 (15), 153 (29), 149 (18), 145 (64), 131 (12), 118 (11), 117 (100), 115 (34), 87 (23), 75 (11). HRMS (ESIpos): m/z calcd for $C_{30}H_{56}O_4Si_3Na$: 587.3379, found: 587.3378.

Dienylsilane 157. An aliquot of a stock solution of benzyl dimethyl silane (1 M in CH_2Cl_2 , 5.3 μ L,



5.3 μ mol) was added to a solution of $[Cp^*RuCl]_4$ (4.2 mg, 15.3 μ mol) and enyne **142** (4.0 mg, 5.1 μ mol) in CH_2Cl_2 (0.2 mL). The resulting dark brown solution was stirred for 2 h at rt before all volatiles were removed in vacuo.

The residue was purified by flash chromatography (hexanes/*t*-butyl methyl ether 4:1 to 3:1) to yield the title compound β -**157** as a pale yellow oil (1.2 mg, 25%). $[\alpha]_D^{20} = -23.8$ ($c = 0.08$, $CHCl_3$). 1H NMR (600 MHz, $CDCl_3$): see Table 4.6. ^{13}C NMR (150 MHz, $CDCl_3$): see Table 4.6. IR (film): $\tilde{\nu} = 3537, 2954, 2927, 2855, 1743, 1462, 1373, 1249, 1093, 1058, 1005, 947, 833, 776, 699$ cm^{-1} . MS (ESIpos) m/z (%): 952.6 (100 (M+NH₄)). HRMS (ESIpos): m/z calcd for $C_{48}H_{86}O_{10}Si_4Na$: 957.5190, found: 957.5196.

Table 4.6. ^1H and ^{13}C NMR data of **157** (1.2 mg in 0.25 mL CDCl_3); chagosensine numbering.*

atom n°	^1H NMR (600 MHz, CDCl_3)					^{13}C NMR (150 MHz, CDCl_3)	
	δ [ppm]	m	J [Hz]	COSY	NOESY	δ [ppm]	HMBC
1	-	-	-	-	-	173.2	20
2	3.98	d	9.1	3	(3), 4b, 23	82.9	(3), 4a, 23
3	2.39	ddq	11.4, 9.0, 6.5	2, 4(a)b, 23	(2), 4a, (5), 23	39.8	2, 4b, 23
4a	1.97	ddd	11.4, 6.5, 5.3	(3), 4b, 5	3, 4b, 5	36.9	23
4b	1.69	q	11.4	3, 4a, 5	(2), 4a, (6), 7, 23	80.9	(6), 7, 4b
5	4.36	ddd	10.7, 5.3, 2.0	4(a)b	3, 4a, 6, 7, 7-TBS	76.3	4b, 5
6	3.42	dd	7.7, 2.0	7	5, 7, 8, 6-TBS	69.0	6, 9
7	5.01	ddd	9.7, 7.7, 1.0	6,8	(6), 9, 6-TBS	132.3	7
8	5.35	dd	11.4, 9.7	7,9	21, 22, 6-TBS	134.3	7, 11
9	6.02	ddd	11.4, 1.2, 1.0	8	-	138.8	8, 21, 22
10	-	-	-	-	-	145.0	9, 12-OH
11	6.55	dd	10.1, 1.4	12	7, 12-OH, 13	72.8	12-OH, 14a
12	4.05	ddd	10.0, 7.8, 4.6	11, 12-OH	21, 22, (24)	-	-
12-OH	2.67	d	7.8	12	11	81.2	11, 12-OH
13	4.01	m	-	14	11, 12-OH, 15	35.2	-
14a	2.00	ddd	14.0, 9.4, 4.8	13, 14b, 15	(12), (13), 15	74.2	14b, 17b
14b	1.91	ddd	13.8, 6.2, 1.5	13, 14a, 15	13, (15)	81.4	14, 17
15	5.38	ddd	5.0, 3.8, 1.5	14a(b)	2, 14a, 6-TBS	60.8	-
16	4.01	m	-	17	6-TBS, 15, 17-TBS	170.2	19
17a	3.74	m	-	17b	16, 17b	21.3	-
17b	3.70	m	-	17a	15, 16	52.0	-
18	-	-	-	-	-	-0.9	22, 24a
19	2.07	s	-	-	20	-1.5	21, 24b
20	3.73	s	-	-	-	17.5	2, 4b
21	0.21	s	-	-	26, 9, 12	26.8	21, 22, 26
22	0.072	s	-	-	26, 9, 24, 6-TBS	139.7	24ab, 27
23	1.21	d	6.6	3	2, 3, 4b, 6-TBS	128.5	21, 22, 28
24a	2.28	d	13.7	24b	12, 21, 22, 26	128.3	24ab, 28
24b	2.21	d	13.7	24a	9, (12), 21, 22, 26	124.4	26, (27)
25	-	-	-	-	-	-	-
26	6.98	d	7.0	27	21, 22, 24ab, 27	-	-
27	7.19	dd	8.3, 7.0	26, 28	26, 28	-	-
28	7.07	t	7.4	(26), 27	27	-	-

* The C10-C11 double bond geometry can be unambiguously assigned as *trans* from NOESY experiments and ^{29}Si -HR-HMBC measurements: ^1H NMR (500 MHz, CDCl_3): δ = 6.55 ($^3J_{\text{SiH}}$ = 14.5 Hz, H-11). The signals of the TBS groups are not listed and appear as follows: ^1H NMR (600 MHz, CDCl_3): δ = 0.89 (s, 9H), 0.86 (s, 9H), 0.85 (s, 9H), 0.07 (s, 3H), 0.06 (s, 3H), 0.05 (s, 3H), 0.03 (s, 3H), 0.02 (s, 3H), 0.01 ppm (s, 3H). ^{13}C NMR (150 MHz, CDCl_3): δ = 26.4 (3C), 26.1 (3C), 25.9 (3C), 18.4, 18.3, 18.2, -2.8, -3.7, -3.8, -4.6, -5.3, -5.4 ppm.

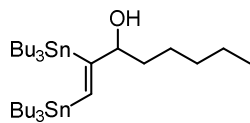
Table 4.7. ^1H and ^{13}C NMR data of **158** (2.1 mg in 0.25 mL CDCl_3); chagosensine numbering.*

atom n°	^1H NMR (600 MHz, CDCl_3)					^{13}C NMR (150 MHz, CDCl_3)	
	δ [ppm]	m	J [Hz]	COSY	NOESY	δ [ppm]	HMBC
1	-	-	-	-	-	173.4	20
2	3.78	d	8.9	3	4a, (6), 23	82.4	4b, 23
3	2.10	m	-	2, 4, 23	4a, (5), 23, 24, 25	39.8	2, 4a, 23
4a	1.29	ddd	11.6, 7.0, 5.6	3, 4b, (5)	3, 4b, 5, (7), 23	37.2	23
4b	0.86	m	-	3, 4a, 5	(2), 4a, 6, 7		
5	3.63	ddd	10.3, 7.9, 5.5	4a(b), 6	3, 4b, (6)	81.6	(3), 4a, 6
6	3.38	dd	7.8, 2.2	5	4a, 6-TBS, 7	80.8	4a, (7)
7	3.51	dd	8.5, 2.2	8	5, 6, 7-TBS	75.3	(5), 6, 9
8	5.82	dd	15.2, 8.5	7,9	(5), 7, 10, 6-TBS	137.7	6, (7), 10
9	6.00	dd	15.2, 10.7	8, 10	7, 22, 7-TBS	130.8	7, (10)
10	6.99	d	10.6	9	8, 12, (13), (22)	143.0	8, (9)
11	-	-	-	-	-	146.9	9, (10)
12	4.22	t	5.3	13, 16	12-OH, 14a, 22	81.4	10, (14a)
12-OH	2.40	d	5.4	12	12, 22	-	-
13	4.11	ddd	9.6, 6.0, 5.6	12, 14	10, 14a, 22	81.8	(14a)
14a	2.02	m	-	13, 14b, 15	(12), 14b, 15	35.4	-
14b	1.93	ddd	13.9, 6.2, 1.6	13, 14a	13, 14a, (15)		
15	5.34	ddd	5.2, 4.0, 1.6	14a, 16	14a(b), 16	74.0	14b, 17
16	3.81	ddd	7.5, 5.5, 3.9	15, 17	15, 17, (19), (22)	81.2	14, 17
17a	3.55	dd	10.1, 7.4	16, 17b	(16), 17b	60.9	-
17b	3.45	dd	10.1, 5.5	16, 17a	16, 17a, 17-TBS		
18	-	-	-	-	-	170.2	19
19	2.02	s	-	-	12, 16, 17-TBS	21.2	-
20	3.76	s	-	-	(3), 4b	51.9	-
21	-	-	-	-	-	140.0	22, 24, 25
22	7.56	m	-	24, 25	9, 13, 17b, 24, 25	137.2	24, 25
23	1.07	d	6.6	3	2, 3, 4b, 24, 25	17.3	2, 4a
24	7.33	m	-	22	(3), 22, 23, 7-TBS	128.7	22
25	7.33	m	-	22	(3), 22, 23, 7-TBS	128.9	22

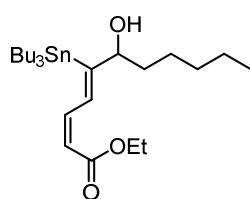
* The C10-C11 double bond geometry can be unambiguously assigned as *trans* from NOESY experiments and tin-proton coupling: ^1H NMR (600 MHz, CDCl_3): δ = 6.99 ($^3J_{\text{SnH}}$ = 148 Hz, H-10), 6.00 ($^4J_{\text{SnH}}$ = 7.5 Hz, H-9), 5.82 ($^5J_{\text{SnH}}$ = 3.5 Hz, H-8). The signals of the TBS groups are not listed and appear as follows: ^1H NMR (600 MHz, CDCl_3): δ = 0.88 (s, 9H), 0.83 (s, 9H), 0.75 (s, 9H), 0.04 (s, 3H), 0.00 (s, 3H), -0.226 (s, 3H), -0.231 (s, 3H), -0.02 (s, 3H), -0.03 ppm (s, 3H). ^{13}C NMR (150 MHz, CDCl_3): δ = 26.3 (3C), 26.1 (3C), 25.9 (3C), 18.7, 18.34, 18.28, -4.1, -4.2, -4.57, -4.64, -5.3, -5.4 ppm.

4.3.9 Synthesis of the Macrolactone 174

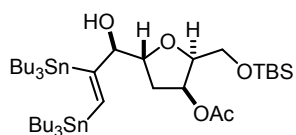
Bis-stannane 160. A solution of 1-octin-3-ol (58 μ L, 0.4 mmol) in THF (1 mL) was added to a solution of Pd(*t*-BuNC)₂Cl₂ (14 mg, 40 μ mol, 10 mol%) in THF (1 mL). Hexabutyliditin (0.22 mL, 0.44 mmol) was added in one portion and the resulting mixture stirred at rt for 7 h. The solvent was evaporated and the residue purified by flash chromatography (hexanes/Et₃N 200:1) to yield the bis-stannane **160** as a yellow oil (239 mg, 85%). ¹H NMR (300 MHz, CDCl₃): δ = 6.73 (d, *J* = 1.2 Hz, *J*_{SnH} = 179, 66.8 Hz, 1H), 4.05 (tdd, *J* = 6.5, 3.6, 1.1 Hz, 1H), 2.52 (q, *J* = 7.2 Hz, 1H), 1.52–1.44 (m, 15H), 1.37–1.30 (m, 17H), 1.03 (t, *J* = 7.2 Hz, 3H), 0.92–0.87 (m, 12H), 0.90 (t, *J* = 7.2 Hz, 9H), 0.89 ppm (t, *J* = 7.2 Hz, 9H). ¹³C NMR (75 MHz, CDCl₃): δ = 172.0, 140.3, 84.0, 37.3, 32.0, 29.5 (3C), 29.3 (3C), 27.8 (3C), 27.6 (3C), 25.7, 22.8, 14.2, 13.8 (6C), 11.3 (3C), 11.0 ppm (3C). ¹¹⁹Sn NMR (112 MHz, CDCl₃): δ = –60.5, –65.5 ppm. IR (film): $\tilde{\nu}$ = 3464, 2955, 2921, 2871, 2854, 1463, 1376, 1340 1291, 1071, 1021, 961, 863, 826, 666, 594 cm⁻¹. MS (ESIpos) *m/z* (%): 731.3 (100 (M+Na)). HRMS (ESIpos): *m/z* calcd for C₃₂H₆₈OSn₂Na: 731.3205, found: 731.3212.



Dienylstannane 162. DMF was degassed by three freeze-pump-thaw cycles prior to use. Tetrabutylammonium diphenylphosphinate (52.1 mg, 11.3 mmol) was placed in a Schlenk tube, which was evacuated and flame-dried. A solution of bis-stannane **160** (50.0 mg, 70.8 μ mol) in degassed DMF (0.5 mL) was added, followed by Pd(PPh₃)₄ (16.4 mg, 14.2 μ mol). The resulting mixture was stirred at rt for 5 min before CuTC (20.2 mg, 106 μ mol) was introduced, followed by a solution of ethyl 3-*cis*-iodoacrylate (17.0 mg, 76.3 μ mol) in degassed DMF (0.5 mL). The resulting mixture was stirred at rt for 1 h before the reaction was quenched with water (3 mL). The aqueous layer was separated and extracted with *t*-butyl methyl ether (3 \times 5 mL). The combined extracts were dried over Na₂SO₄, filtered and concentrated. The residue was purified by flash chromatography (hexanes/*t*-butyl methyl ether/Et₃N 95:5:0.5) to yield the title compound **162** as a colorless oil (21.5 mg, 59%). ¹H NMR (300 MHz, CDCl₃): δ = 7.94 (d, *J* = 11.5 Hz, *J*_{SnH} = 113 Hz, 1H), 6.57 (t, *J* = 11.4 Hz, 1H), 5.70 (dd, *J* = 11.3, 1.1 Hz, 1H), 4.32 (t, *J* = 6.2 Hz, 1H), 4.19 (q, *J* = 7.1 Hz, 2H), 1.61 (brs, 1H), 1.52–1.44 (m, 6H), 1.40–1.22 (m, 18H), 1.05–0.97 (m, 5H), 0.89 ppm (t, *J* = 7.2 Hz, 12H). ¹³C NMR (75 MHz, CDCl₃): δ = 166.4, 144.9, 134.7, 130.2, 117.9, 79.9, 60.2, 37.5, 31.9, 29.3 (3C), 27.5 (3C), 25.6, 22.8, 14.5, 1.45, 13.8 (3C), 11.8 ppm (3C). ¹¹⁹Sn NMR (112 MHz, CDCl₃): δ = –53.6 ppm. IR (film): $\tilde{\nu}$ = 3483, 2956, 2925, 2855, 1716, 1613, 1561, 1463, 1179, 1027, 821, 671, 596 cm⁻¹. MS (ESIpos) *m/z* (%): 539.3 (100 (M+Na)). HRMS (ESIpos): *m/z* calcd for C₂₅H₄₈O₃SnNa: 539.2517, found: 539.2522.



Bis-stannane 163. A solution of alkyne **123** (24 mg, 73 μmol) in THF (0.2 mL) was added to a solution



of $\text{Pd}(t\text{-BuNC})_2\text{Cl}_2$ (5.0 mg, 15 μmol , 20 mol%) in THF (0.2 mL).

Hexabutylditin (41 μL , 80 μmol) was added in one portion and the resulting mixture was stirred at rt for 14 h. The solvent was evaporated

and the residue purified by flash chromatography (hexanes/*t*-butyl methyl ether/ Et_3N 50:1:0.5) to

yield the bis-stannane **163** as a colorless oil (50 mg, 75%). $[\alpha]_{\text{D}}^{20} = +15.8$ ($c = 1.0$, CHCl_3). ^1H NMR (400

MHz, C_6D_6): $\delta = 7.02$ (d, $J = 1.2$ Hz, $J_{\text{SnH}} = 177$, 67.4 Hz, 1H), 5.42 (ddd, $J = 5.3$, 3.6, 1.6 Hz, 1H),

4.33–4.26 (m, 1H), 4.02–3.89 (m, 2H), 3.85–3.79 (m, 2H), 2.77 (brs, 1H), 2.01 (ddd, $J = 14.0$, 6.4, 1.6

Hz, 1H), 1.90–1.82 (m, 1H), 1.79–1.70 (m, 6H), 1.68 (s, 3H), 1.70–1.62 (m, 6H), 1.54–1.39 (m, 12H),

1.27–1.19 (m, 6H), 1.18–1.10 (m, 6H), 1.03–0.97 (m, 18H), 0.97 (s, 9H), 0.07 (s, 3H), 0.05 ppm (s, 3H).

^{13}C NMR (100 MHz, C_6D_6): $\delta = 169.7$, 169.2, 144.2, 87.8, 81.6, 81.1, 74.5, 61.6, 36.0, 29.9 (3C), 29.8

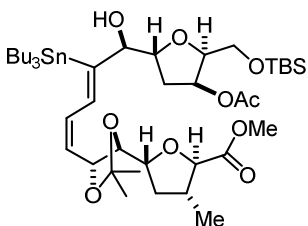
(3C), 28.1 (3C), 27.9 (3C), 26.0 (3C), 20.6, 18.5, 14.04 (3C), 14.02 (3C), 12.1 (3C), 11.5 (3C), –5.2, –5.3

ppm. ^{119}Sn NMR (150 MHz, C_6D_6): $\delta = -59.3$, –67.3 ppm. IR (film): $\tilde{\nu} = 3498$, 2955, 2925, 2855, 1746,

1463, 1375, 1232, 1071, 938, 837, 777, 667, 595 cm^{-1} . MS (ESIpos) m/z (%): 933.4 (100 (M+Na)).

HRMS (ESIpos): m/z calcd for $\text{C}_{40}\text{H}_{82}\text{O}_5\text{SiSn}_2\text{Na}$: 933.3866, found: 933.3874.

Dienylstannane 168. DMF was carefully degassed by three freeze-pump-thaw cycles prior to use.



Tetrabutylammonium diphenylphosphinate (23.3 mg, 50.7 μmol) was

placed in a Schlenk tube, evacuated and flame-dried. A solution of bis-

stannane **163** (41.9 mg, 46.1 μmol) in degassed DMF (0.7 mL) was added,

followed by $\text{Pd}(\text{PPh}_3)_4$ (21.3 mg, 18.4 μmol , 40 mol%). The resulting

mixture was stirred at rt for 5 min before CuTC (9.2 mg, 48 μmol) was

introduced, followed by a solution of vinyl iodide **139** (10.4 mg, 46.1 μmol) in degassed DMF (0.5 mL).

The resulting mixture was stirred at rt for 30 min before the reaction was quenched with water

(3 mL). The aqueous layer was separated and extracted with *t*-butyl methyl ether (3 \times 5 mL). The

combined extracts were dried over Na_2SO_4 , filtered and concentrated. The residue was purified by

flash chromatography (hexanes/*t*-butyl methyl ether 9:1 to 4:1) to yield the title compound **168**

(16.2 mg, 40%) and its regioisomer **169** (9.7 mg, 24%) as a colorless oil each; **169** was fully

characterized at the more stable vinyl chloride stage **171** (*vide infra*). $[\alpha]_{\text{D}}^{20} = +32.0$ ($c = 0.25$, CHCl_3).

^1H NMR (400 MHz, CD_2Cl_2): $\delta = 7.03$ (d, $J = 11.4$ Hz, $J_{\text{SnH}} = 111$ Hz, 1H), 6.17 (td, $J = 11.2$, 1.0 Hz, 1H),

5.59 (t, $J = 10.5$ Hz, 1H), 5.37 (ddd, $J = 5.6$, 3.8, 1.9 Hz, 1H), 5.10 (dd, $J = 9.7$, 5.5 Hz, 1H),

4.13–4.01 (m, 5H), 3.99 (d, $J = 7.9$ Hz, 1H), 3.74 (d, $J = 6.1$ Hz, 2H), 3.71 (s, 3H), 2.62 (d, $J = 2.1$ Hz, 1H),

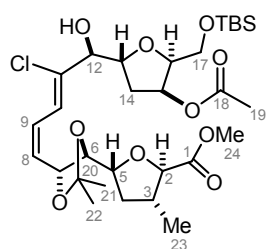
2.31 (dq, $J = 10.0$, 7.4 Hz, 1H), 2.08–2.04 (m, 1H), 2.03 (s, 3H), 1.99–1.87 (m, 2H), 1.52–1.45 (m, 6H),

1.49 (s, 3H), 1.38 (s, 3H), 1.35–1.28 (m, 9H), 1.25–1.21 (m, 1H), 1.16 (d, $J = 6.6$ Hz, 3H), 1.03–0.98 (m,

6H), 0.91–0.89 (m, 6H), 0.88 (s, 9H), 0.06 (s, 3H), 0.05 ppm (s, 3H). ^{13}C NMR (100 MHz, CD_2Cl_2):

δ = 173.4, 170.3, 154.9, 135.2, 132.4, 128.5, 109.7, 83.8, 83.5, 81.7, 81.4, 81.2, 79.5, 74.5, 73.0, 61.6, 52.1, 39.8, 37.5, 36.0, 29.5 (3C), 28.0, 27.7 (3C), 26.0 (3C), 25.8, 21.2, 18.5, 18.1, 13.9 (3C), 12.0 (3C), -5.3, -5.4 ppm. IR (film): $\tilde{\nu}$ = 3507, 2957, 2928, 2856, 1743, 1462, 1375, 1259, 1093, 1020, 799 cm^{-1} . MS (ESIpos) m/z (%): 911.4 (100 (M+Na)). HRMS (ESIpos): m/z calcd for $\text{C}_{42}\text{H}_{76}\text{O}_{10}\text{SiSnNa}$: 911.4121, found: 911.4119.

(Z,Z)-Chlorodiene 170. A solution of dienylstannane **168** (16.2 mg, 18.2 μmol) in THF (0.25 mL) was



added to a suspension of CuCl_2 (12.3 mg, 91.2 μmol) in THF (0.25 mL). 2,6-Lutidine (5.3 μL , 45.6 μmol) was added and the resulting mixture was stirred at rt for 24 h. The reaction was diluted with *t*-butyl methyl ether (2.5 mL) and quenched with aq. sat. NaHCO_3 (3 mL). The aqueous layer was separated and extracted with *t*-butyl methyl ether (3 \times 5 mL). The combined

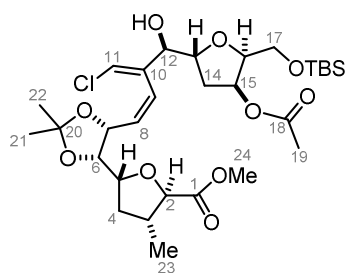
extracts were dried over Na_2SO_4 , filtered and concentrated. The residue was purified by flash chromatography (hexane/*t*-butyl methyl ether 5:1 to 2:1) to yield the title compound **170** as a colorless oil (8.1 mg, 70%). $[\alpha]_{\text{D}}^{20} = +8.2$ ($c = 0.44$, CHCl_3). ^1H NMR (600 MHz, CDCl_3): see Table 4.8. ^{13}C NMR (150 MHz, CDCl_3): see Table 4.8. IR (film): $\tilde{\nu}$ = 3397, 2960, 2926, 2854, 1740, 1669, 1456, 1377, 1260, 1091, 1019, 798 cm^{-1} . MS (ESIpos) m/z (%): 655.3 (100 (M+Na)). HRMS (ESIpos): m/z calcd for $\text{C}_{30}\text{H}_{49}\text{O}_{10}\text{ClSiNa}$: 655.2676, found: 655.2672.

Table 4.8. ^1H and ^{13}C NMR data of **170** (1.0 mg in 0.25 mL CDCl_3); chagosensine numbering.*

atom n°	^1H NMR (600 MHz, CDCl_3)					^{13}C NMR (150 MHz, CDCl_3)	
	δ [ppm]	m	J [Hz]	COSY	NOESY	δ [ppm]	HMBC
1	-	-	-	-	-	173.4	(2), (3), 23
2	4.05	d	7.8	3	4b, 23	83.8	(4a), 23
3	2.37	dq	9.9, 6.9	2, 4, 23	2, 5, 19, 23, (24)	39.6	2, 23
4a	2.06	m	-	(3), 4b, 5	3, 4b, 5, (23)	37.2	23
4b	1.28	m	-	3, 4a, 5	2, 4a, (5), 6, (7)		
5	4.17	dt	9.8, 6.2	4a(b), 6	3, 4a(b), 8,	79.14	4b, (7)
6	4.10	m	-	5, 7	4b, 7, 15, 22	80.8	4b
7	5.00	dd	9.8, 6.4	8	6, 8, 10, 22	73.2	9
8	5.81	dd	11.0, 9.8	7,9	5, (7), 21	130.4	6, 10
9	6.57	t	11.0	8, 10	8	126.5	7
10	6.74	d	11.0	9	2, 12, (13), 21	121.0	8
11	-	-	-	-	-	136.5	9, 10, (13)
12	4.08	t	4.6	12-OH, 13	10, 13, 14, 21	77.5	10
12-OH	2.84	d	4.6	12	-	-	-
13	4.41	ddd	8.4, 7.0, 5.6	12, 14	12, 14, 21	79.06	12, 14a
14a	2.08	m	-	13, 15	12, 15	35.8	-
14b							
15	5.43	ddd	5.6, 5.1, 2.6	14, (16)	14, 16, 17, 19	74.1	(14), 17
16	4.10	m	-	15, 17	4b, 7, 15, (22)	82.0	17
17a	3.75	d	6.4	16	15, 16, 17-TBS	61.2	-
17b							
18	-	-	-	-	-	170.2	19
19	2.07	s	-	-	(23), 17-TBS	21.2	-
20	-	-	-	-	-	110.0	21, 22
21	1.53	s	-	22	(2), 8, 22	27.8	-
22	1.41	s	-	21	6, 7, 21	25.8	-
23	1.19	d	6.6	3	2, 3, 4a, (19), (24)	18.2	2
24	3.73	s	-	-	2	52.1	-

* The signals of the TBS group are not listed and appear as follows: ^1H NMR (600 MHz, CDCl_3): δ = 0.87 (s, 9H), 0.05 (s, 3H), 0.04 ppm (s, 3H). ^{13}C NMR (150 MHz, CDCl_3): δ = 25.9 (3C), 18.4, -5.2, -5.3 ppm.

Chlorodiene 171. Prepared analogously from the corresponding dienylstannane **169** and obtained as

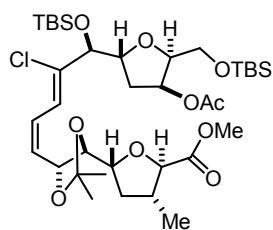


a colorless oil (3.5 mg, 51%). $[\alpha]_D^{20} = -18.3$ ($c = 0.06$, CHCl_3). $^1\text{H NMR}$ (600 MHz, CDCl_3): see Table 4.9. $^{13}\text{C NMR}$ (150 MHz, CDCl_3): see Table 4.9. IR (film): $\tilde{\nu} = 3433, 2959, 2926, 2873, 2855, 1736, 1439, 1373, 1258, 1183, 1069, 1047, 798, 758 \text{ cm}^{-1}$. MS (ESIpos) m/z (%): 655.3 (100 (M+Na)). HRMS (ESIpos): m/z calcd for $\text{C}_{30}\text{H}_{49}\text{O}_{10}\text{ClSiNa}$: 655.2676, found: 655.2672.

Table 4.9. ^1H and ^{13}C NMR data of **171** (1.0 mg in 0.25 mL CDCl_3); chagosensine numbering.*

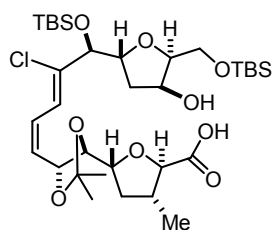
atom n°	$^1\text{H NMR}$ (600 MHz, CDCl_3)					$^{13}\text{C NMR}$ (150 MHz, CDCl_3)	
	δ [ppm]	m	J [Hz]	COSY	NOESY	δ [ppm]	HMBC
1	-	-	-	-	-	173.6	(2), 24
2	4.05	d	7.8	3	14, 21, 23, 24	83.8	(4a), 23
3	2.35	dq	9.8, 7.1	4, 23	2, 4a, 5, 23	39.5	2, 23
4a	2.14	ddd	12.1, 7.4, 6.1	(3), 4b	3, 4b, 5	37.1	23
4b	1.49	ddd	12.1, 9.9, 9.9	3, 4a	4a, (5), 6, 23	79.2	4b, (2)
5	4.25	ddd	9.8, 5.8, 4.6	4, 6	3, 4a(b), 6, 8	79.3	5, 21
6	4.13	dd	6.4, 4.5	5, 7	4b, 5, 7, 22	73.8	9
7	4.72	dd	9.9, 6.6	6, 8	6, (8), 12, 22	131.3	9
8	6.05	dd	11.5, 9.9	7, 9	5, (7), 21	127.6	11
9	6.13	dd	11.6, 1.5	8	13	137.9	8, 11
10	-	-	-	-	-	119.5	9
11	6.38	dd	1.5, 0.8	-	12, 12-OH	77.1	11
12	4.07	m	-	12-OH	7, 11, 12-OH, 14	-	-
12-OH	2.67	d	4.1	12	(11), 12, (13)	80.2	14a
13	4.16	ddd	9.2, 6.4, 6.4	12, 14	9, (11), 12, 14	35.4	-
14a	2.07	ddd	14.1, 6.4, 1.4	14b	13	74.4	14, 17
14b	1.97	ddd	14.1, 9.2, 5.0	14a	12, 15	81.7	14, 17
15	5.38	ddd	5.0, 3.6, 1.2	14, (16)	14, 16, 17	61.1	-
16	4.06	td	6.4, 3.7	15, 17	14b, 15, 17	170.2	19
17a	3.74	m	-	16	15, 16, 17-TBS	21.2	-
17b	-	-	-	-	-	109.4	21, 22
18	-	-	-	-	-	27.5	-
19	2.05	s	-	-	(12), 15, 17-TBS	25.6	21
20	-	-	-	-	-	18.0	2
21	1.48	s	-	22	2, 6, (5), 22	52.0	-
22	1.35	s	-	21	6, 7, 21	-	-
23	1.18	d	6.8	3	2, 3, 4a	-	-
24	3.73	s	-	-	2	-	-

* The signals of the TBS group are not listed and appear as follows: $^1\text{H NMR}$ (600 MHz, CDCl_3): $\delta = 0.87$ (s, 9H), 0.05 (s, 3H), 0.04 ppm (s, 3H). $^{13}\text{C NMR}$ (150 MHz, CDCl_3): $\delta = 25.9$ (3C), 18.4, -5.2, -5.3 ppm.

(Z,Z)-Chlorodiene 172.

2,6-Lutidine (6.8 μL , 59 μmol) and TBSOTf (9.3 μL , 40.5 μmol) were sequentially added to a solution of alcohol **170** (5.7 mg, 9.0 μmol) in CH_2Cl_2 (0.2 mL) at 0 $^\circ\text{C}$. The resulting mixture was stirred at rt for 30 h. The reaction was diluted with *t*-butyl methyl ether (3 mL) and quenched with pH 7 phosphate buffer (3 mL). The aqueous layer was separated and extracted with *t*-butyl methyl ether (3 \times 5 mL). The combined extracts were washed

with brine (10 mL), dried over Na_2SO_4 , filtered and concentrated. The residue was purified by flash chromatography (hexane/*t*-butyl methyl ether 6:1 to 4:1) to yield the title compound **172** as a colorless oil (5.6 mg, 83%). $[\alpha]_{\text{D}}^{20} = +4.8$ ($c = 0.5$, CHCl_3). $^1\text{H NMR}$ (400 MHz, CDCl_3): $\delta = 6.68$ (d, $J = 11.1$ Hz, 1H), 6.55 (td, $J = 11.0$, 1.1 Hz, 1H), 5.77 (ddd, $J = 10.8$, 9.6, 1.0 Hz, 1H), 5.36 (ddd, $J = 5.2$, 3.6, 1.8 Hz, 1H), 4.99 (ddd, $J = 9.6$, 6.4, 1.1 Hz, 1H), 4.36 (ddd, $J = 8.6$, 6.9, 4.5 Hz, 1H), 4.17 (dt, $J = 9.6$, 6.1 Hz, 1H), 4.13–4.07 (m, 2H), 4.05 (d, $J = 7.7$ Hz, 1H), 4.02 (dd, $J = 6.8$, 3.4 Hz, 1H), 3.73 (s, 3H), 3.73–3.70 (m, 2H), 2.37 (dq, $J = 9.5$, 7.1 Hz, 1H), 2.13–2.06 (m, 2H), 2.05 (s, 3H), 2.03–1.98 (m, 1H), 1.53 (s, 3H), 1.39 (s, 3H), 1.30–1.27 (m, 1H), 1.18 (d, $J = 6.6$ Hz, 3H), 0.92 (s, 9H), 0.86 (s, 9H), 0.09 (s, 3H), 0.05 (s, 3H), 0.033 (s, 3H), 0.027 ppm (s, 3H). $^{13}\text{C NMR}$ (100 MHz, CDCl_3): $\delta = 173.4$, 170.4, 137.5, 129.6, 126.7, 120.5, 109.8, 83.8, 81.7, 80.9, 79.2, 79.1, 78.5, 74.4, 73.3, 61.1, 52.1, 39.6, 37.1, 35.0, 27.8, 25.94 (3C), 25.90 (3C), 25.7, 21.2, 18.3 (2C), 18.2, -4.7 , -4.8 , -5.2 , -5.4 ppm. IR (film): $\tilde{\nu} = 2954$, 2929, 2885, 2857, 1741, 1462, 1371, 1248, 1087, 393, 836, 777, 666 cm^{-1} . MS (ESIpos) m/z (%): 769.4 (100 (M+Na)). HRMS (ESIpos): m/z calcd for $\text{C}_{36}\text{H}_{63}\text{O}_{10}\text{ClSi}_2\text{Na}$: 769.3541, found: 769.3538.

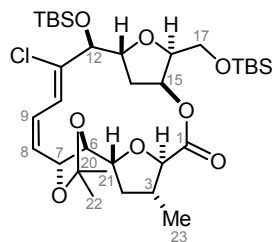
Secoacid 173.

added to a solution of K_2CO_3 (3.0 mg, 22 μmol) in $\text{CH}_2\text{Cl}_2/\text{aq. MeOH}$ (6:1, 1.2 mL) at 0 $^\circ\text{C}$ and the resulting mixture ($\text{CH}_2\text{Cl}_2/\text{MeOH}$ 8:1) was stirred at rt for 48 h. The reaction was quenched with pH 5 phosphate buffer (3 mL). The aqueous layer was separated and extracted with EtOAc (5 \times 5 mL). The combined extracts were dried over Na_2SO_4 , filtered and concentrated. The

residue was purified by flash chromatography (hexane/EtOAc/AcOH 135:65:1) to afford the title compound **173** as a colorless oil (3.5 mg, 79%). $^1\text{H NMR}$ (400 MHz, CDCl_3): $\delta = 6.64$ (d, $J = 11.1$ Hz, 1H), 6.56 (t, $J = 10.8$ Hz, 1H), 5.69 (t, $J = 10.1$ Hz, 1H), 5.01 (dd, $J = 9.4$, 5.4 Hz, 1H), 4.50 (dt, $J = 5.6$, 2.6 Hz, 1H), 4.42 (ddd, $J = 8.6$, 6.6, 4.7 Hz, 1H), 4.29 (ddt, $J = 9.0$, 6.1, 3.3 Hz, 1H), 4.17–4.07 (m, 3H), 3.98 (d, $J = 8.7$ Hz, 1H), 3.94–3.87 (m, 3H), 2.41–2.28 (m, 1H), 2.13–2.03 (m, 1H), 1.99–1.87 (m, 2H), 1.52 (s, 3H), 1.40 (s, 3H), 1.33–1.28 (m, 1H), 1.24 (d, $J = 6.7$ Hz, 3H), 0.91 (s, 9H), 0.89 (s, 9H), 0.09 (s, 6H), 0.08 (s, 3H), 0.04 ppm (s, 3H). $^{13}\text{C NMR}$ (100 MHz, CDCl_3): $\delta = 167.8$, 138.4, 129.1, 126.8, 120.1, 109.9, 83.3, 81.1, 80.8, 79.9, 78.8, 74.1, 73.3, 66.3, 63.0, 39.6, 37.8, 37.5, 27.8, 25.9 (6C), 25.5, 18.4, 18.3,

17.9, -4.7, -4.8, -5.3, -5.4 ppm. MS (ESI^{neg}) m/z (%): 689.3 (100 (M-H)). HRMS (ESI^{neg}): m/z calcd for $C_{33}H_{58}O_9ClSi_2$: 689.3313, found: 689.3321.

Macrolactone 174. A solution of 2-bromo-1-ethylpyridinium tetrafluoroborate (9.1 mg, 33 μ mol) in



dichloroethane (1 mL) was added to a suspension of secoacid **173** (2.3 mg, 3.3 μ mol) and $NaHCO_3$ (35 mg, 0.4 mmol) in dichloroethane (5.6 mL). The reaction mixture was warmed to 80 °C and stirred for 24 h. The reaction was quenched with pH 5 phosphate buffer (3 mL). The aqueous layer was separated and extracted with EtOAc (5 \times 5 mL). The combined extracts were

dried over Na_2SO_4 , filtered and concentrated. The residue was purified by flash chromatography (hexane/EtOAc 19:1 to 15:1) to afford the title compound **174** as a colorless oil (approx. 0.6 mg, 25%). 1H NMR (600 MHz, $CDCl_3$): see Table 4.10. ^{13}C NMR (100 MHz, $CDCl_3$): see Table 4.10. MS (ESI^{pos}) m/z (%): 695.3 (100 (M+Na)). HRMS (ESI^{pos}): m/z calcd for $C_{33}H_{57}O_8ClSi_2Na$: 695.3173, found: 695.3172.

Table 4.10. ^1H and ^{13}C NMR data of macrolactone **174** (0.5 mg in 0.25 mL CDCl_3); chagosensine numbering.*

atom n°	^1H NMR (600 MHz, CDCl_3)					^{13}C NMR (150 MHz, CDCl_3)	
	δ [ppm]	m	J [Hz]	COSY	NOESY	δ [ppm]	HMBC
1	-	-	-	-	-	170.2	15
2	3.89	d	9.2	3	(4b), 15, 23	80.5	23
3	2.80	ddq	9.0, 6.6, 6.2	2, 4(a)b, 23	(2), (4a), 5, 23	37.6	(2), 23
4a	2.16	ddd	12.0, 6.6, 5.1	3, 4b, 5	(3), 4b, 5	36.8	(6), 23
4b	1.57	m	-	3, 4a, 5	(2), 4a, 8, (23)		
5	4.15	m	-	4(a)b, (6)	3, 4a, 6	81.3	4b, (7)
6	4.65	m	7.0, 3.6	(5), 7	5, 7, 10, (22)	78.0	4b
7	5.19	m	-	6, 8	(8), 10, 22	75.4	9
8	5.88	dd	11.0, 5.3	7, 9	4b, (7), 9	130.5	(7), 10
9	6.56	td	11.1, 2.3	8, 10	8	123.4	(10)
10	6.69	d	11.6	9	6, 7, (14a)	123.0	(8)
11	-	-	-	-	-	135.7	12, 13
12	4.40	d	4.1	13	-	75.3	(10), 14b
13	4.37	dd	8.6, 4.2	14b	14b, 12-TBS	82.1	14b
14a	2.52	dd	12.5, 7.8	14b, 15	10, 14b, 15	31.6	12
14b	2.26	ddd	12.0, 10.3, 5.2	13, 14a, 15	13, 14a, (17)		
15	4.92	dt	10.3, 7.9	14, 16	2, (6), 14a, 16	76.1	14(a)b, (13)
16	4.05	m	-	15, 17	15, 17	78.8	14a
17a	3.73	m	-	16	17-TBS	63.0	15
17b							
20	-	-	-	-	-	107.8	21, 22
21	1.48	s	-	-	(8), 22	27.1	-
22	1.34	s	-	-	(6), 7, 21	24.2	-
23	1.12	d	6.4	3	2, 3, (4b)	16.9	2

* The signals of the TBS groups are not listed and appear as follows: ^1H NMR (600 MHz, CDCl_3): δ = 0.92 (s, 9H), 0.90 (s, 9H), 0.083 (s, 3H), 0.082 (s, 3H), 0.054 (s, 3H), 0.045 ppm (s, 3H). ^{13}C NMR (150 MHz, CDCl_3): δ = 26.1 (3C), 25.7 (3C), 18.5, 18.0, -4.8, -5.0, -5.2, -5.3 ppm.

5 Glossary

Ac	acetyl
acac	acetylacetonate
AIBN	azobis- <i>iso</i> -butyronitrile
aq.	aqueous
Ar	aryl
BArF	tetrakis[3,5-bis(trifluoromethyl)phenyl]borate ion
Bn	benzyl
br	broad
b.r.s.m.	based on recovered starting material
Bu	butyl
Bz	benzoyl
calcd	calculated
cat.	catalytic
CD	circular dichroism
cm	centimeter
conc.	concentrated
CSA	camphorsulfonic acid
Cy	cyclohexyl
d	day
d	doublet
d.r.	diastereomeric ratio
DABCO	1,4-diazabicyclo[2.2.2]octane
DBU	1,8-diazabicyclo[5.4.0]undec-7-ene
DCE	1,2-dichloroethane
(DHQD) ₂ PYR	hydroquinidine-2,5-diphenyl-4,6-pyrimidinediyl diether
DIAD	diisopropyl azodicarboxylate
DIBAL-H	diisobutylaluminum hydride
DMA	dimethylacetamide
DMAP	<i>N,N</i> -dimethyl-4-aminopyridine
DMF	dimethylformamide
DMP	Dess-Martin periodinane
DMPU	1,3-dimethyl-3,4,5,6-tetrahydro-2(1H)-pyrimidinone
DMS	dimethyl sulfide
DMSO	dimethyl sulfoxide
<i>ee</i>	enantiomeric excess
<i>ent</i>	enantiomeric
<i>epi</i>	epimeric
equiv	equivalent(s)
Et	ethyl
exp.	experimental
g	gram
GC	gas chromatography
h	hour
hep	heptet
HFIP	hexafluoroisopropanol
HMPA	hexamethylphosphoramide
HPLC	high performance liquid chromatography
HRMS	high resolution mass spectrometry
<i>i</i>	<i>iso</i> (branched)

INT	intermediate
IR	infrared spectroscopy
<i>J</i>	coupling constant
KHMDS	potassium hexamethyldisilazide
L	liter
l.l.s.	longest linear sequence
LDA	lithium diisopropylamide
LiHMDS	lithium hexamethyldisilazide
M	molar
m	multiplet
Me	methyl
Mes	mesityl
mg	milligram
min	minute
mL	milliliter
MOM	methoxymethyl
m.p.	melting point
ms	milisecond
Ms	methanesulfonyl
MS	mass spectrometry
MS	molecular sieves
MTBE	<i>t</i> -methyl ether
μg	microgram
μL	microliter
<i>n</i>	<i>normal</i> (linear)
N	normal (mol/kg)
NaHMDS	sodium hexamethyldisilazide
NCS	<i>N</i> -chloro succinimide
n.d.	not determined
NHC	<i>N</i> -heterocyclic carbene
NME	<i>N</i> -methylephedrine
NMI	<i>N</i> -methylimidazole
NMO	<i>N</i> -methylmorpholine- <i>N</i> -oxide
NMR	nuclear magnetic resonance
4-NO ₂ -Bz	4-nitrobenzoyl
NOE	nuclear Overhauser effect
NOESY	nuclear Overhauser effect spectroscopy
Ph	phenyl
PIDA	phenyliodonium diacetate
pin	pinacol
PG	protecting group
PMB	<i>para</i> -methoxybenzyl
ppm	parts per million
PPTS	pyridinium- <i>para</i> -toluenesulfonate
Pr	propyl
PTSA	<i>p</i> -toluenesulfonic acid
Py	pyridine
q	quartet
quant	quantitative
R	arbitrary organic substituent
r.r.	regioisomeric ratio
rac	racemic

RCAM	ring closing alkyne metathesis
RCM	ring closing (olefin) metathesis
rt	room temperature
s	singlet
s.m.	starting material
sat.	saturated
t	triplet
TBAF	tetra- <i>n</i> -ammonium flouride
TBS	dimethyl- <i>t</i> -silyl
TC	thiophene-2-carboxylate
TDMPP	tris-(2,6-dimethoxyphenyl)phosphine
TEMPO	(2,2,6,6-tetramethyl-piperidin-1-yl)oxyl
TES	triethylsilyl
Tf	trifluoromethanesulfonyl
TFA	trifluoroacetic acid
THF	tetrahydrofurane
TIPS	tri- <i>iso</i> -propylsilyl
TLC	thin layer chromatography
TMS	trimethylsilyl
Tol	<i>ortho</i> -tolyl
TPPO	triphenylphosphine oxide
TS	transition state
Ts	toluenesulfonyl
UV	ultraviolet
(<i>S,S_{FC}</i>)-WalPhos	(<i>S</i>)-1-[(<i>S_{FC}</i>)-2-[2-(diphenylphosphino)-phenyl]-ferrocenyl]-ethylbis-[3,5-bis-(trifluoromethyl)-phenyl]phosphine

6 Bibliography

- [1] (a) A. Fürstner, P. W. Davies, *Angew. Chem. Int. Ed.* **2007**, *46*, 3410; (b) D. J. Gorin, F. D. Toste, *Nature* **2007**, *446*, 395; (c) A. S. K. Hashmi, *Chem. Rev.* **2007**, *107*, 3180.
- [2] A. Fürstner, *Chem. Soc. Rev.* **2009**, *38*, 3208.
- [3] (a) A. S. K. Hashmi, M. Rudolph, *Chem. Soc. Rev.* **2008**, *37*, 1766; (b) M. Rudolph, A. S. K. Hashmi, *Chem. Soc. Rev.* **2012**, *41*, 2448; (c) A. Fürstner, *Acc. Chem. Res.* **2014**, *47*, 925; (d) D. Pflästerer, A. S. K. Hashmi, *Chem. Soc. Rev.* **2016**, *45*, 1331.
- [4] (a) W. Zi, F. Dean Toste, *Chem. Soc. Rev.* **2016**, *45*, 4567; (b) A. Pradal, P. Y. Toullec, V. Michelet, *Synthesis* **2011**, *2011*, 1501; (c) N. D. Shapiro, F. D. Toste, *Synlett* **2010**, *2010*, 675; (d) N. Bongers, N. Krause, *Angew. Chem. Int. Ed.* **2008**, *47*, 2178; (e) R. A. Widenhoefer, *Chem. Eur. J.* **2008**, *14*, 5382; (f) Y.-M. Wang, A. D. Lackner, F. D. Toste, *Acc. Chem. Res.* **2014**, *47*, 889.
- [5] (a) G. L. Hamilton, E. J. Kang, M. Mba, F. D. Toste, *Science* **2007**, *317*, 496; (b) R. L. LaLonde, Z. J. Wang, M. Mba, A. D. Lackner, F. D. Toste, *Angew. Chem. Int. Ed.* **2010**, *49*, 598.
- [6] (a) M. J. Johansson, D. J. Gorin, S. T. Staben, F. D. Toste, *J. Am. Chem. Soc.* **2005**, *127*, 18002; (b) M. P. Muñoz, J. Adrio, J. C. Carretero, A. M. Echavarren, *Organometallics* **2005**, *24*, 1293; (c) M. A. Tarselli, A. R. Chianese, S. J. Lee, M. R. Gagné, *Angew. Chem. Int. Ed.* **2007**, *46*, 6670; (d) Z. Zhang, R. A. Widenhoefer, *Angew. Chem. Int. Ed.* **2007**, *46*, 283.
- [7] (a) I. Alonso, B. Trillo, F. López, S. Montserrat, G. Ujaque, L. Castedo, A. Lledós, J. L. Mascareñas, *J. Am. Chem. Soc.* **2009**, *131*, 13020; (b) H. Teller, S. Flügge, R. Goddard, A. Fürstner, *Angew. Chem. Int. Ed.* **2010**, *49*, 1949; (c) H. Teller, M. Corbet, L. Mantilli, G. Gopakumar, R. Goddard, W. Thiel, A. Fürstner, *J. Am. Chem. Soc.* **2012**, *134*, 15331.
- [8] H. Teller, A. Fürstner, *Chem. Eur. J.* **2011**, *17*, 7764.
- [9] S. Flügge, doctoral thesis, TU Dortmund **2009**.
- [10] (a) N. Krause, C. Winter, *Chem. Rev.* **2011**, *111*, 1994; (b) Z. Zhang, *Gold and Platinum - Catalyzed Hydrofunctionalization of Allenes and Alkenes with Carbon, Oxygen, and Nitrogen Nucleophiles*, BiblioBazaar, **2011**.
- [11] (a) A. S. K. Hashmi, L. Schwarz, J.-H. Choi, T. M. Frost, *Angew. Chem. Int. Ed.* **2000**, *39*, 2285; (b) A. Hoffmann-Röder, N. Krause, *Org. Lett.* **2001**, *3*, 2537; (c) N. Morita, N. Krause, *Org. Lett.* **2004**, *6*, 4121; (d) Z. Zhang, C. Liu, R. E. Kinder, X. Han, H. Qian, R. A. Widenhoefer, *J. Am. Chem. Soc.* **2006**, *128*, 9066; (e) N. Morita, N. Krause, *Angew. Chem. Int. Ed.* **2006**, *45*, 1897; (f) B. Gockel, N. Krause, *Org. Lett.* **2006**, *8*, 4485; (g) C. J. T. Hyland, L. S. Hegedus, *J. Org. Chem.* **2006**, *71*, 8658; (h) T. Watanabe, S. Oishi, N. Fujii, H. Ohno, *Org. Lett.* **2007**, *9*, 4821.
- [12] N. Nishina, Y. Yamamoto, *Tetrahedron* **2009**, *65*, 1799.
- [13] L.-P. Liu, B. Xu, M. S. Mashuta, G. B. Hammond, *J. Am. Chem. Soc.* **2008**, *130*, 17642.
- [14] L.-P. Liu, G. B. Hammond, *Chem. Soc. Rev.* **2012**, *41*, 3129.
- [15] (a) N. Cox, M. R. Uehling, K. T. Haelsig, G. Lalic, *Angew. Chem. Int. Ed.* **2013**, *52*, 4878; (b) D. H. Miles, M. Veguillas, F. D. Toste, *Chem. Sci.* **2013**, *4*, 3427; (c) K. Aikawa, M. Kojima, K. Mikami, *Adv. Synth. Catal.* **2010**, *352*, 3131.
- [16] L. Mantilli, Postdoc Report, Max-Planck-Institut für Kohlenforschung, Mülheim an der Ruhr **2013**. For details see Section 4.2.
- [17] M. K. Ilg, L. M. Wolf, L. Mantilli, C. Farès, W. Thiel, A. Fürstner, *Chem. Eur. J.* **2015**, *21*, 12279.
- [18] (a) G. Zanoni, F. Castronovo, M. Franzini, G. Vidari, E. Giannini, *Chem. Soc. Rev.* **2003**, *32*, 115; (b) G. Cainelli, P. Galletti, D. Giacomini, *Chem. Soc. Rev.* **2009**, *38*, 990; (c) M. Bartók, *Chem.*

- Rev.* **2009**, *110*, 1663; (d) J. Escorihuela, M. I. Burguete, S. V. Luis, *Chem. Soc. Rev.* **2013**, *42*, 5595.
- [19] (a) M. Chiarucci, R. Mocci, L.-D. Syntrivanis, G. Cera, A. Mazzanti, M. Bandini, *Angew. Chem. Int. Ed.* **2013**, *52*, 10850; (b) M.-A. Abadie, X. Trivelli, F. Medina, F. Capet, P. Roussel, F. Agbossou-Niedercorn, C. Michon, *ChemCatChem* **2014**, *6*, 2235.
- [20] D. Wang, R. Cai, S. Sharma, J. Jirak, S. K. Thummanapelli, N. G. Akhmedov, H. Zhang, X. Liu, J. L. Petersen, X. Shi, *J. Am. Chem. Soc.* **2012**, *134*, 9012.
- [21] B. M. Trost, A. Fettes, B. T. Shireman, *J. Am. Chem. Soc.* **2004**, *126*, 2660.
- [22] D. Guillaneux, S.-H. Zhao, O. Samuel, D. Rainford, H. B. Kagan, *J. Am. Chem. Soc.* **1994**, *116*, 9430.
- [23] (a) Z. Wang, Z. Yang, D. Chen, X. Liu, L. Lin, X. Feng, *Angew. Chem. Int. Ed.* **2011**, *50*, 4928; (b) A. Nojiri, N. Kumagai, M. Shibasaki, *J. Am. Chem. Soc.* **2009**, *131*, 3779; (c) G. Lu, T. Yoshino, H. Morimoto, S. Matsunaga, M. Shibasaki, *Angew. Chem. Int. Ed.* **2011**, *50*, 4382; (d) F. Lutz, T. Igarashi, T. Kinoshita, M. Asahina, K. Tsukiyama, T. Kawasaki, K. Soai, *J. Am. Chem. Soc.* **2008**, *130*, 2956.
- [24] (a) T. J. Brown, D. Weber, M. R. Gagné, R. A. Widenhoefer, *J. Am. Chem. Soc.* **2012**, *134*, 9134; (b) G. Seidel, C. W. Lehmann, A. Fürstner, *Angew. Chem. Int. Ed.* **2010**, *49*, 8466.
- [25] T. Satyanarayana, S. Abraham, H. B. Kagan, *Angew. Chem. Int. Ed.* **2009**, *48*, 456.
- [26] H. Yu, F. Xie, Z. Ma, Y. Liu, W. Zhang, *Org. Biomol. Chem.* **2012**, *10*, 5137.
- [27] T. Tanaka, M. Hayashi, *Synthesis* **2008**, *2008*, 3361.
- [28] (a) C. M. Krauter, A. S. K. Hashmi, M. Pernpointner, *ChemCatChem* **2010**, *2*, 1226; (b) J. Zhang, W. Shen, L. Li, M. Li, *Organometallics* **2009**, *28*, 3129.
- [29] N. Haddad, B. Qu, S. Rodriguez, L. van der Veen, D. C. Reeves, N. C. Gonnella, H. Lee, N. Grinberg, S. Ma, D. Krishnamurthy, T. Wunberg, C. H. Senanayake, *Tetrahedron Lett.* **2011**, *52*, 3718.
- [30] J. Zhou, M.-C. Ye, Z.-Z. Huang, Y. Tang, *J. Org. Chem.* **2004**, *69*, 1309.
- [31] (a) W. Adam, Konrad J. Roschmann, Chantu R. Saha-Möller, *Eur. J. Org. Chem.* **2000**, *2000*, 3519; (b) M. Rueping, R. M. Koenigs, I. Atodiresei, *Chem. Eur. J.* **2010**, *16*, 9350; (c) M. Jia, M. Bandini, *ACS Catalysis* **2015**, *5*, 1638.
- [32] (a) J. Lacour, D. Moraleda, *Chem. Commun.* **2009**, 7073; (b) R. J. Phipps, G. L. Hamilton, F. D. Toste, *Nat Chem* **2012**, *4*, 603; (c) M. Mahlau, B. List, *Angew. Chem. Int. Ed.* **2013**, *52*, 518.
- [33] (a) A. Bernardi, G. Colombo, C. Scolastico, *Tetrahedron Lett.* **1996**, *37*, 8921; (b) P. Carbone, G. Desimoni, G. Faita, S. Filippone, P. Righetti, *Tetrahedron* **1998**, *54*, 6099; (c) D. A. Evans, C. S. Burgey, M. C. Kozlowski, S. W. Tregay, *J. Am. Chem. Soc.* **1999**, *121*, 686; (d) D. A. Evans, M. C. Kozlowski, J. A. Murry, C. S. Burgey, K. R. Campos, B. T. Connell, R. J. Staples, *J. Am. Chem. Soc.* **1999**, *121*, 669; (e) J. Barluenga, A. Fernández, A. Diéguez, F. Rodríguez, F. J. Fañanás, *Chem. Eur. J.* **2009**, *15*, 11660.
- [34] M. Bandini, M. Monari, A. Romaniello, M. Tragni, *Chem. Eur. J.* **2010**, *16*, 14272.
- [35] P. W. Davies, N. Martin, *Org. Lett.* **2009**, *11*, 2293.
- [36] G. Kovács, G. Ujaque, A. Lledós, *J. Am. Chem. Soc.* **2008**, *130*, 853.
- [37] Z.-Y. Ding, F. Chen, J. Qin, Y.-M. He, Q.-H. Fan, *Angew. Chem. Int. Ed.* **2012**, *51*, 5706.
- [38] (a) C. P. Casey, S. C. Martins, M. A. Fagan, *J. Am. Chem. Soc.* **2004**, *126*, 5585; (b) N. Abermil, G. r. Masson, J. Zhu, *Org. Lett.* **2009**, *11*, 4648; (c) Y. Inoue, T. Yokoyama, N. Yamasaki, A. Tai, *Nature* **1989**, *341*, 225; (d) Y. Inoue, T. Yokoyama, N. Yamasaki, A. Tai, *J. Am. Chem. Soc.* **1989**, *111*, 6480; (e) M. P. Sibi, U. Gorikunti, M. Liu, *Tetrahedron* **2002**, *58*, 8357; (f) V. S.

- Chan, M. Chiu, R. G. Bergman, F. D. Toste, *J. Am. Chem. Soc.* **2009**, *131*, 6021; (g) N. R. Chaubey, S. K. Ghosh, *RSC Advances* **2011**, *1*, 393.
- [39] S. T. Schneebeli, M. L. Hall, R. Breslow, R. Friesner, *J. Am. Chem. Soc.* **2009**, *131*, 3965.
- [40] (a) J. Otera, K. Sakamoto, T. Tsukamoto, A. Orita, *Tetrahedron Lett.* **1998**, *39*, 3201; (b) R. Saito, S. Naruse, K. Takano, K. Fukuda, A. Katoh, Y. Inoue, *Org. Lett.* **2006**, *8*, 2067.
- [41] H. Buschmann, H.-D. Scharf, N. Hoffmann, P. Esser, *Angew. Chem. Int. Ed.* **1991**, *30*, 477.
- [42] DFT calculations on the SMD-PBE0-D3/def2-TZVP//TPSS-D3/def2-SVP (TZVP for Au) level of theory kindly provided by Dr. Larry M. Wolf, Department of Theoretical Chemistry, Max-Planck-Institut für Kohlenforschung, Mülheim an der Ruhr, Germany.
- [43] O. N. Faza, C. S. López, in *Homogeneous Gold Catalysis* (Ed.: L. M. Slaughter), Springer International Publishing, Cham, **2015**, pp. 213.
- [44] NMR experiments and analysis thereof performed by Dr. Christophe Farès, Department of NMR spectroscopy, Max-Planck-Institut für Kohlenforschung, Mülheim an der Ruhr, Germany.
- [45] (a) T. J. Brown, A. Sugie, M. G. Dickens, R. A. Widenhoefer, *Organometallics* **2010**, *29*, 4207; (b) R. E. M. Brooner, T. J. Brown, R. A. Widenhoefer, *Chem. Eur. J.* **2013**, *19*, 8276.
- [46] (a) M. Messerer, H. Wennemers, *Synlett* **2011**, *2011*, 499; (b) M. Suginome, T. Yamamoto, Y. Nagata, T. Yamada, Y. Akai, *Pure Appl. Chem.* **2012**, *84*, 1759.
- [47] (a) K. Aplander, U. M. Lindström, J. Wennerberg, *Synthesis* **2012**, *44*, 848; (b) Y. Sohtome, B. Shin, N. Horitsugi, R. Takagi, K. Noguchi, K. Nagasawa, *Angew. Chem. Int. Ed.* **2010**, *49*, 7299.
- [48] R. A. Maplestone, M. J. Stone, D. H. Williams, *Gene* **1992**, *115*, 151.
- [49] (a) E. M. Driggers, S. P. Hale, J. Lee, N. K. Terrett, *Nat. Rev. Drug Discov.* **2008**, *7*, 608; (b) F. E. Koehn, G. T. Carter, *Nat. Rev. Drug Discov.* **2005**, *4*, 206.
- [50] S. Danishefsky, *Nat. Prod. Rep.* **2010**, *27*, 1114.
- [51] T. F. Molinski, D. S. Dalisay, S. L. Lievens, J. P. Saludes, *Nat. Rev. Drug Discov.* **2009**, *8*, 69.
- [52] (a) K. J. Weissman, *Nat. Prod. Rep.* **2015**, *32*, 436; (b) K. J. Weissman, *Nat. Chem. Biol.* **2014**, *11*, 660.
- [53] (a) R. D. Norcross, I. Paterson, *Chem. Rev.* **1995**, *95*, 2041; (b) C. A. Kuttruff, M. D. Eastgate, P. S. Baran, *Nat. Prod. Rep.* **2014**, *31*, 419.
- [54] (a) Y. Hirata, D. Uemura, *Pure Appl. Chem.* **1986**, *58*, 701; (b) T. D. Aicher, K. R. Buszek, F. G. Fang, C. J. Forsyth, S. H. Jung, Y. Kishi, M. C. Matelich, P. M. Scola, D. M. Spero, S. K. Yoon, *J. Am. Chem. Soc.* **1992**, *114*, 3162.
- [55] M. J. Towle, K. A. Salvato, J. Budrow, B. F. Wels, G. Kuznetsov, K. K. Aalfs, S. Welsh, W. Zheng, B. M. Seletsky, M. H. Palme, G. J. Habgood, L. A. Singer, L. V. DiPietro, Y. Wang, J. J. Chen, D. A. Quincy, A. Davis, K. Yoshimatsu, Y. Kishi, M. J. Yu, B. A. Littlefield, *Canc. Res.* **2001**, *61*, 1013.
- [56] M. S. Butler, A. A. B. Robertson, M. A. Cooper, *Nat. Prod. Rep.* **2014**, *31*, 1612.
- [57] Y. Qi, S. Ma, *ChemMedChem* **2011**, *6*, 399.
- [58] (a) Atta-ur-Rahman, *Studies in Natural Products Chemistry*, Elsevier Science, **2015**, 353–402; (b) Y. Kato, P. J. Scheuer, *J. Am. Chem. Soc.* **1974**, *96*, 2245.
- [59] (a) Atta-ur-Rahman, *Studies in Natural Products Chemistry*, Elsevier Science, **2008**, 57–100; (b) C. S. Neumann, D. G. Fujimori, C. T. Walsh, *Chem. Biol.* **2008**, *15*, 99.
- [60] (a) M. T. Cabrita, C. Vale, A. P. Rauter, *Mar. Drugs* **2010**, *8*, 2301; (b) G. W. Gribble, *Chem. Soc. Rev.* **1999**, *28*, 335; (c) G. W. Gribble, *Pure Appl. Chem.* **1996**, *68*, 1699.

- [61] (a) R. Bai, Z. A. Cichacz, C. L. Herald, G. R. Pettit, E. Hamel, *Mol. Pharmacol.* **1993**, *44*, 757; (b) A. Lorente, K. Makowski, F. Albericio, M. Álvarez, *Ann. Mar. Biol. Res.* **2014**, *1*, 1.
- [62] K. C. Nicolaou, D. Vourloumis, N. Winssinger, P. S. Baran, *Angew. Chem. Int. Ed.* **2000**, *39*, 44.
- [63] (a) K. C. Nicolaou, S. A. Snyder, *Angew. Chem. Int. Ed.* **2005**, *44*, 1012; (b) Y. Usami, *Mar. Drugs* **2009**, *7*, 314.
- [64] A. Fürstner, G. Seidel, *Angew. Chem. Int. Ed.* **1998**, *37*, 1734.
- [65] A. Fürstner, *Angew. Chem. Int. Ed.* **2013**, *52*, 2794.
- [66] (a) C. E. Laplaza, C. C. Cummins, *Science* **1995**, *268*, 861; (b) C. E. Laplaza, M. J. A. Johnson, J. C. Peters, A. L. Odom, E. Kim, C. C. Cummins, G. N. George, I. J. Pickering, *J. Am. Chem. Soc.* **1996**, *118*, 8623; (c) C. C. Cummins, *Chem. Commun.* **1998**, 1777.
- [67] (a) A. Fürstner, C. Mathes, C. W. Lehmann, *J. Am. Chem. Soc.* **1999**, *121*, 9453; (b) A. Fürstner, C. Mathes, C. W. Lehmann, *Chem. Eur. J.* **2001**, *7*, 5299.
- [68] W. Zhang, S. Kraft, J. S. Moore, *J. Am. Chem. Soc.* **2004**, *126*, 329.
- [69] (a) J. Heppekausen, R. Stade, R. Goddard, A. Fürstner, *J. Am. Chem. Soc.* **2010**, *132*, 11045; (b) J. Heppekausen, R. Stade, A. Kondoh, G. Seidel, R. Goddard, A. Fürstner, *Chem. Eur. J.* **2012**, *18*, 10281.
- [70] (a) K. Micoine, A. Fürstner, *J. Am. Chem. Soc.* **2010**, *132*, 14064; (b) K. Lehr, R. Mariz, L. Leseurre, B. Gabor, A. Fürstner, *Angew. Chem. Int. Ed.* **2011**, *50*, 11373; (c) W. Chaladaj, M. Corbet, A. Fürstner, *Angew. Chem. Int. Ed.* **2012**, *51*, 6929; (d) L. Hoffmeister, T. Fukuda, G. Pototschnig, A. Fürstner, *Chem. Eur. J.* **2015**, *21*, 4529; (e) D. Mailhol, J. Willwacher, N. Kausch-Busies, E. E. Rubitski, Z. Sobol, M. Schuler, M.-H. Lam, S. Musto, F. Loganzo, A. Maderna, A. Fürstner, *J. Am. Chem. Soc.* **2014**, *136*, 15719.
- [71] (a) J. Willwacher, N. Kausch-Busies, A. Fürstner, *Angew. Chem. Int. Ed.* **2012**, *51*, 12041; (b) J. Willwacher, A. Fürstner, *Angew. Chem. Int. Ed.* **2014**, *53*, 4217; (c) M. Fuchs, A. Fürstner, *Angew. Chem. Int. Ed.* **2015**, *54*, 3978.
- [72] (a) M. Yu, C. Wang, A. F. Kyle, P. Jakubec, D. J. Dixon, R. R. Schrock, A. H. Hoveyda, *Nature* **2011**, *479*, 88; (b) X. Shen, T. T. Nguyen, M. J. Koh, D. Xu, A. W. H. Speed, R. R. Schrock, A. H. Hoveyda, *Nature* **2017**, doi:10.1038/nature21043.
- [73] (a) S. Benson, M.-P. Collin, A. Arlt, B. Gabor, R. Goddard, A. Fürstner, *Angew. Chem. Int. Ed.* **2011**, *50*, 8739; (b) G. Valot, C. S. Regens, D. P. O'Malley, E. Godineau, H. Takikawa, A. Fürstner, *Angew. Chem. Int. Ed.* **2013**, *52*, 9534; (c) L. Hoffmeister, P. Persich, A. Fürstner, *Chem. Eur. J.* **2014**, *20*, 4396; (d) A. Ahlers, T. de Haro, B. Gabor, A. Fürstner, *Angew. Chem. Int. Ed.* **2016**, *55*, 1406.
- [74] K. Radkowski, B. Sundararaju, A. Fürstner, *Angew. Chem. Int. Ed.* **2013**, *52*, 355.
- [75] (a) B. Sundararaju, A. Fürstner, *Angew. Chem. Int. Ed.* **2013**, *52*, 14050; (b) S. M. Rummelt, A. Fürstner, *Angew. Chem. Int. Ed.* **2014**, *53*, 3626; (c) F. T. Gylling, F. Alois, *Bull. Chem. Soc. Jpn.* **2016**, *89*, 135.
- [76] S. M. Rummelt, K. Radkowski, D.-A. Roşca, A. Fürstner, *J. Am. Chem. Soc.* **2015**, *137*, 5506.
- [77] S. M. Rummelt, J. Preindl, H. Sommer, A. Fürstner, *Angew. Chem. Int. Ed.* **2015**, *54*, 6241.
- [78] H. Sommer, A. Fürstner, *Org. Lett.* **2016**, *18*, 3210.
- [79] H. Sommer, A. Fürstner, *Chem. Eur. J.* **2017**, *23*, 558.
- [80] T. Řezanka, L. Hanuš, Valery M. Dembitsky, *Eur. J. Org. Chem.* **2003**, *2003*, 4073.
- [81] (a) S. Carmely, Y. Kashman, *Tetrahedron Lett.* **1987**, *28*, 3003; (b) S. Carmely, M. Ilanb, Y. Kashmana, *Tetrahedron* **1989**, *45*, 2193; (c) A. Plubrukarn, D. W. Smith, R. E. Cramer, B. S.

- Davidson, *J. Nat. Prod.* **1997**, *60*, 712; (d) X. Fu, J. R. Barnes, T. Do, F. J. Schmitz, *J. Nat. Prod.* **1997**, *60*, 497.
- [82] D. Chuck Dunbar, J. M. Rimoldi, A. M. Clark, M. Kelly, M. T. Hamann, *Tetrahedron* **2000**, *56*, 8795.
- [83] F. Kong, D. J. Faulkner, *J. Org. Chem.* **1993**, *58*, 970.
- [84] L. C. Lo, N. Berova, K. Nakanishi, G. Schlingmann, G. T. Carter, D. B. Borders, *J. Am. Chem. Soc.* **1992**, *114*, 7371.
- [85] (a) W. N. Haworth, W. G. M. Jones, L. F. Wiggins, *J. Chem. Soc.* **1945**, *1*; (b) J. H. Udding, K. C. J. M. Tuijp, M. N. A. van Zanden, H. Hiemstra, W. N. Speckamp, *J. Org. Chem.* **1994**, *59*, 1993.
- [86] J. Kobayashi, M. Tsuda, M. Ishibashi, H. Shigemori, T. Yamasu, H. Hirota, T. Sasaki, *J. Antibiot.* **1991**, *44*, 1259.
- [87] N. Takada, H. Sato, K. Suenaga, H. Arimoto, K. Yamada, K. Ueda, D. Uemura, *Tetrahedron Lett.* **1999**, *40*, 6309.
- [88] H. Kigoshi, M. Kita, S. Ogawa, M. Itoh, D. Uemura, *Org. Lett.* **2003**, *5*, 957.
- [89] S. L. Mooberry, G. Tien, A. H. Hernandez, A. Plubrukarn, B. S. Davidson, *Canc. Res.* **1999**, *59*, 653.
- [90] A. Gollner, J. Mulzer, *Org. Lett.* **2008**, *10*, 4701.
- [91] (a) A. Arlt, S. Benson, S. Schulthoff, B. Gabor, A. Fürstner, *Chem. Eur. J.* **2013**, *19*, 3596; (b) K. Gebauer, A. Fürstner, *Angew. Chem. Int. Ed.* **2014**, *53*, 6393.
- [92] (a) P. Persich, J. Llavera, R. Lhermet, T. de Haro, R. Stade, A. Kondoh, A. Fürstner, *Chem. Eur. J.* **2013**, *19*, 13047; (b) S. Schaubach, K. Gebauer, F. Ungeheuer, L. Hoffmeister, M. K. Ilg, C. Wirtz, A. Fürstner, *Chem. Eur. J.* **2016**, *22*, 8494.
- [93] J. Heppekaufen, A. Fürstner, *Angew. Chem. Int. Ed.* **2011**, *50*, 7829.
- [94] J. M. Hoover, S. S. Stahl, *J. Am. Chem. Soc.* **2011**, *133*, 16901.
- [95] K. J. Ralston, H. C. Ramstadius, R. C. Brewster, H. S. Niblock, A. N. Hulme, *Angew. Chem. Int. Ed.* **2015**, *54*, 7086.
- [96] S. Schaubach, doctoral thesis, TU Dortmund **2016**.
- [97] B. M. Trost, C. J. Li, *Modern Alkyne Chemistry: Catalytic and Atom-Economic Transformations*, Wiley, **2014**.
- [98] (a) K. Jyothish, W. Zhang, *Angew. Chem. Int. Ed.* **2011**, *50*, 3435; (b) K. Jyothish, W. Zhang, *Angew. Chem.* **2011**, *123*, 3497; (c) H. Yang, Z. Liu, W. Zhang, *Adv. Synth. Catal.* **2013**, *355*, 885.
- [99] D.-A. Roşca, K. Radkowski, L. M. Wolf, M. Wagh, R. Goddard, W. Thiel, A. Fürstner, *J. Am. Chem. Soc.* **2017**, [accepted article].
- [100] U. Schubert, E. Kunz, B. Harkers, J. Willnecker, J. Meyer, *J. Am. Chem. Soc.* **1989**, *111*, 2572.
- [101] (a) T. Takeda, F. Kanamori, H. Matsusita, T. Fujiwara, *Tetrahedron Lett.* **1991**, *32*, 6563; (b) D. Madec, J.-P. Férézou, *Eur. J. Org. Chem.* **2006**, *2006*, 92.
- [102] Dr. Jakub Flasz performed the experiments leading to **N10** and **N13** once; they were later upscaled during this PhD research. The yields and analytical data obtained during this scale-up are reported.
- [103] J. Flasz, Postdoc-Report, Max-Planck-Institut für Kohlenforschung, Mülheim an der Ruhr **2015**.
- [104] A. Whitehead, M. D. McReynolds, J. D. Moore, P. R. Hanson, *Org. Lett.* **2005**, *7*, 3375.

- [105] (a) M. Kiyotada, M. Masatoshi, N. Tetsuro, *Bull. Chem. Soc. Jpn.* **1973**, *46*, 562; (b) S. D. Rychnovsky, G. Griesgraber, S. Zeller, D. J. Skalitzky, *J. Org. Chem.* **1991**, *56*, 5161; (c) S. D. Rychnovsky, G. Griesgraber, J. P. Powers, *Org. Synth.* **2000**, *77*, 1.
- [106] (a) T. Ikariya, Y. Ishii, H. Kawano, T. Arai, M. Saburi, S. Yoshikawa, S. Akutagawa, *J. Chem. Soc., Chem. Commun.* **1985**, 922; (b) R. Noyori, T. Ohkuma, M. Kitamura, H. Takaya, N. Sayo, H. Kumobayashi, S. Akutagawa, *J. Am. Chem. Soc.* **1987**, *109*, 5856; (c) M. Kitamura, T. Ohkuma, S. Inoue, N. Sayo, H. Kumobayashi, S. Akutagawa, T. Ohta, H. Takaya, R. Noyori, *J. Am. Chem. Soc.* **1988**, *110*, 629; (d) R. Noyori, T. Ohkuma, *Angew. Chem. Int. Ed.* **2001**, *40*, 40.
- [107] (a) G. Singh, A. Meyer, J. Aubé, *J. Org. Chem.* **2014**, *79*, 452; (b) G. Singh, J. Aubé, *Org. Biomol. Chem.* **2016**, *14*, 4299.
- [108] E. J. Corey, M. Chaykovsky, *J. Am. Chem. Soc.* **1965**, *87*, 1353.
- [109] I. Satoshi, M. Teruaki, *Chem. Lett.* **1990**, *19*, 67.
- [110] C. Palmer, N. A. Morra, A. C. Stevens, B. Bajtos, B. P. Machin, B. L. Pagenkopf, *Org. Lett.* **2009**, *11*, 5614.
- [111] N. A. Morra, B. L. Pagenkopf, *Tetrahedron* **2013**, *69*, 8632.
- [112] J. D. Hicks, W. R. Roush, *Org. Lett.* **2008**, *10*, 681.
- [113] C. Schwartz, J. Raible, K. Mott, P. H. Dussault, *Org. Lett.* **2006**, *8*, 3199.
- [114] M. González, Z. Gándara, A. Martínez, G. Gómez, Y. Fall, *Synthesis* **2013**, *45*, 1693.
- [115] (a) D. E. Frantz, R. Fässler, E. M. Carreira, *J. Am. Chem. Soc.* **2000**, *122*, 1806; (b) D. Boyall, D. E. Frantz, E. M. Carreira, *Org. Lett.* **2002**, *4*, 2605.
- [116] S. Schaubach, K. Michigami, A. Fürstner, *Synthesis* **2017**, *49*, 202.
- [117] (a) J. Wu, J. S. Panek, *Angew. Chem. Int. Ed.* **2010**, *49*, 6165; (b) O. Kubo, D. P. Canterbury, G. C. Micalizio, *Org. Lett.* **2012**, *14*, 5748.
- [118] T. R. Hoye, C. S. Jeffrey, F. Shao, *Nat. Protocols* **2007**, *2*, 2451.
- [119] R. N. Harris, P. Sundararaman, C. Djerassi, *J. Am. Chem. Soc.* **1983**, *105*, 2408.
- [120] T. Katsuki, K. B. Sharpless, *J. Am. Chem. Soc.* **1980**, *102*, 5974.
- [121] C. Oger, L. Balas, T. Durand, J.-M. Galano, *Chem. Rev.* **2013**, *113*, 1313.
- [122] M. Moreno-Mañas, A. Trius, *Tetrahedron* **1981**, *37*, 3009.
- [123] Y. Gao, J. M. Klunder, R. M. Hanson, H. Masamune, S. Y. Ko, K. B. Sharpless, *J. Am. Chem. Soc.* **1987**, *109*, 5765.
- [124] W. T. Lambert, G. H. Hanson, F. Benayoud, S. D. Burke, *J. Org. Chem.* **2005**, *70*, 9382.
- [125] D. G. Vanga, K. P. Kaliappan, *RSC Advances* **2014**, *4*, 12716.
- [126] P. J. Walsh, M. C. Kozlowski, *Fundamentals of Asymmetric Catalysis*, University Science Books, **2009**, 355-356; and literature therein.
- [127] D. B. Dess, J. C. Martin, *J. Org. Chem.* **1983**, *48*, 4155.
- [128] S. D. Meyer, S. L. Schreiber, *J. Org. Chem.* **1994**, *59*, 7549.
- [129] G. Tojo, M. I. Fernandez, *Oxidation of Alcohols to Aldehydes and Ketones: A Guide to Current Common Practice*, Springer US, **2006**.
- [130] T. Kubota, M. Tsuda, J. i. Kobayashi, *Tetrahedron* **2003**, *59*, 1613.
- [131] W. C. Still, C. Gennari, *Tetrahedron Lett.* **1983**, *24*, 4405.
- [132] S. Gupta, L. Poepelman, C. L. Hinman, J. Bretz, R. A. Hudson, L. M. V. Tillekeratne, *Biorg. Med. Chem.* **2010**, *18*, 849.
- [133] (a) P. L. Anelli, F. Montanari, S. Quici, *Org. Synth.* **1990**, *69*, 212; (b) R. M. Leanna, T. J. Sowin, H. E. Morton, *Tetrahedron Lett.* **1992**, *33*, 5029.

- [134] (a) S. V. Ley, J. Norman, W. P. Griffith, S. P. Marsden, *Synthesis* **1994**, 1994, 639; (b) F. Cominetti, A. Deagostino, C. Prandi, P. Venturello, *Tetrahedron* **1998**, 54, 14603.
- [135] J. R. Parikh, W. v. E. Doering, *J. Am. Chem. Soc.* **1967**, 89, 5505.
- [136] (a) S. G. Hentges, K. B. Sharpless, *J. Am. Chem. Soc.* **1980**, 102, 4263; (b) H. C. Kolb, M. S. VanNieuwenhze, K. B. Sharpless, *Chem. Rev.* **1994**, 94, 2483.
- [137] (a) L. Wang, K. B. Sharpless, *J. Am. Chem. Soc.* **1992**, 114, 7568; (b) T. Das, T. Mahapatra, S. Nanda, *Tetrahedron Lett.* **2012**, 53, 1186; (c) L. Ermolenko, N. A. Sasaki, *J. Org. Chem.* **2006**, 71, 693.
- [138] G. A. Crispino, K. S. Jeong, H. C. Kolb, Z. M. Wang, D. Xu, K. B. Sharpless, *J. Org. Chem.* **1993**, 58, 3785.
- [139] T. R. Hoyer, A. W. Aspaas, B. M. Eklov, T. D. Ryba, *Org. Lett.* **2005**, 7, 2205.
- [140] (a) M. P. Paudyal, N. P. Rath, C. D. Spilling, *Org. Lett.* **2010**, 12, 2954; (b) G. Valot, D. Mailhol, C. S. Regens, D. P. O'Malley, E. Godineau, H. Takikawa, P. Philipps, A. Fürstner, *Chem. Eur. J.* **2015**, 21, 2398.
- [141] S. E. Denmark, T. Bui, *Proc. Natl. Acad. Sci. USA* **2004**, 101, 5439.
- [142] (a) A. B. Northrup, D. W. C. MacMillan, *J. Am. Chem. Soc.* **2002**, 124, 6798; (b) A. B. Northrup, D. W. C. MacMillan, *Science* **2004**, 305, 1752; (c) A. B. Northrup, I. K. Mangion, F. Hettche, D. W. C. MacMillan, *Angew. Chem. Int. Ed.* **2004**, 43, 2152; (d) J. Carpenter, A. B. Northrup, D. Chung, J. J. M. Wiener, S.-G. Kim, D. W. C. MacMillan, *Angew. Chem. Int. Ed.* **2008**, 47, 3568; (e) B. M. Trost, C. S. Brindle, *Chem. Soc. Rev.* **2010**, 39, 1600.
- [143] J. A. Lafontaine, D. P. Provencal, C. Gardelli, J. W. Leahy, *J. Org. Chem.* **2003**, 68, 4215.
- [144] S. Hanessian, X. Mi, *Synlett* **2010**, 2010, 761.
- [145] M. Christmann, S. Bräse, *Asymmetric Synthesis: The Essentials*, Wiley, **2007**.
- [146] J. B. Baudin, G. Hareau, S. A. Julia, O. Ruel, *Tetrahedron Lett.* **1991**, 32, 1175.
- [147] C. Aïssa, *Eur. J. Org. Chem.* **2009**, 2009, 1831.
- [148] P. J. Kocienski, A. Bell, P. R. Blakemore, *Synlett* **2000**, 2000, 365.
- [149] P. R. Blakemore, W. J. Cole, P. J. Kociński, A. Morley, *Synlett* **1998**, 1998, 26.
- [150] J. Willwacher, doctoral thesis, TU Dortmund **2015**.
- [151] G. Stork, K. Zhao, *Tetrahedron Lett.* **1989**, 30, 2173.
- [152] G. Seidel, A. Fürstner, *Chem. Commun.* **2012**, 48, 2055.
- [153] Y. Shin, J.-H. Fournier, A. Brückner, C. Madiraju, R. Balachandran, B. S. Raccor, M. C. Edler, E. Hamel, Rachel P. Sikorski, A. Vogt, B. W. Day, D. P. Curran, *Tetrahedron* **2007**, 63, 8537.
- [154] A.-K. C. Schmidt, C. B. W. Stark, *Org. Lett.* **2011**, 13, 4164.
- [155] M. Heinrich, projected doctoral thesis, TU Dortmund.
- [156] (a) B. M. Trost, M. T. Sorum, C. Chan, G. Rühler, *J. Am. Chem. Soc.* **1997**, 119, 698; (b) B. M. Trost, J. T. Masters, *Chem. Soc. Rev.* **2016**.
- [157] N. Tsukada, S. Ninomiya, Y. Aoyama, Y. Inoue, *Org. Lett.* **2007**, 9, 2919.
- [158] (a) B. M. Trost, B. R. Taft, J. T. Masters, J.-P. Lumb, *J. Am. Chem. Soc.* **2011**, 133, 8502; (b) B. M. Trost, J. T. Masters, B. R. Taft, J.-P. Lumb, *Chem. Sci.* **2016**, 7, 6217.
- [159] O. Mitsunobu, *Synthesis* **1981**, 1981, 1.
- [160] (a) K. C. K. Swamy, N. N. B. Kumar, E. Balaraman, K. V. P. P. Kumar, *Chem. Rev.* **2009**, 109, 2551; (b) A. B. Smith, G. R. Ott, *J. Am. Chem. Soc.* **1996**, 118, 13095.
- [161] L. A. Paquette, Z. Gao, Z. Ni, G. F. Smith, *J. Am. Chem. Soc.* **1998**, 120, 2543.
- [162] T. Nakata, G. Schmid, B. Vranesic, M. Okigawa, T. Smith-Palmer, Y. Kishi, *J. Am. Chem. Soc.* **1978**, 100, 2933.

- [163] B. H. Lipshutz, D. F. Harvey, *Synth. Commun.* **1982**, *12*, 267.
- [164] (a) Y. Guindon, C. Yoakim, H. E. Morton, *Tetrahedron Lett.* **1983**, *24*, 2969; (b) Y. Quindon, H. E. Morton, C. Yoakim, *Tetrahedron Lett.* **1983**, *24*, 3969.
- [165] A. Letort, unpublished work, Max-Planck-Institut für Kohlenforschung, Mülheim an der Ruhr **2016**.
- [166] G. Gao, D. Moore, R.-G. Xie, L. Pu, *Org. Lett.* **2002**, *4*, 4143.
- [167] (a) B. M. Trost, A. Quintard, *Angew. Chem. Int. Ed.* **2012**, *51*, 6704; (b) B. M. Trost, M. J. Bartlett, A. H. Weiss, A. J. von Wangelin, V. S. Chan, *Chem. Eur. J.* **2012**, *18*, 16498.
- [168] D. L. Hughes, R. A. Reamer, *J. Org. Chem.* **1996**, *61*, 2967.
- [169] N. Kojima, Y. Suga, T. Matsumoto, T. Tanaka, A. Akatsuka, T. Yamori, S. Dan, H. Iwasaki, M. Yamashita, *Biorg. Med. Chem.* **2015**, *23*, 1276.
- [170] R. Takita, K. Yakura, T. Ohshima, M. Shibasaki, *J. Am. Chem. Soc.* **2005**, *127*, 13760.
- [171] F. W. Walker, E. C. Ashby, *J. Am. Chem. Soc.* **1969**, *91*, 3845.
- [172] (a) D. J. Cram, F. A. A. Elhafez, *J. Am. Chem. Soc.* **1952**, *74*, 5828; (b) M. T. Reetz, M. Hüllmann, T. Seitz, *Angew. Chem. Int. Ed.* **1987**, *26*, 477.
- [173] (a) H. B. Bürgi, J. D. Dunitz, E. Shefter, *J. Am. Chem. Soc.* **1973**, *95*, 5065; (b) A. Nguyen Trong, O. Eisenstein, J. M. Lefour, M. E. Tran Huu Dau, *J. Am. Chem. Soc.* **1973**, *95*, 6146.
- [174] (a) K. Matsumura, S. Hashiguchi, T. Ikariya, R. Noyori, *J. Am. Chem. Soc.* **1997**, *119*, 8738; (b) A. M. Hayes, D. J. Morris, G. J. Clarkson, M. Wills, *J. Am. Chem. Soc.* **2005**, *127*, 7318; (c) K. J. Hale, S. Manaviazar, J. George, *Chem. Commun.* **2010**, *46*, 4021.
- [175] I. Yuh-ichiro, K. Hideki, F. Ken'ichi, O. Tatsuo, N. Koichi, *Bull. Chem. Soc. Jpn.* **1989**, *62*, 845.
- [176] L. Bialy, H. Waldmann, *Chem. Eur. J.* **2004**, *10*, 2759.
- [177] H. Sasaki, D. Boyall, E. M. Carreira, *Helv. Chim. Acta* **2001**, *84*, 964.
- [178] D. Seyferth, A. W. Dow, H. Menzel, T. C. Flood, *J. Am. Chem. Soc.* **1968**, *90*, 1080.
- [179] (a) J. B. Epp, T. S. Widlanski, *J. Org. Chem.* **1999**, *64*, 293; (b) A. Vescovi, A. Knoll, U. Koert, *Org. Biomol. Chem.* **2003**, *1*, 2983.
- [180] (a) K. Sonogashira, Y. Tohda, N. Hagihara, *Tetrahedron Lett.* **1975**, *16*, 4467; (b) R. Chinchilla, C. Nájera, *Chem. Rev.* **2007**, *107*, 874.
- [181] (a) T. M. Brütsch, P. Bucher, K.-H. Altmann, *Chem. Eur. J.* **2016**, *22*, 1292; (b) M. O. Duffey, A. LeTiran, J. P. Morken, *J. Am. Chem. Soc.* **2003**, *125*, 1458.
- [182] F. Bohlmann, H. Schönowsky, E. Inhoffen, G. Grau, *Chem. Ber.* **1964**, *97*, 794.
- [183] D. Strand, T. Rein, *Org. Lett.* **2005**, *7*, 199.
- [184] J. S. Clark, G. Yang, A. P. Osnowski, *Org. Lett.* **2013**, *15*, 1464.
- [185] A. Soheili, J. Albaneze-Walker, J. A. Murry, P. G. Dormer, D. L. Hughes, *Org. Lett.* **2003**, *5*, 4191.
- [186] (a) J.-H. Li, X.-D. Zhang, Y.-X. Xie, *Eur. J. Org. Chem.* **2005**, *2005*, 4256; (b) J. M. Chalker, C. S. C. Wood, B. G. Davis, *J. Am. Chem. Soc.* **2009**, *131*, 16346.
- [187] H. Hofmeister, K. Annen, H. Laurent, R. Wiechert, *Angew. Chem. Int. Ed.* **1984**, *23*, 727.
- [188] V. Farina, S. I. Hauck, *J. Org. Chem.* **1991**, *56*, 4317.
- [189] M. Holmes, D. Kwon, M. Taron, R. Britton, *Org. Lett.* **2015**, *17*, 3868.
- [190] F. Kleinbeck, E. M. Carreira, *Angew. Chem. Int. Ed.* **2009**, *48*, 578.
- [191] (a) T. P. Gill, K. R. Mann, *Organometallics* **1982**, *1*, 485; (b) A. Schmid, H. Piotrowski, T. Lindel, *Eur. J. Inorg. Chem.* **2003**, *2003*, 2255.
- [192] B. M. Trost, R. C. Livingston, *J. Am. Chem. Soc.* **1995**, *117*, 9586.

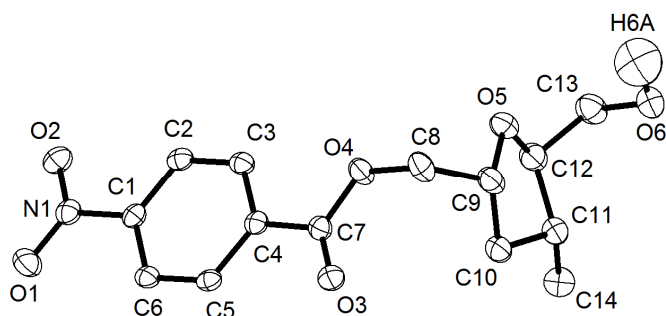
- [193] (a) H. E. Ensley, R. R. Buescher, K. Lee, *J. Org. Chem.* **1982**, *47*, 404; (b) M. S. Oderinde, R. D. J. Froese, M. G. Organ, *Angew. Chem. Int. Ed.* **2013**, *52*, 11334.
- [194] (a) P. Dimopoulos, A. Athlan, S. Manaviazar, J. George, M. Walters, L. Lazarides, A. E. Aliev, K. J. Hale, *Org. Lett.* **2005**, *7*, 5369; (b) P. Dimopoulos, J. George, D. A. Tocher, S. Manaviazar, K. J. Hale, *Org. Lett.* **2005**, *7*, 5377.
- [195] D.-A. Roşca, unpublished work, Max-Planck-Institut für Kohlenforschung, Mülheim an der Ruhr **2016**.
- [196] (a) K. J. Hale, M. Grabski, S. Manaviazar, M. Maczka, *Org. Lett.* **2014**, *16*, 1164; (b) S. Manaviazar, K. J. Hale, A. LeFranc, *Tetrahedron Lett.* **2011**, *52*, 2080; (c) K. J. Hale, M. Maczka, A. Kaur, S. Manaviazar, M. Ostovar, M. Grabski, *Org. Lett.* **2014**, *16*, 1168.
- [197] D. P. Curran, T. R. McFadden, *J. Am. Chem. Soc.* **2016**, *138*, 7741.
- [198] (a) D. A. Petrone, J. Ye, M. Lautens, *Chem. Rev.* **2016**, *116*, 8003; (b) I. Beletskaya, C. Moberg, *Chem. Rev.* **1999**, *99*, 3435; (c) R. Barbeyron, E. Benedetti, J. Cossy, J.-J. Vasseur, S. Arseniyadis, M. Smietana, *Tetrahedron* **2014**, *70*, 8431.
- [199] (a) M. F. Lappert, B. Prokai, *J. Organomet. Chem.* **1964**, *1*, 384; (b) N. Zhou, Q. Wang, A. J. Lough, H. Yan, *Can. J. Chem.* **2012**, *90*, 625; (c) R. S. Yalagala, H. Yan, *Tetrahedron Lett.* **2014**, *55*, 4830; (d) J. R. Lawson, E. R. Clark, I. A. Cade, S. A. Solomon, M. J. Ingleson, *Angew. Chem. Int. Ed.* **2013**, *52*, 7518.
- [200] M. L. Ho, A. B. Flynn, W. W. Ogilvie, *J. Org. Chem.* **2007**, *72*, 977.
- [201] After a short survey of different available halometalations on (protected) propargylic alcohols by postdoctoral researcher Dr. Aurélien Letort and myself, the unprecedented approach was abandoned.
- [202] (a) T. Ohmura, K. Oshima, H. Taniguchi, M. Suginome, *J. Am. Chem. Soc.* **2010**, *132*, 12194; (b) P. Wang, X.-L. Yeo, T.-P. Loh, *J. Am. Chem. Soc.* **2011**, *133*, 1254; (c) W. Su, T.-J. Gong, Q. Zhang, Q. Zhang, B. Xiao, Y. Fu, *ACS Catalysis* **2016**, *6*, 6417; (d) C. Gryparis, M. Stratakis, *Org. Lett.* **2014**, *16*, 1430; (e) N. Saito, K. Saito, H. Sato, Y. Sato, *Adv. Synth. Catal.* **2013**, *355*, 853; (f) H. Yoshida, *ACS Catalysis* **2016**, *6*, 1799; (g) M. Oestreich, E. Hartmann, M. Mewald, *Chem. Rev.* **2013**, *113*, 402.
- [203] (a) T. Ishiyama, N. Matsuda, N. Miyaura, A. Suzuki, *J. Am. Chem. Soc.* **1993**, *115*, 11018; (b) T. Ishiyama, N. Matsuda, M. Murata, F. Ozawa, A. Suzuki, N. Miyaura, *Organometallics* **1996**, *15*, 713; (c) M. Niestroj, W. P. Neumann, T. N. Mitchell, *J. Organomet. Chem.* **1996**, *519*, 45; (d) T. N. Mitchell, A. Amamria, H. Killing, D. Rutschow, *J. Organomet. Chem.* **1983**, *241*, C45; (e) T. N. Mitchell, K. Kwetkat, D. Rutschow, U. Schneider, *Tetrahedron* **1989**, *45*, 969; (f) J. Mancuso, M. Lautens, *Org. Lett.* **2003**, *5*, 1653; (g) S. Braune, U. Kazmaier, *Angew. Chem. Int. Ed.* **2003**, *42*, 306.
- [204] (a) S.-K. Kang, Y.-T. Lee, S.-H. Lee, *Tetrahedron Lett.* **1999**, *40*, 3573; (b) N. B. Carter, R. Mabon, J. B. Sweeney, *Synlett* **2006**, *2006*, 1577.
- [205] A. Fürstner, J.-A. Funel, M. Tremblay, L. C. Bouchez, C. Nevado, M. Waser, J. Ackerstaff, C. C. Stimson, *Chem. Commun.* **2008**, 2873.
- [206] (a) P. Espinet, A. M. Echavarren, *Angew. Chem. Int. Ed.* **2004**, *43*, 4704; (b) G. D. Allred, L. S. Liebeskind, *J. Am. Chem. Soc.* **1996**, *118*, 2748.
- [207] J. Srogl, G. D. Allred, L. S. Liebeskind, *J. Am. Chem. Soc.* **1997**, *119*, 12376.
- [208] (a) K. C. Nicolaou, P. G. Bulger, D. Sarlah, *Angew. Chem. Int. Ed.* **2005**, *44*, 4442; (b) E. O. Onyango, J. Tsurumoto, N. Imai, K. Takahashi, J. Ishihara, S. Hatakeyama, *Angew. Chem. Int.*

- Ed.* **2007**, *46*, 6703; (c) A. B. Smith, T. M. Razler, G. R. Pettit, J.-C. Chapuis, *Org. Lett.* **2005**, *7*, 4403.
- [209] N. Kanoh, S. Itoh, K. Fujita, K. Sakanishi, R. Sugiyama, Y. Terajima, Y. Iwabuchi, S. Nishimura, H. Kakeya, *Chem. Eur. J.* **2016**, *22*, 8586.
- [210] T. P. Blaisdell, J. P. Morken, *J. Am. Chem. Soc.* **2015**, *137*, 8712.
- [211] (a) A. Parenty, X. Moreau, J. M. Campagne, *Chem. Rev.* **2006**, *106*, 911; (b) A. Parenty, X. Moreau, G. Niel, J. M. Campagne, *Chem. Rev.* **2013**, *113*, PR1.
- [212] S. Benson, M.-P. Collin, G. W. O'Neil, J. Ceccon, B. Fasching, M. D. B. Fenster, C. Godbout, K. Radkowski, R. Goddard, A. Fürstner, *Angew. Chem. Int. Ed.* **2009**, *48*, 9946.
- [213] W. Zhu, M. Jiménez, W.-H. Jung, D. P. Camarco, R. Balachandran, A. Vogt, B. W. Day, D. P. Curran, *J. Am. Chem. Soc.* **2010**, *132*, 9175.
- [214] It needs to be mentioned at this point that due to impurities (mainly softener in 'distilled' solvents for chromatography and ethanol in anhydrous toluene), the precious material was unexpectedly reduced, thus it is refrained from interpreting yields on this exceedingly small scale.
- [215] (a) A. B. Smith, S. Dong, J. B. Brennehan, R. J. Fox, *J. Am. Chem. Soc.* **2009**, *131*, 12109; (b) T. Mukaiyama, M. Usui, K. Saigo, *Chem. Lett.* **1976**, *5*, 49; (c) D. A. Evans, J. T. Starr, *J. Am. Chem. Soc.* **2003**, *125*, 13531.
- [216] J. M. Schomaker, B. Borhan, *J. Am. Chem. Soc.* **2008**, *130*, 12228.
- [217] G. Storch, O. Trapp, *Angew. Chem. Int. Ed.* **2015**, *54*, 3580.
- [218] D. Seyferth, J. K. Heeren, G. Singh, S. O. Grim, W. B. Hughes, *J. Organomet. Chem.* **1966**, *5*, 267.
- [219] H. Nöth, H. Vahrenkamp, *J. Organomet. Chem.* **1968**, *11*, 399.
- [220] F. Tellier, R. Sauvêtre, J.-F. Normant, *J. Organomet. Chem.* **1985**, *292*, 19.
- [221] (a) S. Otsuka, A. Nakamura, Y. Tatsuno, *J. Am. Chem. Soc.* **1969**, *91*, 6994; (b) S. Otsuka, Y. Tatsuno, K. Ataka, *J. Am. Chem. Soc.* **1971**, *93*, 6705.
- [222] B. M. Trost, A. B. Pinkerton, M. Seidel, *J. Am. Chem. Soc.* **2001**, *123*, 12466.
- [223] Z. Zhang, C. F. Bender, R. A. Widenhoefer, *Org. Lett.* **2007**, *9*, 2887.
- [224] M. Murakami, S. Kadowaki, T. Matsuda, *Org. Lett.* **2005**, *7*, 3953.
- [225] J. Löfstedt, J. Franzén, J.-E. Bäckvall, *J. Org. Chem.* **2001**, *66*, 8015.
- [226] K. Aikawa, M. Kojima, K. Mikami, *Adv. Synth. Catal.* **2011**, *353*, 2882.
- [227] J. L. Arbour, H. S. Rzepa, A. J. P. White, K. K. Hii, *Chem. Commun.* **2009**, *0*, 7125.
- [228] T. Inokuchi, S. Matsumoto, S. Torii, *J. Org. Chem.* **1991**, *56*, 2416.
- [229] H. Fujioka, T. Okitsu, Y. Sawama, N. Murata, R. Li, Y. Kita, *J. Am. Chem. Soc.* **2006**, *128*, 5930.
- [230] M. J. Cryle, P. R. Ortiz de Montellano, J. J. De Voss, *J. Org. Chem.* **2005**, *70*, 2455.
- [231] (a) P. Fristrup, T. Jensen, J. Hoppe, P.-O. Norrby, *Chem. Eur. J.* **2006**, *12*, 5352; (b) L. F. Hatch, S. S. Nesbitt, *J. Am. Chem. Soc.* **1950**, *72*, 727.
- [232] S. A. Ali, M. Z. N. Iman, *J. Chem. Res.* **2008**, *2008*, 38.

7 Appendix

7.1 Crystallographic Data

Compound 68



Identification code (intern)	9052	
Empirical formula	$C_{14}H_{17}NO_6$	
Color	colorless	
Formula weight	$295.28 \text{ g} \cdot \text{mol}^{-1}$	
Temperature	100 K	
Wavelength	1.54178 \AA	
Crystal system	triclinic	
Space group	$P 1, (\text{no. } 2)$	
Unit cell dimensions	$a = 5.9280(5) \text{ \AA}$	$\alpha = 78.427(3)^\circ$
	$b = 7.3798(6) \text{ \AA}$	$\beta = 84.323(3)^\circ$
	$c = 16.2463(13) \text{ \AA}$	$\gamma = 86.923(4)^\circ$
Volume	$692.45(10) \text{ \AA}^3$	
Z	2	
Density (calcd)	$1.416 \text{ Mg} \cdot \text{m}^{-3}$	
Absorption coefficient	0.944 mm^{-1}	
F(000)	312 e	
Crystal size	$0.17 \times 0.15 \times 0.05 \text{ mm}^3$	
θ range for data collection	2.788 to 67.699° .	
Index ranges	$-6 \leq h \leq 7, -8 \leq k \leq 8, -19 \leq l \leq 19$	
Reflections collected	29024	
Independent reflections	2417 [$R_{\text{int}} = 0.0443$]	
Reflections with $I > 2\sigma(I)$	2128	
Completeness to $\theta = 67.679^\circ$	96.4%	

Absorption correction	Gaussian	
Max. and min. transmission	0.95709 and 0.88038	
Refinement method	Full-matrix least-squares on F^2	
Data / restraints / parameters	2417 / 0 / 194	
Goodness-of-fit on F^2	1.052	
Final R indices [$I > 2\sigma(I)$]	$R_1 = 0.0384$	$wR^2 = 0.1046$
R indices (all data)	$R_1 = 0.0441$	$wR^2 = 0.1094$
Extinction coefficient	0	
Largest diff. peak and hole	0.196 and $-0.291 \text{ e} \cdot \text{\AA}^{-3}$	

7.2 Calibration of HPLC-MS for RCAM

In order to obtain quantitative results during analytical HPLC-MS reaction monitoring, the device was calibrated as follows. Two independent stock solutions (1.57 mg and 2.36 mg) of the starting material **92** in HPLC-grade MeCN (392 μL and 500 μL) were prepared and dilution series performed (Table 7.1). After recording the respective HPLC chromatograms (two for each concentration), the concentrations (c in mg/mL) were plotted against the averaged area points (Figure 7.1). A straight calibration line was obtained, which can be used to determine the quantity of starting material in the HPLC trace of attempted RCAM reactions. To this end, the area points determined from a certain measurement can be inserted into the linear equation and the corresponding mass approximated *via* the concentration.

Table 7.1. Data acquired for enyne-yne **92**.

Entry	c [mg/mL]	Area Points ($\times 1000$)	Area Points ($\times 1000$)	\emptyset Area Points ($\times 1000$)
1	4.00	5067.96	5067.96	5067.96
2	2.00	2832.76	2676.90	2754.83
3	1.00	1338.63	1338.97	1338.80
4	0.50	874.49	767.48	820.98
5	0.25	316.14	318.02	317.08
6	0.125	153.01	159.05	156.03

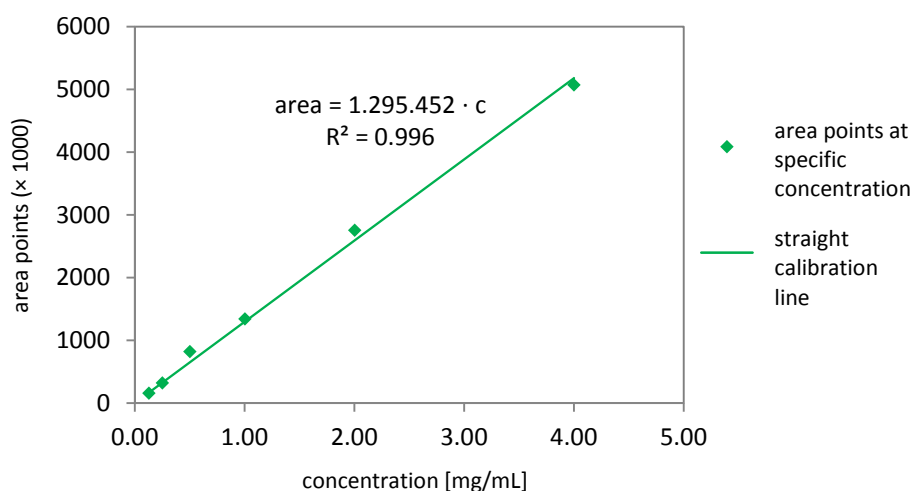


Figure 7.1. Straight calibration line for **92**.

The same procedure was carried out for the desired product **93b** in order to obtain the amount of product formed in the RCAM reaction (Table 7.2, Figure 7.2). Two independent stock solutions (1.19 mg and 1.36 mg) of the product **93b** in HPLC-grade MeCN (297 μ L and 500 μ L) were prepared and dilution series performed as described above.

Table 7.2. Data acquired for cyclic enyne **93b**.

Entry	c [mg/mL]	Area Points (× 1000)	Area Points (× 1000)	\emptyset Area Points (× 1000)
1	2.80	4195.12	4195.12	4195.12
2	1.40	2097.30	2088.91	2093.10
3	0.70	1057.20	1043.43	1050.31
4	0.35	504.22	509.18	506.70
5	0.18	262.01	267.24	264.63
6	0.09	134.73	118.60	126.67

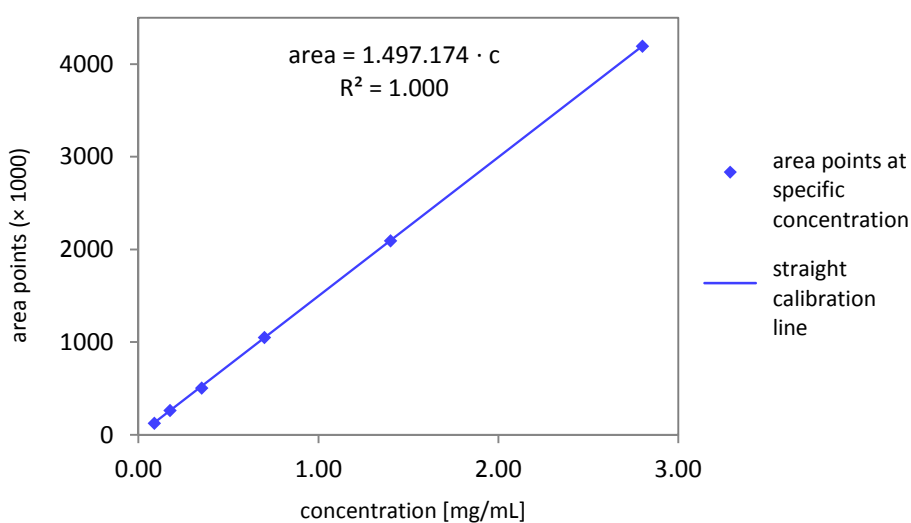


Figure 7.2. Straight calibration line for **93b**.